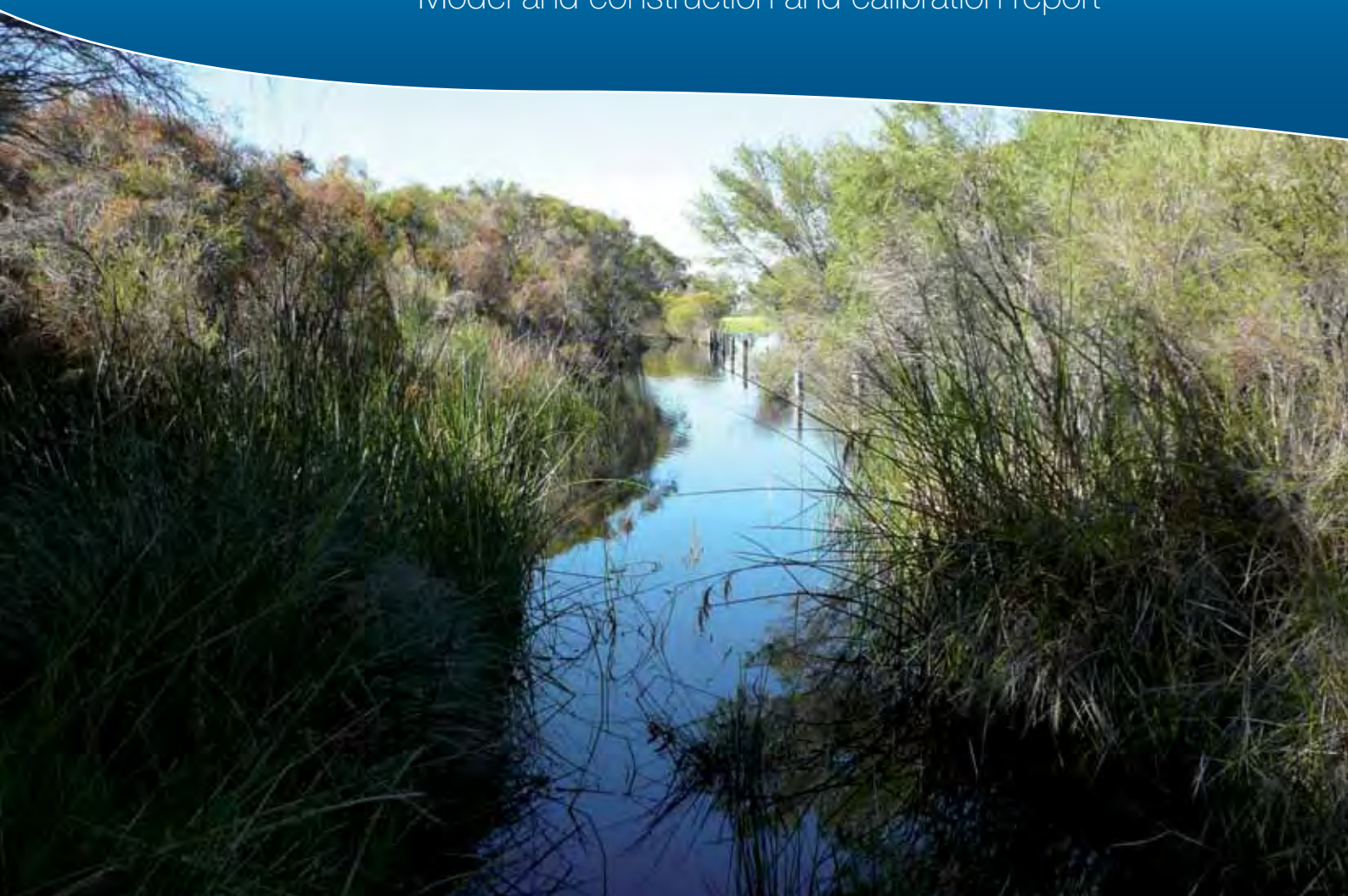




Government of **Western Australia**
Department of **Water**

Murray hydrological studies: surface water, groundwater and environmental water

Model and construction and calibration report



Looking after all our water needs

Water Science
technical series

Report no. WST 25
May 2010

Murray hydrological studies: surface water, groundwater and environmental water

Model construction and calibration report

Department of Water

Water Science Branch Technical Series

Report no. 25

May 2010

Department of Water

168 St Georges Terrace

Perth Western Australia 6000

Telephone +61 8 6364 7600

Facsimile +61 8 6364 7601

<http://www.water.wa.gov.au>

© Government of Western Australia 2010

May 2010

This work is copyright. You may download, display, print and reproduce this material in unaltered form only (retaining this notice) for your personal, non-commercial use or use within your organisation. Apart from any use as permitted under the *Copyright Act 1968*, all other rights are reserved. Requests and inquiries concerning reproduction and rights should be addressed to the Department of Water.

ISSN 1836-2869 (print)

ISSN 1836-2877 (online)

ISBN 978-1-921736-34-6 (print)

ISBN 978-1-921736-35-3 (online)

Acknowledgements

The Department of Water would like to thank the following people for their contribution to this publication. Philip Commander, Penny Wallace-Bell, Carey Johnston, Sandie McHugh, Cahit Yesertener and the technical advisory group from the Department of Water for assistance with geological interpretation and conceptualisation. Neil Milligan from CyMod Solutions for assistance with calibration. Peter Muirden from the Department of Water for guidance and project steering.

Reference details

The recommended reference for this publication is: Hall, J, Kretschmer, P, Quinton, B & Marillier, B, 2009, *Murray hydrological studies: surface water, groundwater and environmental water – model construction and calibration report*, Water Science Technical Series, Report no. 25, Department of Water, Western Australia.

Disclaimer

This document has been published by the Department of Water. Any representation, statement, opinion or advice expressed or implied in this publication is made in good faith and on the basis that the Department of Water and its employees are not liable for any damage or loss whatsoever which may occur as a result of action taken or not taken, as the case may be in respect of any representation, statement, opinion or advice referred to herein. Professional advice should be obtained before applying the information contained in this document to particular circumstances.

For more information about this report, contact Joel Hall, Water Science Branch, the Department of Water, Western Australia.

Cover photograph: Wetland along Scott Road, facing east, J Hall (2010).

Contents

Contents.....	i
Summary.....	v
1 Introduction	1
1.1 Project objective.....	2
Groundwater and surface water studies.....	2
Ecological water requirements and ecological study.....	2
Integration	3
1.2 Scope of work	3
2 Mike SHE for the Murray study area	6
Overland flow	7
Channel flow.....	8
Unsaturated flow/evapotranspiration model	8
Saturated flow	10
Interaction processes	11
3 Model construction	12
3.1 Simulation periods	12
3.2 Model domain and grid	12
3.3 Topography.....	13
3.4 Rainfall and evapotranspiration.....	13
3.5 Evapotranspiration model.....	15
3.6 Channel flow model (Mike 11).....	16
River network	16
Cross-sections.....	17
Boundaries	17
Hydrodynamics.....	18
3.7 Overland flow model	18
3.8 Unsaturated flow model	19
3.9 Saturated flow model	19
Geological layers.....	19
Geological lenses	19
Groundwater abstraction	22
Computational layers (vertical discretisation)	22
Boundary conditions.....	23
Drainage (saturated zone).....	24
4 Model calibration and validation	25
4.1 Calibration methods.....	25
4.2 Calibration bores.....	26
4.3 Calibration results	27
4.4 Validation bores	28
4.5 Validation results.....	28
4.6 Calibrated parameters	30
Unsaturated zone parameters	30
Land-use parameters	31
Channel flow parameters.....	32
Overland flow parameters	32
Saturated zone parameters.....	33

Saturated zone drainage parameters	34
4.7 Calibration discussion	34
Calibration bores	36
Rivers and lakes	37
Limitations and uncertainties	38
5 Water balance	40
6 Sensitivity analysis	41
7 Wetland models	45
Model set-up	45
Land use	45
Boundary conditions	46
7.1 Model calibration	46
Barragup Swamp model	47
Scott Road model	48
Elliot Road model	50
Lakes Road model	51
Phillips Road model	53
7.2 Wetland calibration discussion	55
7.3 Wetland water balances	55
8 Conclusions and recommendations	57
8.1 Regional model	57
8.2 Wetland models	59
9 References	61
Figures	63

Appendices

Appendix A: Calibration plots and statistics	92
Appendix B: Validation bore time-series and statistics	120
Appendix C: Barragup Swamp calibration statistics and plots	187
Appendix D: Scott Road wetland system calibration statistics and plots	196
Appendix E: Elliot Road wetland system calibration statistics and plots	218
Appendix F: Lakes Road wetland system calibration statistics and plots	228
Appendix G: Phillips Road wetland system calibration statistics and plots	253

Tables

Table 3-1: Model domain and grid values	12
Table 3-2: Initial values for LAI and average root-depth estimates from Xu et al. (2009)	15
Table 3-3: Hydraulic parameter ranges for geological lenses within the Superficial aquifer	22
Table 4-1: Calibration statistics for the observed versus modelled heads in the Murray Mike SHE model	27
Table 4-2: Calibration statistics for the observed versus modelled heads in the Murray Mike SHE model	27

Table 4-3: Validation statistics for the observed versus modelled heads in the Murray regional mode.....	29
Table 4-4: Validation statistics for the observed versus modelled heads in the Murray regional model.....	29
Table 4-5: Unsaturated zone model (two-layer model) calibrated parameters.....	31
Table 4-6: Evapotranspiration model calibrated parameters.....	32
Table 4-7: Mike 11 calibrated parameters.....	32
Table 4-8: Overland flow model calibrated parameters.....	32
Table 4-9: Saturated zone model calibrated hydraulic parameters.....	33
Table 4-10: Calibrated drainage parameters.....	34
Table 5-1: Average annual water balance for the entire model domain, 1978 - 2007.....	40
Table 6-1: Parameters and values used in the sensitivity analysis.....	43
Table 7-1: Wetland model set-up parameters.....	45
Table 7-2: Barragup Swamp model land-use parameters.....	47
Table 7-3: Barragup Swamp model unsaturated zone parameters.....	48
Table 7-4: Scott Road model land-use parameters.....	49
Table 7-5: Scott Road model unsaturated zone parameters.....	49
Table 7-6: Elliot Road model land-use parameters.....	50
Table 7-7: Elliot Road model unsaturated zone parameters.....	51
Table 7-8: Lakes Road model land-use parameters.....	52
Table 7-9: Lakes Road model unsaturated zone parameters.....	52
Table 7-10: Phillips Road wetland model land-use parameters.....	54
Table 7-11: Phillips Road wetland model unsaturated zone parameters.....	54
Table 7-12: Wetland model water balances.....	56
Table 8-1: Calibration error summary for the Murray regional model.....	57
Table 8-2: Wetland model set-up parameters.....	59
Table 8-3: Calibration error summary for the wetland models.....	59

Figures

Figure 1-1: Murray study area boundary and Murray DWMP boundary.....	64
Figure 3-1: Murray modelling domain and boundary cells.....	65
Figure 3-2: Surface topography for the Murray regional model at 200 m grid size.....	65
Figure 3-3: SILO rainfall locations and climate zones for the Murray regional model.....	66
Figure 3-4: Climate zones (evapotranspiration and rainfall) for the Murray regional model.....	67
Figure 3-5: Average annual rainfall (1985 – 2009) and Penman-Monteith evapotranspiration for the nine climate zones in the Murray study area and for the Pinjarra rainfall gauging station (9596).....	14
Figure 3-6: Annual rainfall (1985 – 2009) for the nine climate zones in the Murray study area and the Pinjarra rainfall gauging station (9596).....	14
Figure 3-7: Monthly rainfall (1985 – 2009) for the nine climate zones in the Murray study area and for the Pinjarra rainfall gauging station (9596).....	15
Figure 3-8: Land-use categories for the Murray regional model.....	67
Figure 3-9: Land-use categories re-sampled for the 200m model grid.....	68
Figure 3-10: Annual rotation scheme for grazing land use (non-irrigated) LAI.....	16
Figure 3-11: Mike 11 channel nodes, cross sections and boundary locations.....	68
Figure 3-12: Mike 11 channel network.....	69
Figure 3-13: Soil zones for the unsaturated zone model in the Murray regional model.....	69
Figure 3-14: Rockingham Sand: top of geological formation (mAHD).....	70
Figure 3-15: Rockingham Sand: base of geological formation (mAHD).....	70
Figure 3-16: Ascot Formation: top of geological formation (mAHD).....	71
Figure 3-17: Ascot Formation: base of geological formation (mAHD).....	71
Figure 3-18: Yoganup Formation: top of geological formation (mAHD).....	72
Figure 3-19: Yoganup Formation: base of geological formation (mAHD).....	72
Figure 3-20: Guildford Clay: top of geological formation (mAHD).....	73
Figure 3-21: Guildford Clay: base of geological formation (mAHD).....	73

Figure 3-22: Bassendean Sand: top of geological formation (mAHD).....	74
Figure 3-23: Bassendean Sand: base of geological formation (mAHD).....	74
Figure 3-24: Tamala Limestone: top of geological formation (mAHD)	75
Figure 3-25: Tamala Limestone: base of geological formation (mAHD).....	75
Figure 3-26: Alluvium, estuarine deposits and swamp deposits: top of formation (mAHD)	76
Figure 3-27 Alluvium, estuarine deposits and swamp deposits: base of formation (mAHD)	76
Figure 3-28: Colluvium: top of geological formation (mAHD)	77
Figure 3-29: Colluvium: base of geological formation (mAHD).....	77
Figure 3-30: Mine clays: top of geological formation (mAHD)	78
Figure 3-31: Mine clays: base of geological formation (mAHD)	78
Figure 3-32: Superficial aquifer abstraction bores and sub-regions	79
Figure 3-33: Base of computational layer 1(mAHD)	80
Figure 3-34: Base of computational layer 2 (mAHD)	80
Figure 3-35: Time-varying fixed-head boundary condition on the western boundary I	23
Figure 4-1: Calibration monitoring bore locations	81
Figure 4-2: Calibration scatter plot for the observed versus modelled heads in the Murray Mike SHE model.....	28
Figure 4-3: Validation monitoring bore locations.....	82
Figure 4-4: Validation scatter plot for the observed versus modelled heads in the Murray regional model	30
Figure 4-5: Computational layer 1 - thickness (m)	83
Figure 4-6: Computational layer 2 - thickness (m)	83
Figure 4-7: Computational layer 1 – horizontal hydraulic conductivity (m/day)	84
Figure 4-8: Computational layer 2 – horizontal hydraulic conductivity (m/day)	84
Figure 4-9: Computational layer 1 – vertical hydraulic conductivity (m/day)	85
Figure 4-10: Computational layer 2 – vertical hydraulic conductivity (m/day)	85
Figure 4-11: Computational layer 1 – specific yield	86
Figure 4-12: Computational layer 2 – specific yield	86
Figure 4-13: Computational layer 1 – transmissivity (m ² /day)	87
Figure 4-14: Computational layer 2 – transmissivity (m ² /day)	87
Figure 6-1: Scale sensitivity values resulting from the sensitivity analysis.....	44
Figure 7-1: Domain for individual wetland models	88
Figure 7-2: Barragup wetland model: land use and monitoring locations.....	89
Figure 7-3: Scott Road model: land use, monitoring and Mike 11 channel locations	89
Figure 7-4: Elliot Road model: land use and monitoring locations.....	90
Figure 7-5: Scott Road model: land use, monitoring and Mike 11 channel locations	90
Figure 7-6: Phillips Road model: land use, monitoring and Mike 11 channel locations	91
Figure 7-7: Irrigation rate for the Pinjarra golf course	54
Figure 7-8: Phillips Road model: soil type and irrigation area	91

Summary

This *construction and calibration report* is the second of three reports that comprise the 'groundwater studies' component of the Murray drainage and water management plan (DWMP). The 'groundwater studies' project aims to develop and calibrate a regional-scale groundwater model and finer-scaled wetland models, and to use the models to run various development, drainage and climate scenarios.

This report outlines the process of construction and calibration of a regional transient numerical model for the Murray study area, and for five finer-scaled wetland models within the Murray DWMP area. The report involves detailed explanation and discussion of

- the selection process for the model code and a description of the model
- the construction of the numerical model based on the outcome of the conceptual model
- a description of the calibration process, including calibration results (both quantitative and qualitative)
- the calibrated parameters, errors in the calibration and the limitations of the model
- water balances for the regional and wetland models
- a sensitivity analysis of the major model parameters
- future modelling and monitoring recommendations based on the results of the calibration and sensitivity analysis.

Murray regional model

The Murray regional model was constructed using the modelling software package Mike SHE, and was based on the conceptual hydrogeology and hydrology described in the *conceptual model report* (phase I of the 'groundwater studies' project component). The model was constructed using available geological, hydrogeological, hydrological, soil and land-use information. The Murray regional model consists of unsaturated zone, saturated zone, channel flow and overland flow components. It has a constant grid spacing of 200 m, and covers an area of approximately 722 km².

The calibration period was from 1985 – 2000 and validation was from 2000 – 2009. The normalised root mean square (RMS) error for the calibrated model was 2.02%. The RMS was 0.80 m, and the absolute residual mean (mean absolute error) and the residual mean error (mean error) were 0.55 m and 0.07 m respectively. The average absolute error was 0.52 m, defined as the difference between the predicted and measured water levels. The maximum positive error in the aquifer in predicted head was 2.80 m and the maximum negative error was -2.83 m. The model calibration satisfied the criteria of a water balance error <0.05%, an iteration residual error <0.1% and a scaled RMS error <5%.

Most of the simulated heads at the monitoring bores in the Superficial aquifer had a response consistent with measured data. The monitoring bores maintained correct trends and the magnitude of the error was constant.

Areas of significant error are:

- Near the edge of the Rockingham Sand paleochannel. The exact location of the edge is poorly understood, and it is likely there is error induced by the sudden increase in transmissivity.
- Those of low topography and high watertable, where minimum groundwater levels are close to sea level. The root-depth parameter for vegetation in the pasture and native vegetation surrounding these bores is likely to cause errors, as roots are not likely to remain within the groundwater table.
- In the south-east of the modelling area, where monitoring bores are likely to be affected by pumping from the Cattamarra Coal Measures, as this deeper aquifer has shown a steady decline of over 10 m in potentiometric head over the past three decades.
- Along the Darling Fault, where there are few measurements and the geology and hydrogeology is poorly understood.

The model predicted a gross recharge rate of 41% of rainfall and a net recharge of 12.3% for the regional model domain over the period 1978 – 2007. The lower net recharge rate is reflective of the high watertable in the Murray regional model domain, and large evaporative flux from the superficial groundwater.

The sensitivity analysis indicated that the model is sensitive to horizontal conductivity in the saturated zone, and to most parameters apart from LAI in the unsaturated zone (including root-depth, saturated soil capacity, and field capacity). The model was insensitive to vertical hydraulic conductivity, specific yield, LAI and overland flow parameters.

The Murray regional model has a spatial resolution of 200 m and a temporal resolution of one day. Based on these structural limitations of the model, the errors discussed in the previous section and the quality of the calibration, the model is considered suitable for:

- Evaluating changes in the water balance due to drainage changes and land-use changes (changes in recharge, drainage, evapotranspiration, horizontal flow etc.).
- The relative assessment of regional and subregional impacts due to changes in drainage, and abstraction from the shallow aquifer.
- District-scale groundwater-level evaluation (AAMGL, AAMinGL etc.) under various climate scenarios. This includes determining areas of seasonal waterlogging and inundation. However, the inherent model error needs to be considered when using groundwater levels derived from the regional model. If the error is deemed too large for the purpose of the application, a localised model with a finer grid should be constructed and calibrated to achieve appropriate model accuracy.

The model's structural limitations suggest that the Murray regional model is not the preferred platform for the following applications: wetland or lake assessment, flood modelling, detailed drainage modelling, abstraction or sustainable yields from the Leederville aquifer.

Wetland models

Eight key wetlands were selected to have their ecological water requirement (EWR) defined, a process involving detailed assessment of the water regime required to maintain the ecological values of the wetlands. Five separate wetland models were used to model the eight key wetlands. The models used hydraulic parameters, geologic layers and boundary conditions that were consistent with the calibrated Murray regional model, and applied at a finer grid scale. The five models were set up with grids ranging from 30 – 50 m.

The calibration period for each of the wetland models was from 2000 – 2009 and due to the limited data there was no validation period. The model calibration satisfied the criteria of a water balance error <0.1% and an iteration residual error <0.1% for all wetland models. The scaled RMS was below 5% for the Lakes Road model. It was recognised that the criteria of 5% was difficult to achieve in all models, as ranges in groundwater head were small for some models due to limited groundwater data.

Based on the model's structural limitations, the errors discussed in the previous section and the quality of the calibration, the wetland models are considered suitable for predicting changes in wetland water levels and for predicting wetland water regimes for various climate and land-use change scenarios; however, errors in the calibration need to be considered when interpreting modelling results.

1 Introduction

The Western Australian Planning Commission, in consultation with local government authorities, has placed a high priority on developing structure plans for areas of urban growth. These plans will guide future development and the management of environmental issues. A key step in a structure plan's implementation is the creation of a drainage and water management plan (DWMP) that embraces water sensitive urban design (WSUD) and best management practices and provides a framework for more site-specific water management plans. A DWMP addresses the following aspects of the total water cycle:

- protection of significant environmental assets within the structure plan area, including meeting their water requirements and managing potential impacts from development
- water demands, supply options, opportunities for conservation and demand management measures and wastewater management
- surface runoff, including both peak event (flood) management and WSUD principles to be applied to frequent events
- groundwater, including the impact of urbanisation, variation in climate, installation of drainage to manage maximum annual groundwater levels, potential impacts on the environment and the potential to use groundwater as a resource
- water quality management, which includes source control of pollution inputs by catchment management, acid sulfate soil management, control of contaminated discharges from industrial areas and management of nutrient exports from surface runoff and groundwater through structural measures.

As part of the Murray region DWMP, the Department of Water's Drainage and Waterways Branch has instigated the following projects:

1. floodplain development study including inundation and local catchment stormwater modelling
2. groundwater studies including regional pre-development groundwater levels, water balance modelling, climate impacts and extent of current waterlogged areas
3. ecological water requirements (EWRs) for wetlands within the study area
4. preparation of a DWMP for the DWMP study area

GHD Pty Ltd has been contracted to write the DWMP for the Murray region, which will integrate the results of the other studies. The Department of Water's Water Science Branch has been commissioned to deliver the 'groundwater studies' project, as well as to provide the hydrological deliverables of the 'ecological water requirements and ecological study' component of the project.

The DWMP area includes a portion of the Swan Coastal Plain centred on Ravenswood, where there is relatively flat terrain, significant waterlogging, wetlands of significance, and risk of riverine flooding. The study area extends from the Nambelup Brook catchment in the north, Lower Serpentine River and Peel Inlet/Harvey Estuary in the west, Fautleroy Drain catchment in the south and the Murray River/Darling Range foothills in the east.

The area specified for the groundwater studies, designated 'modelling boundary' in Figure 1-1, is larger than the DWMP area, and is referred to as the 'Murray study area' in this report. The Murray study area extends east to the Darling Fault, west to the Indian Ocean and Peel-Harvey estuary and approximately 5 km north and south of the DWMP study area to the boundary of Dirk Brook and Caris Drain.

1.1 Project objective

Groundwater and surface water studies

The purpose of the groundwater study is to develop and calibrate a regional-scale groundwater model, and to use this model to run various climate and land-use change scenarios. The groundwater study had been re-named *Murray hydrological studies: surface water, groundwater and environmental water*, due to the region's high degree of surface water/groundwater interaction, the requirement to study both parts of its water regime, and the need to determine environmental water requirements (EWRs) for its wetlands. The model will thus be an integrated surface water/groundwater model, and will reflect the nature of the local environment which has wetlands of significant size and value.

The primary objectives of the groundwater studies are to:

- deliver a calibrated regional-scale groundwater model
- develop and run a suite of scenarios
- deliver associated maps and ESRI shapefiles.

The project requirements include the modelling of various climate scenarios, pre- and post-development scenarios, and WSUD construction philosophies to determine:

- maximum, minimum, average annual maximum and average annual minimum groundwater levels (MaxGL, MinGL, AAMaxGL and AAMinGL)
- water balance modelling including changes in groundwater discharges, interaction with surface water and environmental water
- likely impacts of acid sulfate soils (ASS)
- reuse opportunities such as community bores and surface detention
- likely areas of waterlogging
- water balance modelling including flows in drains and tributaries
- flood, drought, wet, dry and average year impacts
- impacts on water-dependent ecosystems (wetlands) and ecology
- guidance for drainage design (surface water and groundwater infrastructure).

Ecological water requirements and ecological study

The purpose of the EWR component of the study is to provide a detailed hydrological assessment of key wetlands within the study area, which will be used to determine wetland water levels under various climate and land-use conditions. EWRs are defined as the water

regimes needed to maintain the ecological values of water-dependent systems at a low level of risk. It is necessary that EWRs are primarily based on the water requirements of wetland vegetation, with limited consideration of other factors. This EWR project requires a detailed vegetation survey, analysis and subsequent report. GHD has been contracted to conduct the vegetation study, analyse the hydrological regimes and write the report.

For this EWR project, the delivery of the hydrological components of the EWRs will include the estimated surface water and groundwater inflows, outflows and water levels from the modelling of eight key wetlands selected by the Drainage and Waterways Branch. The vegetation science component, drilling, monitoring, analysis and reporting will be delivered by GHD.

Integration

The regional model of the study area will primarily provide groundwater levels, but also information on surface water flows, groundwater interactions, waterlogging, and MinGL, MaxGL, AAMaxGL and AAMinGL for all modelled scenarios. This will allow a controlled groundwater level (CGL) to be determined, taking into account the wetland EWRs.

The Water Science Branch's specific deliverables for the EWR project will be to describe the current and predicted hydrology for each of the wetlands, taking into account land use and climate change. The ecological team from GHD can then assess the potential impacts on the wetlands. An EWR will be specified for each wetland in collaboration with the ecological team.

1.2 Scope of work

The scope of the surface water and groundwater hydrological studies and EWR hydrological studies can be broadly divided into three phases. Each phase will have its own detailed scientific report, which will be reviewed before the next phase is undertaken. The three phases involved in the surface water and groundwater component of the study include:

1. Developing a conceptual groundwater/surface water model and steady-state water balance model for the Murray study area, including:
 - a review of relevant literature
 - description of the study area
 - description of the climate and hydrology
 - interpretation and development of a three-dimensional conceptual model of the geology
 - definition of all aquifers and major hydrogeological processes
 - a description of the hydrological and hydrogeological processes and parameters
 - a numerical steady-state water balance conceptual model that includes surface water, groundwater and the interaction between them.

This project phase is described in the *conceptual model report* (Hall et al. 2010a).

2. Constructing and calibrating a regional transient numerical model for the Murray study area. This will involve the simulation of surface water in relevant waterways and groundwater flow in each aquifer, the calculation of a water budget for each of the aquifers and the determination of groundwater-level contours. This phase will involve:
 - the selection process for the model code and description of the model
 - a description of the construction of the numerical model, which will be based on the outcome of the conceptual model
 - a description of the calibration process, including calibration results (both quantitative and qualitative). Calibration results will be assessed against calibration criteria
 - the calibrated parameters will be presented; the errors in the calibration and the limitations of the model will be discussed
 - the water balance for the regional model and the DWMP area will be presented and discussed
 - a sensitivity analysis of the major model parameters will be undertaken, and sensitivities will be discussed with respect to the model's predictive capabilities.

Phase 2 will be described in this report.

3. A suite of predictive runs will be undertaken to determine the change to water budgets and groundwater levels under various climate and land-use scenarios. This phase will follow on from phase 2 and will be described in a subsequent *land development, drainage and climate scenario report* (Hall et al. 2010b).

The three phases of the EWR hydrological studies component of the project have the following scope:

1. Characterisation and conceptualisation of the wetlands included in the EWR. Determination of the appropriate drivers for wetland water levels was based on available literature and data gathered from hydrogeological measurements and stratigraphy interpretation from GHD's recent drilling program. This project phase is described in the *conceptual model report* (Hall et al. 2010a).
2. Construction and calibration of finer-grid-scale wetland models using modelling results from phase 2 of the surface water and groundwater studies. Detailed calibration of fine-scaled models was completed using data collected during the 2009 winter by Department of Water staff. Boundary conditions for wetland models were taken from the regional model. This phase involved:
 - a description of each of the wetland models, including the set-up, boundary conditions and model components
 - an outline of the calibration process for each of the wetland models, including the parameters that were calibrated; presentation of the calibration results for each of the individual wetland models; and discussion of the calibration error and limitations of the wetland modelling
 - a detailed water balance for each of the wetland models.

This phase will be described in the following report.

3. Phase 3 involves a suite of predictive runs to determine the change in wetland water levels and water balances in the wetlands under various drainage and climate scenarios. This phase is described in the *land development, drainage and climate scenario report* (Hall et al. 2010b).

2 Mike SHE for the Murray study area

Mike SHE was selected as the most appropriate tool for the transient numerical modelling exercise. Mike SHE is an advanced, flexible framework for hydrologic modelling that includes a full suite of pre- and post-processing tools and a flexible mix of advanced and simple solution techniques for each of the hydrologic processes (Refsgaard et al. 1995). Mike SHE is a deterministic physical-based distributed model; the hydrological processes are modelled by finite difference representations of the partial differential equations for the conservation of mass, momentum and energy, in addition to some empirical equations. Mike SHE includes a suite of interacting process models. Those models included in the Murray modelling project are the:

- saturated zone model
- overland flow model
- channel flow model
- unsaturated zone model
- evapotranspiration model.

Processes within the models can be represented at different levels of spatial distribution and complexity. Each of the models in Mike SHE has the ability to utilise physics-based code that solves the partial differential equations describing mass flow and momentum transfer.

Parameters in these equations can be obtained from measurement and used in the model (e.g. the Saint Venant equations for open-channel flow and the Darcy equation for saturated flow in porous media).

There are, however, important limitations to the applicability of such physics-based models. For example:

- it is widely recognised that such models require a significant amount of data and the cost of data acquisition may be high
- the relative complexity of the physics-based solution requires substantial execution time
- the relative complexity may lead to over-paramatised descriptions for simple applications.

Therefore, it is often practical to use simplified process descriptions for some of the hydrologic procedures. A complete physical-based flow description for all processes in one model is rarely necessary. A sensible methodology is to use physical-based flow descriptions for only those processes that are important, and simpler, faster, less data-demanding methods for the less important processes. The downside is that the parameters in the simpler methods are usually no longer physically meaningful and must be calibrated.

The modular approach used in the Mike SHE code makes it possible to implement multiple descriptions for each of the hydrologic processes. In the simplest case, Mike SHE can use fully distributed conceptual approaches to model the watershed processes. For advanced applications, Mike SHE can simulate all the processes using physics based methods.

Alternatively, Mike SHE can combine conceptual and physically based methods depending on data availability and project needs. The flexibility in Mike SHE's process-based framework allows each process to be solved at its own relevant spatial and temporal scale.

The Murray DWMP requires a regional groundwater model, and the study area covers 722 km². For a model of this spatial scale, it is not appropriate to use physical-based equations for all hydrological processes. Physical-based processes are used for the saturated zone and channel flow models, but simpler empirical techniques are used for the unsaturated zone, evapotranspiration and overland flow components.

The type and complexity of each of the process models used in the Murray modelling project and the reasons for adopting the methodology are outlined below.

Overland flow

Overland flow simulates the movement of ponded surface water across the topography. It can be used to calculate flow on a floodplain or runoff to streams. The exact route and quantity is determined by the topography and flow resistance, as well as the losses due to evaporation and infiltration along the flow path.

The overland flow module is required when using Mike SHE's channel flow model, because it provides lateral runoff to the waterways. Mike SHE's overland flow module uses finite difference methods to solve the overland flow equations. The finite difference method uses the diffusive wave approximation of the Saint Venant equations. There are two solution methods available:

- successive over-relaxation (SOR) numerical solution
- explicit numerical solution.

The choice of method is a trade-off between accuracy and solution time. The SOR solver is generally faster because it can run with larger timesteps, and significantly reduces the model run-time. The explicit method is generally more accurate than the SOR method, but is often constrained to smaller timesteps. For the Murray model, the SOR method was selected to improve model run-time. It is recognised that while overland flow is likely to be an important flux, flood modelling and detailed overland analysis is not a project objective.

The overland flow model interacts with the saturated zone model, the unsaturated zone model, and the channel flow model. When the phreatic surface rises to meet the land surface, excessive water from the saturated zone model will then form part of the overland flow model. Also, if rainfall is more intense than the soil infiltration, the excessive rainfall will form part of the overland flow model. Water in the overland flow model will move via the topography from cell to cell according to the diffusive wave approximation equations. The water will run to local depressions where it will either infiltrate or evaporate, or it will run to a river link, where it will become part of the channel flow model. The overland flow model provides the catchment surface-flow component of the channel flow model. Parameters required for estimation and calibration for the overland flow model include the Manning number (Manning's 'M', which is the inverse of the channel roughness, known as Manning's 'n') and the detention storage.

Channel flow

Mike SHE uses Mike 11 to simulate channel flow. Mike 11 belongs to the Danish Hydrological Institute's suite of modelling tools, and is a dynamic model for river and channel hydraulics. Mike 11 includes comprehensive facilities for modelling complex channel networks, lakes and reservoirs and river structures. The hydrologic components of Mike SHE are directly coupled to Mike 11. The Mike SHE – Mike 11 coupling enables:

- one-dimensional simulation of river flows and water levels using the fully dynamic Saint Venant equations
- simulation of a wide range of hydraulic control structures, such as weirs, gates and culverts
- dynamic overland flooding flow to and from the Mike 11 river network
- full dynamic coupling of surface and subsurface flow processes in Mike 11 and Mike SHE.

Mike 11 is a one-dimensional model and consists of a set of nodes along a river reach, each with a series of properties. Water will flow from node to node, and nodes are linked together to form the river network. Nodes contain physical properties such as river cross-section geometry, floodplain topography, channel and floodplain roughness and/or structure geometry. Time-series data can be stored at the nodes, including boundary conditions (Q-h, flow time-series, constant head etc.) or calibration data.

The general assumptions in the Mike 11 model are for incompressible and homogenous fluid with one-dimensional flow. A small bottom slope is assumed, with small longitudinal variations of cross-sectional parameters and hydrostatic pressure distribution. There are three solutions to the conservation of momentum equations solved in the Mike 11 model: the fully dynamic wave equation (full Saint Venant equations), the diffusive wave equation which ignores the momentum flux, and the kinematic wave equation which ignores momentum and pressure fluxes in the solution to the Saint Venant equations. The latter two solutions are simplified versions of the fully dynamic wave equation, and have faster execution times. However, they are only appropriate in relatively fast-moving waterbodies, where backwater effects are not important. In the Murray study area, there is very little slope and channel flow is likely to have large backwater effects in many of the catchment's flat regions. As such, the use of the fully dynamic wave equation was required in the Murray Mike SHE model.

The main parameters to modify during the calibration process are the river bed roughness (Manning's ' n ') and the leakage coefficient between the river bed and the surrounding aquifer. However, the calibration process also involves the development of a Mike 11 network that is of sufficient scale to account for all of the drainage in the Murray study area.

Unsaturated flow/evapotranspiration model

The unsaturated flow model and evapotranspiration model are coupled in Mike SHE, with the main purpose of providing an estimate of the actual evapotranspiration and the amount of

water that recharges the saturated zone. There are three methods in Mike SHE to calculate unsaturated flow:

1. Richards equation: used when detailed unsaturated-zone water content profile is required or if the soils have significant capillary potential.
2. Gravity flow: used when the main purpose of the unsaturated zone is to provide recharge and overland flow, and if the soils are predominantly coarse.
3. Two-layer water balance: useful when the watertable is 'shallow' and a simple water balance of the unsaturated zone is required. 'Shallow' is when the infiltration time is less than or close to the groundwater timestep.

The two-layer water balance method is an alternative to more complex unsaturated flow processes, and is suitable for the Murray modelling project. The two-layer unsaturated zone evapotranspiration (UZ/ET) module in Mike SHE is a simplification of the Kristensen and Jensen evapotranspiration model, which is based on empirically derived equations that follow the work of Kristensen and Jensen (1975) undertaken at Denmark's Royal Veterinary and Agricultural University. The module also uses a formulation presented in Yann and Smith (1994). It is primarily suited to areas where topsoils are coarse and the watertable is shallow. The two-layer model is also useful for large-scale models and where detailed soil data is not available.

The two-layer UZ/ET model divides the unsaturated zone into a root zone, from which evapotranspiration can occur, and a zone below the root zone, where evapotranspiration does not occur. The module is particularly useful for areas with a shallow groundwater table, such as swamps or wetland areas, where the actual evapotranspiration rate is close to the potential rate. In areas with deeper or drier unsaturated zones, the model does not realistically represent the flow dynamics in the unsaturated zone. The model only considers average conditions and does not account for the relation between unsaturated hydraulic conductivity and soil moisture content and thereby the ability of the soil to transport water to the roots. The two-layer approach simply assumes that if sufficient water is available in the root zone, then the water will be available for evapotranspiration. However, it is usually possible to calibrate the input parameters so that the model performs reasonably well under most conditions.

The calculation of evapotranspiration uses meteorological (Penman Monteith evapotranspiration data as a primary input, Allen et al. 1998) and vegetative data to predict the total evapotranspiration and net rainfall due to:

- interception of rainfall by the canopy
- drainage from the canopy to the soil surface
- evaporation from the canopy surface
- evaporation from the soil surface

- uptake of water by plant roots and its transpiration, based on soil moisture in the unsaturated root zone.

In MIKE SHE, the evapotranspiration processes are split and modelled in the following order:

- a proportion of the rainfall is intercepted by the vegetation canopy, from which part of the water evaporates
- the remaining water reaches the soil surface, producing either surface water runoff or percolating to the unsaturated zone
- part of the infiltrating water is evaporated from the upper part of the root zone or transpired by the plant roots
- the remainder of the infiltrating water recharges the groundwater in the saturated zone.

The two 'layers' in the two-layer UZ/ET approach represent average conditions in the unsaturated zone. The vegetation is described in terms of leaf area index (LAI) and root depth. LAI describes the area of leaves above the unit area of the ground surface. Generalised time-varying functions of the LAI for most crops and types of vegetation are available in the literature. In Mike SHE, the temporal variation of the LAI for each vegetation type is required. Root depth is defined as the maximum depth of active roots in the root zone. The soil properties include a constant infiltration capacity and the soil moisture content at the wilting point, field capacity and saturation. The output is an estimate of the actual evapotranspiration and the groundwater recharge.

Saturated flow

The saturated zone component of Mike SHE calculates the saturated subsurface flow in the catchment. Mike SHE allows for a fully three-dimensional flow in a heterogeneous aquifer shifting between unconfined and confined conditions. The spatial and temporal values of the hydraulic head are described mathematically by the three-dimensional Darcy equation and solved numerically by an iterative implicit finite difference technique.

Mike SHE allows the subsurface geologic model to be developed independently of the numerical model. The parameters for the numerical grid are interpolated from the grid's independent values during pre-processing.

The geologic model can include both geologic layers and lenses. The former cover the entire model domain and the latter may exist in only parts of the model area. Both geologic layers and lenses are assigned geologic parameters as either distributed values or as constant values.

The geologic model is interpolated to the model grid during pre-processing by a two-step process:

- 1) the horizontal geologic distribution is interpolated to the horizontal model grid
- 2) the vertical geologic distribution is interpolated to the vertical model grid.

The upper boundary of the top layer is always either the infiltration/exfiltration boundary, which in Mike SHE is calculated by the unsaturated zone component. The lower boundary of the bottom layer is always considered as impermeable. In Mike SHE, the rest of the boundary conditions can be divided into two types: internal and outer. If the boundary is an outer boundary then it is defined on the boundary of the model domain. Internal boundaries, on the other hand, must be inside the model domain.

Interaction processes

The coupling between Mike 11 and Mike SHE is made via river links, which are located on the edges of adjacent grid cells. The river link network is created by the pre-processor, based on the Mike 11 coupling reaches (a coupling reach is a Mike 11 river reach that has been selected to interact with the Mike SHE model). The entire river system is always included in the hydraulic model, but Mike SHE will only exchange water with the coupling reaches. Mike 11 will exchange water with both the saturated zone model and the overland flow model. The Murray model allows for water to exchange from the Mike 11 rivers to the Mike SHE saturated zone via the river bed along the river links, and from the Mike SHE saturated zone to the Mike 11 rivers via the river bed to the Mike 11 nodes.

The overland flow model will calculate the surface runoff and provide lateral runoff to the rivers in the Mike 11 network. The overland flow model will also interact with the unsaturated zone model, and infiltration and evapotranspiration is calculated from overland flow and the unsaturated zone model at each timestep.

The saturated zone component calculates the recharge/discharge between ponded water and the saturated zone without the unsaturated zone, if the phreatic surface is above the ground surface. Otherwise the saturated zone receives recharge from the unsaturated zone model. All model flux processes and algorithms are documented in the Mike SHE technical reference guide (DHI 2009).

3 Model construction

Model construction involves the transformation of the conceptual model into a mathematical form that can be used to simulate groundwater heads and flows. The required outcome is an interactive model with features to represent the hydrogeological framework, hydraulic properties, hydrological processes and boundary conditions as designed in the conceptualisation stage. The model's design is based on the conceptual model's development, with some simplifications to achieve either better calibrations, better representations of the hydraulic processes, or a better model run-time.

3.1 Simulation periods

The period 1985 – 2000 was used as the calibration period, and the validation period was from 2000 – 2009. Most T-series bores (the northern calibration bores) have data from 1975 – current, whereas the southern Harvey-Shallow (HS) series of bores have data from 1988 – current. The calibration period was determined using the period of appropriate length and available data. A spin-up period of five years (1980 – 1985) was used to stabilise stores from initial conditions.

3.2 Model domain and grid

A grid size of 200 m x 200 m was selected for the model. Mike SHE has a constant grid, and the model does not support finer grid spacing in different regions of the model that require finer detail. However, Mike SHE allows for smaller regions of the model to be easily extracted from the model domain and executed at a finer grid scale, importing boundary conditions from the regional model if required. The model domain consists of 1660 internal cells and 614 boundary cells, and is shown in Figure 3-1. Co-ordinates, values and parameters relating to the model domain and grid are shown in Table 3-1. All model layers have consistent map projections of GDA 1994 MGA Zone 50.

Table 3-1: Model domain and grid values

Cell size	200 m
Map projection	GDA 1994 MGA Zone 50
X minimum	375387
X maximum	405589
Y minimum	6381976
Y maximum	6412770
Total model area	720 km ²
Number of cells X direction	155
Number of cells Y direction	155

3.3 Topography

The topography is the layer most used in the Mike SHE model. It is the upper layer for the saturated zone model and the unsaturated zone model, and it is used to determine the flow direction and velocity in the overland flow model.

Recently LiDAR (light detection and ranging) was flown and analysed for the Swan Coastal Plain (which included the entire Murray domain). LiDAR is an aircraft-based remote sensing technique, using laser-driven pulses of light and multi-spectral cameras to scan and process digital information about a landscape. The digital elevation model (DEM) that is processed from LiDAR data is of 1 m horizontal resolution and 0.15 m vertical resolution.

The DEM was re-sampled to the 200 m model grid, which leads to simplifications and some potential errors. For example, small sand dunes and raised roads and verges which are anomalies in a generally flat landscape will be effectively removed in the re-sampling process. The re-sampled topography for the model grid is shown in Figure 3-2.

3.4 Rainfall and evapotranspiration

Rainfall and evapotranspiration are the primary hydrologic drivers of the Mike SHE model. Spatially, they can either be homogeneous over the entire catchment, or they can vary by assigning a rainfall and evapotranspiration file to separate climate zones. The conceptual model identified an increasing rainfall gradient from west-north-west to east-south-east in the Murray study area. Therefore it was important to capture the gradient in the numerical model, and a spatially homogeneous rainfall input was inadequate. SILO data-drill rainfall and evapotranspiration data were used as the inputs. The data-drill accesses grids of data interpolated from point observations by the Bureau of Meteorology. Interpolations are calculated by splining and Kriging techniques. The data in the data-drill are all synthetic; that is, no original meteorological station data remains in the calculated grid fields. The data-drill provides meteorological variables interpolated to 0.05° spatial resolution (approximately 5 km).

Twenty-five SILO data-drill locations were present within the model domain, which is more than the model's spatial requirements. Nine stations were selected to use in the modelling project, and the domain divided into 'climate zones' which were each assigned a data-drill site. Figure 3-3 shows the climate zones, the used and unused data-drill locations, and the location of the Pinjarra rainfall gauging station. The rainfall stations re-sampled to the 200 m grid for the numerical model are shown in Figure 3-4.

Data from the SILO data-drill for each of the nine climate zones in the model domain were analysed alongside the gauging station data at Pinjarra (station 9596). Figure 3-5 shows the average annual rainfall (1985 – 2009) for each of the nine data-drill locations used in the modelling and for the Pinjarra site. There is very little variation in the evapotranspiration data (less than 4% difference between the maximum and minimum sites); however, the rainfall data exhibits an increasing trend from the north-west to the south-east (zone 1 has 15% less rainfall than zone 9), as identified in the conceptual model.

The variation in rainfall sites from year to year is shown in Figure 3-6 (annual variation), and in Figure 3-7 (monthly variation).

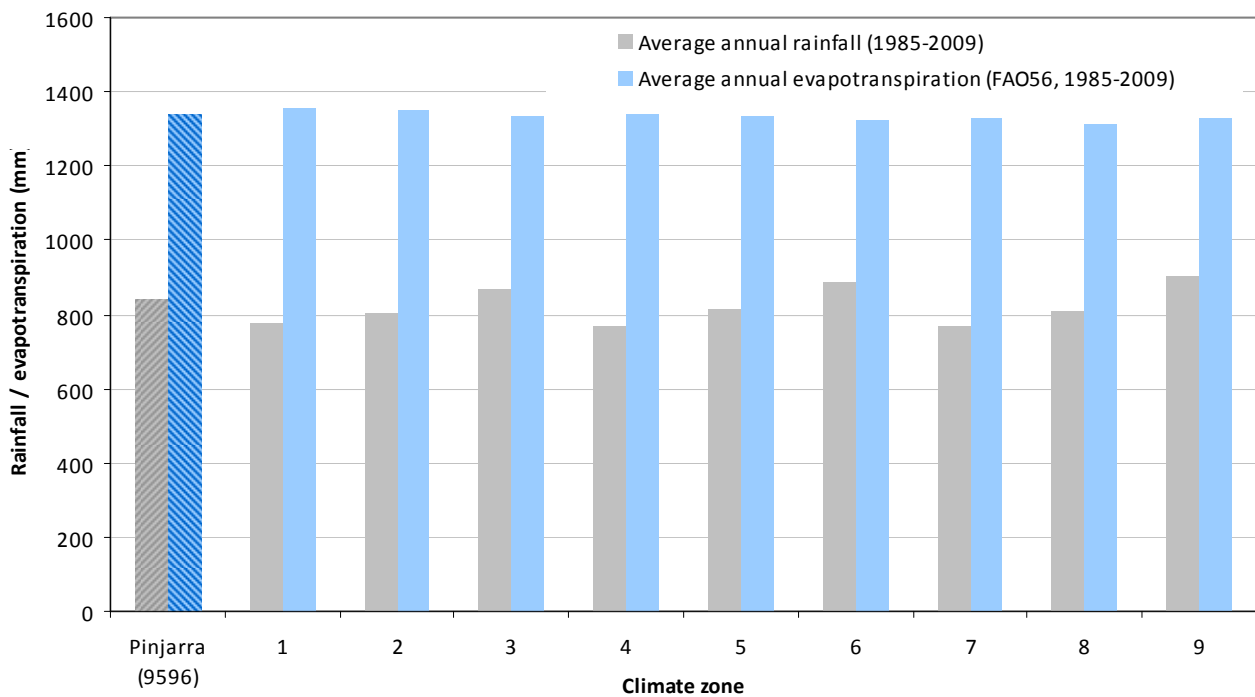


Figure 3-5: Average annual rainfall (1985 - 2009) and Penman-Monteith evapotranspiration for the nine climate zones in the Murray study area and for the Pinjarra rainfall gauging station (9596)

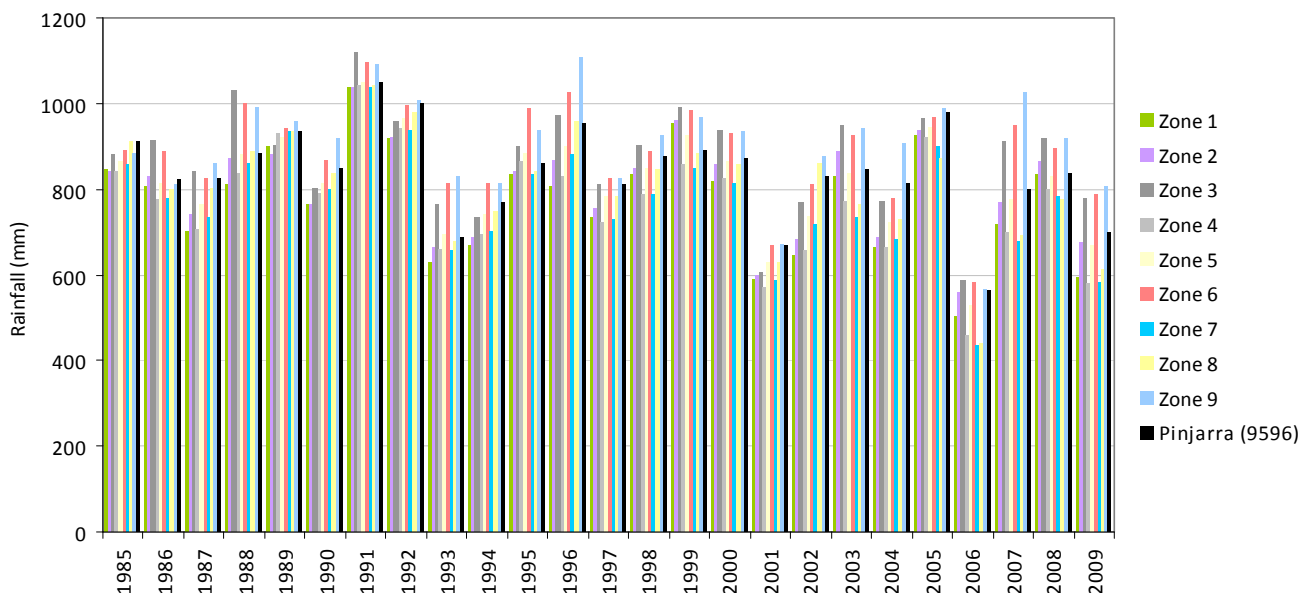


Figure 3-6: Annual rainfall (1985 - 2009) for the nine climate zones in the Murray study area and the Pinjarra rainfall gauging station (9596)

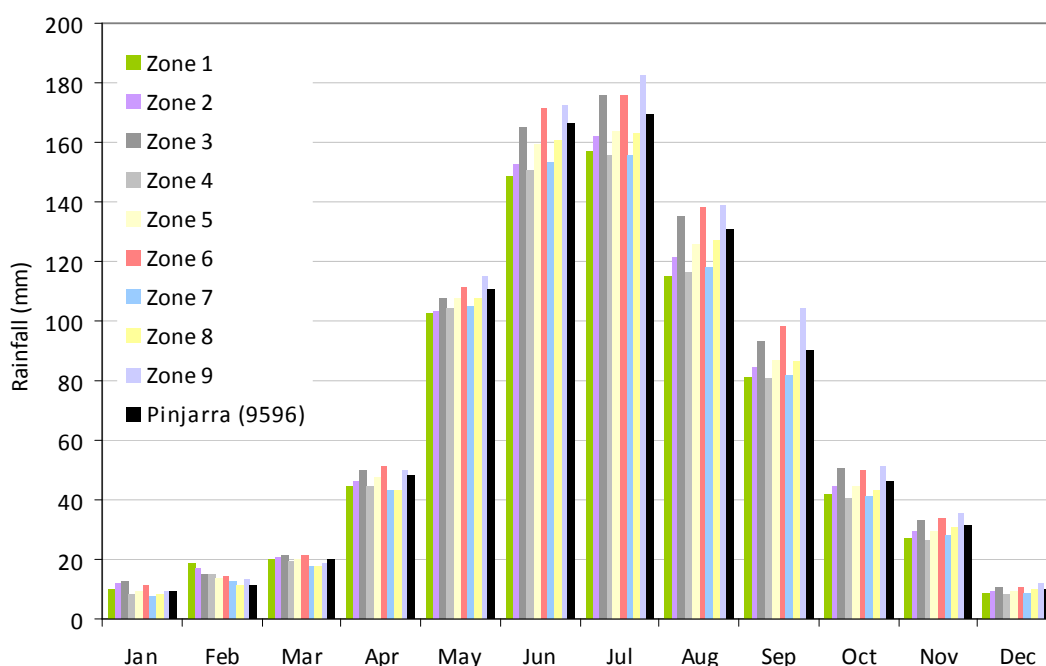


Figure 3-7: Monthly rainfall (1985 - 2009) for the nine climate zones in the Murray study area and for the Pinjarra rainfall gauging station (9596)

3.5 Evapotranspiration model

The requirements for the evapotranspiration model include root depth and leaf area index (LAI). The catchment land use was divided into five categories, each with corresponding values for LAI and deep-rooted vegetation. The land use for the Murray study area was taken from the conceptual model report, and re-categorised into five groupings (Figure 3-8). This was re-sampled to the 200 m grid by the Mike SHE pre-processor. The modelling land-use categories at the 200 m scale are shown in Figure 3-9. The initial values for root depth and LAI were taken from the work undertaken by Xu et al. (2009) for the vertical flux component of the PRAMS model, and are shown in Table 3-2.

Table 3-2: Initial values for LAI and average root-depth estimates from Xu et al. (2009)

Murray land-use category	Equivalent VFM category	Leaf area index (LAI)	Root depth (mm)
Bare / urban	-	0.0	0
Plantation	Pine - medium density	1.8	12 000
Native vegetation	Banksia - high density	1.3	10 000
Grazing (irrigated)	Pasture	3.0	1000
Grazing (non-irrigated)	Pasture	0 – 3.0*	1000

* Represents range of values from rotation scheme

With the exception of annual pasture, all land-use classes use a constant LAI and root depth throughout the simulation. The values for LAI are subject to calibration in the model within the bounds of available literature. For annual pasture, an annual trend of LAI is assigned that

follows normal pasture growth and senescence in monthly increments (Xu et al. 2009). The annual LAI profile for pasture is shown in Figure 3-10.

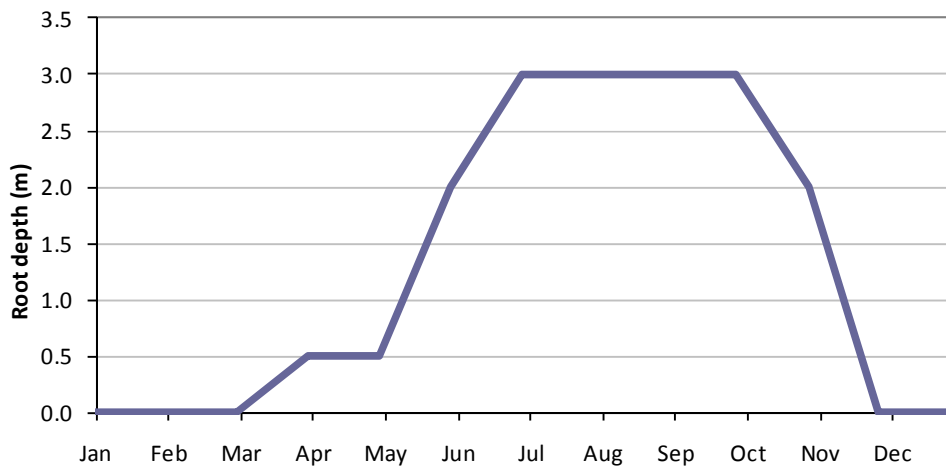


Figure 3-10: Annual rotation scheme for grazing land use (non-irrigated) LAI

3.6 Channel flow model (Mike 11)

Mike 11 is the channel flow model used by Mike SHE. It is a one-dimensional model and consists of a set of nodes along a river reach. Water will flow from node to node, and nodes are linked together to form the river network. Nodes contain physical properties such as river cross-section geometry, floodplain topography, channel and floodplain roughness and/or structure geometry. Time-series data can be stored at the nodes, including boundary conditions (Q-h, flow time-series, constant head etc.) or calibration data. The Mike 11 simulation file for the Murray model requires four physical data editors: a river network editor, a cross-section editor, a boundary file editor and a hydraulic parameter editor.

River network

The Mike 11 river network editor functions to provide editing facilities for data defining the river network such as:

- digitisation of points and connection of river branches
- definition of weirs, culverts and other hydraulic structures
- definition of interaction processes between the river network and the overland flow and saturated zone models.

The river network editor provides an overview of all data included in the river model simulation, and spatially represents locations of cross-section data, boundary data, and computational node data (Figure 3-11). The extent of the hydrological network, as defined by the river network file, is shown in Figure 3-12.

The Mike 11 network in the Murray regional model consists of 11 775 points and 114 branches. There were no hydraulic structures entered into the model. While it is recognised that there are many weirs, culverts, bridges and other miscellaneous structures within the

study region – which would be important if detailed flood mapping were an output of the Mike 11 model – they are not likely to be critical to maximum groundwater level and long-term water balance analysis. The primary purpose of the Mike 11 model in the Murray study region was to drain the groundwater from the superficial aquifer, and prevent the overland flow moving to local depressions. As such, detailed analysis and implementation of structures was not considered relevant for the Murray regional model.

Cross-sections

The river cross-section data comprises both raw and processed data. The raw data describes the physical shape of a cross-section using (x, z) co-ordinates. For much of the model, the co-ordinates were obtained using the Mike 11 GIS extension. Mike 11 GIS is an extension to ESRI's ArcMap, which takes advantage of ArcMap's many GIS functionalities and provides a number of useful tools in relation to Mike 11 modelling. The primary use of Mike 11 GIS includes graphical data preparation of the network and cross-section input data files for Mike 11. Mike 11 GIS allows streamlines to be traced directly onto the waterways and the automatic sampling of cross-sections using the topographical raster (the LiDAR in the case of the Murray regional model). This allows for many cross-sections to be applied to the Mike 11 model without requiring large amounts of survey data. The LiDAR was flown in late summer, so most waterways in the model domain were dry at the time. However, the lower reaches of the Murray and Serpentine rivers have water in them year-round. Detailed survey data from each of these reaches was provided by the Department of Water, and manually entered into the Mike 11 cross-section file.

Boundaries

The boundary conditions in Mike 11 are defined by the combined use of time-series data and specifications made on locations of boundary points and boundary types. Three types of boundary conditions were put into the Murray Mike 11 model, which were:

- **Inflow boundaries:** these were implemented at the upper end of a first-order reach (i.e. a reach that had no upstream reach connected to it). Most reaches had constant no-inflow boundaries; however, there were seven reaches that entered the Murray regional model with significant flow, for which a time-varying flow was implemented as the inflow boundary conditions. The flow was derived from the catchment rainfall-runoff model SQUARE (Hall et al. 2010), and was calibrated using SILO data-drill data. The reaches that received dynamic inflow boundaries include the Serpentine River, Murray River, Oakley Brook, North Dandalup River, North Dandalup Tributary and Conjurunup Brook.
- **Water level boundaries:** these were implemented on the downstream end of reaches entering the Peel Inlet. These boundaries were time-varying fixed-head boundary conditions, and represented the level of the Peel Inlet and Harvey Estuary. Rivers that required these boundaries included the Serpentine River, Murray River, Coolup Drain, Southern Drain and two other minor drains. The water level boundary was taken from the tidal-derived water levels in the Peel Inlet. The derivation of the tide levels is outlined in the *conceptual model report*.

- **Head-discharge boundaries:** head-discharge (or Q-h) boundaries were implemented at the downstream vertex of reaches that did not have a water level that was controlled by the Peel Inlet level. In each case, the Q-h relationship was taken from the processed cross-section data, which is available in the Mike 11 cross-section editor.

Hydrodynamics

The hydrodynamic editor offers the possibility of specifying user-defined values for a number of variables used during the hydrodynamic computation. The hydrodynamic variables able to be specified in the hydrodynamic editor include initial conditions, wind, bed resistance, and wave approximation technique. The Murray Mike 11 model assumed no wind, and initial conditions were set using a steady-state solution. The Manning's roughness coefficient ' n ' was used to define bed roughness, and a global value of 0.035 was implemented for both rivers and channels in the Murray regional model. The wave approximation was specified in the hydrodynamic file, and a choice of kinematic, diffusive wave or fully dynamic solutions were available. The fully dynamic wave solution (first order) was necessary for the model, with a minimum timestep of three minutes. The kinematic and diffusive wave approximations are simpler and more computationally efficient solutions to the fully dynamic equation; however, they do not work well when backwater effects are present in the river network. The Murray modelling domain, which has little slope and large areas of waterlogging, is prone to backwater effects, and hence these approximations did not converge when applied to the Murray Mike 11 model.

3.7 Overland flow model

The successive over-relaxation (SOR) method of solving the finite difference equations for overland flow is used in the Murray regional model. The method uses the Stickler roughness coefficient to solve the finite-difference equations, and is equivalent to the Manning M. The Manning M is the inverse of the commonly used Manning n . The value of n is typically in the range of 0.01 (smooth channels) to 0.10 (thickly vegetated channels), which correspond to values of M between 100 and 10 respectively. A global Manning's M value of 20 was chosen for the Murray model, a typical value for pasture or sparse vegetation.

Detention storage is the only other parameter in the overland flow module. This is used to limit the amount of water that can flow over the ground surface. The depth of ponded water must exceed the detention storage before water will flow as sheetflow to the adjacent cell. For example, if the detention storage is set equal to 2 mm, then the depth of water on the surface must exceed 2 mm before it will be able to flow as overland flow. This is equivalent to the trapping of surface water in small ponds or depressions within a grid cell. Water trapped in detention storage continues to be available for infiltration to the unsaturated zone and to evapotranspiration. A detention storage value of 2 mm was used in the Murray regional model.

3.8 Unsaturated flow model

Soil zones for the unsaturated flow model were developed for the Murray regional model. The classification of soils was constrained by the existing soil units in the Department of Agriculture and Food's Soil Landscape Units dataset. The sandy units of the study area consist of the Bassendean, Spearwood and Quindalup soil units (generally associated with the Bassendean, Tamala, and Safety Bay Sand geologic units). The Pinjarra soils, generally associated with the Guildford Clay and alluvium, consist of duplex soils with higher quantities of clay sediments. The locations of the model's soil units are shown in Figure 3-13.

The unsaturated zone model had five parameters to calibrate:

- **Water content at saturation** is the maximum water content of the soil, which is approximately equal to the porosity.
- **Water content at field capacity** is the water content at which vertical flow becomes negligible. In practice, this is the water content that is reached when the soil can freely drain. It should be noted that the difference between the water content at saturation and the water content at field capacity should be approximately equal to the specific yield of the corresponding geological layer.
- **Water content at wilting point** is the lowest water content whereby plants can extract water from the soil. The difference between the water content at field capacity and the water content at wilting point is the plant-available moisture.
- **Saturated hydraulic conductivity** is equal to the vertical infiltration rate of the soil.

The two-layer unsaturated zone model only considers average conditions and does not account for the relation between unsaturated hydraulic conductivity and soil moisture content and, thereby, the ability of the soil to transport water to the roots. The model assumes that if sufficient water is available in the root zone, the water will be available for evapotranspiration.

3.9 Saturated flow model

Geological layers

In Mike SHE, each geological aquifer is required to span the entire model domain, and is entered as a 'geological layer'. Only one geological layer was entered into the model and was labelled the 'superficial' layer, representing the Superficial Aquifer. The detailed conceptual geology and hydrogeology was later entered as aquifer units, labelled 'geological lenses' in Mike SHE, which form within the geological layer. The top of the geological layer was the surface topography and the base of the model was the top of the Leederville Formation.

Geological lenses

Each of the eight geologic members that constitute the aquifer units within the superficial formation were entered into the Murray regional model as geological lenses. The block

model presented in the *conceptual model report* was used to define the upper and lower levels, and the extent of each of the formations. The upper and lower levels from the block model were re-sampled to the 200 m model domain grid for the numerical model. The formations that were explicitly represented by the Murray regional model included:

- The **Rockingham Sand** formed during the Tertiary period between the Leederville and superficial formations. The formation consists of medium- to coarse-grained sand. The main channel is in the north-western portion of the catchment. The top and base of the Rockingham Sand lens, as represented in the numerical model, is shown in figures 3-14 and 3-15.
- The **Ascot Formation** exists as a relatively thin layer in the southern half of the catchment, and comprises grey, poorly-sorted, medium-grained sands with shell remains throughout. The top and base of the Ascot Formation, as represented in the numerical model, is shown in figures 3-16 and 3-17.
- The **Yoganup Formation** consists of white, yellowish-brown and orange-brown, poorly sorted, fine to very coarse sands and clayey sands. It overlies the Leederville Formation on the study area's eastern margin. The top and base of the Yoganup Formation, as represented in the numerical model, is shown in figures 3-18 and 3-19.
- The **Guildford Clay** is predominantly of fluvial origin and is generally constrained to within 5 to 10 km of the Darling Scarp. Guildford Clay is described as pale grey, blue, but mostly brown, silty and slightly sandy clay. The top and base of the Guildford Clay, as represented in the numerical model, is shown in figures 3-20 and 3-21.
- **Bassendean Sand** covers most of the study area. Bassendean Sand is pale grey to white, and occasionally brown, moderately-sorted, fine- to medium-grained quartz sand with traces of heavy minerals. A layer of friable, mostly weakly limonite cemented sand known as 'coffee rock' is commonly present at or near the watertable. The formation is interpreted to exist as a thin veneer and the uppermost layer over much of the study region east of the Tamala Limestone; however, it is up to 30 m thick in the central area due to stranded dunes. The top and base of the Bassendean Sand formation, as represented in the numerical model, is shown in figures 3-22 and 3-23.
- The **Tamala Limestone** is composed of limestone, calcarenite and sand, with minor clay and shell beds. The limestone contains numerous solution channels that form a karst aquifer. Below approximately +3 mAHD the formation contains marine and lacustrine sediments. On its western side it is unconformably overlain by the Safety Bay Sand. Depending on the height of the dunes, its thickness is up to 50 m in the study area. The top and base of the Tamala Limestone formation, as represented in the numerical model, is shown in figures 3-24 and 3-25.
- The **alluvium, estuarine and swamp deposits** are associated with the many rivers, lakes and wetlands that exist within the study area. These deposits consist of clays, silts and sand, which is angular to rounded, poorly sorted and often containing gravel and pebbles (Pennington Scott 2009). Peaty and sandy swamp deposits are

associated with the numerous wetlands, often having a dark brown, grey to black colour and being organic rich. The distribution of the alluvium, estuarine and swamp deposits, as represented in the numerical model, is shown in figures 3-26 and 3-27.

- A layer of **colluvium**, which lies along the edge of the Darling Scarp, is identifiable as fragments of granite, laterite and clays unconformably overlying the Guildford Clay, Yoganup Formation and Precambrian rocks. The grain size can range from coarse pebbly sand to poorly sorted silty sand and clay. The colluvium's thickness is highly variable but rarely exceeds 5 m. The distribution of colluvium, as represented in the numerical model, is shown in figures 3-28 and 3-29.
- The **mine clays** are associated with the ALCOA refineries' tailings dams, which consist of low permeability clays. Standard conductivity rates for heavy clays were assumed for this region. The distribution of mine clays, as represented in the numerical model, is shown in figures 3-30 and 3-31.

Hydrogeological specifications of each of the aquifer units are described in detail in the *conceptual model report* (Hall et al. 2010). There are two formations that were not defined explicitly in the numerical model but were included in the conceptual geology: the Safety Bay Sand and the Gnamptara Sand. These two formations were assumed to have similar hydraulic properties, as they were both medium-grained sands. All regions in the superficial layer that were not assigned to a specific lens were assigned the properties of Gnamptara Sand, thus ensuring there were no voids within the geologic model.

A review of the available data for the above formations within the Superficial aquifer in the Murray regional model domain was completed as part of the conceptual model. The summary of that review is shown in Table 3-3, which shows the initial value of hydraulic conductivity and specific yield for the selected formations. Typically a ratio of 10:1 horizontal to vertical hydraulic conductivity has been used to define the value for vertical hydraulic conductivity. These ranges represent best estimates of the upper and lower bounds for aquifer properties that may be assigned during calibration.

Table 3-3: Hydraulic parameter ranges for geological lenses within the Superficial aquifer.

Stratigraphy	K_H (range) (m/day)	K_z (range) (m/day)	S_V	S_s
Gnangara	20	2.0	0.22	1×10^{-6}
Bassendean	5 to 15	0.5 to 1.5	0.21	1×10^{-6}
Tamala	7 to 1000	0.7 to 100	0.27	1×10^{-6}
Guildford	0.001 to 2	0.0001 to 0.2	0.07	5×10^{-5}
Yoganup	0.1 to 10	0.01 to 1	0.10	1×10^{-6}
Ascot	1 to 28	0.1 to 2.8	0.23	1×10^{-6}
Colluvium	1	0.1	0.10	5×10^{-5}
Alluvium	0.1 to 12	0.01 to 0.12	0.20	5×10^{-5}
Mine Clays	0.01 to 1	0.001 to 0.0001	0.05	5×10^{-5}
Rockingham	20	2.0	0.25	1×10^{-6}

Groundwater abstraction

Groundwater abstraction was modelled in the Superficial aquifer. The conceptual model identified groundwater abstraction as a minor flux in the total water balance, and an aggregated approach to abstraction was adopted for the numerical model.

The model was divided spatially into 38 groundwater abstraction regions. Abstraction identified in the conceptual model from 1043 draw-points in the Superficial aquifer was aggregated within each of the groundwater abstraction regions. The abstraction was entered as a single location in the centroid of each of the regions. In each location, the abstraction was assumed to occur only between November and April, and a constant rate of abstraction was assumed during this time period. The location of the abstraction regions for the Murray regional model is shown in Figure 3-32.

Computational layers (vertical discretisation)

The Murray regional model comprises two computational layers – these are designed to capture head differences in the paired bores within the Superficial aquifer. The Mike SHE saturated zone model does not accommodate drying cells in the first computational layer. Therefore it is a requirement that the groundwater level always be within the first computational layer.

A surface 1 m below the minimum groundwater level was used to define the base of the first computational layer. The extra metre below the minimum groundwater level was used to ensure that water levels did not fall below the base of the first computational layer during predictive scenarios. The elevation of the base of the first computational layer is shown in Figure 3-33.

The base of the second computational layer was defined by the top of the Leederville Formation, and is the base of the numerical model. The base of the second computational layer is shown in Figure 3-34.

Boundary conditions

Hydrogeological model boundaries are important constraints to groundwater flow and recharge. The saturated zone model in the Murray regional model uses a fixed-head boundary condition on its western border, and no-flow boundary conditions on the north, south and eastern borders.

The Darling Fault forms the model's eastern boundary. The Darling Fault separates the coastal plain sediments from the Yilgarn Block's basement rocks and is often covered with a thin layer of weathered alluvial sediment. Groundwater flow from the basement rock is negligible. Groundwater flow in the weathered sediments is generally limited and discharges into the drains originating on the Darling Plateau or infiltrates into the coastal plain, across the Darling Fault. Water in the drains contributes to groundwater recharge or becomes evaporation loss. Drainage water crossing the eastern boundary is implemented as 'boundary conditions' to the Mike 11 channel flow model, and the rainfall-runoff model SQUARE was used to determine the daily flows at each of these locations. The eastern boundary of the saturated zone model was assumed to be a no-flow boundary coincident with the Darling Fault.

The western boundary of the model comprises the Indian Ocean in the north, Peel Inlet in the centre and Harvey Estuary to the south. A time-varying fixed-head boundary condition was applied to this boundary. The monthly levels were derived from measurements taken in the Peel Inlet, the Harvey Estuary and the Indian Ocean, and are shown in Figure 3-35. A detailed derivation of this time-series is outlined in the *conceptual model report* (Hall et al. 2010)

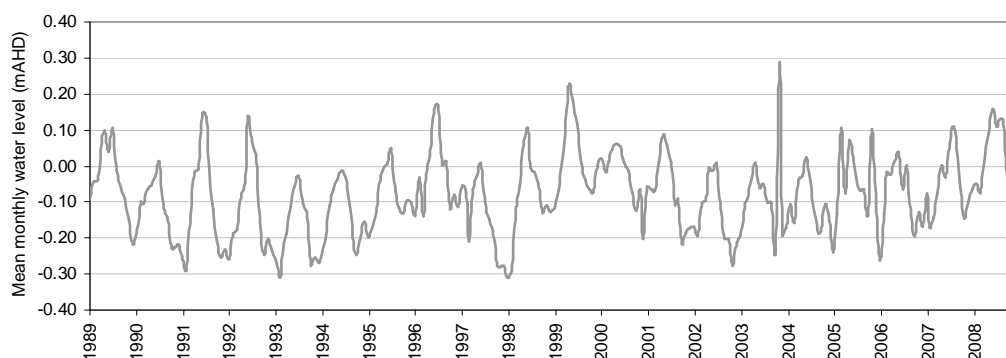


Figure 3-35: Time-varying fixed-head boundary condition on the western boundary of the model

The model's northern and southern boundaries were perpendicular to groundwater flow-lines, and no-flow boundary conditions were implemented.

Drainage (saturated zone)

In addition to the drainage in the channel flow model, the saturated zone model also contains a drainage component. The drainage comprises a set level below the ground surface (the surface of the saturated zone model), and a drain constant. Water will drain from grid to grid according to the topography and drain constant, until it leads to a local depression, the model boundary or a Mike 11 channel. The purpose of the drainage component is to account for drainage from the saturated zone due to the change in topography within the 200 m grid. A constant drain level of 0.2 m bgl was used as an initial value in the Murray regional model, with a drain constant of 0.1 (/d). The drain depth is a calibrated parameter that is necessary to meet surface water budgets in waterways.

4 Model calibration and validation

Calibration is the process by which the independent variables (parameters and fluxes) of a model are adjusted, within realistic limits, to produce the best match between simulated and measured data (from groundwater level monitoring and surface flow monitoring). Calibration aims to solve a problem inversely by adjusting the unknowns (parameters and fluxes) until the solution matches the knowns (heads).

The Murray regional model is a high-complexity model, and calibration to measured data before use for prediction simulations is a fundamental requirement. The calibration performance is presented in qualitative and quantitative terms in comparison with agreed target criteria. The model calibration and validation methods are based on the *Murray-Darling Basin Commission groundwater flow modelling guidelines* (Middlemis 2000). The four calibration criteria described below have been used to assess the calibration result:

- **Water balance:** the single maximum cumulative error of the water balance of the Superficial aquifer of less than 1%. The difference between the total modelled inflow and the total modelled outflow (water balance error) will be less than 0.1%.
- **Iteration residual error:** the iteration convergence criterion should be one or two orders of magnitude smaller than the head resolution. Here the criterion is <0.1%.
- **Qualitative measures:**
 - modelled versus measured groundwater hydrographs for each calibration bore
 - residual error plot for each calibration bore
 - scattergram of measured versus modelled heads.
- **Quantitative measures:**
 - Root mean square (RMS) error between measured hydraulic-head and modelled hydraulic-head will be less than 5% of the measured hydraulic-head drop across the model area. The error will not be spatially biased. Final calibration results will report the RMS error, mean absolute error, the mean error and the coefficient of determination.
 - Final calibration for each bore will report mean error, mean absolute error, RMS error, standard deviation of residuals, correlation coefficient (R), and Nash Sutcliffe efficiency (R^2).

4.1 Calibration methods

The calibration period was from 1 June 1985 – 31 May 2000, and the validation period from 1 June 2000 – 1 October 2009. It was necessary to validate to as late as possible in 2009 to incorporate the latest groundwater measurements in many of the recently completed bores, which have one to two years of data.

Modelled and measured groundwater levels were compared over the selected calibration time-period. Selected model parameters were adjusted both manually and automatically to

minimise the difference between the modelled and measured data. The manual iterative technique was based on the conceptual hydrogeology, and the results of the calibration/validation are consistent with the model conceptualisation and the project objectives.

The following processes were used to calibrate the model:

1. Review of the model's construction, ensuring that geology from bore logs was represented in the numerical model, and that geological and computational layers were consistent with the conceptual model.
2. Initial model sensitivity was undertaken to determine the model's response to changes in model parameters (such as vertical hydraulic conductivity, horizontal hydraulic conductivity, leaf area index (LAI), root depth, and unsaturated zone parameters).
3. Review of water balances to determine validity of recharge, evapotranspiration, drainage and horizontal flow.
4. Review of the error in predicted water levels in the calibration bores.
5. Adjustment of saturated zone model parameters, land-use parameters and unsaturated zone model over a five-year period (1985 – 1990) within reasonable ranges as identified in the conceptual model. Return to step three to review the model.
6. When the amplitude in the groundwater levels was close to the measured groundwater amplitude, and the water balance was close to the conceptual water balance, the model was simulated from 1985 – 2000, with changes in the land use and hydraulic parameters undertaken to reduce error in bores. Repeat steps three and four.
7. When the calibration criteria was achieved and most remaining errors were small or intractable (did not respond to changes in model parameters), the calibration process was complete.

Model calibration results were assessed using the calibration measures (targets) outlined above.

4.2 Calibration bores

Hydrographs from 27 bores were considered suitable for model calibration. The calibration bores were selected based on the quality and quantity of the water level data, the depth at which the bores were completed, and an assessment of whether the bores adequately reflected regional water levels. These consisted of two series of bores: the 't-series' bores, 15 of which were used and are located in the study area's northern region; and the 'Harvey Shallow' (HS) bores, 12 of which were used and are located in the model's southern region. The location of the calibration bores is shown in Figure 4-1. Most bores were sampled biannually, quarterly or monthly. Data was not available for calibration of groundwater heads at a sub-monthly scale.

4.3 Calibration results

The simulation period for the calibration was from 1 June 1985 – 31 May 2000 (5478 days). The model was calibrated against 27 groundwater bores. The calibration targets described in Section 4.1 were achieved. The normalised RMS error for the calibrated model is 2.02%. The RMS is 0.80 m, and the absolute residual mean (mean absolute error) and the residual mean error (mean error) are 0.55 m and 0.07 m respectively. Table 4-1 and Table 4-2 show the calibration statistics and summary, and Figure 4-2 shows the normalised RMS for the modelled versus observed heads. Figure 4-2 shows a generally random distribution around the unity slope.

The average absolute error is 0.52 m, and is defined as the difference between the predicted and measured water levels. The maximum positive error in the aquifer in predicted head is 2.80 m and the maximum negative error is -2.83 m.

Table 4-1: Calibration statistics for the observed versus modelled heads in the Murray Mike SHE model

Description	Observed	Modelled	Residual	Abs residual
sum (m)	18679	18538	140.4	
average (m)	12.21	12.12	0.09	0.52
median (m)	7.09	7.55	0.03	0.34
min (m)	-0.59	-0.28	-2.83	
max (m)	33.79	33.88	2.80	
range (m)	34.38	34.16	5.63	

Table 4-2: Calibration statistics for the observed versus modelled heads in the Murray Mike SHE model

Description	Symbol	Value
Count	n	1530
Sum of squares (m ²)	SSQ	848
Mean sum of squares (m ²)	MSSQ	0.55
Root mean square (m)	RMS	0.74
Scaled root mean square (%)	SRMS	2.17
Sum of residuals (m)	SRMS	796.4
Mean sum of residuals (m)	MSR	0.52
Scaled mean sum of residuals (%)	SMSR	1.51
Coefficient of determination ()	CD	1.01

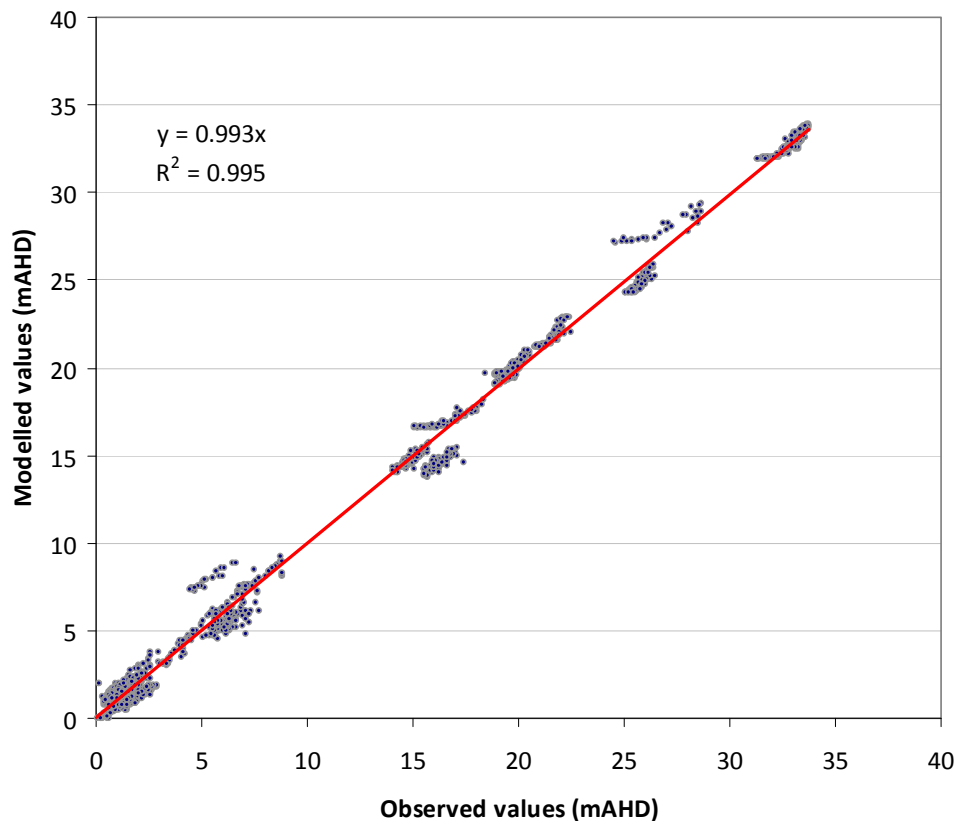


Figure 4-2: Calibration scatter plot for the observed versus modelled heads in the Murray Mike SHE model

4.4 Validation bores

The model validation included all bores that were used in model calibration, and an additional 40 bores with monthly water level recordings from 2008, or from the start of 2009 to present. The location of all validation bores is shown in Figure 4-3.

The selection of validation bores was based on the quality and quantity of the water level data, the depth at which the bores were completed, and an assessment of whether the bores adequately reflected regional water levels.

4.5 Validation results

Model validation is used to assess the model's predictive capability by testing it against data that are independent from the calibration data. The simulation period for the validation was from 1 June 2000 – 15 November 2009 (3454 days). The model was validated against 67 groundwater bores. The normalised RMS error for the validation period model is 2.03%. The RMS is 0.87 m, and the absolute residual mean (mean absolute error) and the residual mean error (mean error) are 0.58 m and 0.10 m respectively. Table 4-3 and Table 4-4 show the calibration statistics and summary, and Figure 4-4 shows the normalised RMS for the modelled versus observed heads.

Table 4-3: Validation statistics for the observed versus modelled heads in the Murray regional mode.

Description	Observed	Modelled	Residual	Abs residual
sum (m)	14537	14408	128.8	
average (m)	10.95	10.86	0.10	0.58
median (m)	7.01	7.08	0.06	0.39
min (m)	-0.51	-0.45	-3.14	
max (m)	42.53	42.20	4.06	
range (m)	43.04	42.65	7.19	

Table 4-4: Validation statistics for the observed versus modelled heads in the Murray regional model

Description	Symbol	Value
Count	n	1327
Sum of squares (m ²)	SSQ	1013
Mean sum of squares (m ²)	MSSQ	0.76
Root mean square (m)	RMS	0.87
Scaled root mean square (%)	SRMS	2.03
Sum of residuals (m)	SRMS	767.3
Mean sum of residuals (m)	MSR	0.58
Scaled mean sum of residuals (%)	SMSR	1.34
Coefficient of determination ()	CD	0.97

The model validation results show similar errors to the calibration results. The scaled RMS is marginally smaller for the validation period; however, the validation period has larger errors in residuals and the maximum and minimum errors are larger also. The validation bores included bores from the scarp in the catchment's west (HS110 and HS103), which has geology that was not represented by the calibration bores – so model uncertainty in the region at the scarp is large, and this is where the validation error was also large. This accounts for a small portion of the modelling area, and is not likely to affect most of the Murray DWMP area adversely.

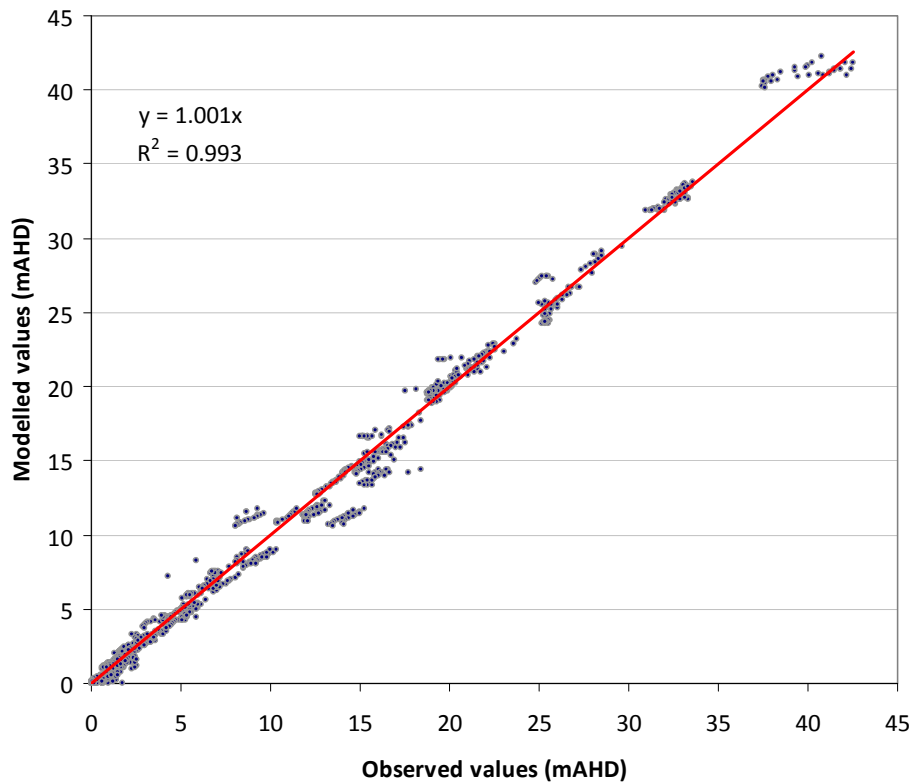


Figure 4-4: Validation scatter plot for the observed versus modelled heads in the Murray regional model

4.6 Calibrated parameters

The calibrated model parameters are the result of manual adjustments to achieve best fit between observed and modelled groundwater levels and surface water flows, within the limits imposed in the conceptual model. For the Murray regional model, parameters from the unsaturated zone model (including LAI and root depth), parameters from the overland flow model, and parameters from the saturated zone model were adjusted for calibration. Boundary conditions were not adjusted during calibration. A summary of the calibrated parameters for each of the Mike SHE model components are presented below.

Unsaturated zone parameters

Calibration of the input parameters in the two-layer unsaturated zone model was required to meet the model's recharge requirements. The calibrated unsaturated zone parameters are shown in Table 4-5. As mentioned in Section 2, the two-layer model has an unsaturated zone component and an evapotranspiration component. The evapotranspiration component is driven by the vegetation, which is characterised by LAI as well as root depth. In addition there is a parameter describing the evapotranspiration extinction depth. If the capillary fringe reaches the bottom of the root zone, then water removed from the root zone by evapotranspiration will be replaced by water drawn up by capillary action. The

evapotranspiration extinction depth is then the maximum depth where evapotranspiration can be removed from the saturated zone by the roots; that is, the root depth plus the thickness of the capillary fringe. A calibrated value of 0.3 m was determined for the evapotranspiration extinction depth (uniform over the modelling region), which is reasonable for sands and clayey sands. The difference between the water content at saturation and the water content at field capacity should be similar to the specific yield of the soil. Values of specific yield of 0.28, 0.21 and 0.17 for the Spearwood, Bassendean and Pinjarra sands represent typical values for coarse-grained sands to clayey sands.

Table 4-5: Unsaturated zone model (two-layer model) calibrated parameters

Parameter	Spearwood	Bassendean	Pinjarra
Water content at saturation	0.33	0.30	0.37
Water content at field capacity	0.05	0.09	0.20
Water content at wilting point	0.03	0.03	0.13
Saturated hydraulic conductivity (m/day)	1.00	0.10	0.05

Land-use parameters

The calibrated values for root depth and LAI are shown in Table 4-6. The LAI values for grazing and irrigated land uses were similar to those presented by Xu et al. (2009) for the PRAMS vertical flux model. The LAI value for 'plantation' corresponded to that of 'medium-level pine forest', while the LAI for 'native vegetation' was significantly higher than that of 'high-density banksia woodland' presented in PRAMS. However, native vegetation in the Murray catchment is generally coarser than the banksia woodland of the northern Swan Coastal Plain due to higher rainfall in the region, and its LAI is likely to reflect this.

The calibrated root depths for 'native vegetation' and 'plantation' were significantly lower than the original values taken from the PRAMS vertical flux model project. It is unlikely that roots are present below the watertable. Analysis of the depth to maximum groundwater level revealed that for most areas of the Murray catchment, the watertable was within 2 m of the ground surface. The PRAMS values were developed specifically for the northern Swan Coastal Plain around the Gnangara Mound, where the depth to the watertable is regularly more than 8 – 10 m. A root depth of 2 m was considered appropriate for the Murray regional model. The root depth of the grazing pasture was increased by 20%, due to the prominence of perennials and sparse trees in the catchment which are not represented in the 200 m land-use grid.

Table 4-6: Evapotranspiration model calibrated parameters

Land use category	Leaf area index (LAI)	Root depth (mm)
Bare / urban	2.0	1000
Plantation	1.5	2000
Native vegetation	1.5	2000
Grazing (irrigated)	3.0	1200
Grazing (non-irrigated)	0 – 3.0*	0 – 1200*

* Represents range of values from rotation scheme

Channel flow parameters

The channel flow model (Mike 11) uses two main parameters: the bed resistance (Manning's n) and the conductance of water from the saturated zone to the channel bed and vice versa. The conductance was calibrated to a value of 20 m/day, which corresponds closely to the horizontal hydraulic conductivity of the Bassendean Sand, and the bed resistance was assigned the original value of $0.035 \text{ s/m}^{1/3}$. The bed resistance parameter was insensitive and a value of $0.035 \text{ s/m}^{1/3}$ was adopted which represents channels and rivers with sand bottoms. Table 4-7 shows the channel flow parameters.

Table 4-7: Mike 11 calibrated parameters

Rivers and lakes model (Mike 11)	Distribution	Value
Bed resistance (Mannings n) [$\text{s/m}^{1/3}$]	Uniform	0.035
Conductance (m/day)	Aquifer + Bed	20.0
Wave approximation	Uniform	Fully dynamic

Overland flow parameters

Table 4-8 shows the calibrated overland flow parameters. For the overland flow model, a resistance parameter (Manning's M) of $20 \text{ m}^{1/3}/\text{s}$ was used. This is a typical value for pasture or sparse native vegetation, which makes up most of the catchment. A Manning's M value of $20 \text{ m}^{1/3}/\text{s}$ was also used for pasture and sparse vegetation in the flood model that formed part of the greater Murray DWMP project (GHD 2010).

Table 4-8: Overland flow model calibrated parameters

Overland flow model	Distribution	Value
Manning number - ' M ' [$\text{m}^{1/3}/\text{s}$]	Uniform	20
Detention storage (mm)	Uniform	2

Saturated zone parameters

Calibrated hydraulic parameters for each of the geological lenses are shown in Table 4-9. For most geological formations, hydraulic parameter values were assigned in accordance with the distribution of the geological units as defined in the *conceptual model report*. The Gngangara, Rockingham and Bassendean sands had calibrated hydraulic properties that were outside of the ranges of the values presented in the *conceptual model report*.

The value for the horizontal hydraulic conductivity for the Gngangara Sand was reduced from 20 m/day to 8 m/day. It was recognised that the value of 20 m/day was determined for clean sands close to the Gngangara Mound, north of Perth. The Gngangara Sand within the Murray region has higher quantities of silt, and is likely to have lower values of hydraulic conductivity, although pump test data is not available. A value of 8 m/day is appropriate for the relatively clean, medium-grained sands to silty sands that were observed in the Murray region.

The vertical hydraulic conductivity for the Bassendean Sand was reduced to 0.1 m/day to reflect the presence of indurated sands and clay lenses that were observed throughout this unit.

The hydraulic conductivity of the Rockingham Sand was reduced from 20 m/day to 7 m/day. The presence of the Rockingham paleochannel gives rise to a zone of increased transmissivity that affects bore levels near the channel's edge. This edge is poorly defined and errors in its definition will give rise to errors in the groundwater heads in these regions. The value of K_H was reduced to 7m/day and K_Z was reduced to 0.1 m/d to minimise the errors at the paleochannel's edge. The value of 20 m/day for the Rockingham formation was used in the PRAMS model (Davidson & Yu 2009), however there has not been a pump test on the Rockingham Sand to verify this figure.

It is recommended that pump tests for the Rockingham, Bassendean and Gngangara sands are undertaken in the Murray region to validate the hydraulic parameters used in the modelling.

Table 4-9: Saturated zone model calibrated hydraulic parameters

Saturated zone model	K_h (m/d)	K_z (m/d)	S_y
Gngangara	8.0	1.20	0.25
Bassendean	10.0	0.10	0.21
Tamala	80.0	8.00	0.25
Guildford	2.0	0.05	0.12
Yoganup	4.1	0.41	0.20
Ascot	9.7	1.20	0.25
Colluvium	2.0	0.02	0.05
Alluvium	10.0	0.05	0.20
Mine Clays	0.1	0.001	0.07
Rockingham Sands	7.0	0.10	0.20

Figure 4-5 to Figure 4-14 show the spatial representation of the calibrated saturated zone model parameters for computational layers one and two respectively.

Saturated zone drainage parameters

The drainage component of the saturated zone model contained two parameters: the drain level and the drain time constant. Values for these two parameters were adjusted to meet the catchment water balance, in particular the delivery of surface water to the waterways. The drain level was adjusted from 0.2 m bgl to 0.15 m bgl, and the drain time constant remained at 0.1 (/d) (Table 4-10).

Table 4-10: Calibrated drainage parameters

Drainage parameters	Value
Drain level (m bgl)	0.15
Time constant (/d)	0.1

4.7 Calibration discussion

The Murray regional model has a domain area of 722 km². Most of the simulated heads at the monitoring bores have responses consistent in amplitude and level with the measured data. However, a model of this size will have various inherent errors due to the simplifications required to produce a large-scale numerical model. The errors are deficiencies in either the calibration process or the conceptual model. Deficiencies in the conceptual model can result in localised areas of high error, systematic errors over large areas, and errors that are intractable or insensitive to parameter variations. Some of the main sources of errors in the conceptual model are listed below.

- Parameter variation within geological layers:** each geologic lens was assumed to be homogenous; however, the properties of a geologic unit are likely to be heterogeneous. This is particularly the case for the Bassendean Sand, which covers a large portion of the Superficial aquifer in the Murray DWMP area. Bassendean Sand has varying quantities of indurated sand at or around the groundwater table and lenses of sandy clay or clayey sand throughout the unit's subsurface. The presence of these layers is likely to impede groundwater flow in localised subareas within the model, but without accurate mapping of these units and testing of the hydraulic properties, they are difficult to quantify both spatially and hydraulically. The variation in hydraulic properties within a geologic unit is also particularly relevant to the Tamala Limestone, which is karstic and has values of hydraulic conductivity known to vary by up to two orders of magnitude. The calibration process involves a single value for each of these parameters being assigned to each geologic unit. It is recommended that if fine-scale modelling projects are undertaken that require greater precision in calibration, then further drilling and pump tests be undertaken to improve the resolution and hydraulic characterisation of the subsurface geology.

- **Inadequate mapping of geological layers:** the geology was mapped using more than 500 bore interpretations, as outlined in the *conceptual model report*. However, there were regions within the model where bore locations were sparse and long-distance interpolations were required. There will be some error with the interpolation of the geological lenses, particularly where bore data is sparse on the model's eastern margin.
- **Leakage across the bottom computational layer:** the model assumes no leakage to the Leederville aquifer (which is not part of the model). The *conceptual model report* states that the flux is small enough to be disregarded. While this is likely to be true for the overall domain, localised connections of either upward or downward fluxes are likely to exist. For example, a sandy part of the Superficial aquifer may be in direct contact with a sand lens within the Leederville aquifer. These small-scale features are not accounted for. The superficial formation and Rockingham Sand lie in unconformable contact with the underlying Leederville Formation, which is composed of the Mariginiup Member and the Wanneroo Member within the study area. Davidson (1995) mapped the extent of these members north of a line through the Murray and South Dandalup rivers. This work illustrated the Mariginiup Member unconformably underlying the superficial formation east of a line trending north-north-east through the junction of the North and South Dandalup rivers. Drilling undertaken south of the Murray River intersected the Mariginiup Member in HS80A immediately below the Ascot Formation, extending this north-easterly trend south of the Murray River. The Mariginiup Member is composed of interbedded clays and generally thin sandy beds and therefore it is not a formation typically associated with high recharge rates. The potential for recharge to occur is further diminished by much of its exposure to the superficial formation and contact with the low-permeability Yoganup Formation and Guildford Clay. West of the Mariginiup Formation the Wanneroo Member is present below the superficial formation and the Rockingham Sand aquifer. The potential for recharge to the Wanneroo Member is likely to be higher than the Mariginiup Member due to it consisting of larger interbedded sand lenses. The overlying formations also tend to be much more sandy in these areas with the Rockingham, Gngangara and Bassendean sands all having high hydraulic conductivities. The hydraulic connection between the Superficial and Leederville aquifers is evidenced in several ways. Regionally a seasonal response to rainfall is observed in all bores screened within the Leederville. Also, various piezometers in the Superficial aquifer show a difference in hydraulic head – that difference is always negative (downward), indicating possible leakage to the Leederville.
- **Groundwater abstraction:** the groundwater abstraction was modelled by aggregating bores and abstraction in a coarse grid across the modelling surface. Errors are likely to be inherent in the model when this approach is used, because the location of the abstraction is not precise. The error due to the imprecise abstraction locations in the Murray regional model is not likely to be large, given that abstraction is a minor flux in the total water balance. However, it is recommended that if detailed models are undertaken at a finer grid scale, abstraction bores should be placed in their precise locations.

- **Root depth and LAI:** The Murray regional model was particularly sensitive to root depth and LAI. Initial values for root depth were taken from studies mostly centred on the Gnangara region (north of Perth), which is where most of metropolitan Western Australia's groundwater resources are found. Values for root depth and LAI are likely to be similar between the Murray and Gnangara regions for pasture (irrigated and annual); however, the native vegetation is significantly different in the Murray domain compared with the Gnangara region. The Gnangara region has mostly deep-rooted (8 – 10 m) banksia woodland, and is centred on areas with large depths to the watertable. Native vegetation in the Murray regional model consists mostly of melaleuca and small eucalypt species, as well as low-lying shrubs and sedges. Values of root depth for many of these species are poorly understood, yet it is not likely that rooting depths would remain below the groundwater table for extended periods of time. Maximum root depth for native vegetation and plantations was calibrated to a value of 2000 mm for the Murray regional model, which represents the average thickness of the unsaturated zone. While this is a reasonable approximation, it is likely that in some areas roots will be deeper such as in sand dunes, and other regions with larger depths to the watertable. Also, for areas with a very shallow watertable, it is not likely that pasture will have root depth of 1000 mm. If further calibration or model refinement is to be undertaken, further analysis of root depth in pasture and native vegetation within the Murray study area is recommended.

The model error is amenable to additional calibration. However, further calibration should only be done after verifying root depth and LAI of vegetation within the domain, updating and improving the licensed abstraction data, refining the mapping of the geological layers within the model, and modifying the hydraulic parameters for the base of the model.

Calibration bores

Bores that achieved a poor or intractable calibration, negative values for Nash-Sutcliffe efficiencies (R^2) or low correlation values are discussed individually below, with possible reasons given for the uncertainty in prediction.

T590 and T650 are located near the edge of the Rockingham Sand paleochannel and both under-predict groundwater heads. It is likely that much of the under-prediction can be attributed to the interpretation of the paleochannel edge's location and the steepness of its sides. The error may be induced by the sudden increase in transmissivity and resulting lowering of the head arising from increasing the aquifer thickness from ~15 m to ~60 m as water flows into the paleochannel. An additional geologic investigation is recommended along the edge of the Rockingham Sand paleochannel to improve the geologic model in this hydraulically sensitive area.

At T630, the model over-predicts groundwater heads, but has reasonable amplitude. At T540, the model under-predicts but has reasonable amplitude. Both bores are within the Tamala Limestone, and are likely to be affected by the heterogeneous nature of this geological formation. Also, it is possible that unlicensed abstraction may be contributing to the over-prediction in the T630 (it is in a region surrounded by medium-density urban residential land use).

T670 under-predicts the groundwater minimums and over-predicts the amplitude. The bore is on a road verge, along a thin strip where there is a local mound and no vegetation. The model re-samples the land use at a 200 m grid (see figures 3-8 and 3-9) and, in this case, the road verge is too small to appear on the re-sampled land-use grid. Therefore the land use surrounding the bore is assumed to be 'grazing' and the model assigns a root depth of 1 m for bore T670 (approx 0.6 m deeper than what is assigned to bare ground). The excessive root depth and LAI surrounding this bore is likely to contribute to the lower minimums and over-predicted amplitudes.

HS55A and HS59A both under-predict the minimum groundwater level. Both bores are located on topography that is low-lying, have minimum groundwater levels that are close to sea level, and have perennially high watertables (URS 2008). Root depth in the pasture and native vegetation surrounding these bores is not likely to be 1000 m, as the roots are not likely to be within the groundwater table. However, it is very difficult to assign a root depth based on the groundwater depth, when the groundwater depth is likely to depend on the root depth, and there are no studies of root depth in these areas. If model refinement is to be undertaken in areas of very shallow watertable, it is recommended that further analysis of root depth in the pasture and native vegetation of these regions is undertaken within the Murray regional model domain.

HS52 appears to be affected by pumping, because a decreasing trend in minimum groundwater level and increasing amplitude is occurring in this bore. It is likely that an increased downward head gradient to underlying aquifers is responsible for this change. HS52 is screened within the Superficial aquifer and located close to sub-cropping Cattamarra Coal Measures. The hydraulic head of the underlying Cattamarra aquifer has declined from around 21 mAHD in 1970 to around 8 mAHD at the end of 2007, as recorded in Alcoa Refinery monitoring bore ES006A (Rockwater 2009). In addition, Alcoa Refinery monitoring bore ES043A screened in the Leederville aquifer shows declines of 4 – 5 mAHD in summer minimums since the early 1990s (Rockwater 2009).

Rivers and lakes

The version of the Mike 11 network shown in Figure 3-11 is the final version used in the calibration. A simplified version of the network that only contained the Murray study area's major rivers was initially implemented. However, in the simplified version the surface water component of the water balance was not sufficient when compared with the conceptual surface water balance, because for most of the catchment (which has a very low slope and is characterised by undulating dunal systems) overland water would flow to a local depression where it would infiltrate or evaporate – rather than flow to a drain where it would form part of the surface water balance. Drains in the Murray region often cut through the local topography, as they were designed to alleviate waterlogging in the pastoral regions of the Swan Coastal Plain. To satisfy the surface water balance, it was necessary to include many of the study area's major drains and waterways, in order to convey the water to the major surface waterbodies. This procedure increased the contributing catchment area to each of the major waterways. There are other methods in Mike SHE that will artificially 'force' water to drain to specific Mike 11 points from regions of the model (e.g. by using Grid Codes, see

the *Mike SHE technical manual*, DHI 2005); however, these methods require a drain level to be entered to the model, which could constrain the maximum groundwater levels in locations near drains. By developing a more complex Mike 11 network, the drain levels reflect the topography and effects on the surrounding groundwater levels are more realistic. The increase in model run-time between the most simple and most complex Mike 11 model is approximately 30%.

Limitations and uncertainties

The calibration of a groundwater model does not ensure it is an accurate representation of the system. The appropriateness and correctness of the conceptual hydrogeological model is typically more important than achieving a small error between simulated and observed heads and flows. The model's application should be constrained by the limitations inherent in the underlying conceptual model.

The Murray regional model has a spatial resolution of 200 m and a temporal resolution of one day. Based on these structural limitations of the model, the errors discussed in the previous section and the quality of the calibration, the model is considered suitable for:

- Evaluating changes in the water balance due to drainage changes and land-use changes (changes in recharge, drainage, evapotranspiration, horizontal flow etc.).
- The relative assessment of regional and subregional impacts due to changes in drainage, and abstraction from the shallow aquifer.
- District-scale groundwater-level evaluation (AAMaxGL, AAMinGL etc.) under various climate scenarios. This includes determining areas of seasonal waterlogging and inundation. However, the inherent model error needs to be considered when using groundwater levels derived from the regional model. If the error is deemed too large for the purpose of the application, a localised model with a finer grid should be constructed and recalibrated to achieve appropriate model error.

The model's structural limitations suggest that the Murray regional model is **not** the preferred platform for the following applications:

- **Wetland or lake assessment:** when features are similar in scale to the horizontal and vertical resolution of the model, they are not suitable for evaluation under the current Murray regional model platform. However, the Murray regional model can act as a basis for developing higher-resolution subregional and local models that can be more appropriate for these types of evaluations.
- **Flood modelling:** although the Mike SHE model has appropriate modules to undertake detailed flood modelling and floodplain mapping, the 200 m grid in the Murray regional model is too coarse for this type of application. Furthermore, the water levels in the major waterways have not been calibrated to flood events (1 in 100, 1 in 200 etc.), and weirs, bridges and culverts have not been explicitly included in the Mike 11 model. Therefore use of the Murray regional model for flood applications is not considered suitable.
- **Detailed drainage modelling:** this includes the detailed modelling of individual subsurface drains, and potential development drainage scenarios. Drainage cannot

be modelled at a grid scale finer than that of the saturated zone model (200 m), so any drainage that is likely to be at a finer scale than 200 m is not considered a suitable scenario for the Murray regional model. However, the Murray regional model can act as a basis for developing higher-resolution subregional and local models that can be more appropriate for these types of evaluations.

- **Abstraction or sustainable yields from the Leederville aquifer:** according to the conceptual model, flows between the Superficial and Leederville aquifers were not of sufficient magnitude to affect the groundwater heads in the Superficial aquifer. The numerical model was constructed with the base of the Superficial aquifer as the base of the model, and no flow was assumed to transfer through this boundary. Therefore, modelling groundwater abstraction from deeper and confined aquifers is not possible using the Murray regional model. If a model that includes abstraction or sustainable yield from deeper aquifers is desired, it is recommended that the Murray regional model be used as a basis for deeper aquifer models, where layers representing deeper aquifers could be incorporated into the model and calibrated to appropriate deep groundwater bores.

5 Water balance

The average annual water balance for the Murray regional model was calculated for the period from January 1978 to December 2007. The water balance was calculated for the Murray DWMP area by using the post-processing water-balance tool included in the Mike SHE software package (Mike Zero) suite of tools. The flow rate and source of flow components were integrated over the period to obtain cumulative volumes.

The water balance was determined for both the total regional model domain and the Murray DWMP area. The water balance for the major groundwater fluxes and for the surface and groundwater fluxes is presented in Table 5-1. The water balance for the superficial groundwater is consistent with the conceptual hydrogeological model (DoW 2010). An error of <0.05% for the model domain satisfies the calibration criteria.

Table 5-1: Average annual water balance for the entire model domain, 1978 - 2007

Flux	Total model domain		Murray DWMP area	
	(mm)	(%)	(mm)	(%)
Water balance for superficial groundwater				
Net recharge	103.8	100.0%	87.6	87.1%
Flow through	-12.2	-11.8%	13.0	12.9%
Abstraction	-14.3	-13.8%	-9.9	-9.8%
Drainage	-76.2	-73.4%	-90.5	-90.0%
Storage	-1.0	-1.0%	-1.1	-1.1%
Error	0.0	0.0%	-0.9	-0.9%
Water balance for surface water and groundwater				
Rainfall	843.6	100.0%	849.0	98.5%
Surface water flow	-82.7	-9.8%	-96.3	-11.2%
Flow through (groundwater)	-12.2	-1.5%	13.0	1.5%
Evapotranspiration	-733.1	-86.9%	-755.2	-87.6%
Storage	-1.3	-0.2%	-1.4	-0.2%
Error	0.0	0.0%	-0.9	-0.1%

The model predicted a gross recharge rate of 41% for the total regional model domain, which is marginally less than the 49% predicted in the conceptual model. The conceptual model did not account for waterlogging inhibiting recharge, and it was recognised that 49% was likely to be an upper limit. Recharge rates reflected those of the conceptual model, and of previous studies (Xu et al. 2009 predicted 45% recharge under annual pasture for sand soils in the PRAMS vertical flux model). A net recharge rate of 103 mm (12.3% of rainfall) is lower than the predicted gross recharge (41%), and reflects the high watertable in the Murray regional model domain, as well as the large evaporative flux from the superficial groundwater.

The model under-predicts surface water flow, particularly surface runoff, when compared with the conceptual water balance. It is likely that this is related to lack of resolution in the surface water model (Mike 11), and is difficult to remedy with a 200 m grid size. However, the prediction of the baseflow component of the water balance was adequate; and the water balance of the superficial groundwater component of the model was satisfactory.

6 Sensitivity analysis

Sensitivity analysis describes the procedure for quantifying the impact on an aquifer's simulated response due to an incremental variation in a model parameter or a model stress. The objective of a sensitivity analysis is to identify those parameters that are most important in determining aquifer behaviours. If parameters can be ranked in order of importance, then priorities can be set for focusing field investigations on key parameters to reduce model uncertainty. A sensitivity analysis is undertaken by systematically changing calibrated aquifer parameters and determining the effect these changes have on observed data (i.e. bores where the model has been calibrated to measured heads). The Murray regional model is a high-complexity numerical model and, as such, a sensitivity analysis conducted by perturbation is extremely demanding computationally. Only a limited selective analysis is justified for anticipated key parameters. The change in the simulated heads due to these variations is an estimate of the calibrated model's sensitivity to that parameter.

The sensitivity analysis was undertaken using the following procedure:

1. A decision was made on the model inputs and parameters to be included in the analysis, and the range of variation for each parameter. The inputs and the range of each input for the sensitivity analysis are shown in Table 6-1.
2. Simulations were run for each input varied across its range. This was completed by Danish Hydrological Institute modellers in Sydney, where many computers with relevant licenses were available for the multiple runs required to complete the analysis.
3. Scaled sensitivity values were compared discussed for all parameters included in the sensitivity analysis, and sensitive parameters identified.

The implemented analysis is based on the principles such as the requirements set out in the Murray-Darling Basin Commission's (2001) Groundwater Flow Modelling Guideline.

The sensitivity analysis was carried out with the Auto Calibration Tool AUTOCAL from DHI. AUTOCAL is a generic tool for performing automatic calibration, parameter optimisation, sensitivity analysis and scenario management of Mike SHE's numerical modelling engines. The methodology is described in detail in the Mike User Guide (DHI 2005). AUTOCAL produces a result file that contains the calculated sensitivity coefficients of each parameter with respect to the different output measures and objective functions. It contains in particular:

- the parameter set and corresponding output measures and objective functions for the point where the local sensitivity analysis has been performed
- scaled sensitivity coefficients for each parameter of the specified output measures and objective functions
- parameter covariance matrix in terms of the standard deviations of the parameters and the correlation matrix. It should be noted that the calculated parameter covariance is related to the transformed parameter values and not their native values.

The analysis focuses on the calculation of a sensitivity ranking for the model parameters, and does not consider factors that are not parameters (e.g. model boundaries, source release

history, model time-step etc.). The outcome was a scaled sensitivity coefficient from calculations against groundwater levels for each considered parameter. This allows for the ranking of parameters in order of importance, so that priorities can be set for focusing on the single parameter analysis to compute the range of sensitivity.

In order to compare the local sensitivity coefficients between parameters of different scales of magnitude, scaled sensitivity values were calculated. The scaled sensitivities provide a ranking of the parameters with respect to the importance of the parameters for the considered output measure or objective function. Higher scaled sensitivity values (absolute values) indicate more sensitive parameters. As a general rule, parameters are said to be insensitive if their scaled sensitivity value is less than about 0.01 – 0.02 times the maximum scaled sensitivity value (absolute value).

Since the sensitivity coefficients are evaluated only around the initial parameter set, they reflect the local sensitivities only. At other locations in the parameter space the sensitivity coefficients may be very different, especially if the simulation model is highly non-linear in its parameter-output interaction. The sensitivity analysis provides information on the relative sensitivity of the model to a change in a parameter value, and does not necessarily reflect the actual sensitivity of the real system.

The parameters included in the sensitivity analysis, their calibrated value and their specified upper limits are shown in Table 6-1. The scaled sensitivity coefficients for each of the parameters included in the sensitivity analysis are shown in Figure 6-1. The model is sensitive to horizontal conductivity in the saturated zone, and to most parameters apart from LAI in the unsaturated zone. According to the results, scaled sensitive coefficients with a value below 100 are expected to be insensitive. These include the vertical hydraulic conductivity in the saturated zone (except the Rockingham Sands), the Manning value for overland flow, the Leaf Area Index (LAI), the specific yield, the vertical hydraulic conductivity in the unsaturated zone (apart from the Bassendean Sands).

The sensitivity of the model to horizontal hydraulic conductivity, particularly in Bassendean, Gnangara and Rockingham Sands, highlights the requirement for further local pump tests in these formations to validate model parameters. Root-depth is highly sensitivity and is associated with high uncertainty, and the sensitivity analysis highlights the need for further investigations into root depth within the Murray region. Likewise, soil properties in the unsaturated zone may require further investigation, based on sensitivity analysis results, and local scale studies are likely to require investigation into local unsaturated zone hydraulic properties, including the vertical hydraulic conductivities in the Bassendean Sands.

Table 6-1: Parameters and values used in the sensitivity analysis

Parameter	Catchment parameters	Value	Units	Sens*	Name	Module**	Run
Water content at saturation	Spearwood	0.33	-	0.41	spe_wcs	UZ/ET	1
Water content at saturation	Bassendean	0.3	-	0.38	bass_wcs	UZ/ET	1
Water content at saturation	Pinjarra	0.37	-	0.46	pin_wcs	UZ/ET	1
Water content at field capacity	Spearwood	0.05	-	0.063	spe_wfc	UZ/ET	2
Water content at field capacity	Bassendean	0.09	-	0.11	bass_wfc	UZ/ET	2
Water content at field capacity	Pinjarra	0.2	-	0.25	pin_wfc	UZ/ET	2
Water content at wilting point	Spearwood	0.03	-	0.038	spe_wcw	UZ/ET	3
Water content at wilting point	Bassendean	0.03	-	0.038	bass_wcw	UZ/ET	3
Water content at wilting point	Pinjarra	0.13	-	0.16	pin_wcw	UZ/ET	3
Saturated hydraulic conductivity	Spearwood	1	m/d	3.12	spe_hydcon	UZ/ET	4
Saturated hydraulic conductivity	Bassendean	0.02	m/d	0.10	bass_hydcon	UZ/ET	4
Saturated hydraulic conductivity	Pinjarra	0.05	m/d	0.21	pin_hydcon	UZ/ET	4
Root depth	Bare/urban	1000	mm	1250	RD_bare	UZ/ET	5
Root depth	Irrigated	1200	mm	1500	RD_irr	UZ/ET	5
Root depth	Native	2000	mm	2500	RD_nat	UZ/ET	5
Root depth	Grazing	1000	mm	1250	RD_rd	UZ/ET	5
Root depth	Plantation	2000	mm	2500	RD_plan	UZ/ET	5
LAI	Bare/urban	2	-	3.5	LAI_bare	UZ/ET	6
LAI	Irrigated	3	-	5.3	LAI_irr	UZ/ET	6
LAI	Native	1.5	-	2.6	LAI_nat	UZ/ET	6
LAI	Grazing	1.15	-	1.4	LAI_rd	UZ/ET	6
LAI	Plantation	1.5	-	2.6	LAI_plan	UZ/ET	6
Manning 'M'	Uniform	20	m ^{1/3} /s	30	Manning	OL	7
Detention storage	Uniform	2	mm	3	DetStor	OL	8
Drain level	Uniform	-0.15	m	-0.45	drainLevel	SZ	9
Drain time constant	Uniform	0.1	1/d	0.20	drainTC	SZ	10
Specific yield	Gnangara	0.25	-	0.35	gna_sy	SZ	11
Specific yield	Colluvium	0.05	-	0.07	col_sy	SZ	11
Specific yield	Alluvium	0.2	-	0.28	all_sy	SZ	11
Specific yield	Mining Clay	0.07	-	0.098	mcl_sy	SZ	11
Specific yield	Bassendean	0.21	-	0.29	bas_sy	SZ	11
Specific yield	Tamala	0.25	-	0.35	tam_sy	SZ	11
Specific yield	Guildford	0.12	-	0.17	gui_sy	SZ	11
Specific yield	Yoganup	0.2	-	0.28	yog_sy	SZ	11
Specific yield	Ascot	0.25	-	0.35	asc_sy	SZ	11
Specific yield	Rock	0.2	-	0.28	roc_sy	SZ	11
Hydraulic conductivity – horizontal	Gnangara	8	m/d	20.2	gna_h	SZ	12
Hydraulic conductivity – horizontal	Colluvium	2	m/d	5.8	col_h	SZ	12
Hydraulic conductivity – horizontal	Alluvium	10	m/d	24.8	all_h	SZ	12
Hydraulic conductivity – horizontal	Bassendean	10	m/d	24.8	bas_h	SZ	12
Hydraulic conductivity – horizontal	Tamala	80	m/d	161	tam_h	SZ	12
Hydraulic conductivity – horizontal	Guildford	2	m/d	5.8	gui_h	SZ	12
Hydraulic conductivity – horizontal	Yoganup	4.1	m/d	11.1	yog_h	SZ	12
Hydraulic conductivity – horizontal	Ascot	9.7	m/d	24.0	asc_h	SZ	12
Hydraulic conductivity – horizontal	Rockingham	7	m/d	18.0	roc_h	SZ	12
Hydraulic conductivity – vertical	Gnangara	1.12	m/d	3.5	gna_v	SZ	13
Hydraulic conductivity – vertical	Colluvium	0.02	m/d	0.09	col_v	SZ	13
Hydraulic conductivity – vertical	Alluvium	0.05	m/d	0.21	all_v	SZ	13
Hydraulic conductivity – vertical	Mining Clay	0.001	m/d	0.0062	mcl_v	SZ	13
Hydraulic conductivity – vertical	Bassendean	0.1	m/d	0.39	bas_v	SZ	13
Hydraulic conductivity – vertical	Tamala	8	m/d	20.2	tam_v	SZ	13
Hydraulic conductivity – vertical	Guildford	0.05	m/d	0.21	gui_v	SZ	13
Hydraulic conductivity – vertical	Yoganup	0.41	m/d	1.4	yog_v	SZ	13
Hydraulic conductivity – vertical	Ascot	1.2	m/d	3.7	asc_v	SZ	13
Hydraulic conductivity – vertical	Rockingham	0.1	m/d	0.39	roc_v	SZ	13

* Sens = specified upper limit of the parameter

** Mike SHE modules: UZ/ET = unsaturated zone and evapotranspiration, OL = overland flow, SZ = saturated zone

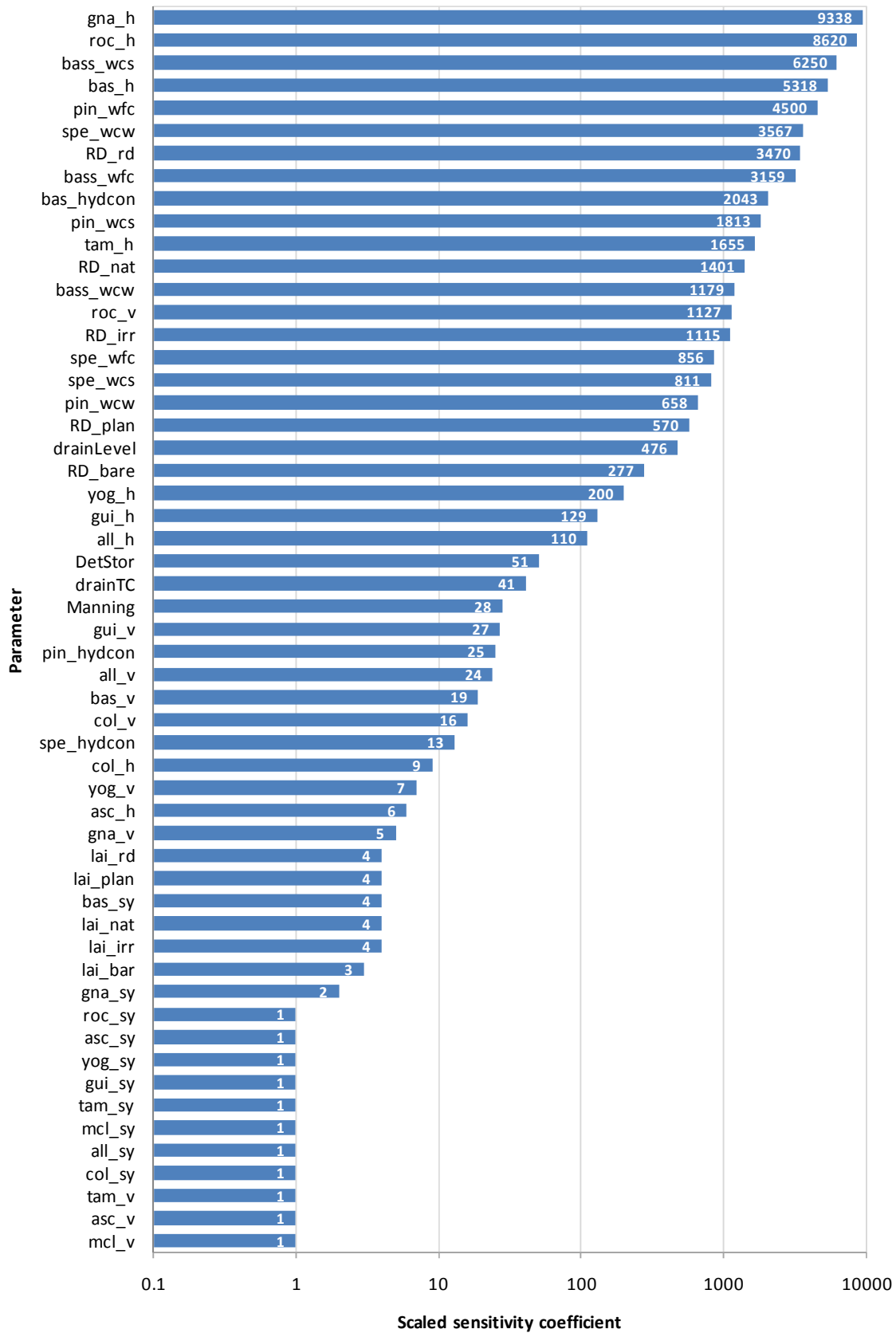


Figure 6-1: Scale sensitivity values resulting from the sensitivity analysis

7 Wetland models

Within the study area, eight key wetlands were selected to have their EWR defined – a process involving detailed assessment of the water regime required to maintain the ecological values of the wetlands. To assess the EWR component, a detailed hydrological assessment of each of the key wetlands was necessary, including conceptual representation of the wetlands and calibrated water level and flow modelling (surface water and groundwater). Various land use and climate change scenarios could then be applied to determine the response of the wetland water regime under those conditions. The selection process and the eight key wetlands are described in detail in the *conceptual model report* (Hall et al. 2010).

The regional model's 200 m grid was too coarse to adequately address the wetland EWR study due to the poor resolution of wetland bathymetry and vegetation. Therefore it was necessary to model the wetlands at a finer grid scale. Five separate wetland models were used to model the eight key wetlands. Scott Road wetland (UFI 5033) and Benden Road wetland (UFI 5724) were included in the same model, as were Lakes Road wetland (UFI 5033), Greyhound Road wetland (UFI 5032) and Airfield wetland (UFI 4835). The model areas and the names given to each of the wetland models are shown in Figure 7-1.

Model set-up

The five models were set up with grids ranging between 30 and 50 m. Co-ordinates, values, and parameters relating to the model domain and grid are shown in Table 7-1. All model layers have consistent map projections of GDA 1994 MGA Zone 50.

Table 7-1: Wetland model set-up parameters

Model set-up parameters	Barragup	Scott Road	Elliot Road	Lakes Road	Phillips Road
Grid size (m)	50	30	40	40	30
Number of internal cells	5466	8254	4960	8593	7319
Number of boundary cells	317	377	287	368	288
Number cells in X direction	104	148	81	115	118
Number cells in Y direction	99	100	64	96	109
Area (km ²)	14.46	7.77	8.31	14.35	6.84

The geology and soil spatial coverages for the wetland models were extracted from the same dataset used in the regional model. The original dataset used in the regional model had a horizontal resolution of 10 m. The geological lenses and computational layers were extracted for the model domain, and re-sampled to the individual wetland model's grid size.

Land use

The sensitivity analysis highlighted the model's sensitivity to land-use parameters (LAI and root depth). The land-use dataset used in the regional model (which was based on the

cadastre spatial coverage) was sufficient for 200 m grid spacing, however it had significant inaccuracies when re-sampled to a grid size of 30 – 50 m. It was therefore necessary to recreate land-use maps at a finer scale for each of the individual wetland models. Figures 7-2 to 7-6 show the land-use coverages used for each of the wetland models.

Boundary conditions

With the exception of the Barragup Swamp model, the wetland model boundaries were defined using the technique described below:

- contours for the average groundwater level from the regional model outputs were overlaid onto the approximate wetland modelling domain
- two wetland boundaries were drawn perpendicular to the groundwater contour lines, and no-flow boundaries were implemented at these boundaries
- the up-gradient and down-gradient boundary conditions were assigned as fixed-head boundary conditions, and a transient fixed-head extracted from the corresponding grid point, climate sequence, and computational layer in the regional model was implemented at each of these boundaries.

The Barragup Swamp model was surrounded by waterbodies that were close to or at sea level. A fixed head boundary condition of 0 mAHD was implemented for the Barragup wetland model.

7.1 Model calibration

Initially, all parameters used in the wetland models were identical to parameters used in the regional model. Parameters for the unsaturated zone and land-use parameters (LAI and root depth) were adjusted for each of the wetland models within reasonable ranges, until calibration criteria were achieved.

The calibration period for the wetland model was from 1 January 2000 – 15 November 2009. A significant portion of the wetland data was measured in the second half of 2009. The time-period of the measurement dataset meant that model validation was not possible for the individual wetland models. It should also be noted that most of the wetland bores and the wetland gauges generally contained data from 1 – 2 years. The 10 year calibration period only applied to regional bores within the wetland models, which generally comprised a minority of the wetland bores.

The calibration performance for the wetland models is presented in qualitative and quantitative terms in comparison with agreed target criteria. The model calibration and validation methods are based on the *Murray-Darling Basin Commission groundwater flow modelling guidelines* (Middlemis 2000). The four calibration measures described below have been used to assess the calibration result:

- **Water balance:** the single maximum cumulative error of the water balance of the Superficial aquifer of less than 1%. The difference between the total modelled inflow and the total modelled outflow (water balance error) will be less than 0.1%.

- **Iteration residual error:** the iteration convergence criterion should be one or two orders of magnitude smaller than the head resolution. Here the criterion is <0.1%.
- **Qualitative measures:**
 - modelled versus measured groundwater hydrographs for each calibration bore
 - residual error plot for each calibration bore
 - scattergram of measured versus modelled heads
 - comparison of aerial photographs and overland water distribution in wetland models at the dates the aerial photographs were taken.
- **Quantitative measures:**
 - Root mean square (RMS) error between measured hydraulic-head and modelled hydraulic-head will be less than 5% of the measured hydraulic-head drop across the model area. Due to the lack of bore data, it is recognised that this will not be achievable in models with very small head drop in observed data, and these will be outlined and explained. The error will not be spatially biased. Final calibration results will report the RMS error, mean absolute error, the mean error and the coefficient of determination.
 - Final calibration for each bore will report mean error, mean absolute error, RMS error, standard deviation of residuals, correlation coefficient (R), and Nash Sutcliffe efficiency (R^2).

Barragup Swamp model

In winter 2009 the Barragup Swamp had four bores drilled in its vicinity (HS087-1A, HS087-1B, HS087-2 and HS087-3). In addition, the model contained two regional bores (HST091B and HS091A) located approximately 500 m north of the wetland, which were completed in mid-2008. Monthly water level measurements in the wetland have been recorded since August 2009, and were taken monthly over the year 1989 for the Bowman Bishaw Gorham report (1990) on the hydrology of Barragup Swamp. The location of the groundwater bores in the Barragup Swamp model is shown in Figure 7-2.

The model was calibrated by adjusting land-use parameters and unsaturated zone parameters within reasonable ranges until calibration criteria were met. An extra land-use field was implemented to account for the open water in Barragup Swamp, and was assigned a root depth and LAI value of zero. The calibrated land-use parameters for Barragup Swamp are shown in Table 7-2. Root depth was increased marginally for native trees in this region to 2600 mm, and reduced for bare soil.

Table 7-2: Barragup Swamp model land-use parameters

Land-use parameters	Native trees	Pasture	Open water	Plantation	Irrigated pasture	Bare/urban
Root depth (mm)	2600	1000	0	2000	400	100
Leaf area index	1.5	0-3.0*	0	1.5	2.5	1.2

*crop rotation scheme (see Figure 3-10)

The values for the unsaturated zone parameters that were calibrated for the Barragup Swamp are shown in Table 7-3. The values were adjusted from the regional model, and represent a sandy soil with marginally more clay content than the soil represented in the regional model. This is reasonable for the Barragup domain, which contains alluvial and estuarine deposits with higher quantities of fine particles than the poorly sorted Bassendean Sand.

Table 7-3: Barragup Swamp model unsaturated zone parameters

Water content at saturation	0.19
Water content at field capacity	0.05
Water content at wilting point	0.03
Saturated hydraulic conductivity (m/day)	0.05

The scaled RMS error for the calibrated Barragup Swamp model is 12.00%. The RMS is 0.15 m and the absolute residual mean (mean absolute error) and residual mean error (mean error) is 0.11 m and -0.05 m respectively.

The average absolute error is 0.11 m, and is defined as the difference between the predicted and measured water levels. The maximum positive error in the aquifer in predicted head is 0.61 m and the maximum negative error is -0.24 m.

The value for the scaled RMS is higher than the criteria of 5%; however, the range of observed values is 1.23 m, which made it very difficult to achieve a scaled RMS of below 5%.

To further ensure calibration accuracy, historical aerial photographs taken in December 2003, December 2005 and December 2006 were compared with the spatial distribution of the modelled overland water within the wetland (see Appendix C). In each case, the distribution of water in the aerial photograph and modelled overland water are closely correlated.

With a mean sum of residuals of 0.11 m, the model is suitable for predicting changes in wetland water levels and for predicting wetland water regimes for various climate and land-use change scenarios. Appendix C contains a detailed report on the calibration statistics, as well as the individual groundwater monitoring bore plots for modelled versus observed values in the Barragup Swamp model.

Scott Road model

The Scott Road model includes the Scott Road wetland (UFI 5180) and the Benden Road wetland (UFI 5724), which is located approximately 1 km to the north-west. The model domain is characterised by low sand dunes and intermittent wetlands and lakes. The land use is primarily annual pasture, with some pockets of native trees throughout. The model has an east-west groundwater gradient.

The Scott Road model used additional data from a series of private bores within the study area, installed for a hydrological investigation in the Nambeelup region (Bowman Bishaw Gorham 2006). The water level data was taken fortnightly for two years, between July 2006

and June 2009. In addition there are two sets of paired groundwater bores with monthly water level readings, drilled by the Department of Water in 2008; and two pairs of Department of Water bores drilled in 2009, also with monthly water level readings. The locations of the bores in the Scott Road model are shown in Figure 7-3.

The modelling domain contained several significant drains that were likely to affect the local hydrology. The drainage was entered into the Mike 11 model, and consisted of a deep drain in the model's north, and a smaller drain south of the Scott Road wetland which eventually drains to Winter Brook. The Mike 11 drainage channels are shown in Figure 7-3.

Calibration of the Scott Road model involved adjusting the land use and unsaturated zone model parameters within reasonable ranges. The land use in the Scott Road model consisted of only three categories: 'native vegetation', 'pasture' and 'waterbody'. The calibrated land-use parameters are shown in Table 7-4.

Table 7-4: Scott Road model land-use parameters

Land-use parameters	Native trees	Pasture	Water body
Root depth (mm)	2000	1000	0
Leaf area index	1.6	0-3.0*	0

*crop rotation scheme (see Figure 3-10)

The calibrated parameters for the unsaturated zone model are shown in Table 7-5, and are reasonable for the sandy soils observed in the Scott Road modelling domain.

Table 7-5: Scott Road model unsaturated zone parameters

Water content at saturation	0.19
Water content at field capacity	0.05
Water content at wilting point	0.03
Saturated hydraulic conductivity (m/day)	0.05

The model achieved a mean absolute sum of residuals of 0.32 m, a mean sum of residuals of 0.19 m and a scaled RMS of 7.52%. The scaled RMS value is marginally higher than the criteria of 5%. Historical aerial photographs taken in December 2003, December 2005 and December 2006 were compared with the spatial distribution of the modelled overland water for both the Scott and Benden wetlands (see Appendix D). The aerial photograph and modelled overland water are closely correlated for Benden Road wetland for all years, whereas water levels in the Scott Road wetland are under-predicted for December 2003 and 2006.

The model can be used to predict changes in wetland water levels and water regimes in the wetland for various climate and land-use change scenarios, yet errors in calibration need to be considered. It is recommended that if further detail is required in this modelling domain, then further calibration should take place once more data is collected at the wetland water gauges and the new monitoring bore locations. Appendix D contains a detailed report on the

calibration statistics, and the individual groundwater monitoring bore plots for modelled versus observed values in the Scott Road model.

It is likely that some error in the model can be attributed to the interpretation of the Rockingham Sand paleochannel, which is located at the modelling domain's northern edge. As mentioned previously, the precise location of the edge and the steepness of its sides are poorly understood, and it is likely there are errors induced by the sudden increase in transmissivity resulting from the paleochannel's presence. An additional geologic investigation is recommended along the edge of the Rockingham Sand paleochannel to improve the geology model, if additional precision in the calibration is required.

Elliot Road model

The Elliot Road wetland system is located in the regional model's northern section. The domain is characterised by sand dunes to the west (which appear to cause a local groundwater mound in the regional model), a relatively shallow Superficial aquifer (depth to the Leederville aquifer is approximately 15 m in the Elliot Road model domain), and a small east-west groundwater gradient.

There is significant drainage in the Elliot Road modelling domain, and a drain to the wetland's south-east is likely to drain the wetland, and is a likely driver for the maximum wetland water levels. A channel flow model for all significant drains in the Elliot Road model is shown in Figure 7-4.

The model domain contains four groundwater bores and two wetland gauges. The bore T560, in the model's northern boundary, contains monthly water level data from 1975. All other bores and wetland gauges had monthly water level recordings from July 2009. The locations of the groundwater bores are shown in Figure 7-4.

The model was calibrated by adjusting unsaturated zone and land-use parameters within reasonable ranges, to achieve a reasonable fit between observed and measured groundwater levels and wetland water levels. Land use in the Elliot Road model comprised only five categories. A new category for native shrubs was implemented, because significant portions of the catchment contain low-lying shrubs, which are likely to have root-depth values between that of native vegetation and pasture. The native vegetation was mostly along the sand dune to the catchment's east, with root depth likely to be higher than 2000 mm for this vegetation, given the depth to groundwater is large in this region. As such, the root depth of native trees was adjusted to 3000 mm. The calibrated land-use parameters are shown in Table 7-6.

Table 7-6: Elliot Road model land-use parameters

Land-use parameters	Native trees	Pasture	Native shrubs	Bare	Irrigated pasture
Root depth (mm)	3000	1000	1700	200	800
Leaf area index	2.5	0-3.0*	1.5	0.8	3

*crop rotation scheme (see Figure 3-10)

The unsaturated zone parameters were adjusted and the water content at saturation was 0.2 and the field capacity was 0.05, which is reasonable for medium- to coarse-grained sand to clayey sand. The calibrated parameters for the unsaturated zone model are shown in Table 7-7.

Table 7-7: Elliot Road model unsaturated zone parameters

Water content at saturation	0.17
Water content at field capacity	0.05
Water content at wilting point	0.03
Saturated hydraulic conductivity (m/day)	0.10

The model achieved a mean absolute sum of residuals of 0.29 m and a scaled RMS of 14.44%. This value is higher than the criteria of 5%. The Elliot Road model had a shortage of water level readings (136 for the entire model, which included 117 from bore T560), which contributed largely to the lack of precision in calibration. Drainage in the model appeared to constrain the water depth in wetter years only, although no measurements were available over these periods. Further data collection is required to confirm the maximum water levels for the Elliot wetland system.

Historical aerial photographs taken in December 2003, December 2005 and December 2006 were compared with the spatial distribution of the modelled overland water for Elliot Road wetland (see Appendix E). The aerial photograph and modelled overland water are closely correlated in each instance.

The model can be used to predict changes in wetland water levels for various climate and land-use change scenarios, although errors in calibration need to be considered. It is recommended that if further detail is required in this modelling domain, then further calibration should take place once more data is collected at the wetland water gauges and the new monitoring bore locations. Appendix E contains a detailed report on the calibration statistics, and the individual groundwater monitoring bore plots for modelled versus observed values in the Elliot Road model.

Lakes Road model

The Lakes Road model contains three wetlands: Lakes Road wetland (UFI 5033), Greyhound Road wetland (UFI 5032) and Airfield wetland (UFI 4835). The model domain is bisected by Lakes Road, and is bounded to the south and the east by Nambeelup Brook. Lakes Road bisects the Airfield wetland and Lakes Road wetland. However, due to road culverts and the sandy substrate, these wetlands remain hydraulically connected. The topography is characterised by low sand dunes with pasture and native vegetation. The groundwater gradient generally slopes toward Nambeelup Brook.

The model contains 15 groundwater monitoring bores and four wetland water level gauges. There is only one groundwater bore with a long-term sampling record (T650); all the other monitoring bores and gauges have records spanning six months to two years.

There is significant surface drainage in the Lakes Road model. The Murray Airfield is located in the model's centre and drains towards the Airfield wetland. There are minor drains that appear to drain Greyhound Road wetland and Lakes Road wetland, and some minor drains that drain to Airfield wetland and Greyhound Road wetland. Also, Nambeelup Brook represents a major groundwater discharge point, and is necessary to include in the model. All relevant drains were represented in a Mike 11 channel flow model, and are shown in Figure 7-5.

The model uses the south-eastern side of Nambeelup Brook as a no-flow boundary condition. The majority of the northern boundary is also a no-flow boundary condition perpendicular to groundwater contours. Transient fixed-head boundary conditions taken from the regional model were used for the western boundary, and for part of the northern boundary. An inflow boundary was also required for Nambeelup Brook, and was extracted from the regional model.

The land use was re-delineated for the Lakes Road model, and is shown in Figure 7-5. An extra land-use category was implemented for native shrubs, which cover a large portion of the study area, and are generally sparse and less than 0.5 m high. They are likely to have a root depth between that of pasture and native trees.

The model was calibrated by adjusting unsaturated zone and land-use parameters within reasonable ranges until calibration criteria were achieved. The calibrated land-use parameters are shown in Table 7-8. Native trees and pasture parameters were not adjusted from the regional model parameters. Native shrubs adopted a root depth of 1300 mm, which is between the values for native trees and pasture.

Table 7-8: Lakes Road model land-use parameters

Land-use parameters	Native trees	Pasture	Native shrubs	Irrigated pasture	Bare
Root depth (mm)	2000	1000	1300	750	300
Leaf area index	1.5	0-3.0*	1.5	2.5	1

*crop rotation scheme (see Figure 3-10)

The unsaturated zone parameters were adjusted and the water content at saturation was 0.25 and the field capacity was 0.12, which is reasonable for medium- to coarse-grained sand to clayey sand. The calibrated parameters for the unsaturated zone model are shown in Table 7-9.

Table 7-9: Lakes Road model unsaturated zone parameters

Water content at saturation	0.25
Water content at field capacity	0.12
Water content at wilting point	0.10
Saturated hydraulic conductivity (m/day)	0.10

The scaled RMS error for the calibrated Lakes Road model is 4.99%, which is below the acceptance criteria of 5%. The RMS is 0.66 m, and the absolute residual mean (mean absolute error) and the residual mean error (mean error) are 0.38 m and 0.49 m respectively. The maximum positive error in the aquifer in predicted head is 1.70 m and the maximum negative error is -0.57 m.

The Lakes Road model is suitable for predicting changes in wetland water levels and for predicting wetland water regimes for various climate and land-use change scenarios. Appendix F contains a detailed report on the calibration statistics, and the individual groundwater monitoring bore plots for modelled versus observed values in the Lakes Road model.

Greyhound Road wetland was limited in depth most years by the level of the drain that discharges water to the wetland's south. The other two wetlands (Lakes Road and Airfield) did not have their maximum level constrained by adjoining drains. The Airfield wetland's northern and southern waterbodies were connected hydraulically by a culvert, and maximum water levels were similar for these two waterbodies.

Phillips Road model

The Phillips Road wetland system is located between the Pinjarra light industrial area and the Pinjarra town centre, approximately 1 km west of the Murray River. The groundwater gradient drains towards the Murray River north and east of the modelling domain. The wetland is surrounded by a light industrial area to the west, Pinjarra golf course to the north-east and the outskirts of residential Pinjarra to the south and south-east (Figure 7-6).

There are four groundwater monitoring bores and one wetland water level gauge within the modelling domain (Figure 7-6). Monitoring bore HS56A is 100 m from the modelling domain, and was moved to be included in the analysis. HS56A contains 10 years of biannual or monthly data, and the remaining monitoring bores have monthly data collected since June 2009.

The Phillips Road model has no-flow boundary conditions on the western and southern boundaries. The northern and eastern boundaries have fixed-head boundaries, and transient fixed-head time-series were extracted from the regional model.

Calibration of the Phillips Road model involved adjusting the land use and unsaturated zone model parameters within reasonable ranges. A reasonable calibration was not achieved until irrigation for the golf course was incorporated into the model. The golf course has a series of unlined lakes that are filled with water abstracted from the Leederville aquifer and used to water the course during the summer months.

The allocation to the golf course is 233 ML/yr, which represents 67% of the rainfall input for the golf course region, and is the cause of a significant groundwater mound beneath the golf course area. The monthly irrigation rate was taken from the metered extraction for 2008–09, and irrigation was applied constantly at the rates shown in Figure 7-7.

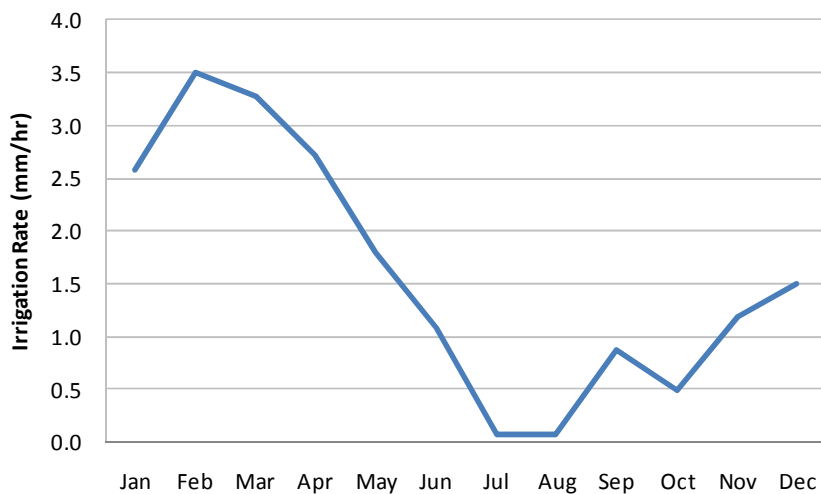


Figure 7-7: Irrigation rate for the Pinjarra golf course

The spatial extent of the irrigation is shown in Figure 7-8. The land use in the Phillips Road model consisted of four categories: 'native vegetation', 'annual pasture', 'irrigated land' and 'bare/urban'. The calibrated land-use parameters are shown in Table 7-10.

Table 7-10: Phillips Road wetland model land-use parameters

Land-use parameters	Native trees	Pasture	Bare / urban	Irrigated pasture
Root depth (mm)	2000	1000	200	650
Leaf area index	1.5	0-3.0*	0.5	2.5

*crop rotation scheme (see Figure 3-10)

According to the Department of Agriculture and Food soils' database, the Phillips model domain contains both Pinjarra soils and Bassendean Sand. The irrigation area and the soils for the Phillips model are shown in Figure 7-7. The calibrated unsaturated zone parameters for the Phillips model area are shown in Table 7-11.

Table 7-11: Phillips Road wetland model unsaturated zone parameters

Unsaturated zone parameters	Bassendean	Pinjarra
Water content at saturation	0.20	0.37
Water content at field capacity	0.06	0.20
Water content at wilting point	0.04	0.13
Saturated hydraulic conductivity (m/day)	0.10	0.10

The scaled RMS error for the calibrated Phillips Road model is 7.97%, which is marginally above the acceptance criteria of 5%. The RMS is 0.47 m, and the absolute residual mean (mean absolute error) and the residual mean error (mean error) is 0.37 m and -0.02 m respectively. The maximum positive error in the aquifer in predicted head is 1.29 m and the maximum negative error is -0.85 m.

The calibration of the Phillips Road model also suffers from having very limited groundwater and wetland water level measurements (62 measurements in total), and four out of the five monitoring locations have data for only half a year.

The historical aerial photograph taken in December 2005 was compared with the spatial distribution of the modelled overland water for Phillips Road wetland at the same time (see Appendix G). The historical photographs indicated there was no water in the wetland in December 2003 and December 2006, and they have not been presented for Phillips Road wetland. The aerial photograph from December 2005 and the modelled overland water are closely correlated.

The Phillips Road model can be used for predicting changes in wetland water levels and for predicting wetland water regimes for various climate and land-use change scenarios; however, errors in the calibration need to be considered when interpreting modelling results. Appendix G contains a detailed report on the calibration statistics, and the individual groundwater monitoring bore plots for modelled versus observed values in the Phillips Road model.

7.2 Wetland calibration discussion

The wetland models were calibrated with limited data, and as such most of the models did not achieve a scaled RMS of below 5%. Most of the bores within the wetland models contained 1 – 2 years of data, and the wetland PLI locations had only 6 months data. The 10 year calibration period only applied to regional bores within the wetland models, which generally comprised a minority of the modelling bores. It is recommended that wetlands gauge boards and groundwater bores be monitored for at least a further two years, and modelling results be validated against future wetland readings, or adjusted accordingly.

7.3 Wetland water balances

The average annual water balance for each of the wetland models was calculated for the period from January 1978 to December 2007. Water balances were calculated for each wetland modelling domain by using the post-processing water-balance tool included in the Mike Zero suite of tools. The flow rate and source of flow components were integrated over the period to obtain cumulative volumes. The water balance for the major groundwater fluxes (water balance for superficial groundwater) and for the total water balance (water balance for surface water and groundwater) is shown in Table 7-12.

Table 7-12: Wetland model water balances

Flux	Elliot Road model		Lakes Road model		Phillips Road model		Scott Road wetland model		Barragup Swamp model	
	(mm)	(%)	(mm)	(%)	(mm)	(%)	(mm)	(%)	(mm)	(%)
Water balance for superficial groundwater										
Net recharge	-107.8	-88.8%	133.1	100.0%	235.1	100.0%	20.5	99.2%	121.7	100.0%
Flow through	121.4	100.0%	-96.0	-72.1%	-197.6	-84.0%	0.2	0.8%	-121.1	-99.5%
Abstraction	0.0	0.0%	0.0	0.0%	0.0	0.0%	0.0	0.0%	0.0	0.0%
Drainage	-13.0	-10.7%	-35.8	-26.9%	-36.4	-15.5%	-19.3	-93.2%	0.0	0.0%
Storage	-0.6	-0.5%	-1.5	-1.1%	-1.2	-0.5%	-1.4	-6.9%	-0.8	-0.7%
Error	0.0	0.0%	-0.1	-0.1%	-0.1	-0.1%	0.0	-0.1%	-0.1	-0.1%
Water balance for surface water and groundwater										
Rainfall	815.7	87.0%	835.0	100.0%	835.8	95.9%	835.1	100.0%	793.5	100.0%
Surface water flow	-191.3	-20.4%	-75.5	-9.0%	-53.5	-6.1%	-138.6	-16.6%	-9.5	-1.2%
Flow through (groundwater)	121.4	13.0%	-96.0	-11.5%	-197.6	-22.7%	0.2	0.0%	-121.1	-15.3%
Evapotranspiration	-743.6	-79.4%	-657.6	-78.8%	-619.4	-71.0%	-693.8	-83.1%	-661.9	-83.4%
Storage	-0.7	-0.1%	-1.6	-0.2%	-1.3	-0.2%	-1.7	-0.2%	-1.0	-0.1%
Error	1.4	0.2%	4.4	0.5%	0.1	0.0%	1.2	0.1%	0.0	0.0%

The error term for all wetland water balances is below 1%, with the exception of the Elliot Road and Lakes Road model for the total water balance. Recharge rates and through-flow quantities agree with both previous studies and the conceptual model. Higher through-flow in the Phillips Road wetland system is attributed to the higher groundwater slope close to the Murray River. The Barragup Swamp model did not include channel flow modules, therefore the drainage component of the groundwater balance is zero. Irrigation was implemented only for the Phillips Road model, and equated to 4.1% of the total model inputs.

8 Conclusions and recommendations

8.1 Regional model

This *construction and calibration report* is the second of three reports that comprise the ‘groundwater studies’ component of the Murray DWMP project. The purpose of the ‘groundwater studies’ project component was to develop and calibrate a regional-scale groundwater model, and to use the model to run various development, drainage and climate scenarios.

The Murray regional model was constructed using the modelling platform Mike SHE, and was based on the conceptual hydrogeology and hydrology described in the Murray *conceptual model report* (Hall et al. 2010). The model was constructed using available geological, hydrogeological, hydrological, soil and land-use information. The Murray regional model consists of unsaturated zone, saturated zone, channel flow and overland flow components. It has a constant grid spacing of 200 m, and covers an area of approximately 722 km².

The calibration period was from 1985 – 2000 and validation was from 2000 – 2009. The model calibration satisfied the criteria of a water balance error <0.05%, an iteration residual error <0.1% and a scaled root mean square (RMS) error <5%. The model calibration error is summarised in Table 8-1.

Table 8-1: Calibration error summary for the Murray regional model

Number of observations	1327
Average absolute error (m)	0.58
Average residual error (m)	0.10
Average RMS error (m)	0.87
Maximum positive error (m)	4.06
Maximum negative error (m)	-3.14
Scaled RMS (%)	2.03

Most of the simulated heads at the monitoring bores in the Superficial aquifer have a response consistent with measured data. The monitoring bores maintain correct trends and the magnitude of the error is constant.

Areas of significant error are:

- Near or within the edge of the Rockingham Sand paleochannel. The exact location of the edge is poorly understood, and it is likely there is error induced by the sudden increase in transmissivity.
- Those of low topography and high watertable, where minimum groundwater levels are close to sea level. The root-depth parameter for vegetation in the pasture and native vegetation surrounding these bores is likely to cause errors, as roots are not likely to remain within the groundwater table. If model refinement is to be done in

areas of very shallow watertable, it is recommended that further analysis of root depth in pasture and native vegetation in these regions is undertaken within the Murray study area.

- In the south-east of the modelling area, where groundwater heads are likely to be affected by pumping from the Cattamarra Coal Measures, as this deeper aquifer has shown a steady decline of over 10 m in potentiometric head over the past three decades.
- Along the Darling Fault, where there are few measurements and the geology and hydrogeology is poorly understood.

The model predicted a gross recharge rate of 41% of rainfall and a net recharge of 12.3% for the regional model domain over the period 1978 – 2007. The lower net recharge rate is reflective of the high watertable in the Murray regional model domain, and large evaporative flux from the superficial groundwater.

The sensitivity analysis indicated that the model is sensitive to horizontal conductivity in the saturated zone, and to most parameters apart from LAI in the unsaturated zone (including root-depth, saturated soil capacity, and field capacity). The model was insensitive to vertical hydraulic conductivity, specific yield, LAI and overland flow parameters.

The sensitivity of the model to horizontal hydraulic conductivity, particularly in Bassendean, Gnangarra and Rockingham Sands, highlights the requirement for further local pump tests in these formations to validate model parameters. Root-depth is highly sensitivity and is associated with high uncertainty, and the sensitivity analysis highlights the need for further investigations into root depth within the Murray region. Likewise, soil properties in the unsaturated zone may require further investigation, based on sensitivity analysis results, and local scale studies are likely to require investigation into local unsaturated zone hydraulic properties.

Based on the structural limitations of the model, the errors discussed in the previous section and the quality of the calibration, the Murray regional model is considered suitable for:

- Evaluating changes in the water balance due to drainage changes and land-use changes (changes in recharge, drainage, evapotranspiration, horizontal flow etc.).
- The relative assessment of regional and subregional impacts due to changes in drainage, and abstraction from the shallow aquifer.
- District-scale groundwater-level evaluation (AAMGL, AAMinGL etc.) under various climate scenarios. This includes determining areas of seasonal waterlogging and inundation. However, the inherent model error needs to be considered when using groundwater levels derived from the regional model. If the error is deemed too large for the purpose of the application, a localised model with a finer grid should be constructed and calibrated to achieve appropriate model accuracy.

The model's structural limitations suggest that the Murray regional model is not the preferred platform for the following applications: wetland or lake assessment, flood modelling, detailed drainage modelling, abstraction or sustainable yields from the Leederville aquifer. Pump-test data is sparse and local data is unavailable for many of the saturated zone formations. It is

recommended that pump tests are undertaken in the Murray region to validate the calibrated hydraulic properties of the Rockingham, Bassendean, and Gnangara Sands.

8.2 Wetland models

Within the study area, eight key wetlands were selected to have their EWR defined; a process involving detailed assessment of the water regime required to maintain the ecological values of the wetlands. Five separate wetland models were used to model the eight key wetlands. Scott Road wetland (UFI 5033) and Benden Road wetland (UFI 5724) were included in the same model, as were Lakes Road wetland (UFI 5033), Greyhound Road wetland (UFI 5032) and Airfield wetland (UFI 4835).

The five models were set up with grids ranging from 30 – 50 m. Co-ordinates, values, and parameters relating to the model domain and grid are shown in Table 8-2.

Table 8-2: Wetland model set-up parameters

Model set-up parameters	Barragup	Scott Road	Elliot Road	Lakes Road	Phillips Road
Grid size (m)	50	30	40	40	30
Number of internal cells	5466	8254	4960	8593	7319
Number of boundary cells	317	377	287	368	288
Number cells in X direction	104	148	81	115	118
Number cells in Y direction	99	100	64	96	109
Area (km ²)	14.46	7.77	8.31	14.35	6.84

The calibration period for each of the wetland models was from 2000 – 2009 and due to the limited data there was no validation period. The model calibration satisfied the criteria of the water balance error <0.1% and the iteration residual error <0.1% for all wetland models. The scaled RMS was below 5% for the Lakes Road model. It was recognised that the criteria of 5% was difficult to achieve in all models, as ranges in groundwater head were small for some models due to limited groundwater data. The model calibration error is summarised in Table 8-1.

Table 8-3: Calibration error summary for the wetland models

	Barragup model	Scott Road model	Elliot Road model	Lakes Road model	Phillips Road model
Number of observations	62	250	136	151	62
Average absolute error (m)	0.11	0.32	0.29	0.49	0.37
Average residual error (m)	-0.05	0.19	0.07	0.38	-0.02
Average RMS error (m)	0.15	0.42	0.39	0.66	0.47
Maximum positive error (m)	0.61	1.27	1.26	1.70	1.29
Maximum negative error (m)	-0.24	-0.90	-0.80	-0.57	-0.85
Scaled RMS (%)	12.00	7.52	14.44	4.99	7.97

Based on the structural limitations of the model, the errors discussed in the previous section and the quality of the calibration, the wetland models are considered suitable for predicting changes in wetland water levels and for predicting wetland water regimes for various climate and land-use change scenarios; however, errors in the calibration need to be considered when interpreting modelling results. To validate modelling results, it is recommended that further measurement of groundwater heads and wetland water levels be undertaken in the wetland modelling regions.

9 References

- Allen, R, Pereria, L, Raes, D & Smith, R 1998, *Crop evapotranspiration – Guidelines for computing crop water requirements – FAO irrigation and drainage paper 56*, Food and Agriculture Organization of the United Nations Rome, 1998
- Bowman Bishaw Gorham 1990, *Summary report Barragup Swamp environmental study*, prepared for the Shire of Murray and the Western Australian Heritage Committee by Bowman Bishaw Gorham, June 1990, 75pp
- 2006, *Nambeelup hydrogeological investigations*, report for the development manager, Clough Property, June 2006
- Commander, DP 1988, *Geology and hydrogeology of the superficial formations and coastal lakes between Harvey and Leschenault inlets (Lake Clifton project)*, Geological Survey of Western Australia, 23, pg 37-50
- Davidson, WA 1984, *A flow-net analysis of the unconfined groundwater in the superficial formations of the southern Perth area, Western Australia*, Geological Survey of Western Australia, record 1984/9
- 1995, *Hydrogeology and groundwater resources of the Perth region, Western Australia*, Geological Survey of Western Australia and the Department of Minerals and Energy, Bulletin 142
- Davidson, WA & Yu, X 2006, Perth regional aquifer modelling system (PRAMS) model development: hydrogeology and groundwater modelling, Department of Water, Western Australia, HG20
- Deeney, AC 1989, *Geology and groundwater resources of the superficial formations between Pinjarra and Bunbury, Perth Basin*, Geological Survey of Western Australia, 26, pg 31-57
- DHI 2005, 'Mike SHE: an integrated hydrological modelling system', documentation and users guide, 375p
- Hall, J, Kretschmer, P, Quinton, B & Marillier, B 2010a, *Murray hydrological studies: surface water, groundwater and environmental water – conceptual model report*, Water Science Technical Series, Report no. 16, Department of Water, Western Australia
- 2010b, *Murray hydrological studies: surface water, groundwater and environmental water – land development, drainage and climate scenario report*, Water Science Technical Series, Report no. 26, Department of Water, Western Australia

- Kelsey, P, Hall, J, Marillier, B, Quinton, B & Shakya, D, in press, Hydrological and nutrient modelling of the Peel-Harvey catchment, Department of Water (in press)
- Middlemis, H 2000, *Murray-Darling Basin Commission groundwater flow modelling guidelines*, Aquaterra Consulting Pty Ltd
- Refsgaard, JC & Knudsen, J 1996, 'Operational validation and intercomparison of different types of hydrological models', *Water Resources Research*, v32(7), p2189-2202.
- Rockwater Pty Ltd 2009, *Pinjarra Refinery: review of groundwater and surface water management for 2008*, report for Alcoa World Alumina Australia, report no. 308.0/09/1
- URS Pty Ltd 2008, Shallow groundwater drilling – Swan Coastal Plain bore completion report (draft), Department of Water, Western Australia
- URS Australia Pty Ltd 2009b, *Peel-Harvey coastal groundwater model WA – model construction and calibration*, prepared for CSIRO
- Xu, C, Canci, M, Martin, M, Donnelly, M & Stokes, R 2009, Perth regional aquifer modelling system (PRAMS) model development: application of the vertical flux model, Hydrogeological record series, Report no. 27, Department of Water, Western Australia
- Yann, J & Smith, K 1994, Simulation of integrated surface water and ground water systems – model formulation, *Water Resources Bulletin*, Vol. 30, No. 5, pp 1-12

Figures

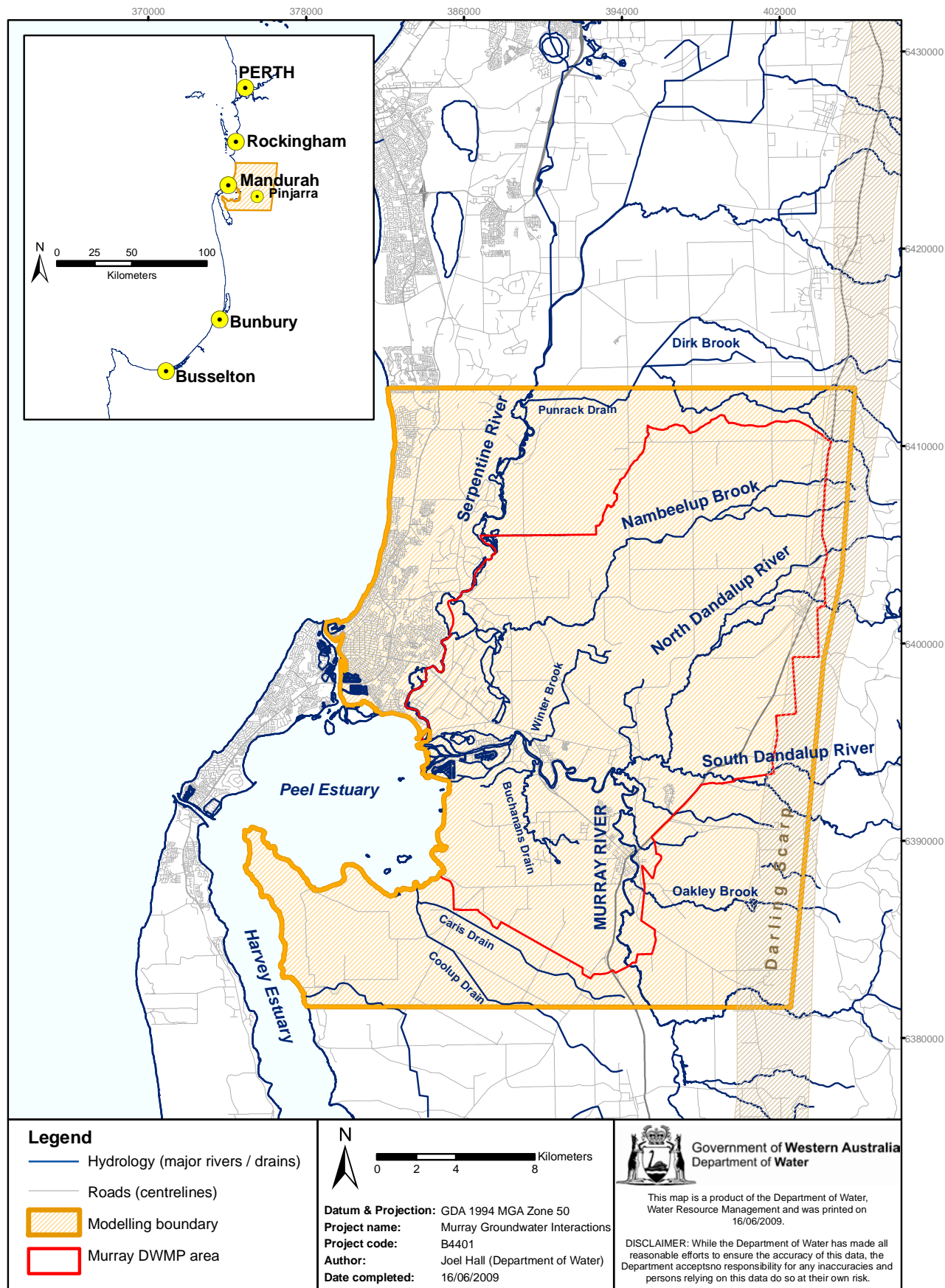


Figure 1-1: Murray study area boundary and Murray DWMP boundary

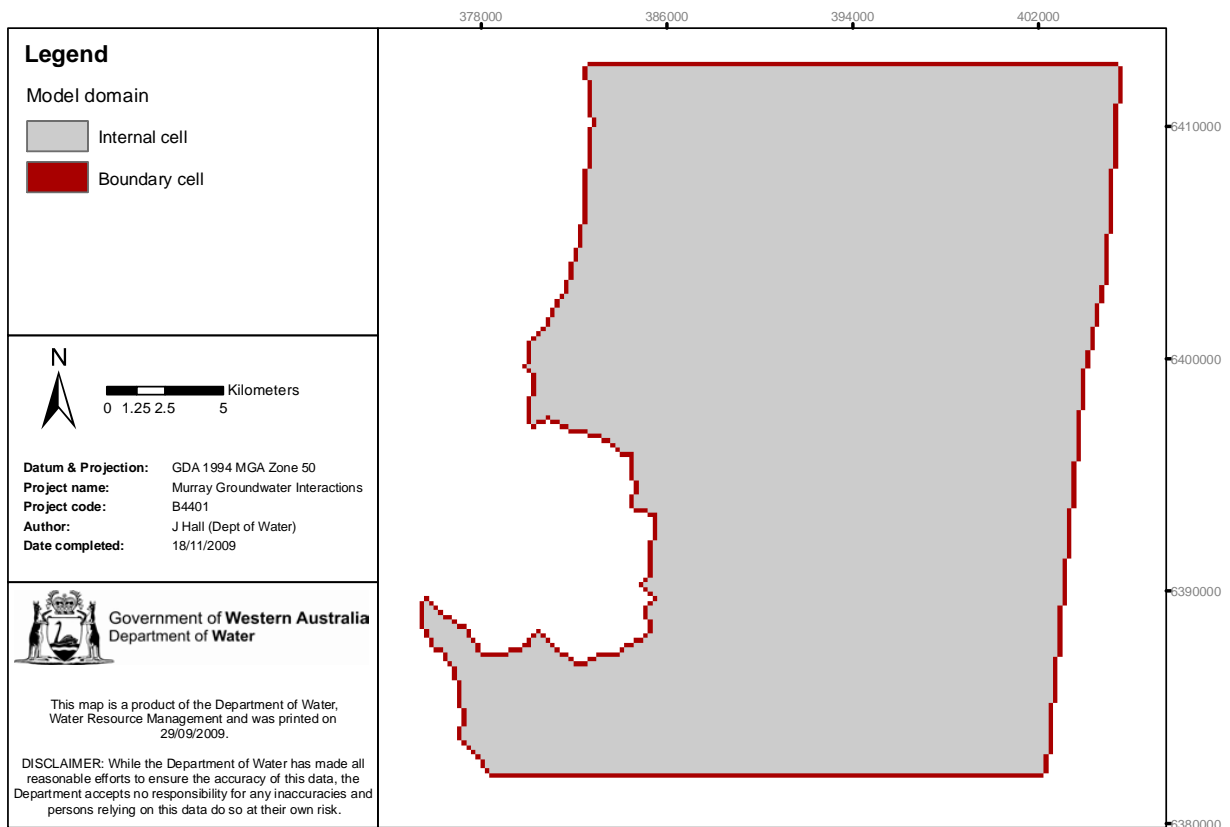


Figure 3-1: Murray modelling domain and boundary cells

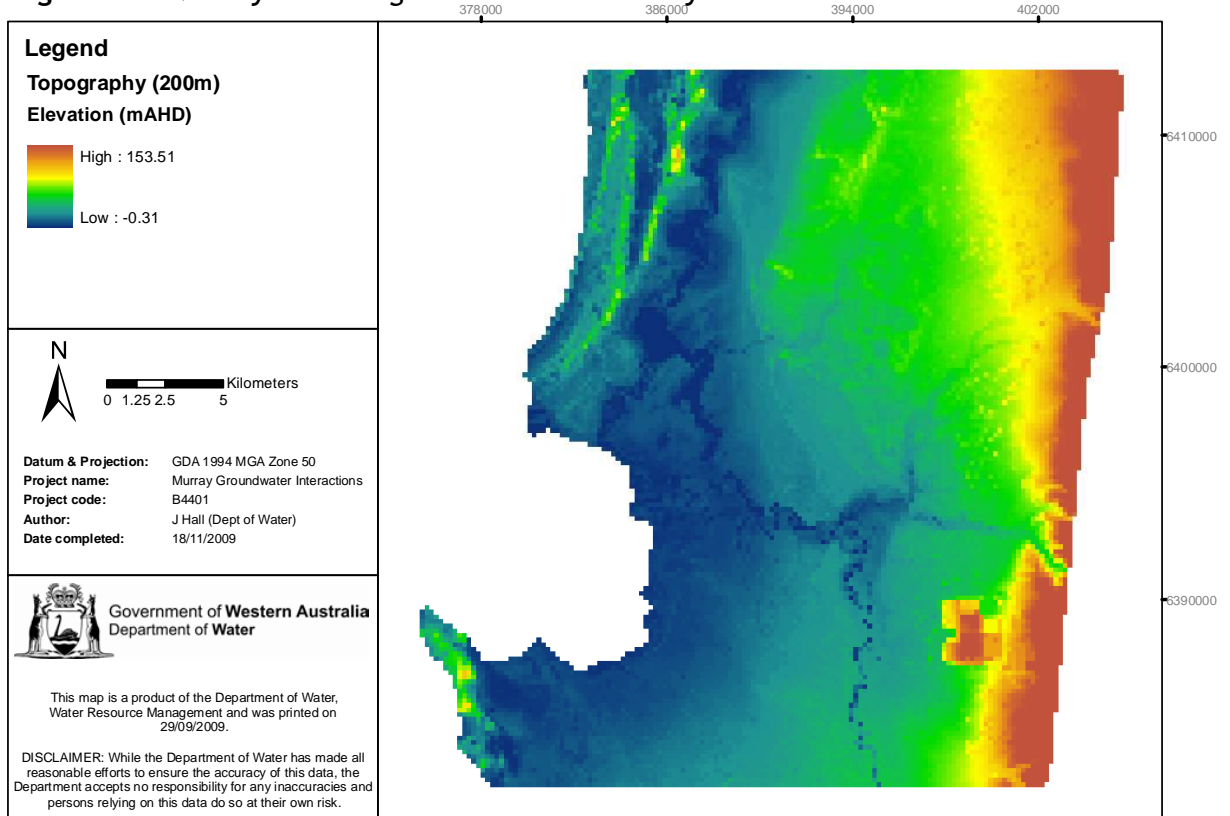


Figure 3-2: Surface topography for the Murray regional model at 200 m grid size

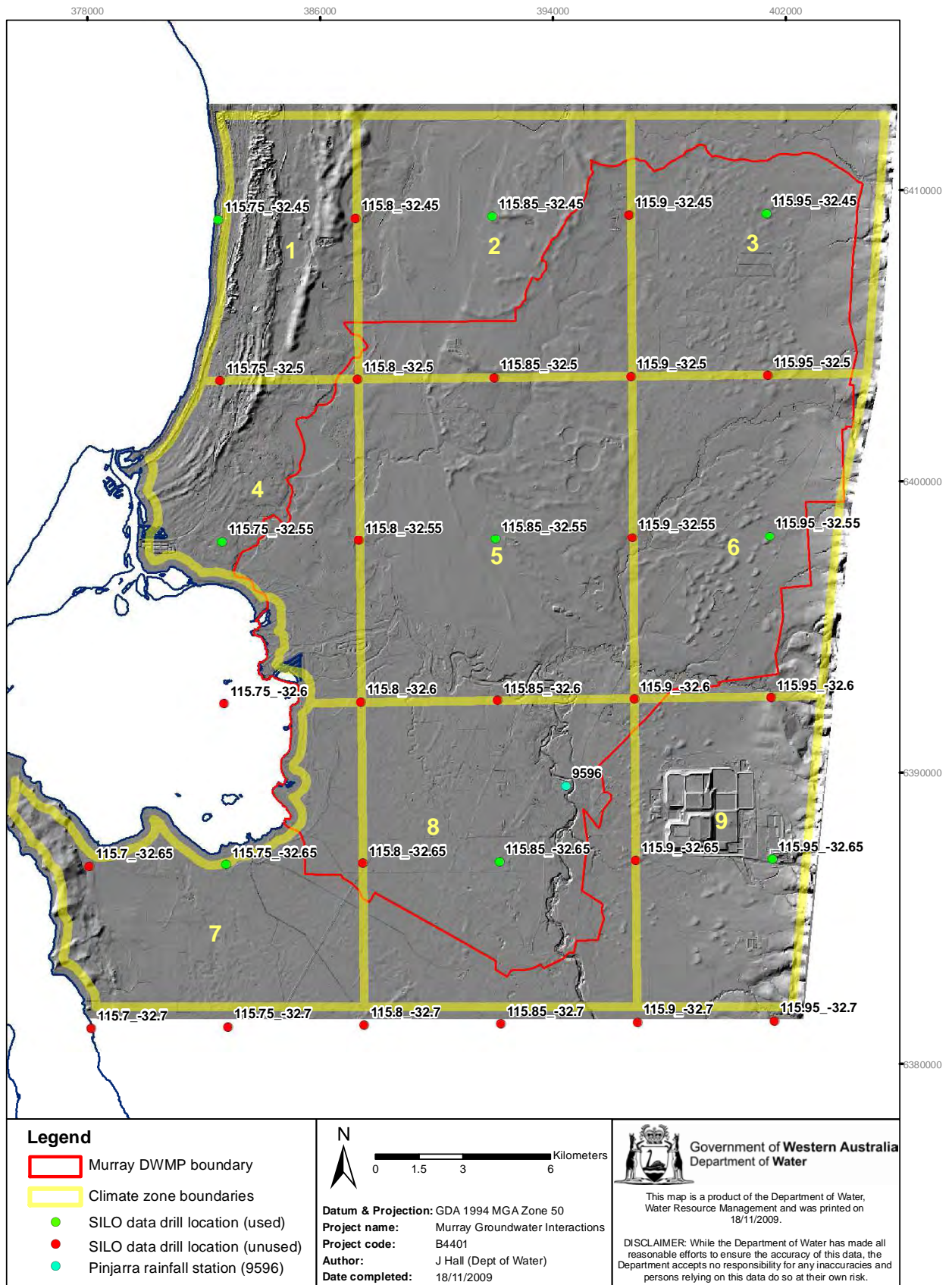


Figure 3-3: SILO rainfall locations and climate zones for the Murray regional model

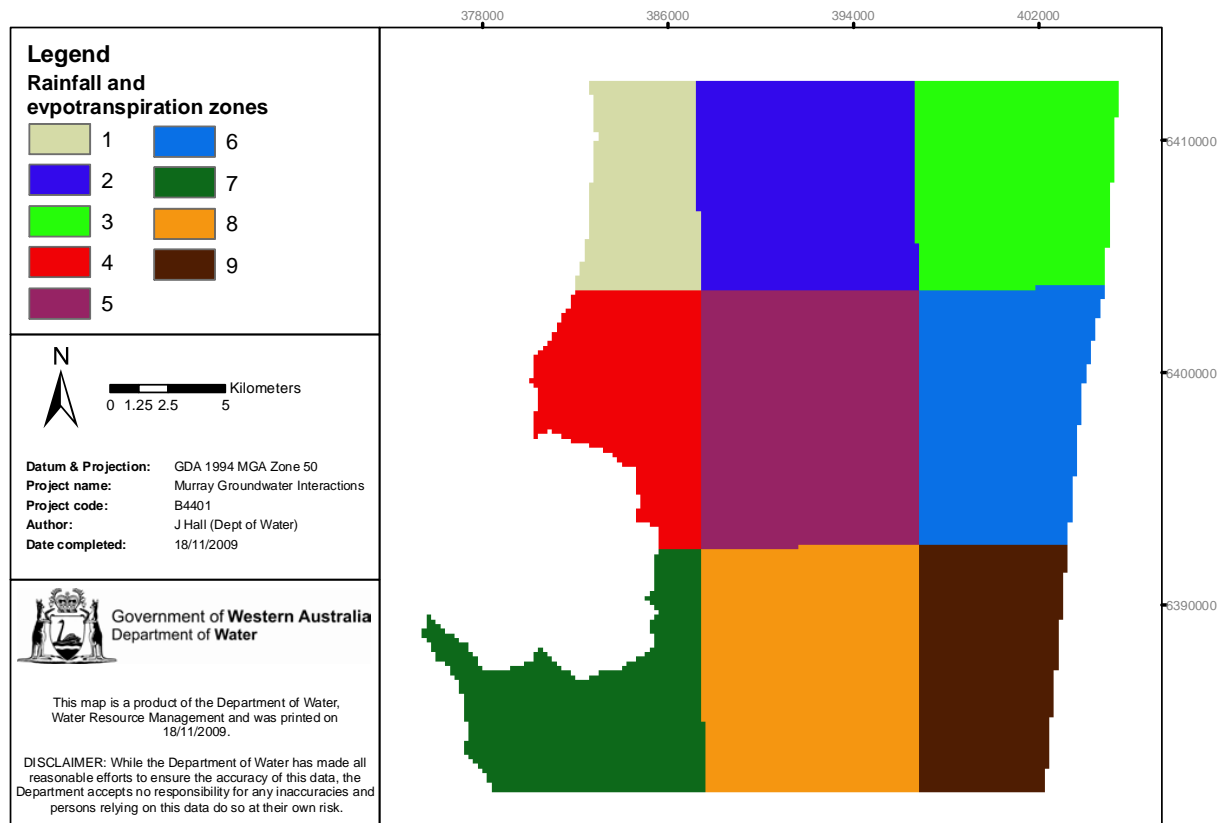


Figure 3-4: Climate zones (evapotranspiration and rainfall) for the Murray regional model

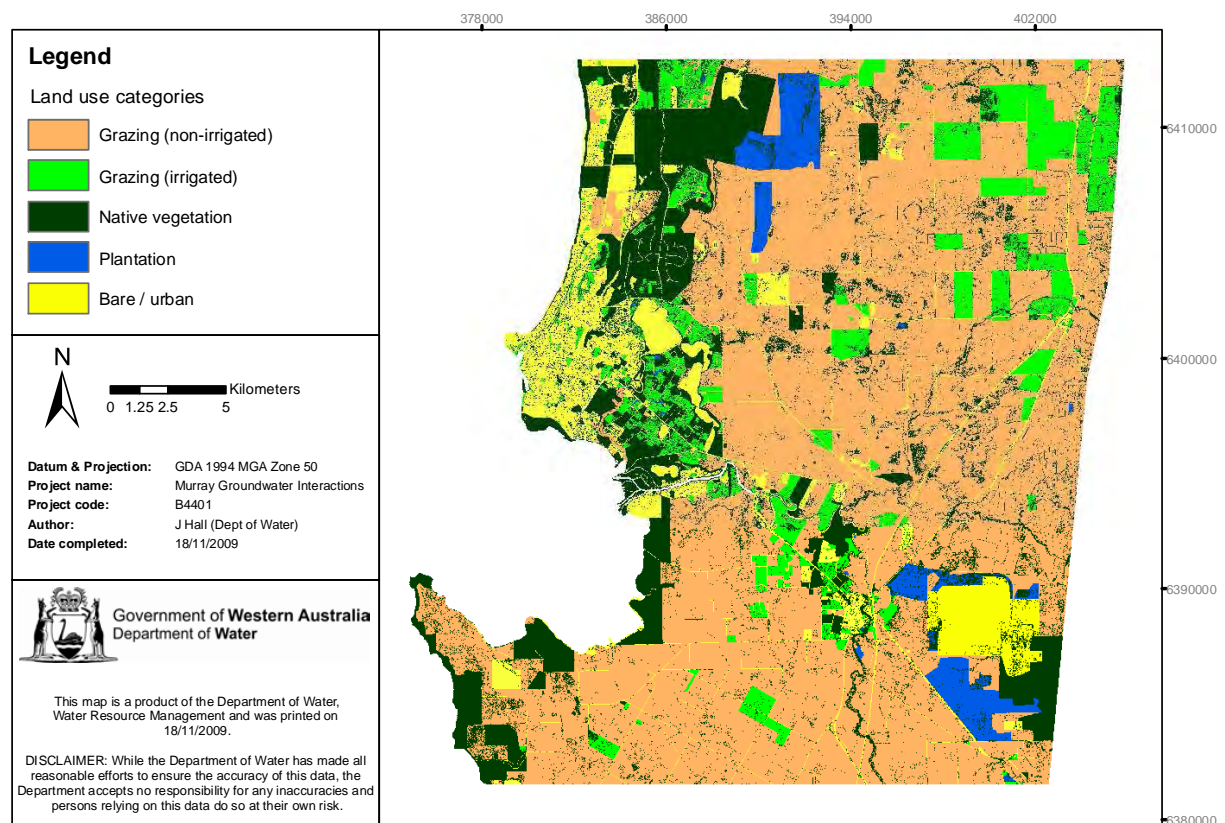


Figure 3-8: Land-use categories for the Murray regional model

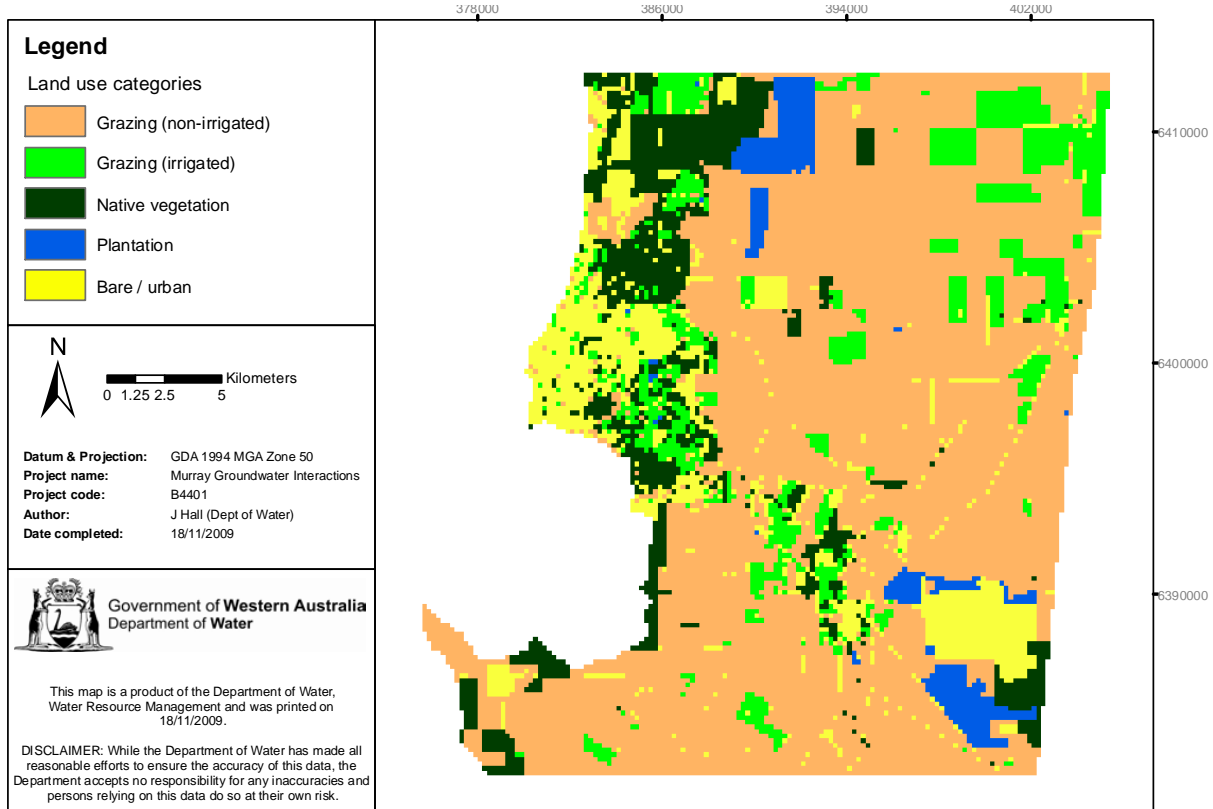


Figure 3-9: Land-use categories re-sampled for the 200m model grid

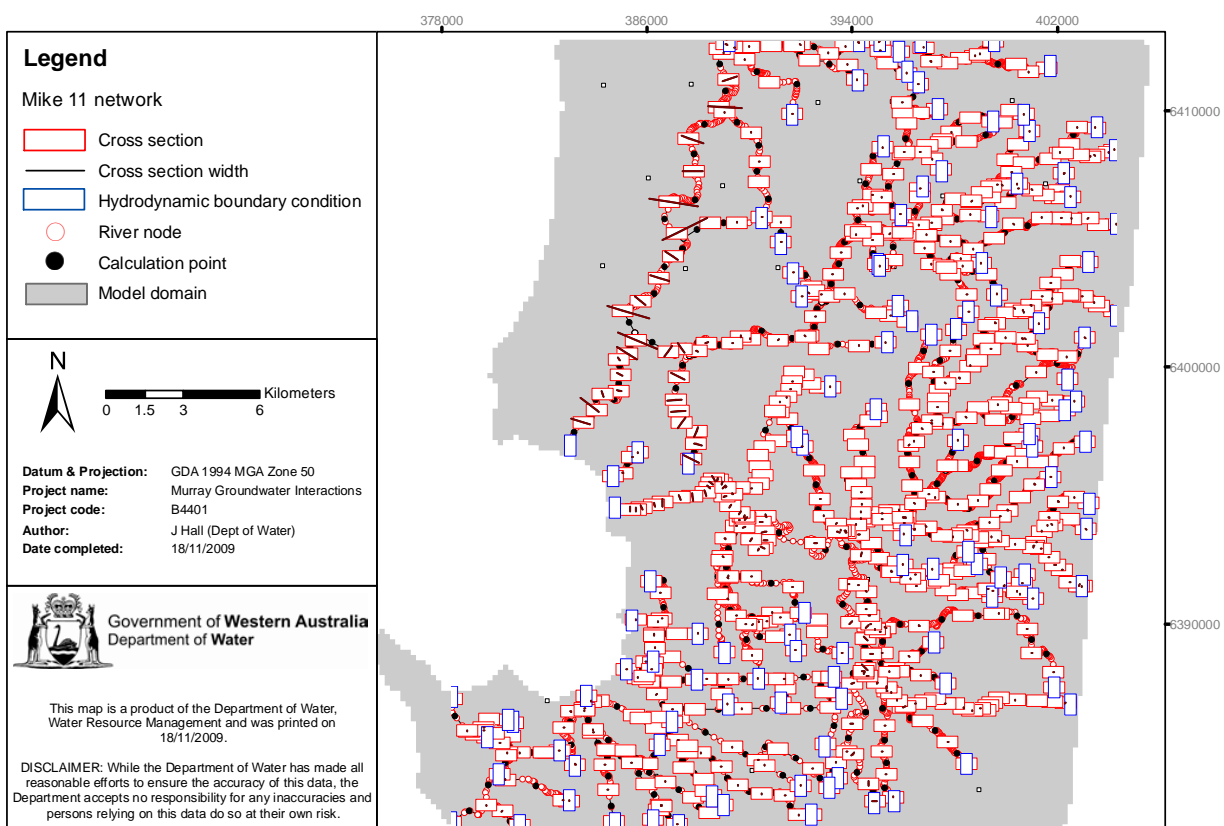


Figure 3-11: Mike 11 channel nodes, cross sections and boundary locations

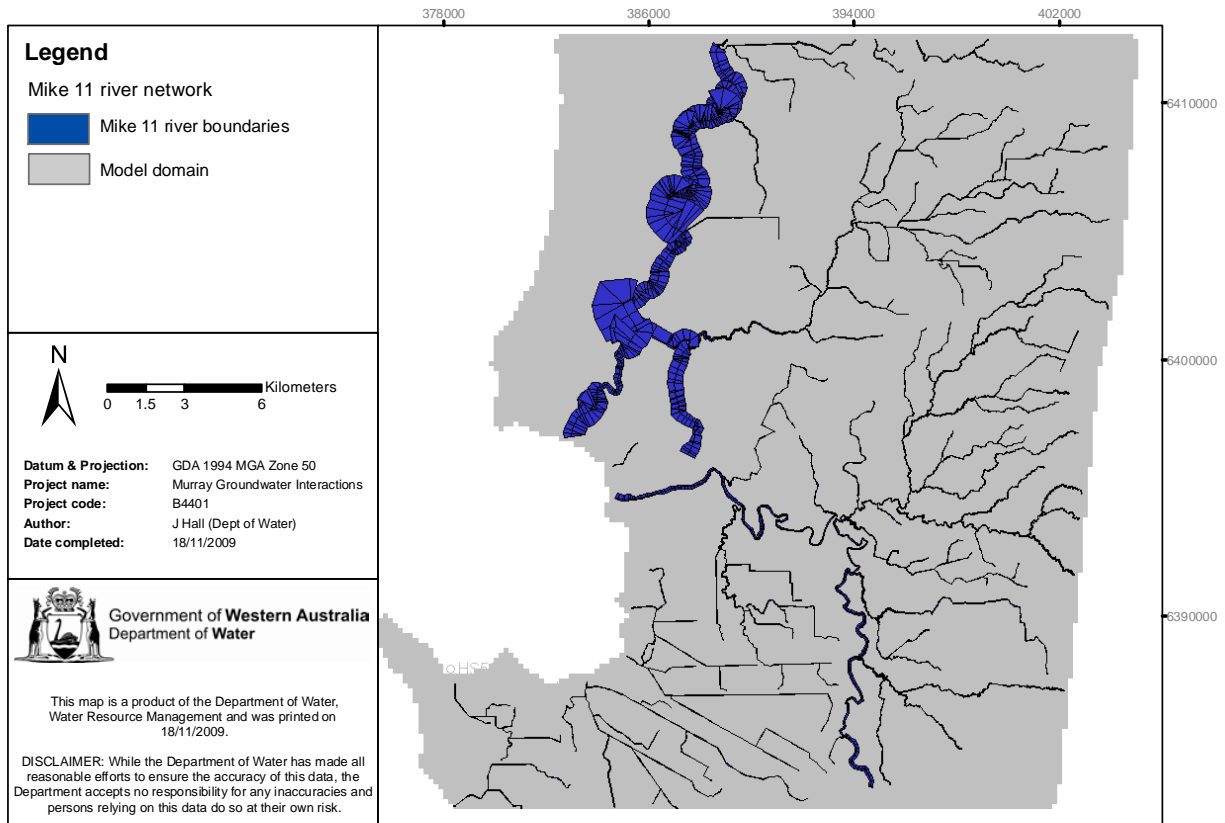


Figure 3-12: Mike 11 channel network

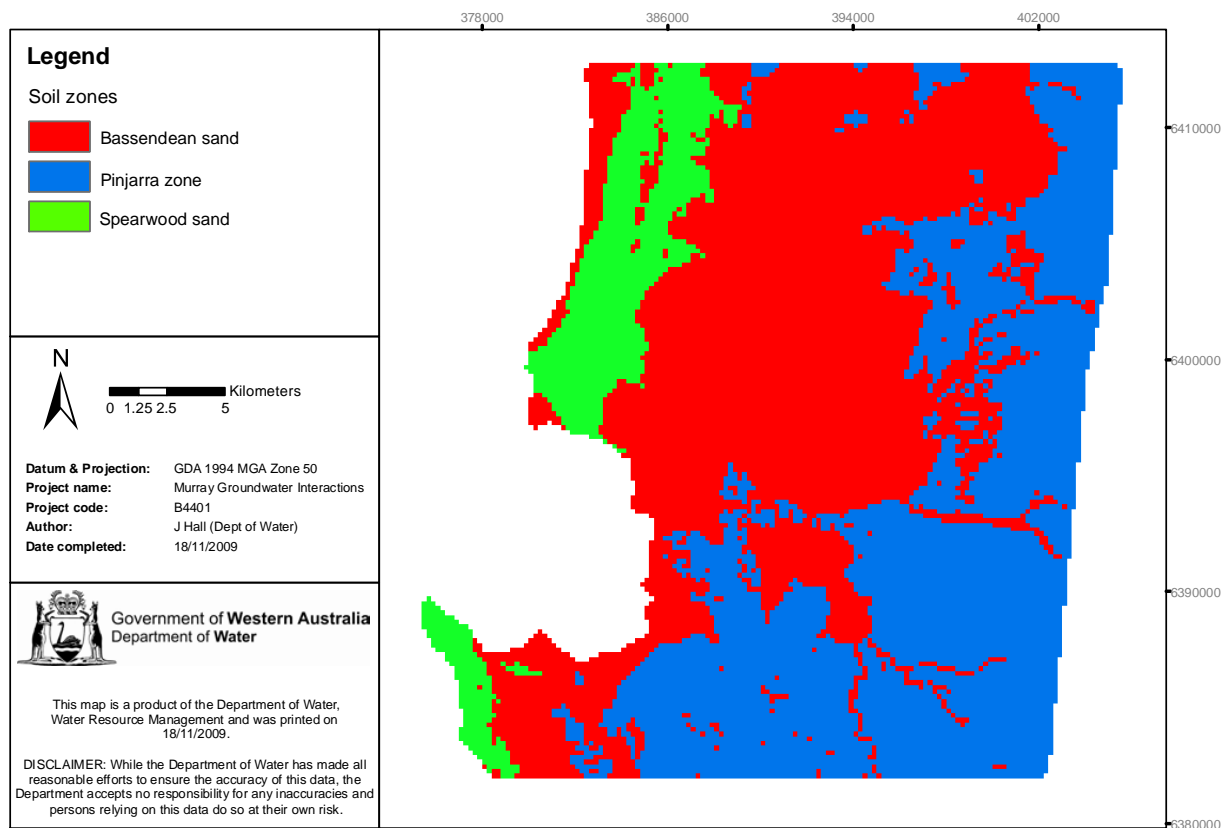


Figure 3-13: Soil zones for the unsaturated zone model in the Murray regional model

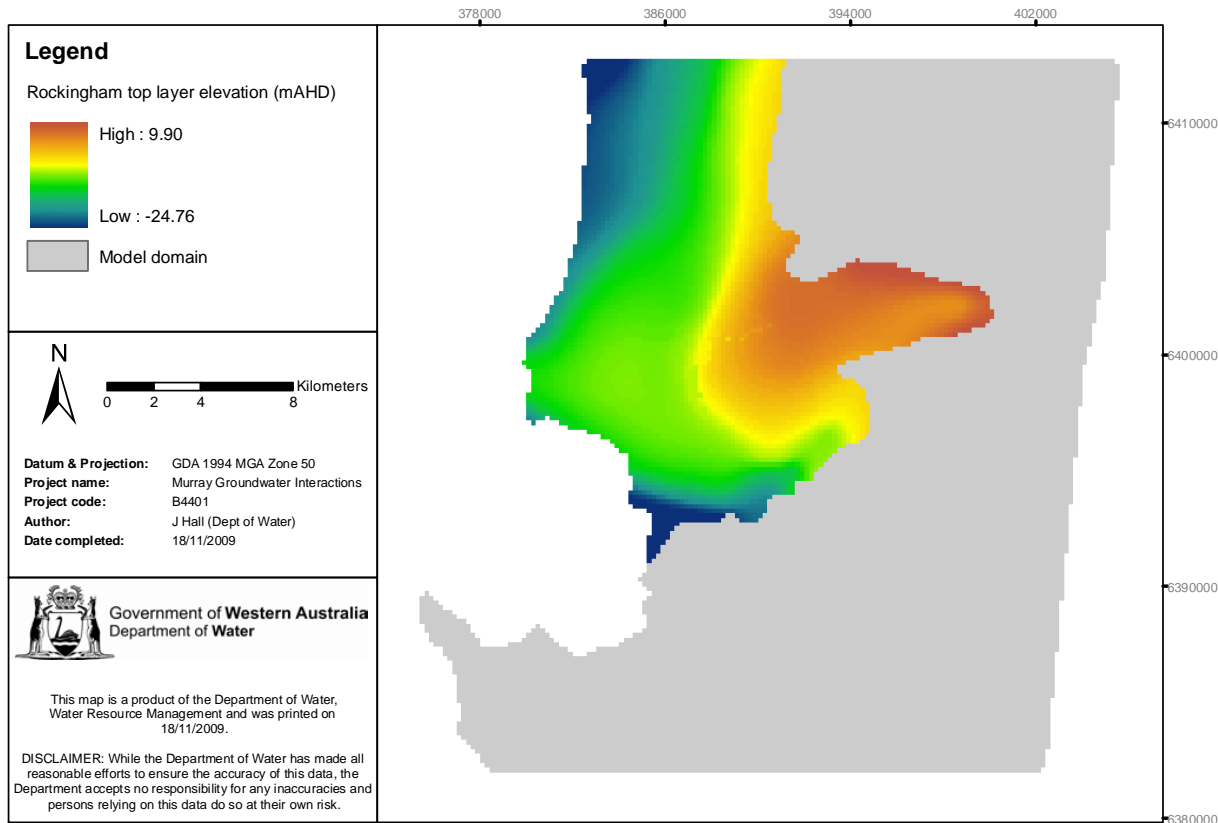


Figure 3-14: Rockingham Sand: top of geological formation (mAHd)

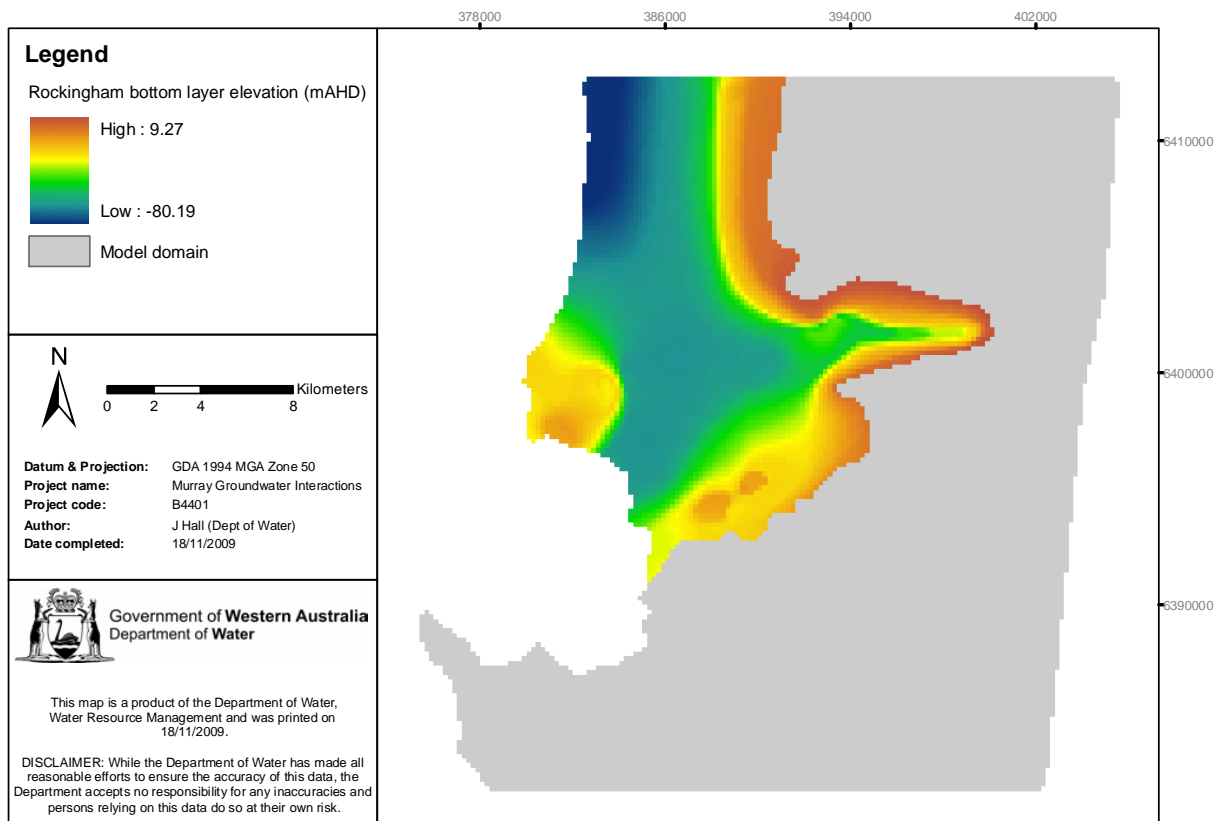


Figure 3-15: Rockingham Sand: base of geological formation (mAHd)

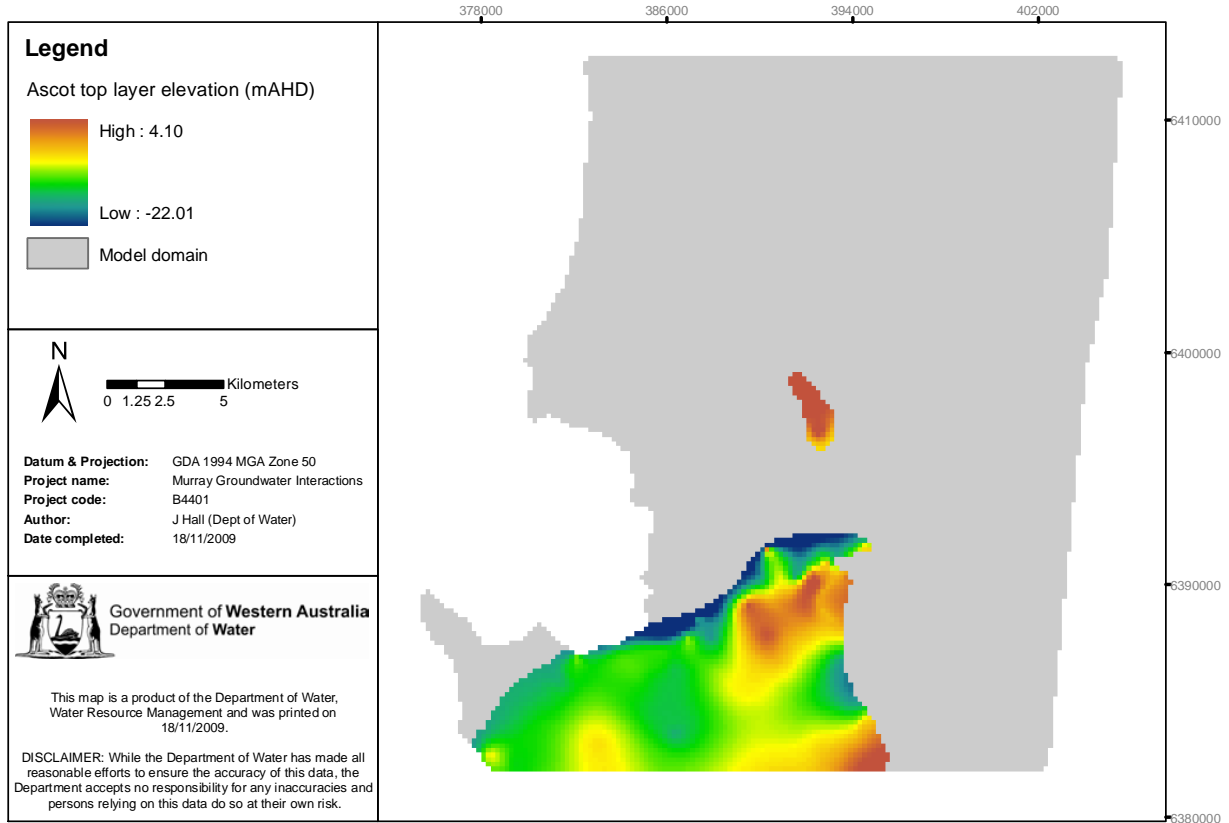


Figure 3-16: Ascot Formation: top of geological formation (mAHD)

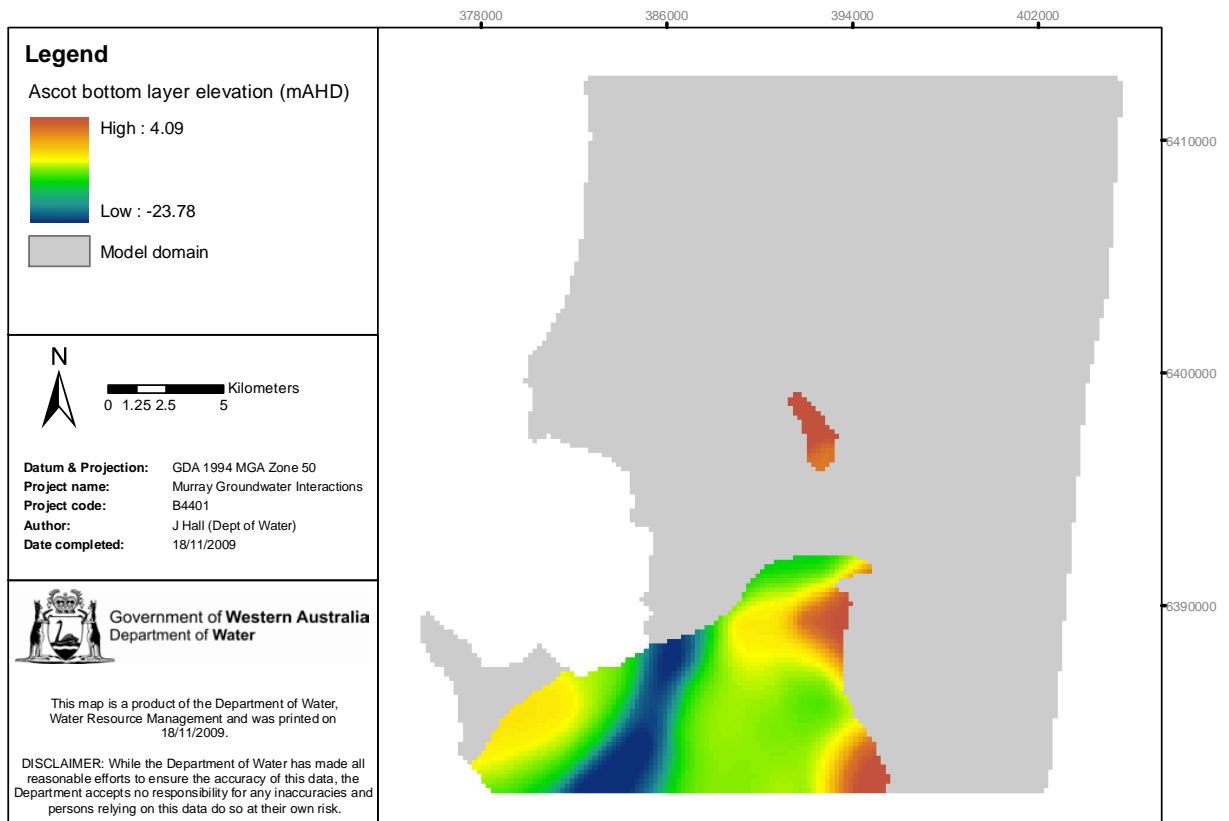


Figure 3-17: Ascot Formation: base of geological formation (mAHD)

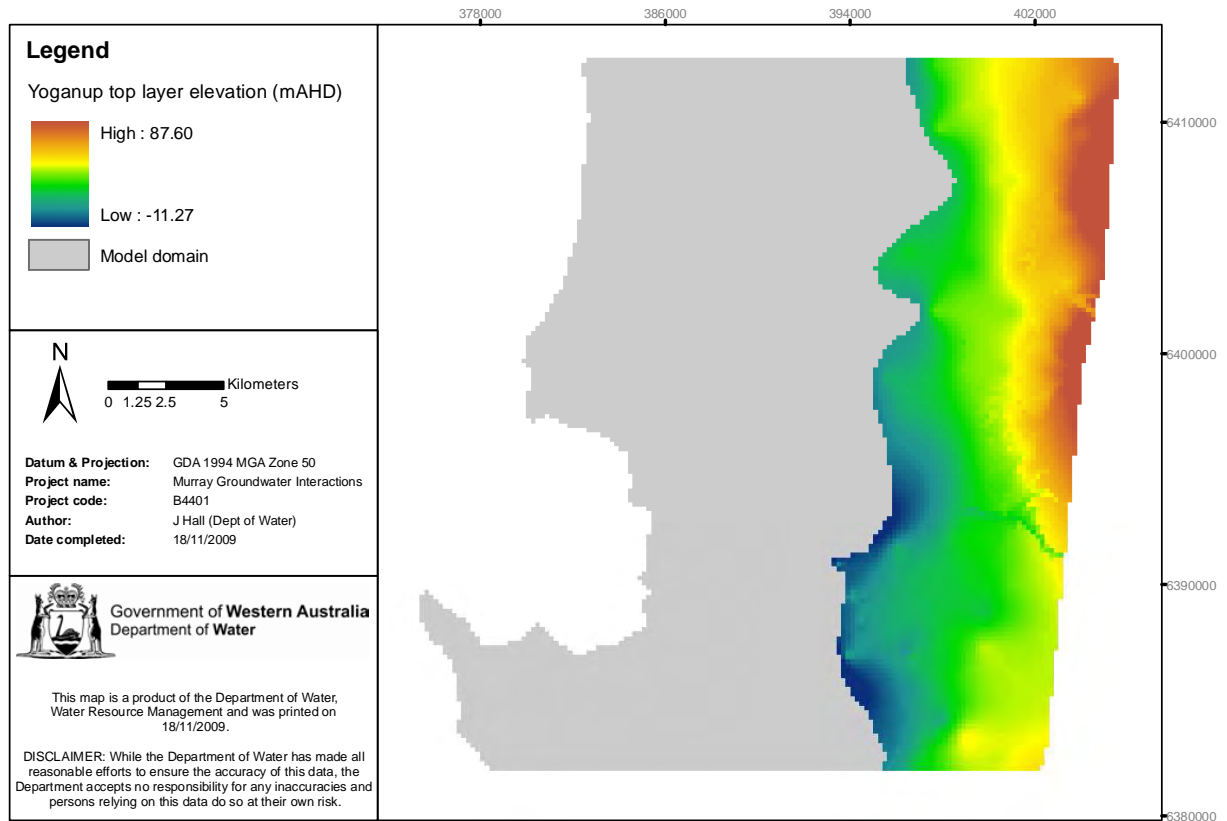


Figure 3-18: Yoganup Formation: top of geological formation (mAHd)

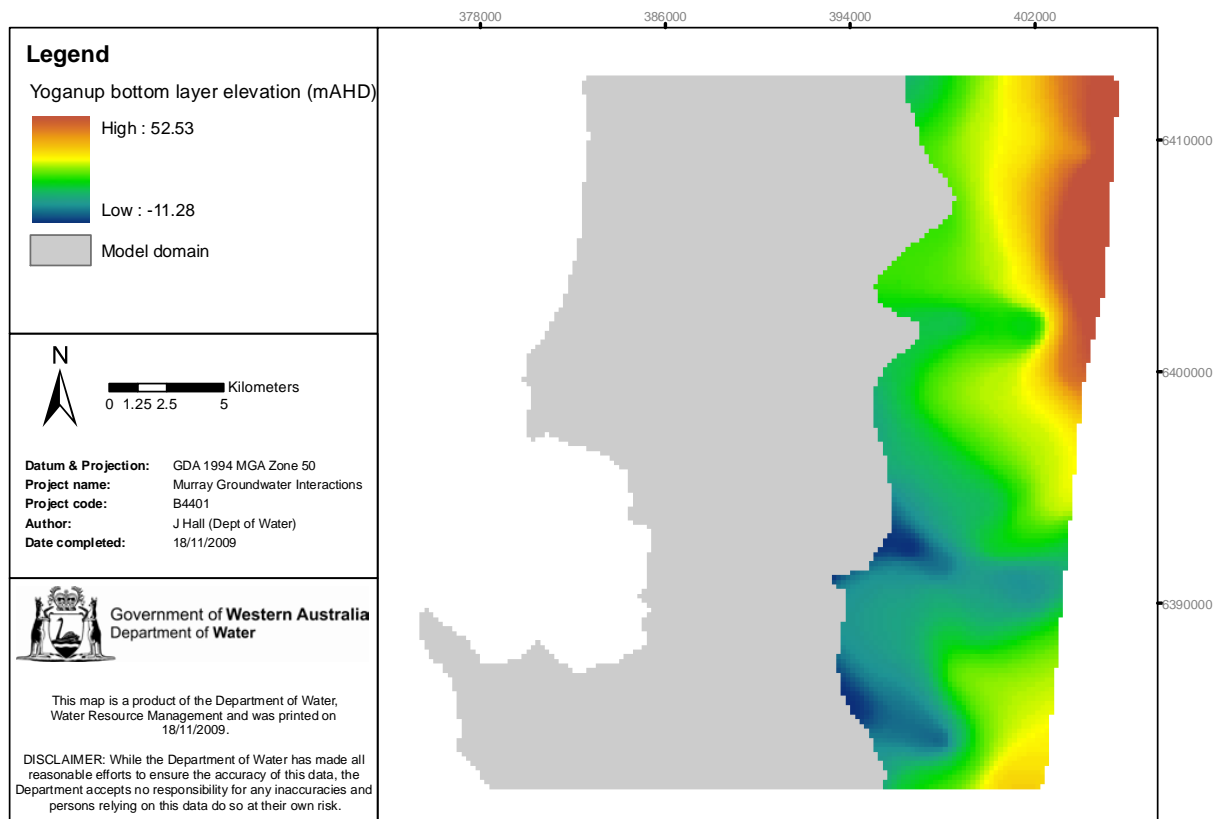


Figure 3-19: Yoganup Formation: base of geological formation (mAHd)

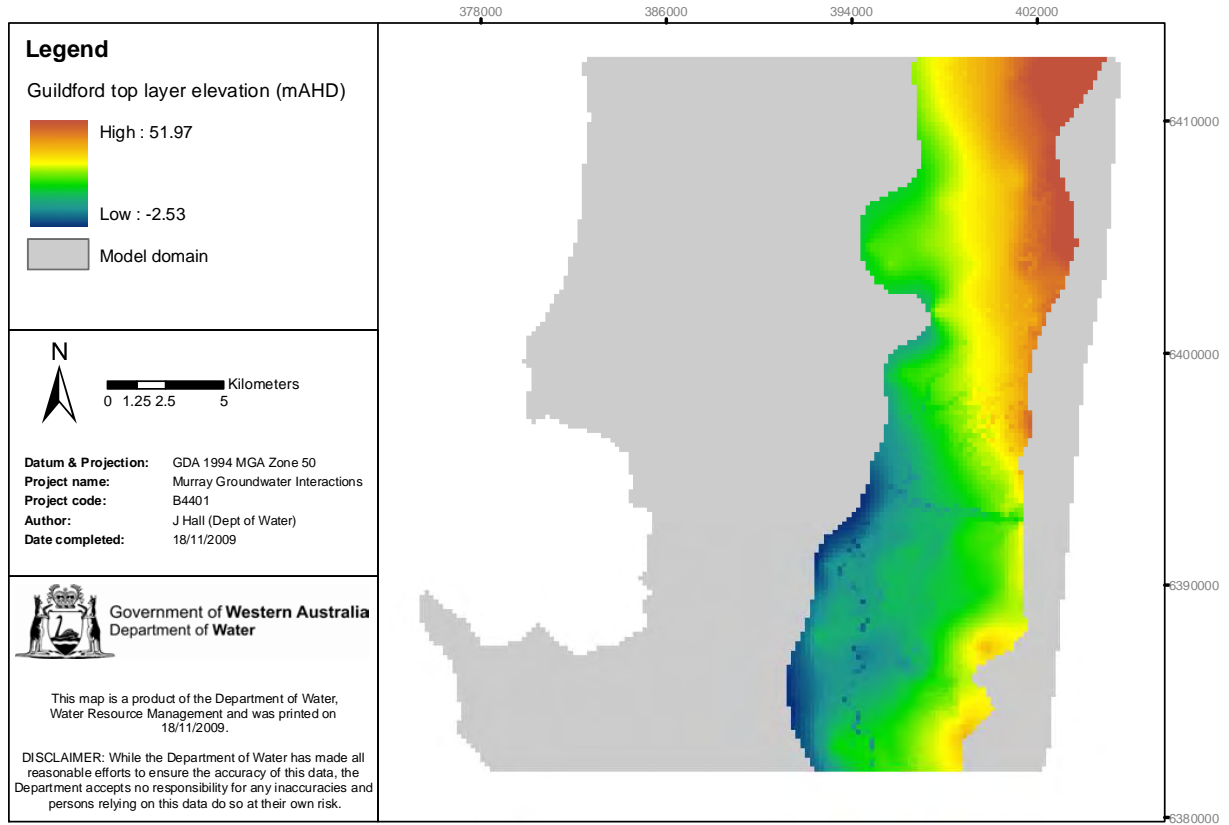


Figure 3-20: Guildford Clay: top of geological formation (mAHd)

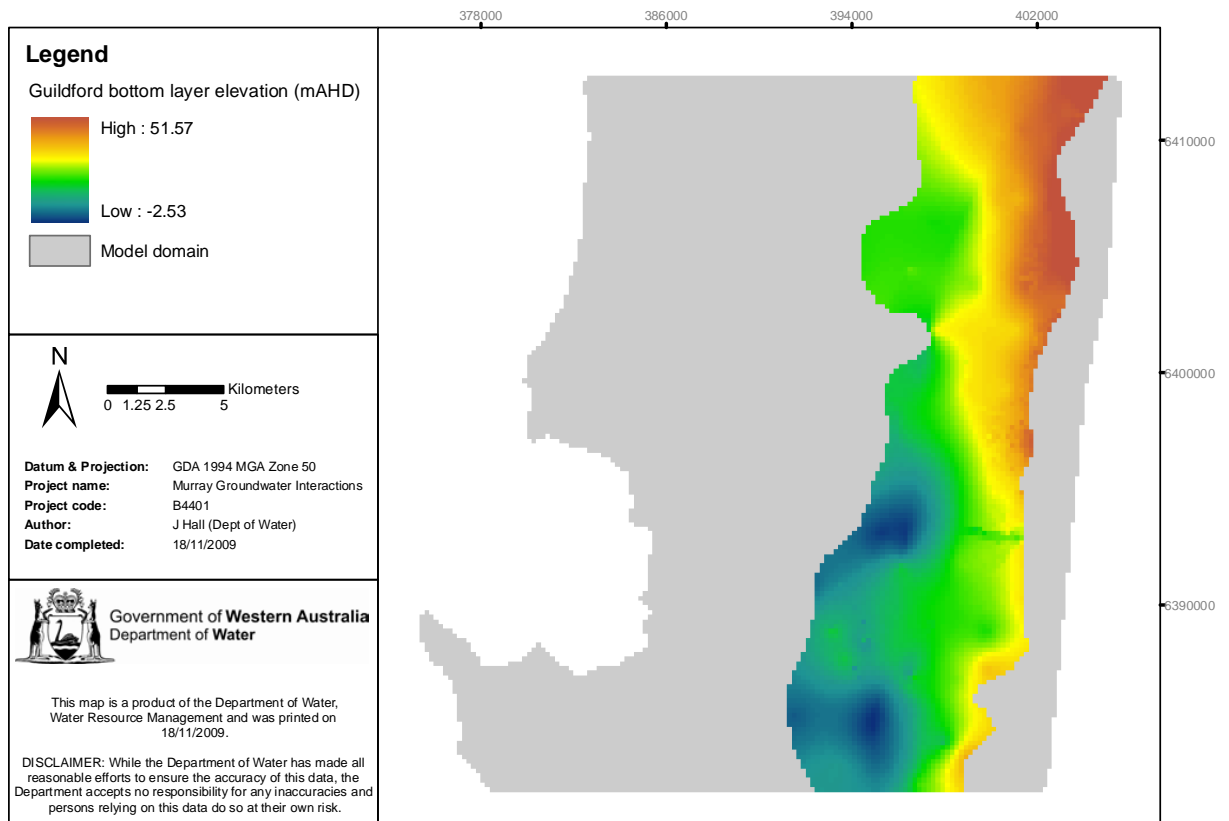


Figure 3-21: Guildford Clay: base of geological formation (mAHd)

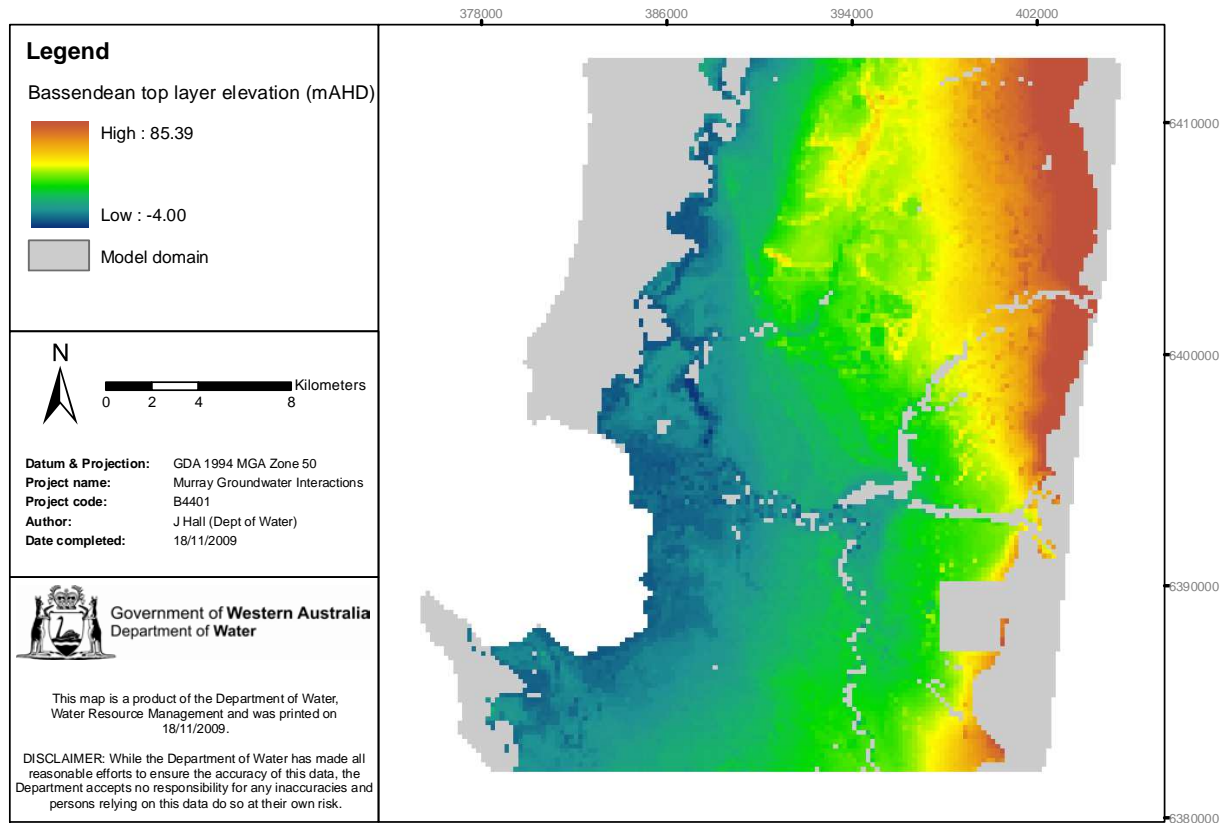


Figure 3-22: Bassendean Sand: top of geological formation (mAHd)

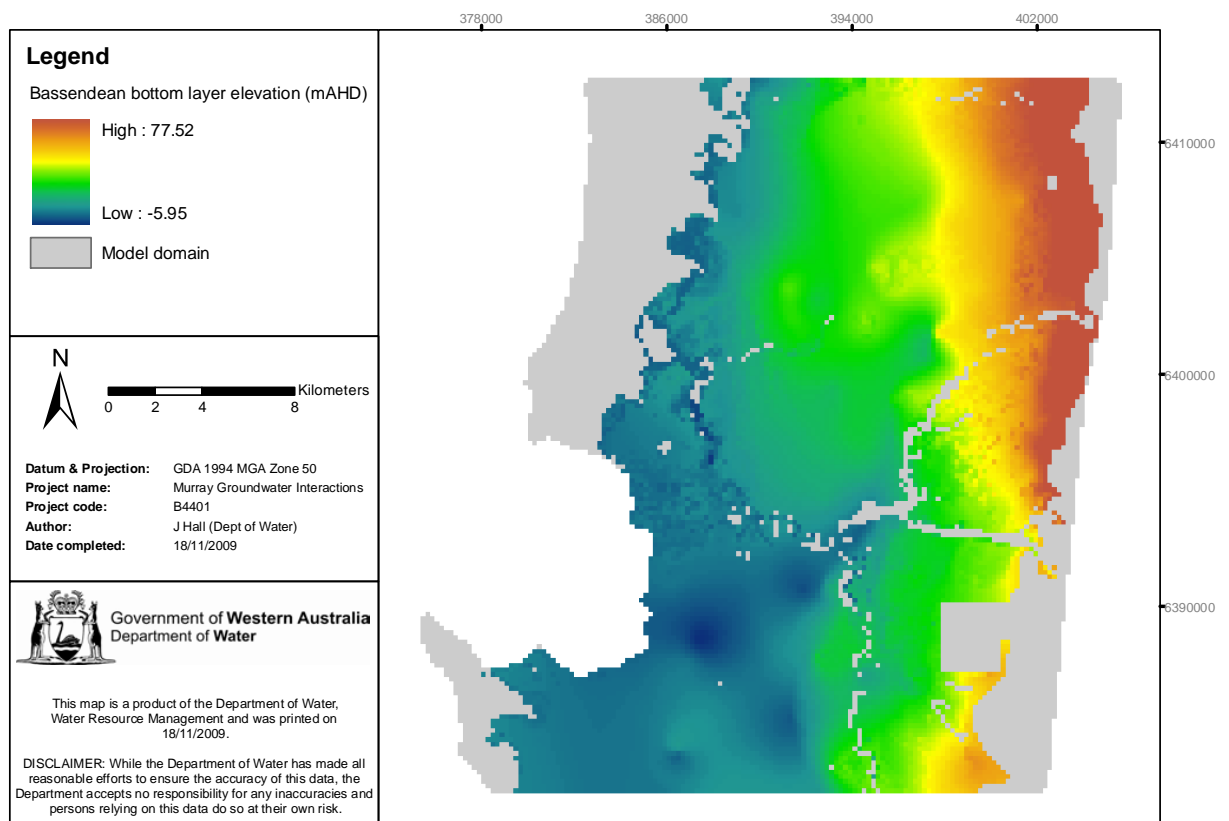


Figure 3-23: Bassendean Sand: base of geological formation (mAHd)

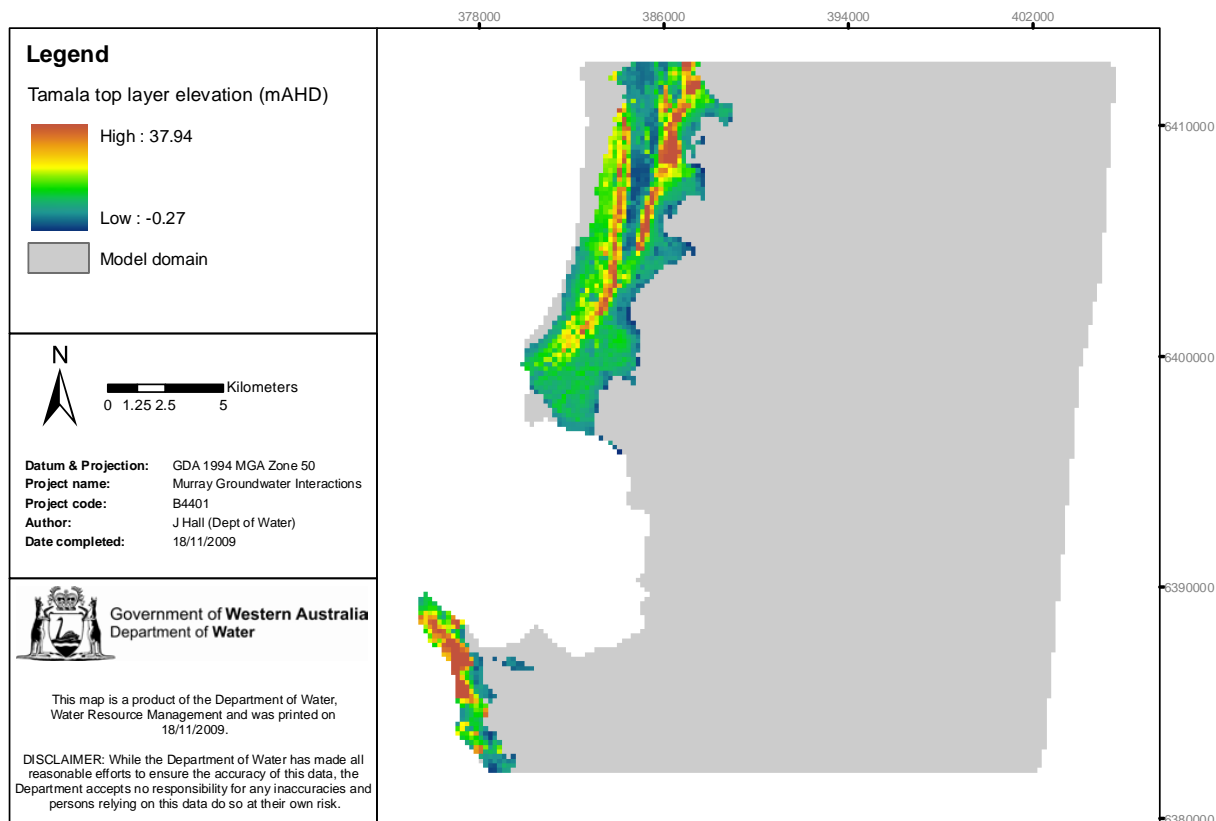


Figure 3-24: Tamala Limestone: top of geological formation (mAHD)

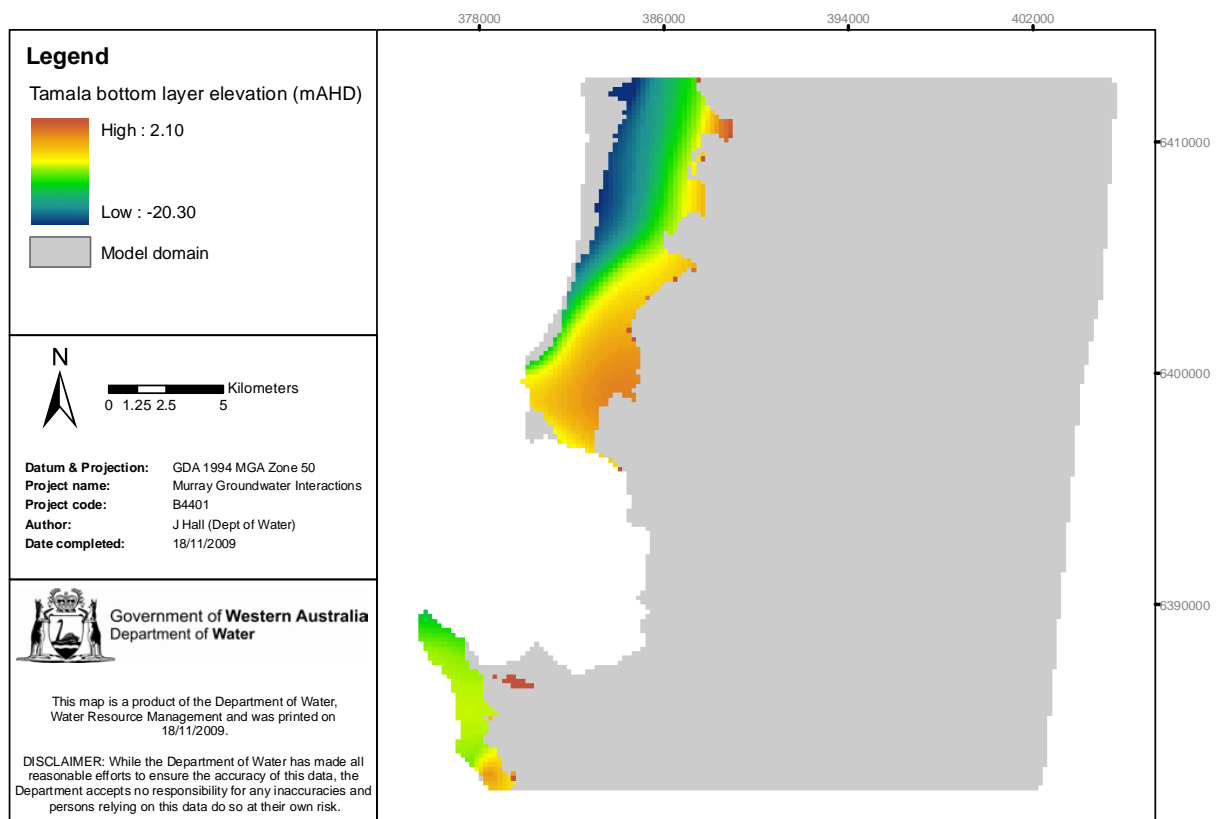


Figure 3-25: Tamala Limestone: base of geological formation (mAHD)

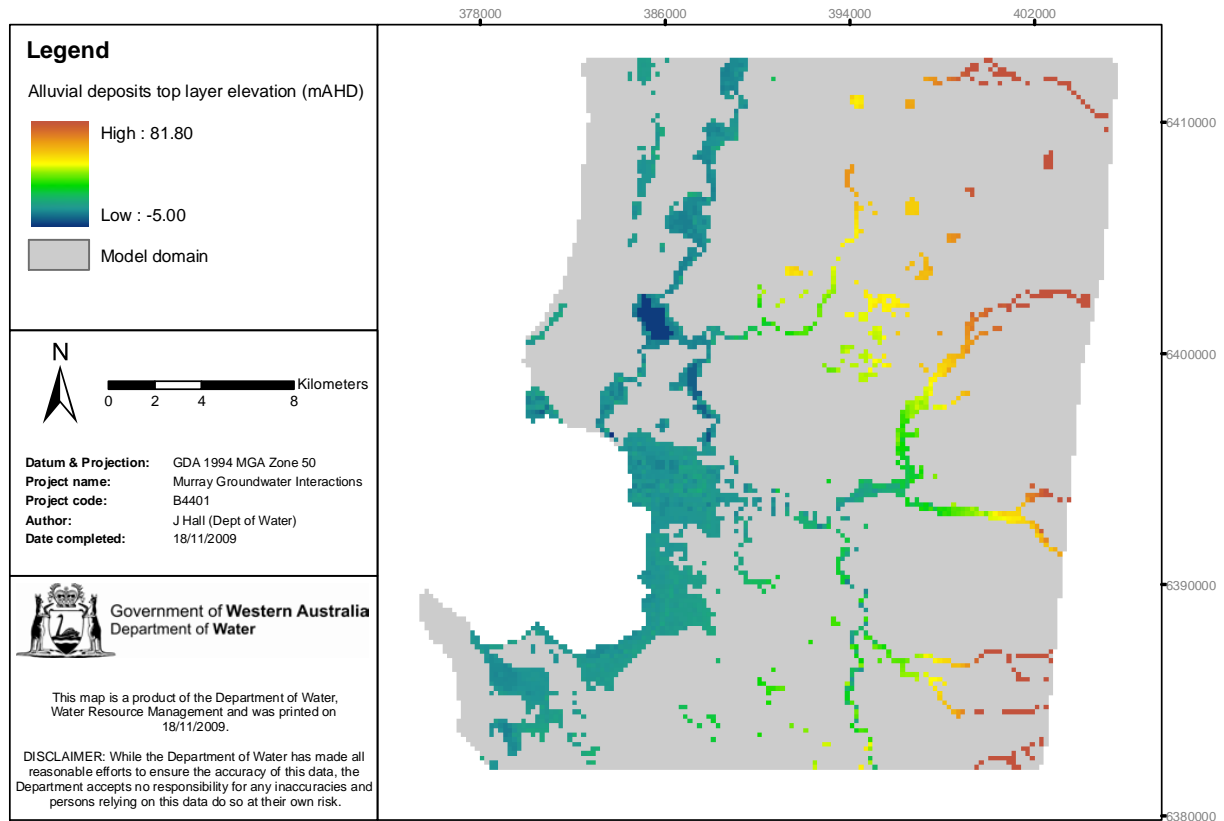


Figure 3-26: Alluvium, estuarine deposits and swamp deposits: top of formation (mAHd)

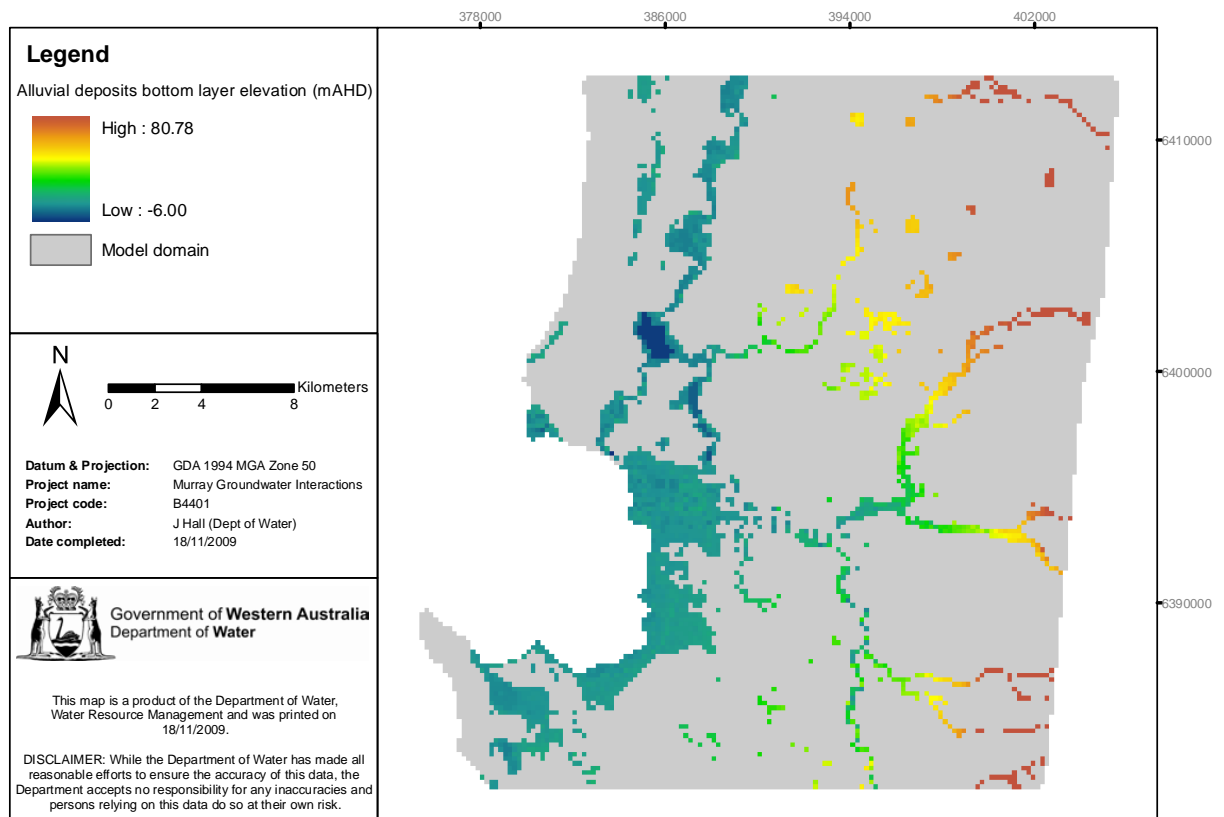


Figure 3-27 Alluvium, estuarine deposits and swamp deposits: base of formation (mAHd)

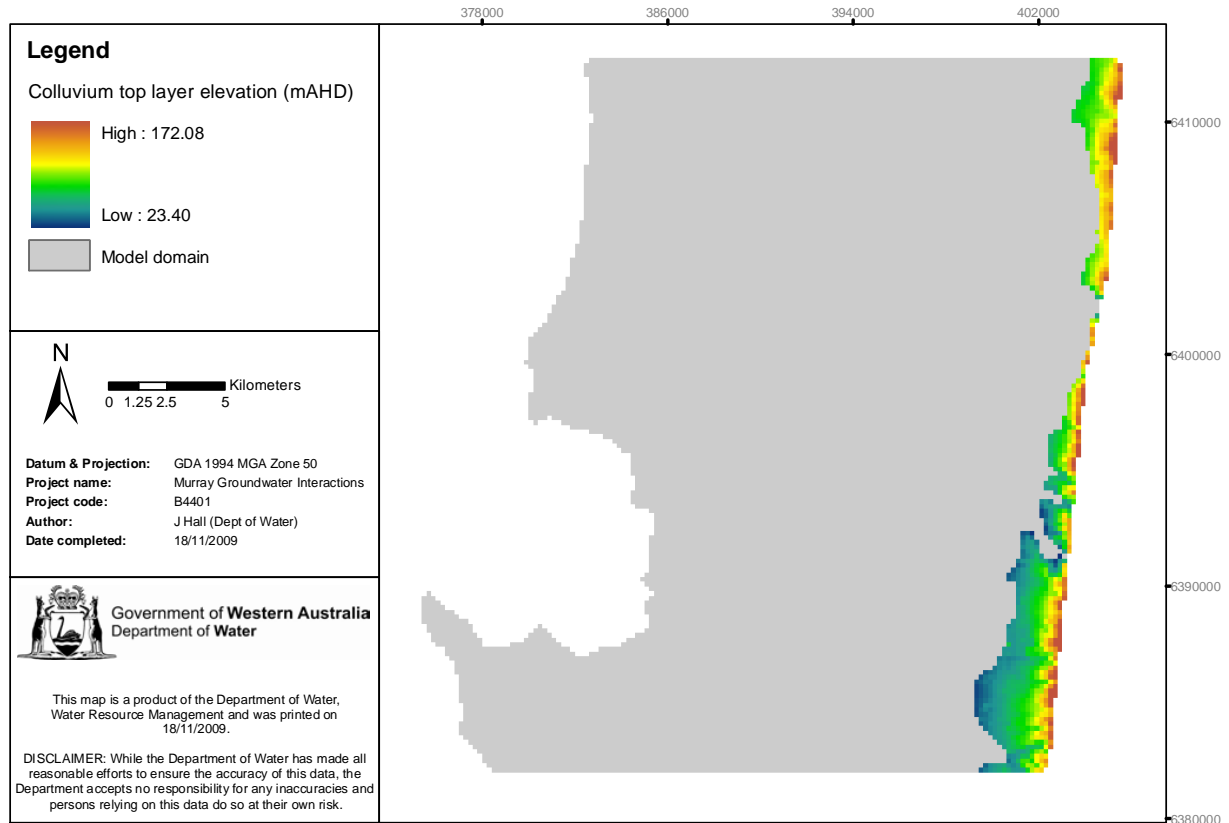


Figure 3-28: Colluvium: top of geological formation (mAHD)

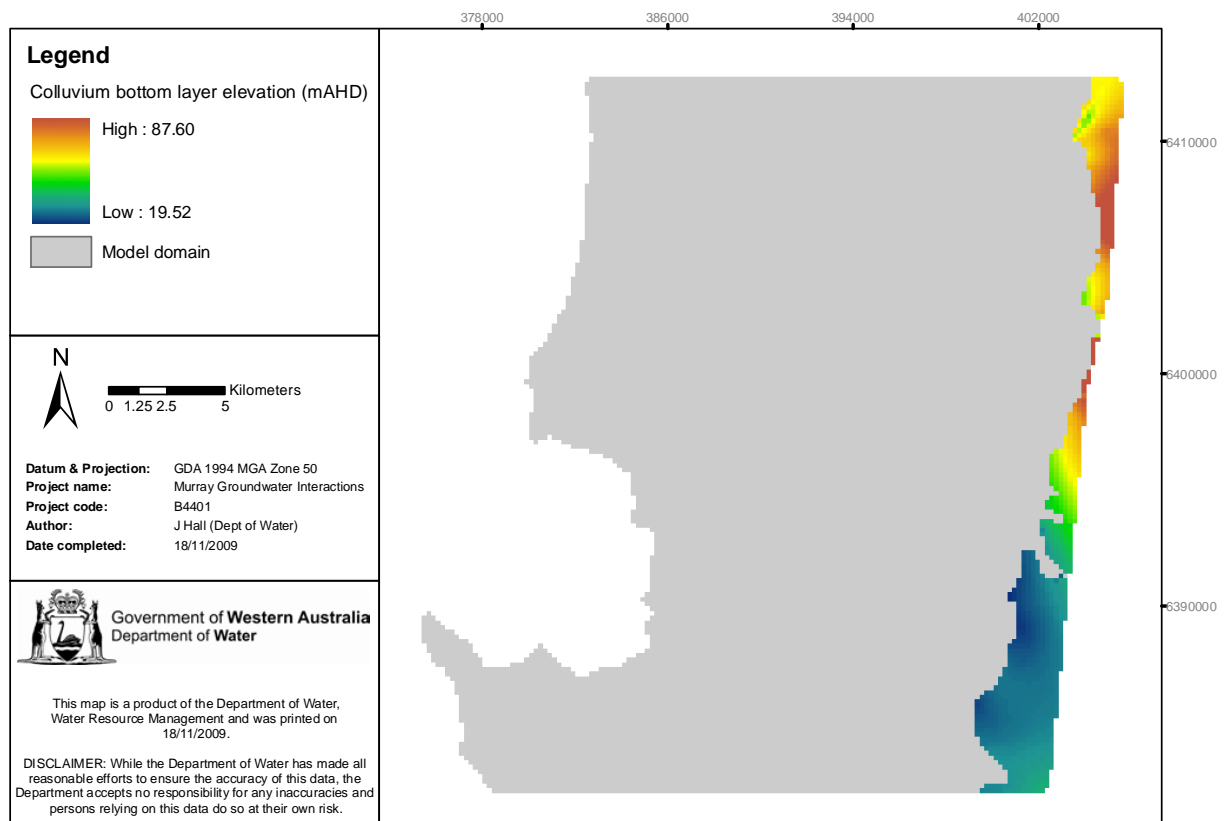


Figure 3-29: Colluvium: base of geological formation (mAHD)

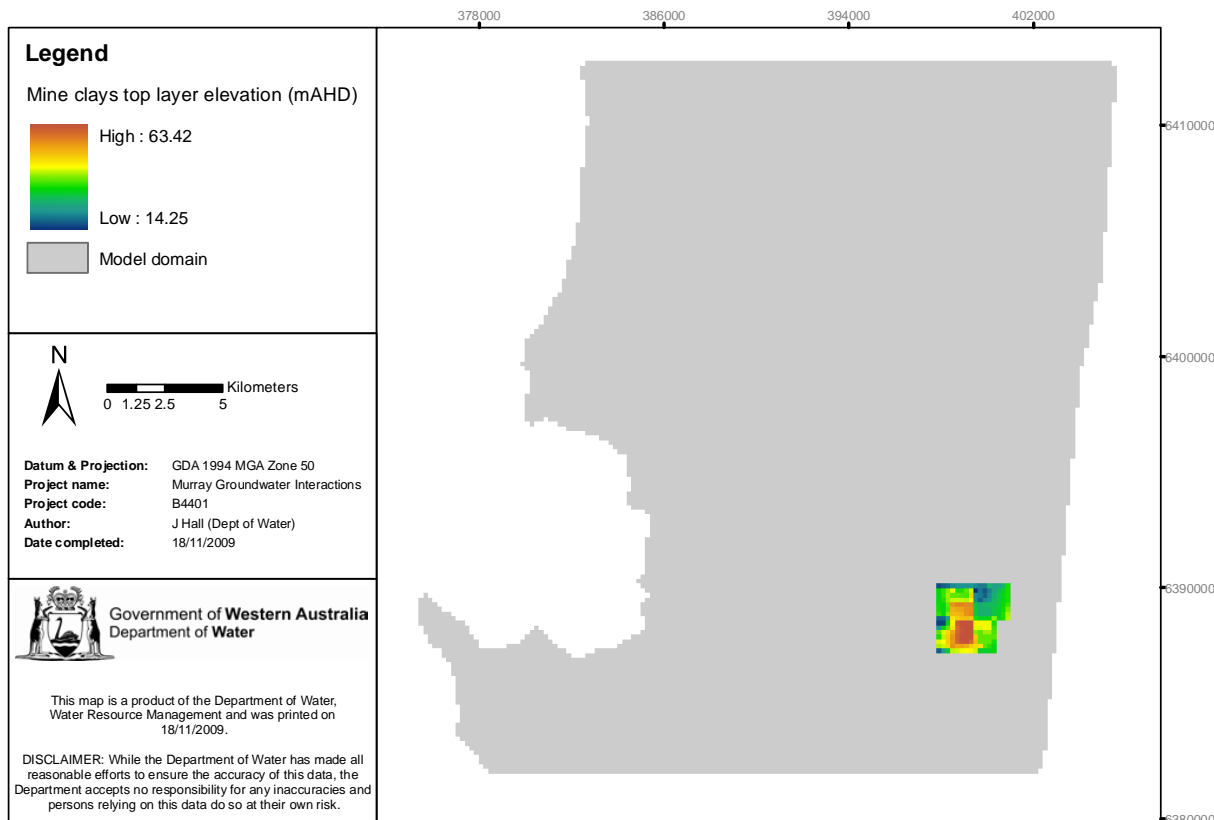


Figure 3-30: Mine clays: top of geological formation (mAHD)

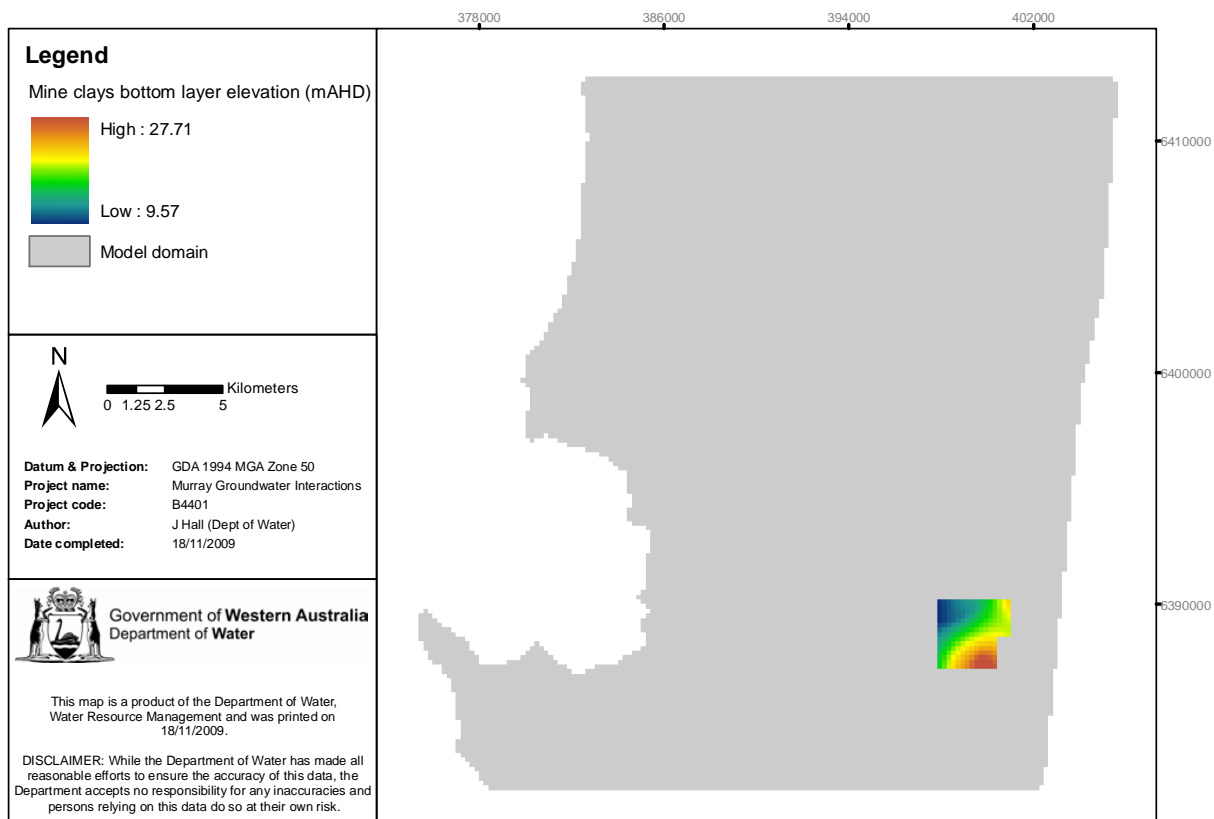


Figure 3-31: Mine clays: base of geological formation (mAHD)

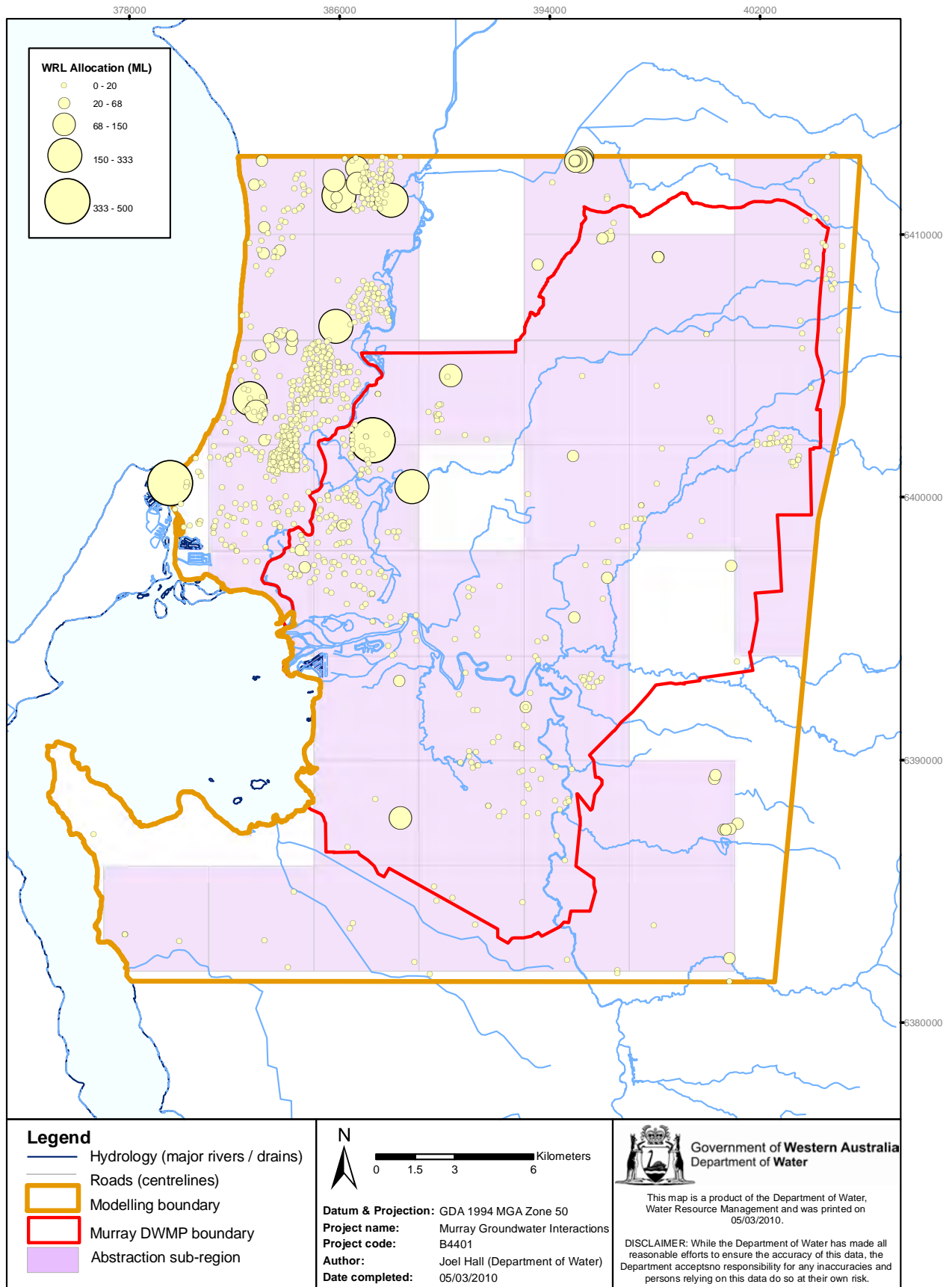


Figure 3-32: Superficial aquifer abstraction bores and sub-regions

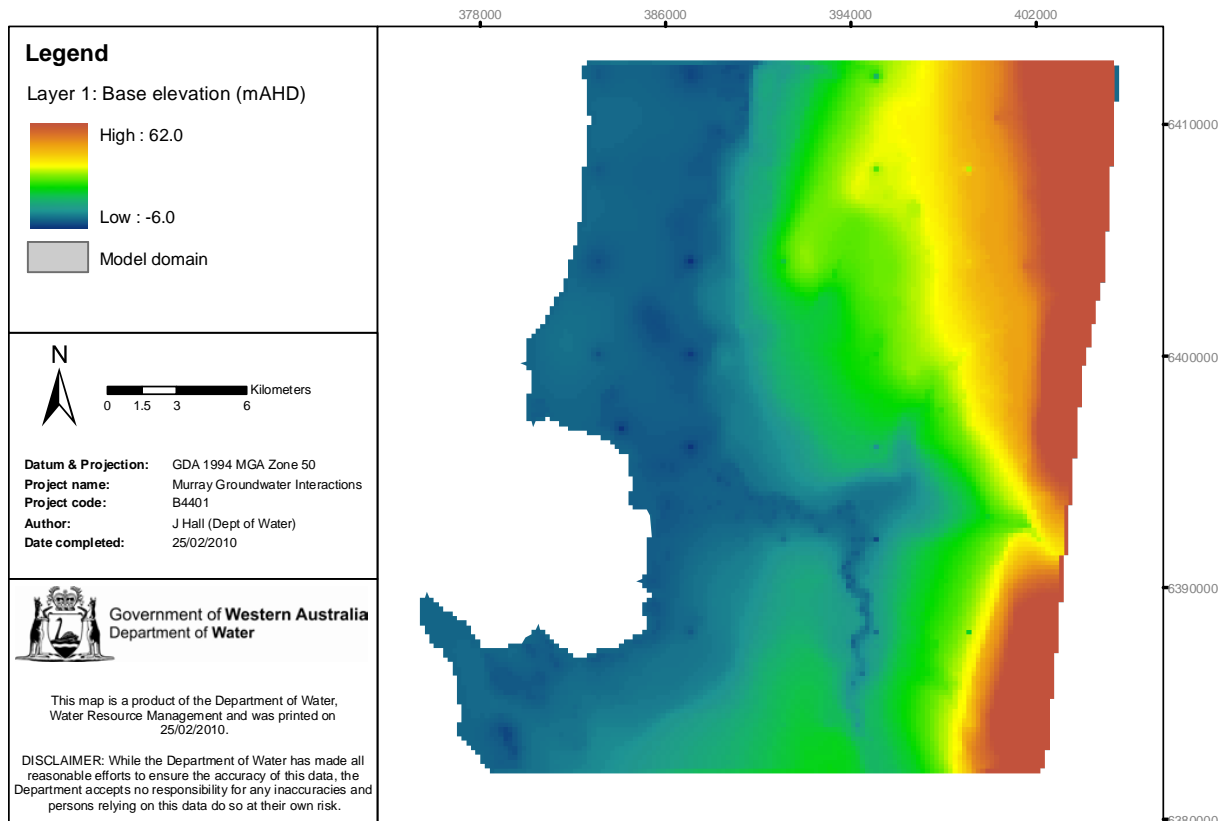


Figure 3-33: Base of computational layer 1(mAHD)

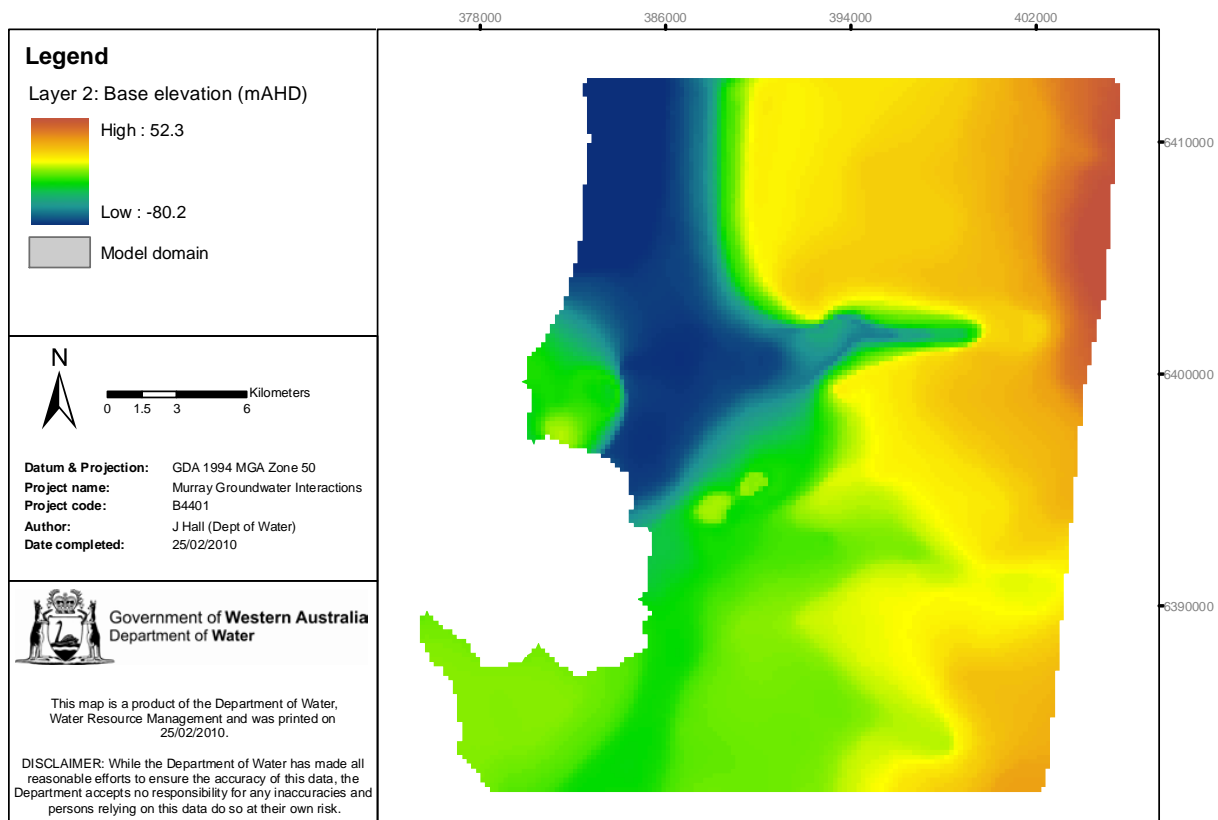


Figure 3-34: Base of computational layer 2 (mAHD)

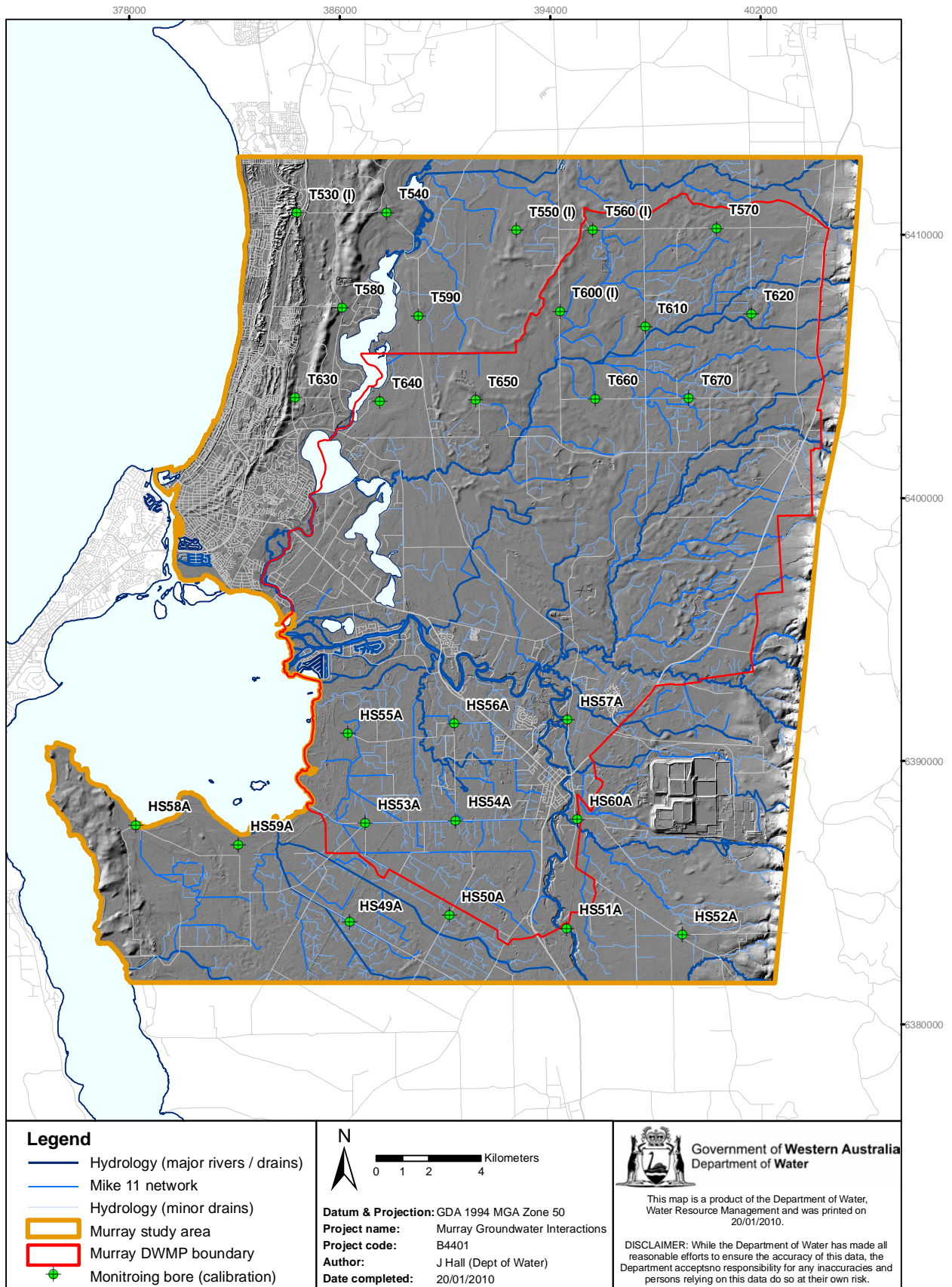


Figure 4-1: Calibration monitoring bore locations

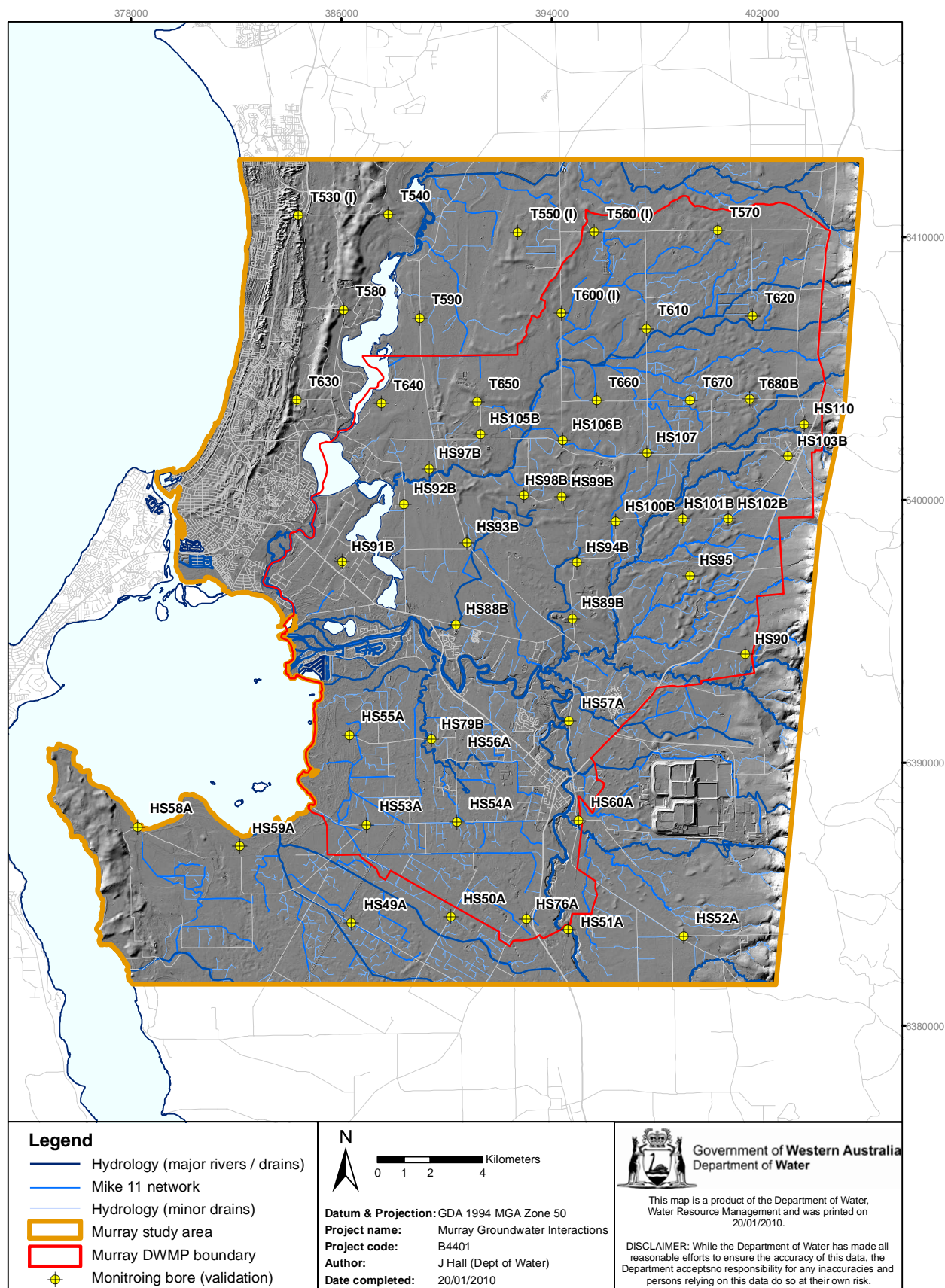


Figure 4-3: Validation monitoring bore locations

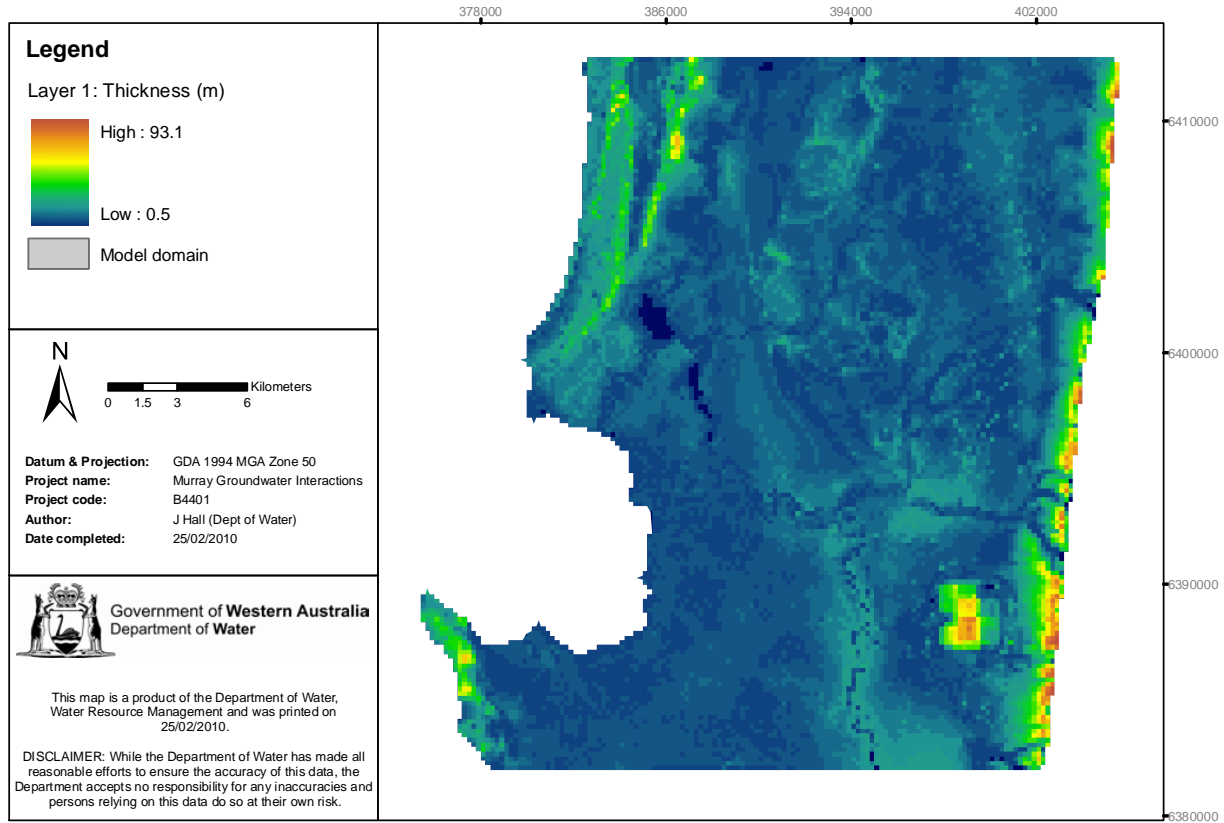


Figure 4-5: Computational layer 1 - thickness (m)

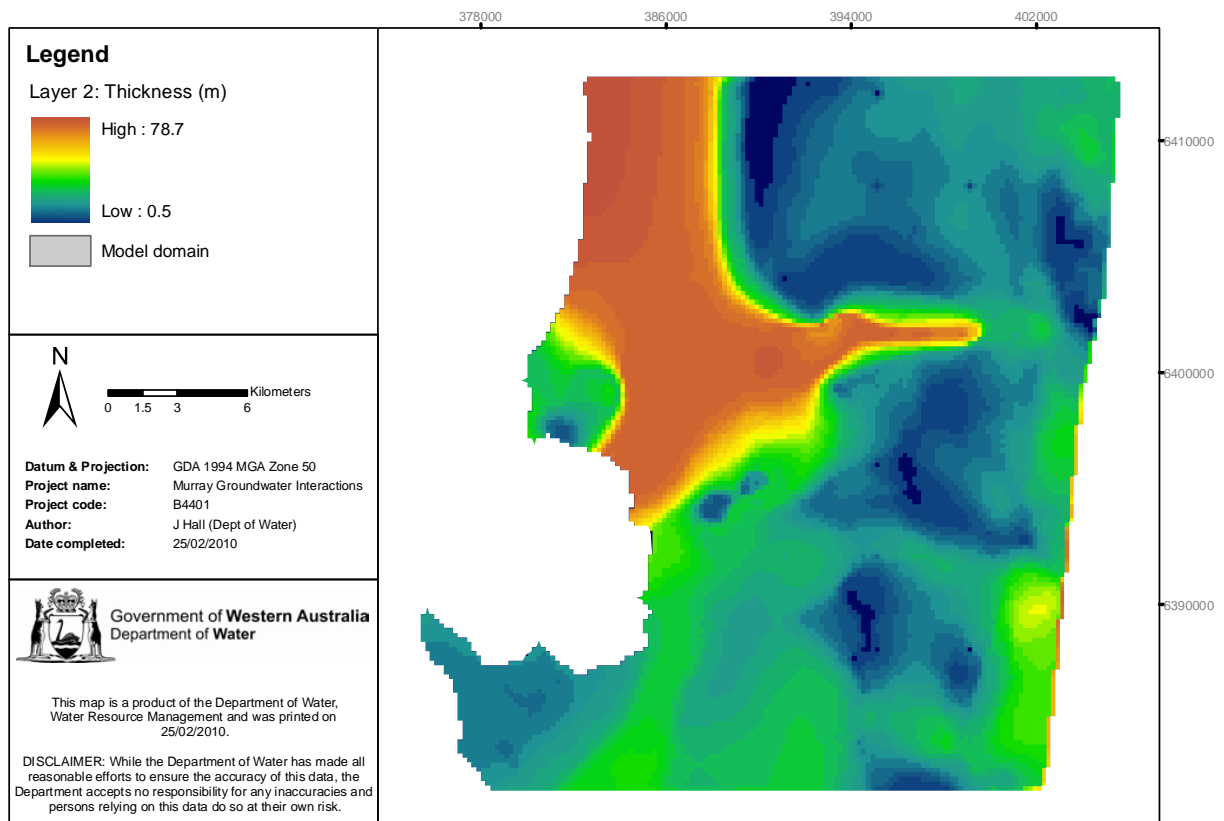


Figure 4-6: Computational layer 2 - thickness (m)

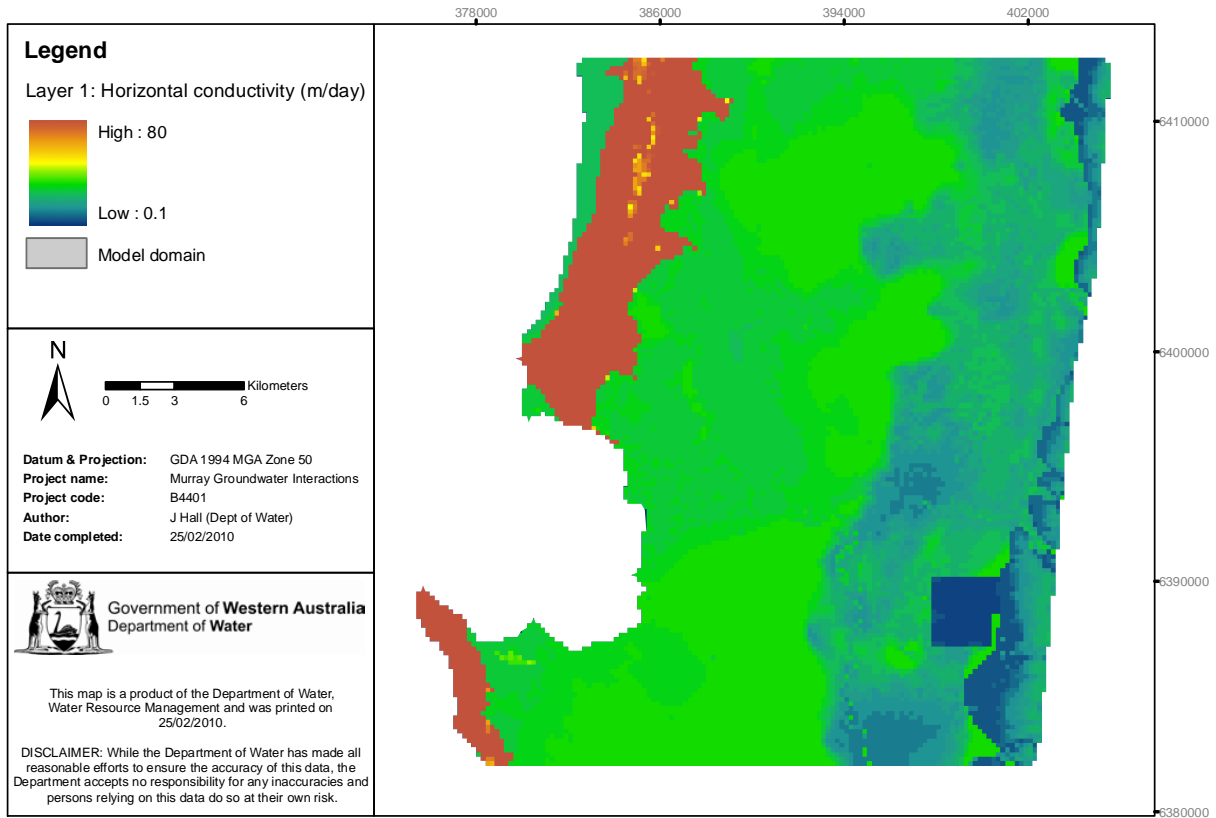


Figure 4-7: Computational layer 1 - horizontal hydraulic conductivity (m/day)

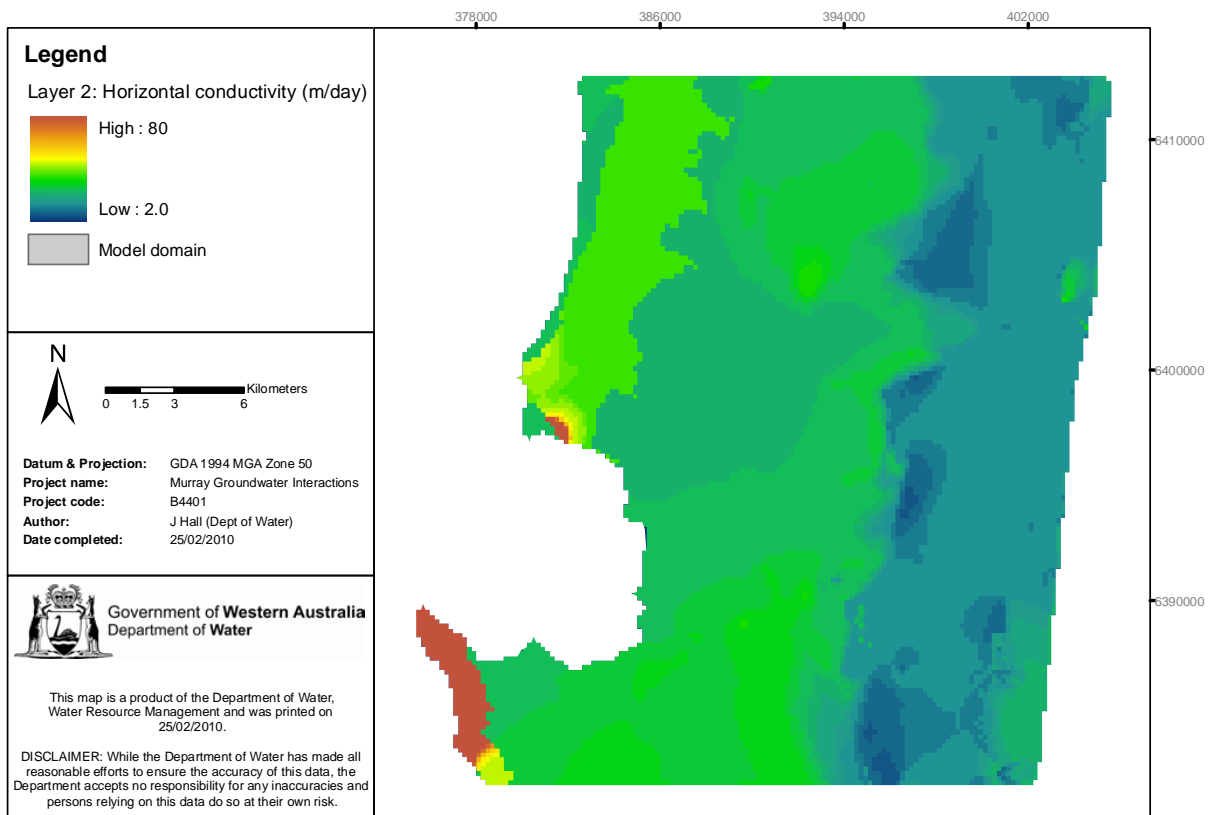


Figure 4-8: Computational layer 2 - horizontal hydraulic conductivity (m/day)

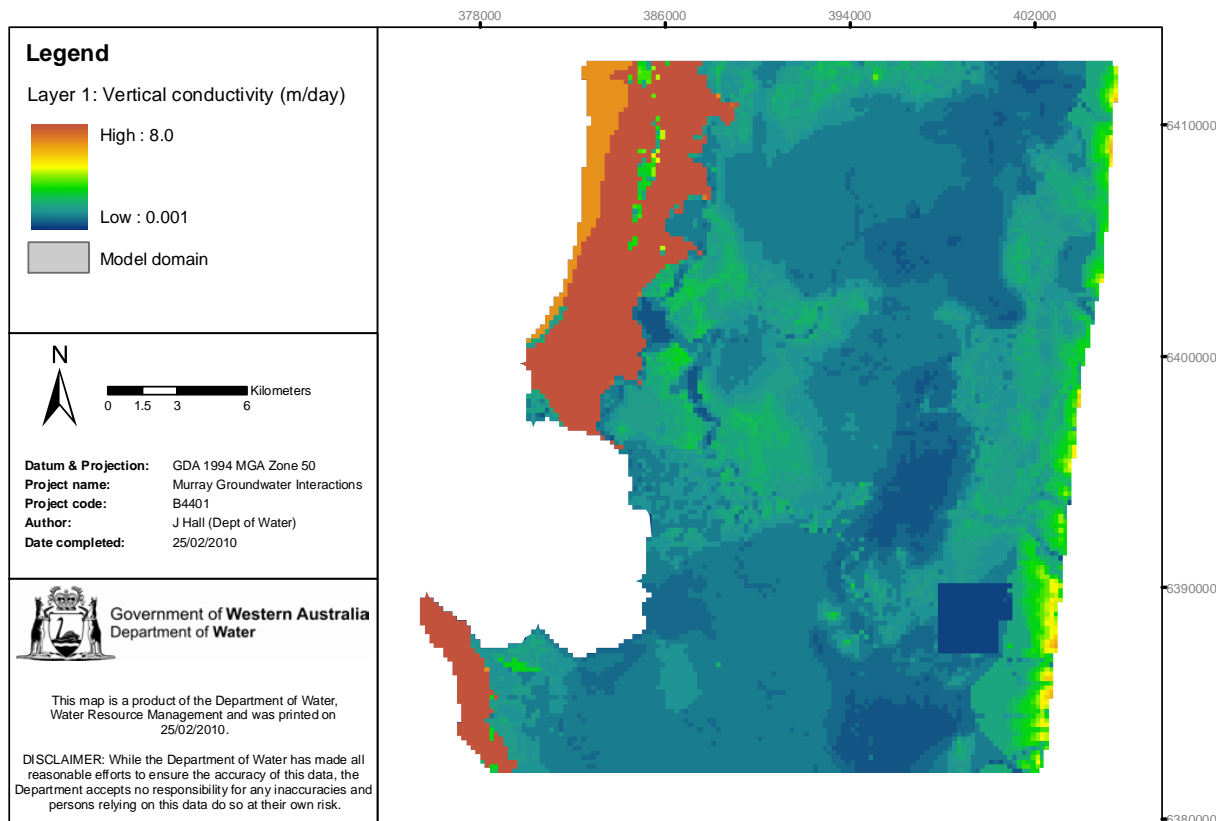


Figure 4-9: Computational layer 1 - vertical hydraulic conductivity (m/day)

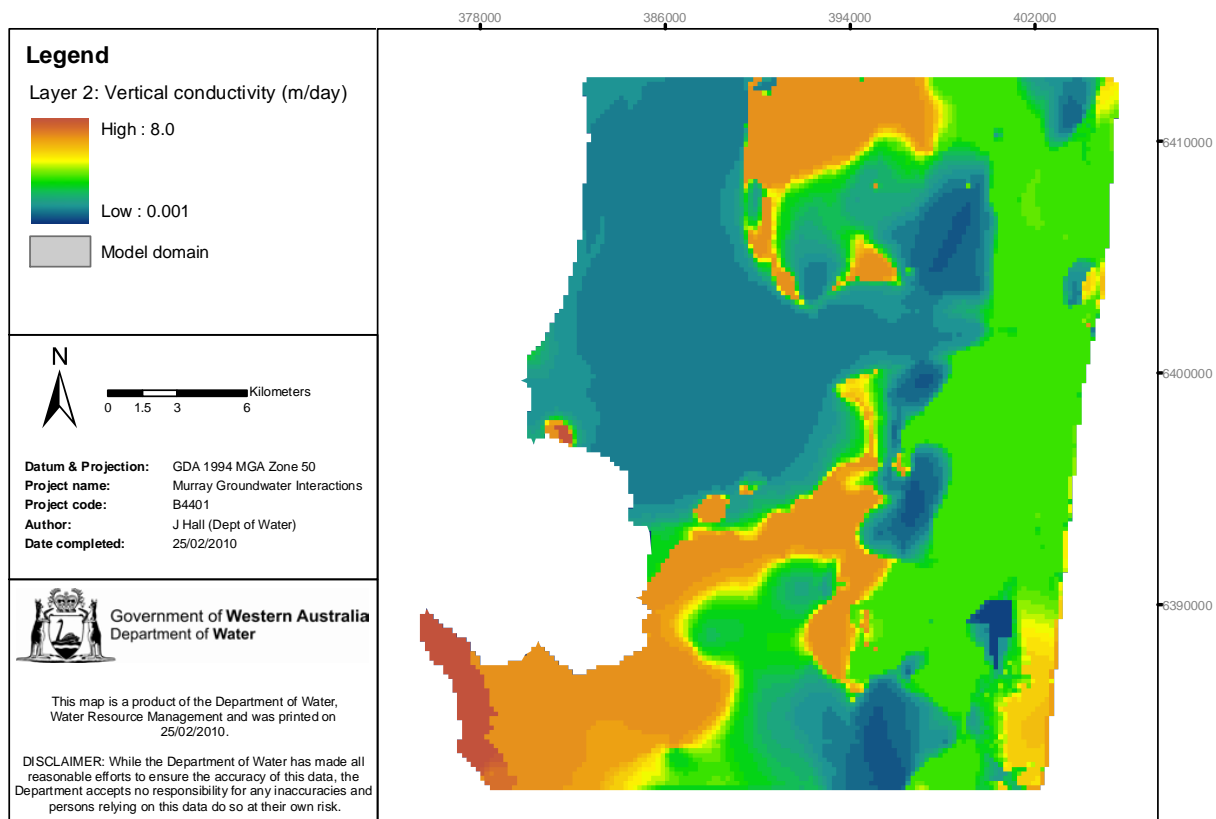


Figure 4-10: Computational layer 2 - vertical hydraulic conductivity (m/day)

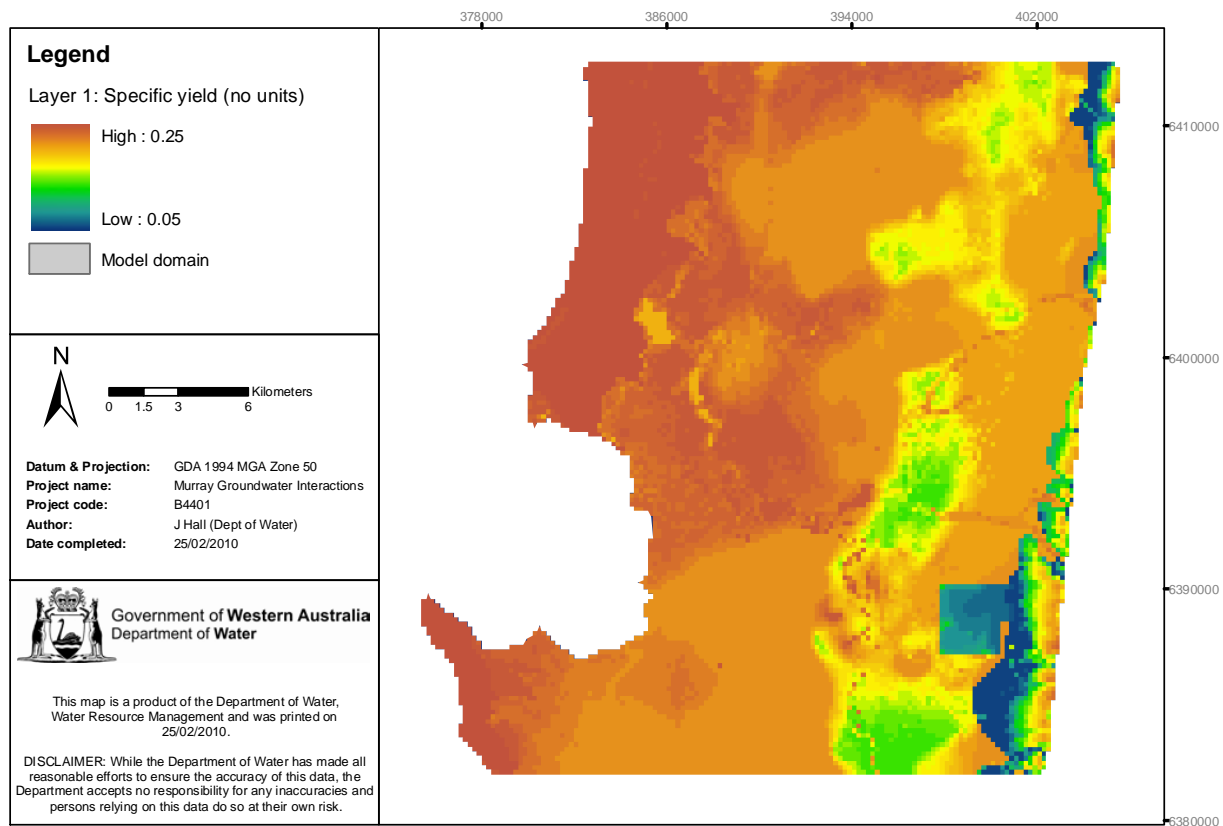


Figure 4-11: Computational layer 1 - specific yield

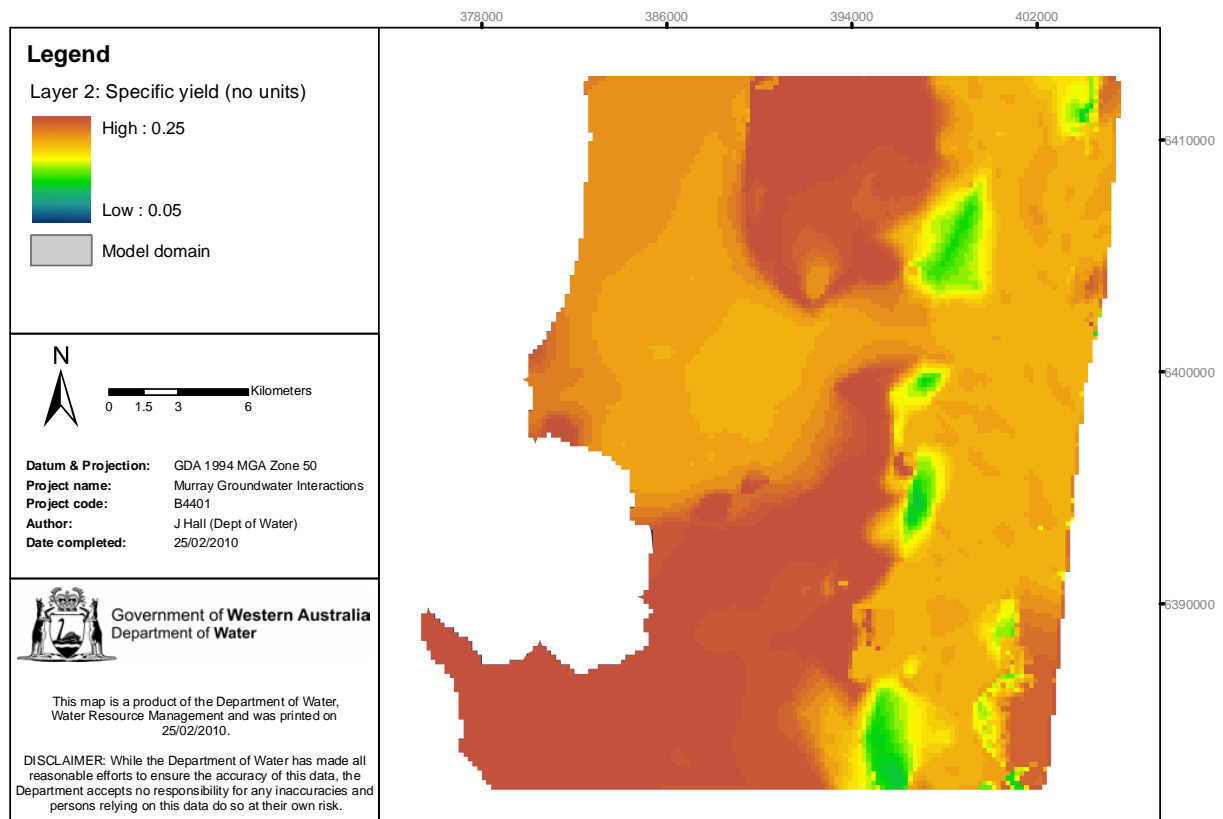


Figure 4-12: Computational layer 2 - specific yield

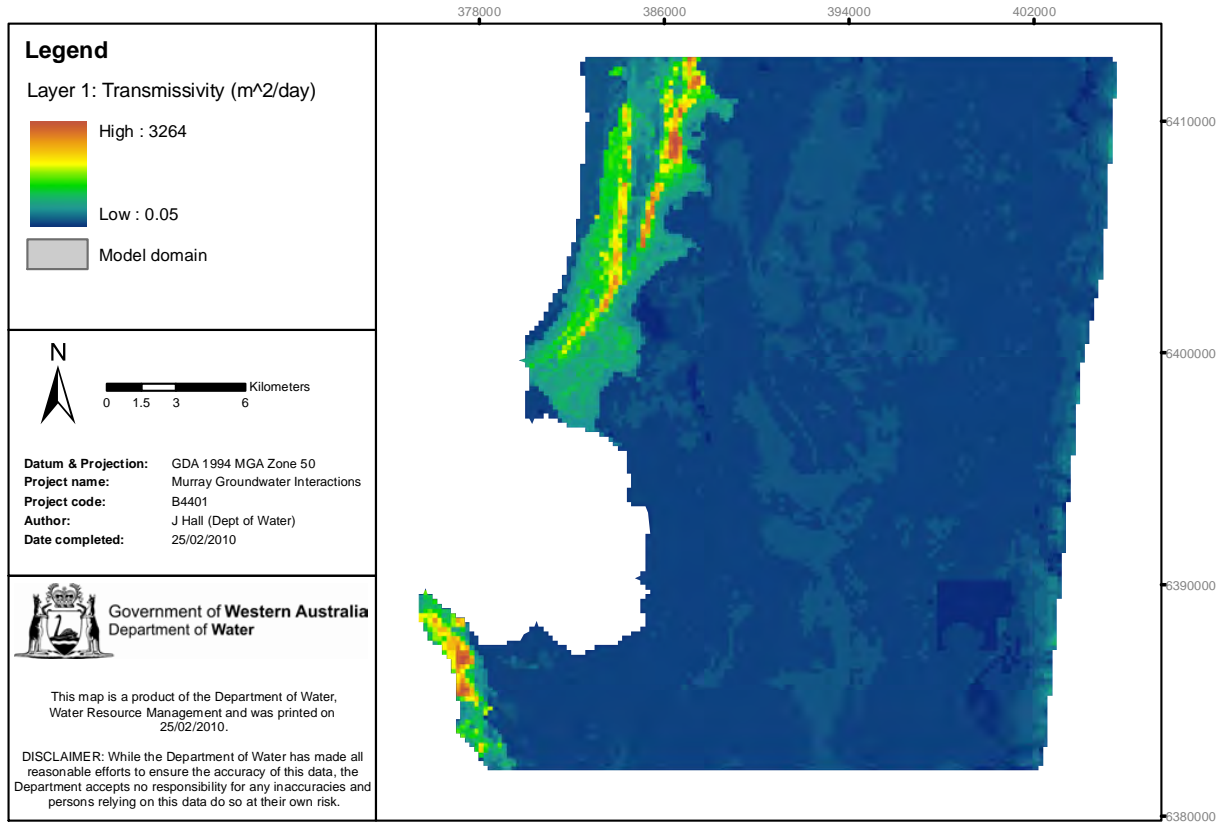


Figure 4-13: Computational layer 1 - transmissivity (m²/day)

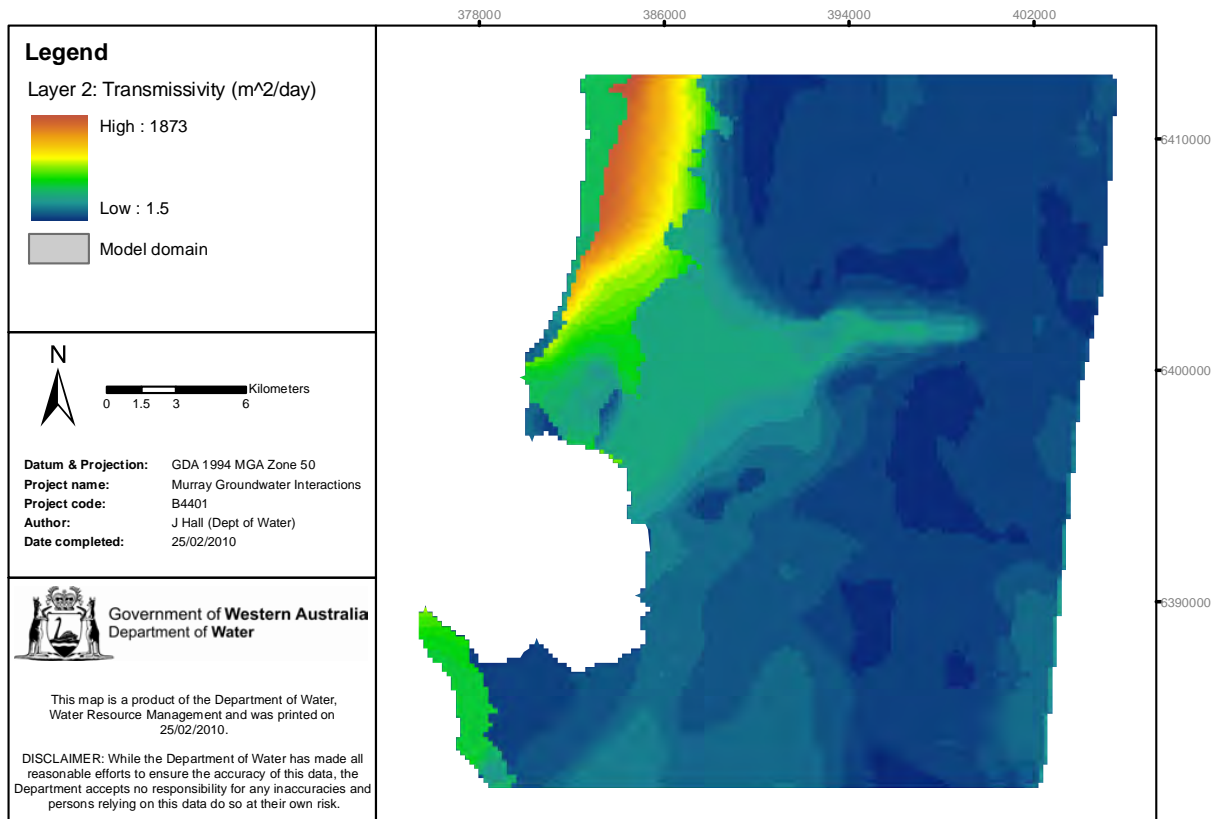


Figure 4-14: Computational layer 2 - transmissivity (m²/day)

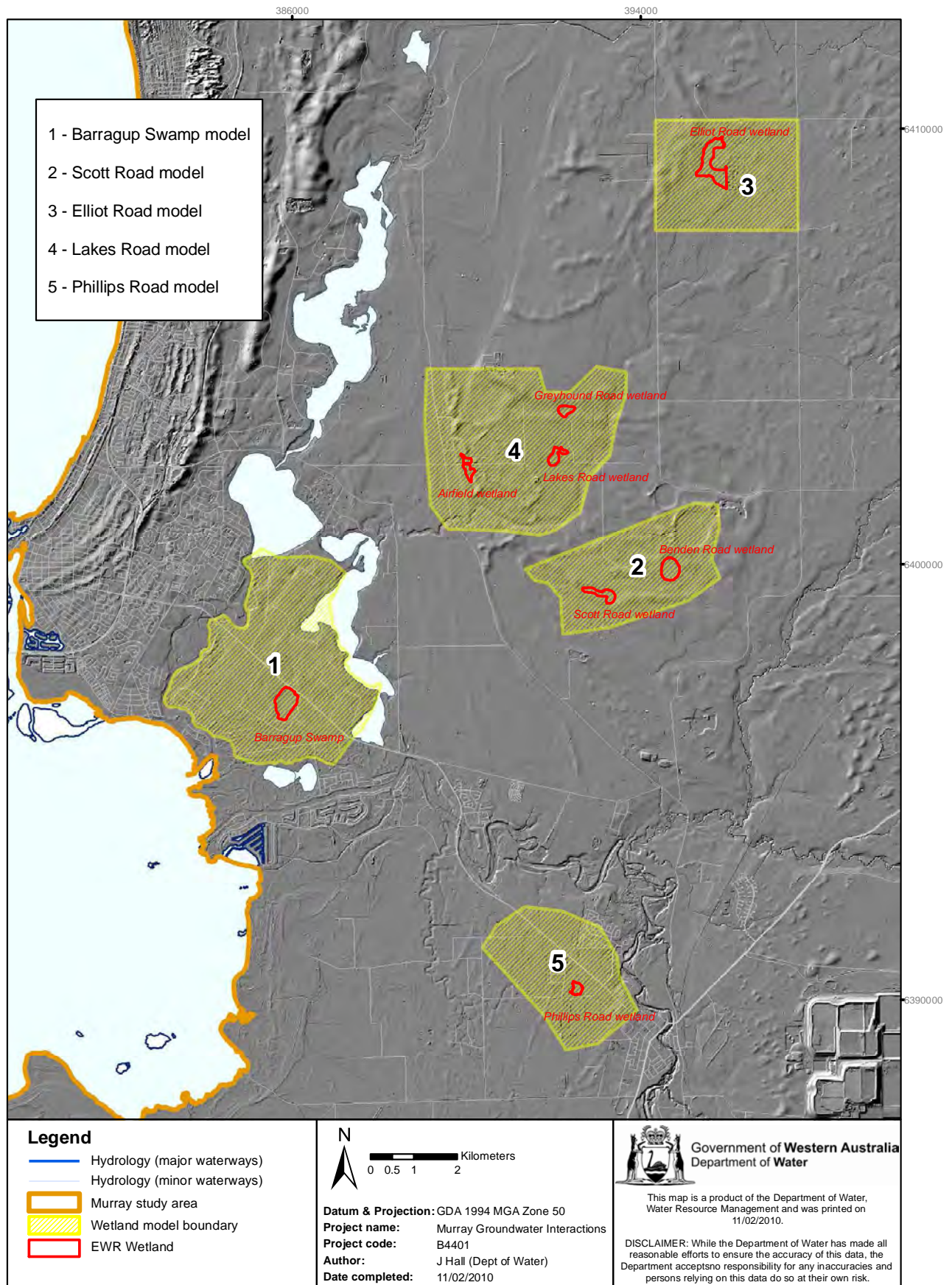


Figure 7-1: Domain for individual wetland models

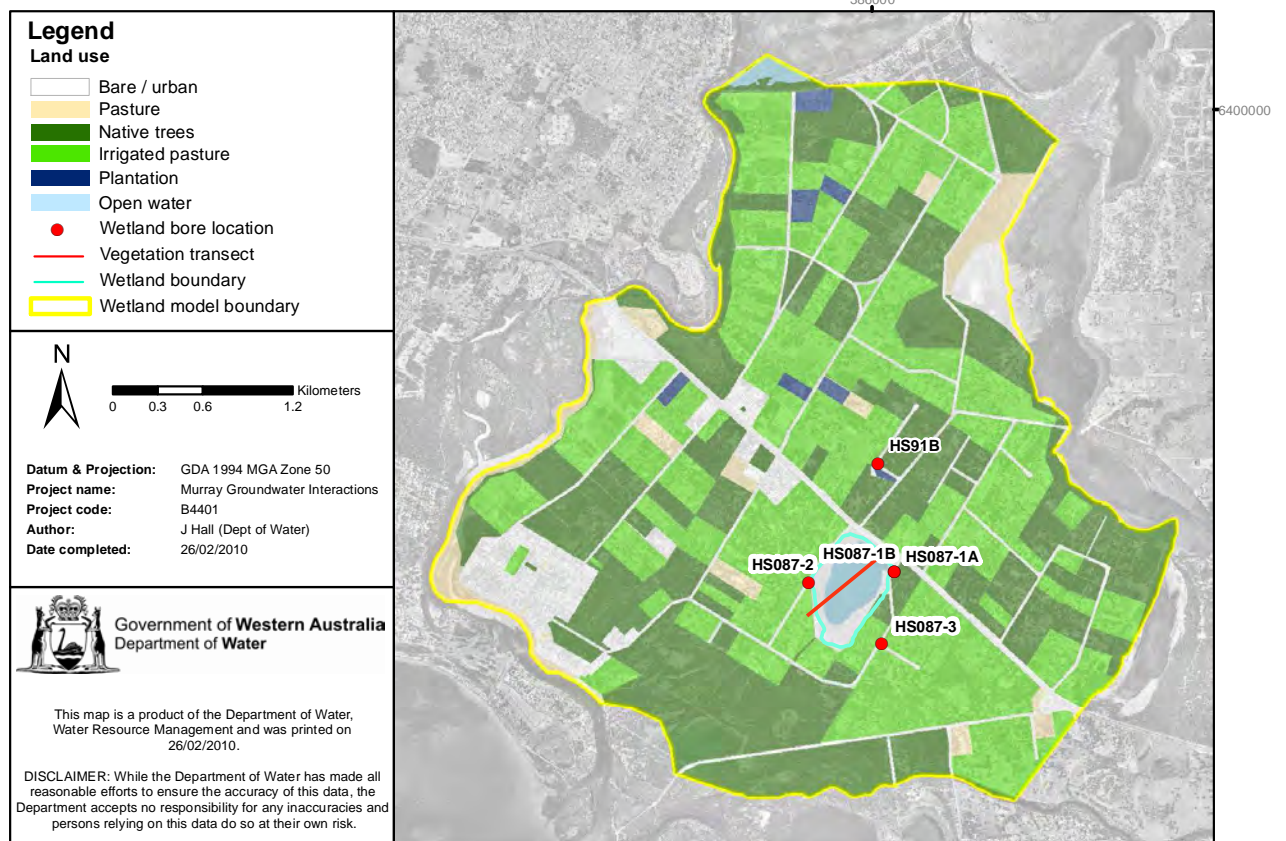


Figure 7-2: Barragup wetland model: land use and monitoring locations

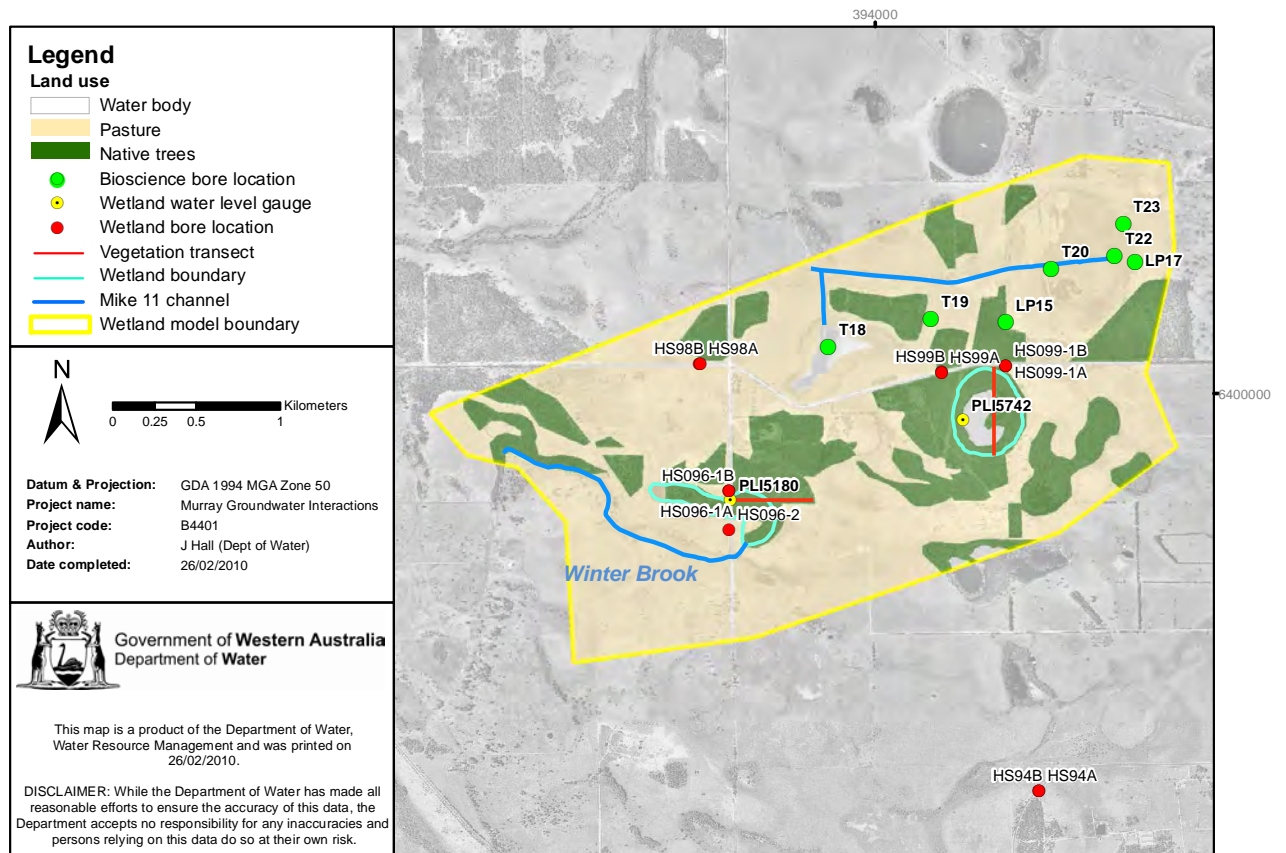


Figure 7-3: Scott Road model: land use, monitoring and Mike 11 channel locations

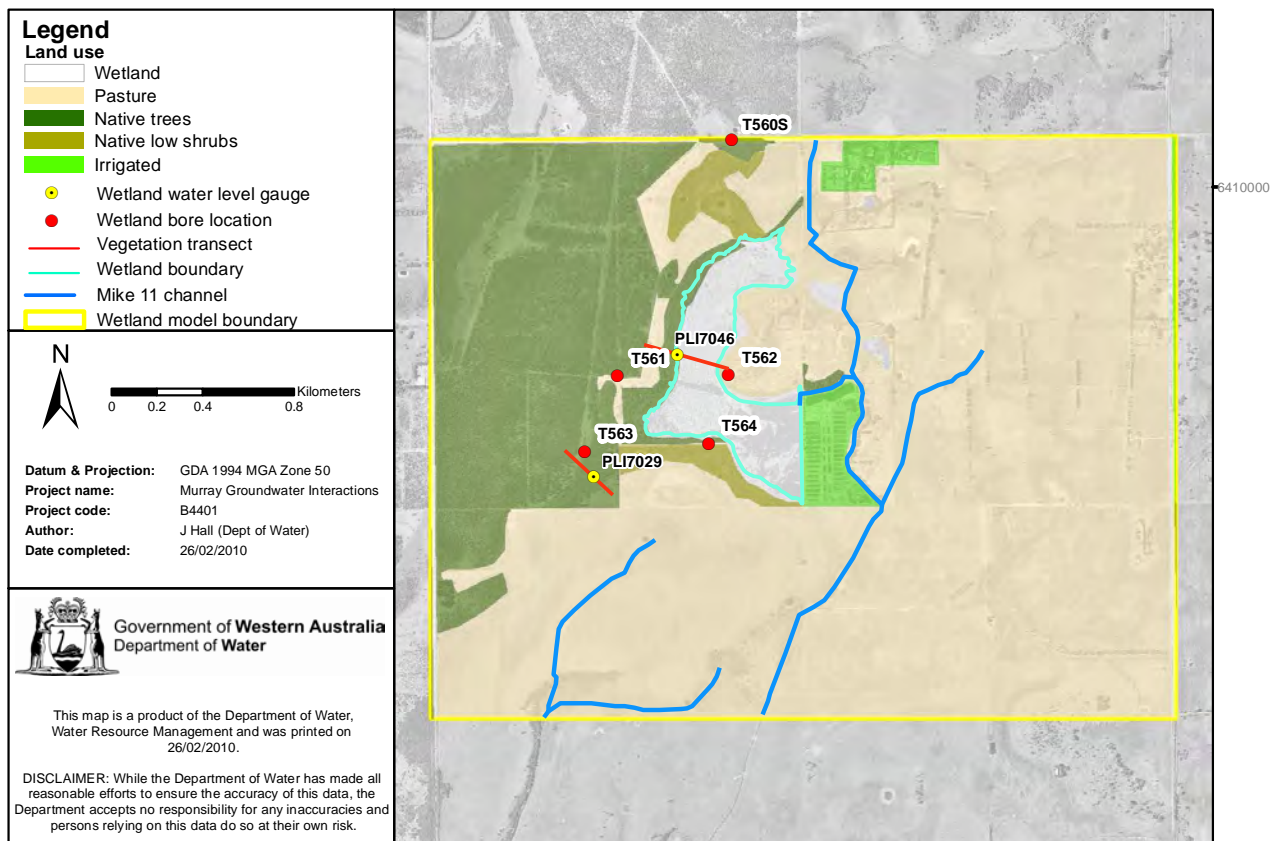


Figure 7-4: Elliot Road model: land use and monitoring locations

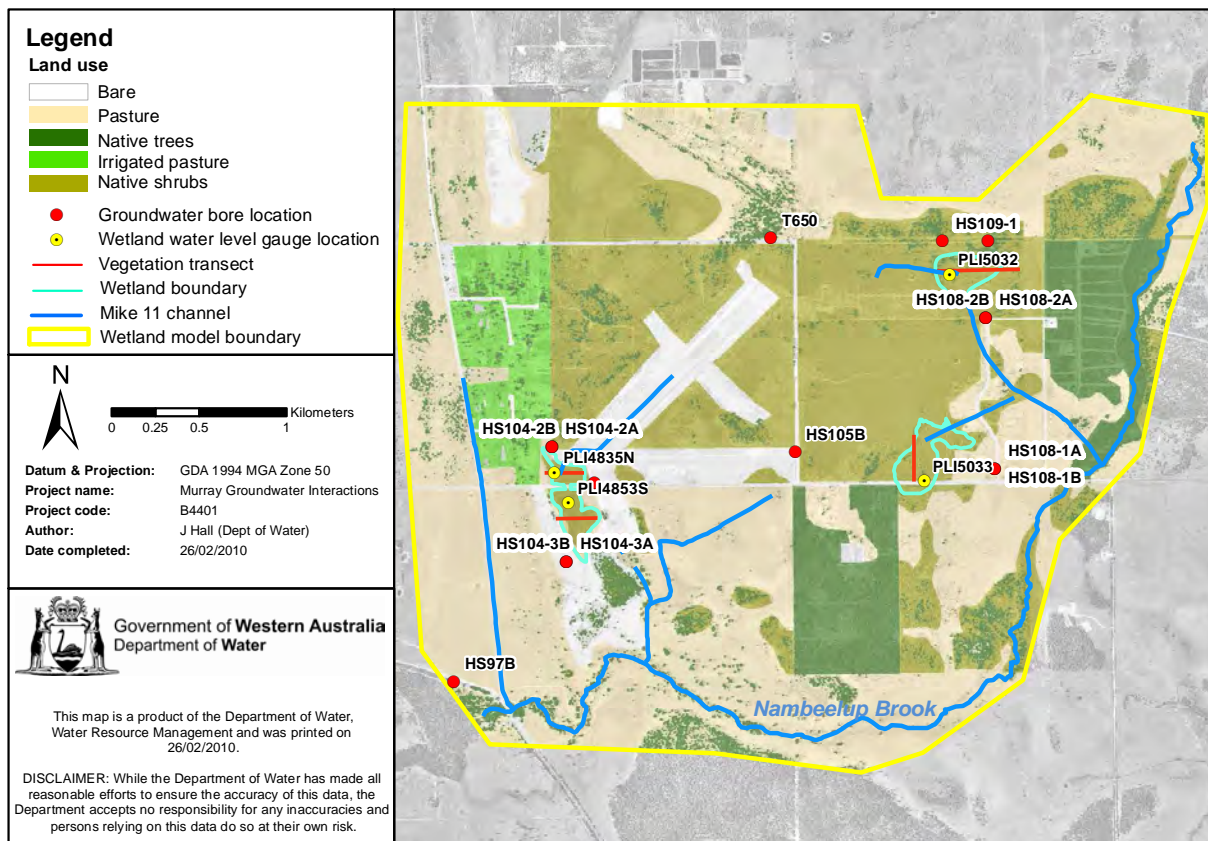


Figure 7-5: Scott Road model: land use, monitoring and Mike 11 channel locations

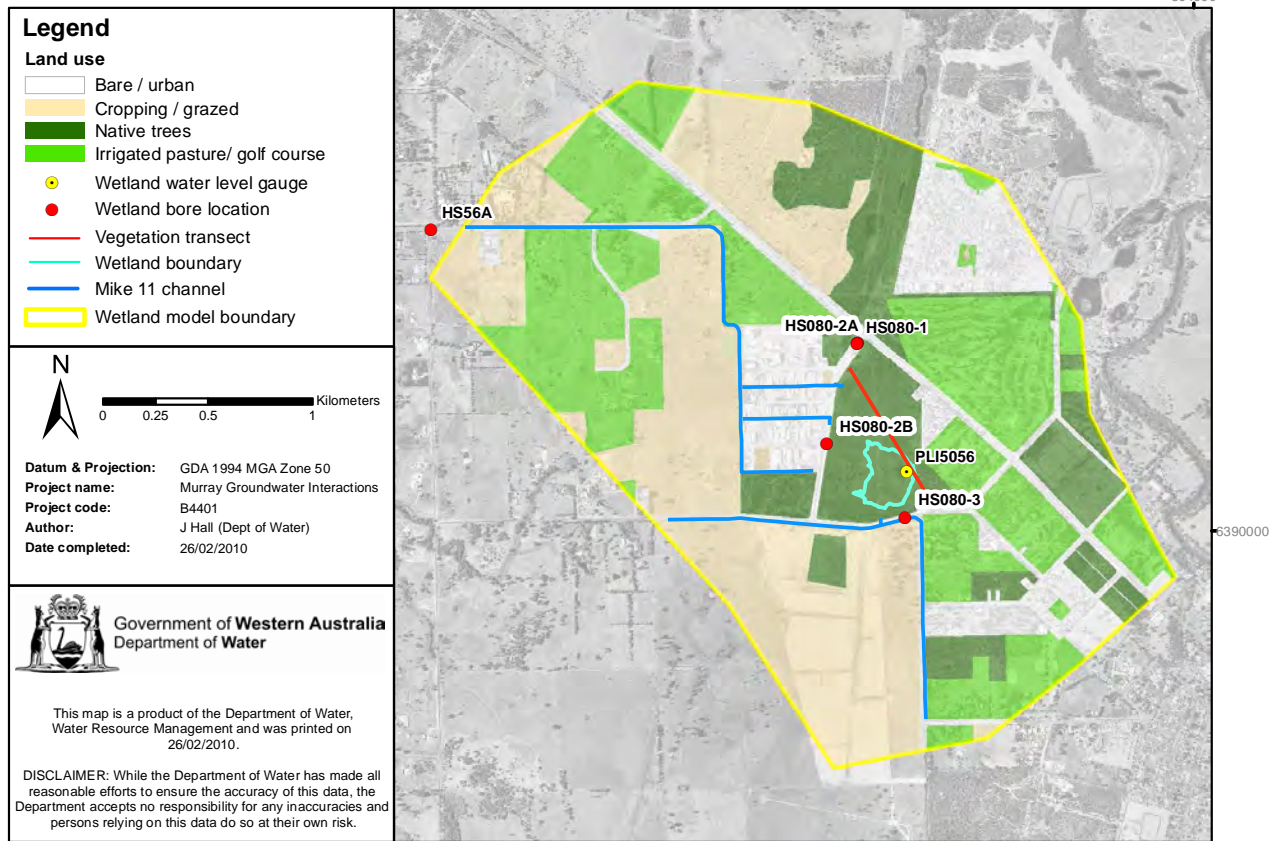


Figure 7-6: Phillips Road model: land use, monitoring and Mike 11 channel locations

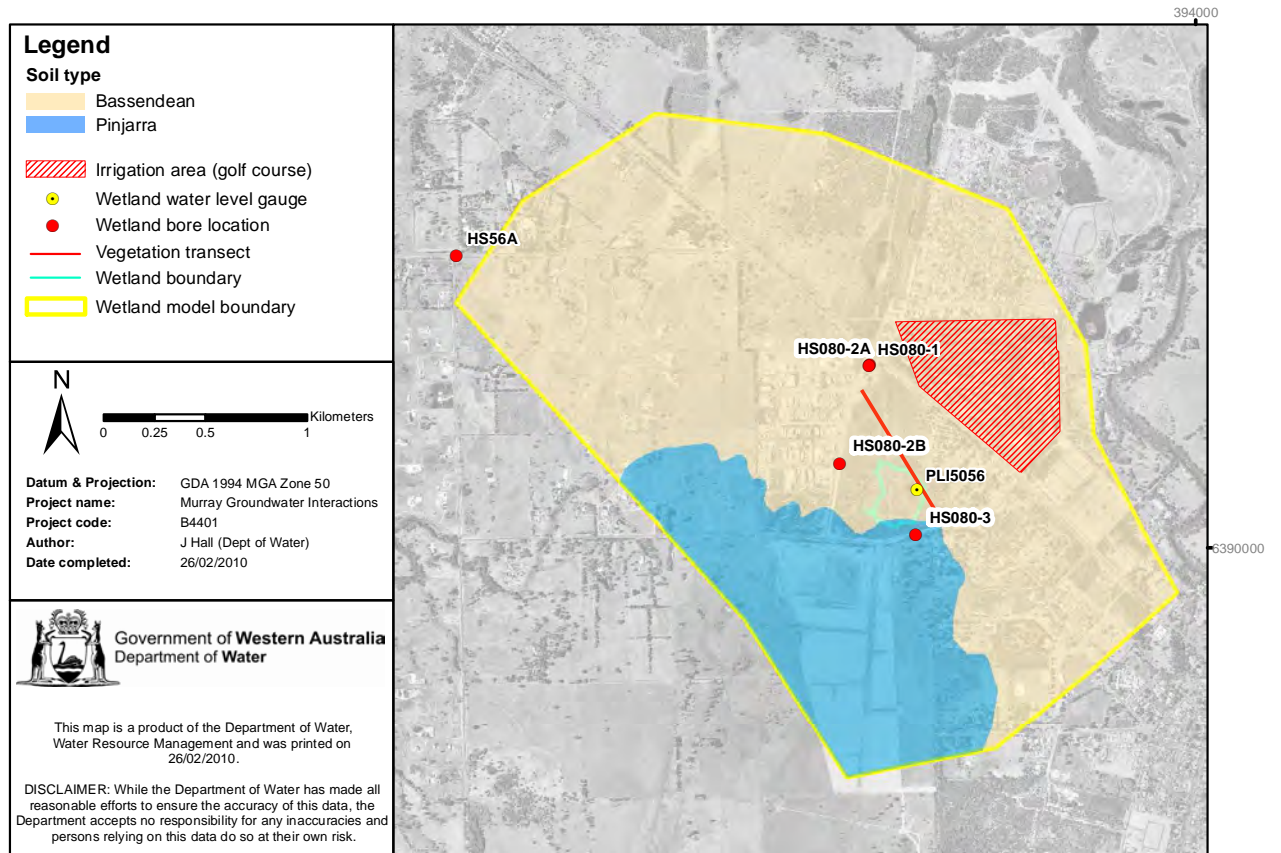
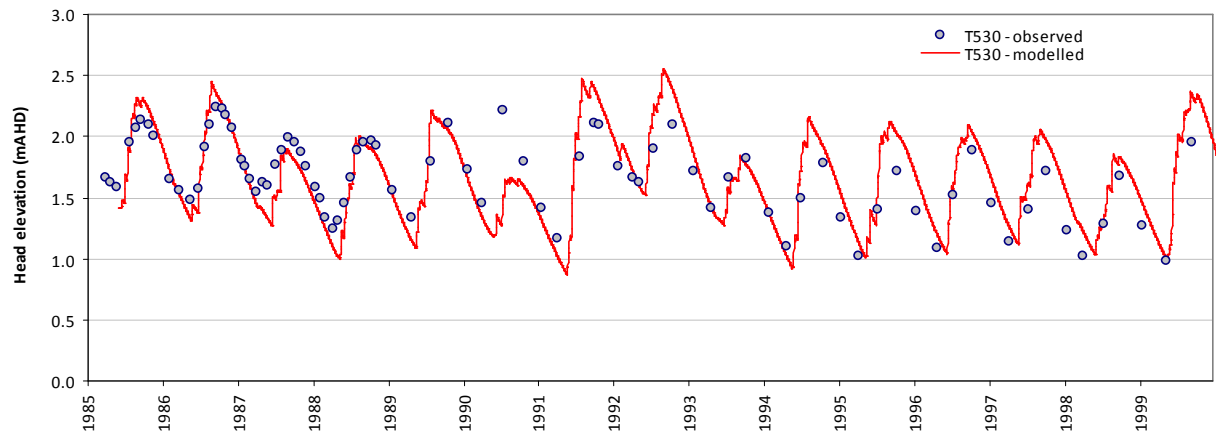


Figure 7-8: Phillips Road model: soil type and irrigation area

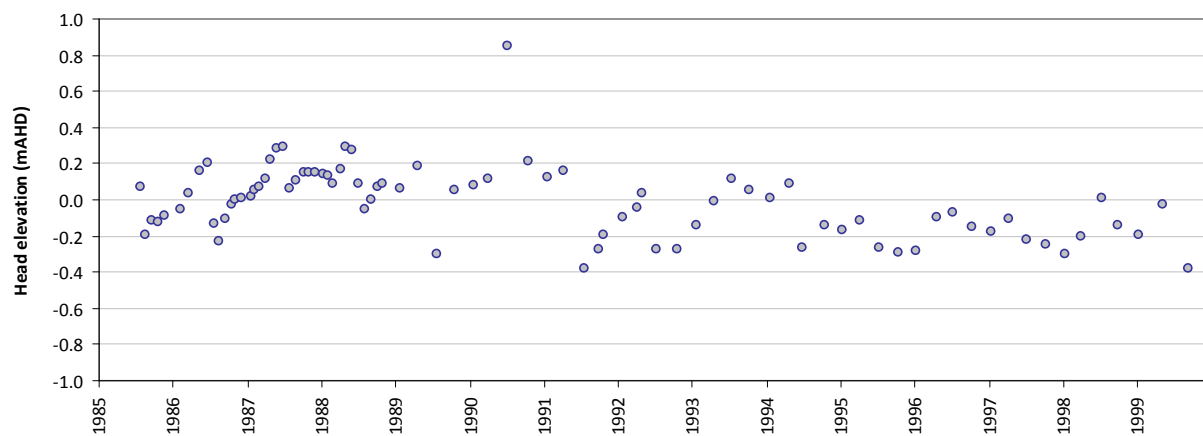
Appendix A: Calibration plots and statistics

T530

Modelled vs observed time-series plot - T530



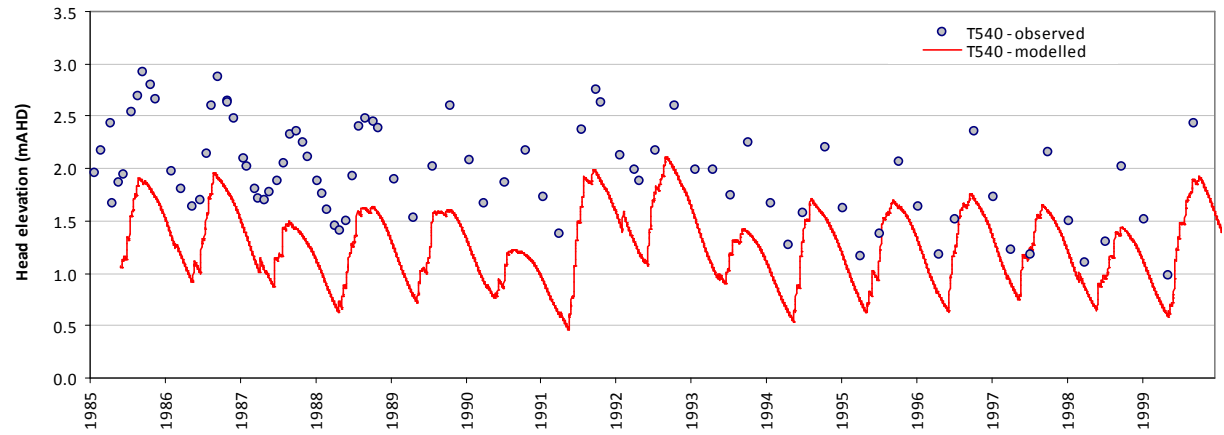
Residual time-series plot - T530



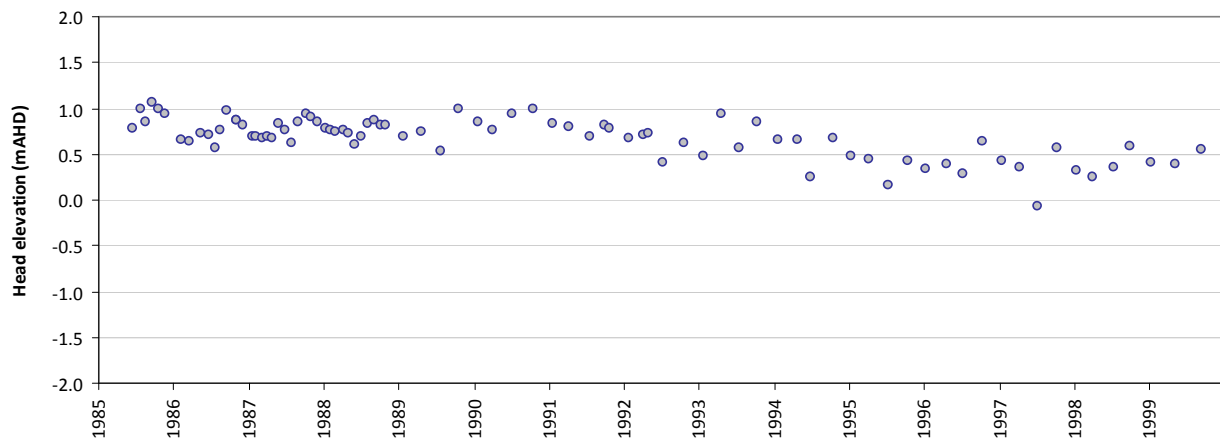
Statistics	
Mean error (ME)	0.67
Mean absolute error (MAE)	0.68
Root mean square error (RMSE)	0.71
Standard deviation of residuals (STDres)	0.22
Correlation coefficient (R)	0.89
Nash Sutcliffe correlation coefficient (R2)	-1.30

T540

Modelled vs observed time-series plot - T540



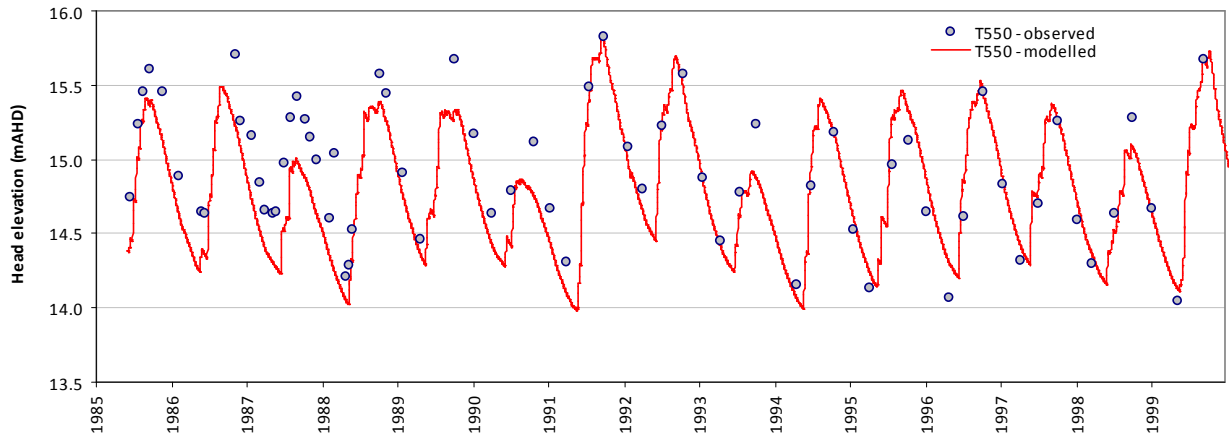
Residual time-series plot - T540



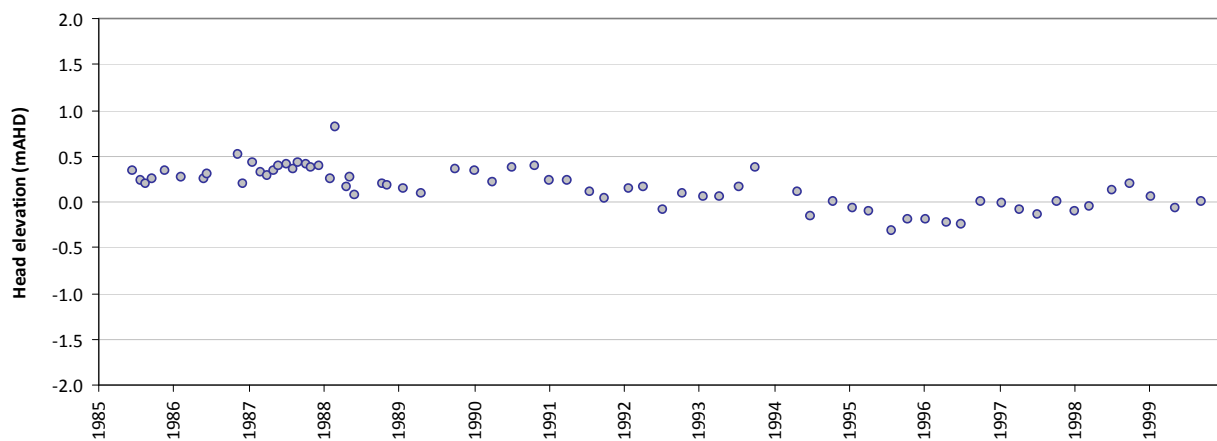
Statistics	
Mean error (ME)	0.67
Mean absolute error (MAE)	0.68
Root mean square error (RMSE)	0.71
Standard deviation of residuals (STDres)	0.22
Correlation coefficient (R)	0.89
Nash Sutcliffe correlation coefficient (R2)	-1.30

T550

Modelled vs observed time-series plot - T550



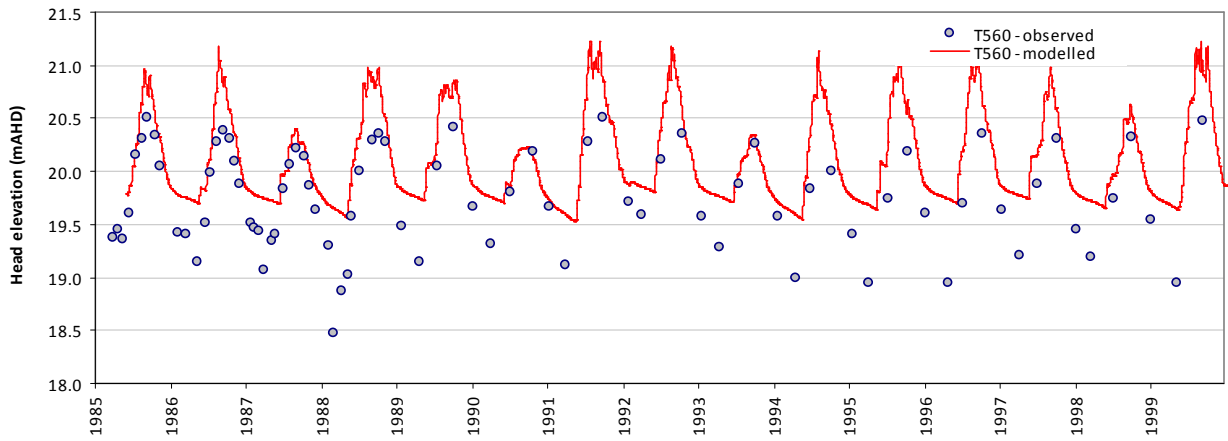
Residual time-series plot - T550



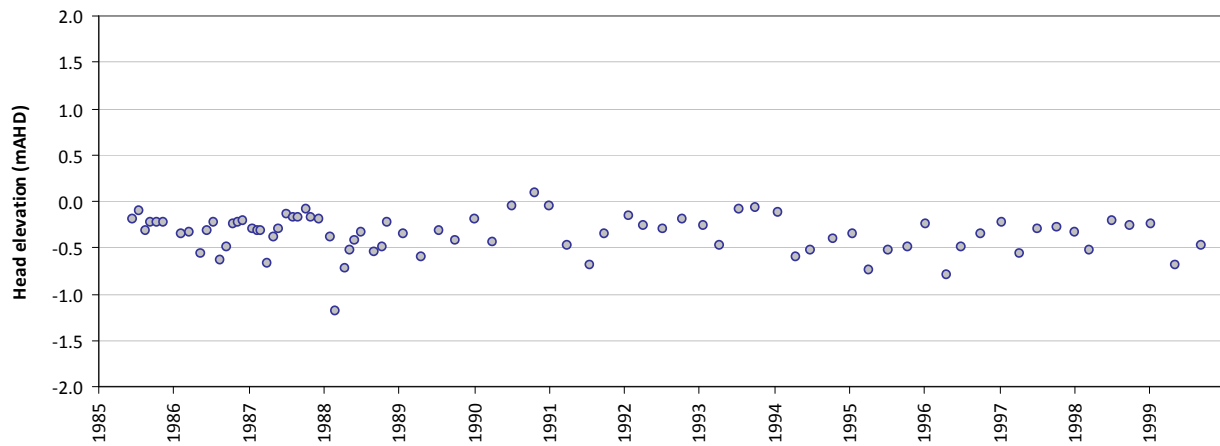
Statistics	
Mean error (ME)	0.16
Mean absolute error (MAE)	0.22
Root mean square error (RMSE)	0.26
Standard deviation of residuals (STDres)	0.21
Correlation coefficient (R)	0.89
Nash Sutcliffe correlation coefficient (R2)	0.65

T560

Modelled vs observed time-series plot - T560



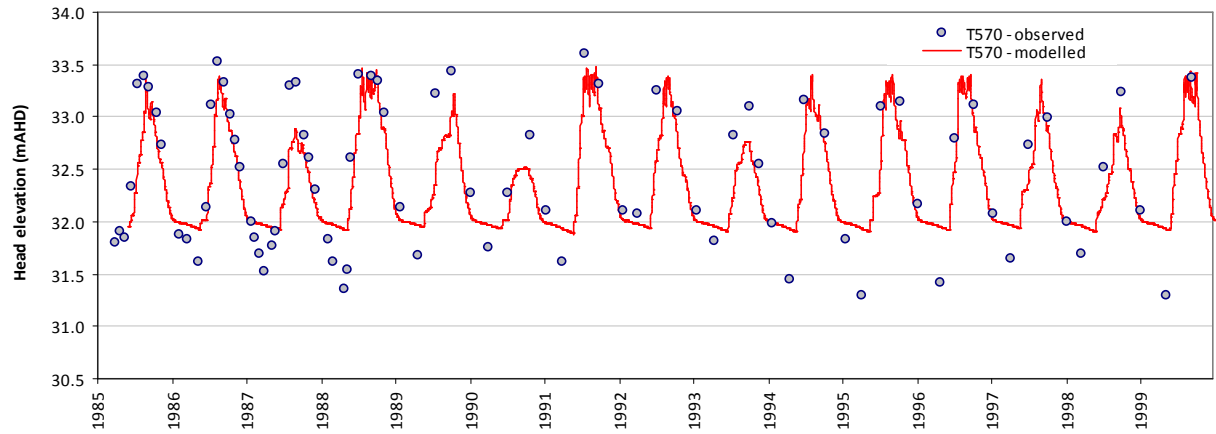
Residual time-series plot - T560



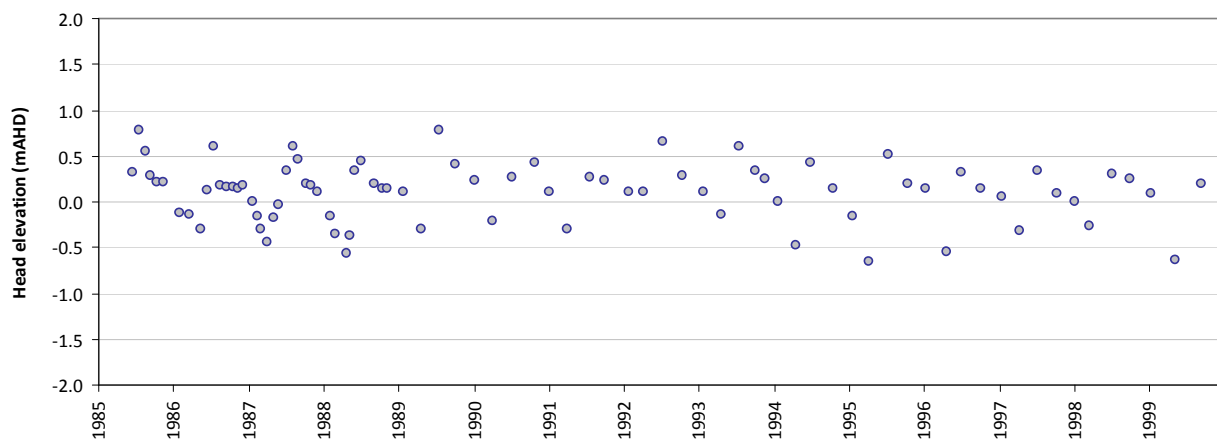
Statistics	
Mean error (ME)	-0.36
Mean absolute error (MAE)	0.36
Root mean square error (RMSE)	0.41
Standard deviation of residuals (STDres)	0.20
Correlation coefficient (R)	0.91
Nash Sutcliffe correlation coefficient (R2)	0.25

T570

Modelled vs observed time-series plot - T570



Residual time-series plot - T570

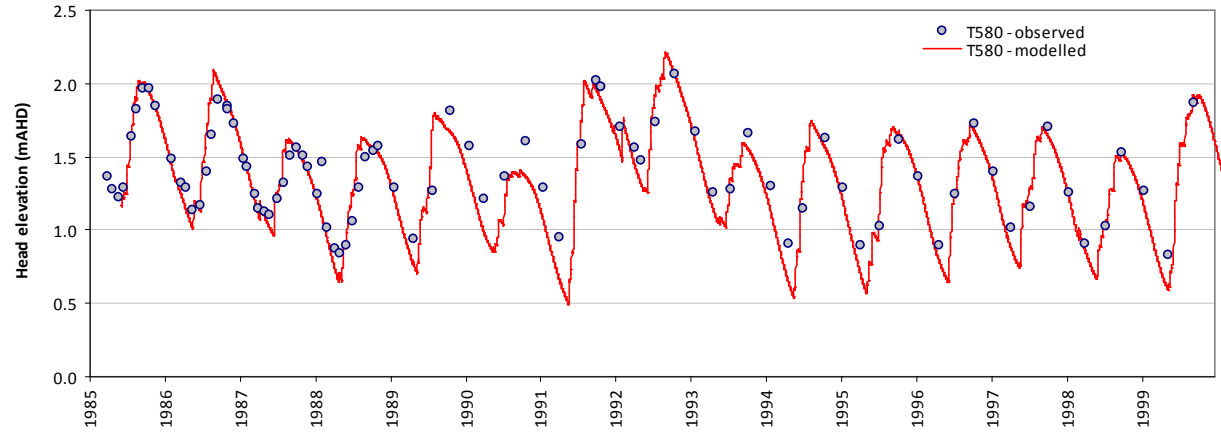


Statistics

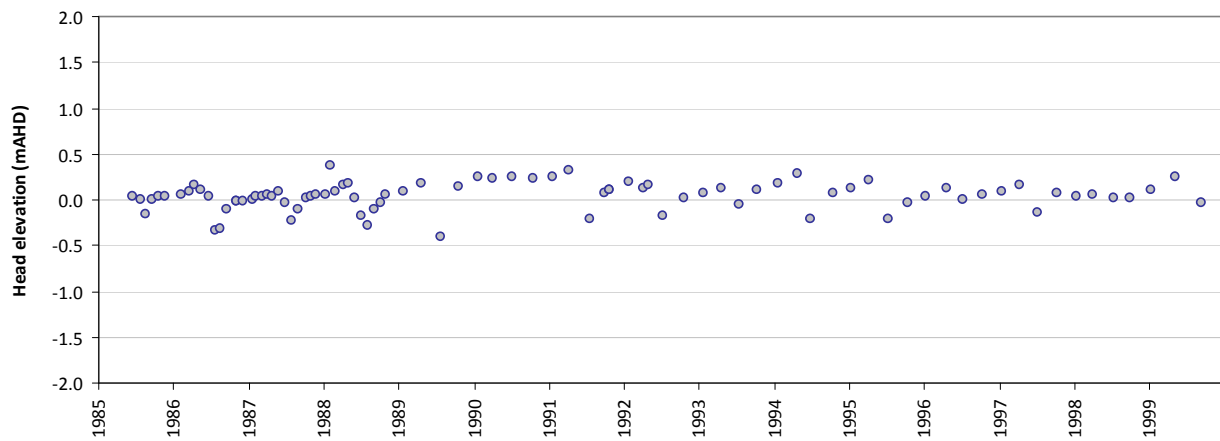
Mean error (ME)	0.10
Mean absolute error (MAE)	0.28
Root mean square error (RMSE)	0.34
Standard deviation of residuals (STDres)	0.32
Correlation coefficient (R)	0.92
Nash Sutcliffe correlation coefficient (R2)	0.75

T580

Modelled vs observed time-series plot - T580



Residual time-series plot - T580

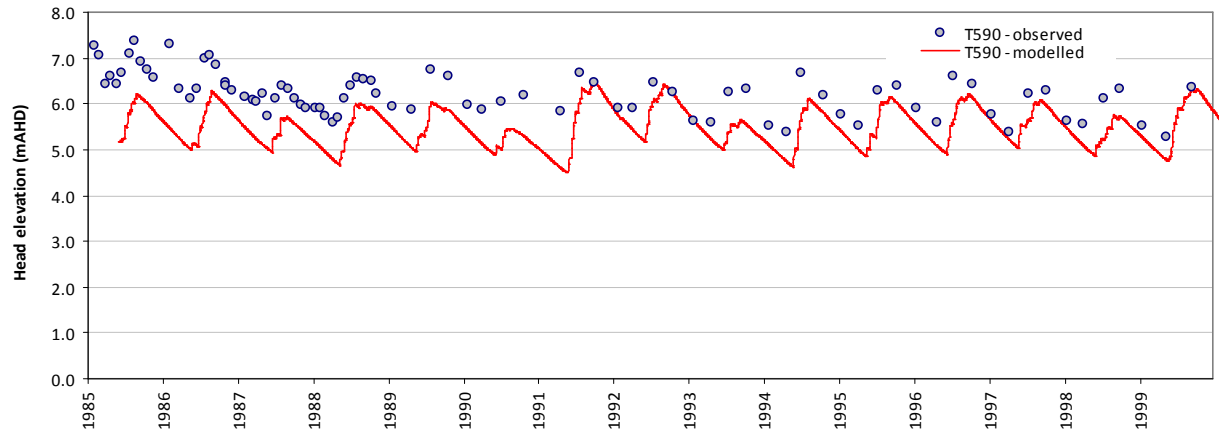


Statistics

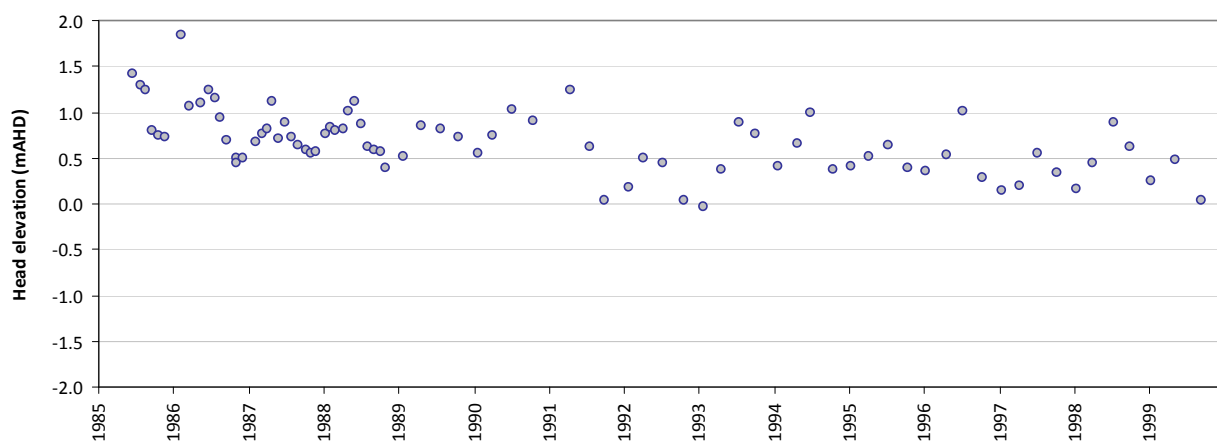
Mean error (ME)	0.04
Mean absolute error (MAE)	0.12
Root mean square error (RMSE)	0.15
Standard deviation of residuals (STDres)	0.14
Correlation coefficient (R)	0.92
Nash Sutcliffe correlation coefficient (R2)	0.78

T590

Modelled vs observed time-series plot - T590



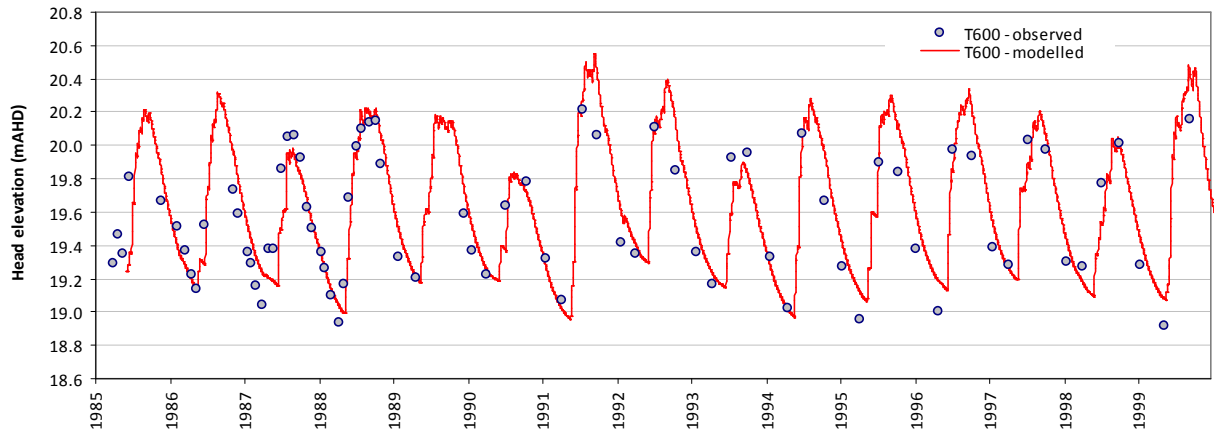
Residual time-series plot - T590



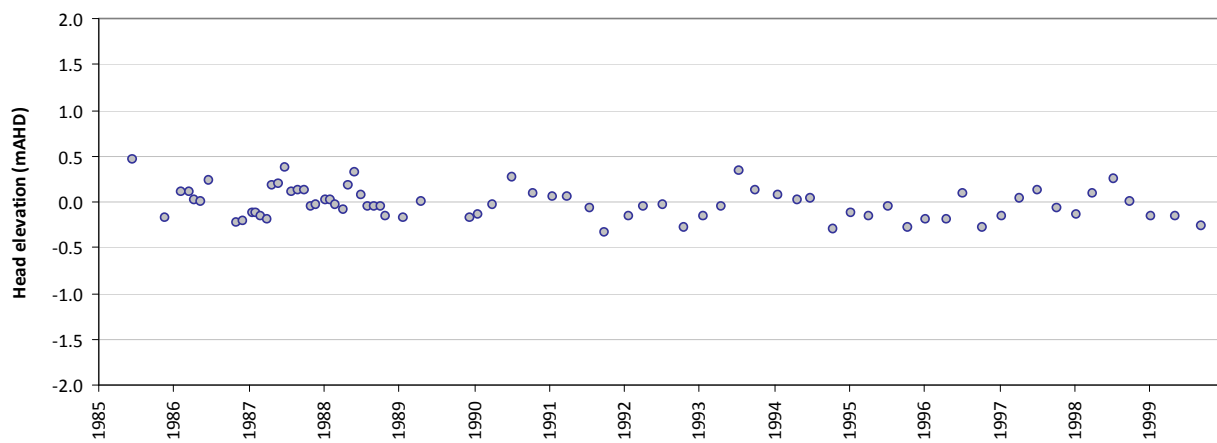
Statistics	
Mean error (ME)	0.67
Mean absolute error (MAE)	0.67
Root mean square error (RMSE)	0.76
Standard deviation of residuals (STDres)	0.34
Correlation coefficient (R)	0.69
Nash Sutcliffe correlation coefficient (R2)	-1.81

T600

Modelled vs observed time-series plot - T600



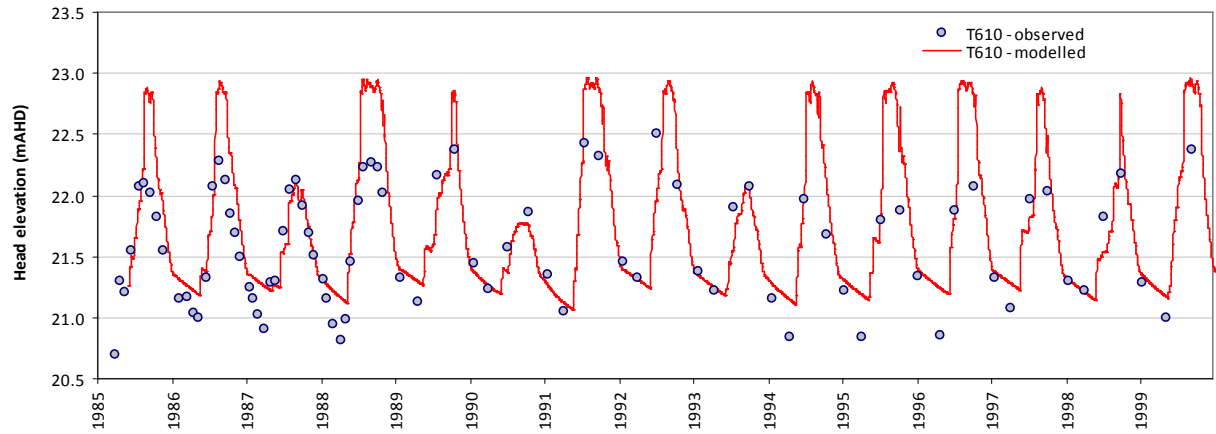
Residual time-series plot - T600



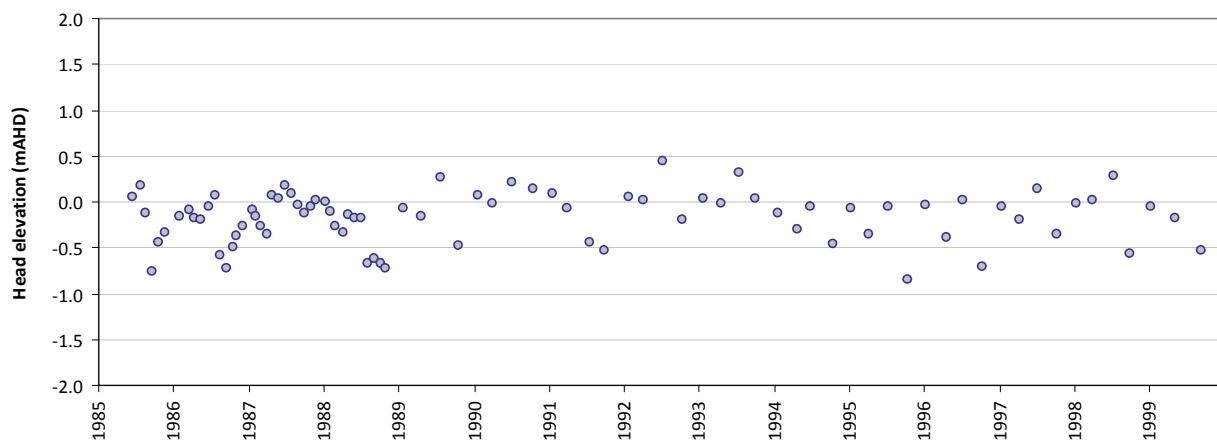
Statistics	
Mean error (ME)	-0.02
Mean absolute error (MAE)	0.14
Root mean square error (RMSE)	0.17
Standard deviation of residuals (STDres)	0.17
Correlation coefficient (R)	0.90
Nash Sutcliffe correlation coefficient (R2)	0.78

T610

Modelled vs observed time-series plot - T610



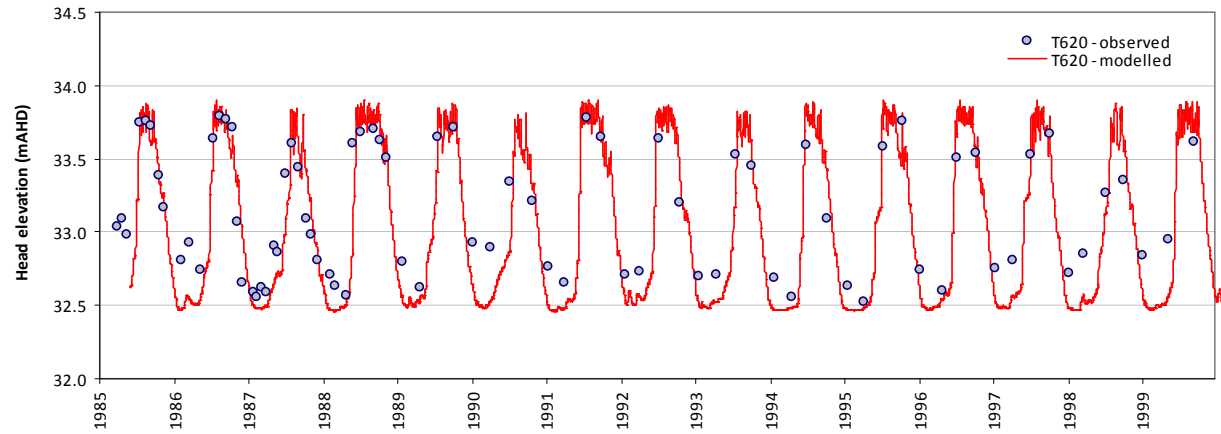
Residual time-series plot - T610



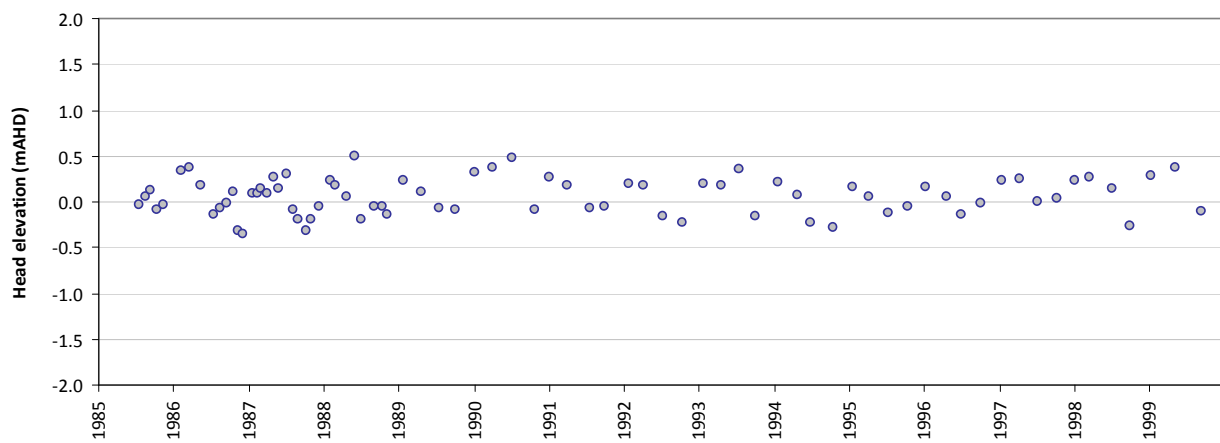
Statistics	
Mean error (ME)	-0.18
Mean absolute error (MAE)	0.25
Root mean square error (RMSE)	0.34
Standard deviation of residuals (STDres)	0.29
Correlation coefficient (R)	0.88
Nash Sutcliffe correlation coefficient (R2)	0.45

T620

Modelled vs observed time-series plot - T620



Residual time-series plot - T620

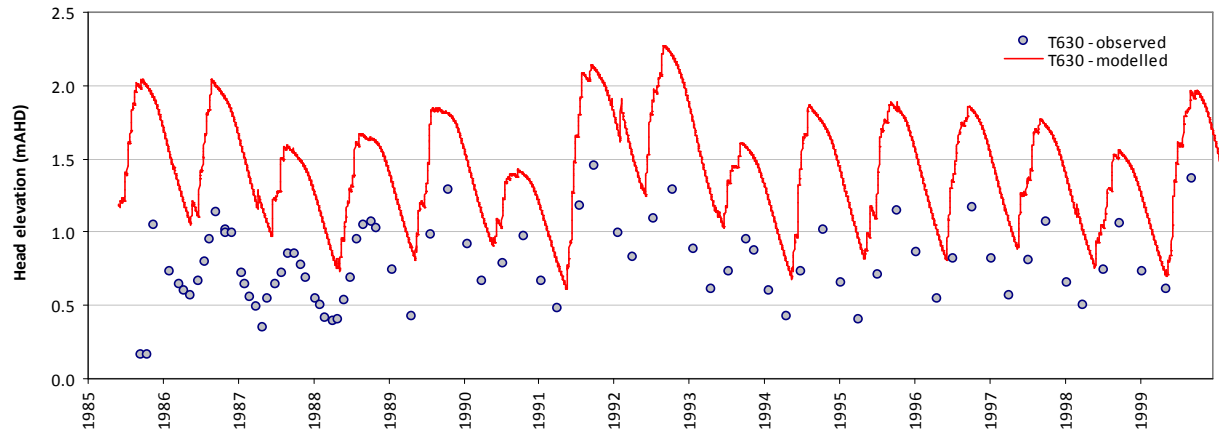


Statistics

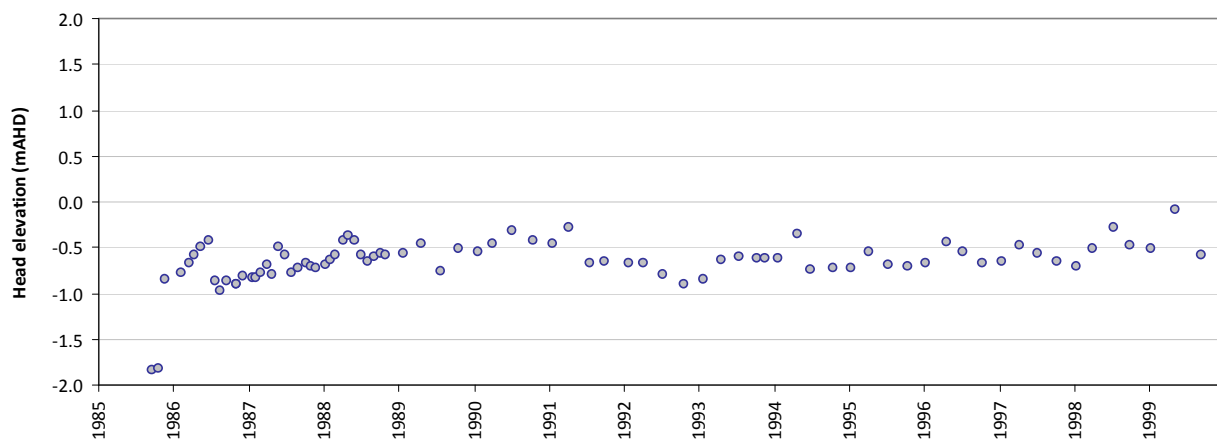
Mean error (ME)	0.06
Mean absolute error (MAE)	0.17
Root mean square error (RMSE)	0.21
Standard deviation of residuals (STDres)	0.20
Correlation coefficient (R)	0.94
Nash Sutcliffe correlation coefficient (R2)	0.77

T630

Modelled vs observed time-series plot - T630



Residual time-series plot - T630

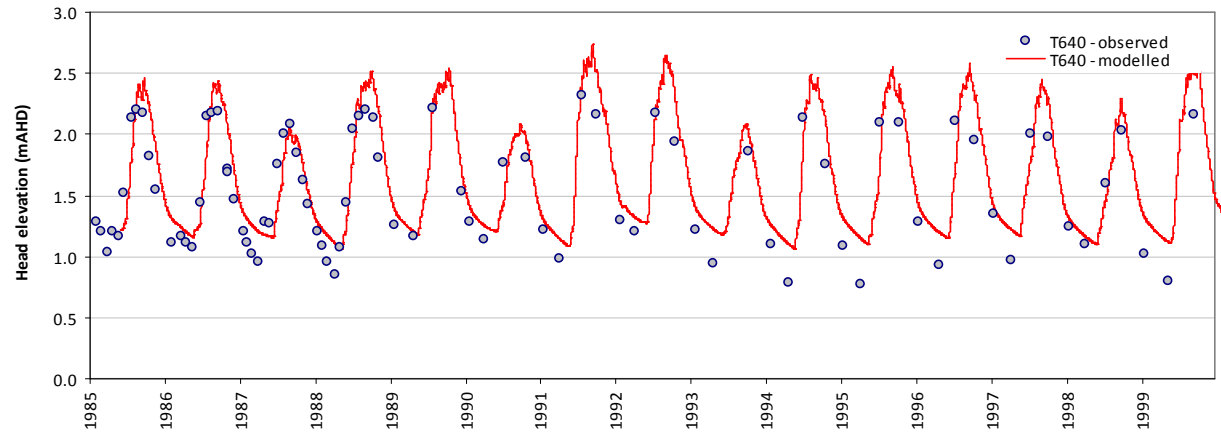


Statistics

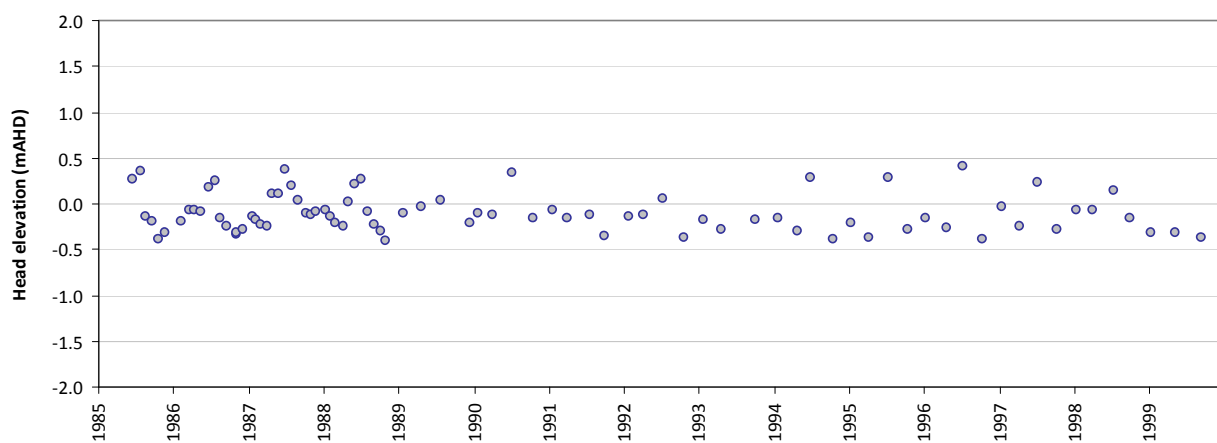
Mean error (ME)	-0.63
Mean absolute error (MAE)	0.63
Root mean square error (RMSE)	0.65
Standard deviation of residuals (STDres)	0.17
Correlation coefficient (R)	0.89
Nash Sutcliffe correlation coefficient (R2)	-5.81

T640

Modelled vs observed time-series plot - T640



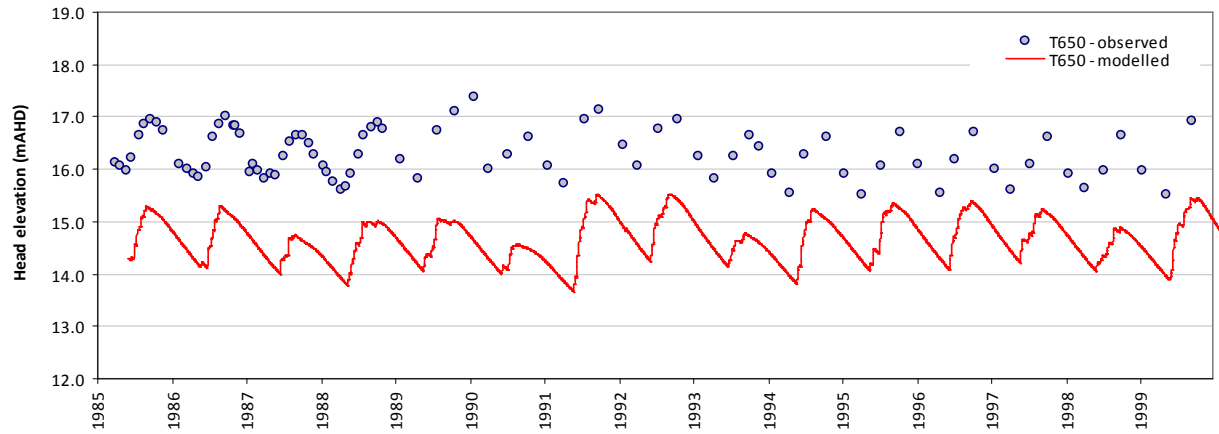
Residual time-series plot - T640



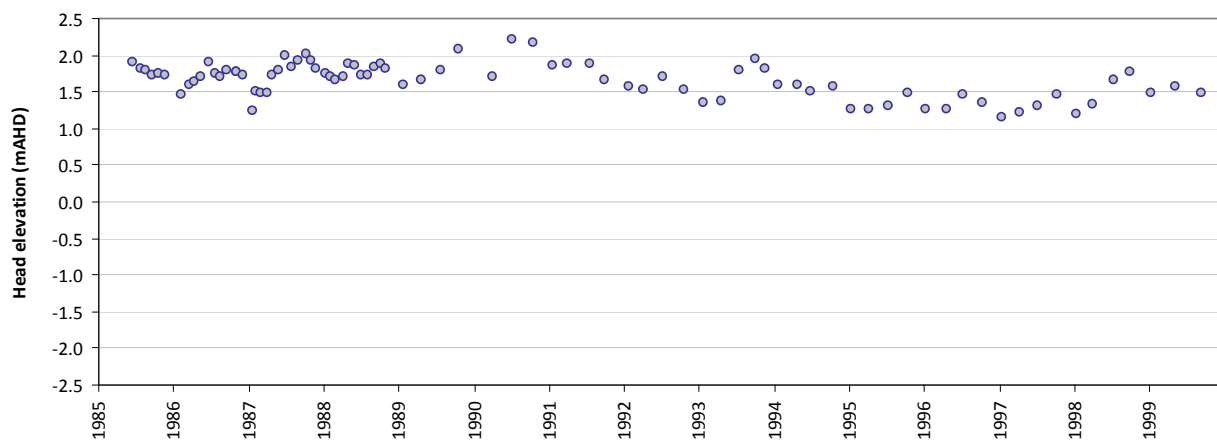
Statistics	
Mean error (ME)	-0.11
Mean absolute error (MAE)	0.21
Root mean square error (RMSE)	0.23
Standard deviation of residuals (STDres)	0.21
Correlation coefficient (R)	0.90
Nash Sutcliffe correlation coefficient (R2)	0.75

T650

Modelled vs observed time-series plot - T650



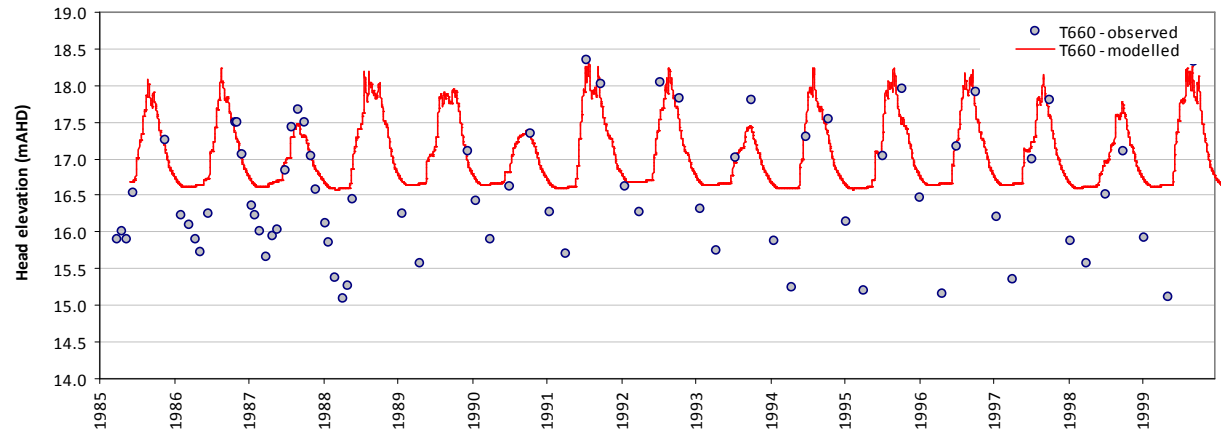
Residual time-series plot - T650



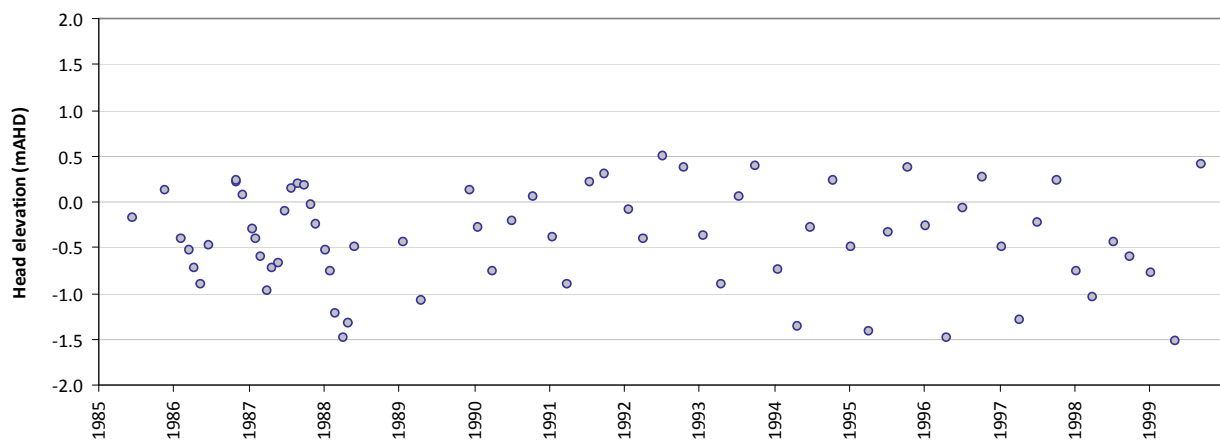
Statistics	
Mean error (ME)	1.67
Mean absolute error (MAE)	1.67
Root mean square error (RMSE)	1.69
Standard deviation of residuals (STDres)	0.26
Correlation coefficient (R)	0.82
Nash Sutcliffe correlation coefficient (R2)	-12.73

T660

Modelled vs observed time-series plot - T660



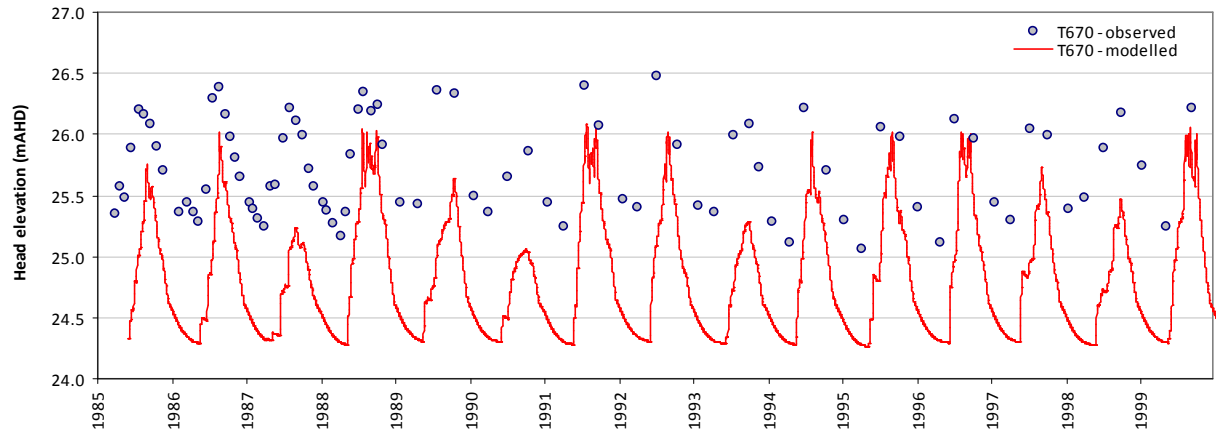
Residual time-series plot - T660



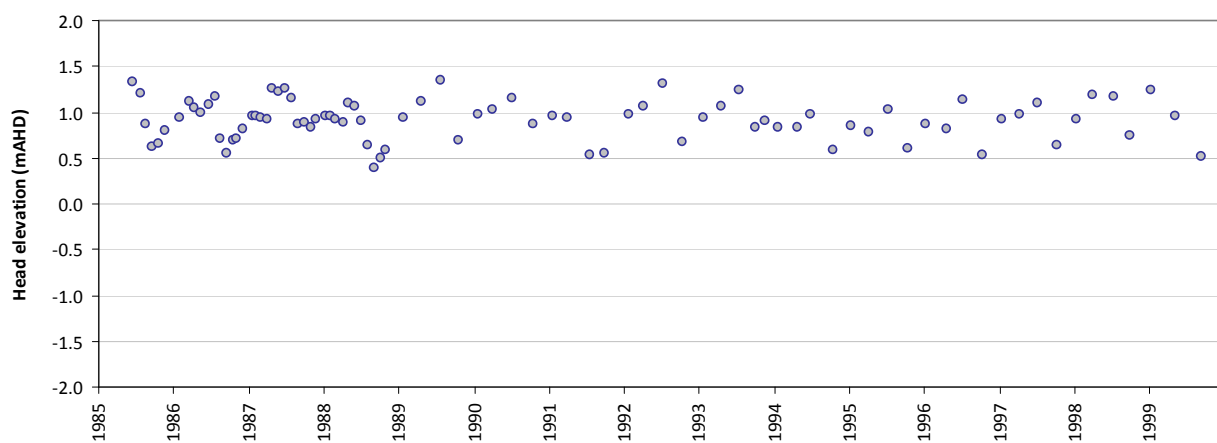
Statistics	
Mean error (ME)	-0.40
Mean absolute error (MAE)	0.53
Root mean square error (RMSE)	0.66
Standard deviation of residuals (STDres)	0.53
Correlation coefficient (R)	0.91
Nash Sutcliffe correlation coefficient (R2)	0.41

T670

Modelled vs observed time-series plot - T670



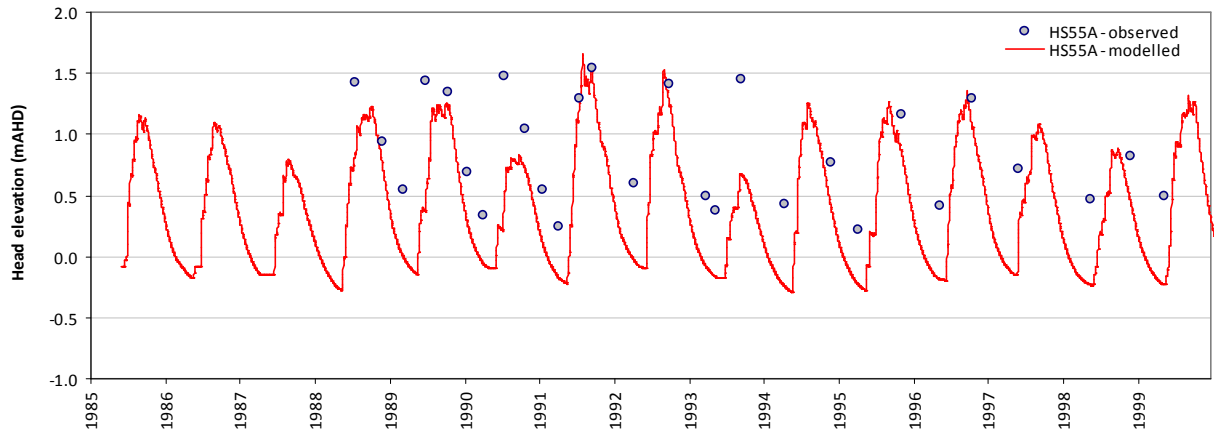
Residual time-series plot - T670



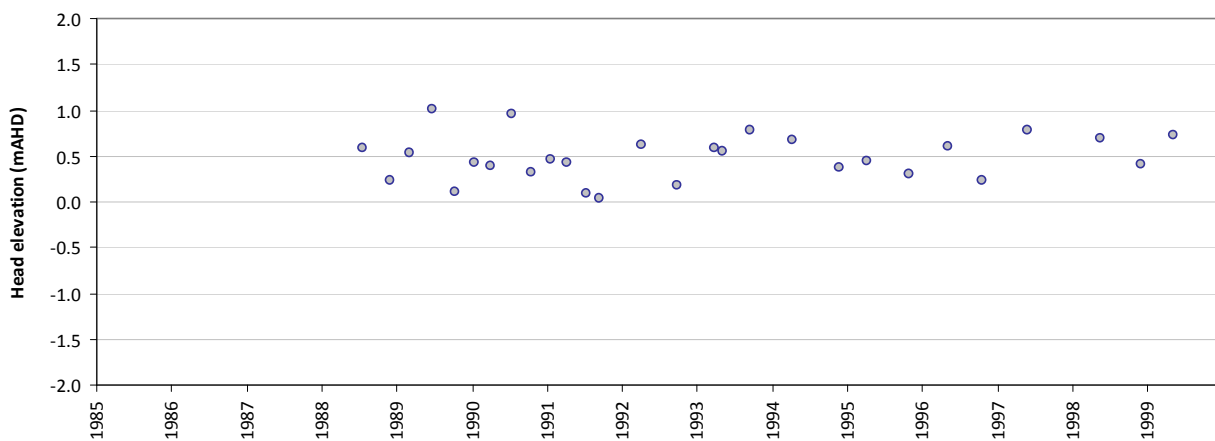
Statistics	
Mean error (ME)	0.91
Mean absolute error (MAE)	0.91
Root mean square error (RMSE)	0.94
Standard deviation of residuals (STDres)	0.22
Correlation coefficient (R)	0.89
Nash Sutcliffe correlation coefficient (R2)	-5.04

HS55A

Modelled vs observed time-series plot - HS55A



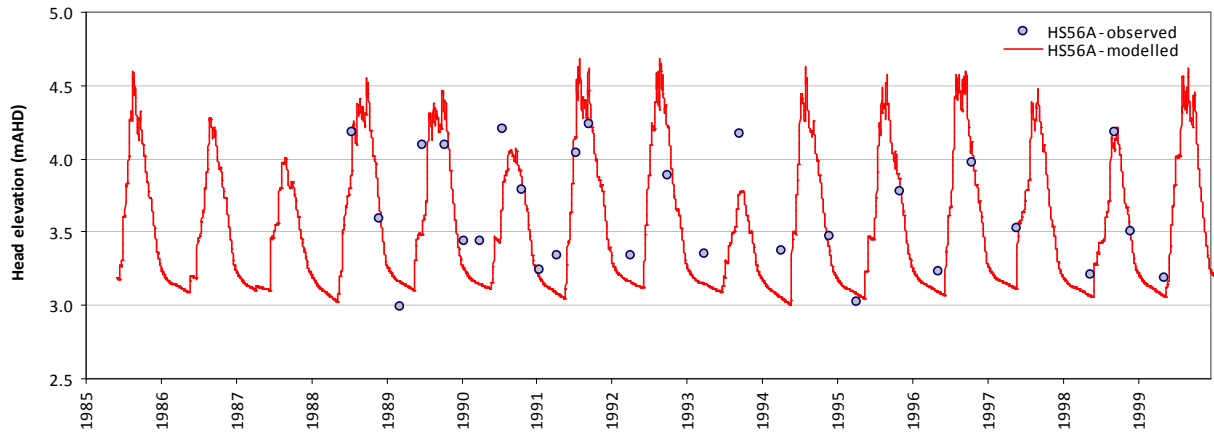
Residual time-series plot - HS55A



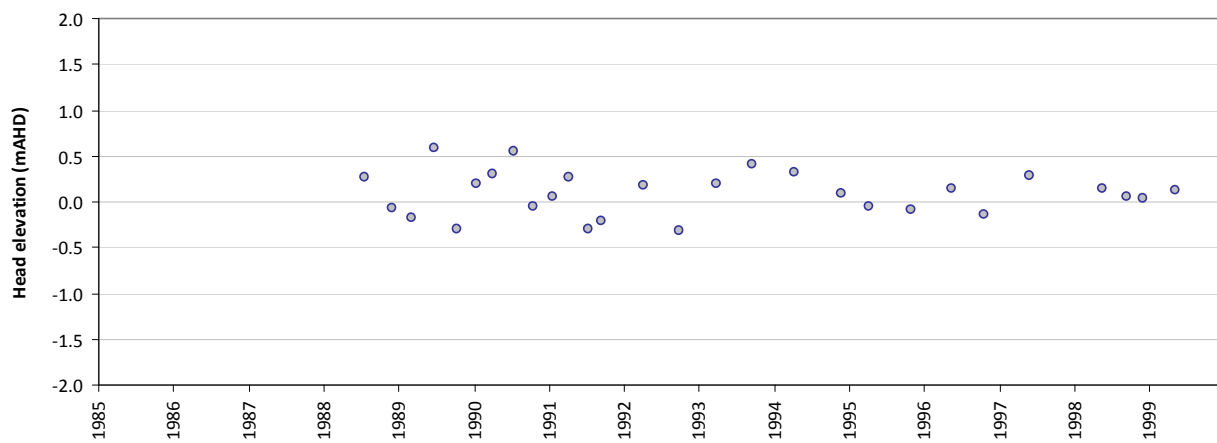
Statistics	
Mean error (ME)	0.50
Mean absolute error (MAE)	0.50
Root mean square error (RMSE)	0.56
Standard deviation of residuals (STDres)	0.25
Correlation coefficient (R)	0.89
Nash Sutcliffe correlation coefficient (R2)	-0.66

HS56A

Modelled vs observed time-series plot - HS56A



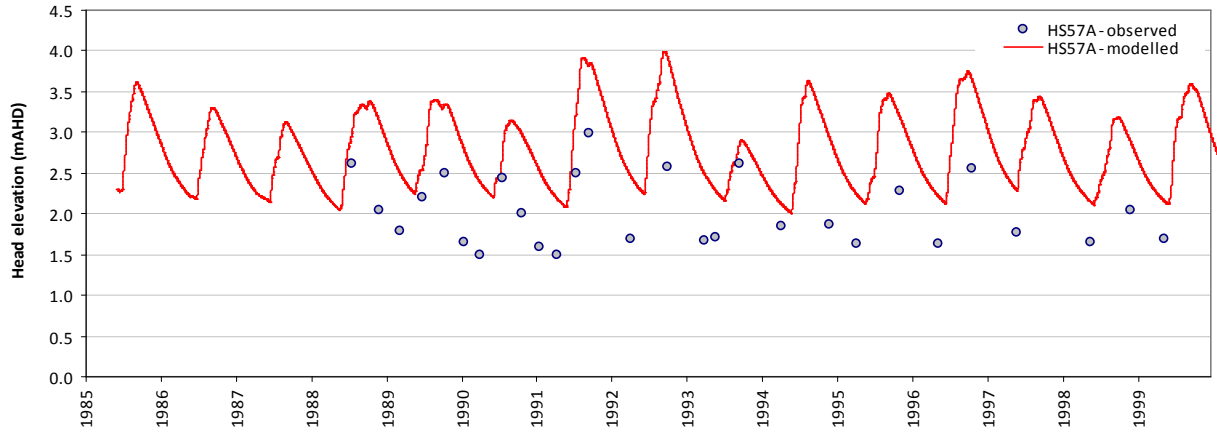
Residual time-series plot - HS56A



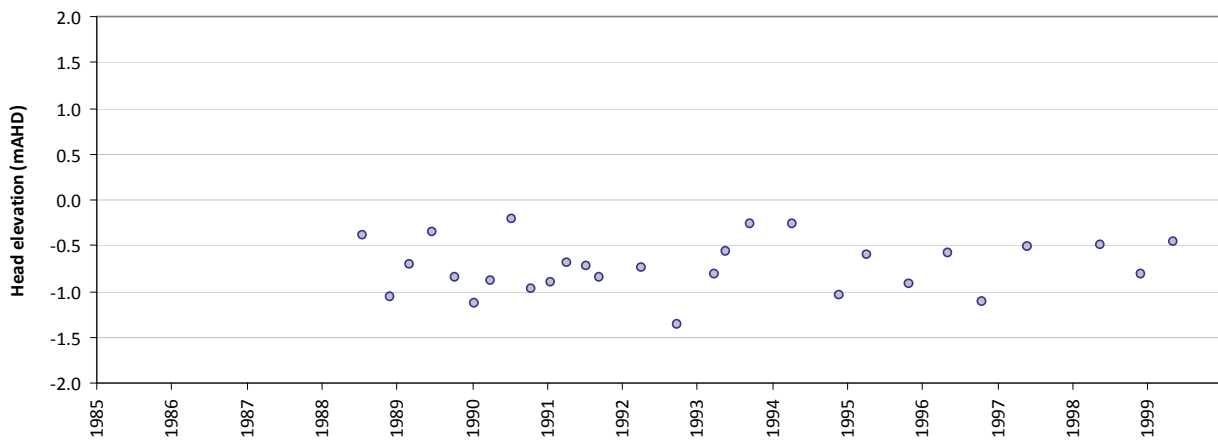
Statistics	
Mean error (ME)	0.10
Mean absolute error (MAE)	0.21
Root mean square error (RMSE)	0.25
Standard deviation of residuals (STDres)	0.23
Correlation coefficient (R)	0.86
Nash Sutcliffe correlation coefficient (R2)	0.58

HS57A

Modelled vs observed time-series plot - HS57A



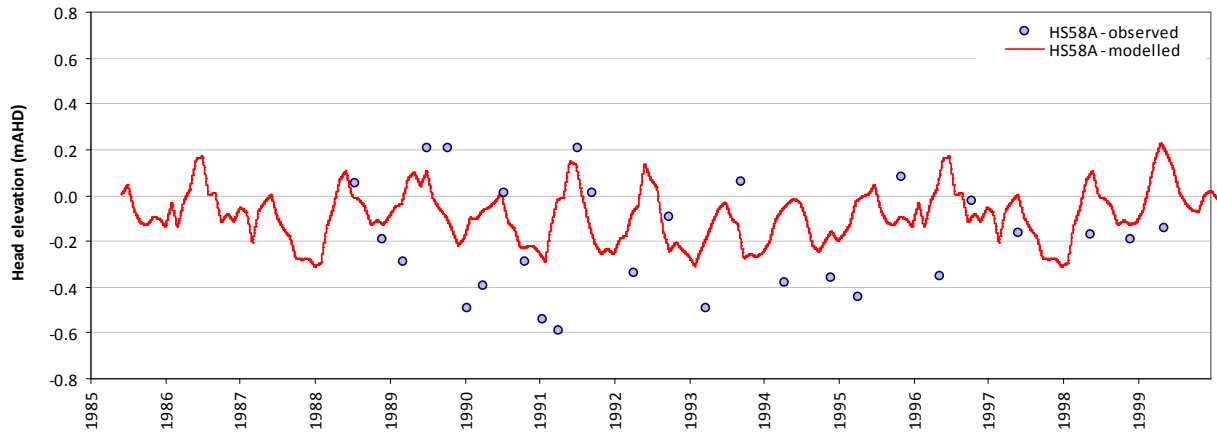
Residual time-series plot - HS57A



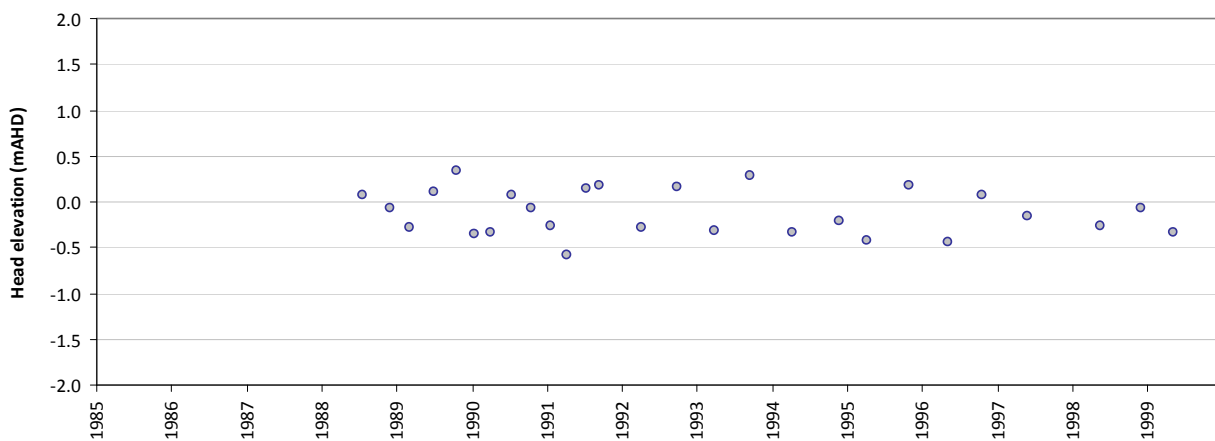
Statistics	
Mean error (ME)	-0.71
Mean absolute error (MAE)	0.71
Root mean square error (RMSE)	0.77
Standard deviation of residuals (STDres)	0.29
Correlation coefficient (R)	0.82
Nash Sutcliffe correlation coefficient (R2)	-2.47

HS58A

Modelled vs observed time-series plot - HS58A



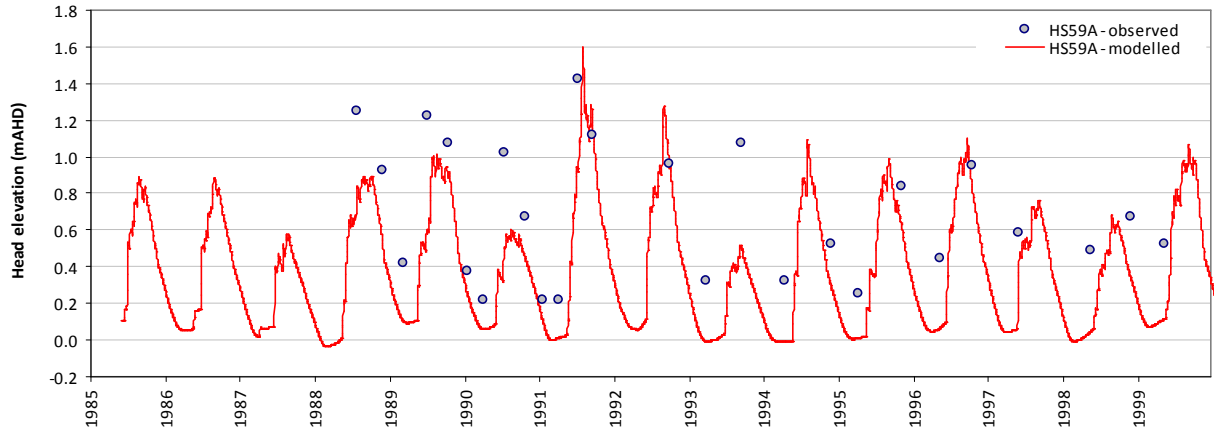
Residual time-series plot - HS58A



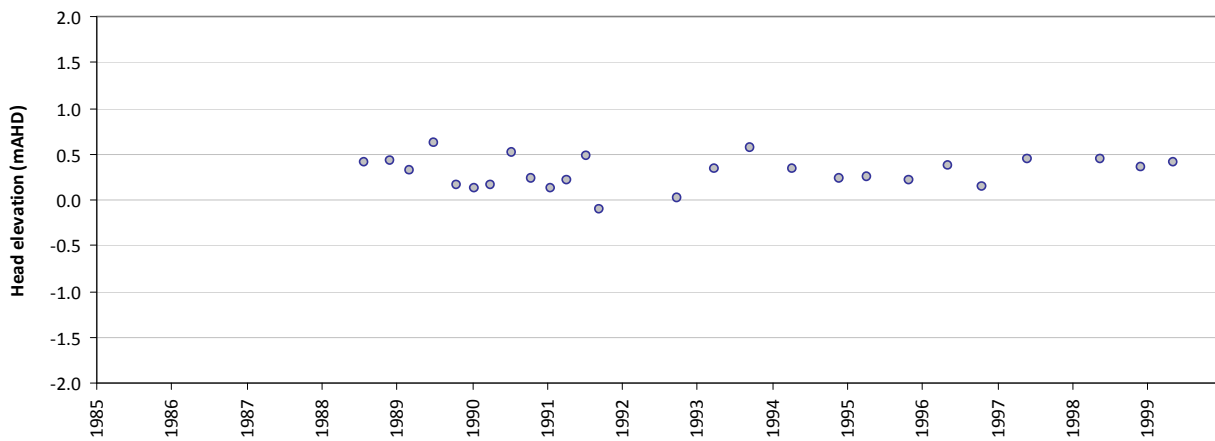
Statistics	
Mean error (ME)	-0.12
Mean absolute error (MAE)	0.24
Root mean square error (RMSE)	0.27
Standard deviation of residuals (STDres)	0.24
Correlation coefficient (R)	0.18
Nash Sutcliffe correlation coefficient (R2)	-0.36

HS59A

Modelled vs observed time-series plot - HS59A



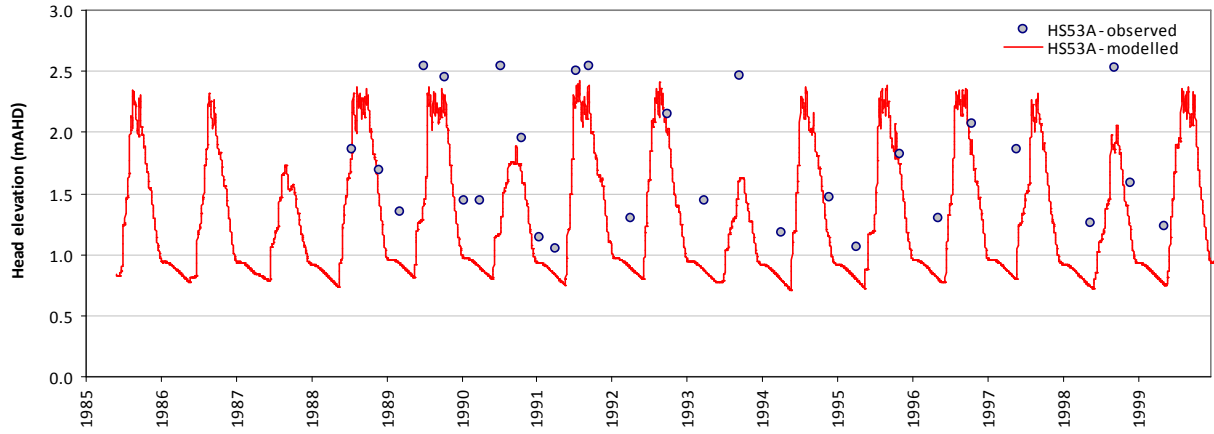
Residual time-series plot - HS59A



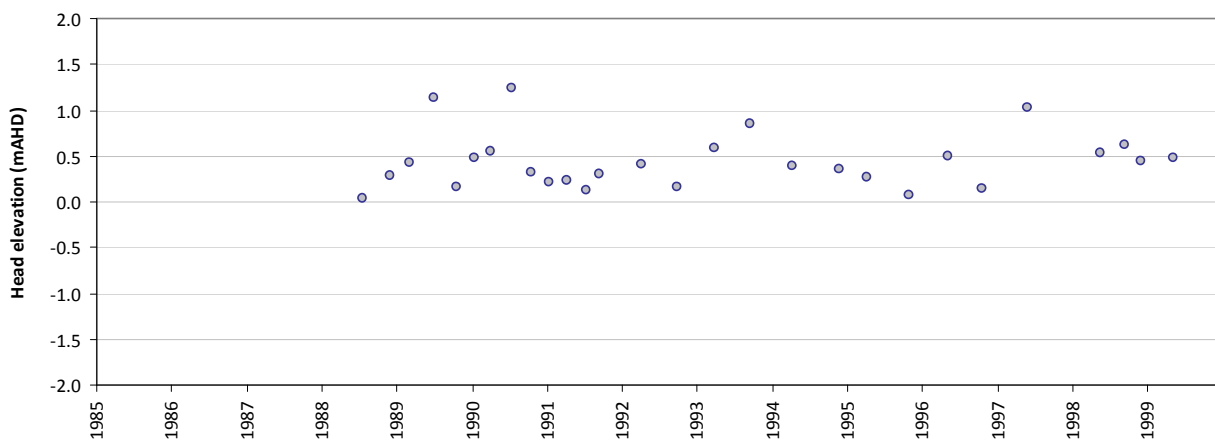
Statistics	
Mean error (ME)	0.31
Mean absolute error (MAE)	0.31
Root mean square error (RMSE)	0.35
Standard deviation of residuals (STDres)	0.17
Correlation coefficient (R)	0.88
Nash Sutcliffe correlation coefficient (R2)	0.03

HS53A

Modelled vs observed time-series plot - HS53A



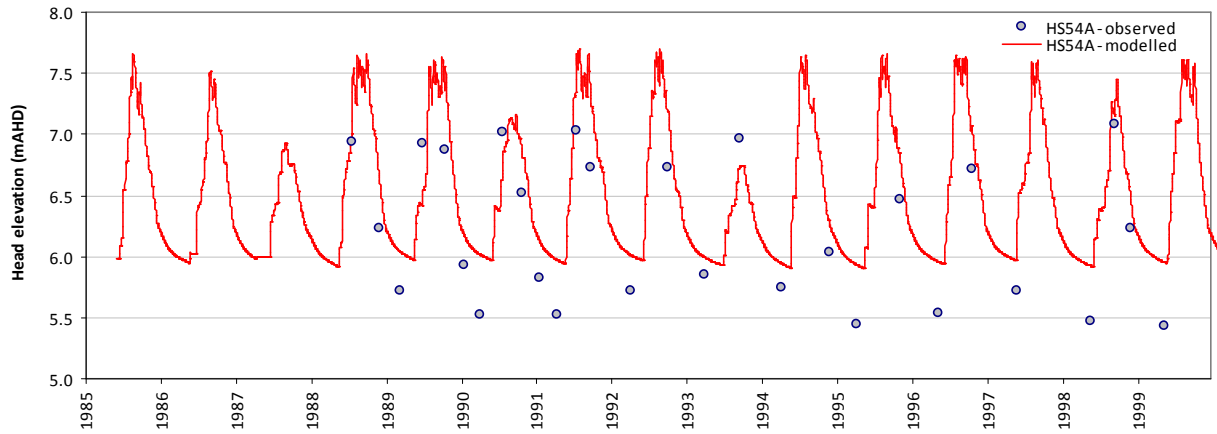
Residual time-series plot - HS53A



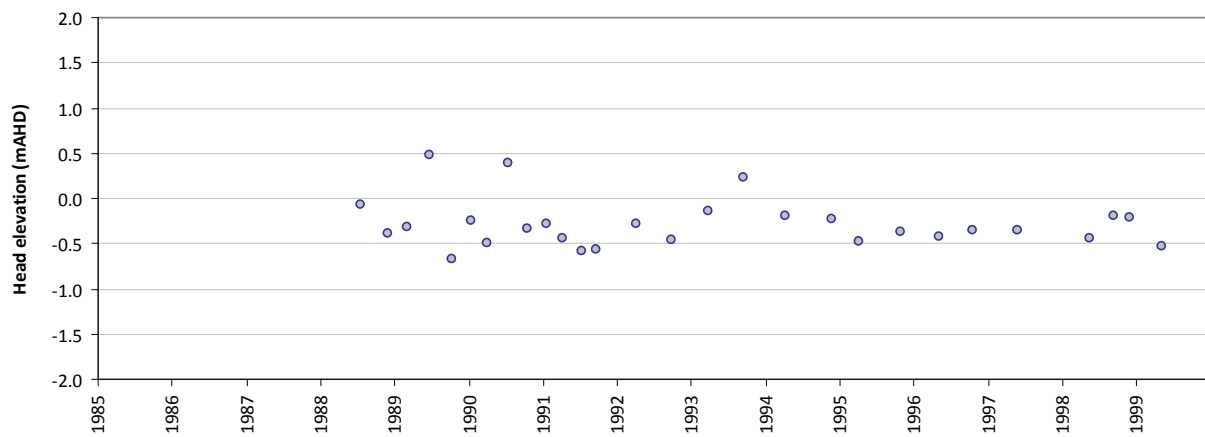
Statistics	
Mean error (ME)	0.45
Mean absolute error (MAE)	0.45
Root mean square error (RMSE)	0.54
Standard deviation of residuals (STDres)	0.30
Correlation coefficient (R)	0.83
Nash Sutcliffe correlation coefficient (R2)	-0.11

HS54A

Modelled vs observed time-series plot - HS54A

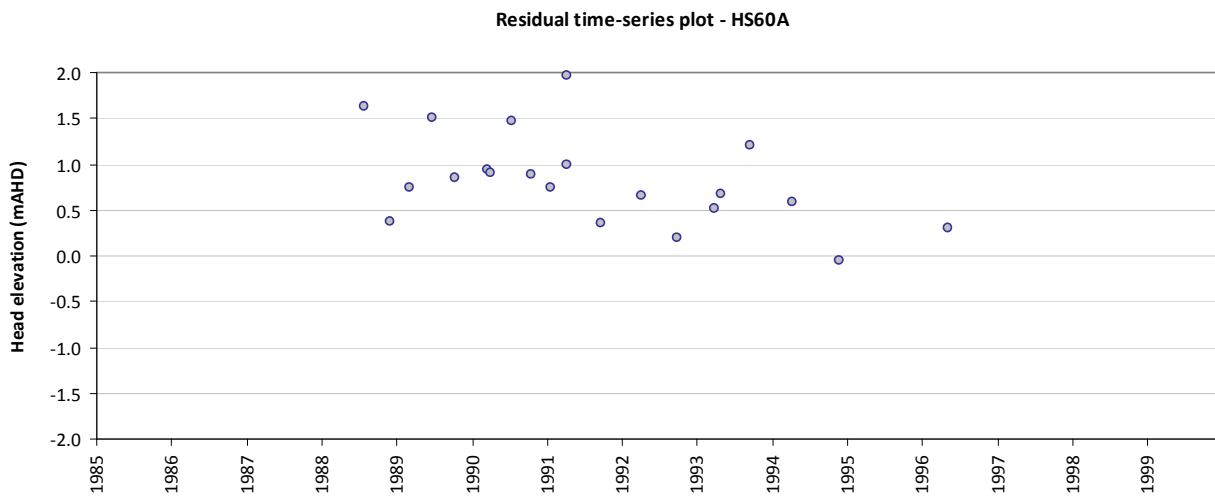
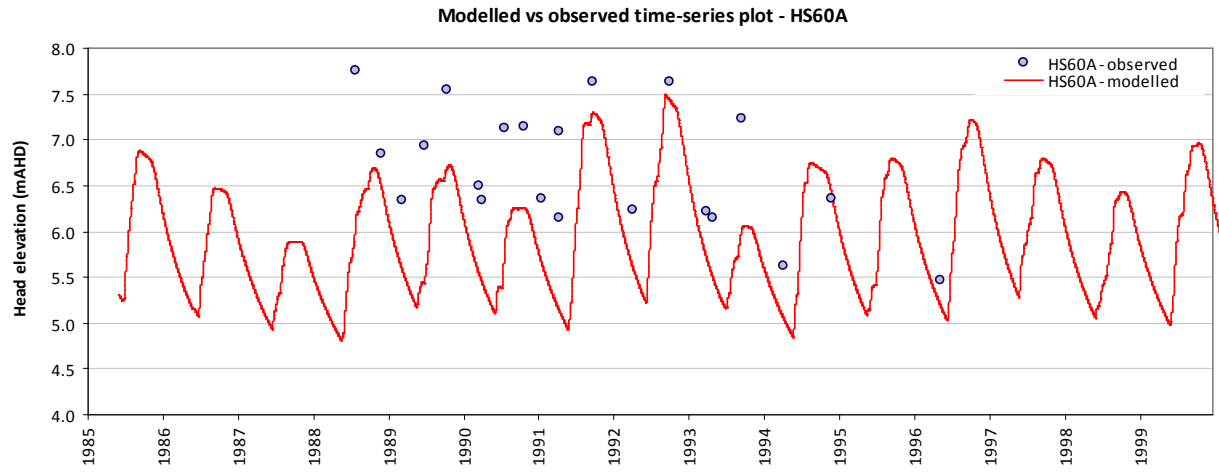


Residual time-series plot - HS54A



Statistics	
Mean error (ME)	-0.28
Mean absolute error (MAE)	0.36
Root mean square error (RMSE)	0.38
Standard deviation of residuals (STDres)	0.26
Correlation coefficient (R)	0.89
Nash Sutcliffe correlation coefficient (R2)	0.57

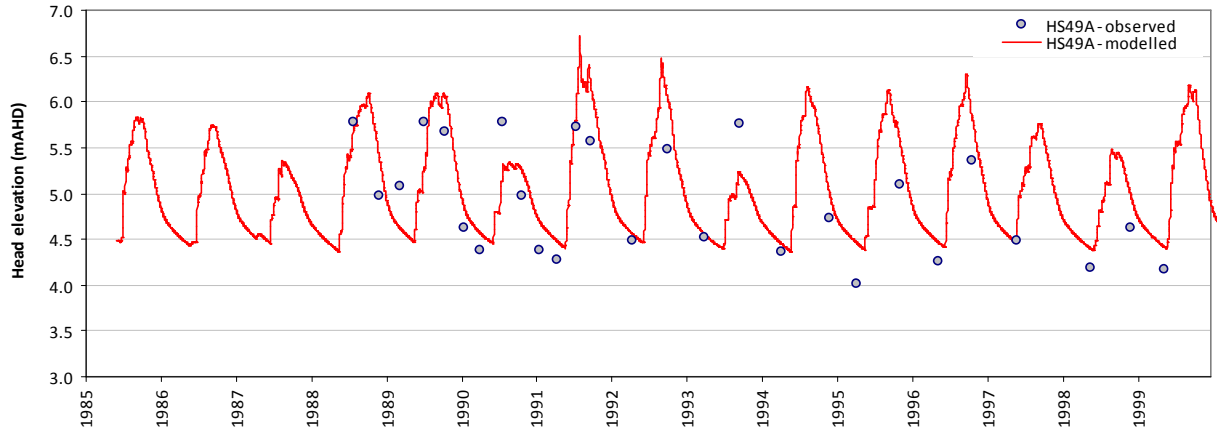
HS60A



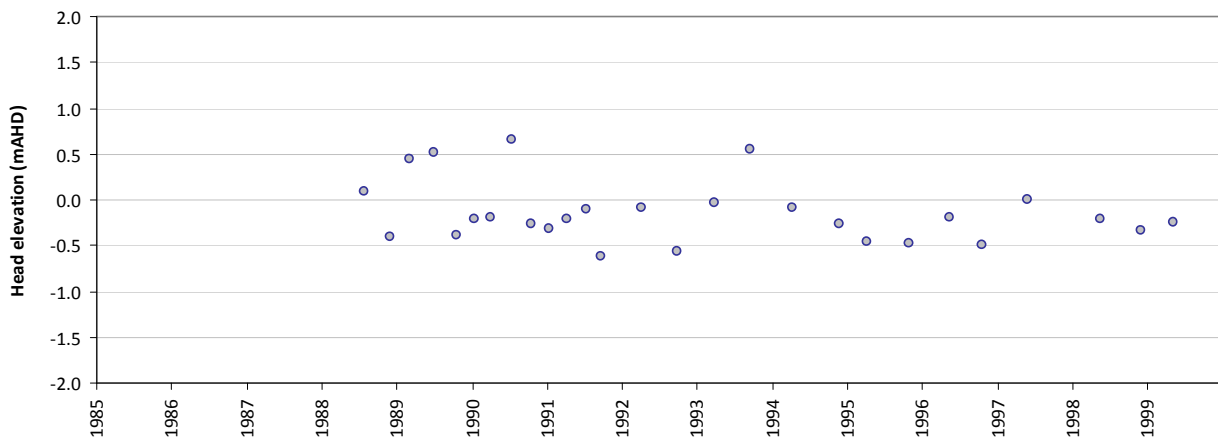
Statistics	
Mean error (ME)	0.83
Mean absolute error (MAE)	0.84
Root mean square error (RMSE)	0.97
Standard deviation of residuals (STDres)	0.50
Correlation coefficient (R)	0.71
Nash Sutcliffe correlation coefficient (R2)	-1.24

HS49A

Modelled vs observed time-series plot - HS49A



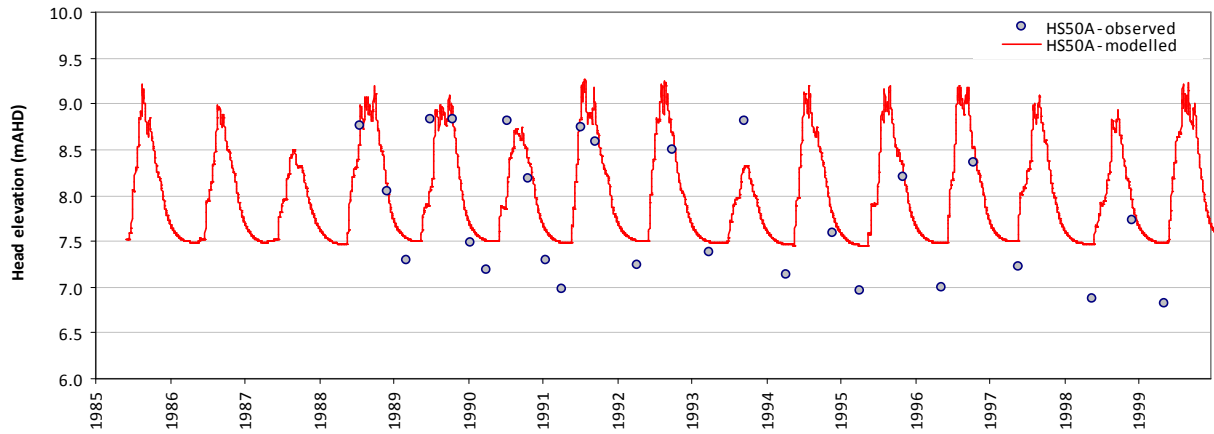
Residual time-series plot - HS49A



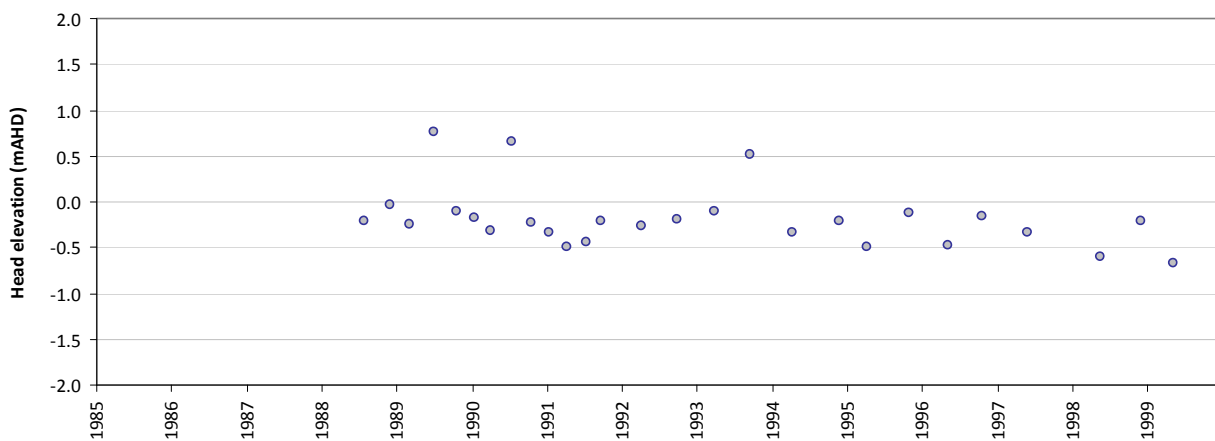
Statistics	
Mean error (ME)	-0.14
Mean absolute error (MAE)	0.31
Root mean square error (RMSE)	0.36
Standard deviation of residuals (STDres)	0.33
Correlation coefficient (R)	0.84
Nash Sutcliffe correlation coefficient (R2)	0.63

HS50A

Modelled vs observed time-series plot - HS50A



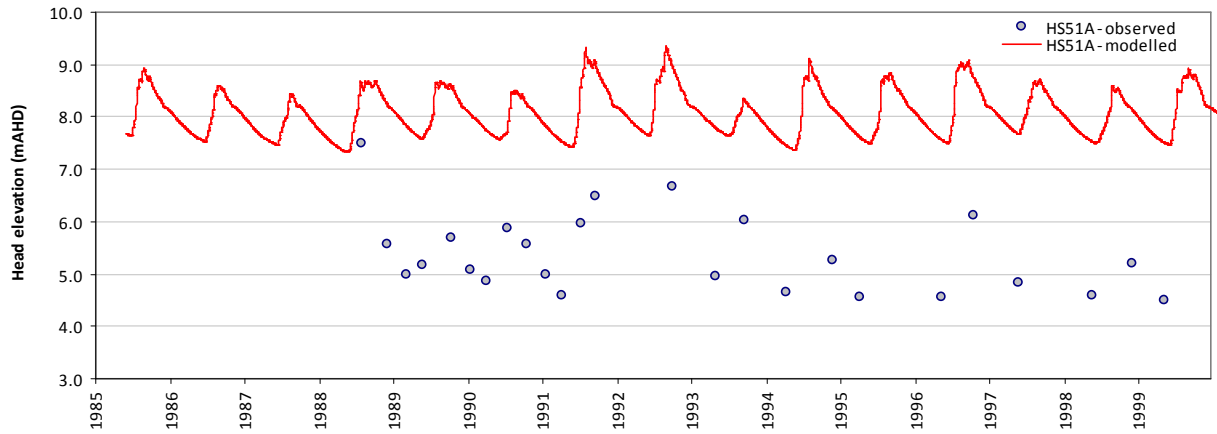
Residual time-series plot - HS50A



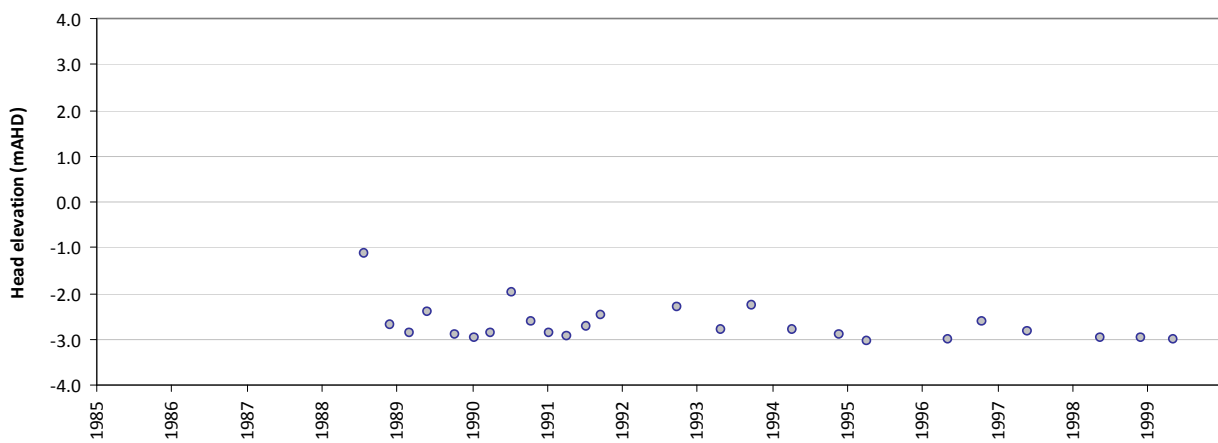
Statistics	
Mean error (ME)	-0.19
Mean absolute error (MAE)	0.33
Root mean square error (RMSE)	0.38
Standard deviation of residuals (STDres)	0.33
Correlation coefficient (R)	0.90
Nash Sutcliffe correlation coefficient (R2)	0.72

HS51A

Modelled vs observed time-series plot - HS51A



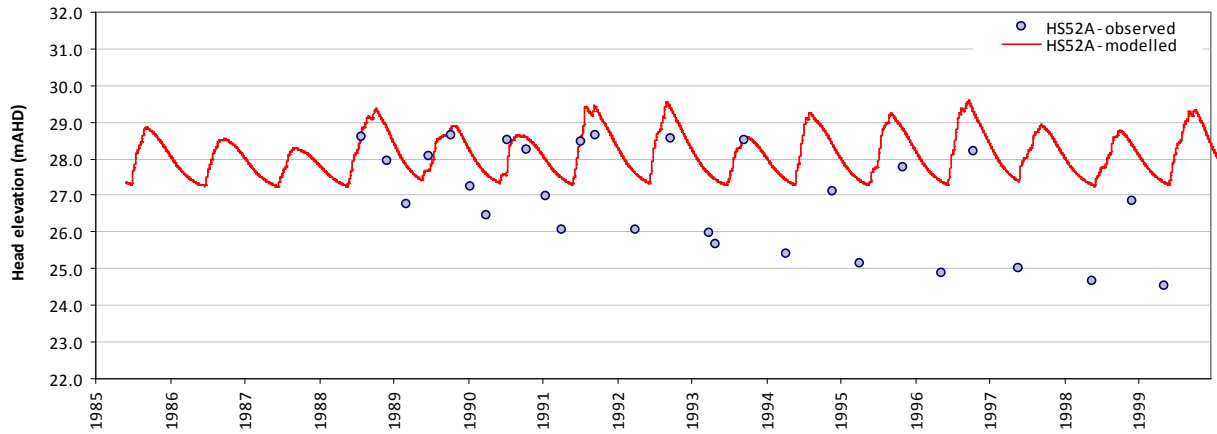
Residual time-series plot - HS51A



Statistics	
Mean error (ME)	-2.69
Mean absolute error (MAE)	2.69
Root mean square error (RMSE)	2.72
Standard deviation of residuals (STDres)	0.41
Correlation coefficient (R)	0.88
Nash Sutcliffe correlation coefficient (R2)	-12.01

HS52A

Modelled vs observed time-series plot - HS52A



Residual time-series plot - HS52A

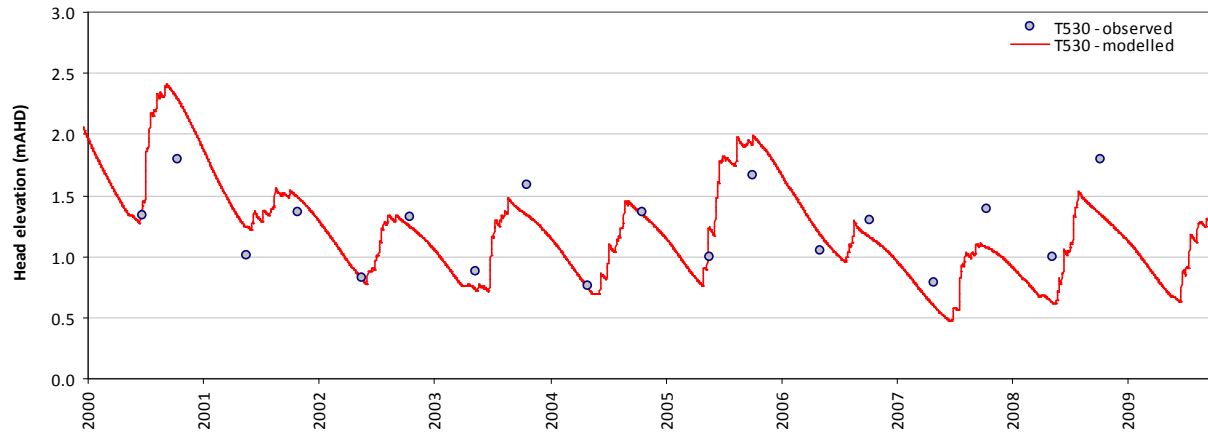


Statistics	
Mean error (ME)	-1.19
Mean absolute error (MAE)	1.25
Root mean square error (RMSE)	1.47
Standard deviation of residuals (STDres)	0.87
Correlation coefficient (R)	0.87
Nash Sutcliffe correlation coefficient (R2)	-0.12

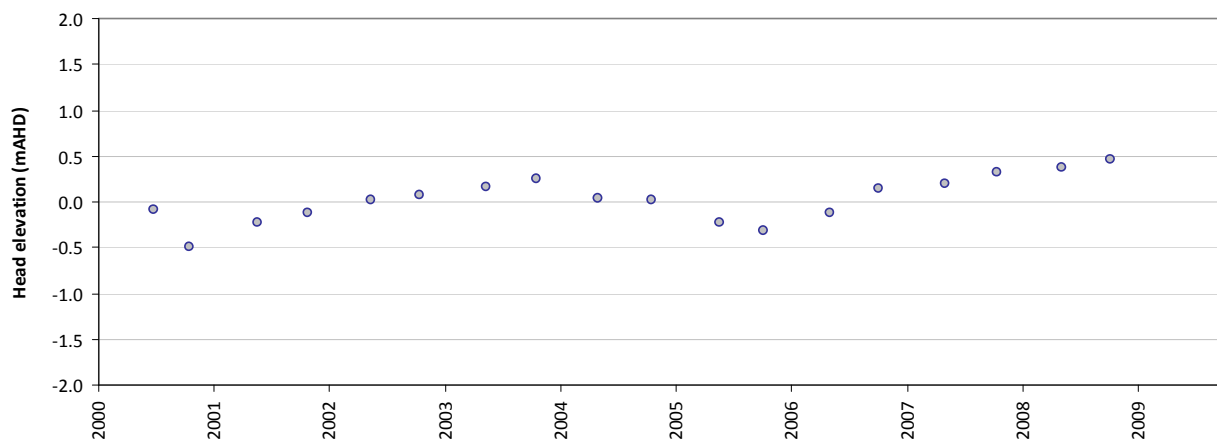
Appendix B: Validation bore time-series and statistics

T530

Modelled vs observed time-series plot - T530



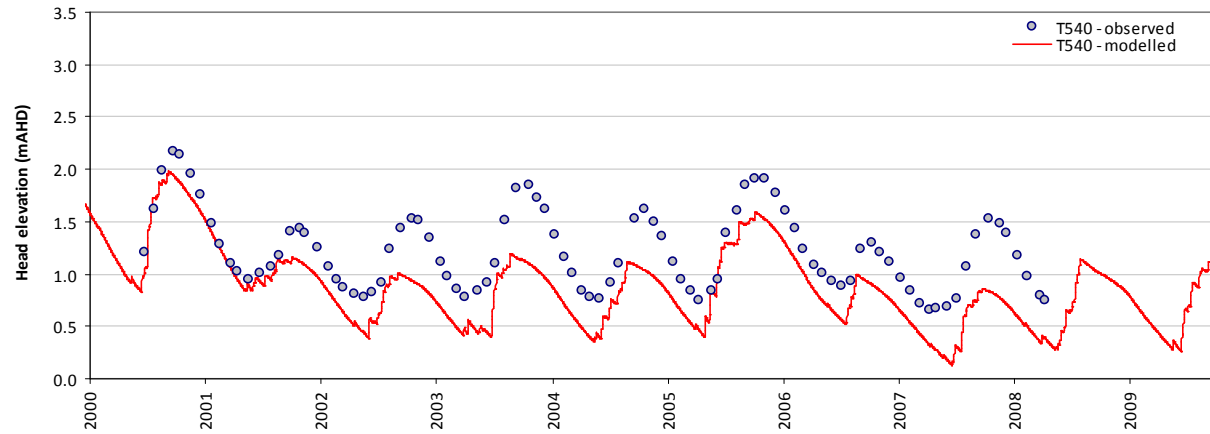
Residual time-series plot - T530



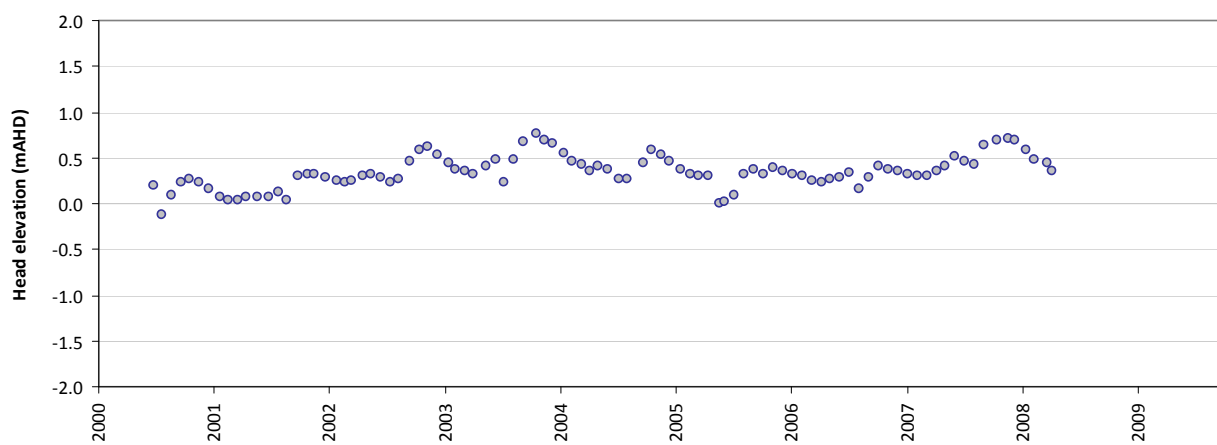
Statistics	
Mean error (ME)	0.02
Mean absolute error (MAE)	0.20
Root mean square error (RMSE)	0.25
Standard deviation of residuals (STDres)	0.25
Correlation coefficient (R)	0.82
Nash Sutcliffe correlation coefficient (R2)	0.43

T540

Modelled vs observed time-series plot - T540



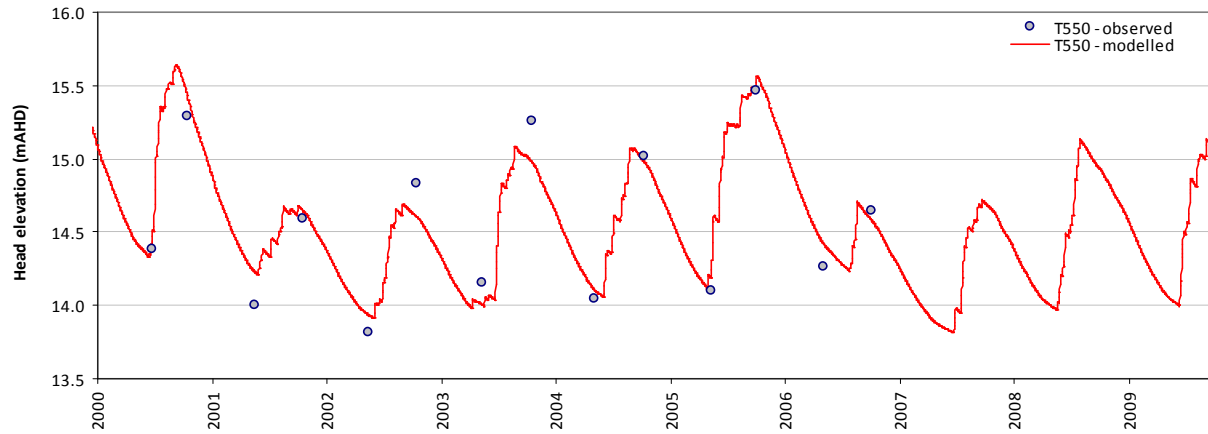
Residual time-series plot - T540



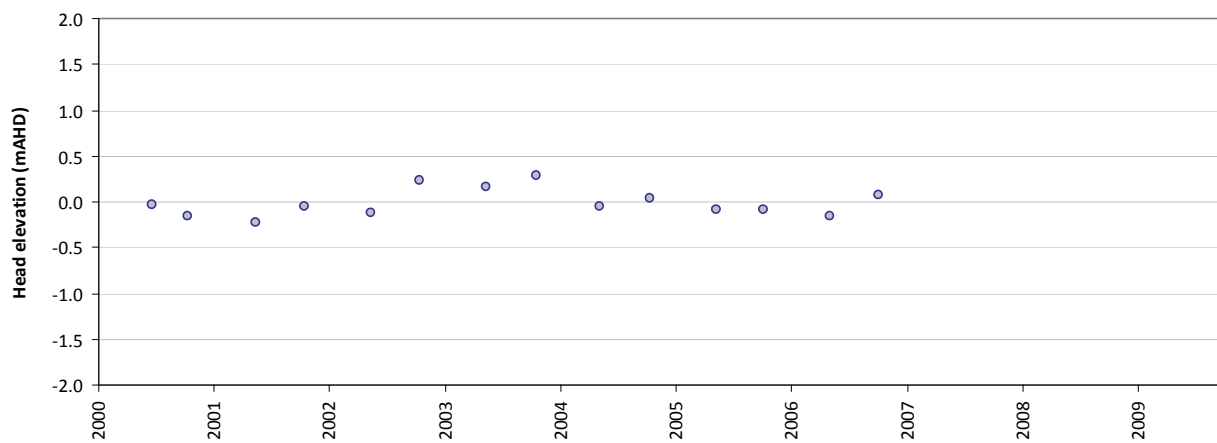
Statistics	
Mean error (ME)	0.34
Mean absolute error (MAE)	0.34
Root mean square error (RMSE)	0.39
Standard deviation of residuals (STDres)	0.18
Correlation coefficient (R)	0.89
Nash Sutcliffe correlation coefficient (R2)	-0.08

T550

Modelled vs observed time-series plot - T550



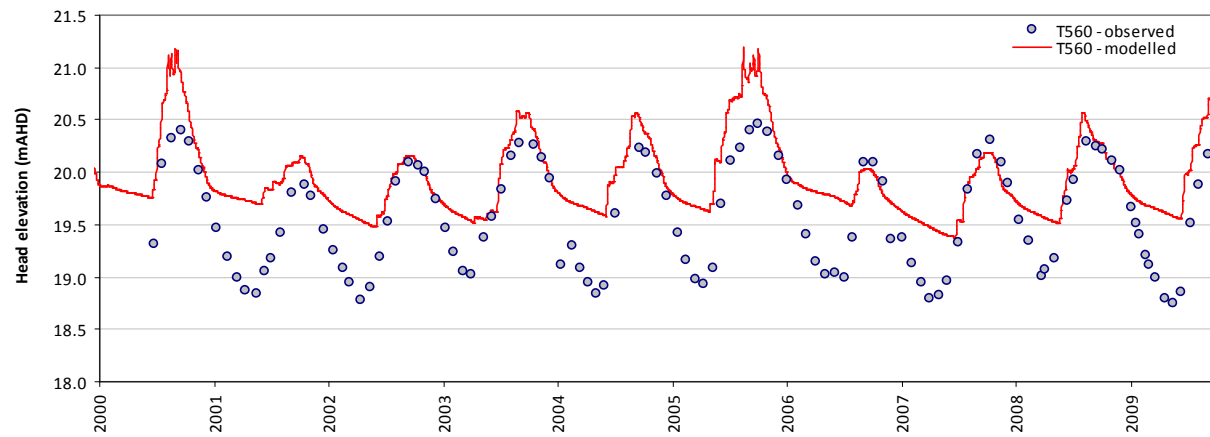
Residual time-series plot - T550



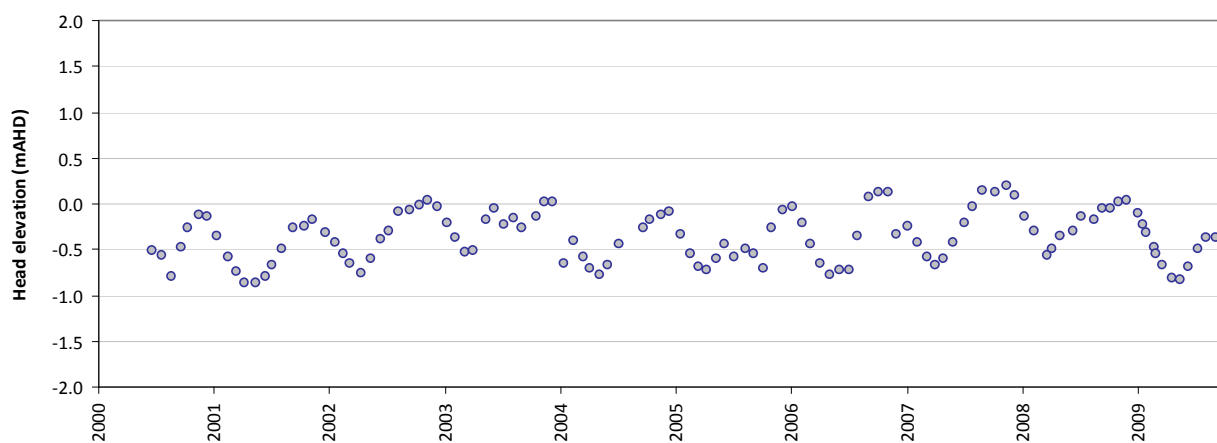
Statistics	
Mean error (ME)	-0.01
Mean absolute error (MAE)	0.13
Root mean square error (RMSE)	0.15
Standard deviation of residuals (STDres)	0.15
Correlation coefficient (R)	0.96
Nash Sutcliffe correlation coefficient (R2)	0.92

T560

Modelled vs observed time-series plot - T560



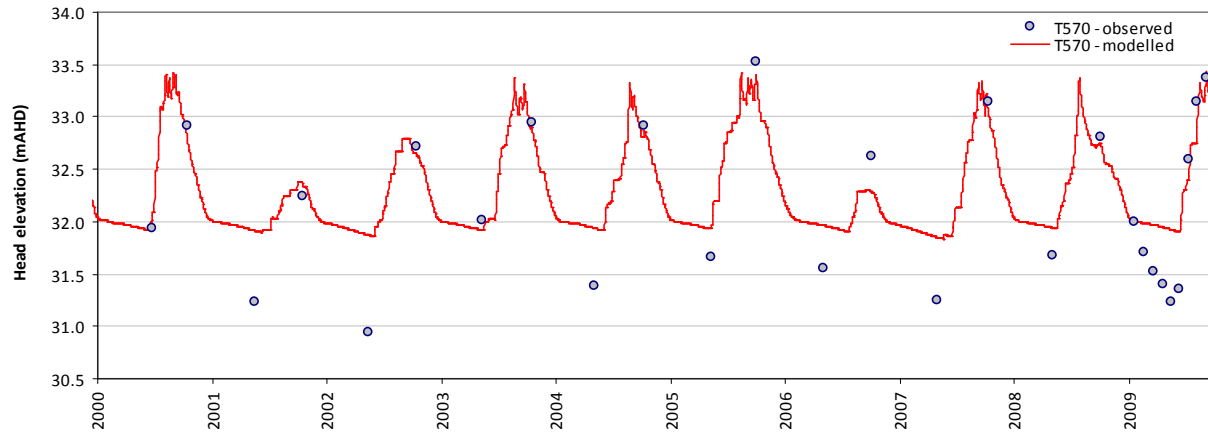
Residual time-series plot - T560



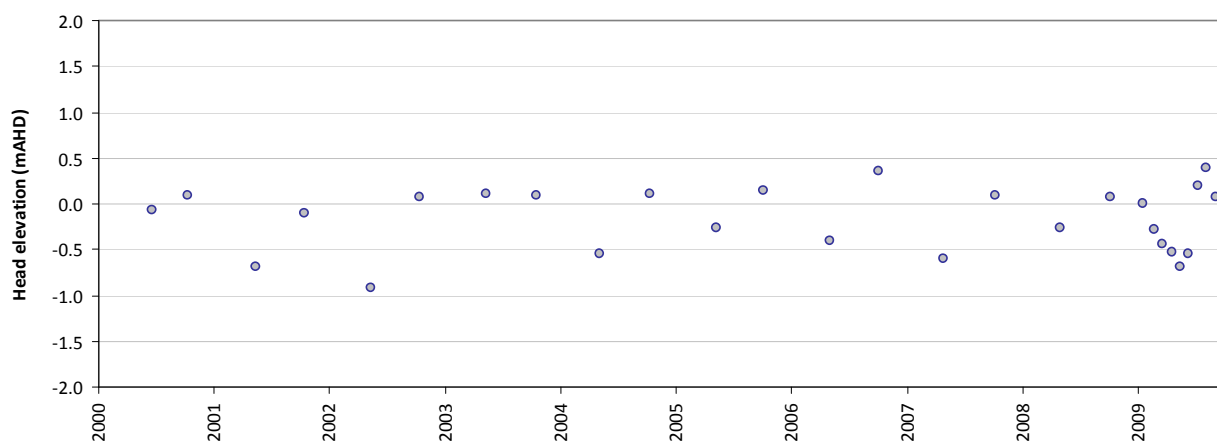
Statistics	
Mean error (ME)	-0.37
Mean absolute error (MAE)	0.38
Root mean square error (RMSE)	0.46
Standard deviation of residuals (STDres)	0.27
Correlation coefficient (R)	0.85
Nash Sutcliffe correlation coefficient (R2)	0.16

T570

Modelled vs observed time-series plot - T570



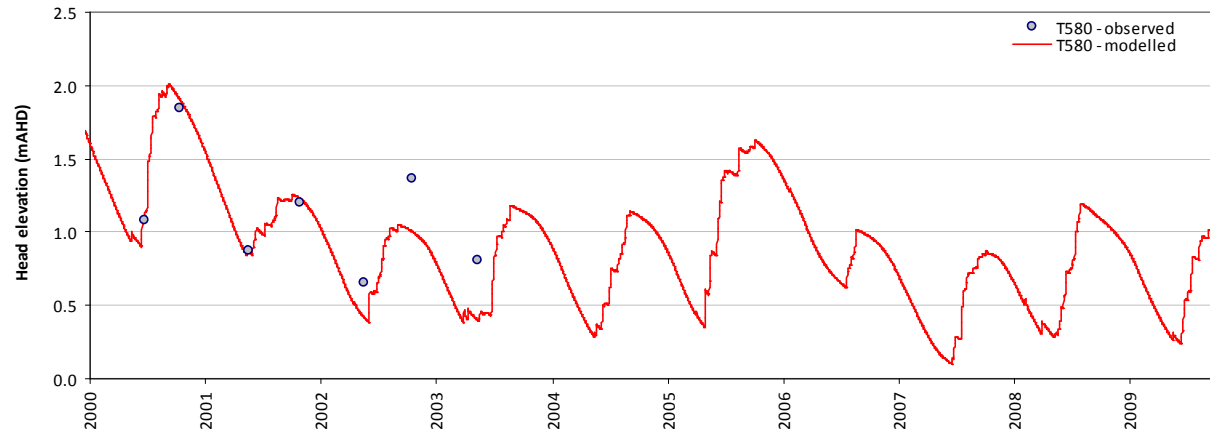
Residual time-series plot - T570



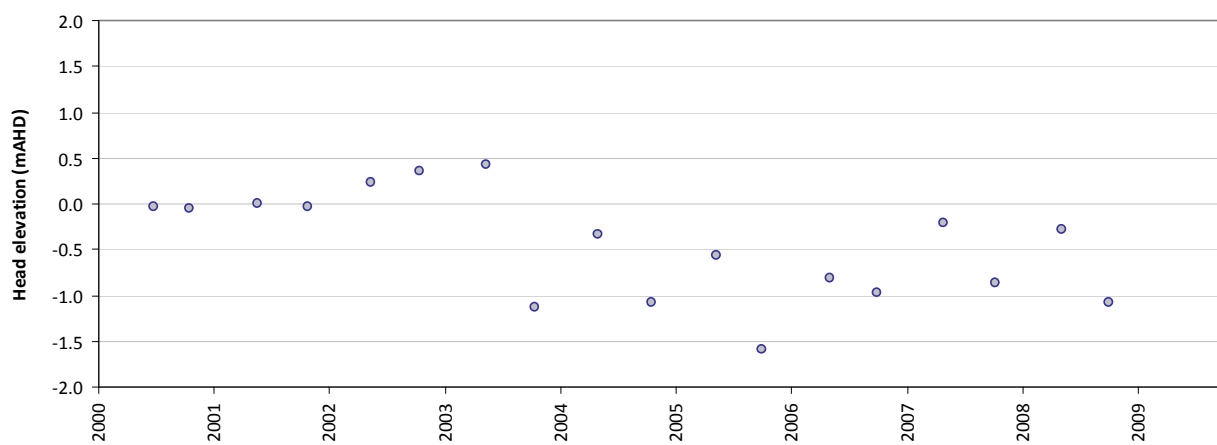
Statistics	
Mean error (ME)	-0.16
Mean absolute error (MAE)	0.30
Root mean square error (RMSE)	0.38
Standard deviation of residuals (STDres)	0.35
Correlation coefficient (R)	0.94
Nash Sutcliffe correlation coefficient (R2)	0.74

T580

Modelled vs observed time-series plot - T580



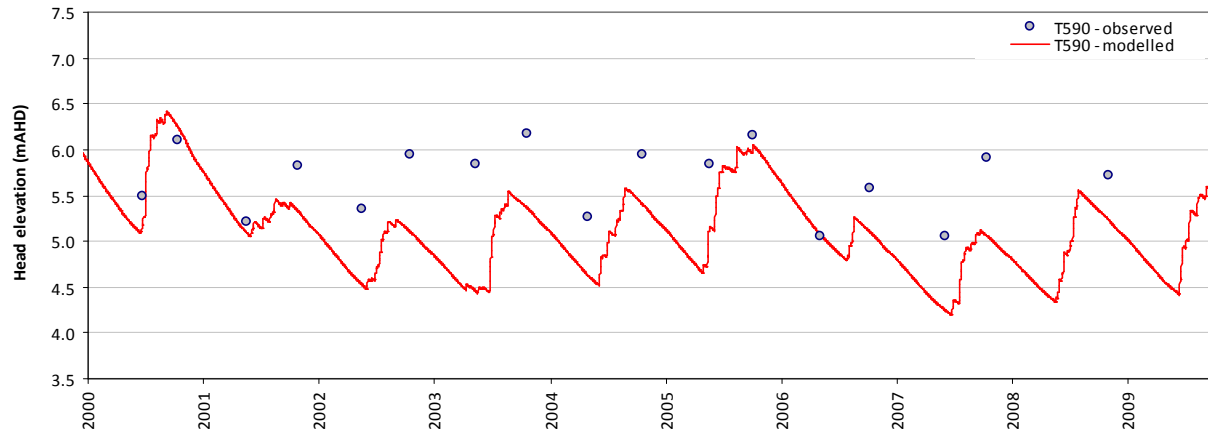
Residual time-series plot - T580



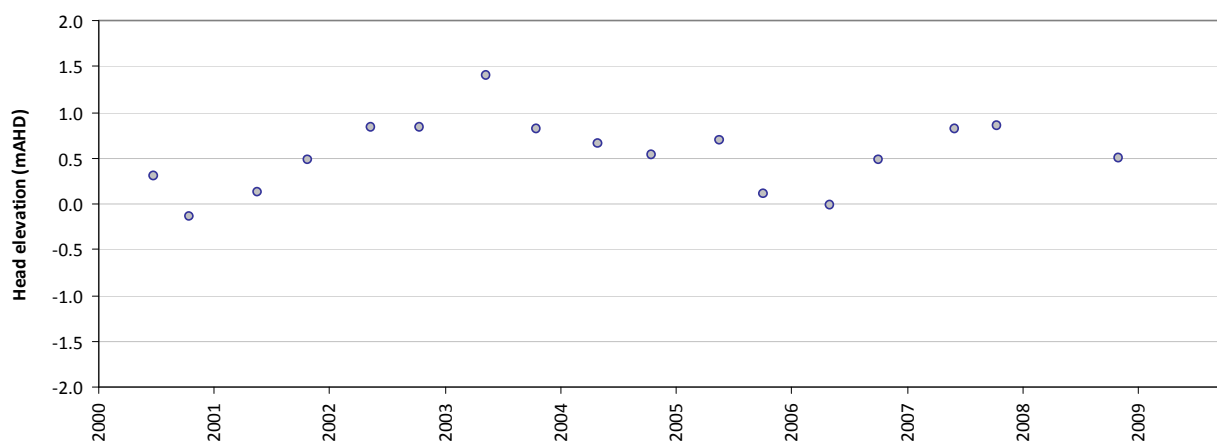
Statistics	
Mean error (ME)	0.19
Mean absolute error (MAE)	0.22
Root mean square error (RMSE)	0.27
Standard deviation of residuals (STDres)	0.20
Correlation coefficient (R)	0.89
Nash Sutcliffe correlation coefficient (R2)	0.41

T590

Modelled vs observed time-series plot - T590



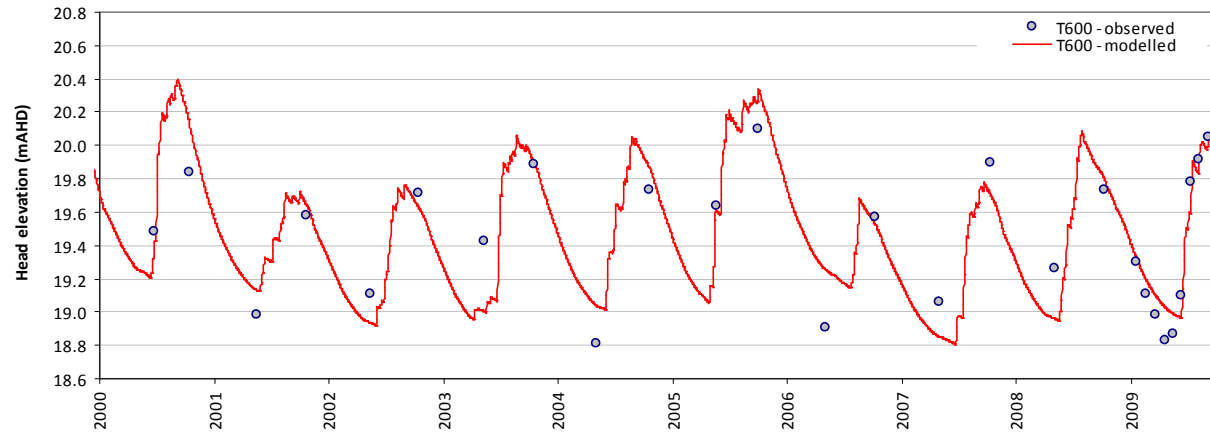
Residual time-series plot - T590



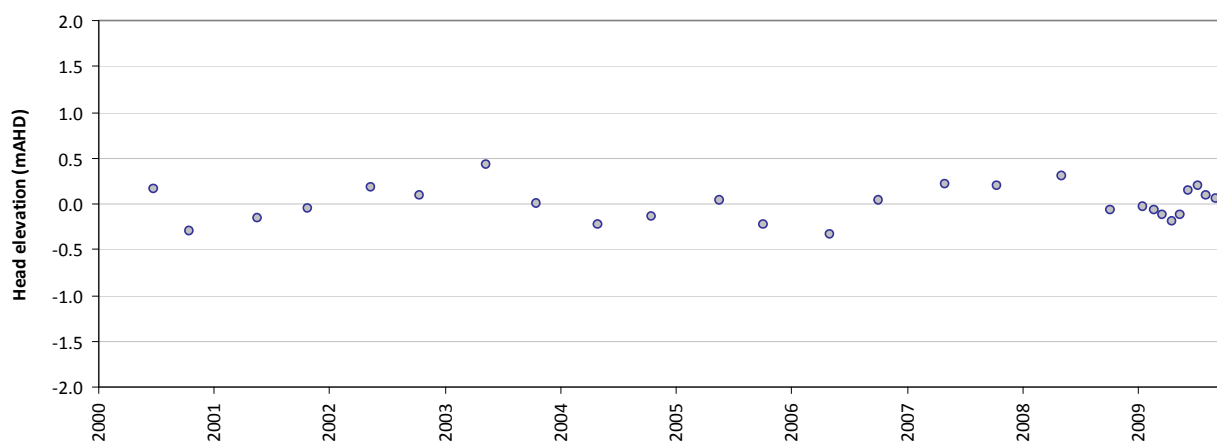
Statistics	
Mean error (ME)	0.54
Mean absolute error (MAE)	0.56
Root mean square error (RMSE)	0.66
Standard deviation of residuals (STDres)	0.37
Correlation coefficient (R)	0.66
Nash Sutcliffe correlation coefficient (R2)	-2.30

T600

Modelled vs observed time-series plot - T600



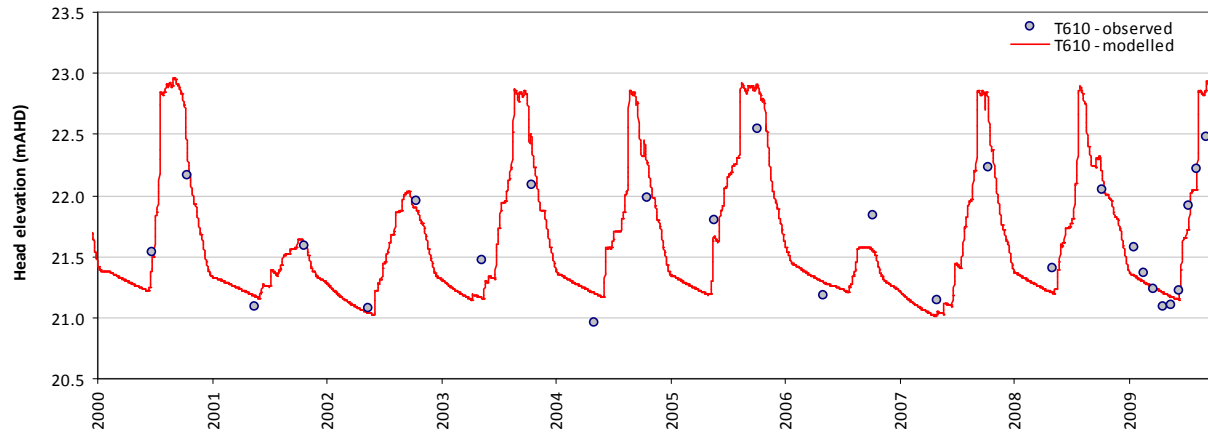
Residual time-series plot - T600



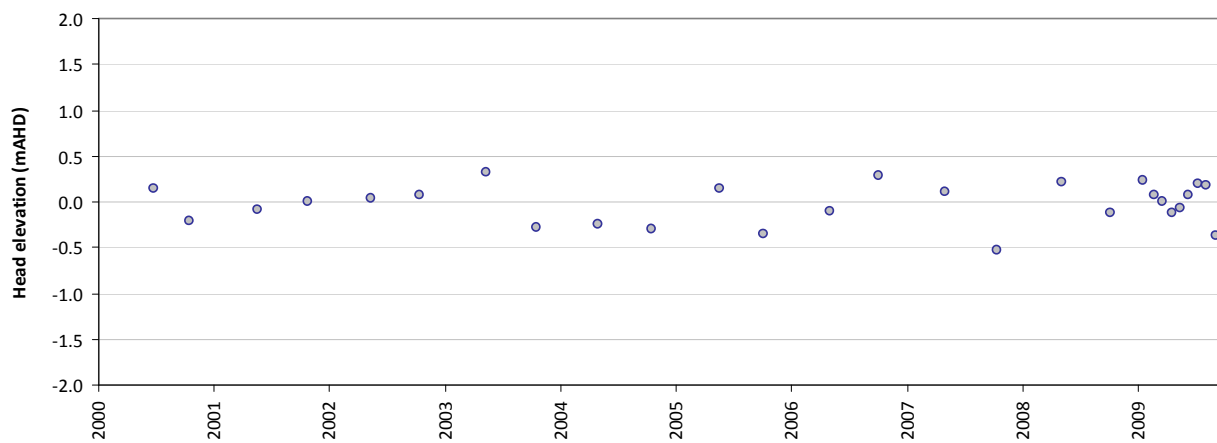
Statistics	
Mean error (ME)	0.00
Mean absolute error (MAE)	0.15
Root mean square error (RMSE)	0.19
Standard deviation of residuals (STDres)	0.19
Correlation coefficient (R)	0.90
Nash Sutcliffe correlation coefficient (R2)	0.79

T610

Modelled vs observed time-series plot - T610



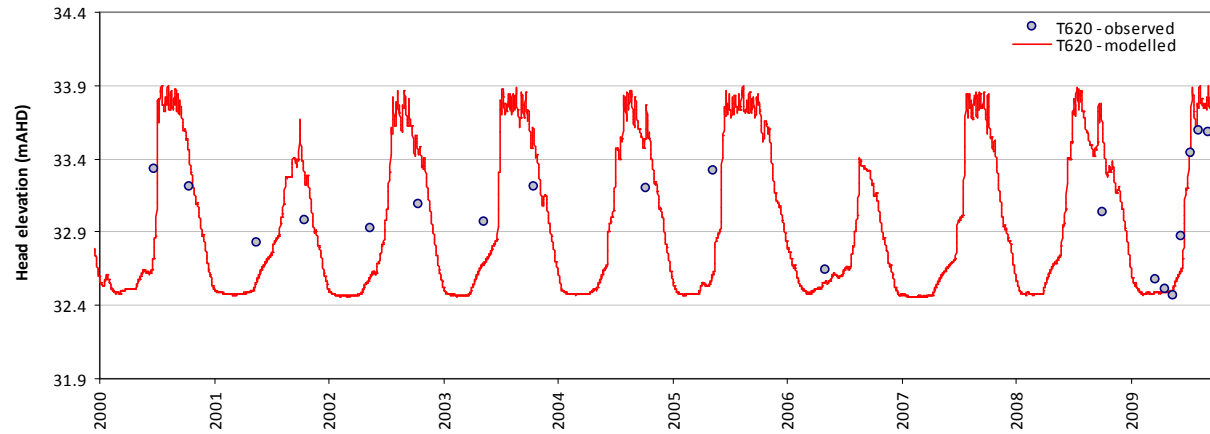
Residual time-series plot - T610



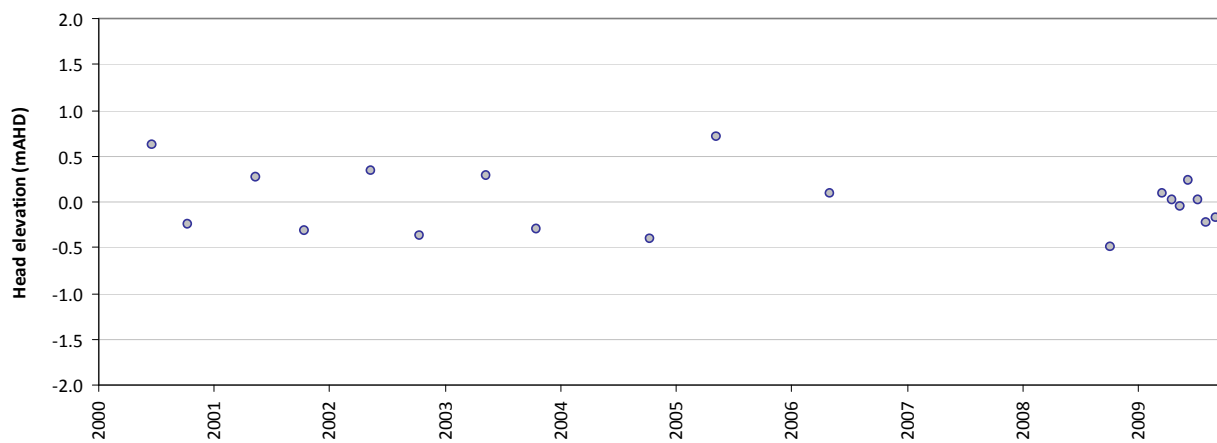
Statistics	
Mean error (ME)	-0.05
Mean absolute error (MAE)	0.20
Root mean square error (RMSE)	0.25
Standard deviation of residuals (STDres)	0.25
Correlation coefficient (R)	0.93
Nash Sutcliffe correlation coefficient (R2)	0.67

T620

Modelled vs observed time-series plot - T620



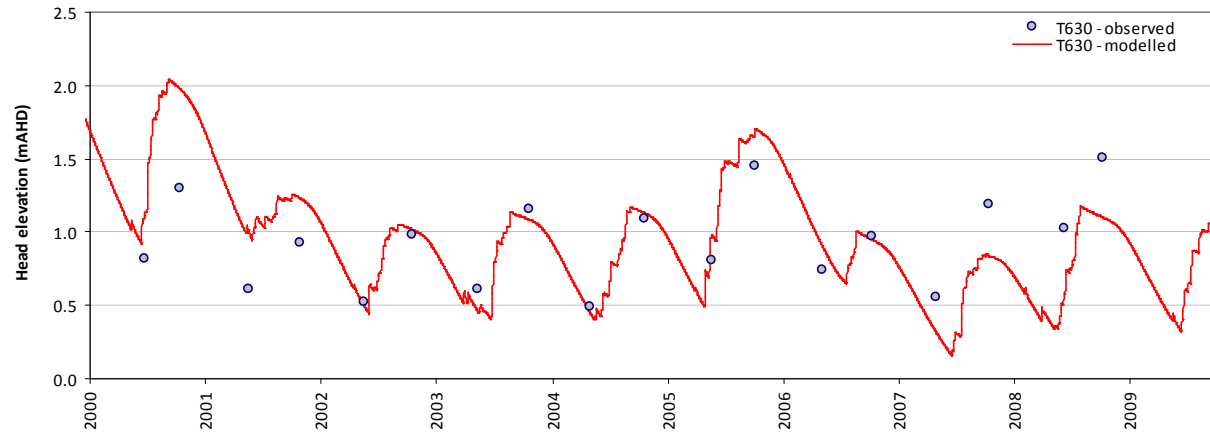
Residual time-series plot - T620



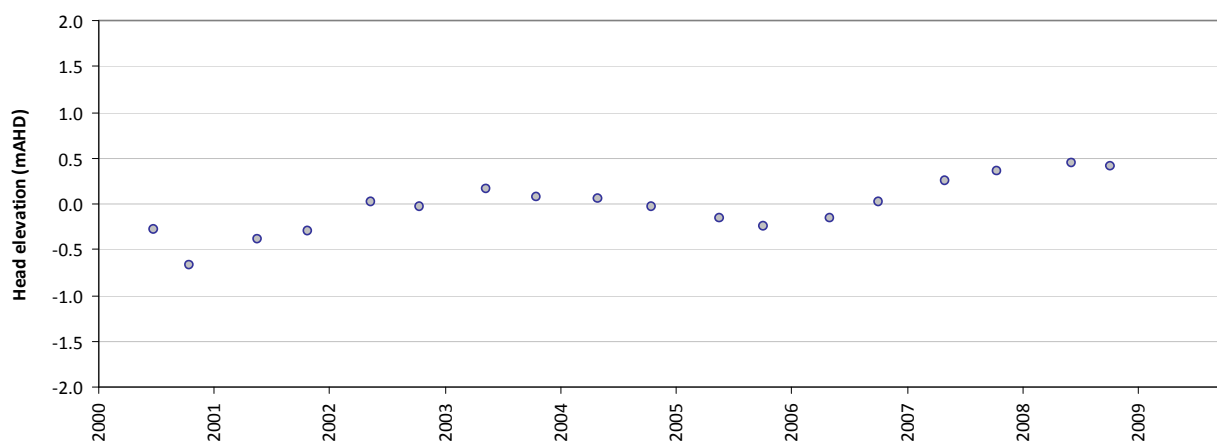
Statistics	
Mean error (ME)	0.00
Mean absolute error (MAE)	0.27
Root mean square error (RMSE)	0.33
Standard deviation of residuals (STDres)	0.33
Correlation coefficient (R)	0.75
Nash Sutcliffe correlation coefficient (R2)	0.02

T630

Modelled vs observed time-series plot - T630



Residual time-series plot - T630

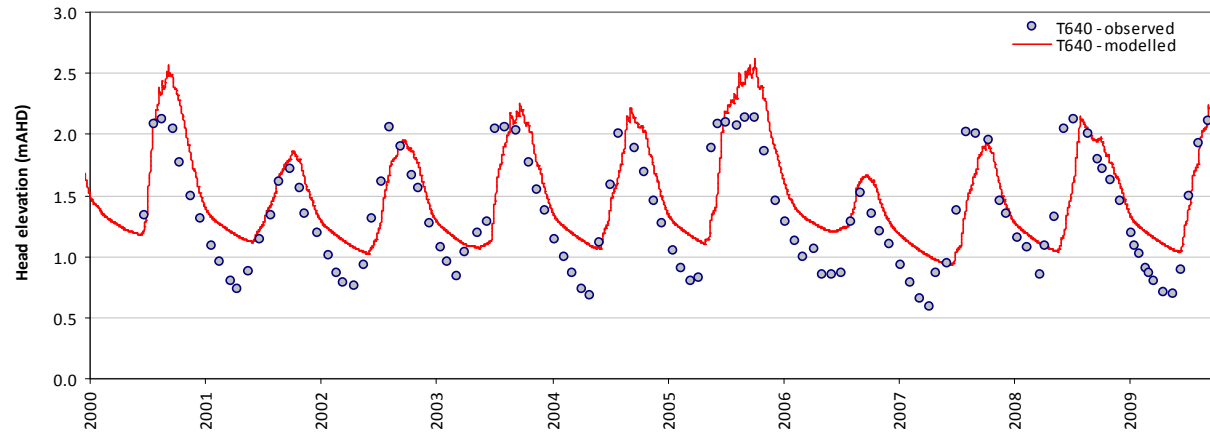


Statistics

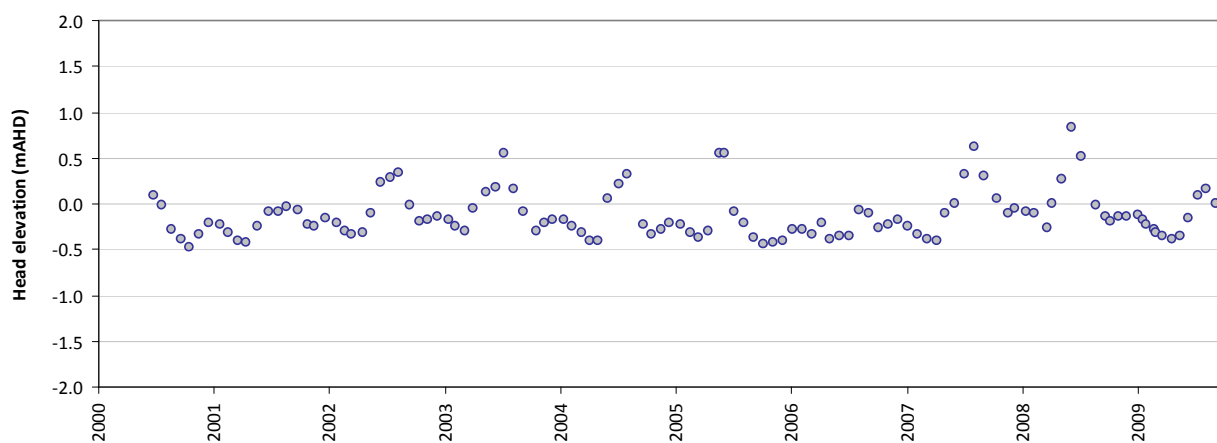
Mean error (ME)	-0.03
Mean absolute error (MAE)	0.23
Root mean square error (RMSE)	0.29
Standard deviation of residuals (STDres)	0.29
Correlation coefficient (R)	0.72
Nash Sutcliffe correlation coefficient (R2)	0.10

T640

Modelled vs observed time-series plot - T640



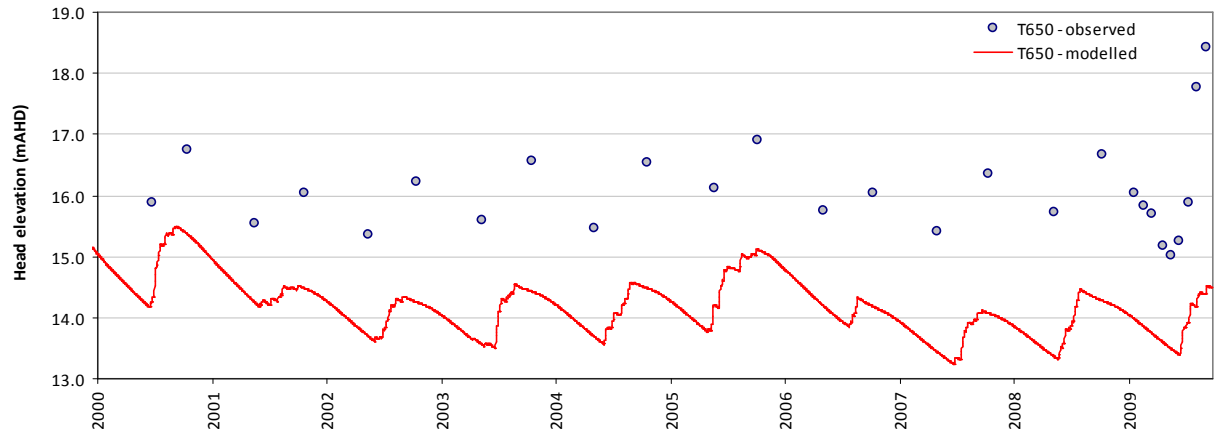
Residual time-series plot - T640



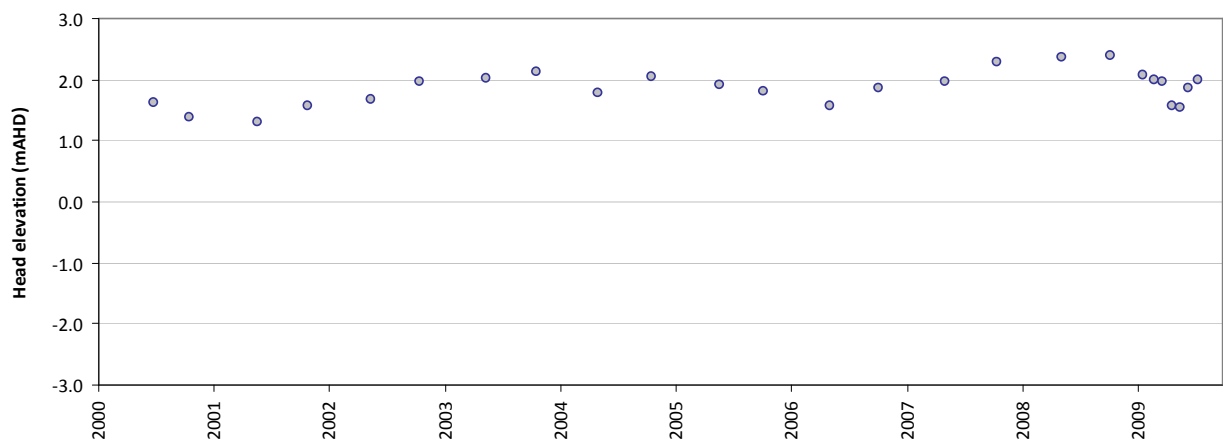
Statistics	
Mean error (ME)	-0.13
Mean absolute error (MAE)	0.25
Root mean square error (RMSE)	0.29
Standard deviation of residuals (STDres)	0.26
Correlation coefficient (R)	0.82
Nash Sutcliffe correlation coefficient (R2)	0.60

T650

Modelled vs observed time-series plot - T650



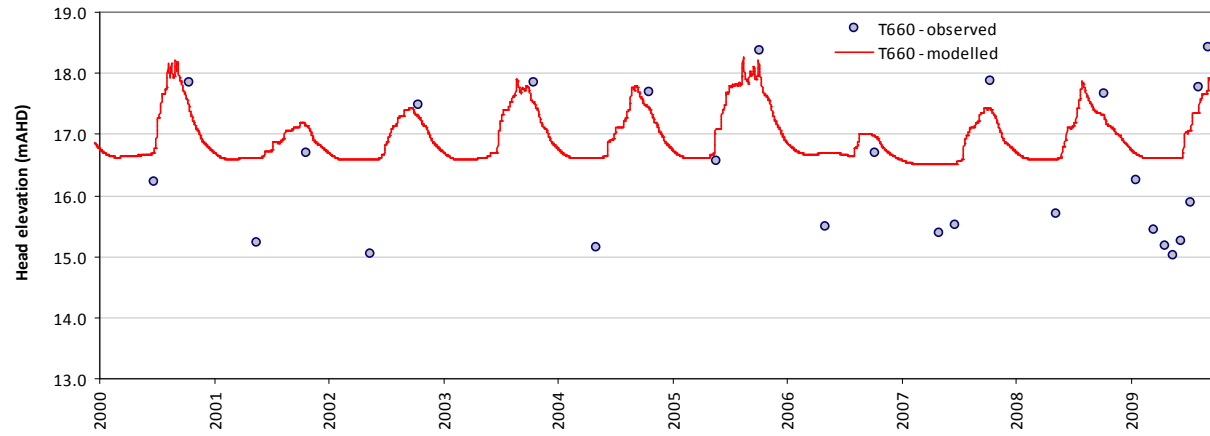
Residual time-series plot - T650



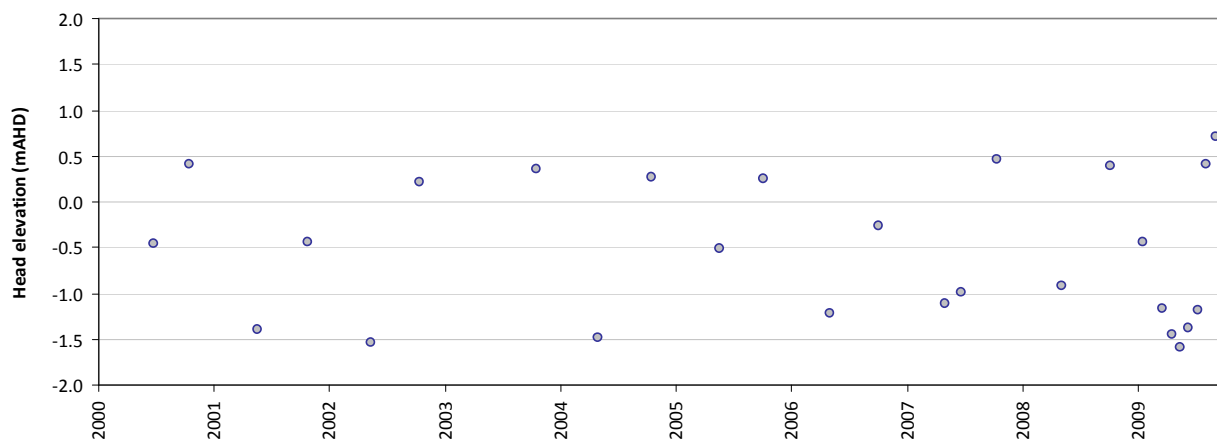
Statistics	
Mean error (ME)	1.94
Mean absolute error (MAE)	1.94
Root mean square error (RMSE)	1.95
Standard deviation of residuals (STDres)	0.27
Correlation coefficient (R)	0.84
Nash Sutcliffe correlation coefficient (R2)	-18.04

T660

Modelled vs observed time-series plot - T660



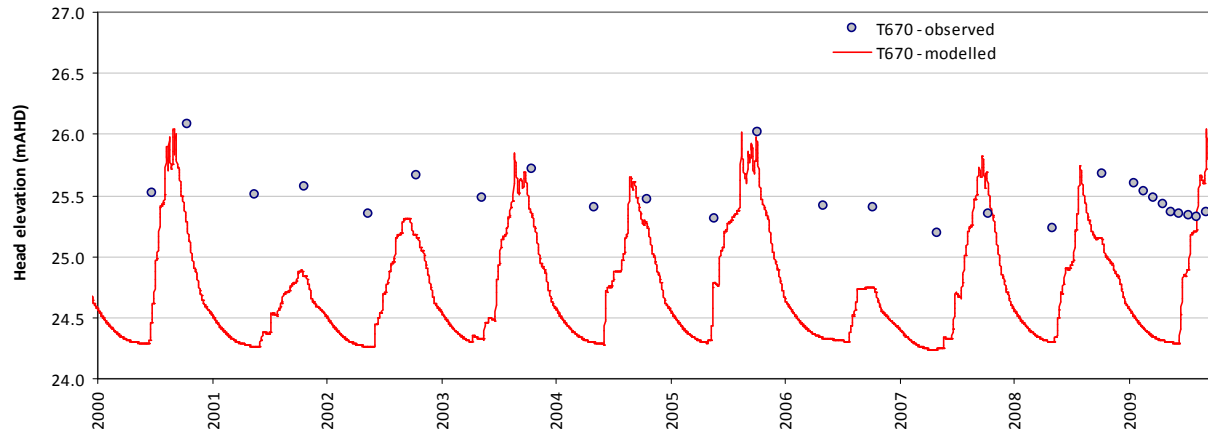
Residual time-series plot - T660



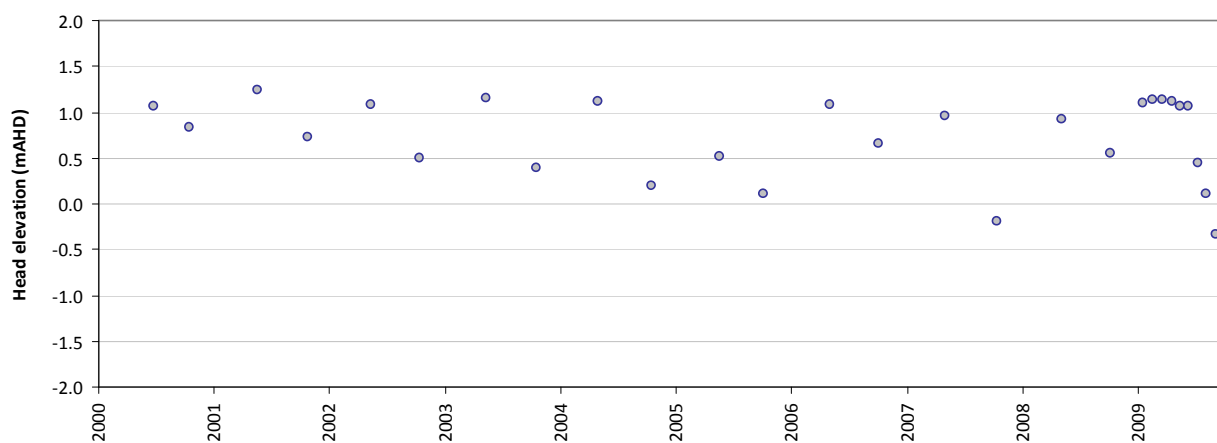
Statistics	
Mean error (ME)	-0.57
Mean absolute error (MAE)	0.82
Root mean square error (RMSE)	0.94
Standard deviation of residuals (STDres)	0.75
Correlation coefficient (R)	0.94
Nash Sutcliffe correlation coefficient (R2)	0.33

T670

Modelled vs observed time-series plot - T670

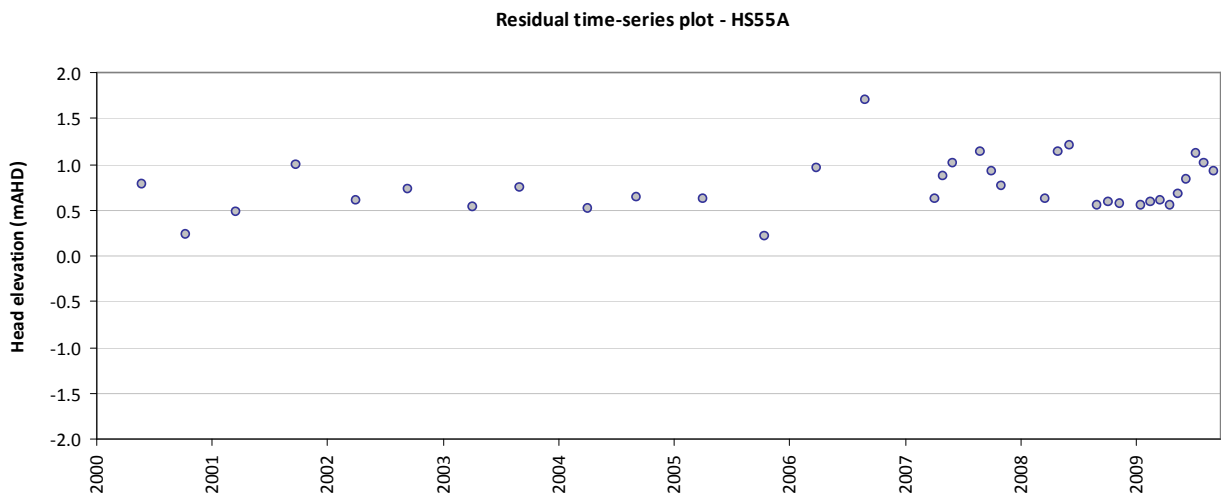
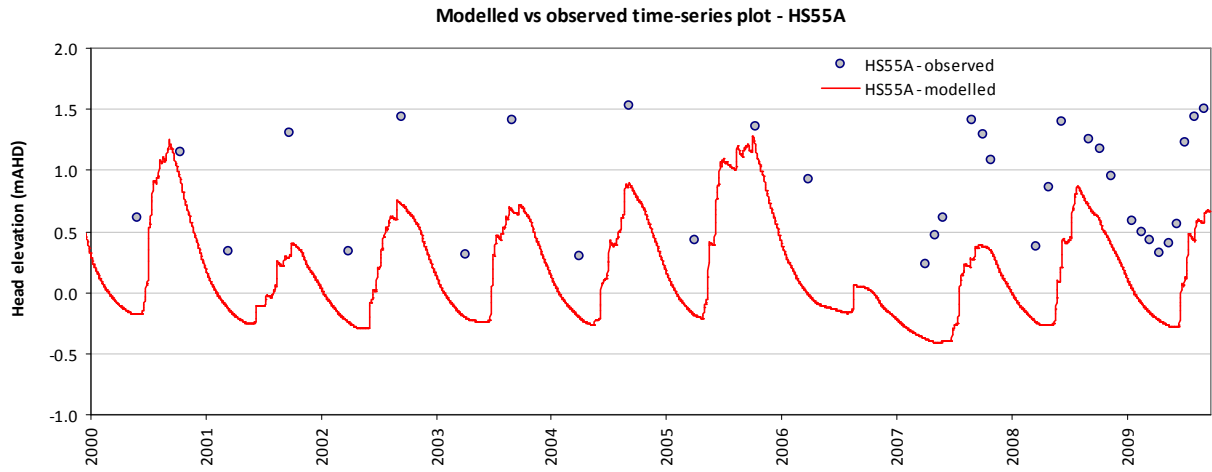


Residual time-series plot - T670



Statistics	
Mean error (ME)	0.73
Mean absolute error (MAE)	0.77
Root mean square error (RMSE)	0.85
Standard deviation of residuals (STDres)	0.44
Correlation coefficient (R)	0.50
Nash Sutcliffe correlation coefficient (R2)	-16.36

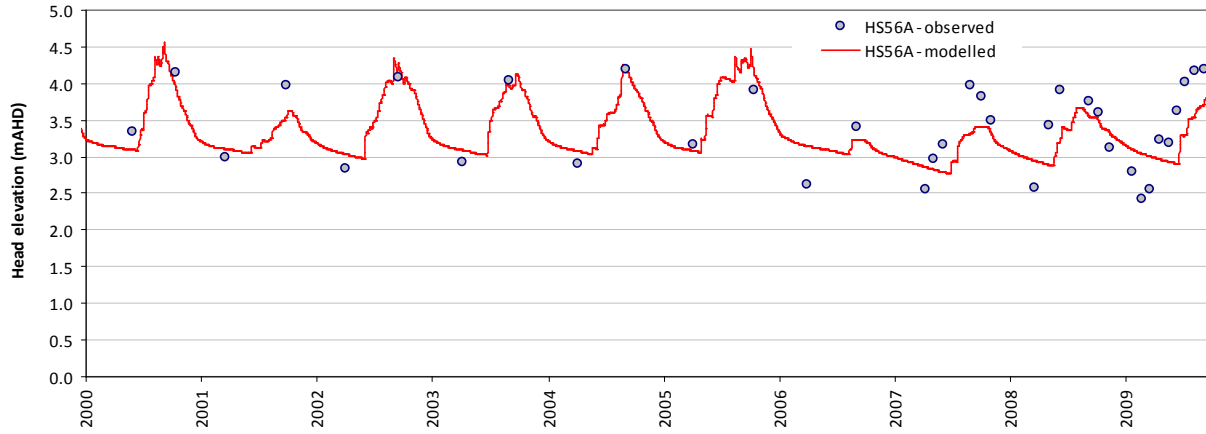
HS55A



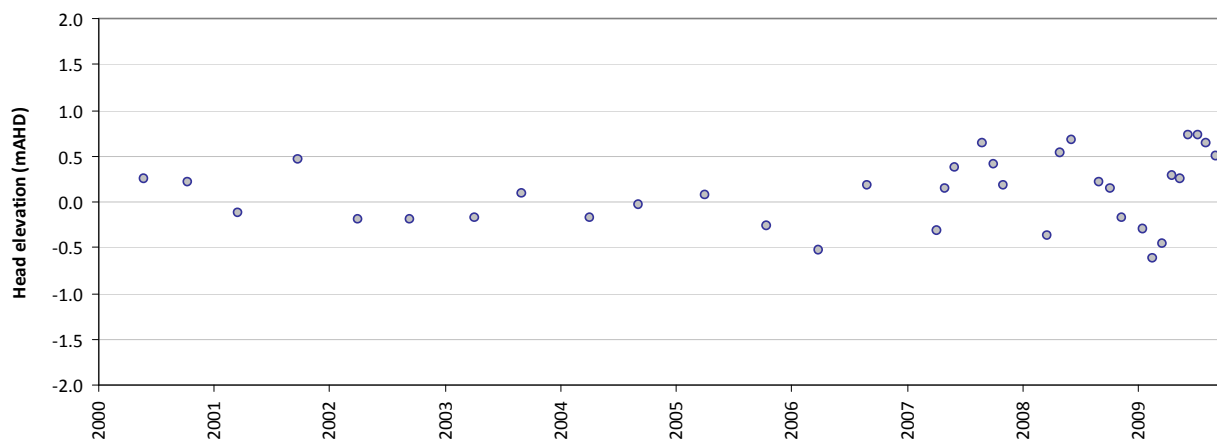
Statistics	
Mean error (ME)	0.75
Mean absolute error (MAE)	0.75
Root mean square error (RMSE)	0.80
Standard deviation of residuals (STDres)	0.29
Correlation coefficient (R)	0.79
Nash Sutcliffe correlation coefficient (R2)	-1.89

HS56A

Modelled vs observed time-series plot - HS56A



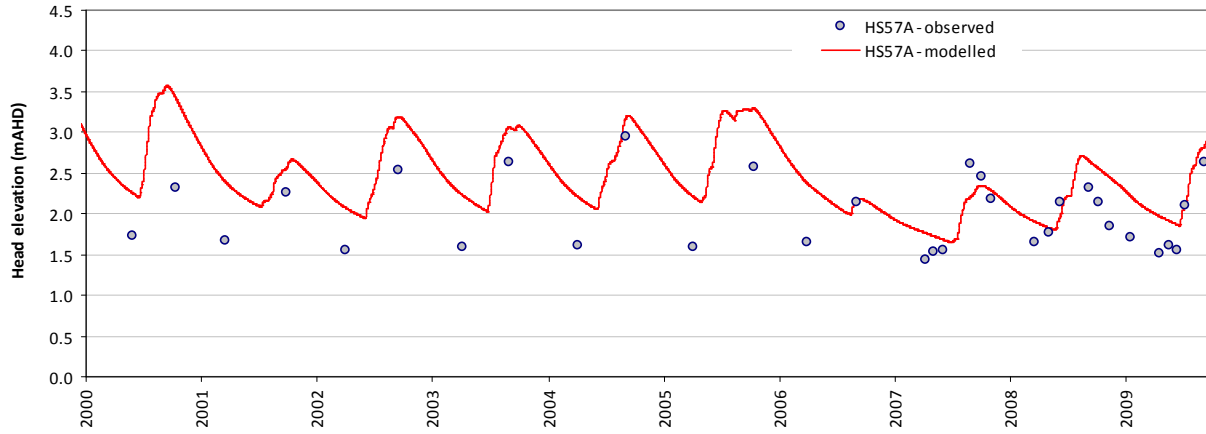
Residual time-series plot - HS56A



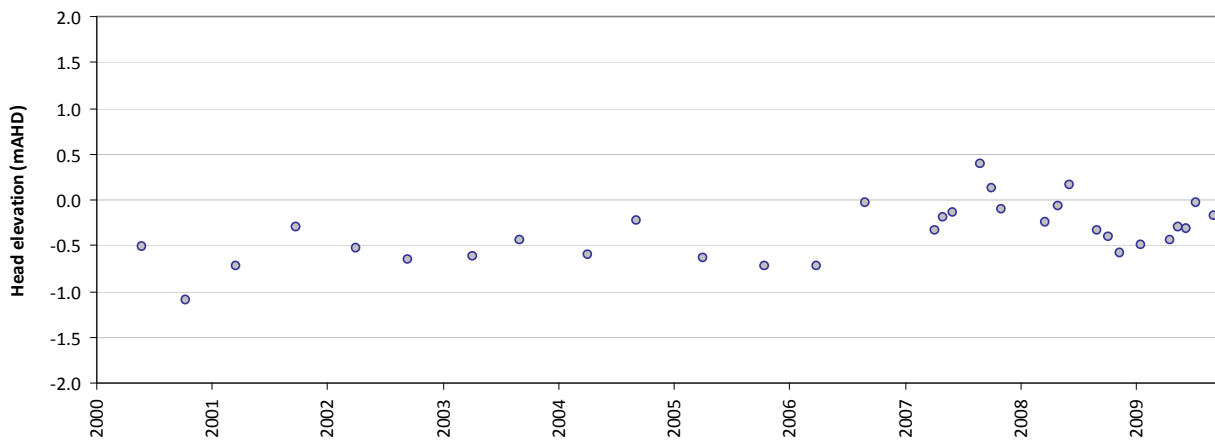
Statistics	
Mean error (ME)	0.02
Mean absolute error (MAE)	0.30
Root mean square error (RMSE)	0.34
Standard deviation of residuals (STDres)	0.34
Correlation coefficient (R)	0.81
Nash Sutcliffe correlation coefficient (R2)	0.64

HS57A

Modelled vs observed time-series plot - HS57A

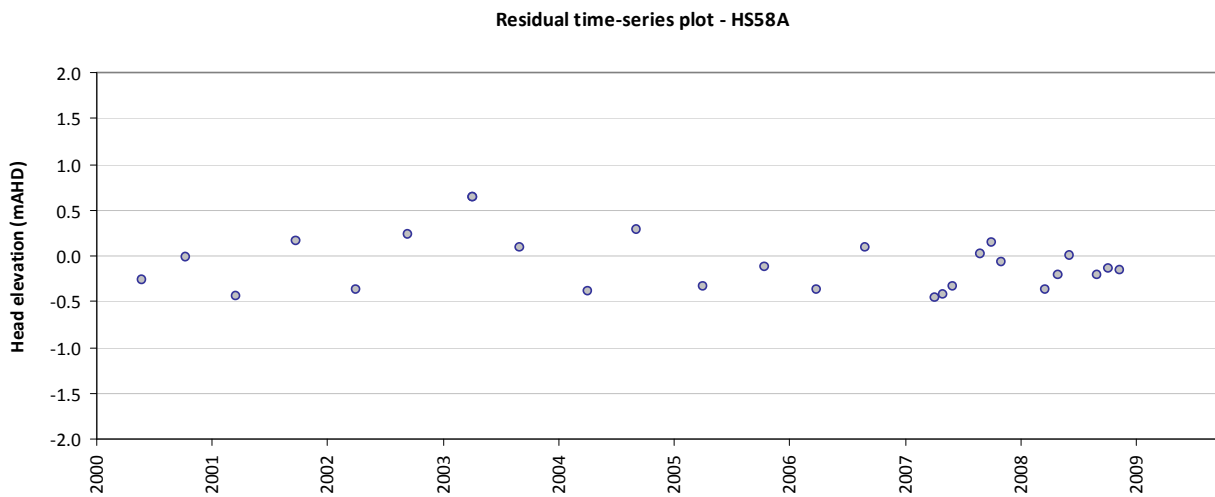
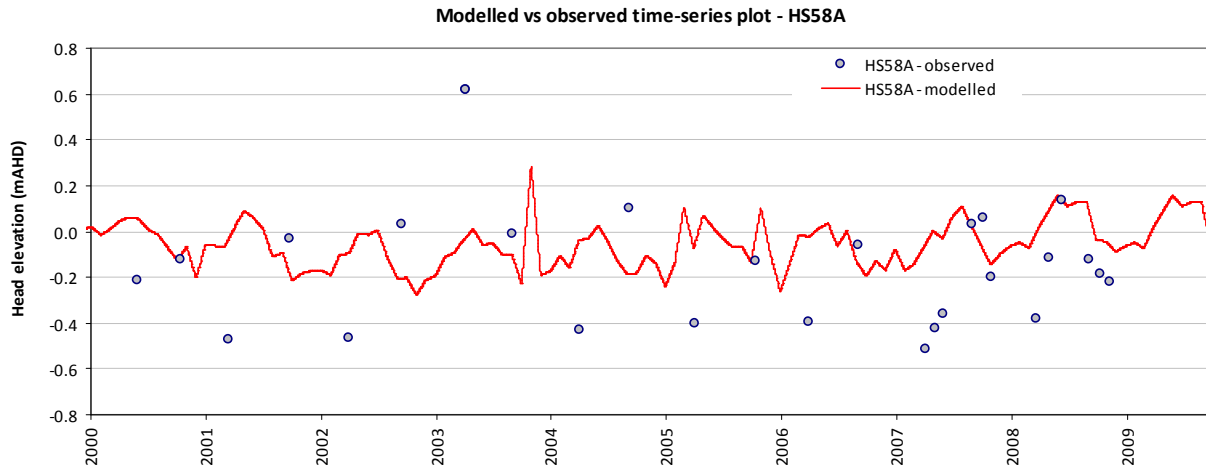


Residual time-series plot - HS57A



Statistics	
Mean error (ME)	-0.36
Mean absolute error (MAE)	0.40
Root mean square error (RMSE)	0.47
Standard deviation of residuals (STDres)	0.31
Correlation coefficient (R)	0.77
Nash Sutcliffe correlation coefficient (R2)	-0.19

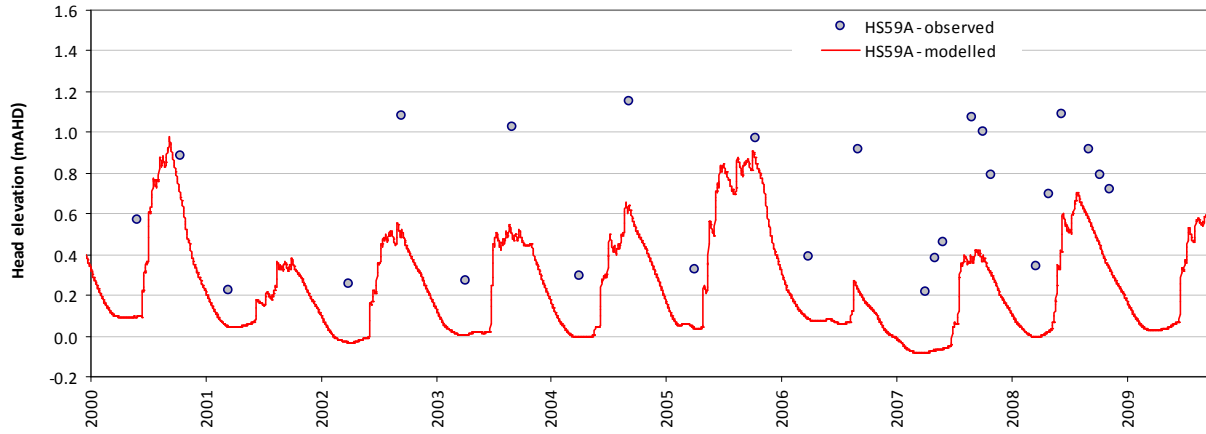
HS58A



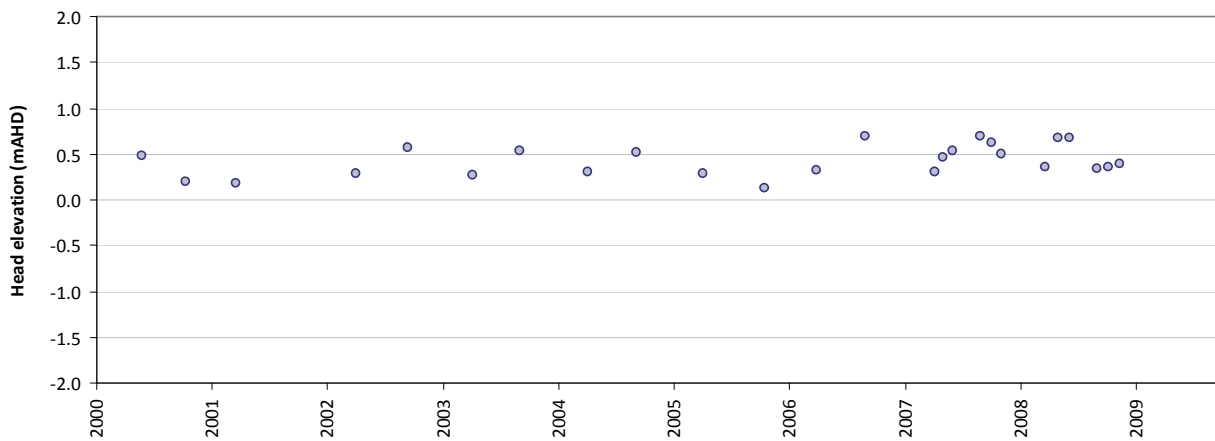
Statistics	
Mean error (ME)	-0.08
Mean absolute error (MAE)	0.26
Root mean square error (RMSE)	0.31
Standard deviation of residuals (STDres)	0.30
Correlation coefficient (R)	-0.01
Nash Sutcliffe correlation coefficient (R2)	-0.17

HS59A

Modelled vs observed time-series plot - HS59A

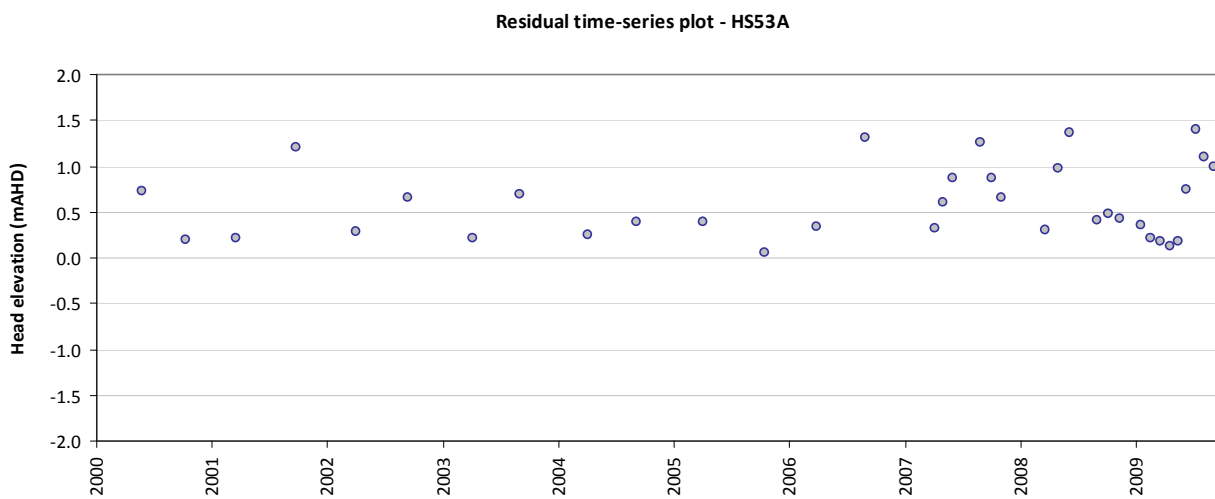
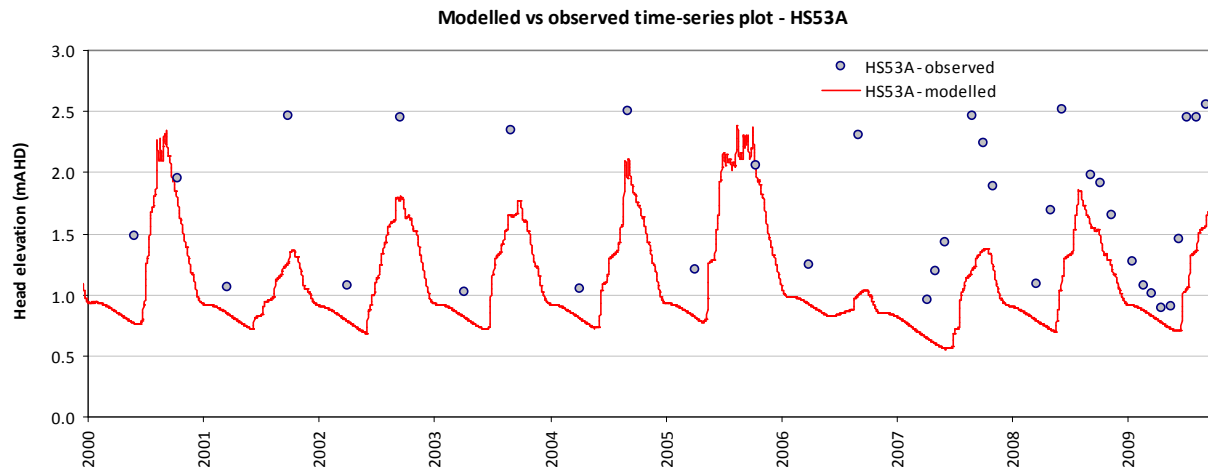


Residual time-series plot - HS59A



Statistics	
Mean error (ME)	0.41
Mean absolute error (MAE)	0.41
Root mean square error (RMSE)	0.45
Standard deviation of residuals (STDres)	0.17
Correlation coefficient (R)	0.86
Nash Sutcliffe correlation coefficient (R2)	-0.82

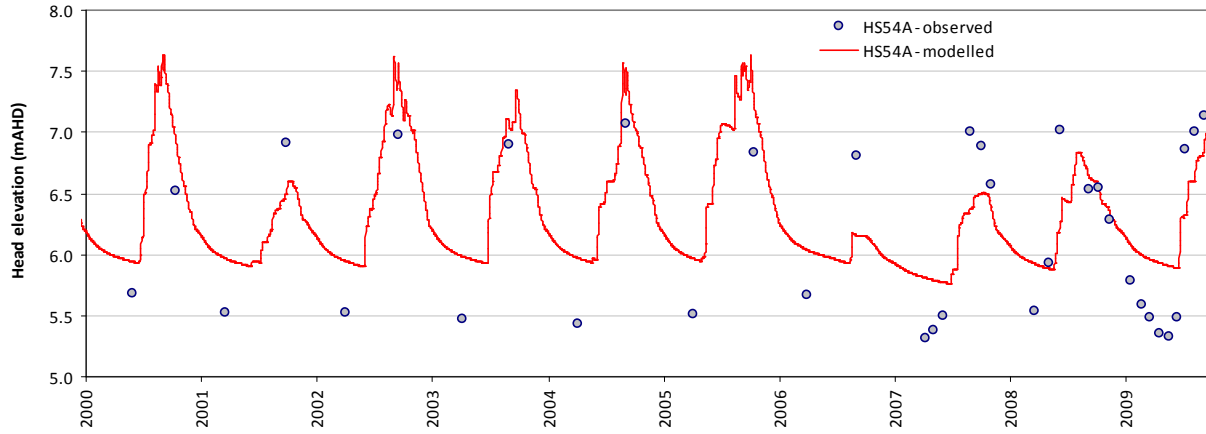
HS53A



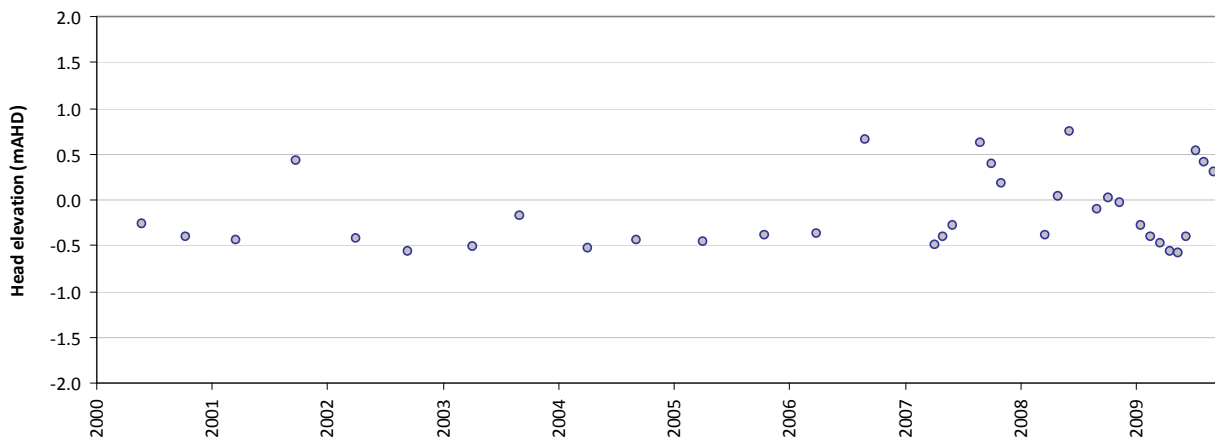
Statistics	
Mean error (ME)	0.58
Mean absolute error (MAE)	0.58
Root mean square error (RMSE)	0.70
Standard deviation of residuals (STDres)	0.40
Correlation coefficient (R)	0.75
Nash Sutcliffe correlation coefficient (R2)	-0.36

HS54A

Modelled vs observed time-series plot - HS54A



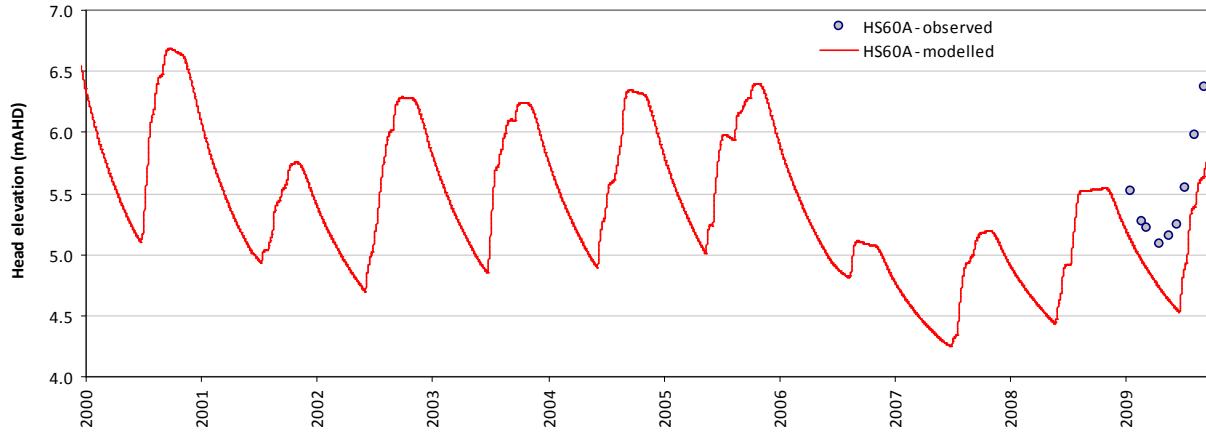
Residual time-series plot - HS54A



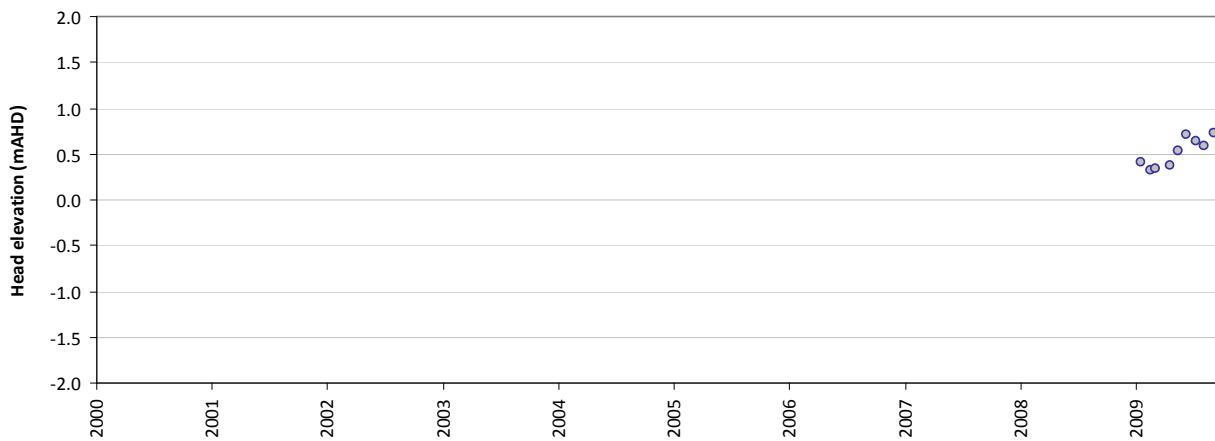
Statistics	
Mean error (ME)	-0.15
Mean absolute error (MAE)	0.40
Root mean square error (RMSE)	0.44
Standard deviation of residuals (STDres)	0.41
Correlation coefficient (R)	0.80
Nash Sutcliffe correlation coefficient (R2)	0.59

HS60A

Modelled vs observed time-series plot - HS60A



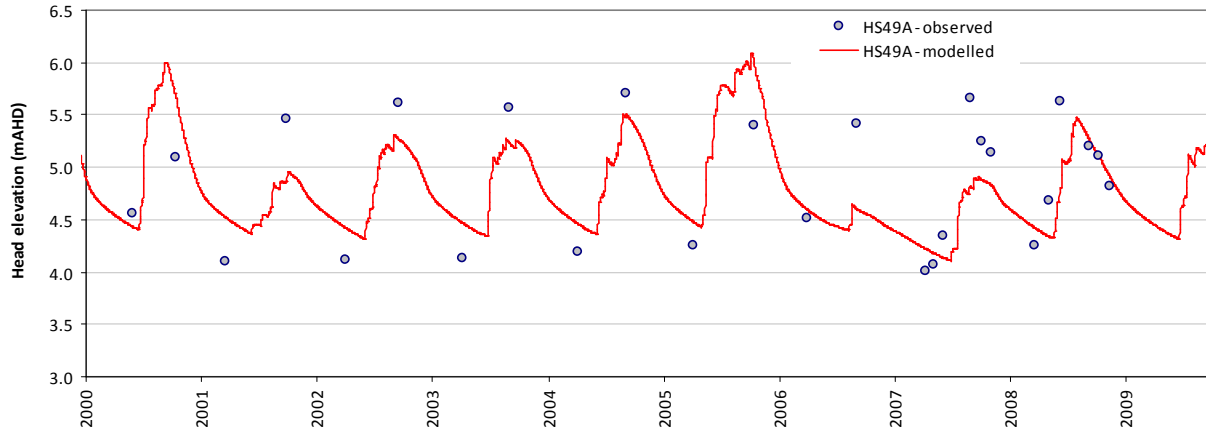
Residual time-series plot - HS60A



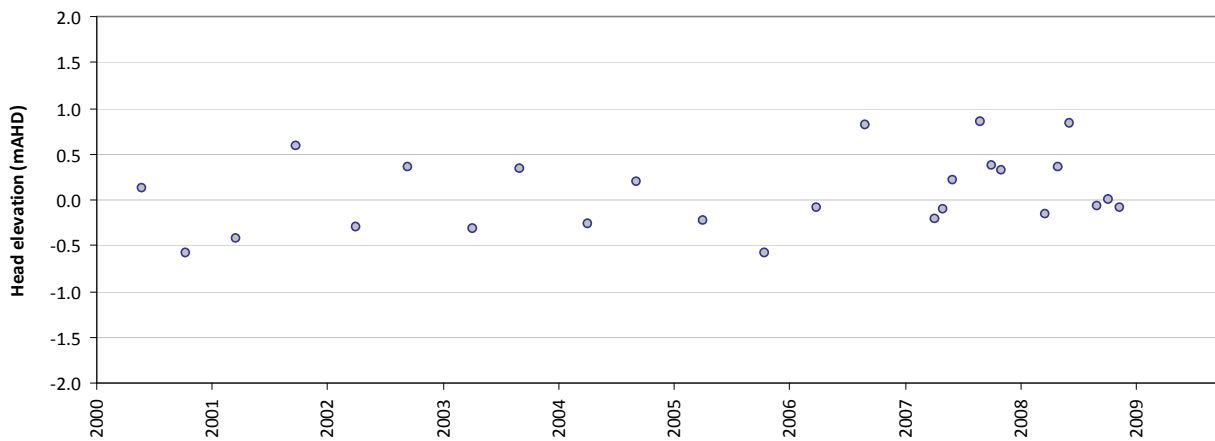
Statistics	
Mean error (ME)	0.52
Mean absolute error (MAE)	0.52
Root mean square error (RMSE)	0.54
Standard deviation of residuals (STDres)	0.14
Correlation coefficient (R)	0.94
Nash Sutcliffe correlation coefficient (R2)	-0.77

HS49A

Modelled vs observed time-series plot - HS49A



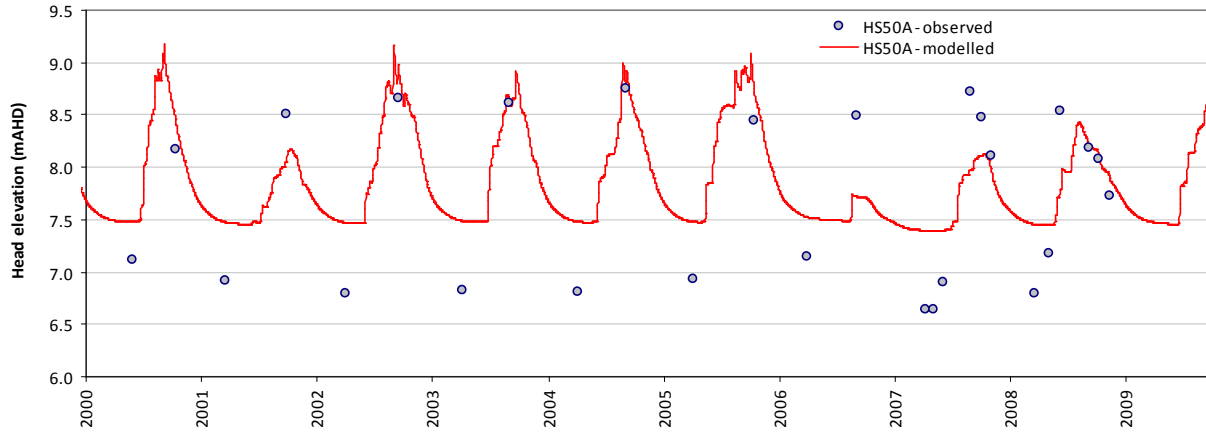
Residual time-series plot - HS49A



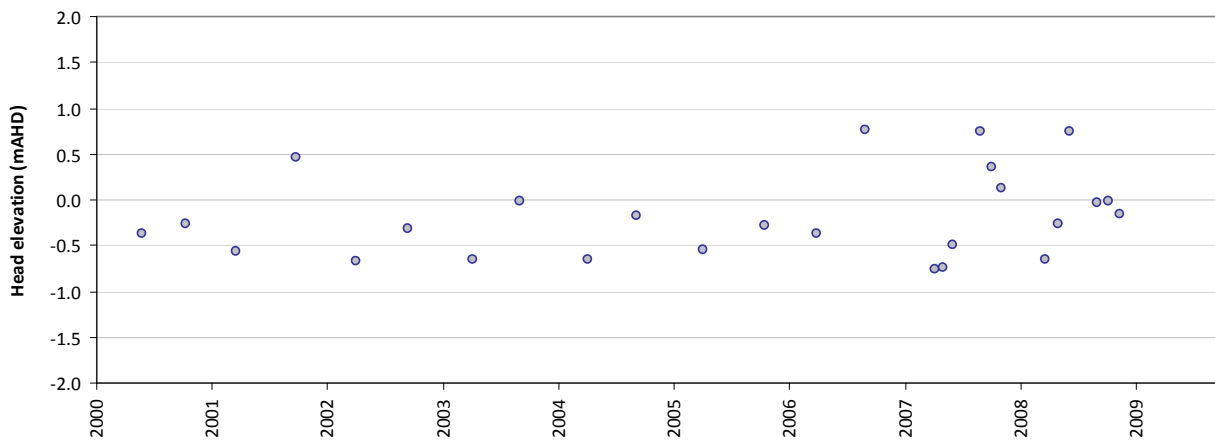
Statistics	
Mean error (ME)	0.05
Mean absolute error (MAE)	0.35
Root mean square error (RMSE)	0.42
Standard deviation of residuals (STDres)	0.41
Correlation coefficient (R)	0.73
Nash Sutcliffe correlation coefficient (R2)	0.53

HS50A

Modelled vs observed time-series plot - HS50A



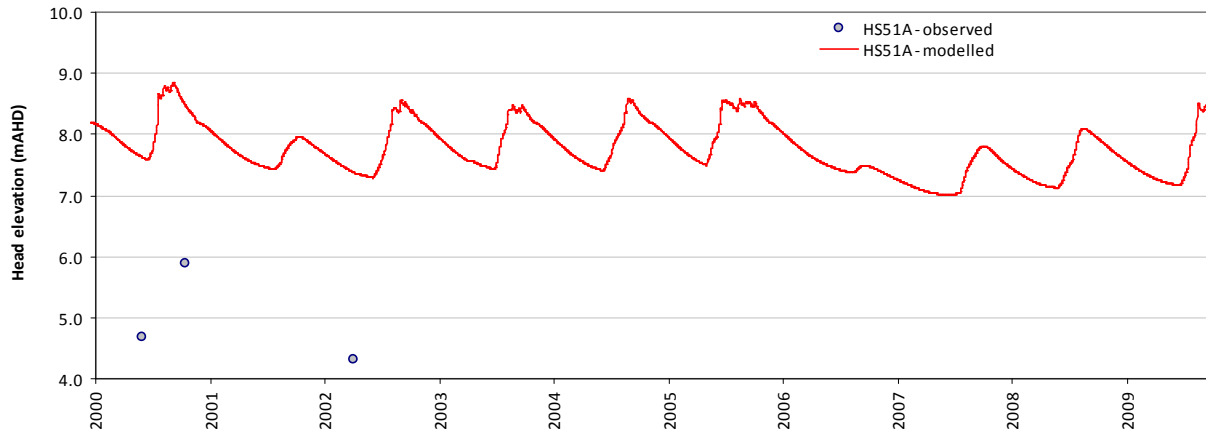
Residual time-series plot - HS50A



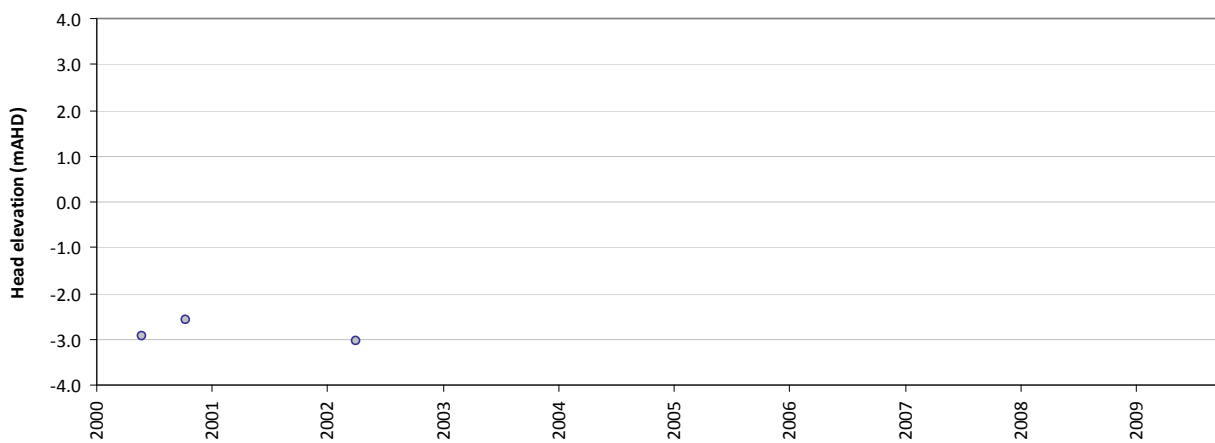
Statistics	
Mean error (ME)	-0.20
Mean absolute error (MAE)	0.45
Root mean square error (RMSE)	0.51
Standard deviation of residuals (STDres)	0.47
Correlation coefficient (R)	0.83
Nash Sutcliffe correlation coefficient (R2)	0.59

HS51A

Modelled vs observed time-series plot - HS51A



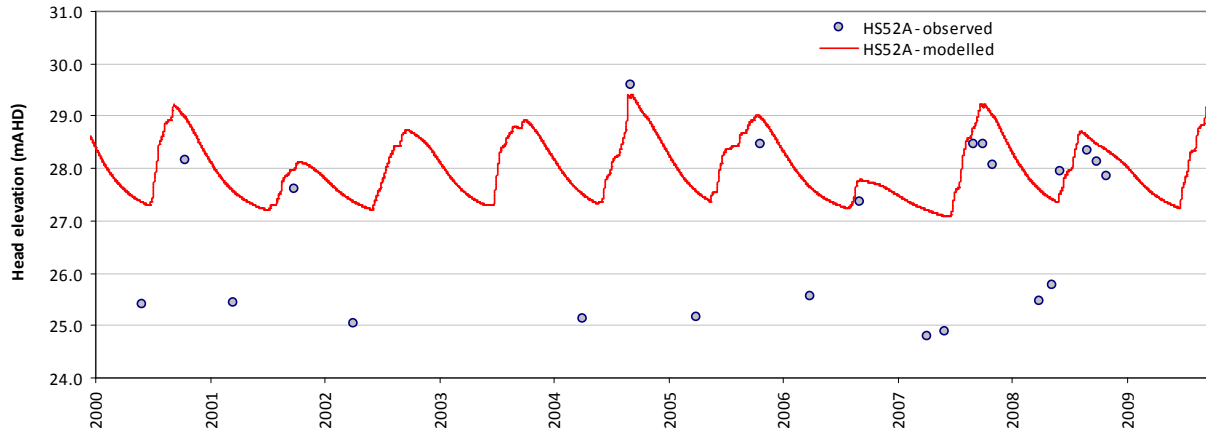
Residual time-series plot - HS51A



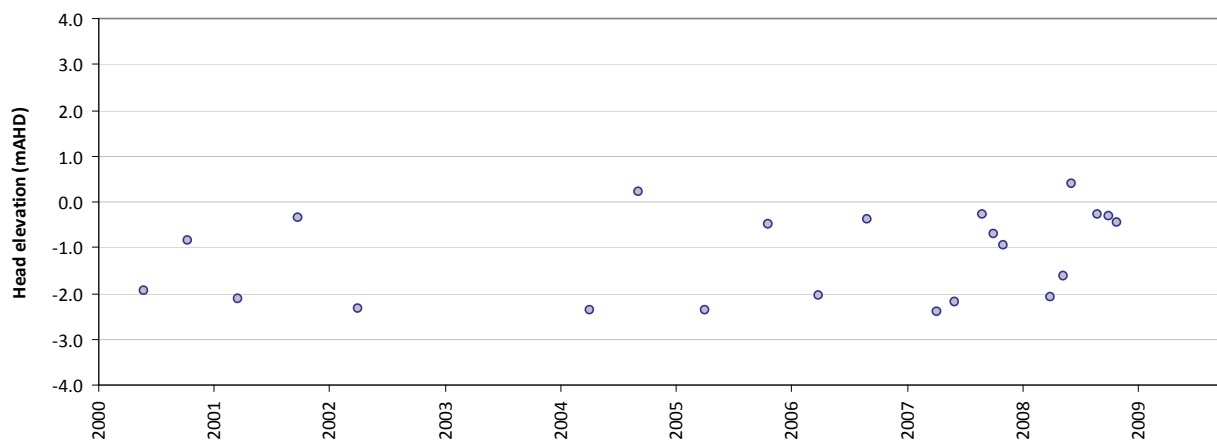
Statistics	
Mean error (ME)	-2.82
Mean absolute error (MAE)	2.82
Root mean square error (RMSE)	2.83
Standard deviation of residuals (STDres)	0.24
Correlation coefficient (R)	1.00
Nash Sutcliffe correlation coefficient (R2)	-11.87

HS52A

Modelled vs observed time-series plot - HS52A



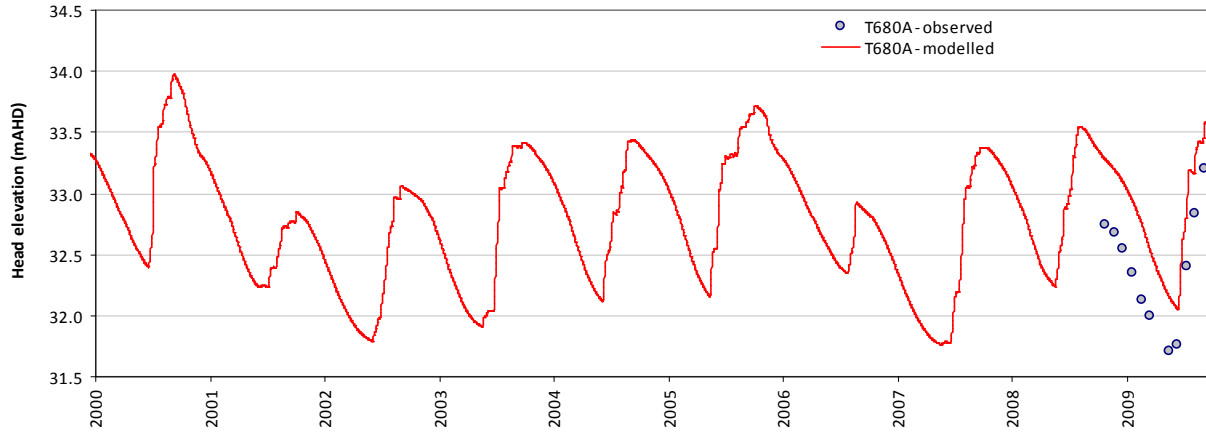
Residual time-series plot - HS52A



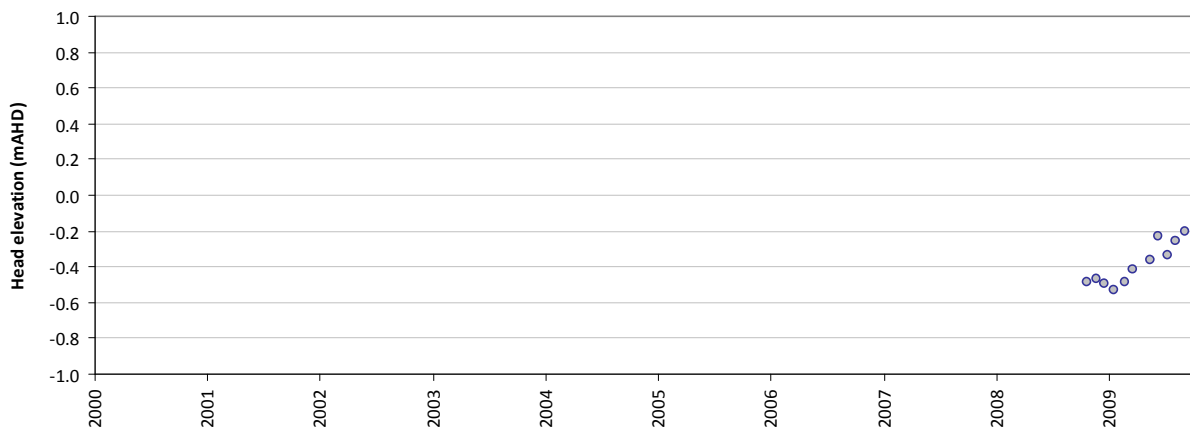
Statistics	
Mean error (ME)	-1.15
Mean absolute error (MAE)	1.21
Root mean square error (RMSE)	1.49
Standard deviation of residuals (STDres)	0.95
Correlation coefficient (R)	0.89
Nash Sutcliffe correlation coefficient (R2)	0.05

T680A

Modelled vs observed time-series plot - T680A



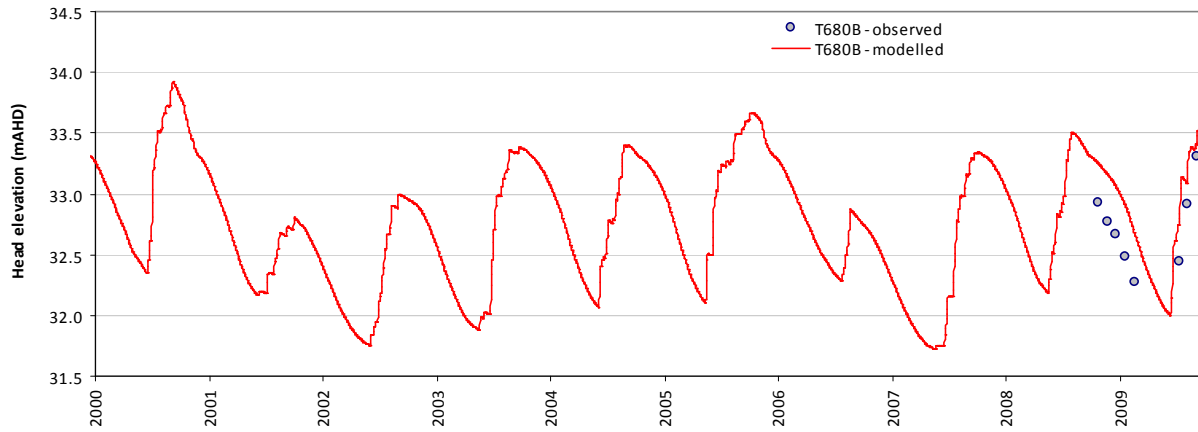
Residual time-series plot - T680A



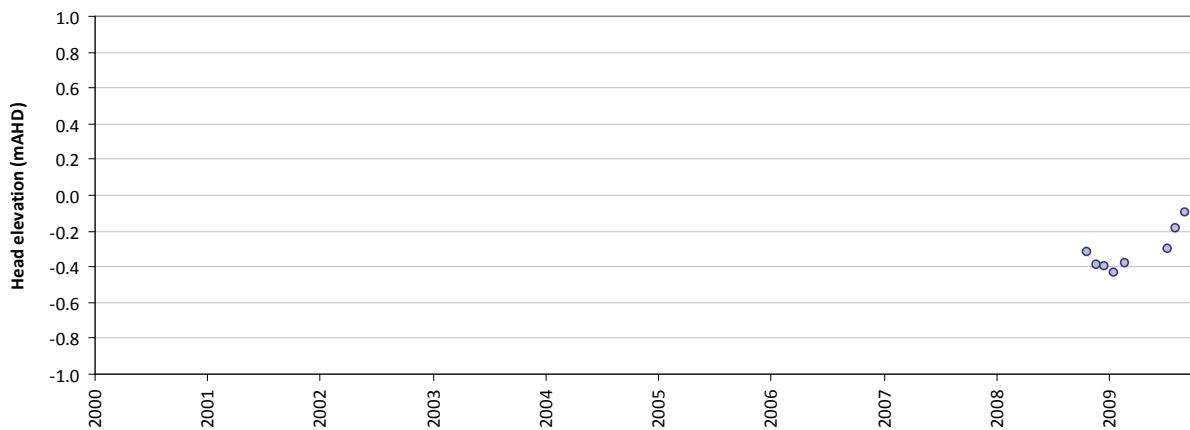
Statistics	
Mean error (ME)	-0.46
Mean absolute error (MAE)	0.46
Root mean square error (RMSE)	0.47
Standard deviation of residuals (STDres)	0.12
Correlation coefficient (R)	0.97
Nash Sutcliffe correlation coefficient (R2)	-0.13

T680B

Modelled vs observed time-series plot - T680B



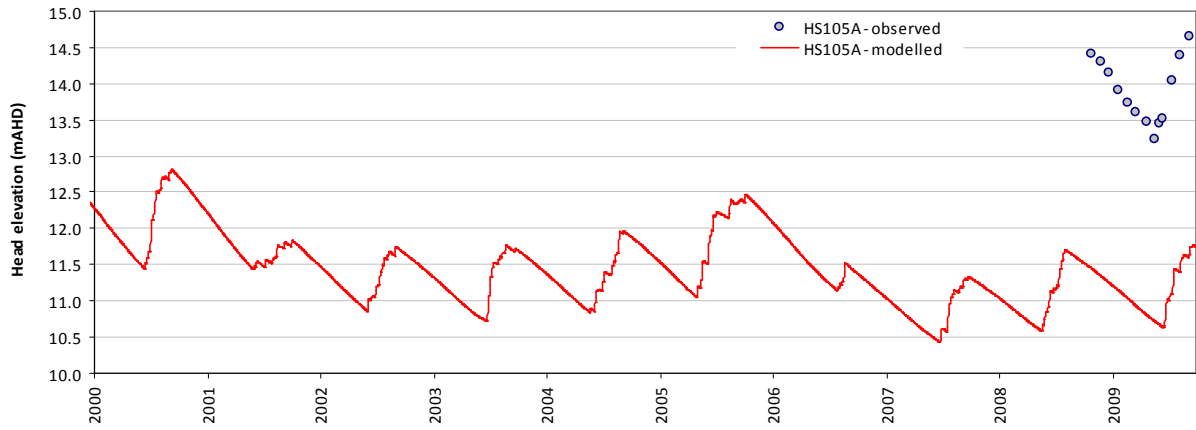
Residual time-series plot - T680B



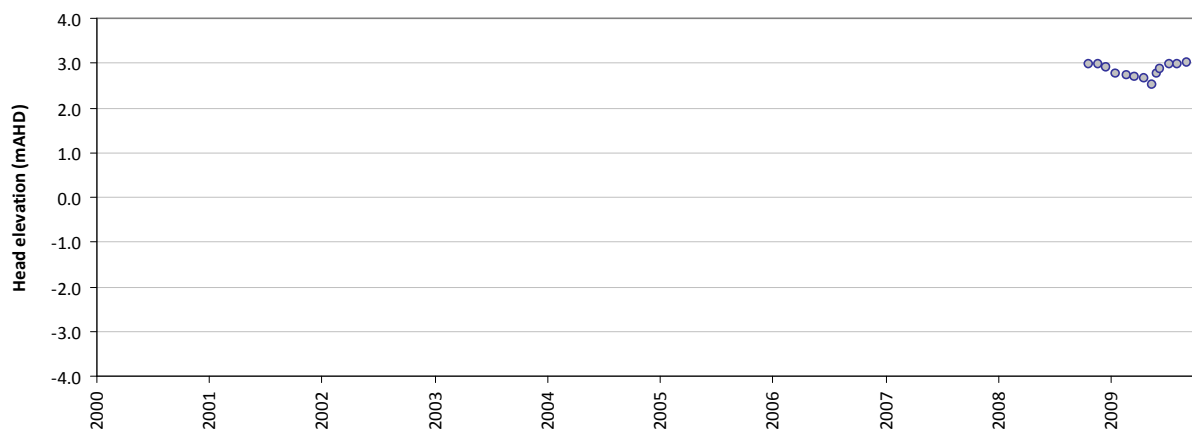
Statistics	
Mean error (ME)	-0.31
Mean absolute error (MAE)	0.31
Root mean square error (RMSE)	0.33
Standard deviation of residuals (STDres)	0.11
Correlation coefficient (R)	0.95
Nash Sutcliffe correlation coefficient (R2)	-0.14

HS105A

Modelled vs observed time-series plot - HS105A



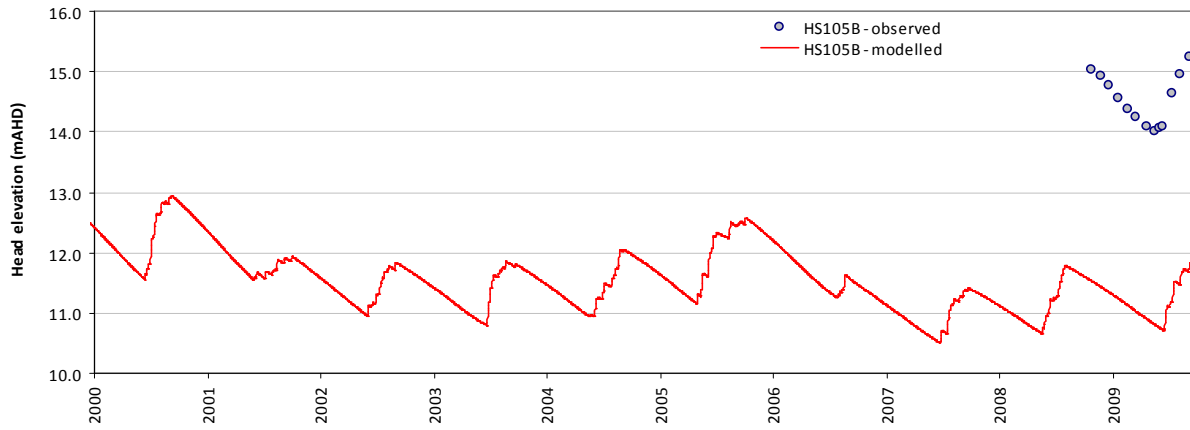
Residual time-series plot - HS105A



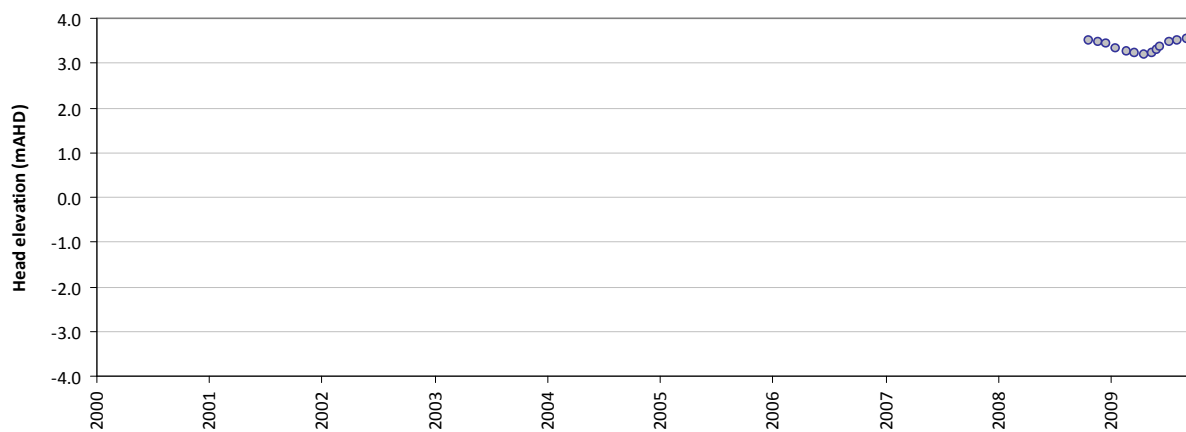
Statistics	
Mean error (ME)	2.83
Mean absolute error (MAE)	2.83
Root mean square error (RMSE)	2.83
Standard deviation of residuals (STDres)	0.15
Correlation coefficient (R)	0.97
Nash Sutcliffe correlation coefficient (R2)	-42.76

HS105B

Modelled vs observed time-series plot - HS105B



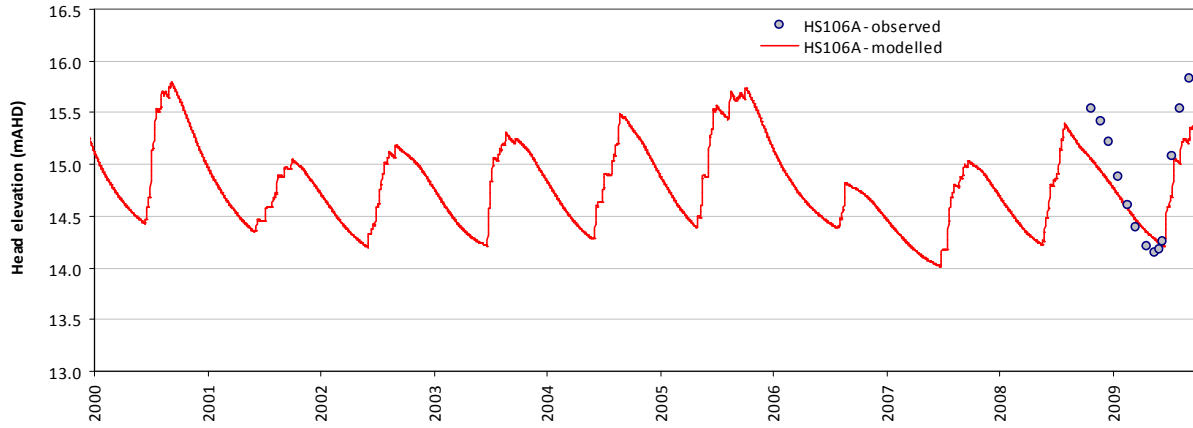
Residual time-series plot - HS105B



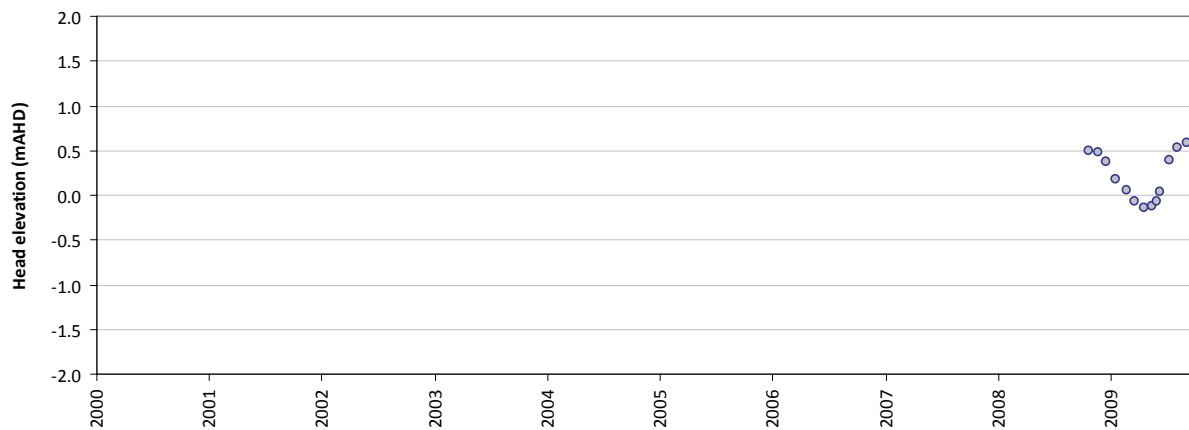
Statistics	
Mean error (ME)	3.37
Mean absolute error (MAE)	3.37
Root mean square error (RMSE)	3.37
Standard deviation of residuals (STDres)	0.12
Correlation coefficient (R)	0.98
Nash Sutcliffe correlation coefficient (R2)	-67.66

HS106A

Modelled vs observed time-series plot - HS106A



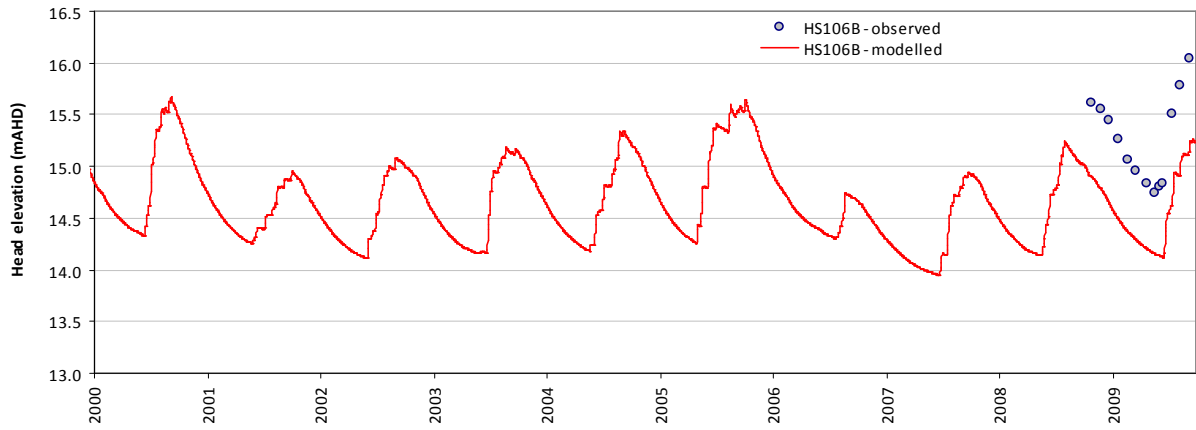
Residual time-series plot - HS106A



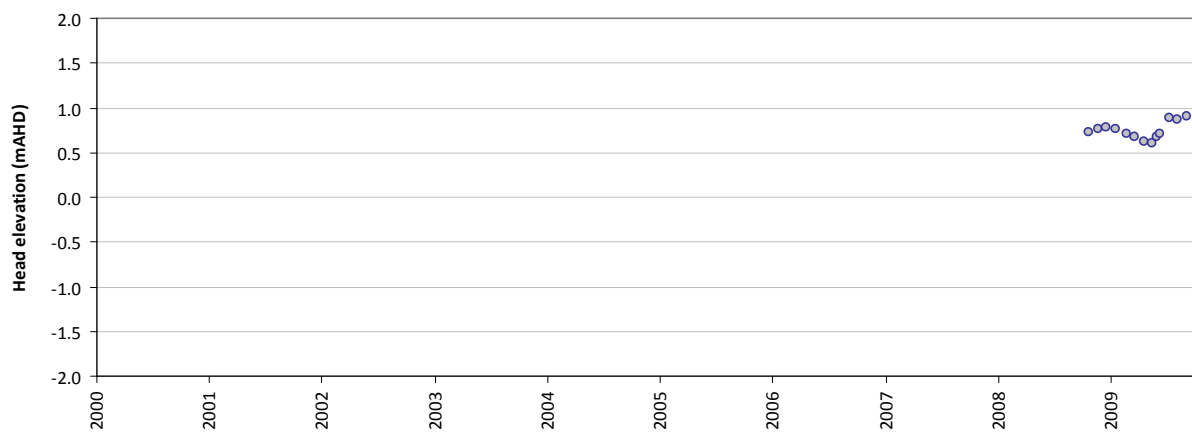
Statistics	
Mean error (ME)	0.21
Mean absolute error (MAE)	0.27
Root mean square error (RMSE)	0.33
Standard deviation of residuals (STDres)	0.26
Correlation coefficient (R)	0.99
Nash Sutcliffe correlation coefficient (R2)	0.67

HS106B

Modelled vs observed time-series plot - HS106B



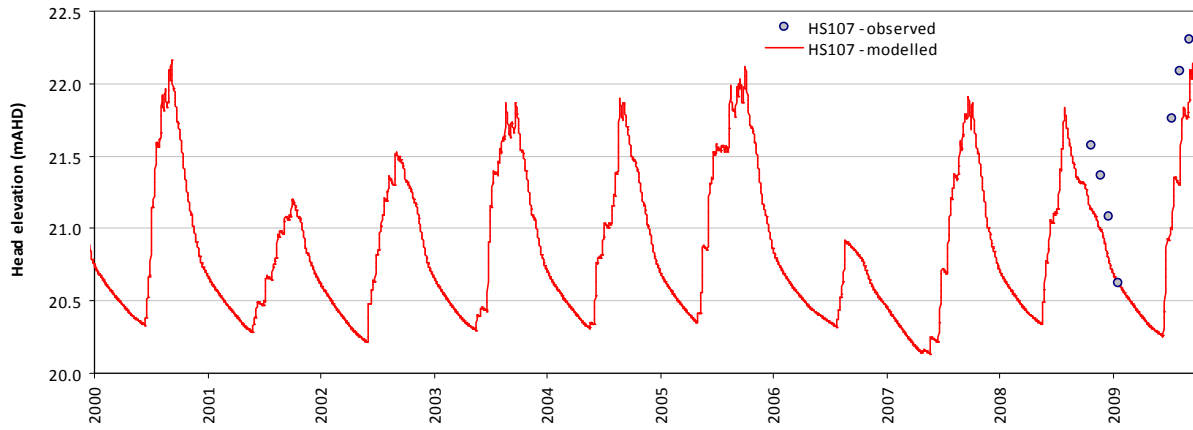
Residual time-series plot - HS106B



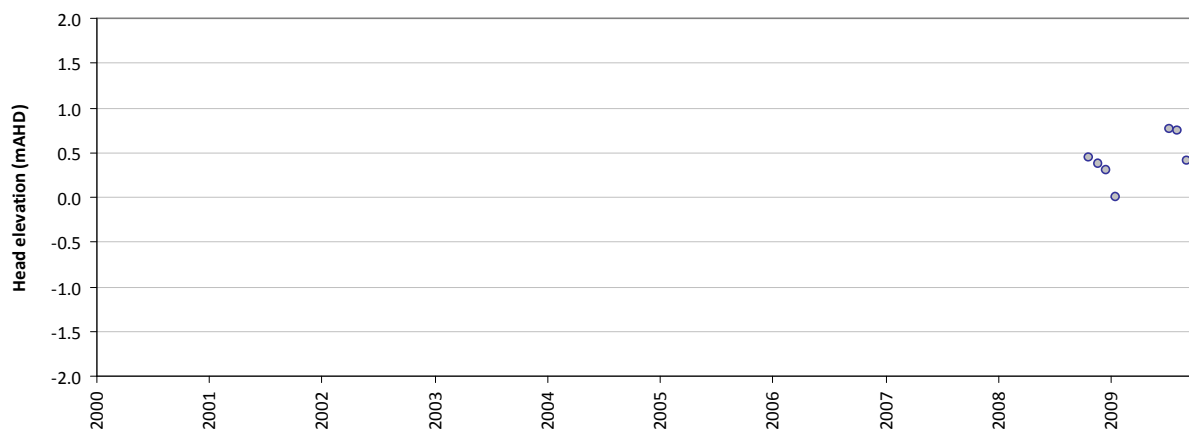
Statistics	
Mean error (ME)	0.74
Mean absolute error (MAE)	0.74
Root mean square error (RMSE)	0.75
Standard deviation of residuals (STDres)	0.09
Correlation coefficient (R)	0.99
Nash Sutcliffe correlation coefficient (R2)	-2.38

HS107

Modelled vs observed time-series plot - HS107

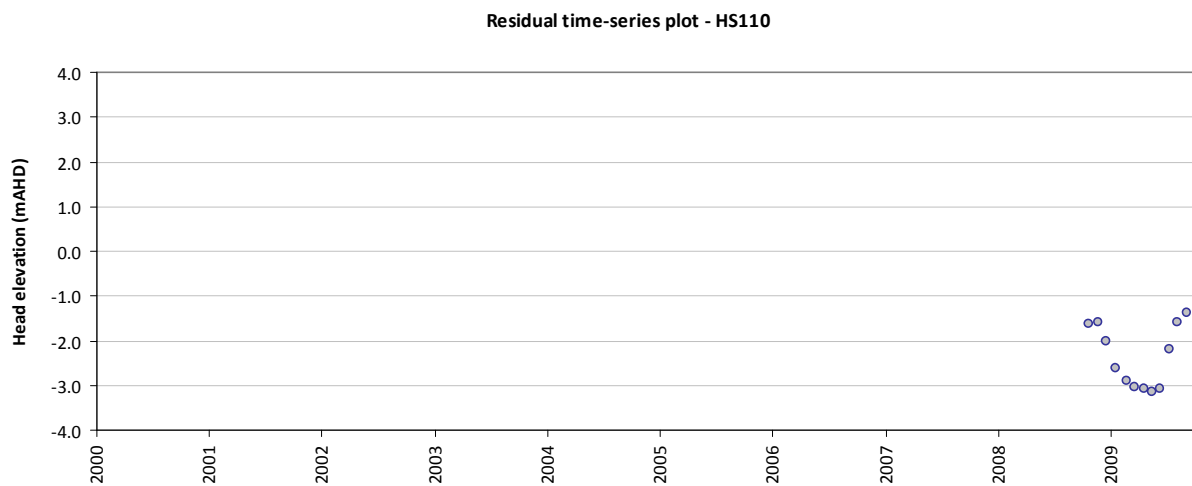
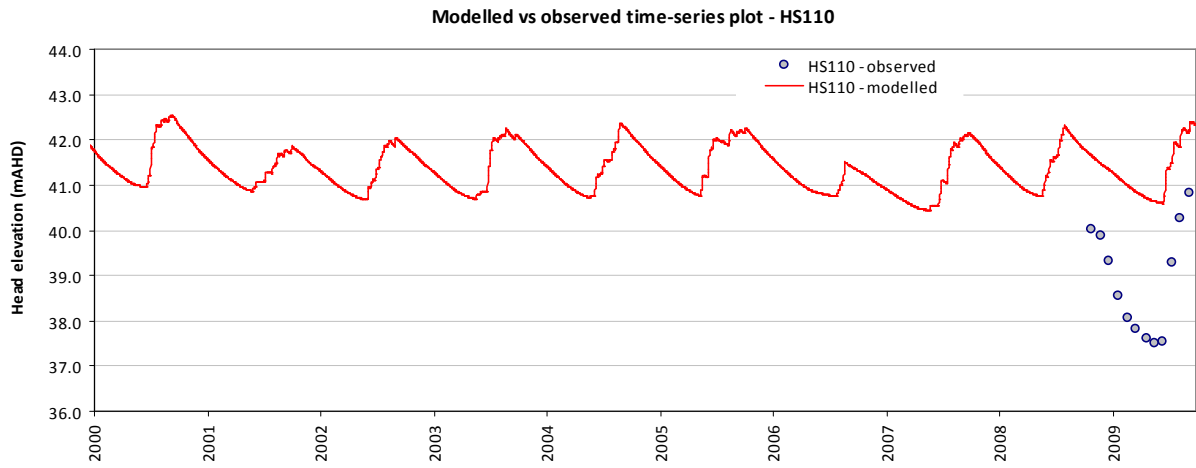


Residual time-series plot - HS107



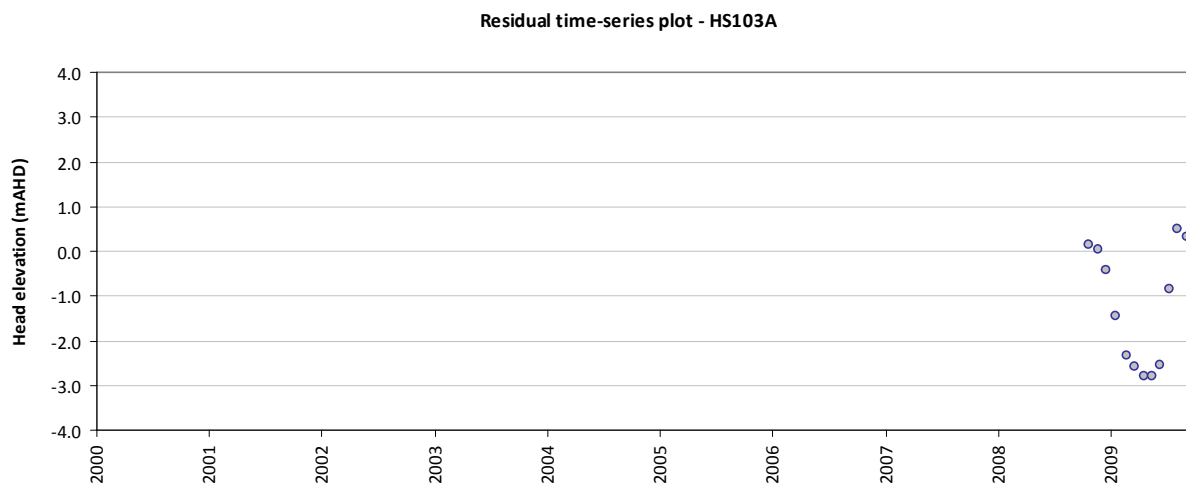
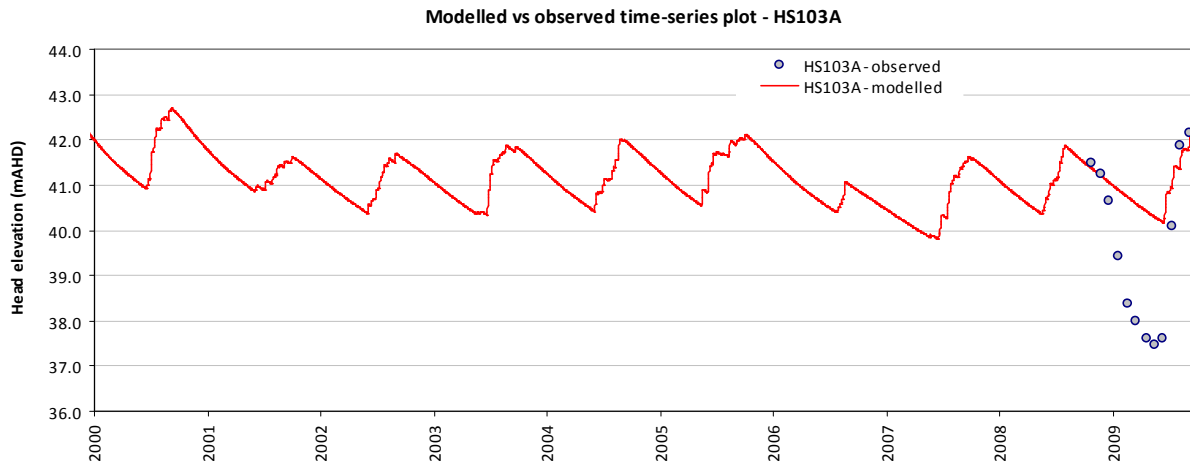
Statistics	
Mean error (ME)	0.43
Mean absolute error (MAE)	0.44
Root mean square error (RMSE)	0.50
Standard deviation of residuals (STDres)	0.25
Correlation coefficient (R)	0.91
Nash Sutcliffe correlation coefficient (R2)	0.12

HS110



Statistics	
Mean error (ME)	-2.35
Mean absolute error (MAE)	2.35
Root mean square error (RMSE)	2.45
Standard deviation of residuals (STDres)	0.67
Correlation coefficient (R)	0.98
Nash Sutcliffe correlation coefficient (R2)	-3.60

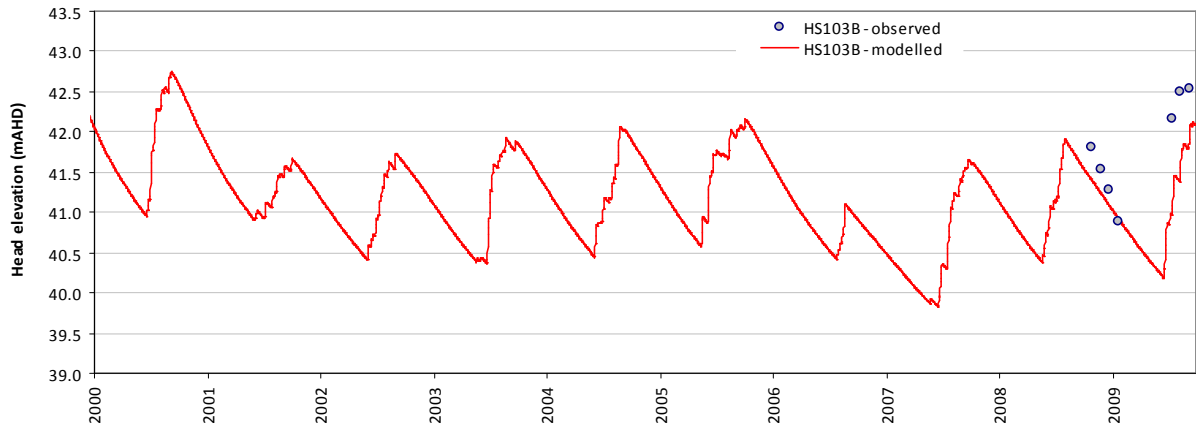
HS103A



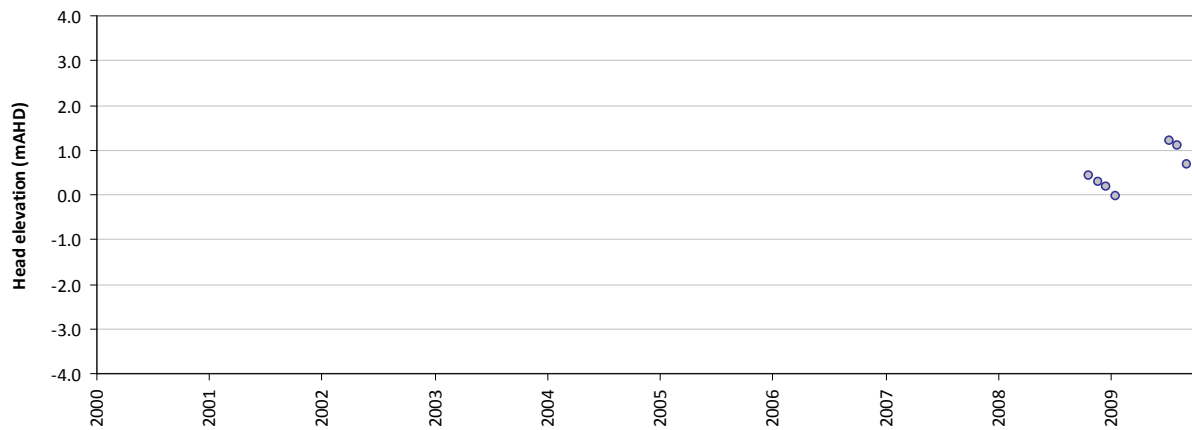
Statistics	
Mean error (ME)	-1.24
Mean absolute error (MAE)	1.41
Root mean square error (RMSE)	1.78
Standard deviation of residuals (STDres)	1.28
Correlation coefficient (R)	0.96
Nash Sutcliffe correlation coefficient (R2)	-0.06

HS103B

Modelled vs observed time-series plot - HS103B



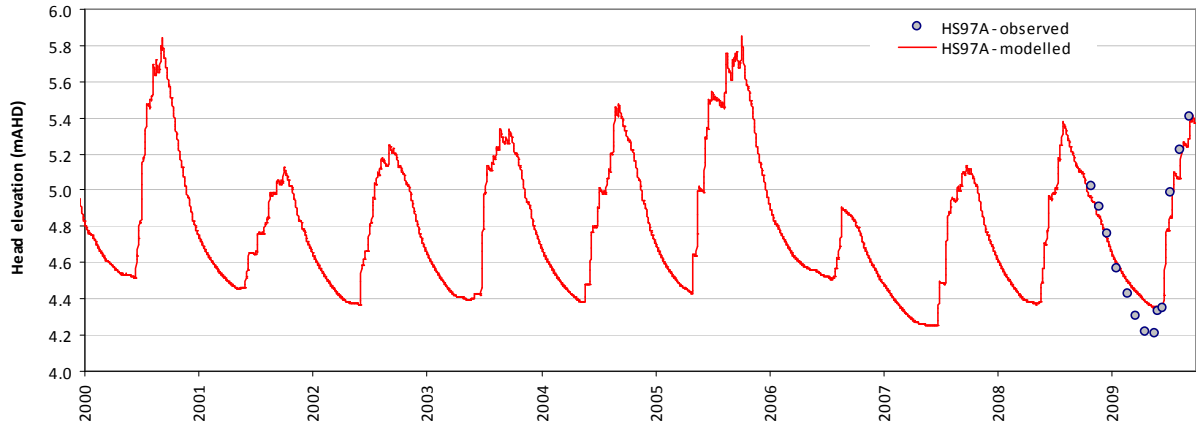
Residual time-series plot - HS103B



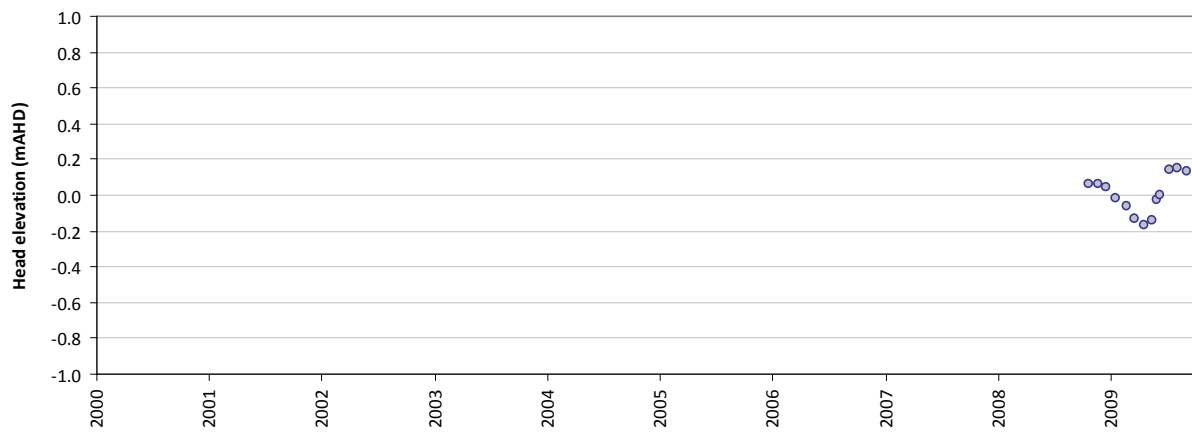
Statistics	
Mean error (ME)	0.55
Mean absolute error (MAE)	0.56
Root mean square error (RMSE)	0.70
Standard deviation of residuals (STDres)	0.44
Correlation coefficient (R)	0.68
Nash Sutcliffe correlation coefficient (R2)	-0.47

HS97A

Modelled vs observed time-series plot - HS97A



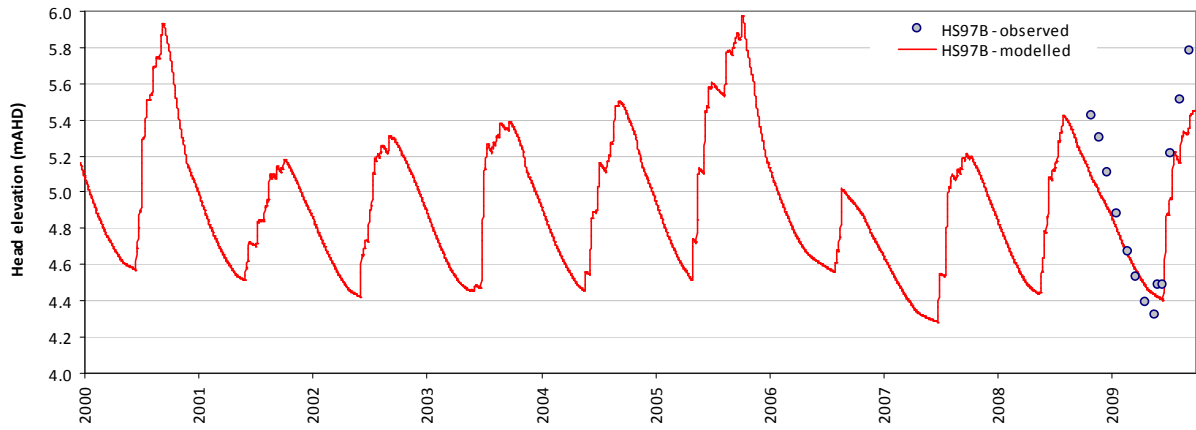
Residual time-series plot - HS97A



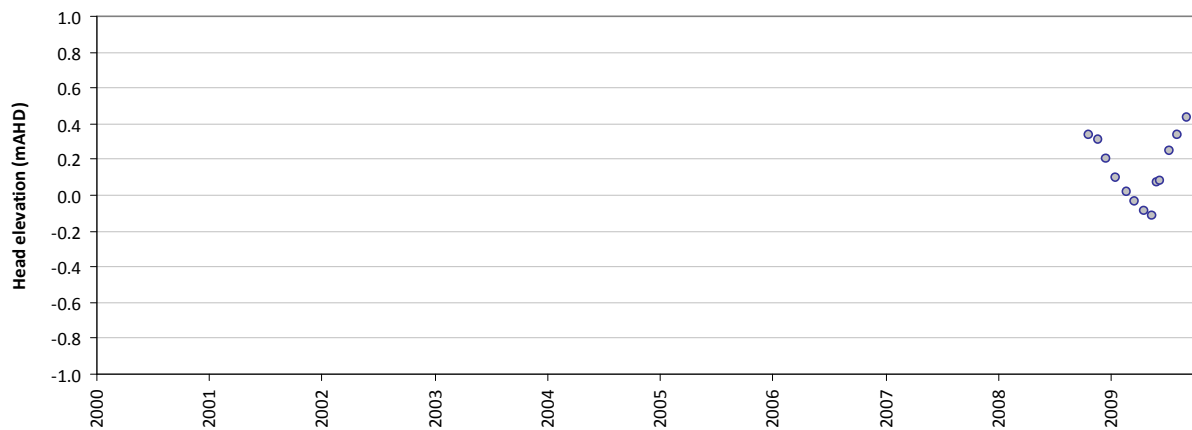
Statistics	
Mean error (ME)	0.00
Mean absolute error (MAE)	0.09
Root mean square error (RMSE)	0.10
Standard deviation of residuals (STDres)	0.10
Correlation coefficient (R)	0.99
Nash Sutcliffe correlation coefficient (R2)	0.93

HS97B

Modelled vs observed time-series plot - HS97B



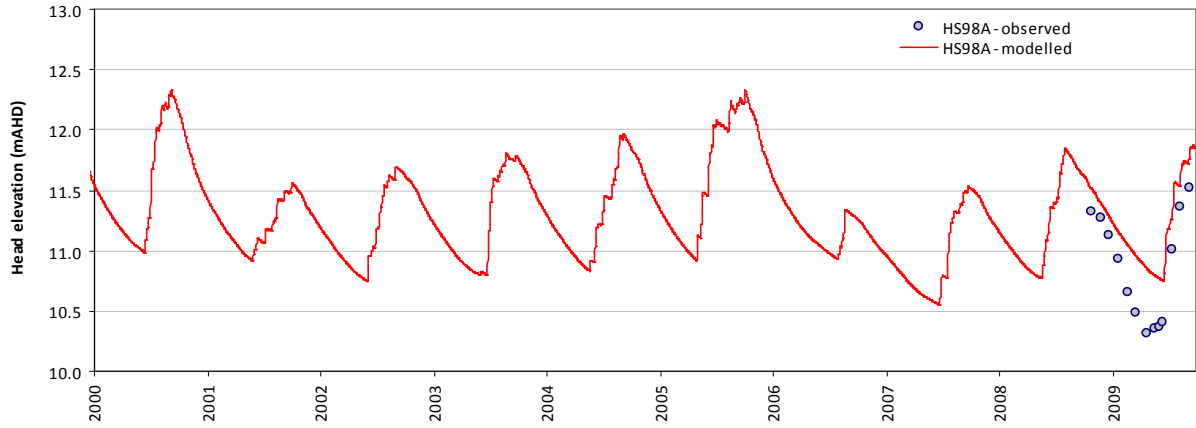
Residual time-series plot - HS97B



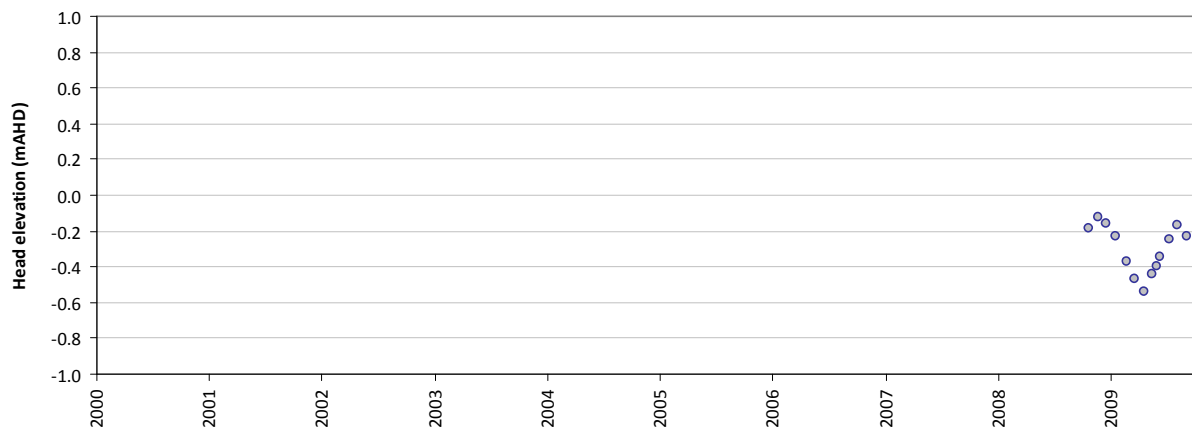
Statistics	
Mean error (ME)	0.14
Mean absolute error (MAE)	0.18
Root mean square error (RMSE)	0.22
Standard deviation of residuals (STDres)	0.17
Correlation coefficient (R)	0.99
Nash Sutcliffe correlation coefficient (R2)	0.77

HS98A

Modelled vs observed time-series plot - HS98A



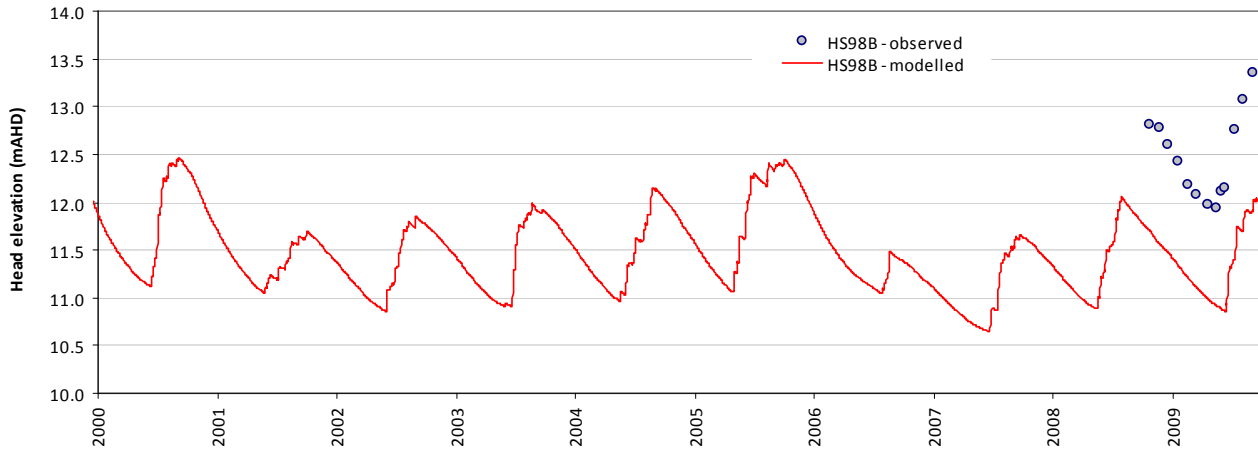
Residual time-series plot - HS98A



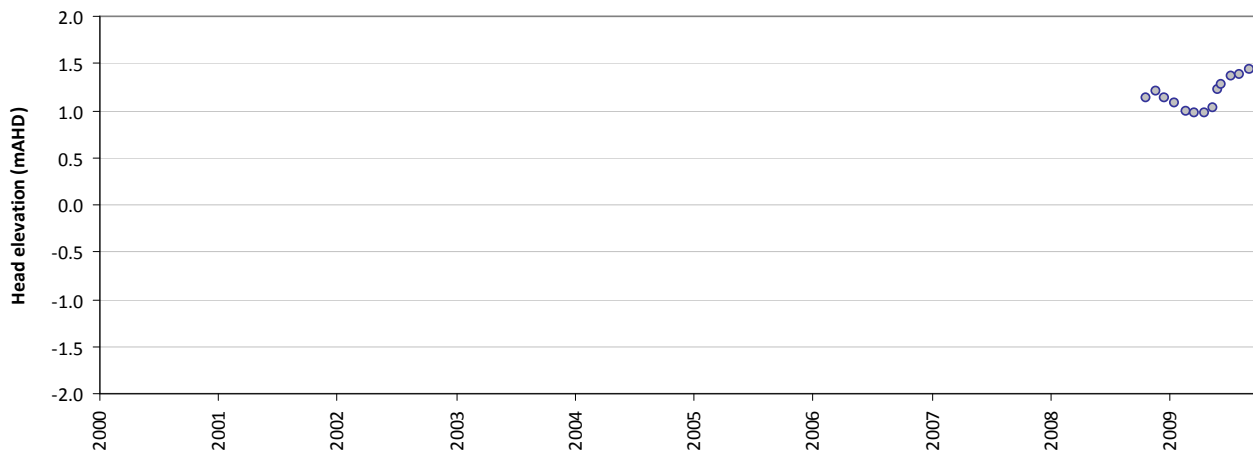
Statistics	
Mean error (ME)	-0.30
Mean absolute error (MAE)	0.30
Root mean square error (RMSE)	0.33
Standard deviation of residuals (STDres)	0.13
Correlation coefficient (R)	0.98
Nash Sutcliffe correlation coefficient (R2)	0.40

HS98B

Modelled vs observed time-series plot - HS98B



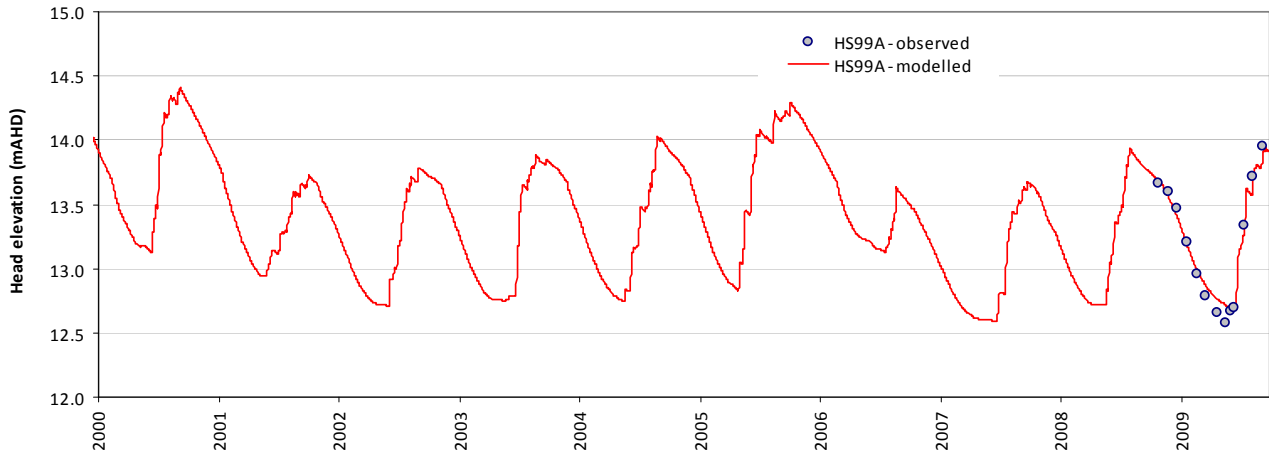
Residual time-series plot - HS98B



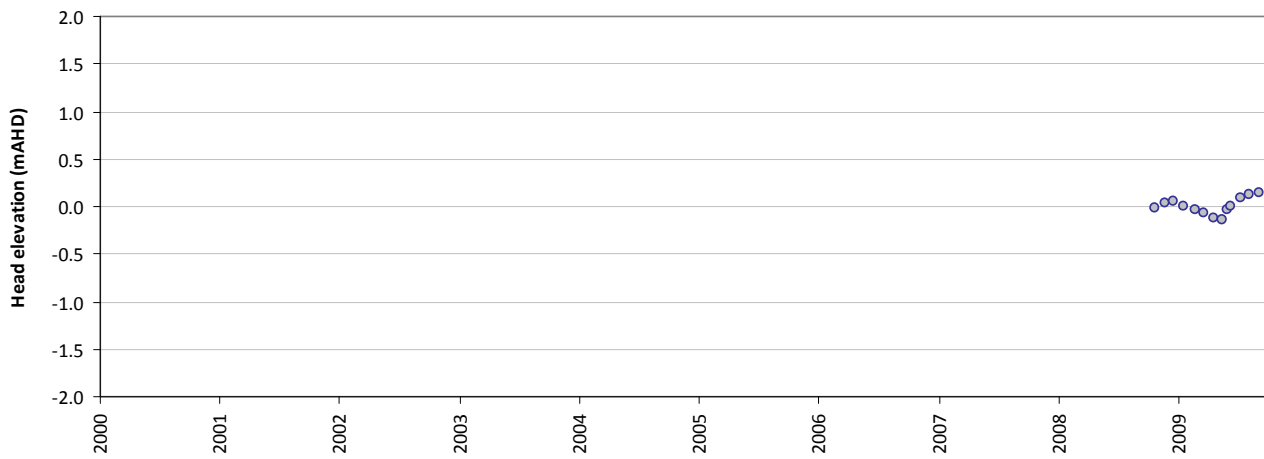
Statistics	
Mean error (ME)	1.17
Mean absolute error (MAE)	1.17
Root mean square error (RMSE)	1.18
Standard deviation of residuals (STDres)	0.16
Correlation coefficient (R)	0.95
Nash Sutcliffe correlation coefficient (R2)	-6.30

HS99A

Modelled vs observed time-series plot - HS99A



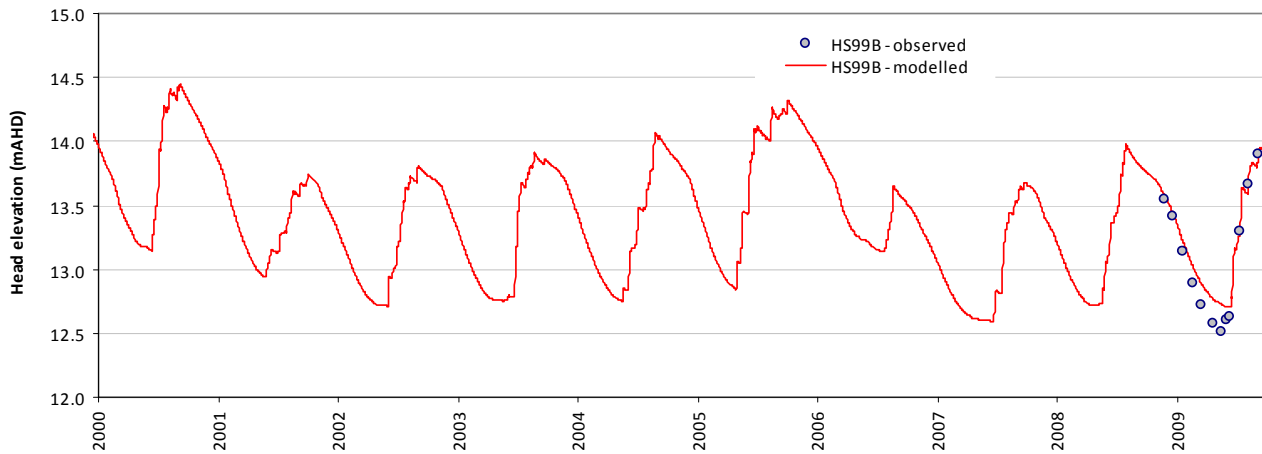
Residual time-series plot - HS99A



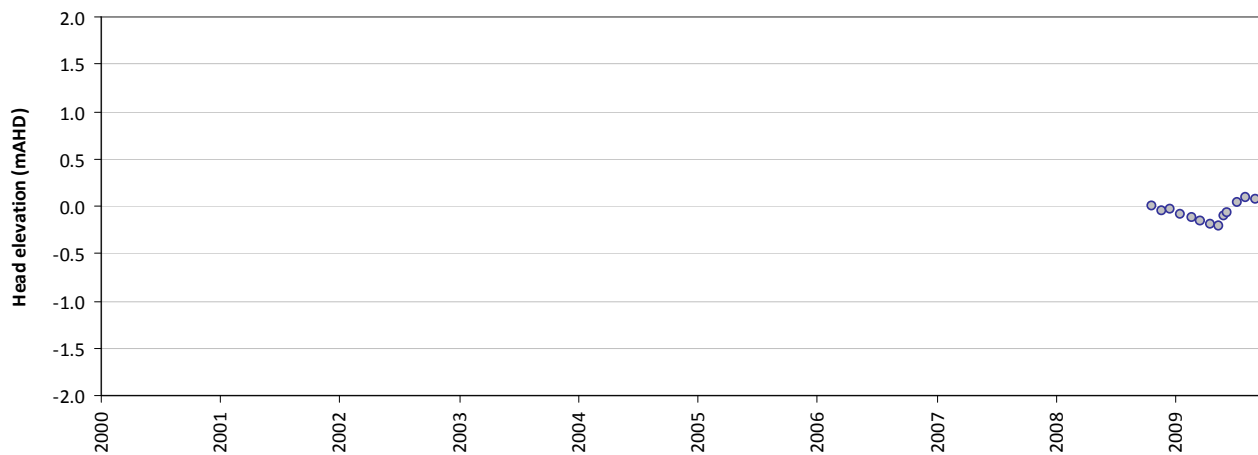
Statistics	
Mean error (ME)	0.00
Mean absolute error (MAE)	0.07
Root mean square error (RMSE)	0.08
Standard deviation of residuals (STDres)	0.08
Correlation coefficient (R)	0.99
Nash Sutcliffe correlation coefficient (R2)	0.97

HS99B

Modelled vs observed time-series plot - HS99B



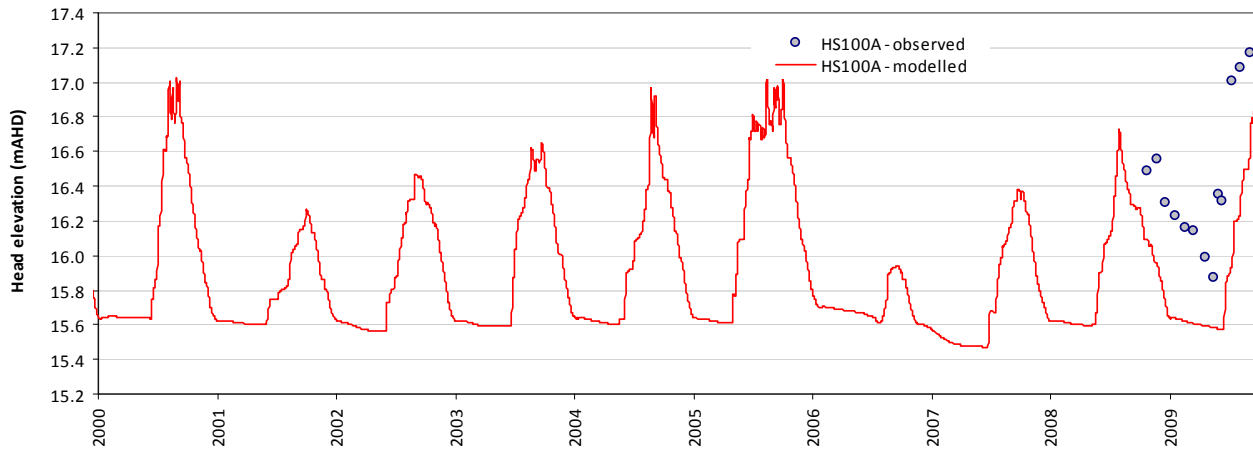
Residual time-series plot - HS99B



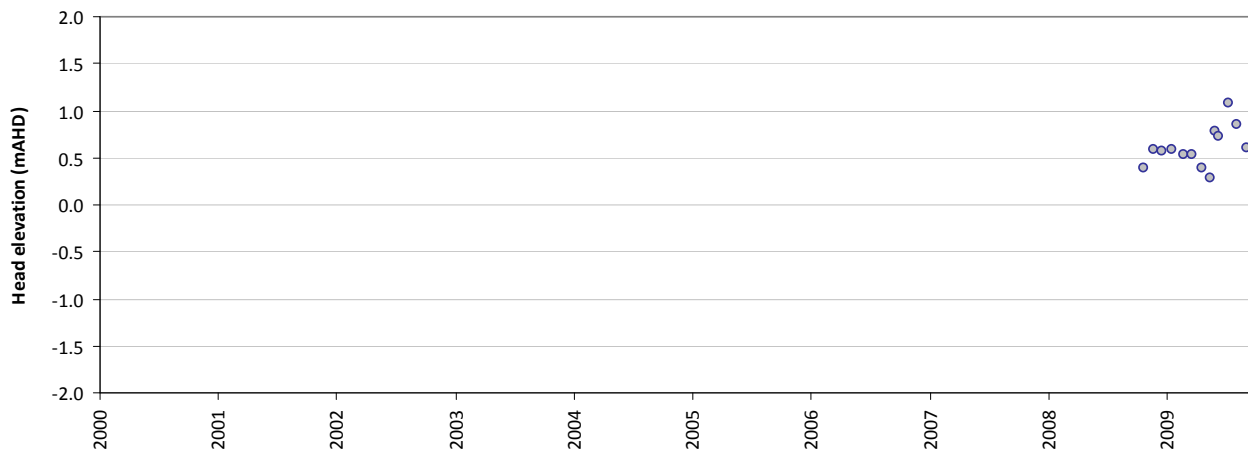
Statistics	
Mean error (ME)	0.02
Mean absolute error (MAE)	0.19
Root mean square error (RMSE)	0.34
Standard deviation of residuals (STDres)	0.34
Correlation coefficient (R)	0.90
Nash Sutcliffe correlation coefficient (R2)	0.73

HS100A

Modelled vs observed time-series plot - HS100A



Residual time-series plot - HS100A

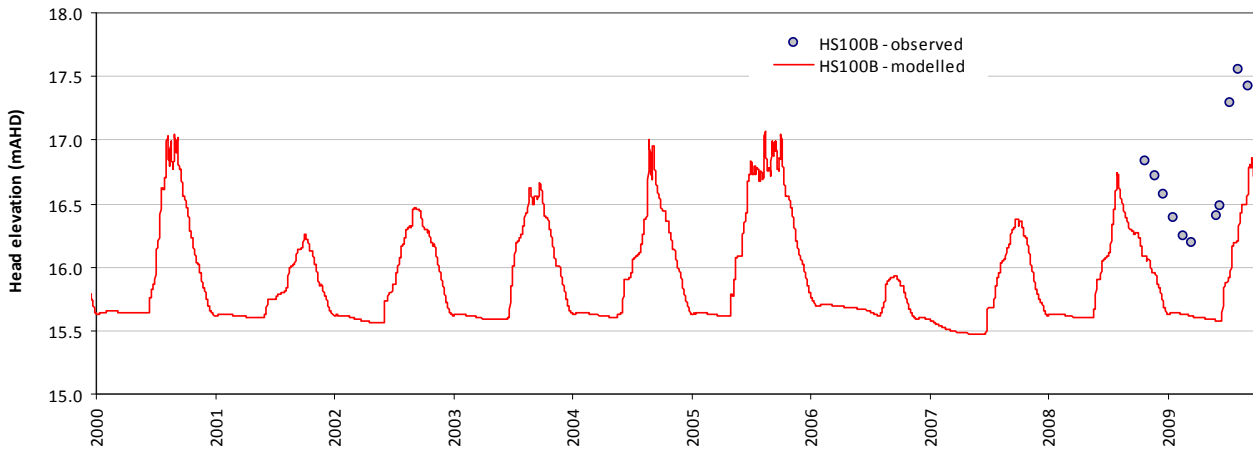


Statistics

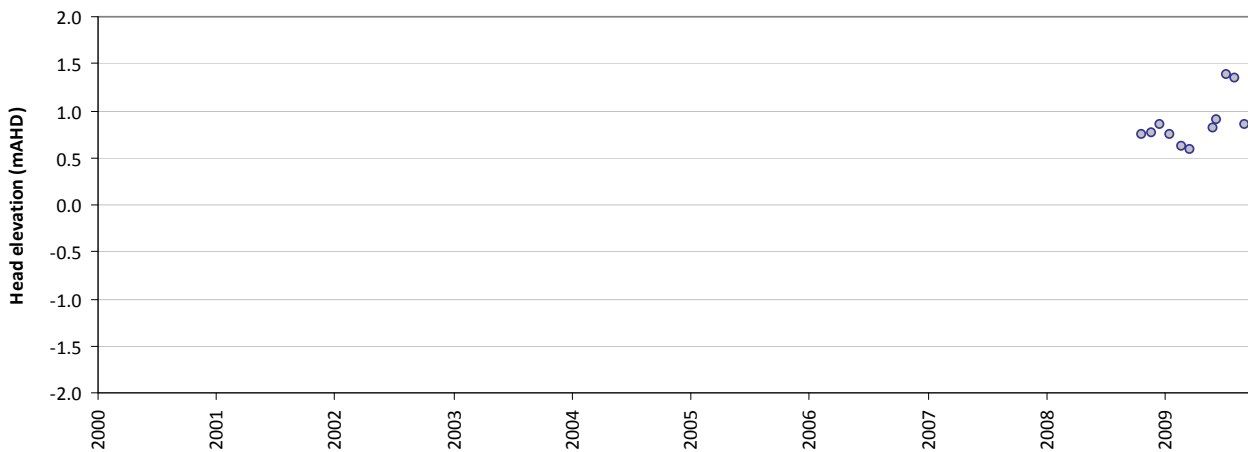
Mean error (ME)	0.61
Mean absolute error (MAE)	0.61
Root mean square error (RMSE)	0.64
Standard deviation of residuals (STDres)	0.20
Correlation coefficient (R)	0.87
Nash Sutcliffe correlation coefficient (R2)	-1.60

HS100B

Modelled vs observed time-series plot - HS100B



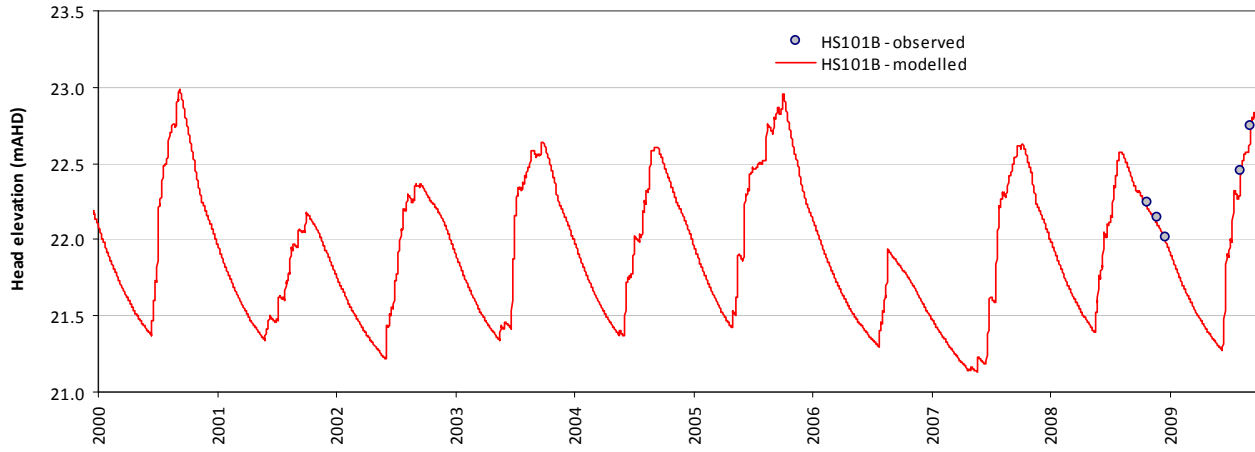
Residual time-series plot - HS100B



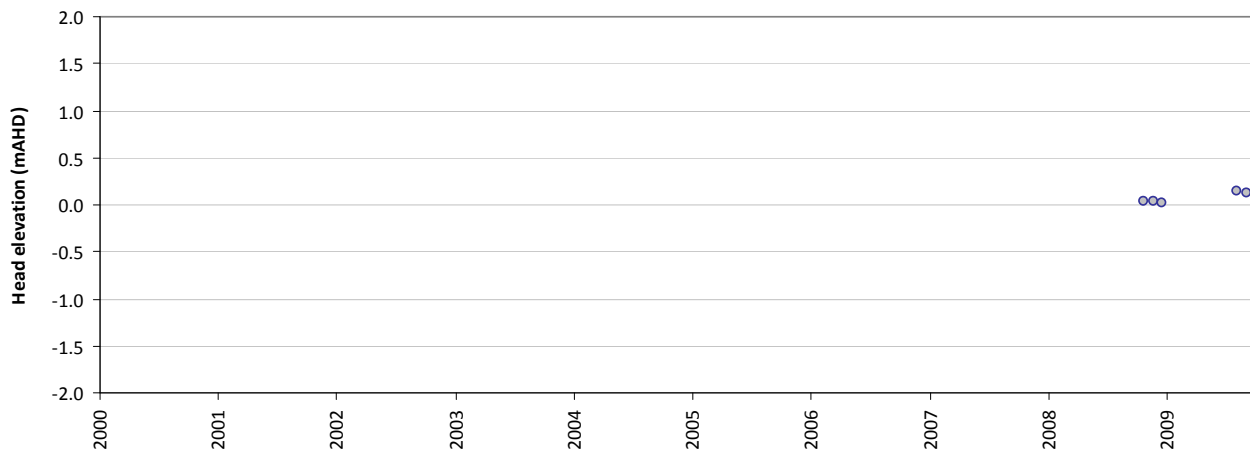
Statistics	
Mean error (ME)	0.87
Mean absolute error (MAE)	0.87
Root mean square error (RMSE)	0.91
Standard deviation of residuals (STDres)	0.25
Correlation coefficient (R)	0.86
Nash Sutcliffe correlation coefficient (R2)	-2.89

HS101B

Modelled vs observed time-series plot - HS101B



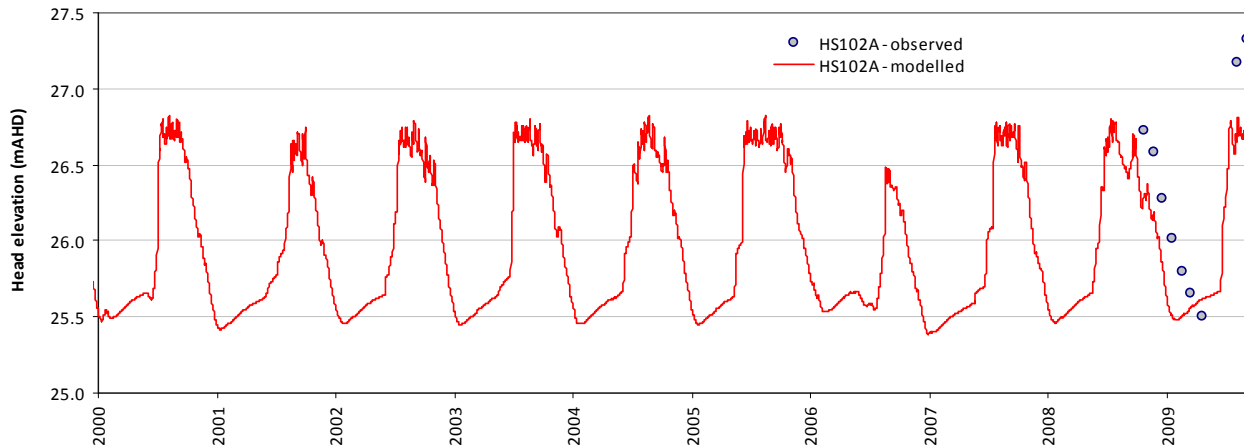
Residual time-series plot - HS101B



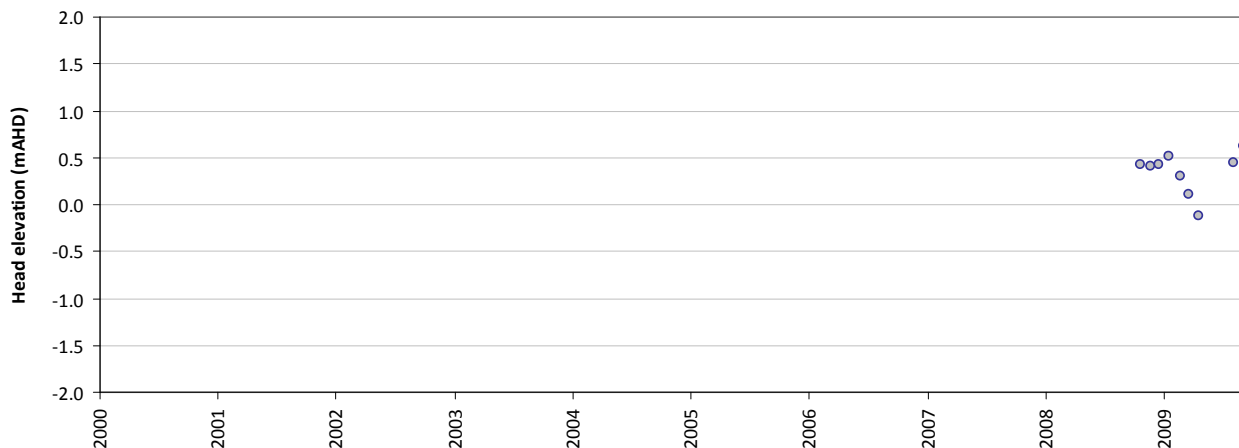
Statistics	
Mean error (ME)	0.07
Mean absolute error (MAE)	0.07
Root mean square error (RMSE)	0.09
Standard deviation of residuals (STDres)	0.05
Correlation coefficient (R)	0.99
Nash Sutcliffe correlation coefficient (R2)	0.88

HS102A

Modelled vs observed time-series plot - HS102A



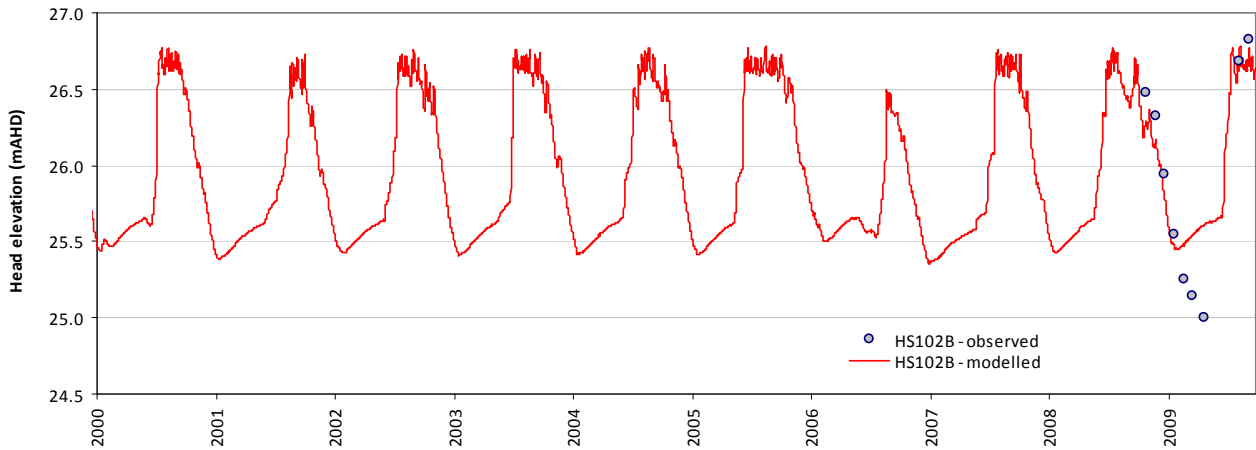
Residual time-series plot - HS102A



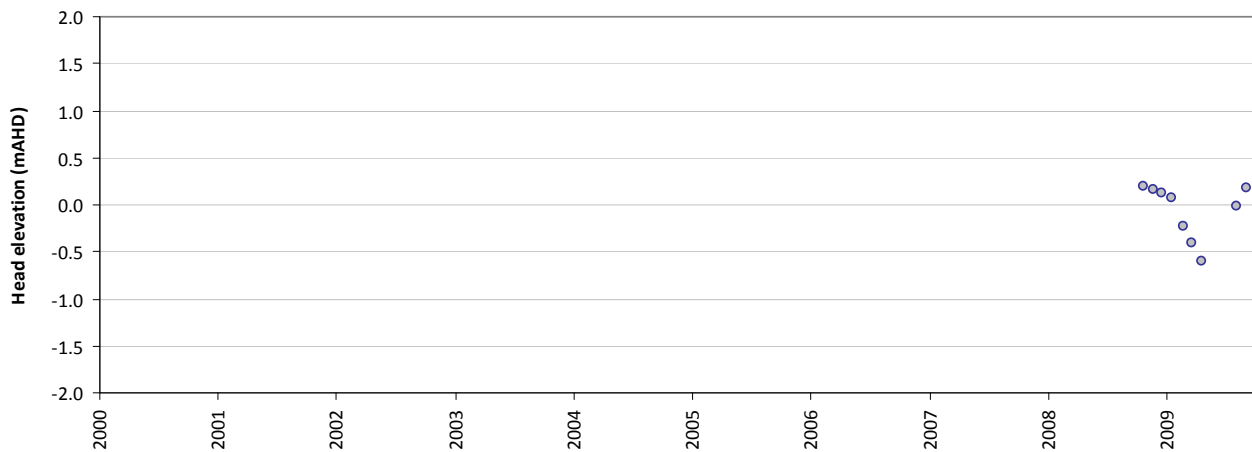
Statistics	
Mean error (ME)	0.35
Mean absolute error (MAE)	0.37
Root mean square error (RMSE)	0.41
Standard deviation of residuals (STDres)	0.21
Correlation coefficient (R)	0.96
Nash Sutcliffe correlation coefficient (R2)	0.56

HS102B

Modelled vs observed time-series plot - HS102B



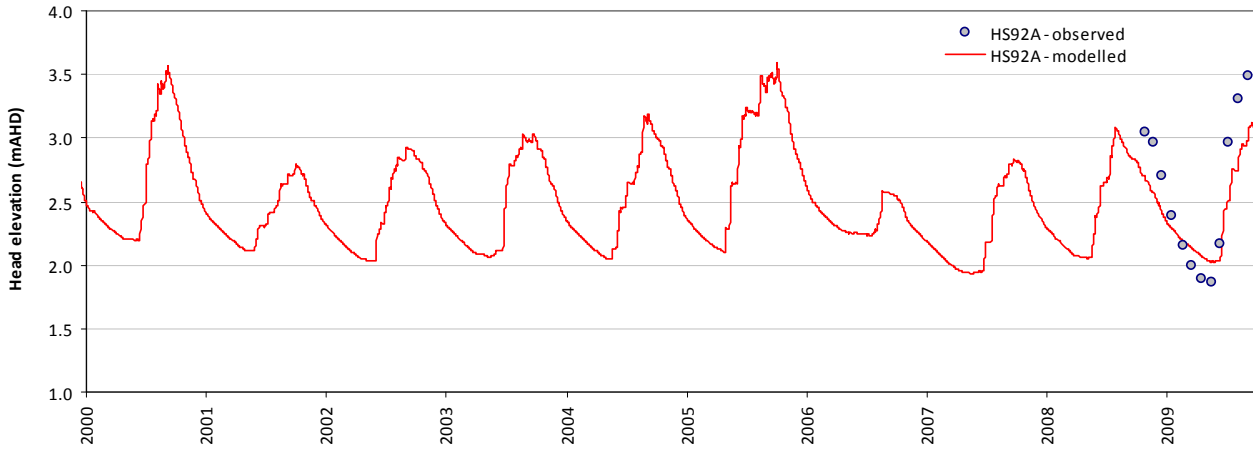
Residual time-series plot - HS102B



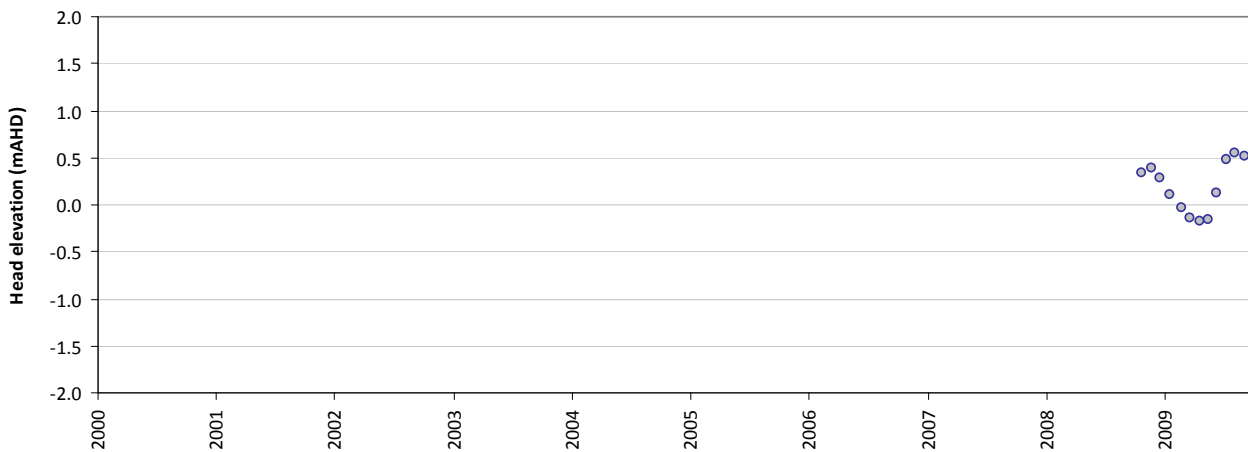
Statistics	
Mean error (ME)	-0.06
Mean absolute error (MAE)	0.22
Root mean square error (RMSE)	0.28
Standard deviation of residuals (STDres)	0.28
Correlation coefficient (R)	0.94
Nash Sutcliffe correlation coefficient (R2)	0.82

HS92A

Modelled vs observed time-series plot - HS92A



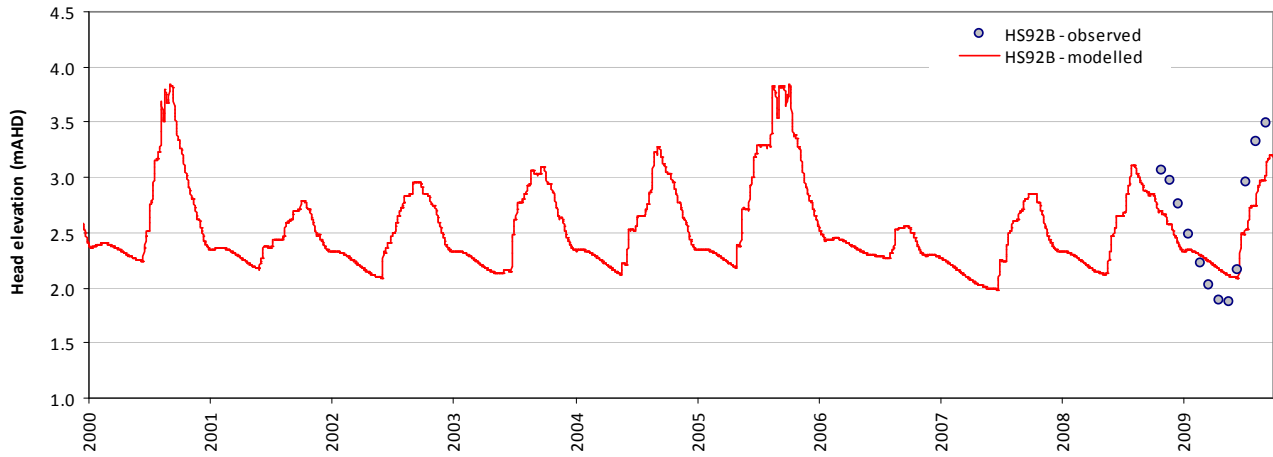
Residual time-series plot - HS92A



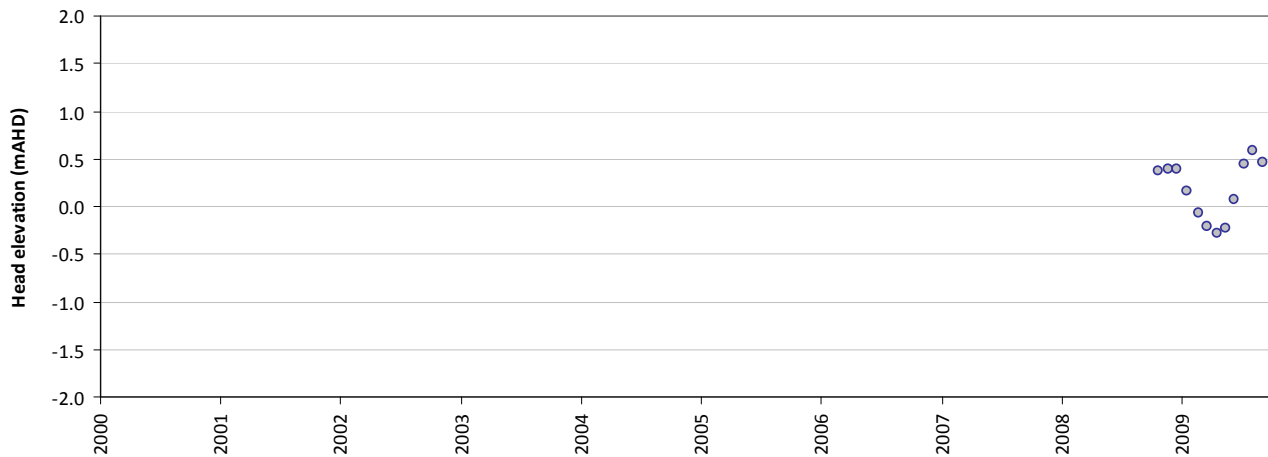
Statistics	
Mean error (ME)	0.19
Mean absolute error (MAE)	0.27
Root mean square error (RMSE)	0.32
Standard deviation of residuals (STDres)	0.26
Correlation coefficient (R)	0.98
Nash Sutcliffe correlation coefficient (R2)	0.65

HS92B

Modelled vs observed time-series plot - HS92B



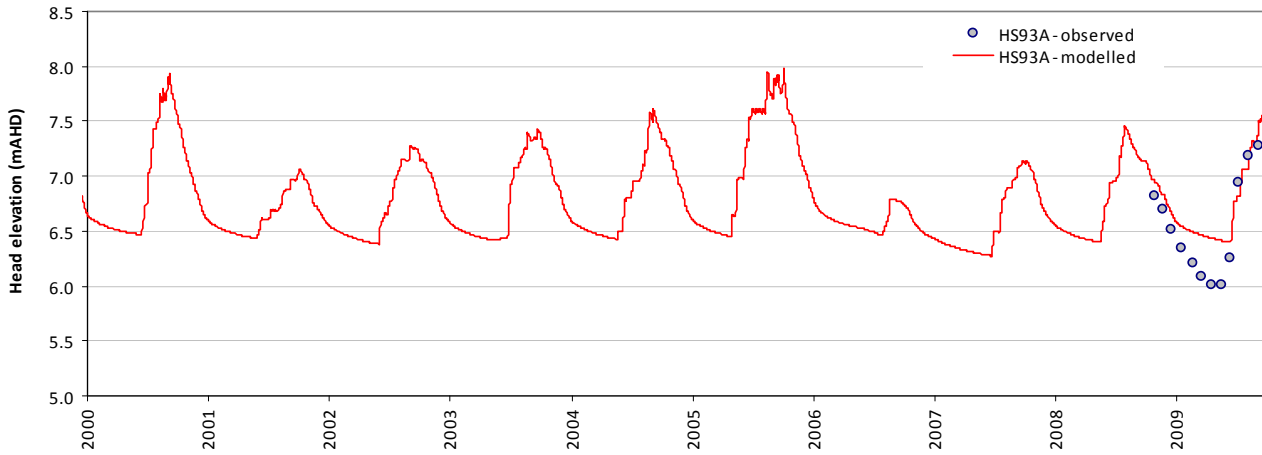
Residual time-series plot - HS92B



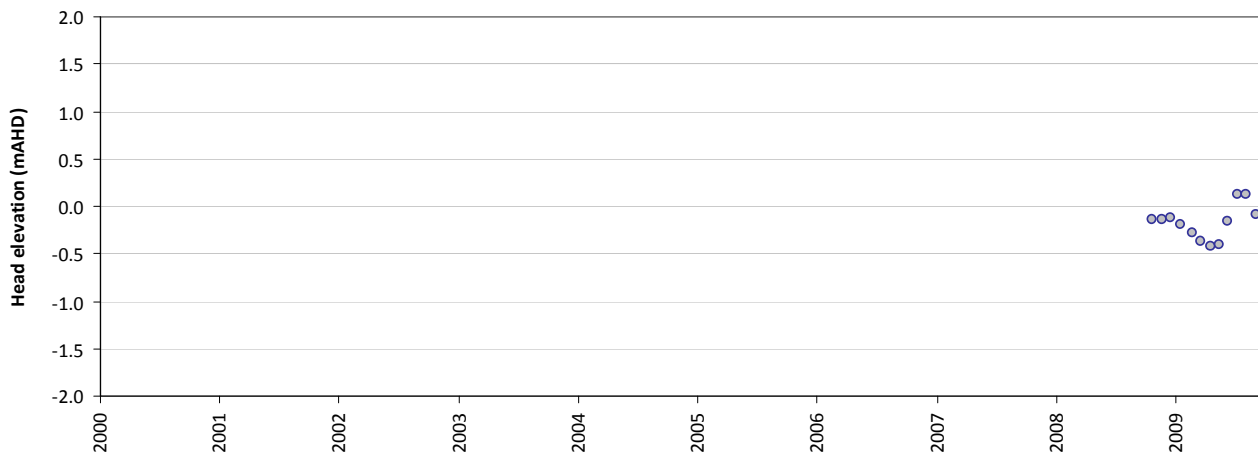
Statistics	
Mean error (ME)	0.17
Mean absolute error (MAE)	0.30
Root mean square error (RMSE)	0.34
Standard deviation of residuals (STDres)	0.30
Correlation coefficient (R)	0.95
Nash Sutcliffe correlation coefficient (R2)	0.61

HS93A

Modelled vs observed time-series plot - HS93A



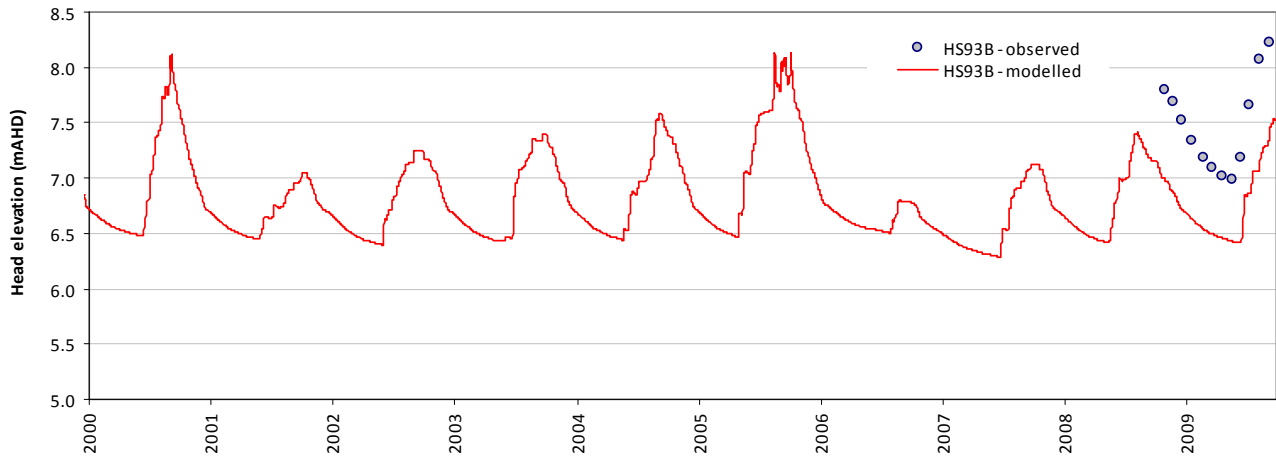
Residual time-series plot - HS93A



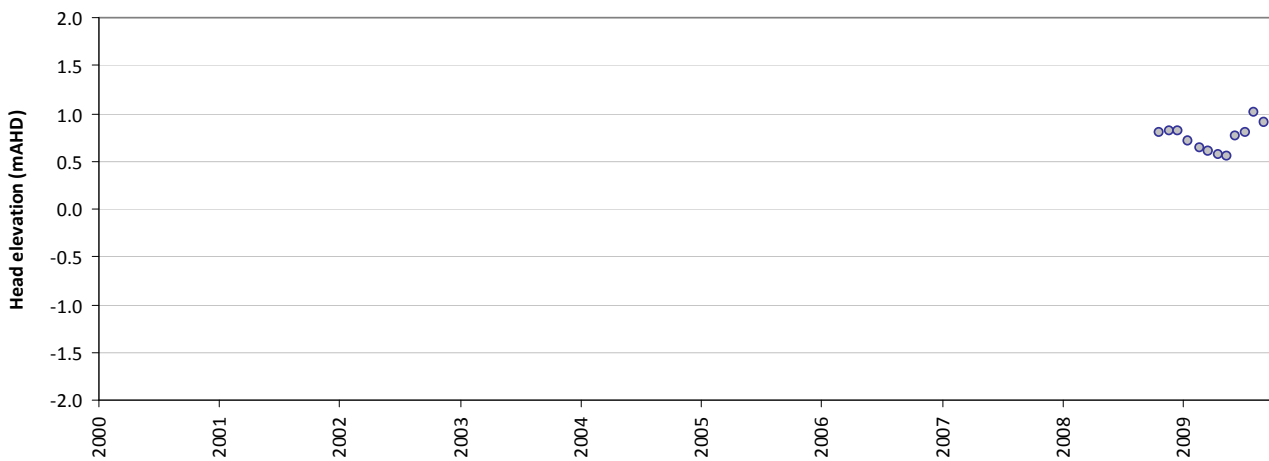
Statistics	
Mean error (ME)	-0.18
Mean absolute error (MAE)	0.22
Root mean square error (RMSE)	0.25
Standard deviation of residuals (STDres)	0.17
Correlation coefficient (R)	0.95
Nash Sutcliffe correlation coefficient (R2)	0.67

HS93B

Modelled vs observed time-series plot - HS93B



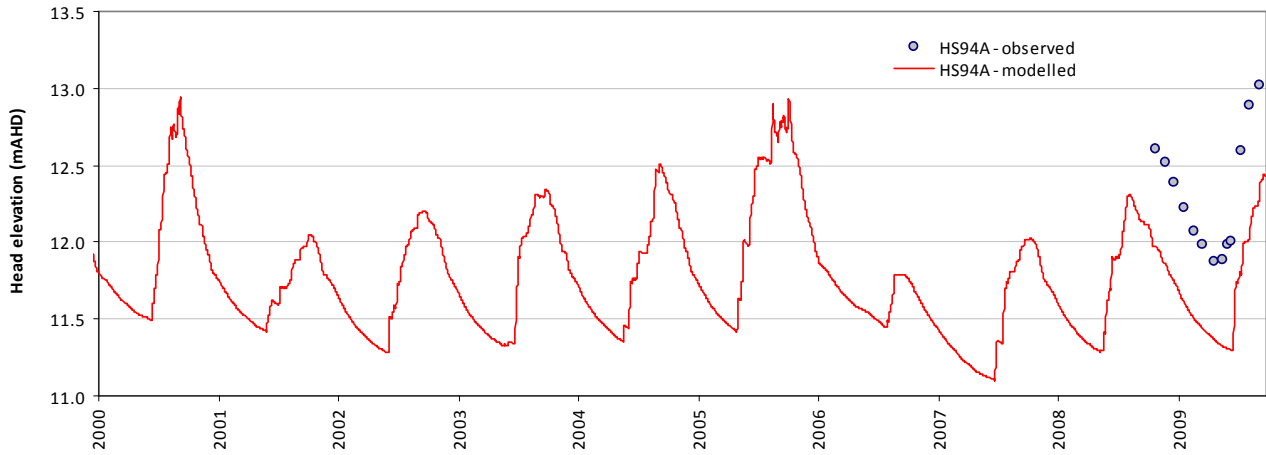
Residual time-series plot - HS93B



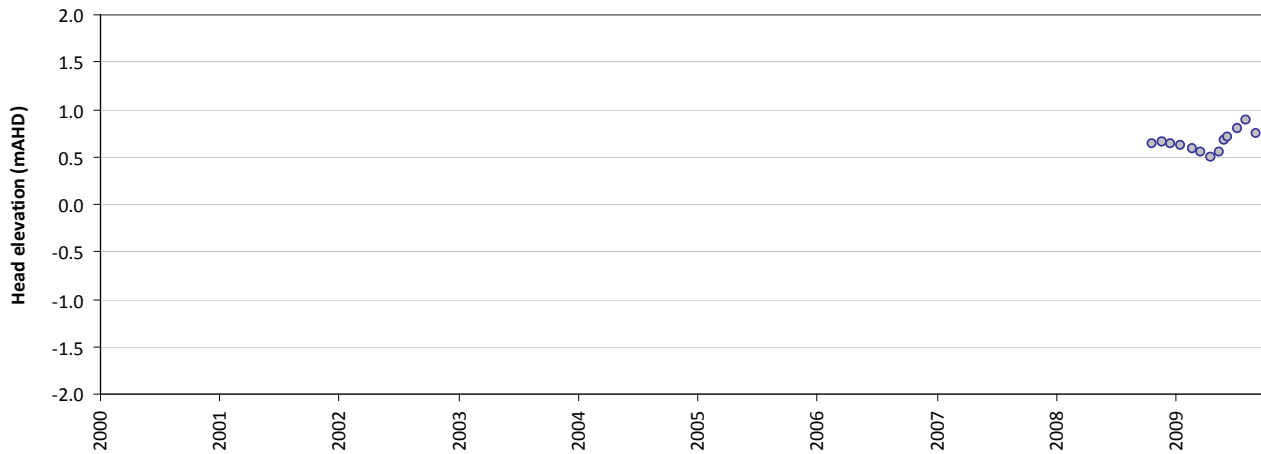
Statistics	
Mean error (ME)	0.75
Mean absolute error (MAE)	0.75
Root mean square error (RMSE)	0.76
Standard deviation of residuals (STDres)	0.13
Correlation coefficient (R)	0.98
Nash Sutcliffe correlation coefficient (R2)	-2.64

HS94A

Modelled vs observed time-series plot - HS94A



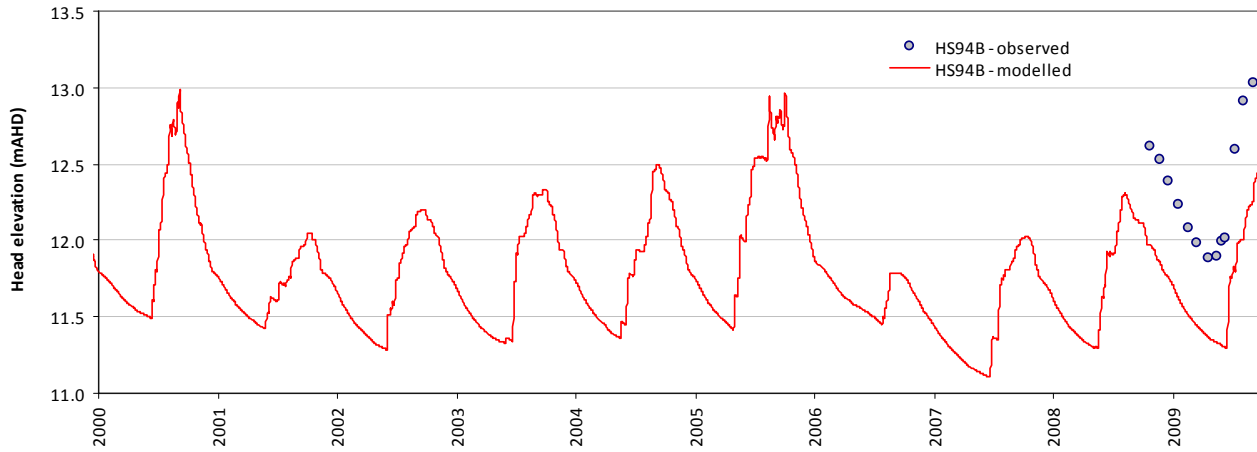
Residual time-series plot - HS94A



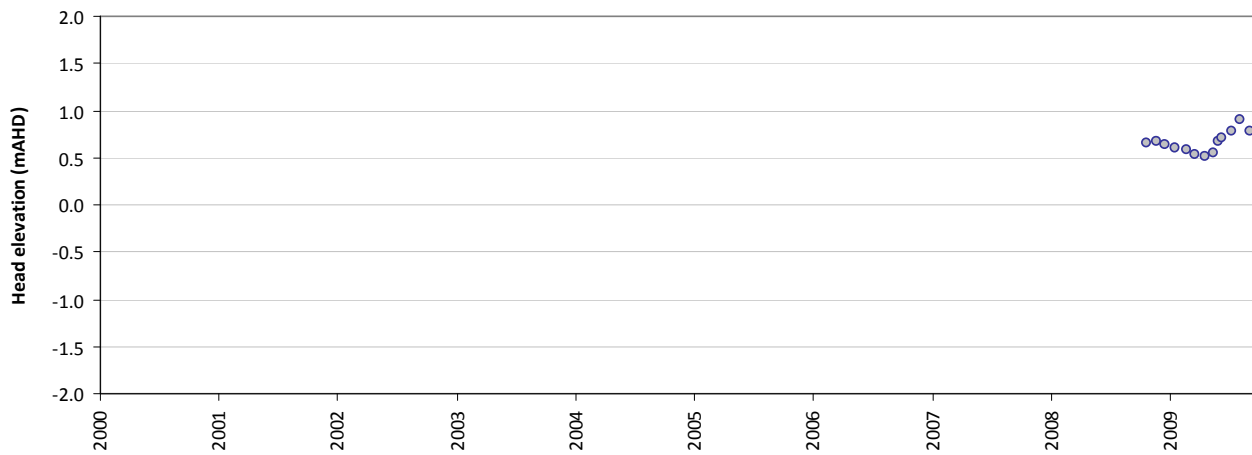
Statistics	
Mean error (ME)	0.66
Mean absolute error (MAE)	0.66
Root mean square error (RMSE)	0.66
Standard deviation of residuals (STDres)	0.10
Correlation coefficient (R)	0.98
Nash Sutcliffe correlation coefficient (R2)	-2.15

HS94B

Modelled vs observed time-series plot - HS94B



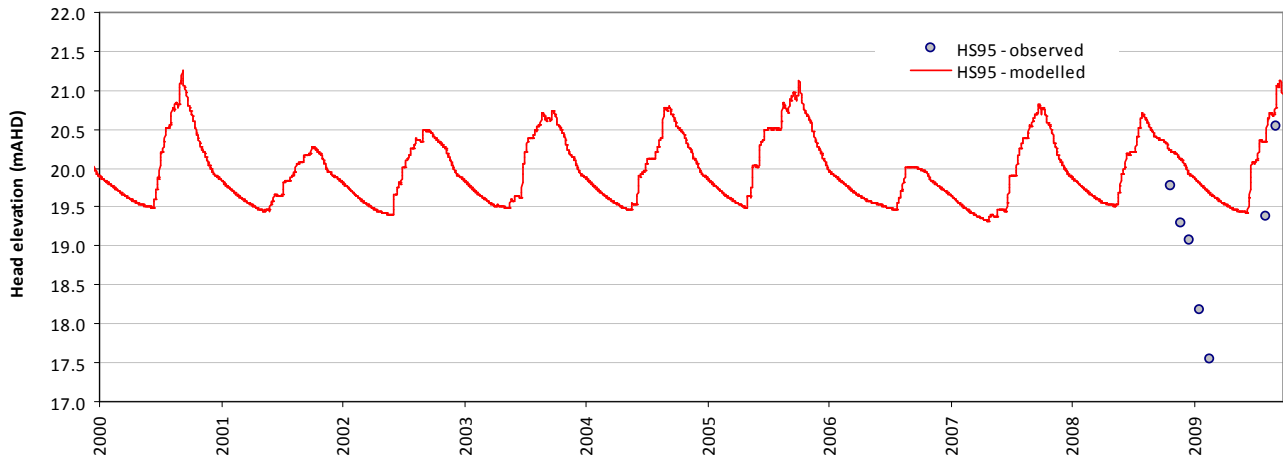
Residual time-series plot - HS94B



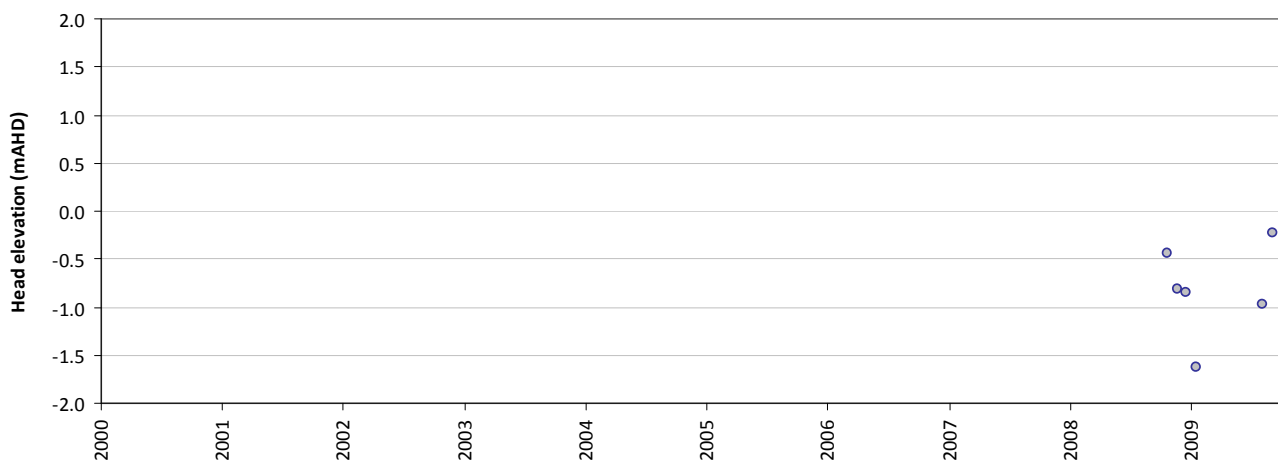
Statistics	
Mean error (ME)	0.66
Mean absolute error (MAE)	0.66
Root mean square error (RMSE)	0.67
Standard deviation of residuals (STDres)	0.11
Correlation coefficient (R)	0.98
Nash Sutcliffe correlation coefficient (R2)	-2.16

HS95

Modelled vs observed time-series plot - HS95



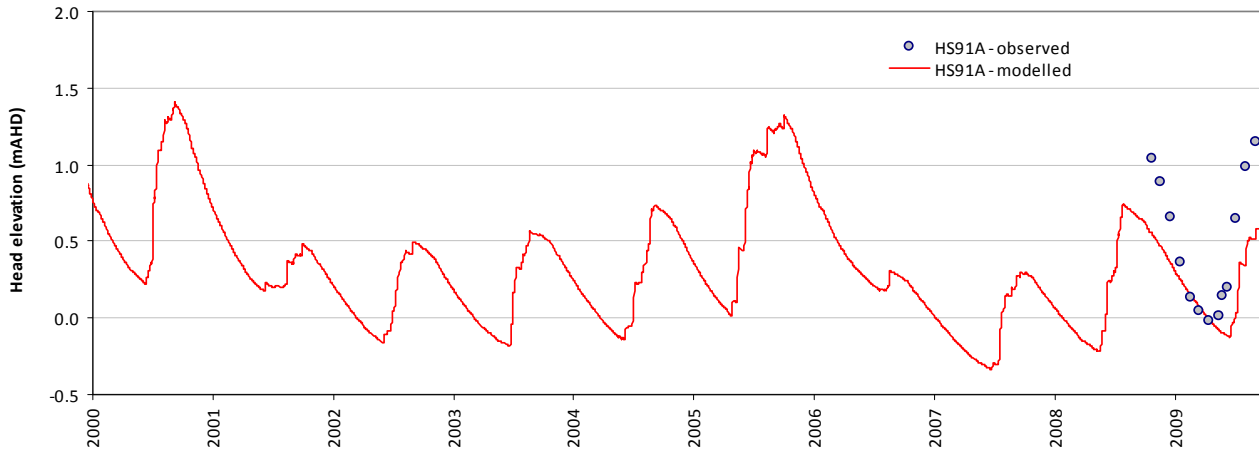
Residual time-series plot - HS95



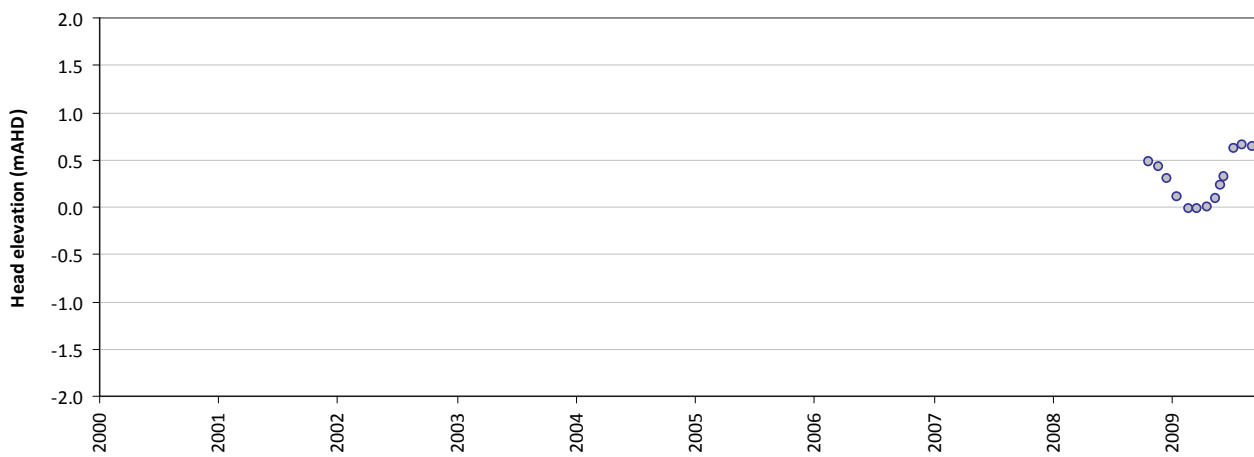
Statistics	
Mean error (ME)	-1.01
Mean absolute error (MAE)	1.01
Root mean square error (RMSE)	1.18
Standard deviation of residuals (STDres)	0.61
Correlation coefficient (R)	0.94
Nash Sutcliffe correlation coefficient (R2)	-0.65

HS91A

Modelled vs observed time-series plot - HS91A



Residual time-series plot - HS91A

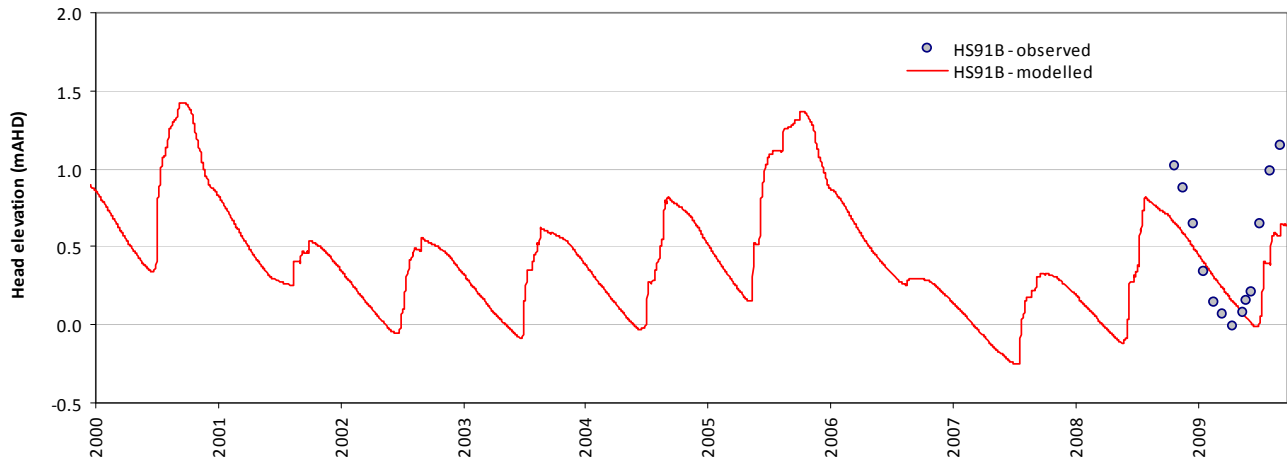


Statistics

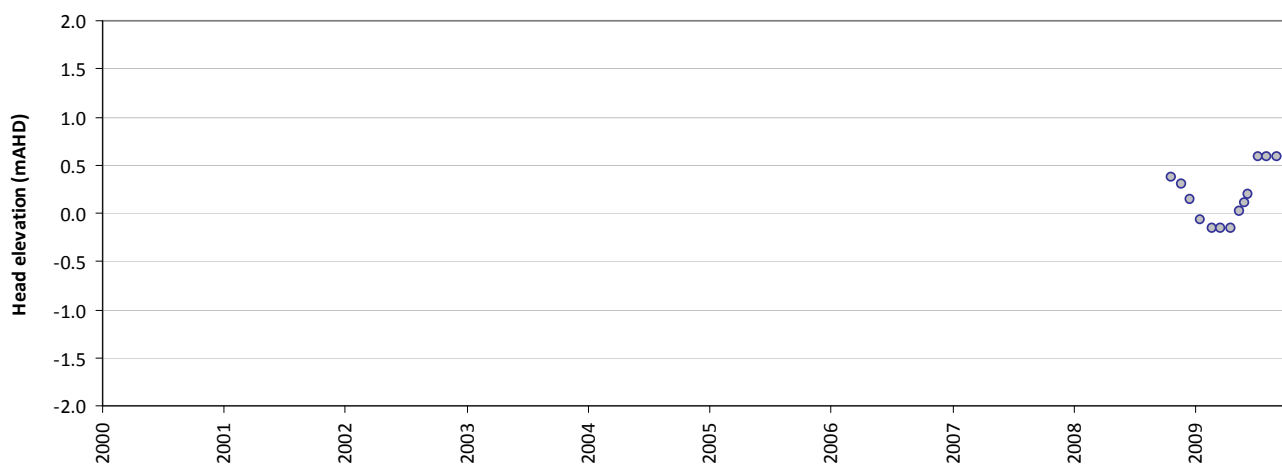
Mean error (ME)	0.29
Mean absolute error (MAE)	0.30
Root mean square error (RMSE)	0.38
Standard deviation of residuals (STDres)	0.24
Correlation coefficient (R)	0.87
Nash Sutcliffe correlation coefficient (R2)	0.17

HS91B

Modelled vs observed time-series plot - HS91B



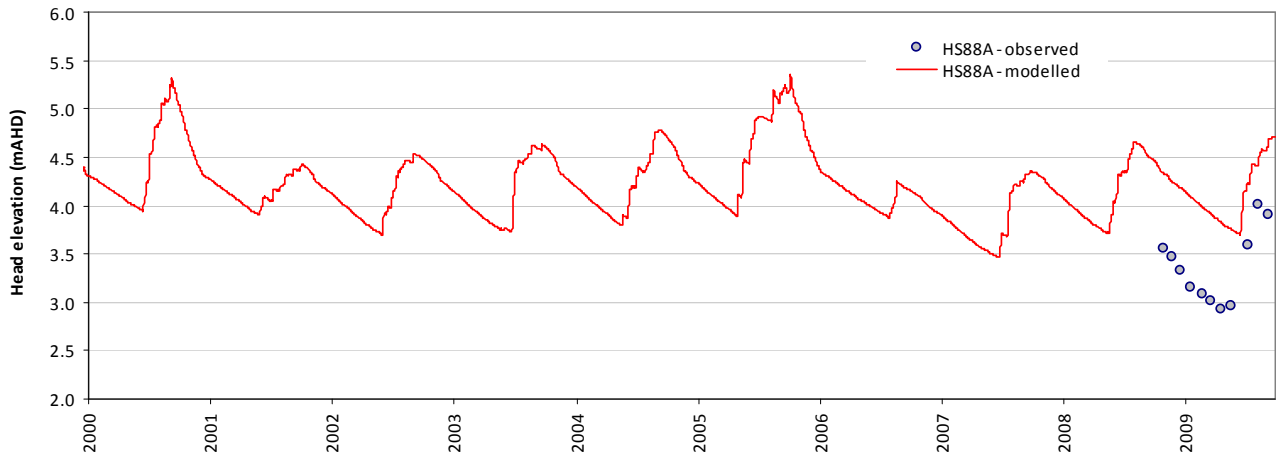
Residual time-series plot - HS91B



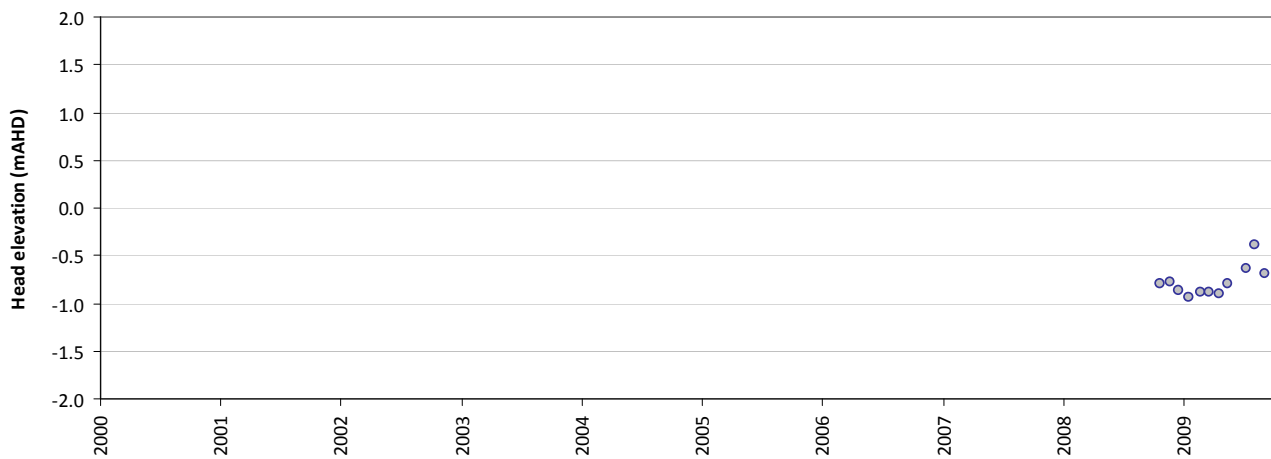
Statistics	
Mean error (ME)	0.18
Mean absolute error (MAE)	0.26
Root mean square error (RMSE)	0.33
Standard deviation of residuals (STDres)	0.28
Correlation coefficient (R)	0.75
Nash Sutcliffe correlation coefficient (R2)	0.33

HS88A

Modelled vs observed time-series plot - HS88A



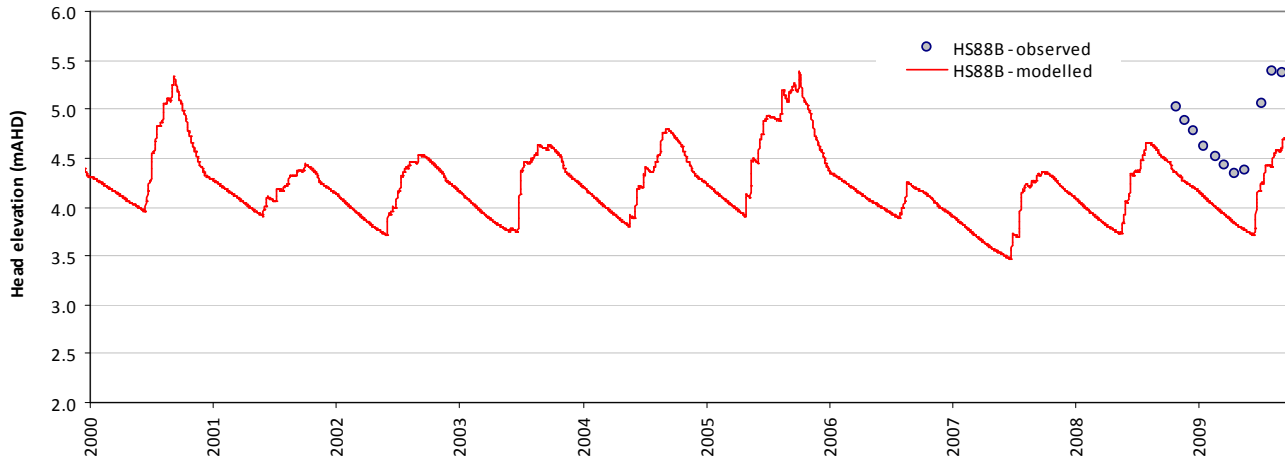
Residual time-series plot - HS88A



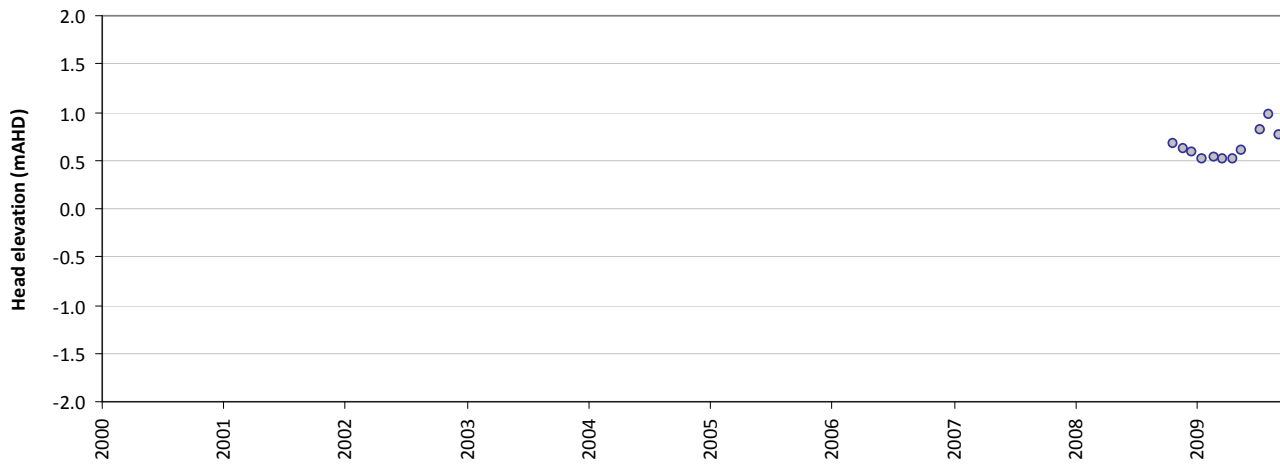
Statistics	
Mean error (ME)	-0.78
Mean absolute error (MAE)	0.78
Root mean square error (RMSE)	0.79
Standard deviation of residuals (STDres)	0.15
Correlation coefficient (R)	0.94
Nash Sutcliffe correlation coefficient (R2)	-3.89

HS88B

Modelled vs observed time-series plot - HS88B



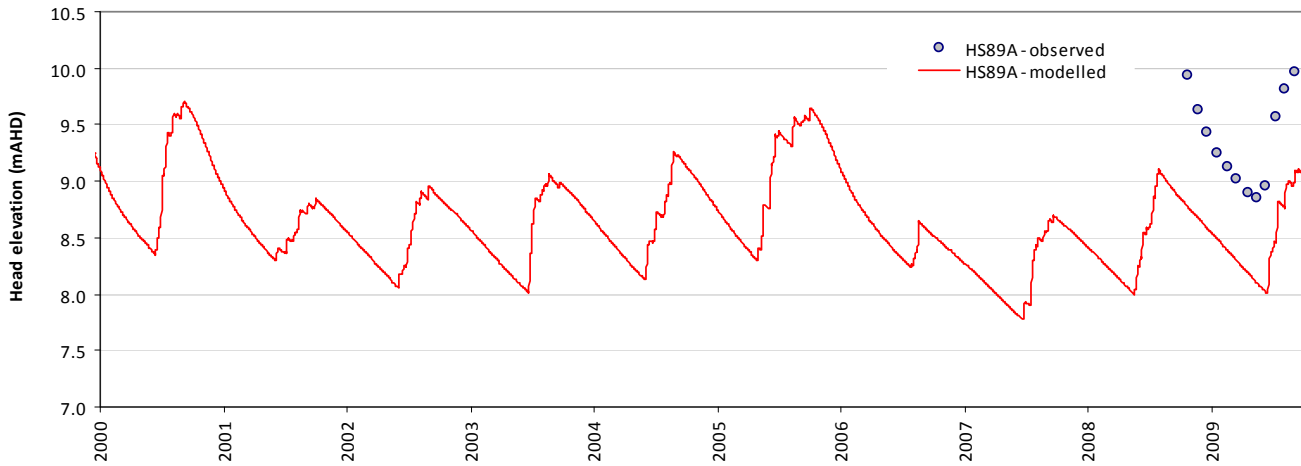
Residual time-series plot - HS88B



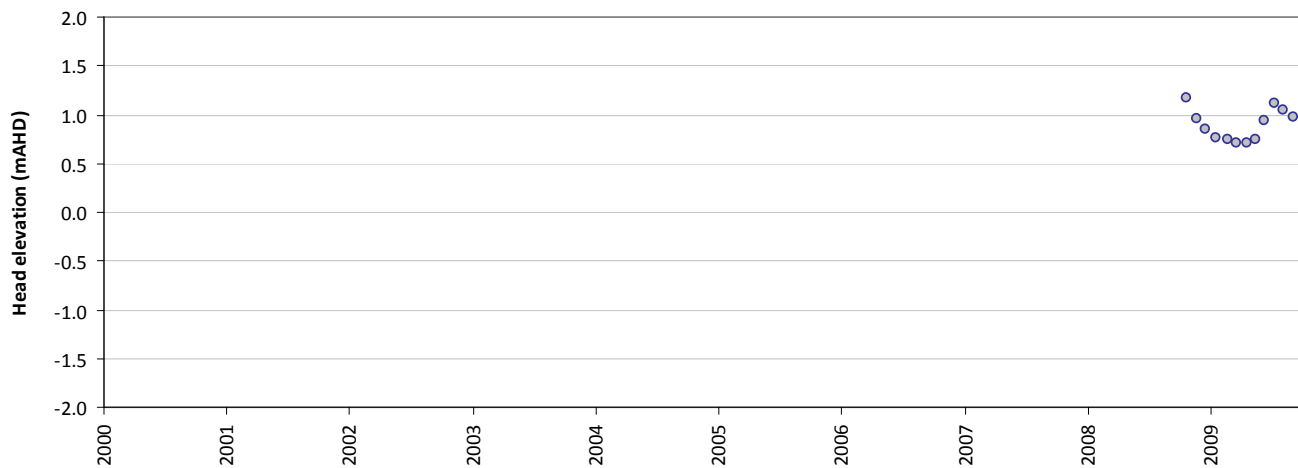
Statistics	
Mean error (ME)	0.65
Mean absolute error (MAE)	0.65
Root mean square error (RMSE)	0.66
Standard deviation of residuals (STDres)	0.14
Correlation coefficient (R)	0.96
Nash Sutcliffe correlation coefficient (R2)	-2.34

HS89A

Modelled vs observed time-series plot - HS89A



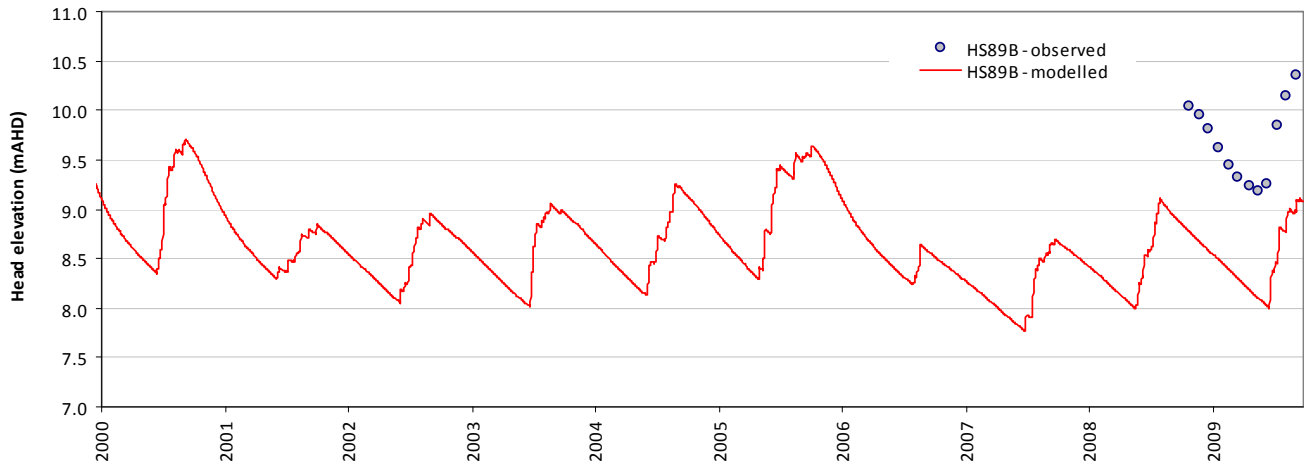
Residual time-series plot - HS89A



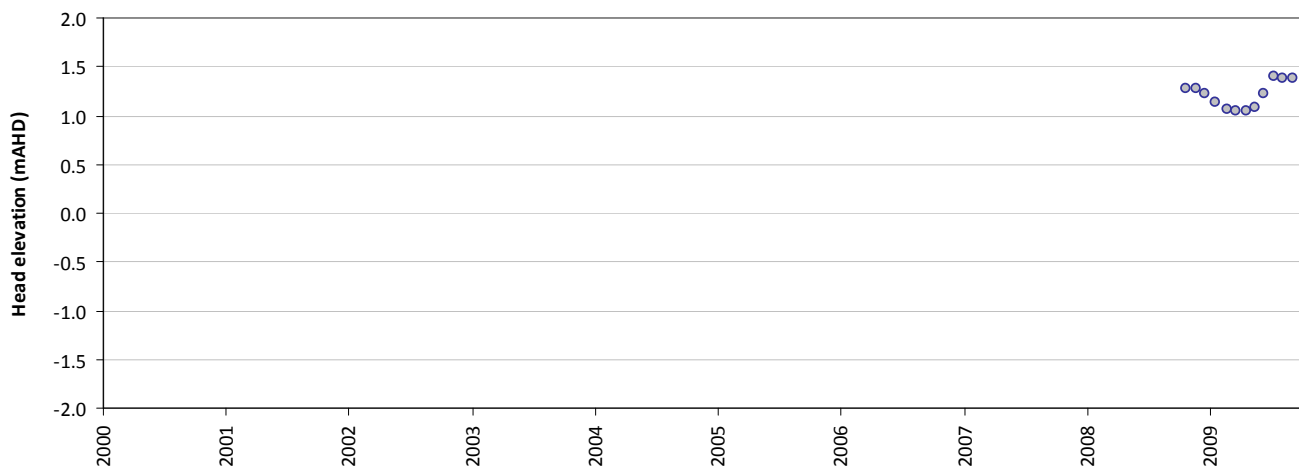
Statistics	
Mean error (ME)	0.89
Mean absolute error (MAE)	0.89
Root mean square error (RMSE)	0.90
Standard deviation of residuals (STDres)	0.15
Correlation coefficient (R)	0.95
Nash Sutcliffe correlation coefficient (R2)	-4.36

HS89B

Modelled vs observed time-series plot - HS89B



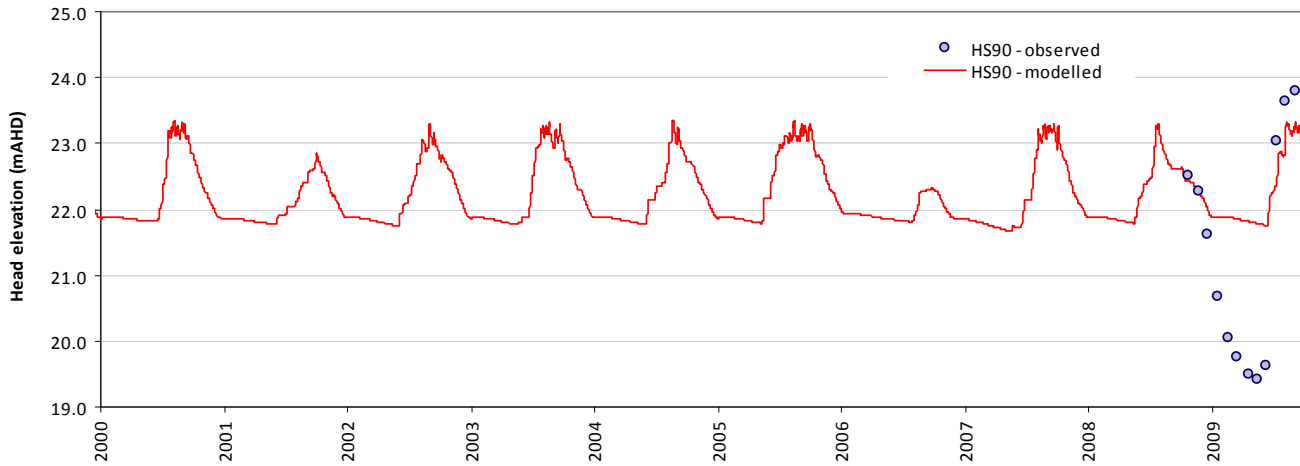
Residual time-series plot - HS89B



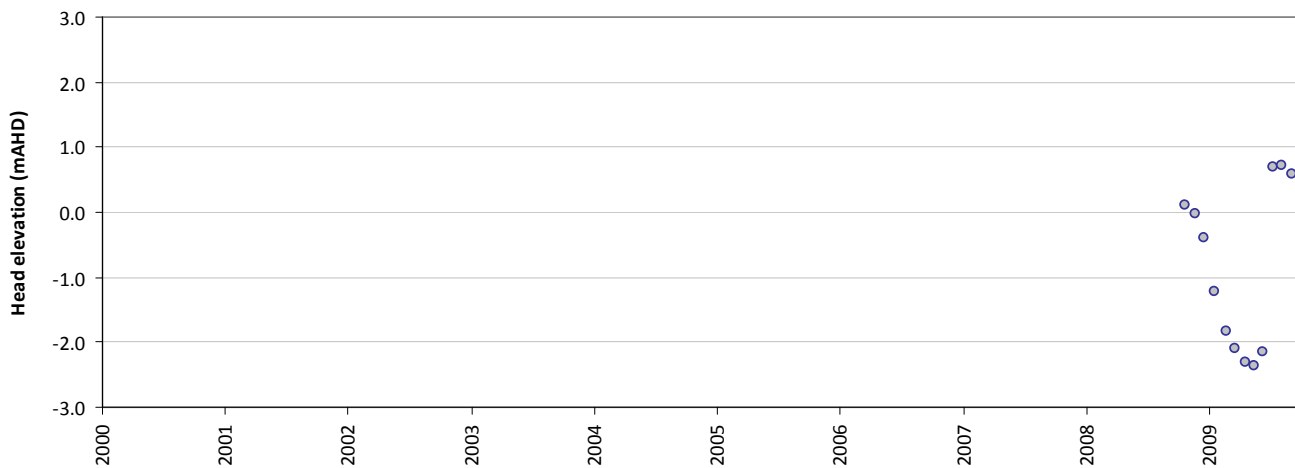
Statistics	
Mean error (ME)	1.21
Mean absolute error (MAE)	1.21
Root mean square error (RMSE)	1.21
Standard deviation of residuals (STDres)	0.13
Correlation coefficient (R)	0.97
Nash Sutcliffe correlation coefficient (R2)	-9.13

HS90

Modelled vs observed time-series plot - HS90



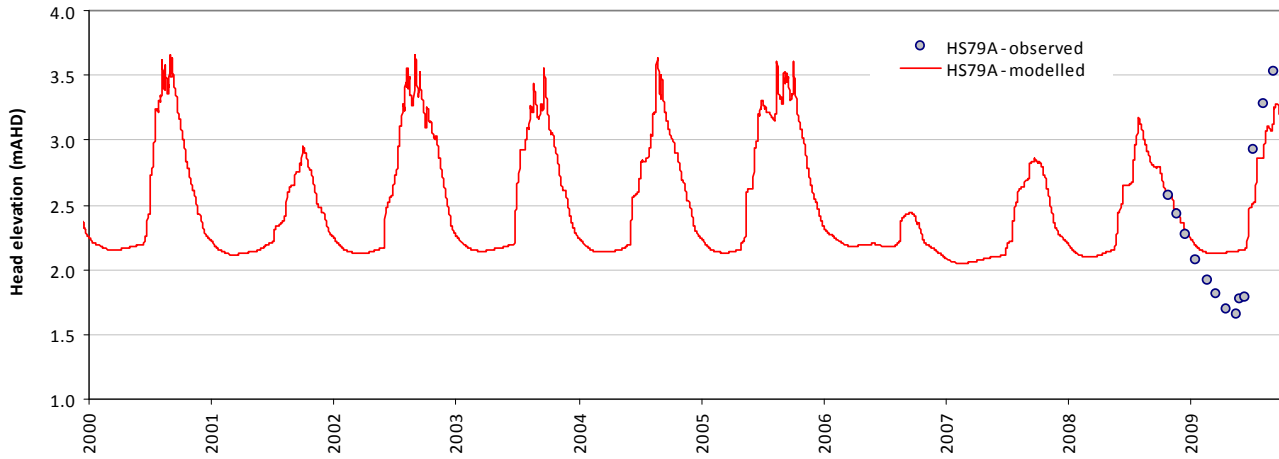
Residual time-series plot - HS90



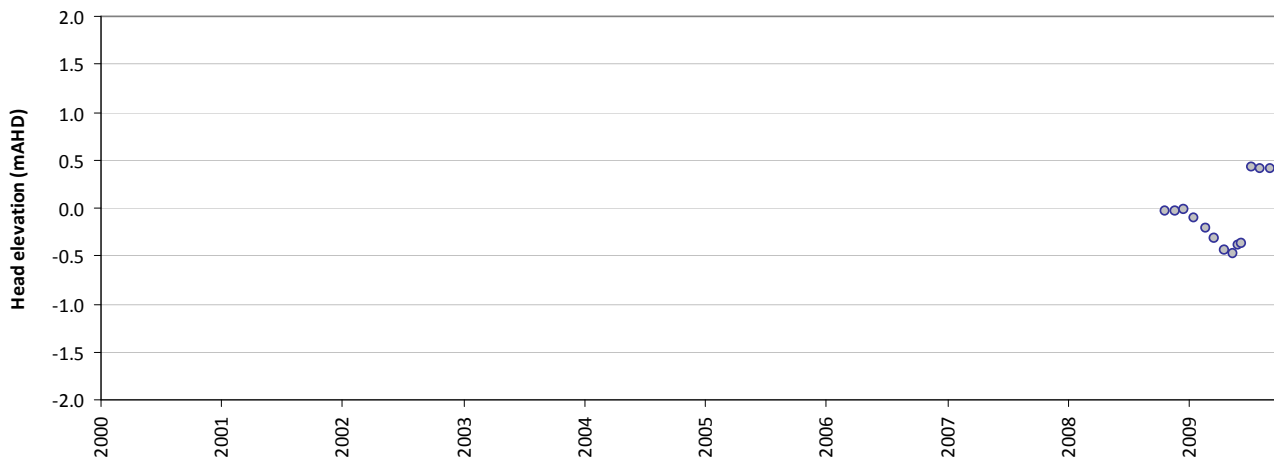
Statistics	
Mean error (ME)	-0.86
Mean absolute error (MAE)	1.21
Root mean square error (RMSE)	1.48
Standard deviation of residuals (STDres)	1.21
Correlation coefficient (R)	0.92
Nash Sutcliffe correlation coefficient (R2)	0.15

HS79A

Modelled vs observed time-series plot - HS79A



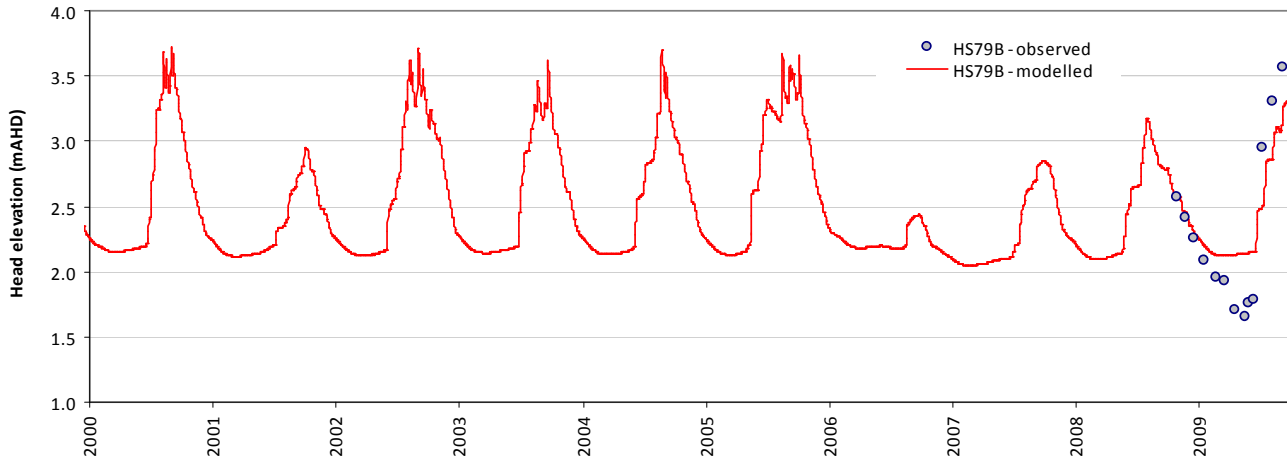
Residual time-series plot - HS79A



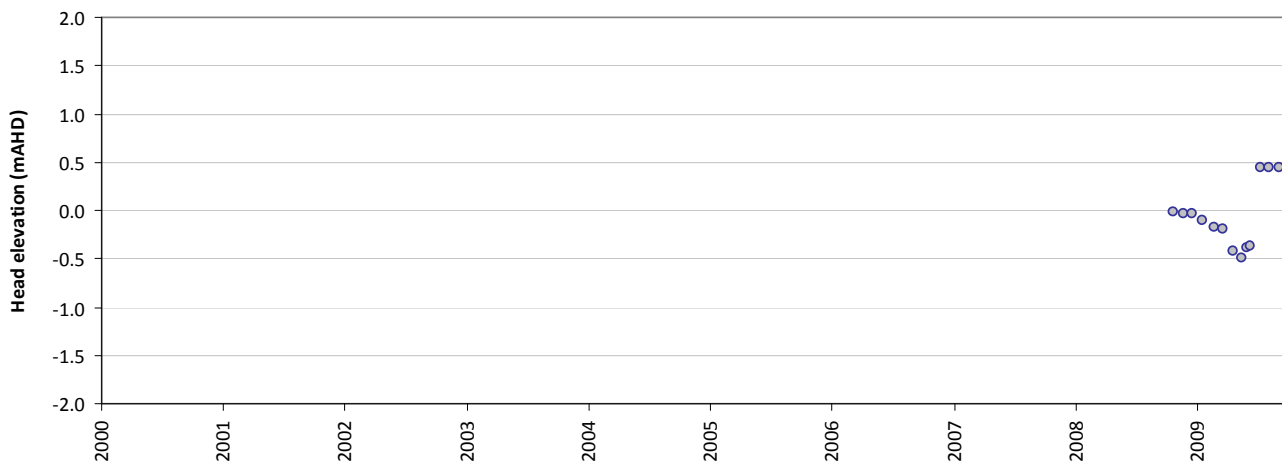
Statistics	
Mean error (ME)	-0.09
Mean absolute error (MAE)	0.28
Root mean square error (RMSE)	0.33
Standard deviation of residuals (STDres)	0.31
Correlation coefficient (R)	0.97
Nash Sutcliffe correlation coefficient (R2)	0.71

HS79B

Modelled vs observed time-series plot - HS79B



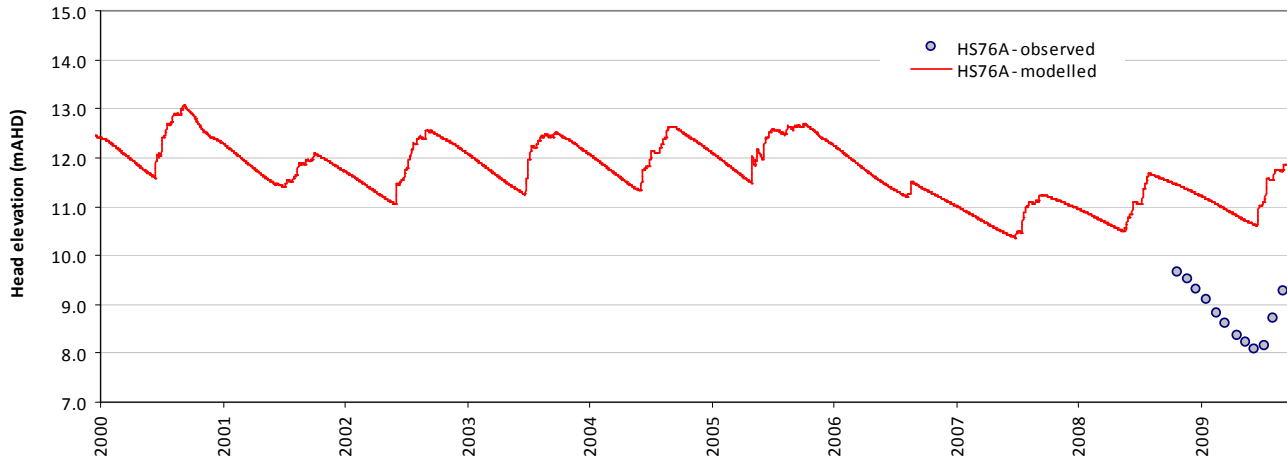
Residual time-series plot - HS79B



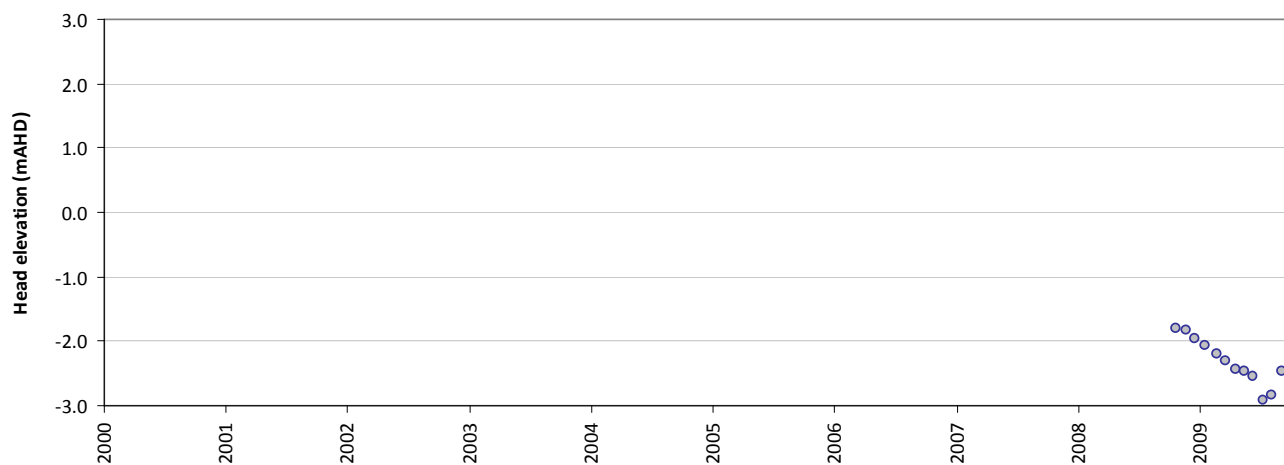
Statistics	
Mean error (ME)	-0.07
Mean absolute error (MAE)	0.28
Root mean square error (RMSE)	0.33
Standard deviation of residuals (STDres)	0.32
Correlation coefficient (R)	0.96
Nash Sutcliffe correlation coefficient (R2)	0.71

HS76A

Modelled vs observed time-series plot - HS76A



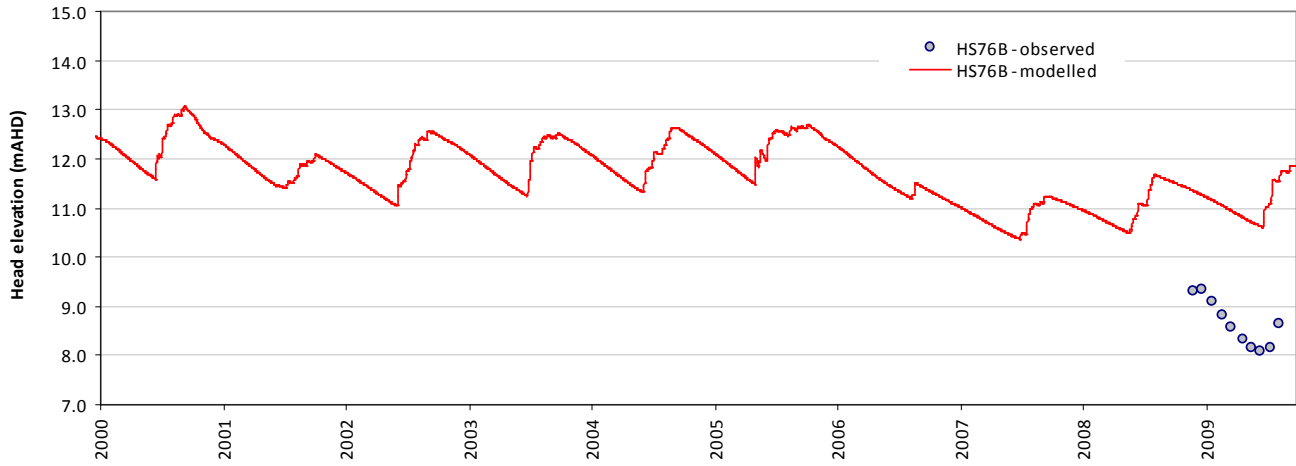
Residual time-series plot - HS76A



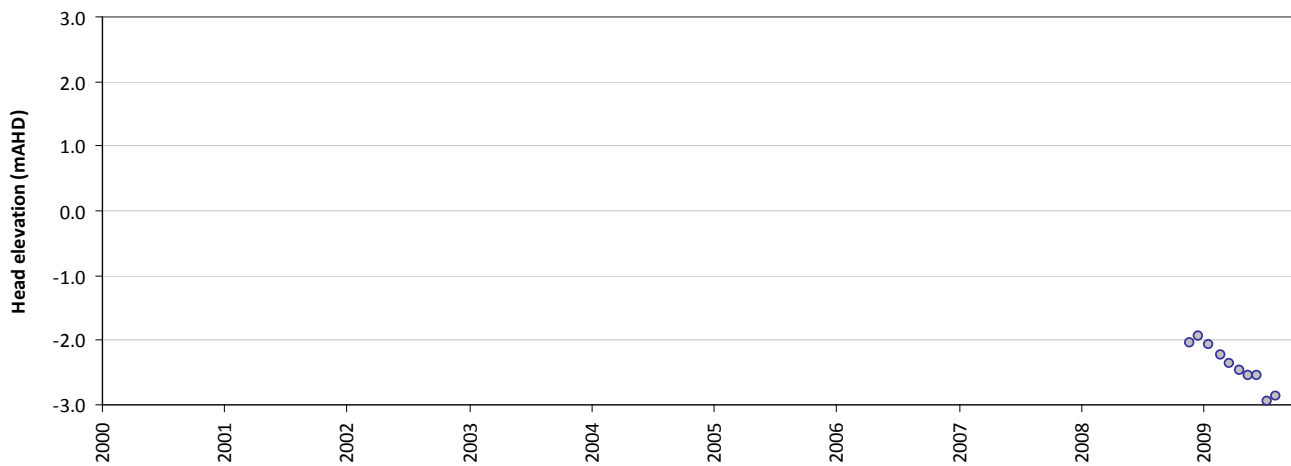
Statistics	
Mean error (ME)	-2.33
Mean absolute error (MAE)	2.33
Root mean square error (RMSE)	2.35
Standard deviation of residuals (STDres)	0.35
Correlation coefficient (R)	0.75
Nash Sutcliffe correlation coefficient (R2)	-19.62

HS76B

Modelled vs observed time-series plot - HS76B



Residual time-series plot - HS76B



Statistics	
Mean error (ME)	-2.41
Mean absolute error (MAE)	2.41
Root mean square error (RMSE)	2.43
Standard deviation of residuals (STDres)	0.32
Correlation coefficient (R)	0.70
Nash Sutcliffe correlation coefficient (R2)	-28.20

Appendix C: Barragup Swamp calibration statistics and plots

Barragup Swamp model calibration statistics

Table C-1: Barragup Swamp model calibration statistic for observed vs modelled heads.

Description	Observed	Modelled	Residual	Abs residual
sum (m)	41	44	-3.01	
average (m)	0.65	0.70	-0.05	0.11
median (m)	0.69	0.71	-0.06	0.10
min (m)	-0.04	-0.08	-0.24	
max (m)	1.19	1.42	0.61	
range (m)	1.23	1.50	0.85	

Table C-1: Barragup Swamp model summary statistic for observed vs modelled heads.

Description	Symbol	Value
Count	n	62
Sum of squares (m ²)	SSQ	1.35
Mean sum of squares (m ²)	MSSQ	0.02
Root mean square (m)	RMS	0.15
Scaled root mean square (%)	SRMS	12.00
Sum of residuals (m)	SRMS	7.1
Mean sum of residuals (m)	MSR	0.11
Scaled mean sum of residuals (%)	SMSR	9.27
Coefficient of determination ()	CD	0.75

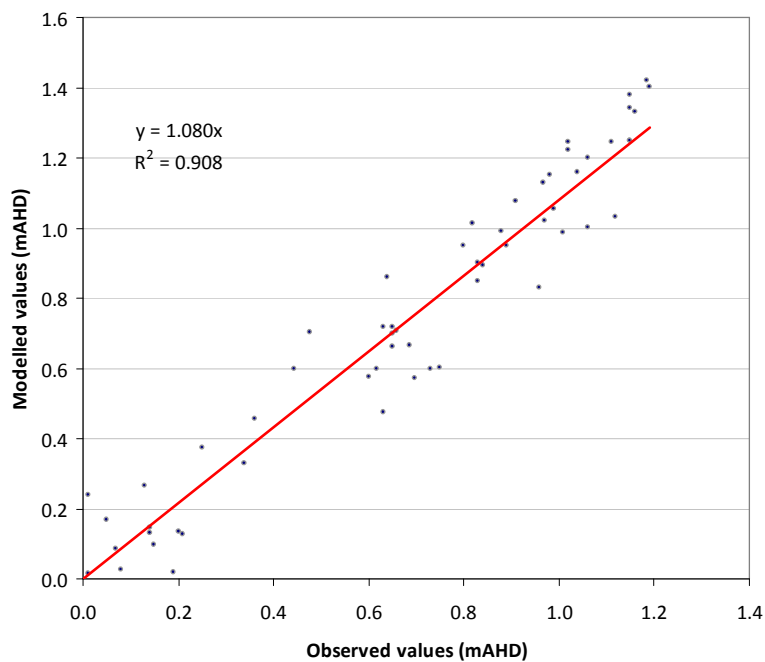


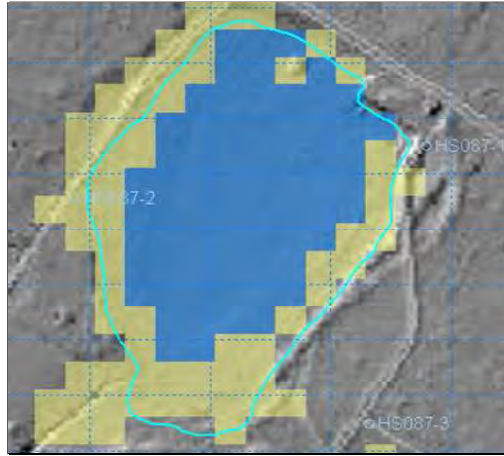
Figure C-1: Barragup Swamp model scatterplot for observed versus modelled groundwater levels

Barragup Swamp aerial photos vs modelled data

Aerial Photo: December 2003



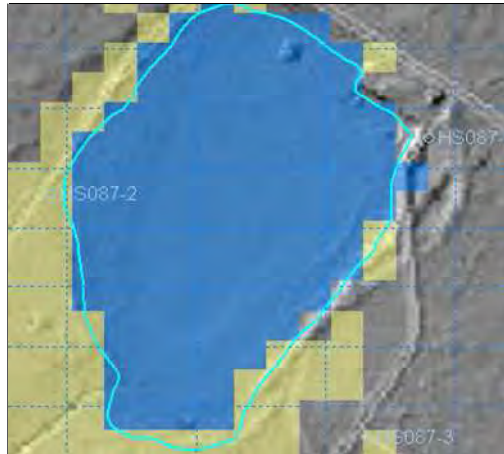
Inundated area: Model



Aerial Photo: December 2005



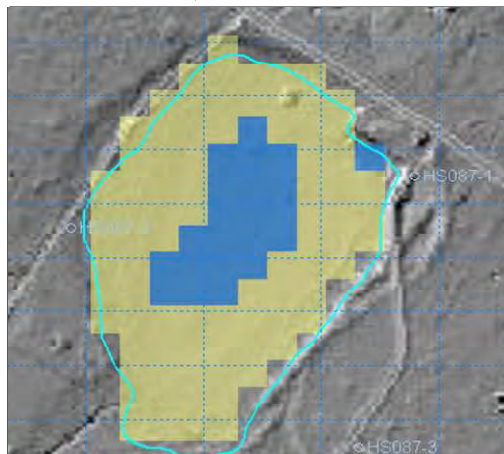
Inundated area: Model



Aerial Photo: December 2006



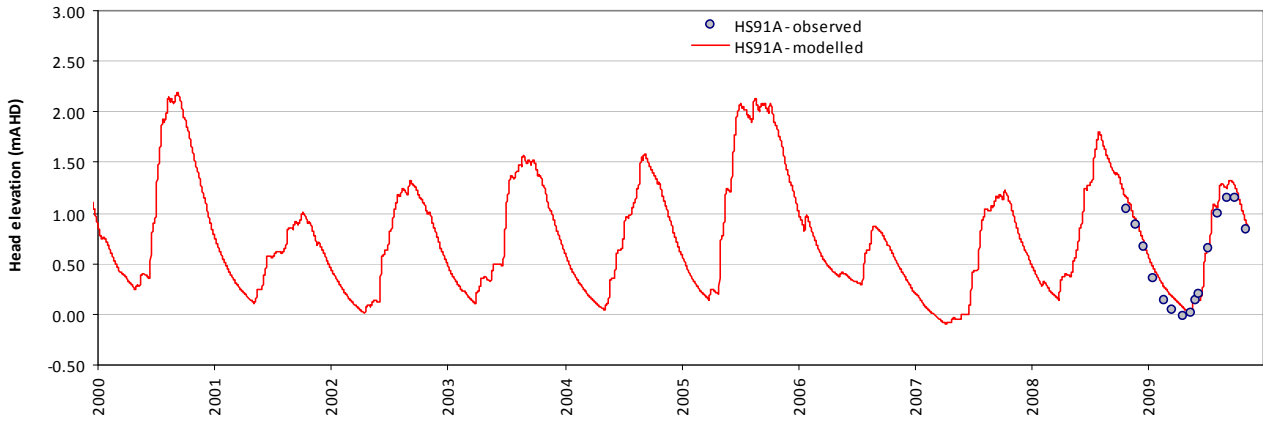
Inundated area: Model



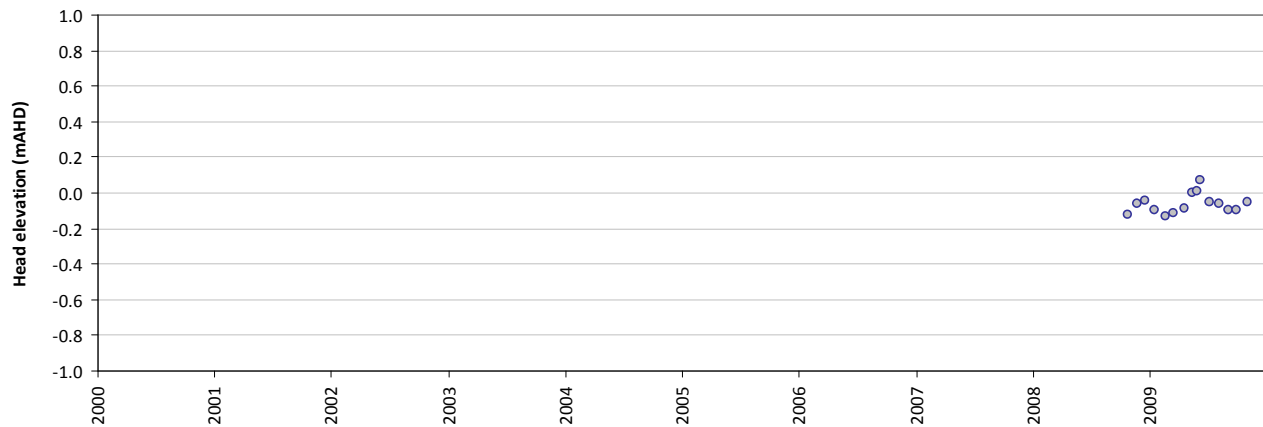
Barragup Swamp model calibration plots

HS91A

Modelled vs observed time-series plot - HS91A



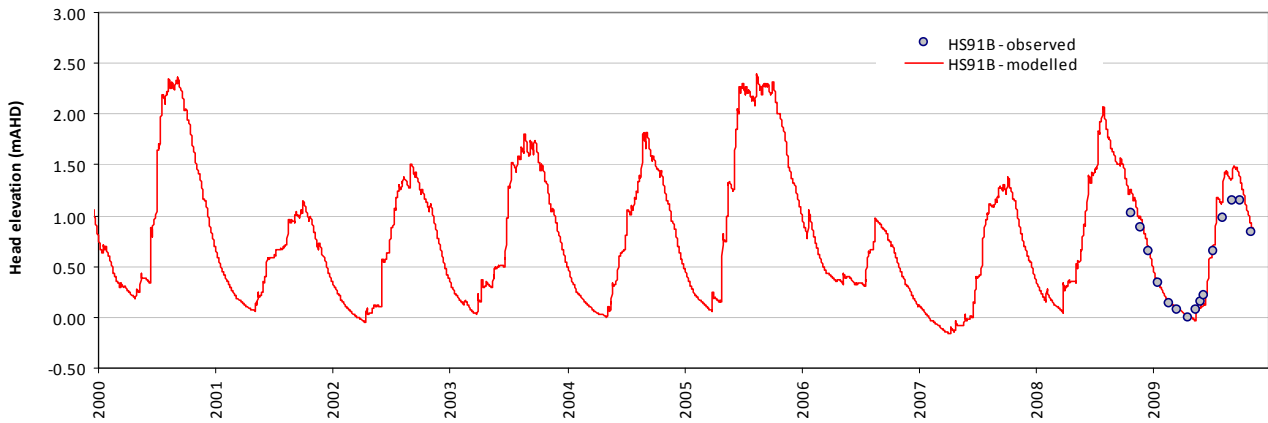
Residual time-series plot - HS91A



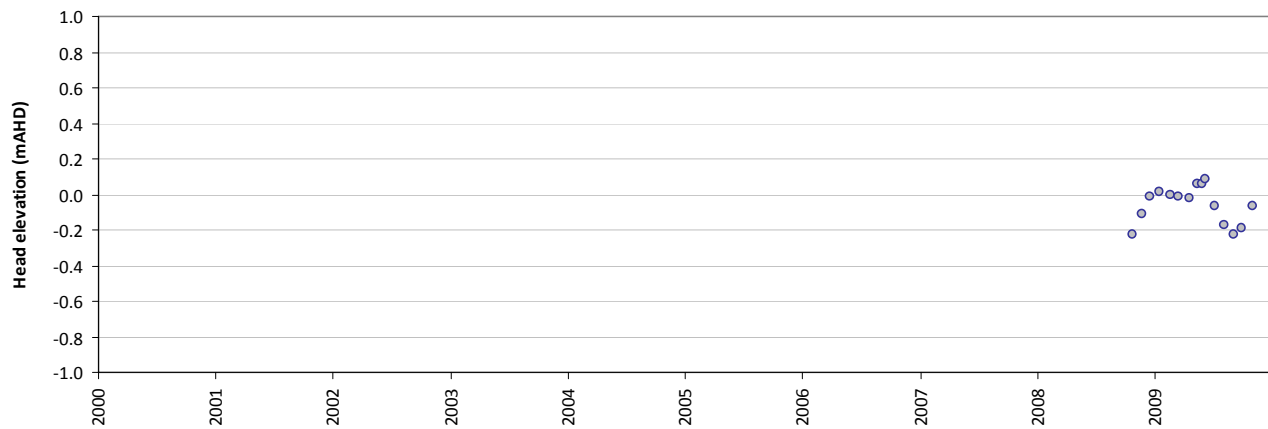
Statistics	
Mean error (ME)	-0.06
Mean absolute error (MAE)	0.07
Root mean square error (RMSE)	0.08
Standard deviation of residuals (STDres)	0.05
Correlation coefficient (R)	0.99
Nash Sutcliffe correlation coefficient (R2)	0.96

HS91B

Modelled vs observed time-series plot - HS91B



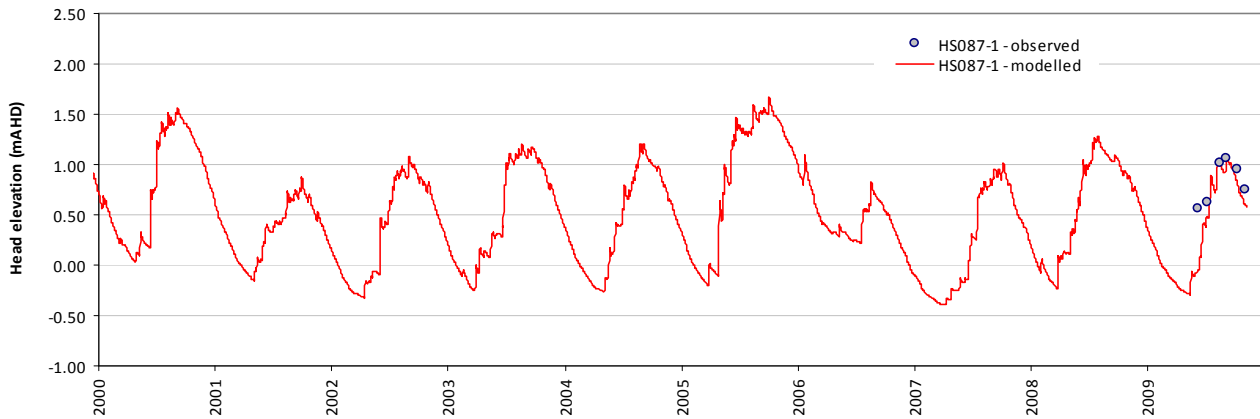
Residual time-series plot - HS91B



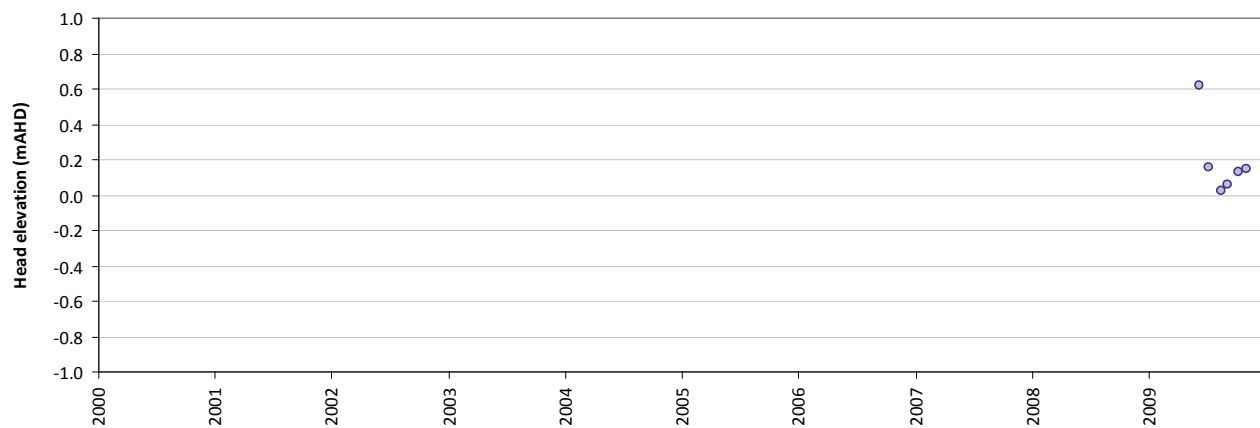
Statistics	
Mean error (ME)	-0.06
Mean absolute error (MAE)	0.09
Root mean square error (RMSE)	0.12
Standard deviation of residuals (STDres)	0.10
Correlation coefficient (R)	1.00
Nash Sutcliffe correlation coefficient (R2)	0.92

HS087-1

Modelled vs observed time-series plot - HS087-1



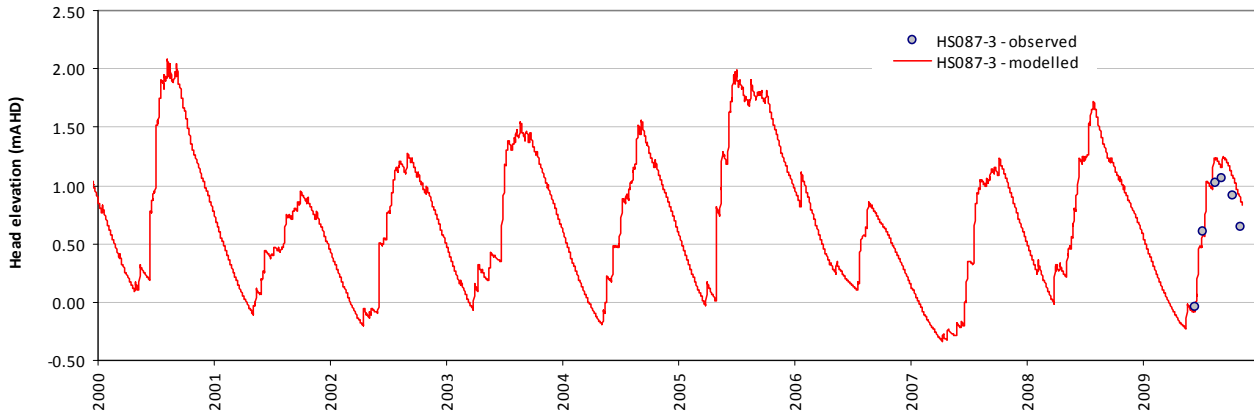
Residual time-series plot - HS087-1



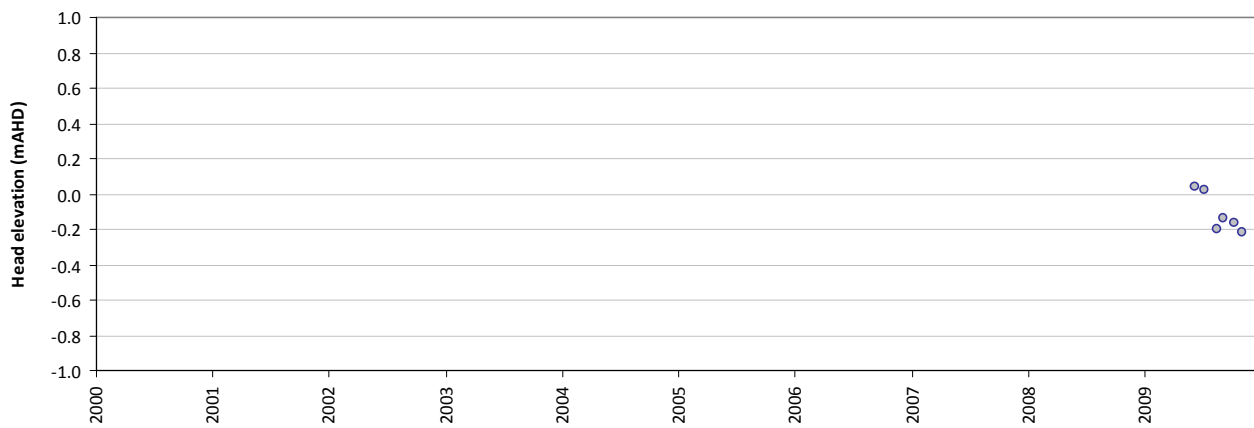
Statistics	
Mean error (ME)	0.22
Mean absolute error (MAE)	0.22
Root mean square error (RMSE)	0.29
Standard deviation of residuals (STDres)	0.19
Correlation coefficient (R)	0.90
Nash Sutcliffe correlation coefficient (R2)	-1.23

HS087-3

Modelled vs observed time-series plot - HS087-3



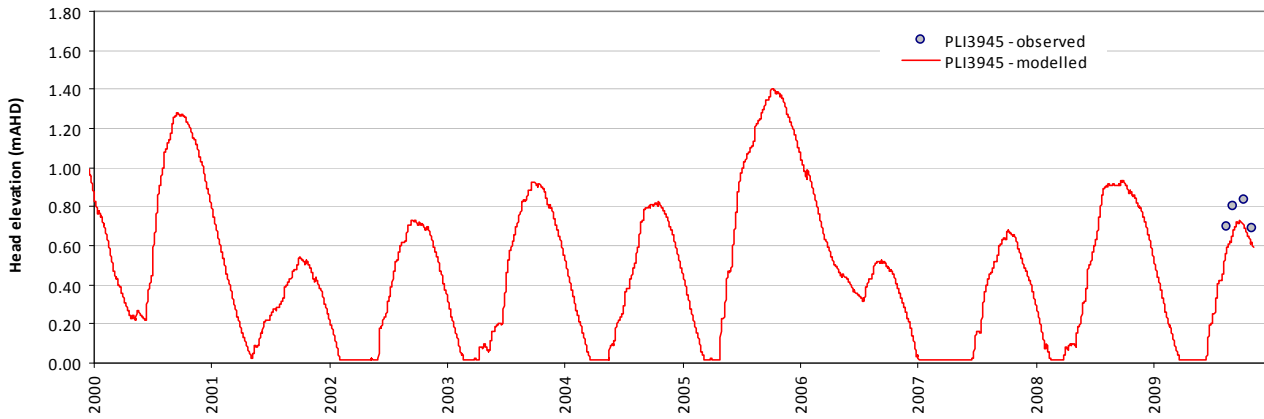
Residual time-series plot - HS087-3



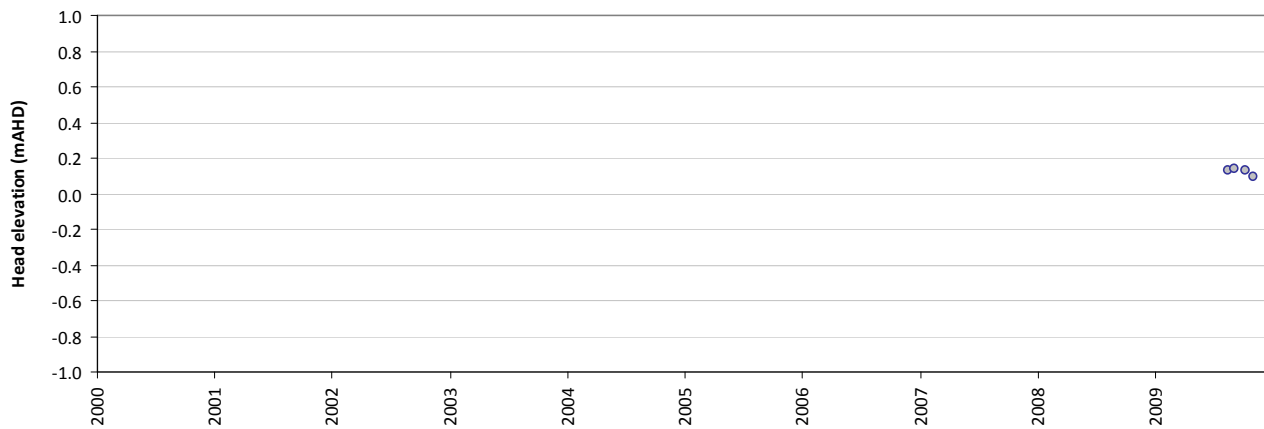
Statistics	
Mean error (ME)	-0.07
Mean absolute error (MAE)	0.11
Root mean square error (RMSE)	0.14
Standard deviation of residuals (STDres)	0.12
Correlation coefficient (R)	0.97
Nash Sutcliffe correlation coefficient (R2)	0.86

PLI3845

Modelled vs observed time-series plot - PLI3945



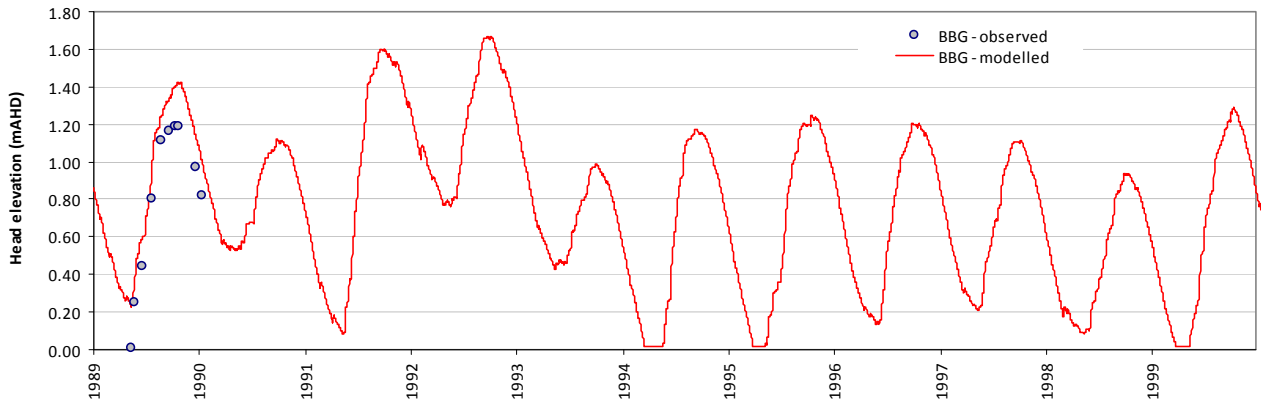
Residual time-series plot - PLI3945



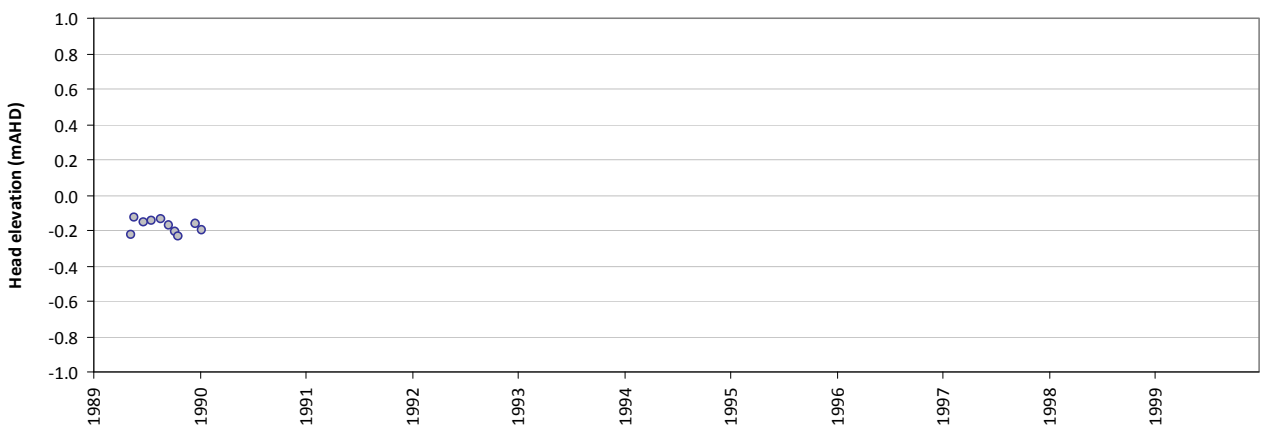
Statistics	
Mean error (ME)	-0.01
Mean absolute error (MAE)	0.10
Root mean square error (RMSE)	0.13
Standard deviation of residuals (STDres)	0.13
Correlation coefficient (R)	-0.69
Nash Sutcliffe correlation coefficient (R2)	-1.23

BBG

Modelled vs observed time-series plot - BBG



Residual time-series plot - BBG



Statistics	
Mean error (ME)	-0.18
Mean absolute error (MAE)	0.18
Root mean square error (RMSE)	0.18
Standard deviation of residuals (STDres)	0.04
Correlation coefficient (R)	1.00
Nash Sutcliffe correlation coefficient (R2)	0.80

Appendix D: Scott Road wetland system calibration statistics and plots

Scott Road wetland system calibration statistics

Table D-1: Scott Road wetland system calibration statistic for observed vs modelled heads.

Description	Observed	Modelled	Residual	Abs residual
sum (m)	3386	3338	47.4	
average (m)	13.54	13.35	0.19	0.32
median (m)	13.64	13.61	0.19	0.27
min (m)	10.32	10.05	-0.90	
max (m)	15.84	15.31	1.27	
range (m)	5.52	5.26	2.17	

Table D-1: Scott Road wetland system summary statistic for observed vs modelled heads.

Description	Symbol	Value
Count	n	250
Sum of squares (m ²)	SSQ	43
Mean sum of squares (m ²)	MSSQ	0.17
Root mean square (m)	RMS	0.42
Scaled root mean square (%)	SRMS	7.52
Sum of residuals (m)	SRMS	79.5
Mean sum of residuals (m)	MSR	0.32
Scaled mean sum of residuals (%)	SMSR	5.76
Coefficient of determination ()	CD	1.08

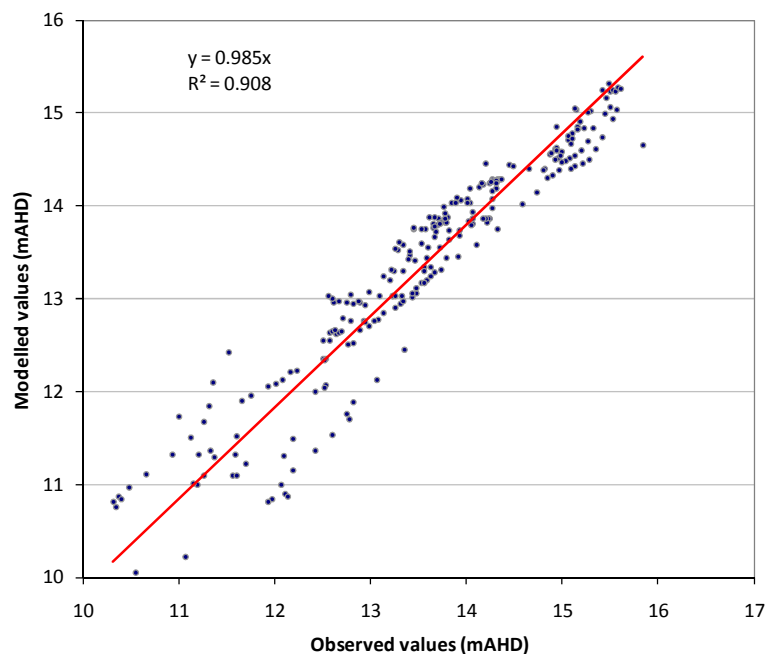


Figure D-1: Scott Road wetland system scatterplot for observed vs modelled groundwater levels

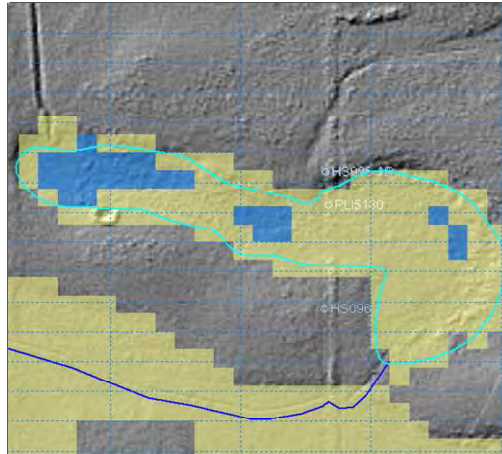
Scott Road wetland aerial photos vs modelled data

Aerial Photo: December 2003



SwanCoastPlain_S_04_40cm_z50.ecw

Inundated area: Model

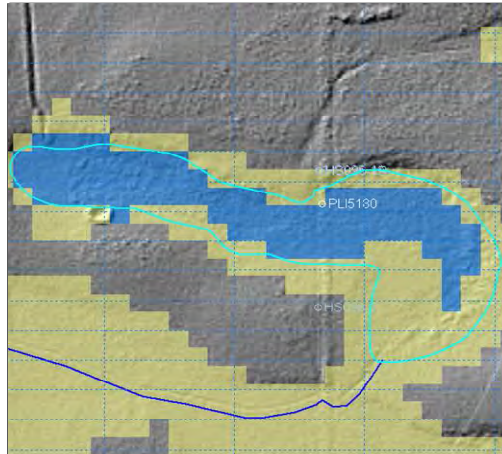


Aerial Photo: December 2005



swancoastplain_South_2006_20cm_z50.ecw

Inundated area: Model

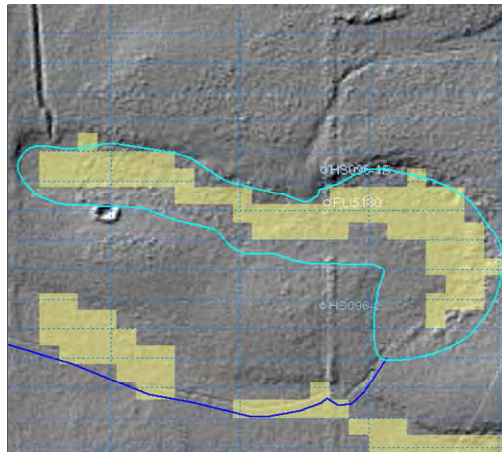


Aerial Photo: December 2006



SwanCoastPlain_South_2007_20cm_z50.ecw

Inundated area: Model

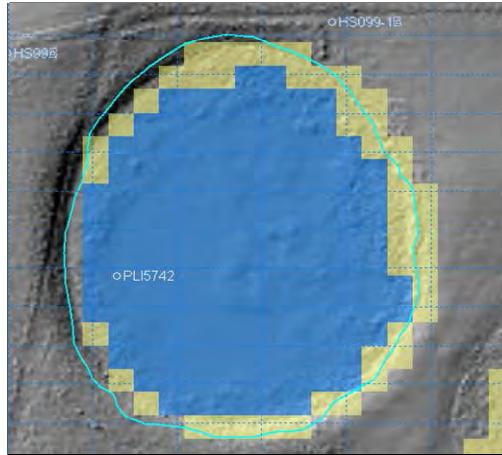


Benden Road wetland aerial photos vs modelled data

Aerial Photo: December 2003



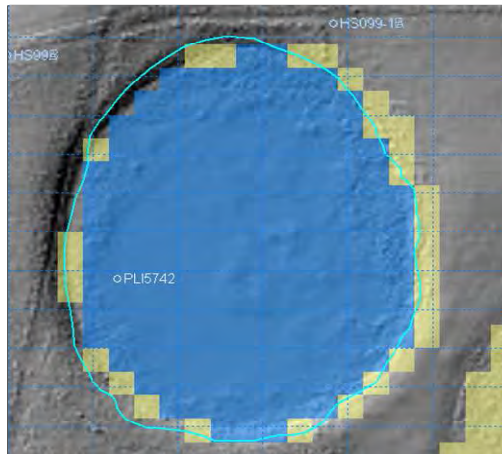
Inundated area: Model



Aerial Photo: December 2005



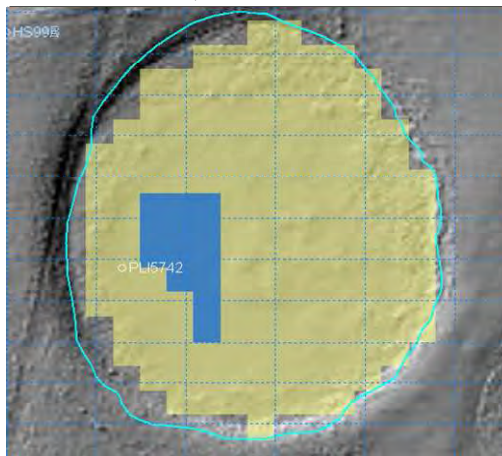
Inundated area: Model



Aerial Photo: December 2006



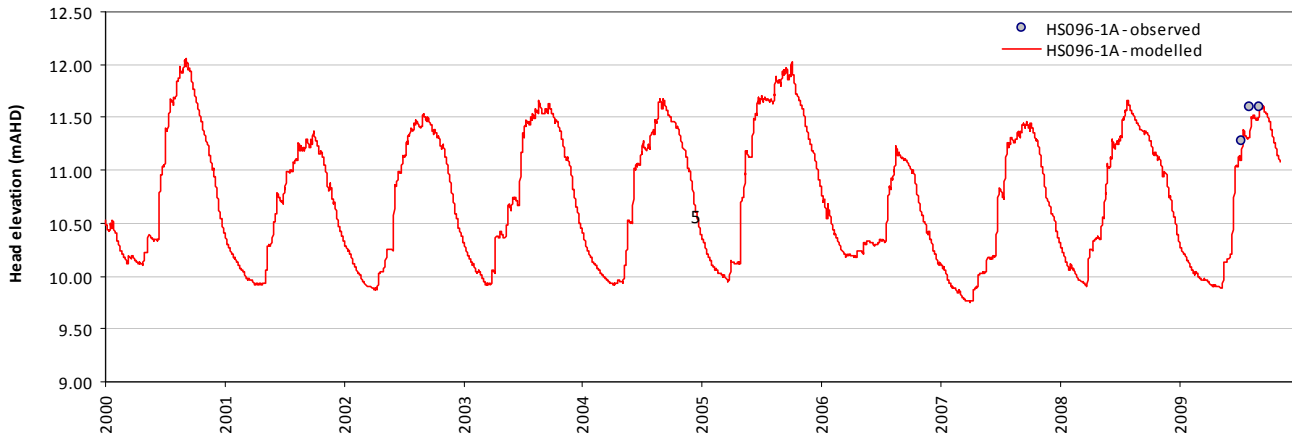
Inundated area: Model



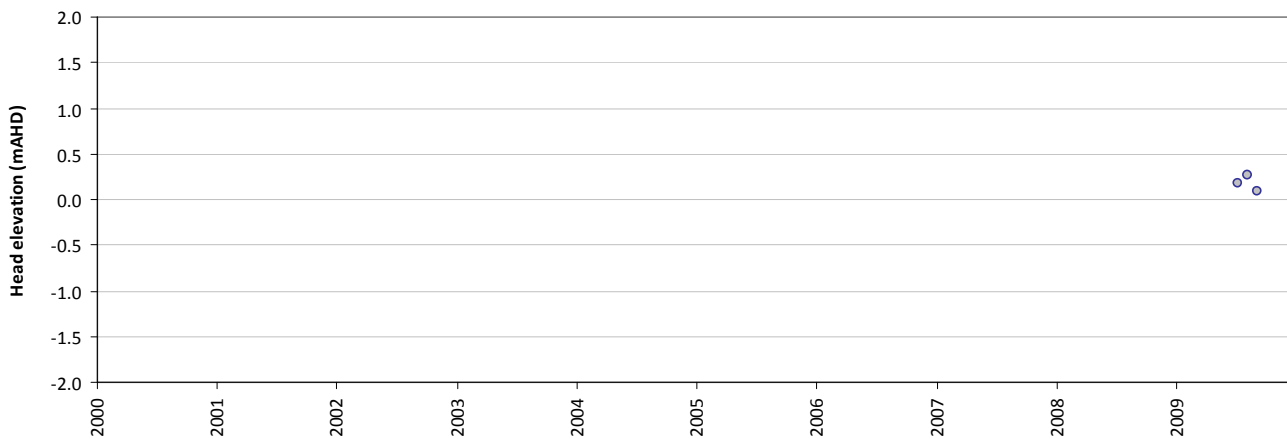
Scott Road wetland system calibration plots

HS096-1A

Modelled vs observed time-series plot - HS096-1A



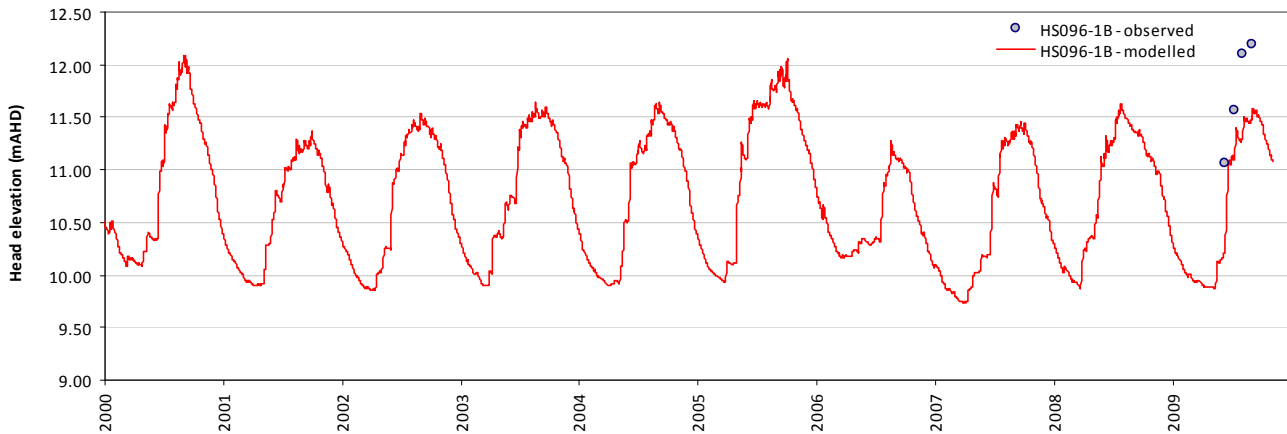
Residual time-series plot - HS096-1A



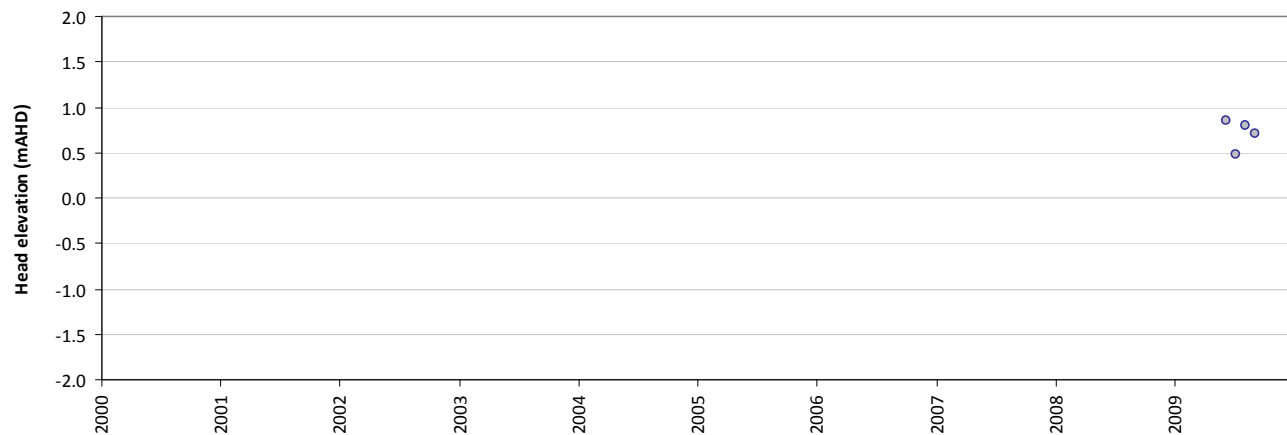
Statistics	
Mean error (ME)	0.18
Mean absolute error (MAE)	0.18
Root mean square error (RMSE)	0.19
Standard deviation of residuals (STDres)	0.08
Correlation coefficient (R)	0.88
Nash Sutcliffe correlation coefficient (R2)	-0.58

HS096-1B

Modelled vs observed time-series plot - HS096-1B



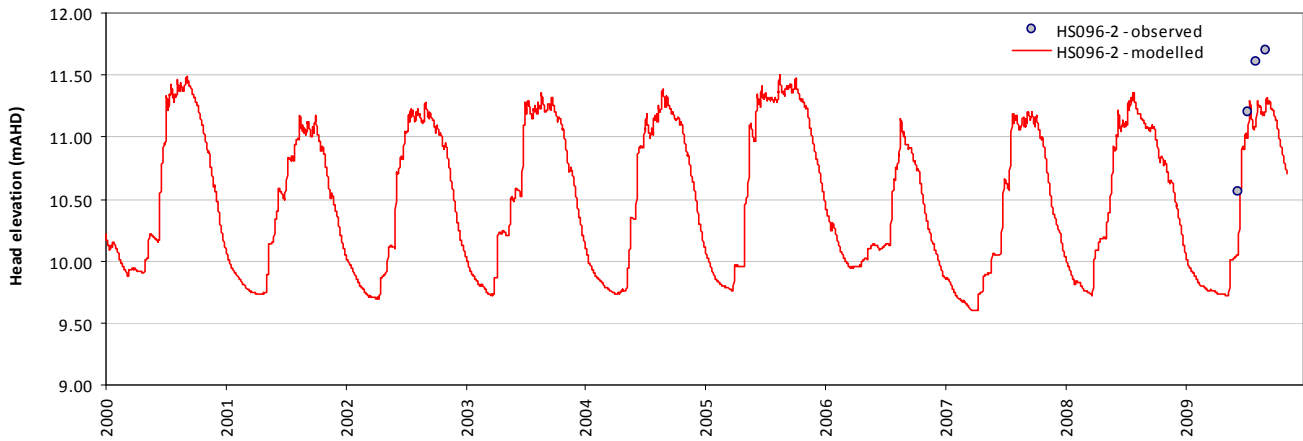
Residual time-series plot - HS096-1B



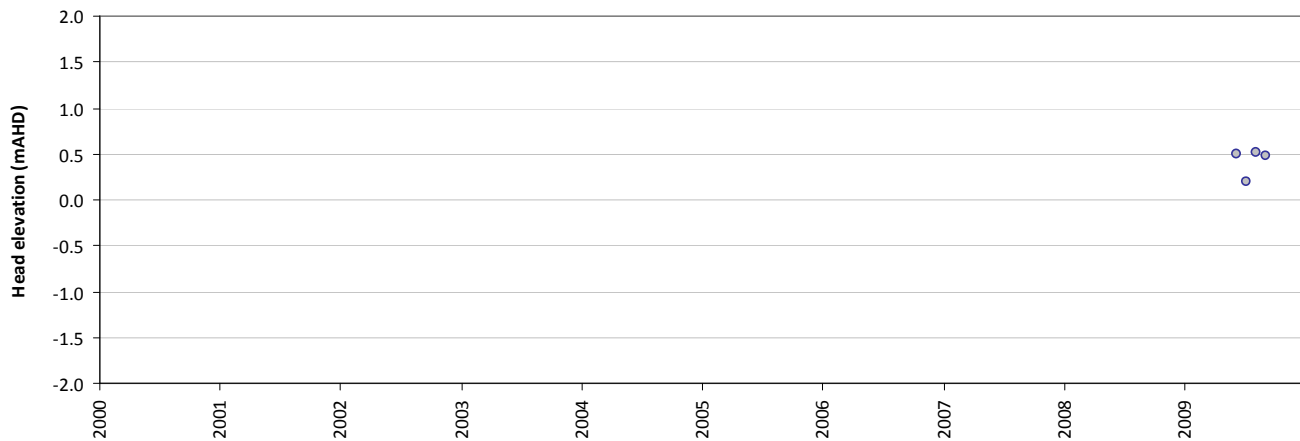
Statistics	
Mean error (ME)	0.71
Mean absolute error (MAE)	0.71
Root mean square error (RMSE)	0.72
Standard deviation of residuals (STDres)	0.15
Correlation coefficient (R)	0.95
Nash Sutcliffe correlation coefficient (R2)	-1.58

HS096-2

Modelled vs observed time-series plot - HS096-2



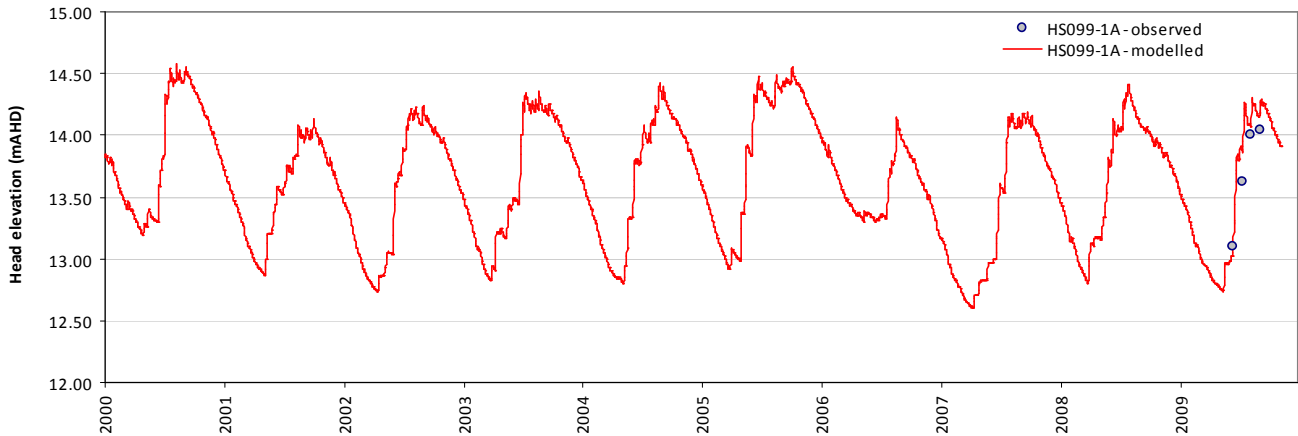
Residual time-series plot - HS096-2



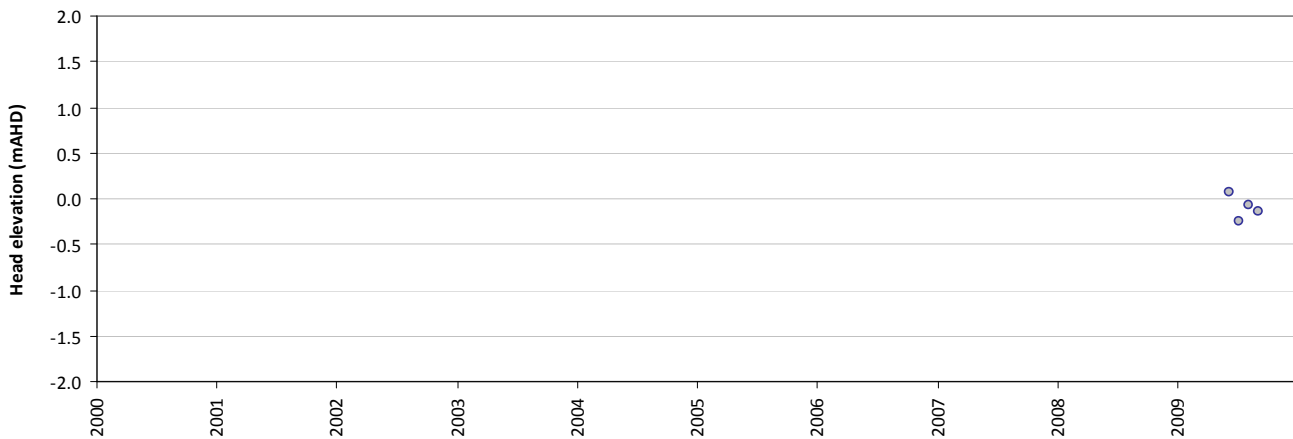
Statistics	
Mean error (ME)	0.42
Mean absolute error (MAE)	0.42
Root mean square error (RMSE)	0.44
Standard deviation of residuals (STDres)	0.13
Correlation coefficient (R)	0.96
Nash Sutcliffe correlation coefficient (R2)	0.02

HS099-1A

Modelled vs observed time-series plot - HS099-1A



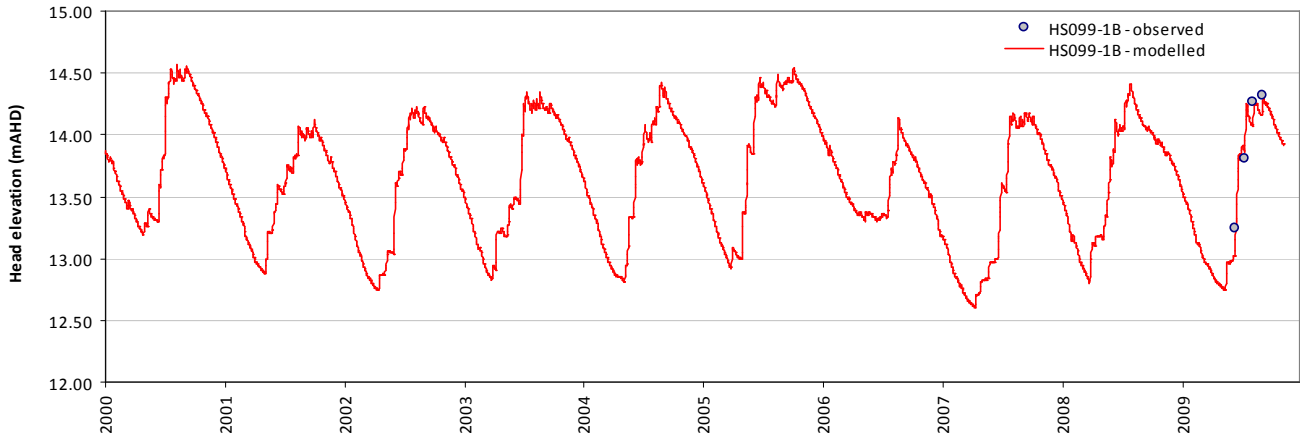
Residual time-series plot - HS099-1A



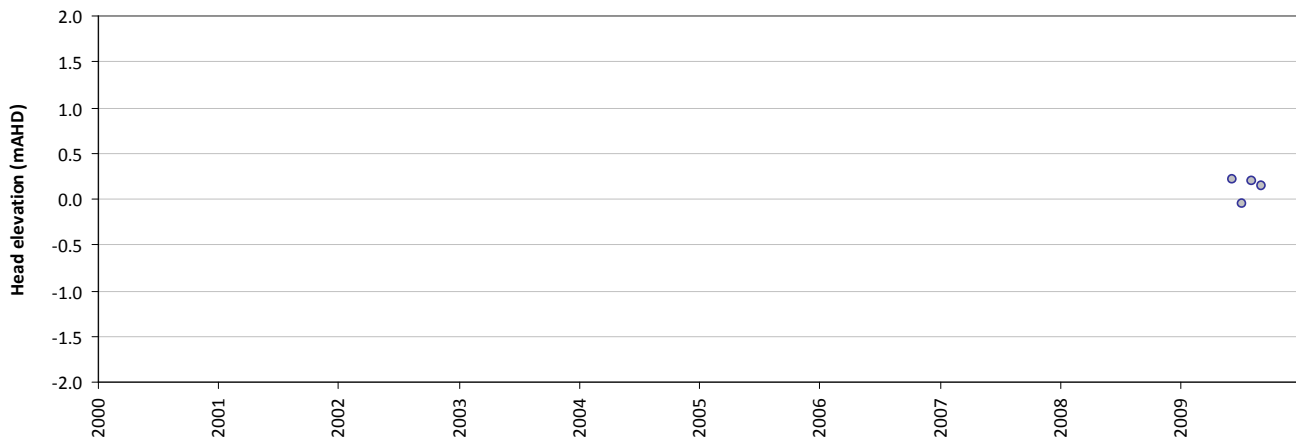
Statistics	
Mean error (ME)	0.12
Mean absolute error (MAE)	0.15
Root mean square error (RMSE)	0.17
Standard deviation of residuals (STDres)	0.11
Correlation coefficient (R)	0.97
Nash Sutcliffe correlation coefficient (R2)	0.86

HS099-1B

Modelled vs observed time-series plot - HS099-1B



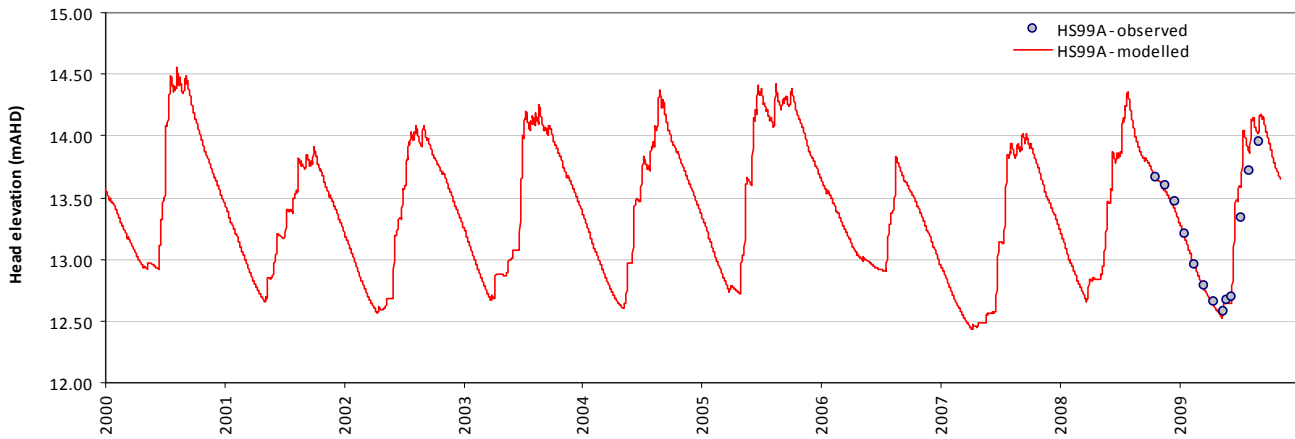
Residual time-series plot - HS099-1B



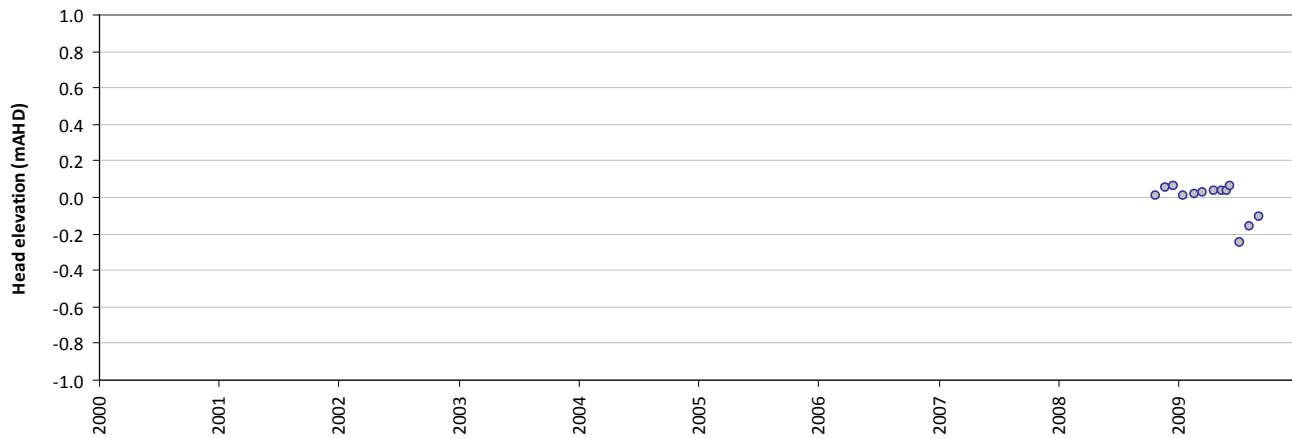
Statistics	
Mean error (ME)	0.12
Mean absolute error (MAE)	0.15
Root mean square error (RMSE)	0.17
Standard deviation of residuals (STDres)	0.11
Correlation coefficient (R)	0.97
Nash Sutcliffe correlation coefficient (R2)	0.86

HS99A

Modelled vs observed time-series plot - HS99A



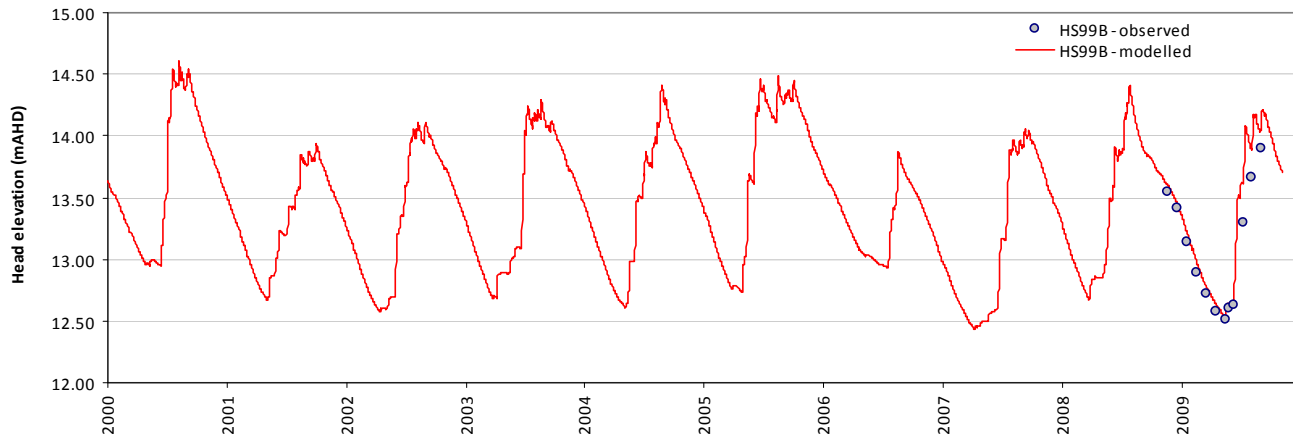
Residual time-series plot - HS99A



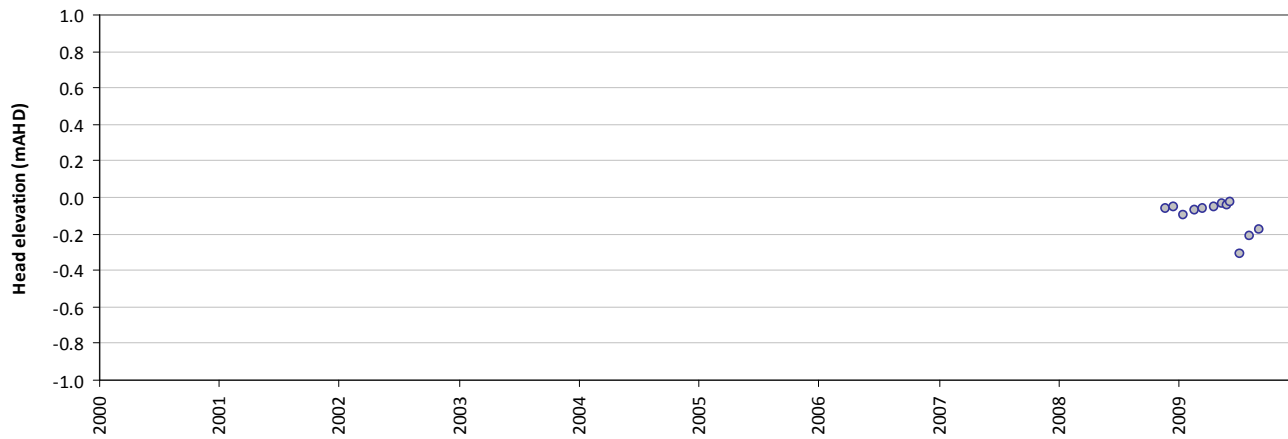
Statistics	
Mean error (ME)	-0.01
Mean absolute error (MAE)	0.06
Root mean square error (RMSE)	0.09
Standard deviation of residuals (STDres)	0.09
Correlation coefficient (R)	0.99
Nash Sutcliffe correlation coefficient (R2)	0.96

HS99B

Modelled vs observed time-series plot - HS99B



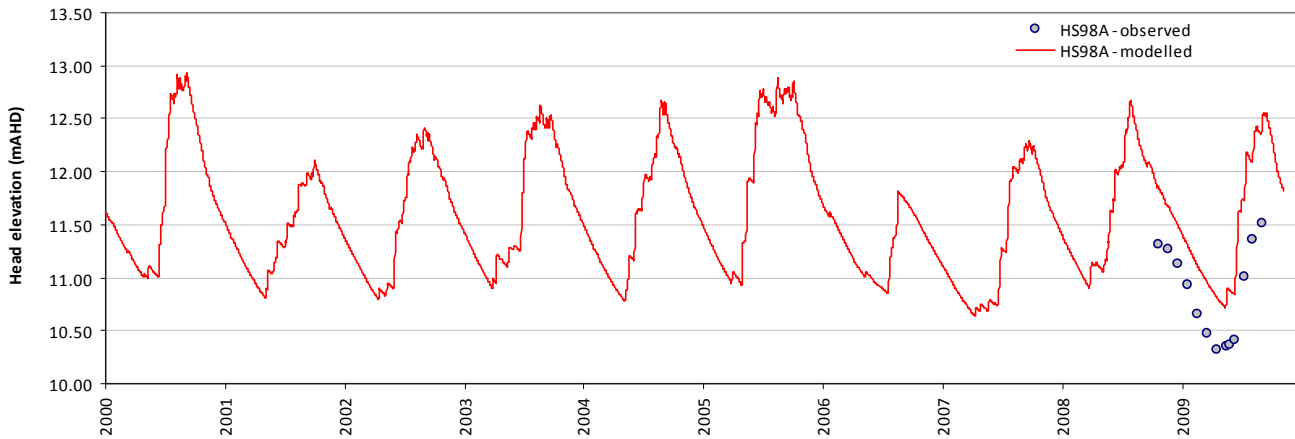
Residual time-series plot - HS99B



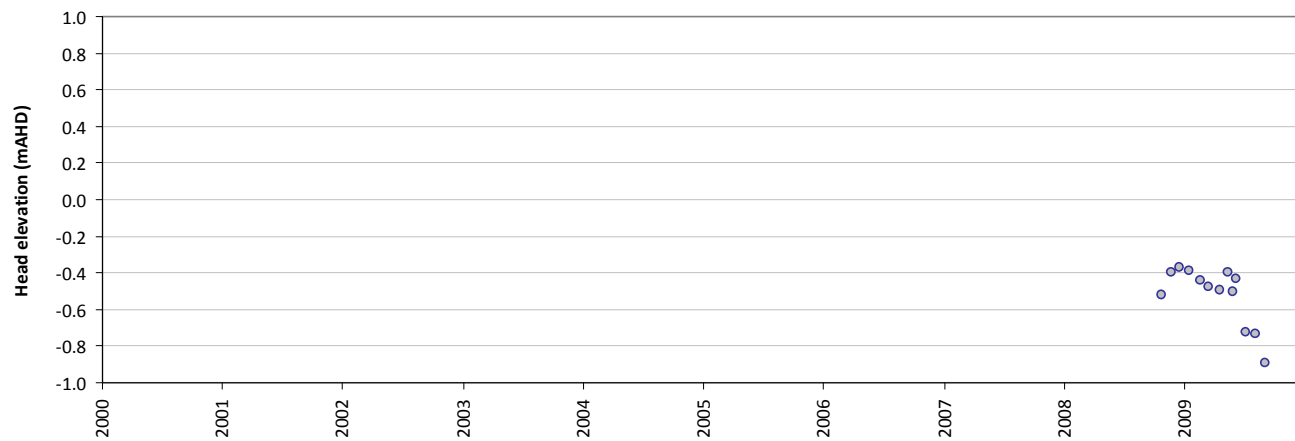
Statistics	
Mean error (ME)	-0.10
Mean absolute error (MAE)	0.10
Root mean square error (RMSE)	0.13
Standard deviation of residuals (STDres)	0.09
Correlation coefficient (R)	0.99
Nash Sutcliffe correlation coefficient (R2)	0.92

HS98A

Modelled vs observed time-series plot - HS98A



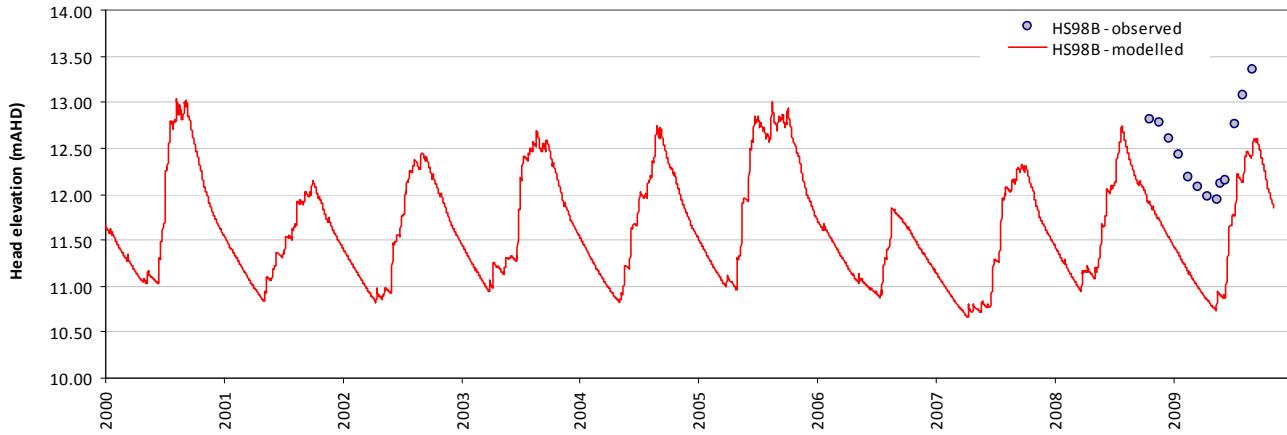
Residual time-series plot - HS98A



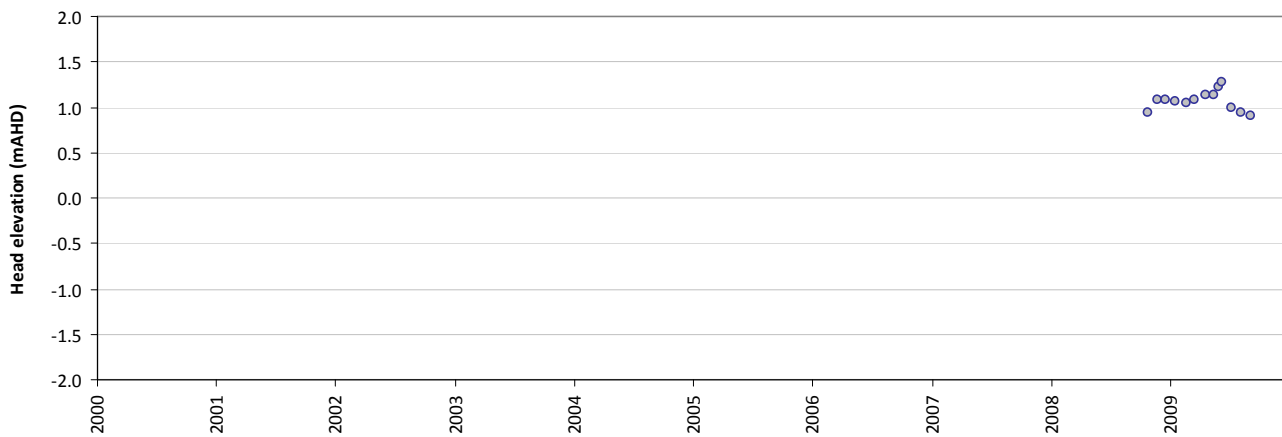
Statistics	
Mean error (ME)	-0.52
Mean absolute error (MAE)	0.52
Root mean square error (RMSE)	0.54
Standard deviation of residuals (STDres)	0.16
Correlation coefficient (R)	0.97
Nash Sutcliffe correlation coefficient (R2)	-0.64

HS98B

Modelled vs observed time-series plot - HS98B



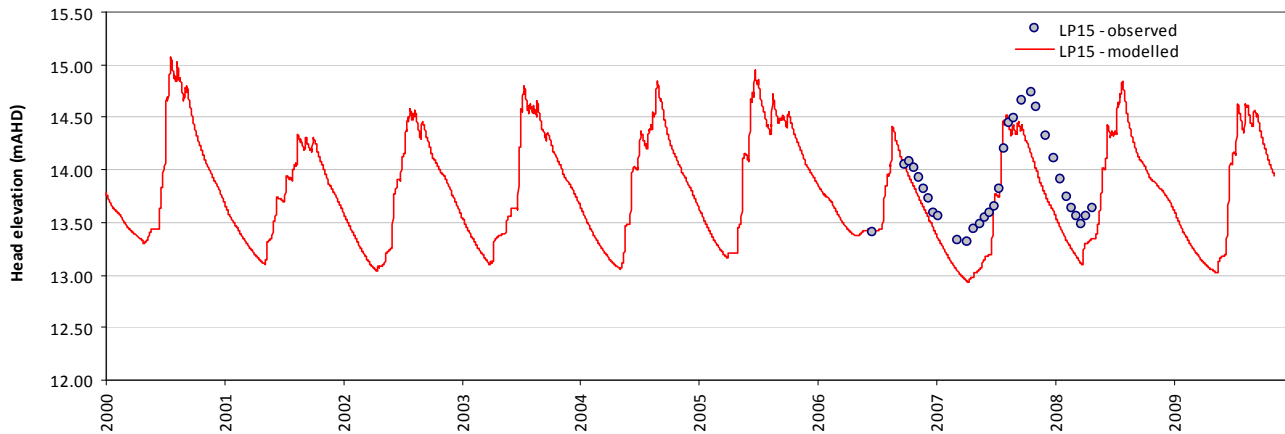
Residual time-series plot - HS98B



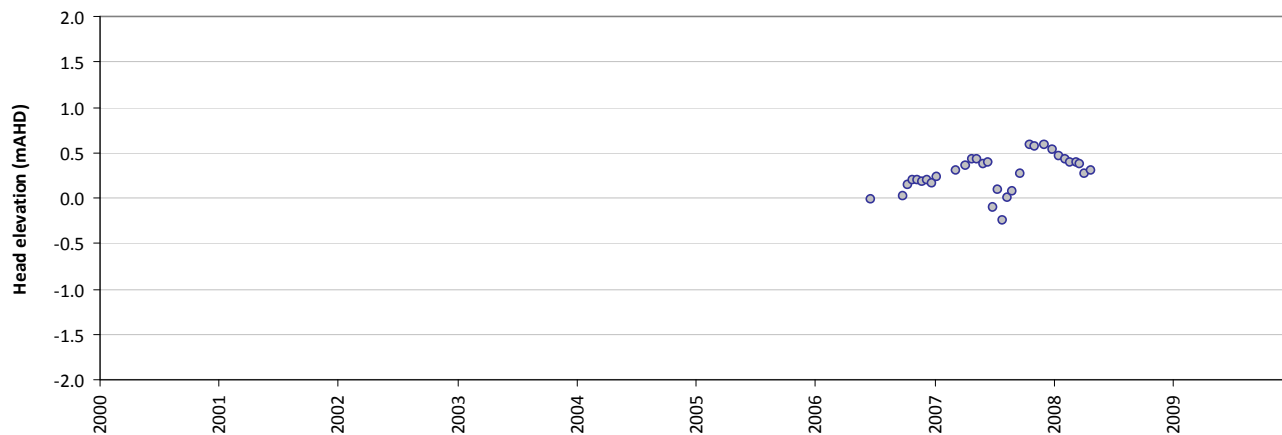
Statistics	
Mean error (ME)	1.07
Mean absolute error (MAE)	1.07
Root mean square error (RMSE)	1.07
Standard deviation of residuals (STDres)	0.10
Correlation coefficient (R)	0.99
Nash Sutcliffe correlation coefficient (R2)	-5.04

LP15

Modelled vs observed time-series plot - LP15



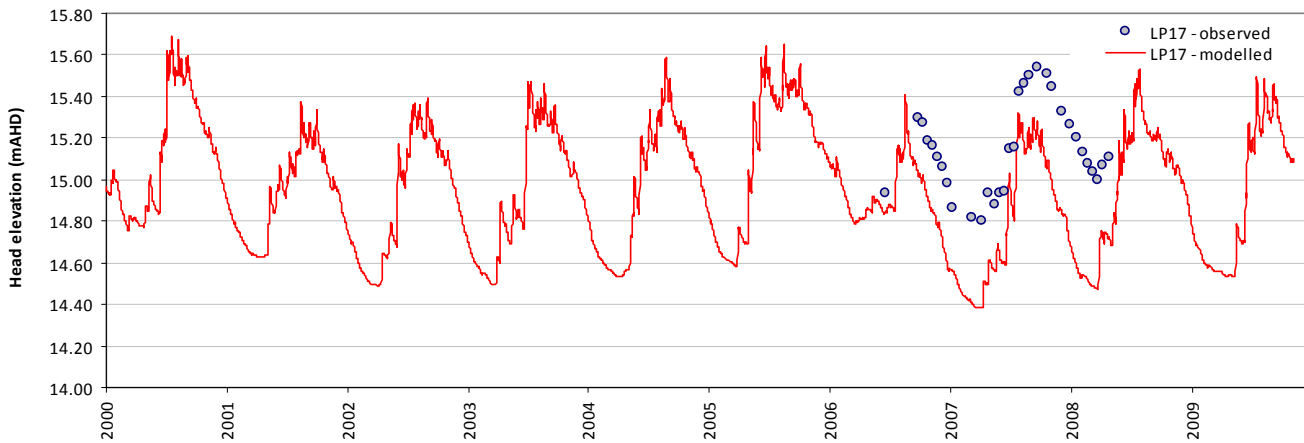
Residual time-series plot - LP15



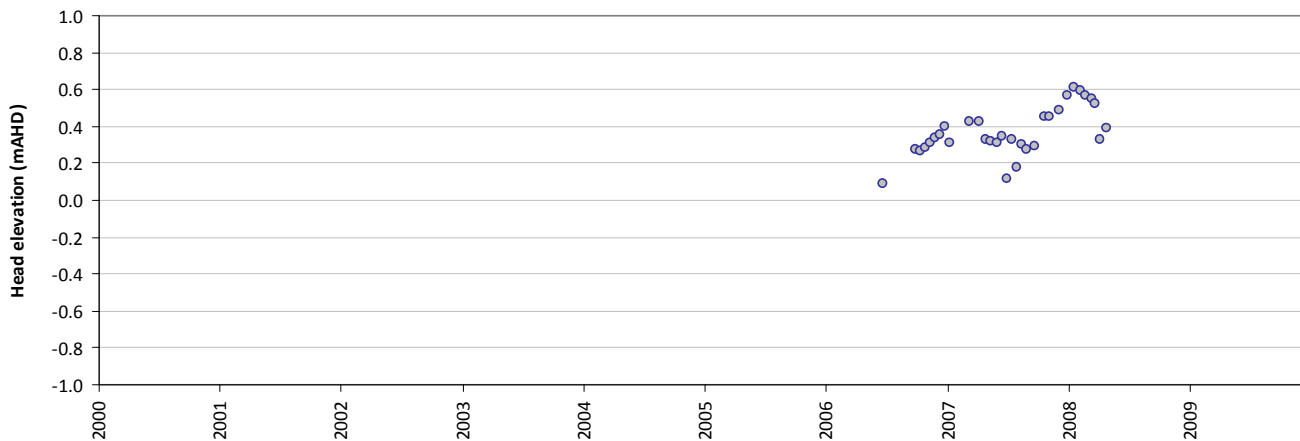
Statistics	
Mean error (ME)	0.27
Mean absolute error (MAE)	0.29
Root mean square error (RMSE)	0.33
Standard deviation of residuals (STDres)	0.20
Correlation coefficient (R)	0.89
Nash Sutcliffe correlation coefficient (R2)	0.31

LP17

Modelled vs observed time-series plot - LP17



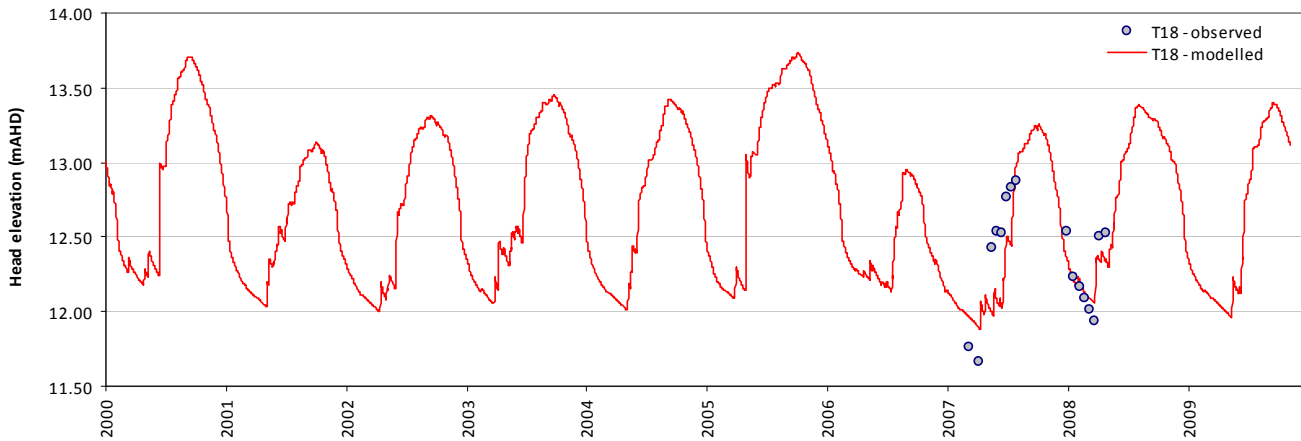
Residual time-series plot - LP17



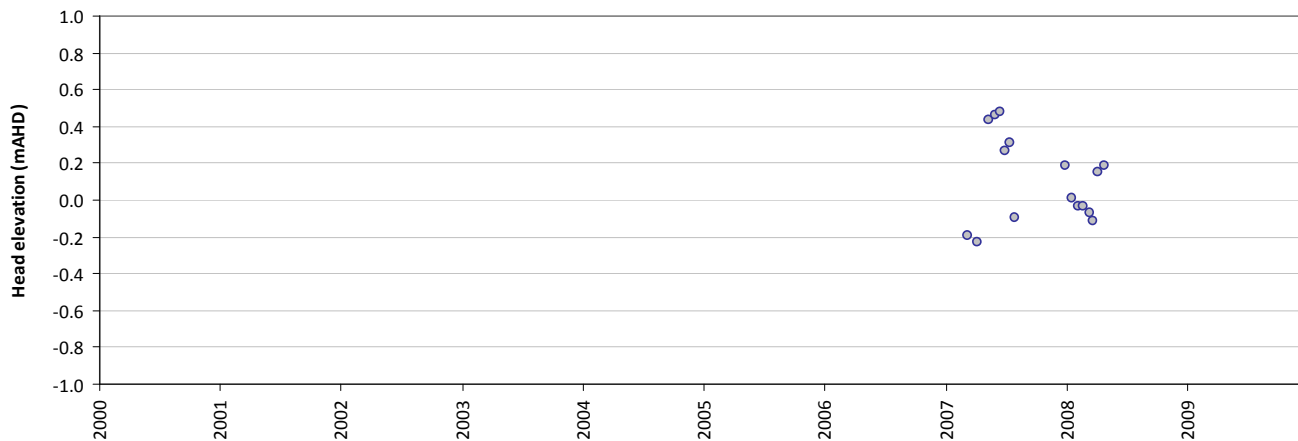
Statistics	
Mean error (ME)	0.37
Mean absolute error (MAE)	0.37
Root mean square error (RMSE)	0.39
Standard deviation of residuals (STDres)	0.13
Correlation coefficient (R)	0.86
Nash Sutcliffe correlation coefficient (R2)	-2.49

T18

Modelled vs observed time-series plot - T18



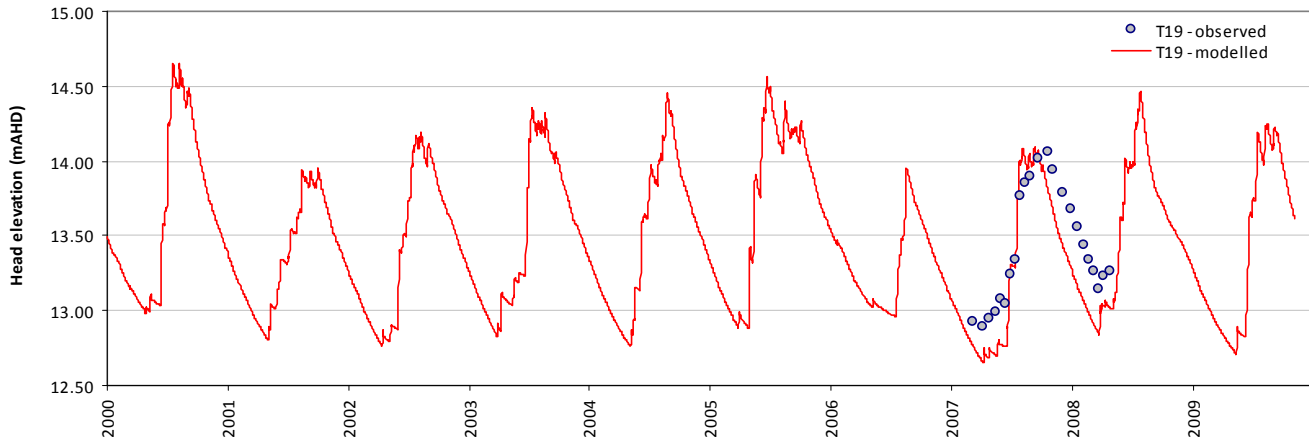
Residual time-series plot - T18



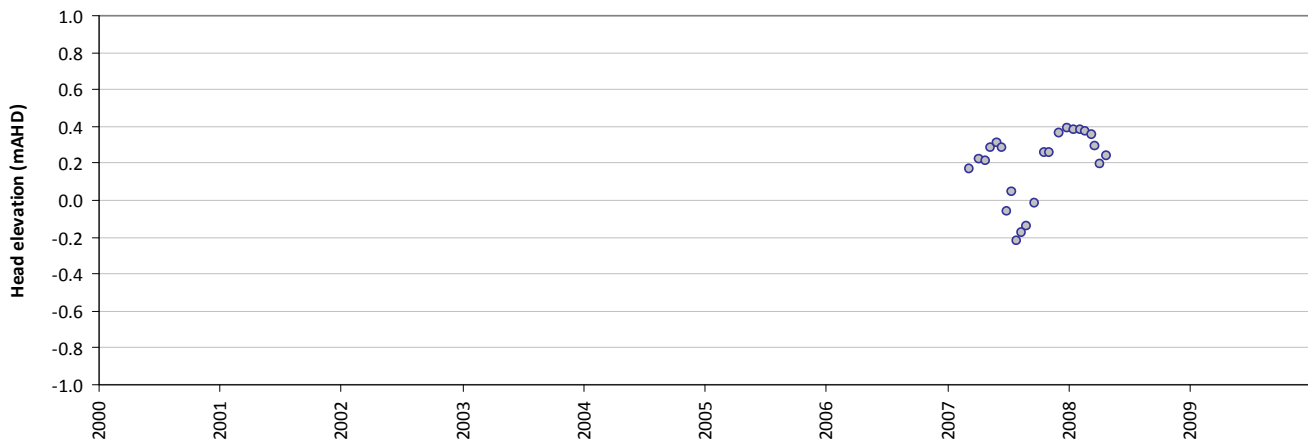
Statistics	
Mean error (ME)	0.11
Mean absolute error (MAE)	0.20
Root mean square error (RMSE)	0.25
Standard deviation of residuals (STDres)	0.23
Correlation coefficient (R)	0.77
Nash Sutcliffe correlation coefficient (R2)	0.50

T19

Modelled vs observed time-series plot - T19



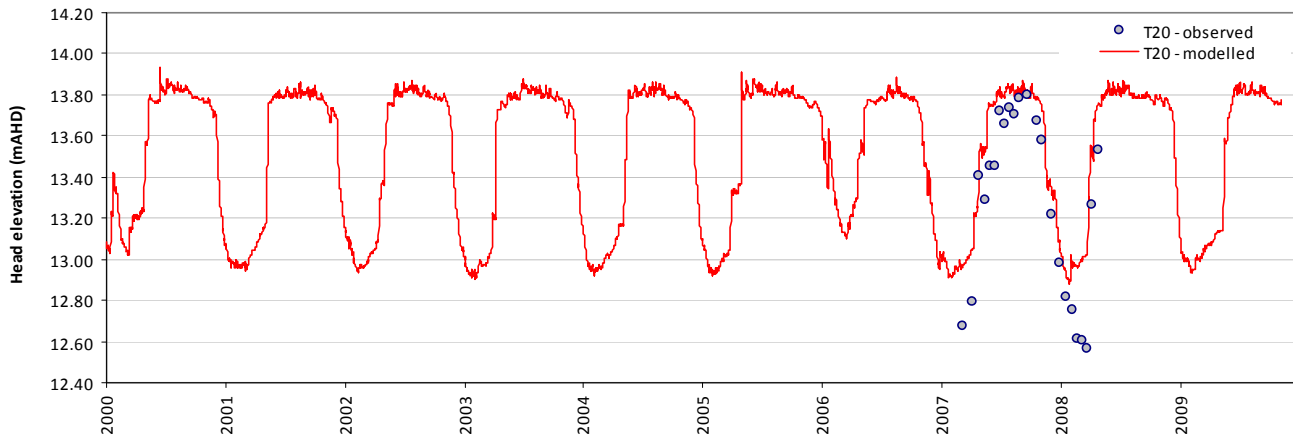
Residual time-series plot - T19



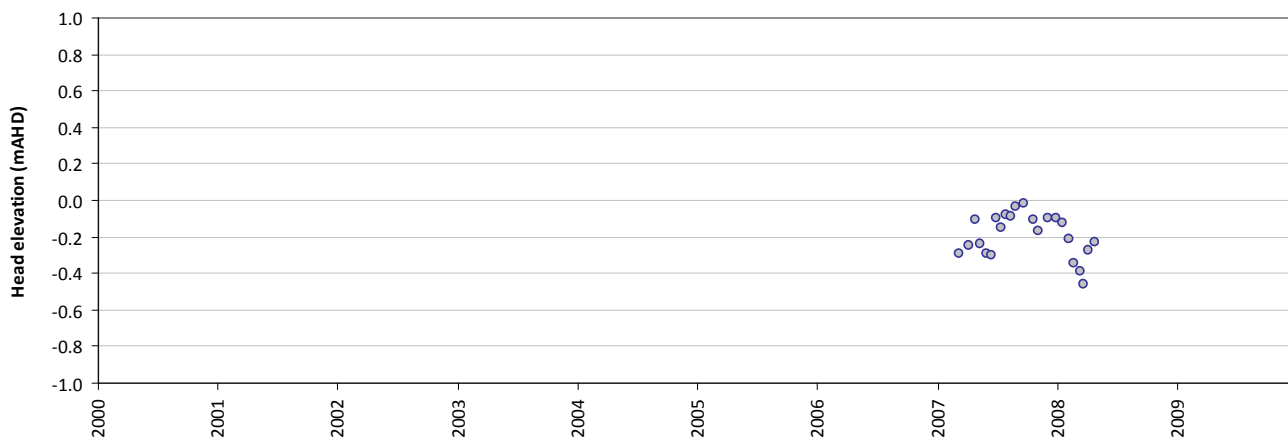
Statistics	
Mean error (ME)	0.19
Mean absolute error (MAE)	0.24
Root mean square error (RMSE)	0.27
Standard deviation of residuals (STDres)	0.18
Correlation coefficient (R)	0.93
Nash Sutcliffe correlation coefficient (R2)	0.49

T20

Modelled vs observed time-series plot - T20



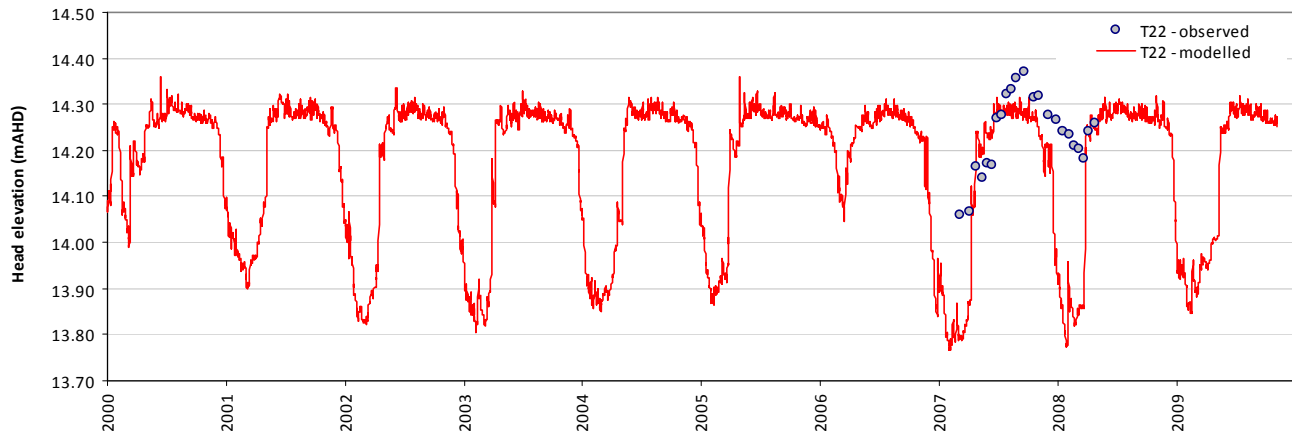
Residual time-series plot - T20



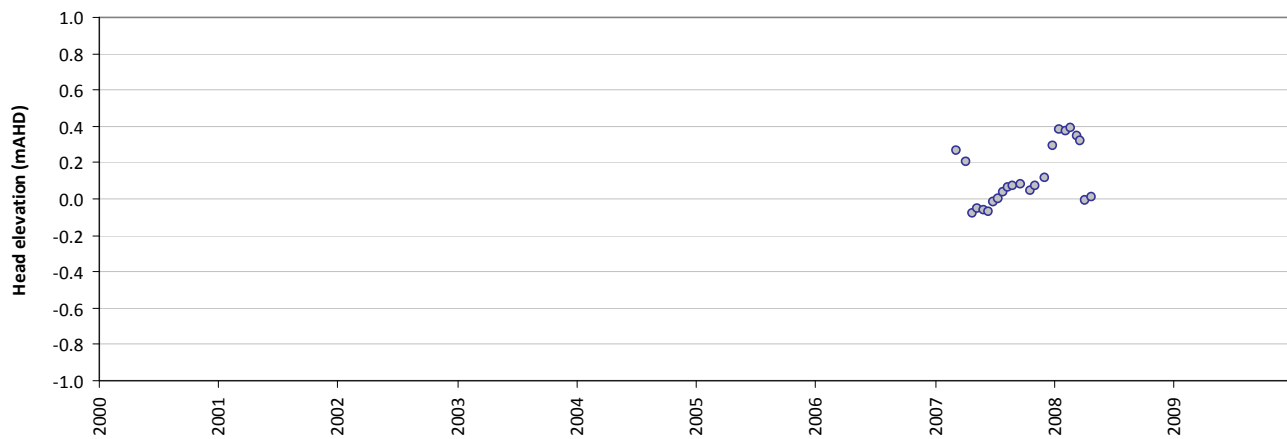
Statistics	
Mean error (ME)	-0.20
Mean absolute error (MAE)	0.20
Root mean square error (RMSE)	0.23
Standard deviation of residuals (STDres)	0.11
Correlation coefficient (R)	0.97
Nash Sutcliffe correlation coefficient (R2)	0.72

T22

Modelled vs observed time-series plot - T22



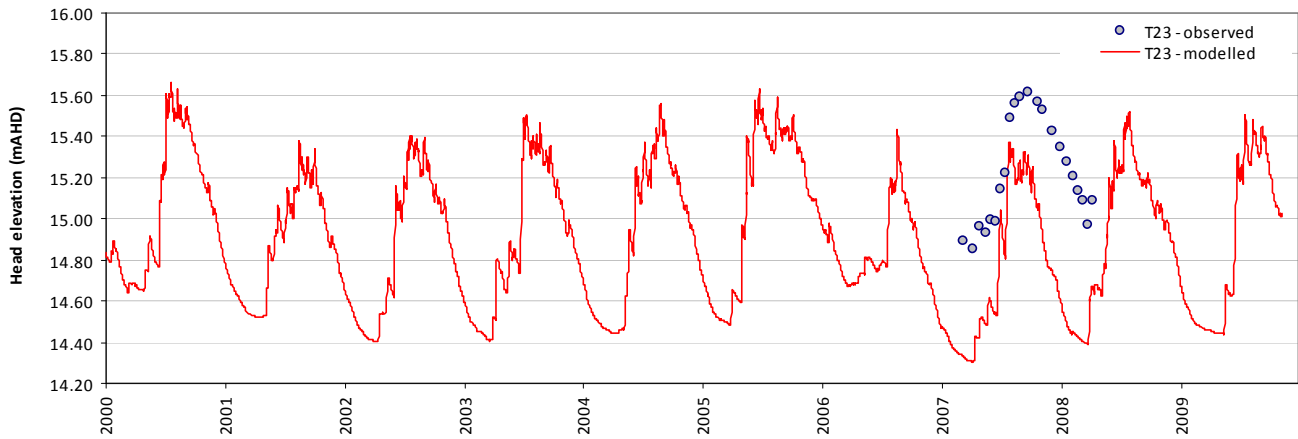
Residual time-series plot - T22



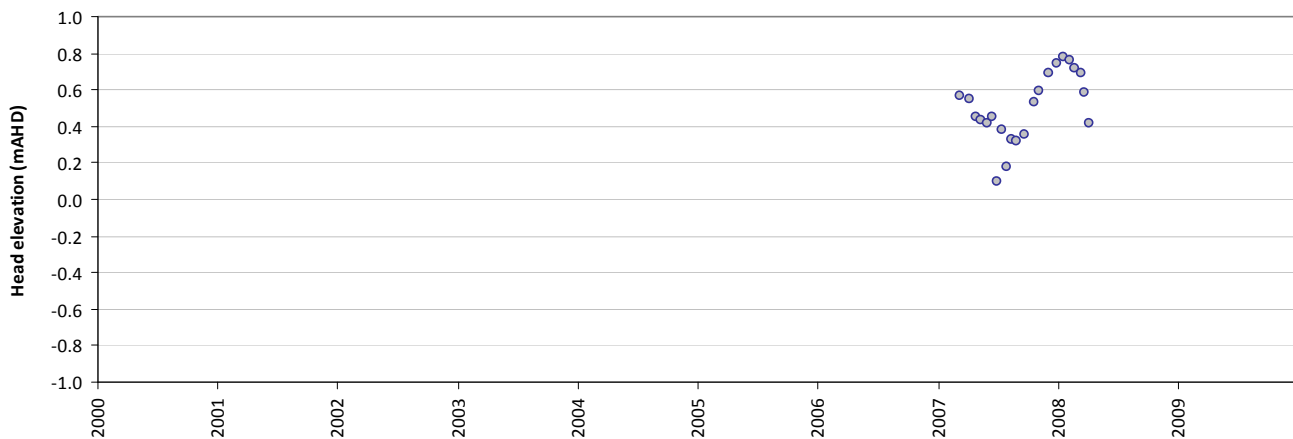
Statistics	
Mean error (ME)	0.12
Mean absolute error (MAE)	0.15
Root mean square error (RMSE)	0.20
Standard deviation of residuals (STDres)	0.16
Correlation coefficient (R)	0.57
Nash Sutcliffe correlation coefficient (R2)	-4.86

T23

Modelled vs observed time-series plot - T23



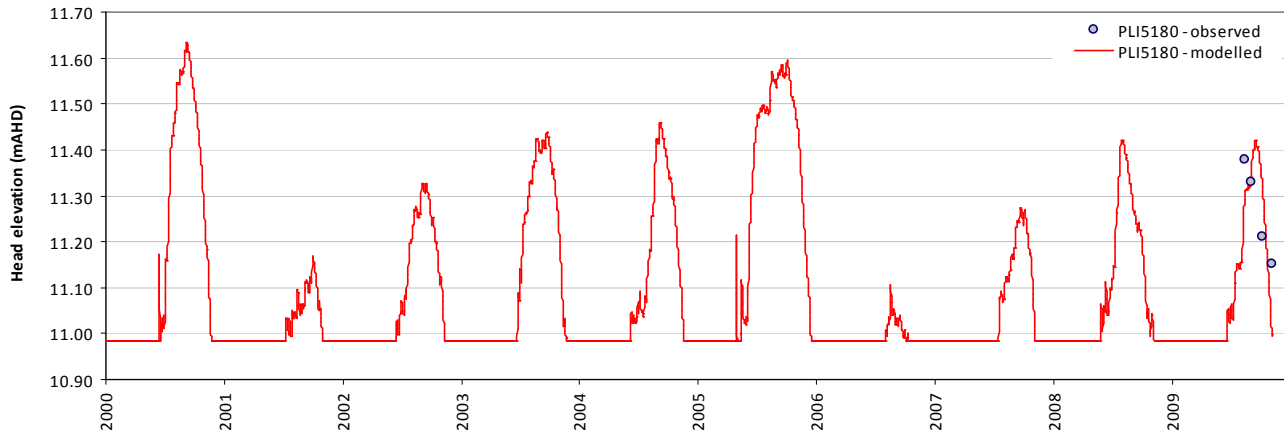
Residual time-series plot - T23



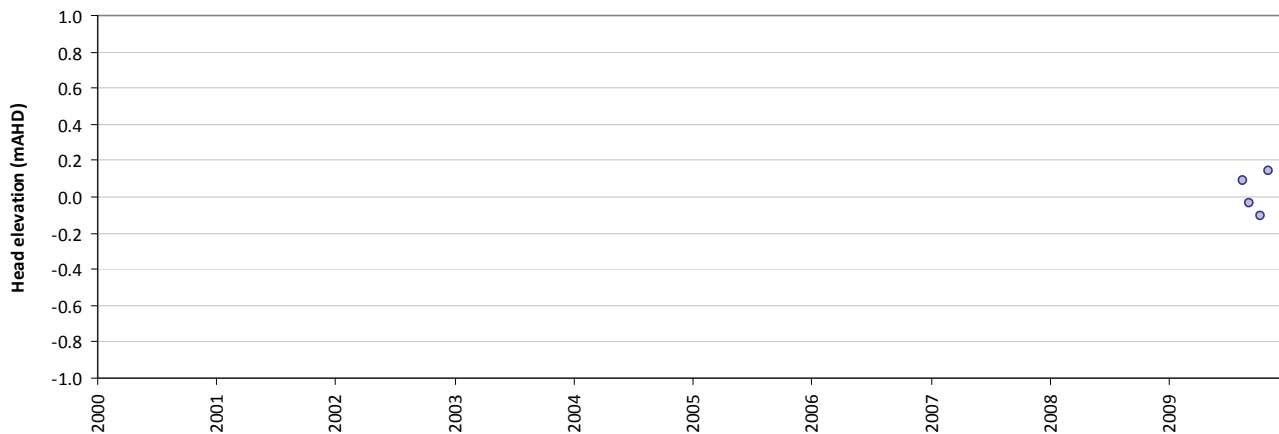
Statistics	
Mean error (ME)	0.53
Mean absolute error (MAE)	0.53
Root mean square error (RMSE)	0.58
Standard deviation of residuals (STDres)	0.23
Correlation coefficient (R)	0.72
Nash Sutcliffe correlation coefficient (R2)	-3.43

PLI5180

Modelled vs observed time-series plot - PLI5180



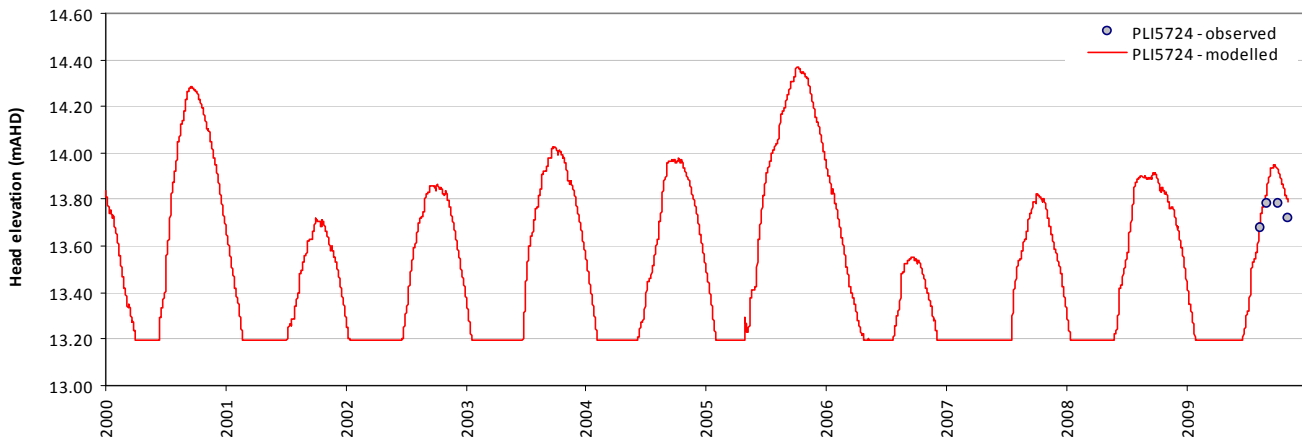
Residual time-series plot - PLI5180



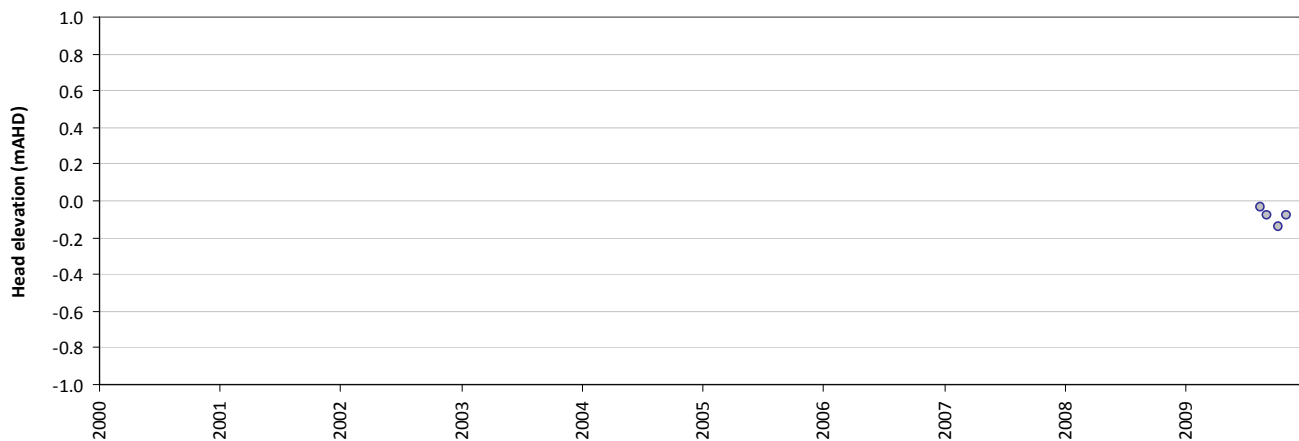
Statistics	
Mean error (ME)	-0.08
Mean absolute error (MAE)	0.08
Root mean square error (RMSE)	0.09
Standard deviation of residuals (STDres)	0.04
Correlation coefficient (R)	0.93
Nash Sutcliffe correlation coefficient (R2)	-3.69

PLI5724

Modelled vs observed time-series plot - PLI5724



Residual time-series plot - PLI5724



Statistics	
Mean error (ME)	0.02
Mean absolute error (MAE)	0.09
Root mean square error (RMSE)	0.10
Standard deviation of residuals (STDres)	0.10
Correlation coefficient (R)	0.68
Nash Sutcliffe correlation coefficient (R2)	-0.23

Appendix E: Elliot Road wetland system calibration statistics and plots

Elliot Road wetland system calibration statistics

Table E-1: Elliot Road wetland system calibration statistic for observed vs modelled heads.

Description	Observed	Modelled	Residual	Abs residual
sum (m)	2692	2682	10.1	
average (m)	19.80	19.72	0.07	0.29
median (m)	19.73	19.75	-0.03	0.22
min (m)	18.69	18.75	-0.80	
max (m)	21.37	21.24	1.26	
range (m)	2.68	2.49	2.06	

Table E-1: Elliot Road wetland system summary statistic for observed vs modelled heads.

Description	Symbol	Value
Count	n	136
Sum of squares (m ²)	SSQ	20
Mean sum of squares (m ²)	MSSQ	0.15
Root mean square (m)	RMS	0.39
Scaled root mean square (%)	SRMS	14.44
Sum of residuals (m)	SRMS	39.1
Mean sum of residuals (m)	MSR	0.29
Scaled mean sum of residuals (%)	SMSR	10.73
Coefficient of determination ()	CD	1.66

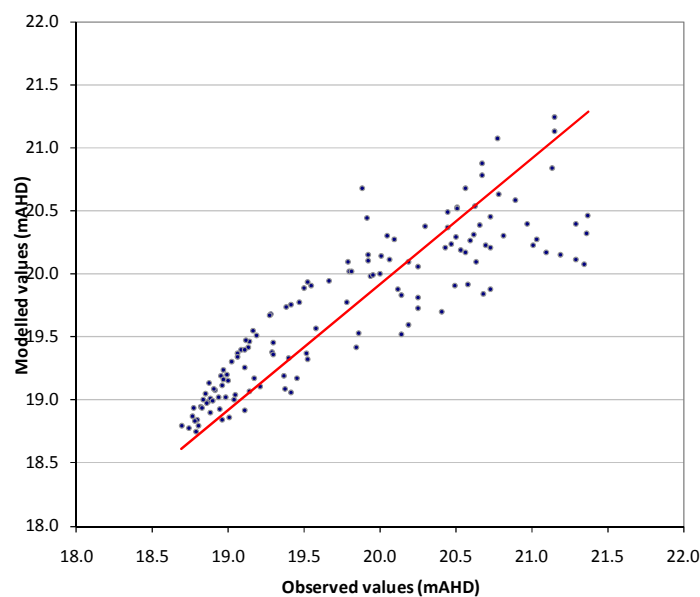


Figure E-1: Elliot Road wetland system scatterplot for observed vs modelled groundwater levels

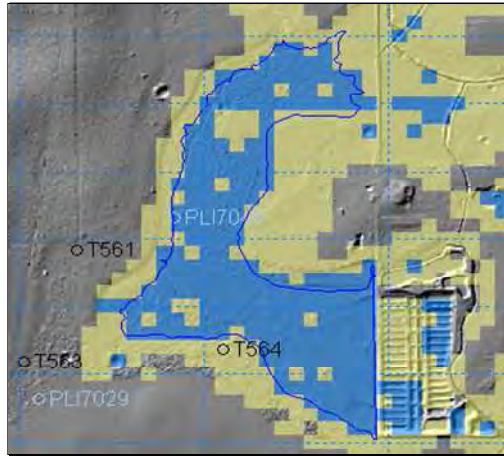
Elliot Road wetland aerial photos vs modelled data

Aerial Photo: December 2003



SwanCoastPlain_S_04_40cm_z50.ecw

Inundated area: Model

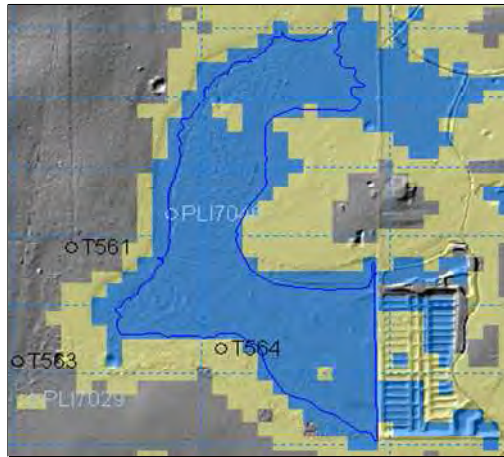


Aerial Photo: December 2005



swancoastplain_South_2006_20cm_z50.ecw

Inundated area: Model

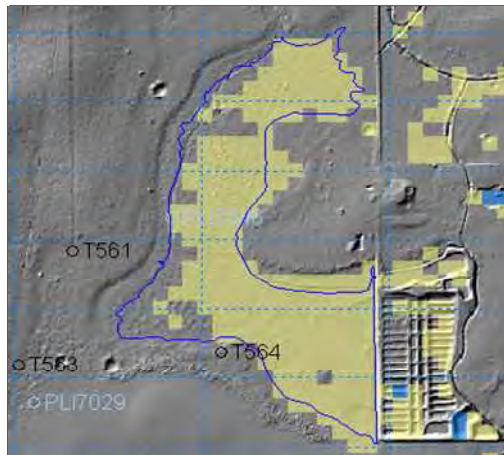


Aerial Photo: December 2006



SwanCoastPlain_South_2007_20cm_z50.ecw

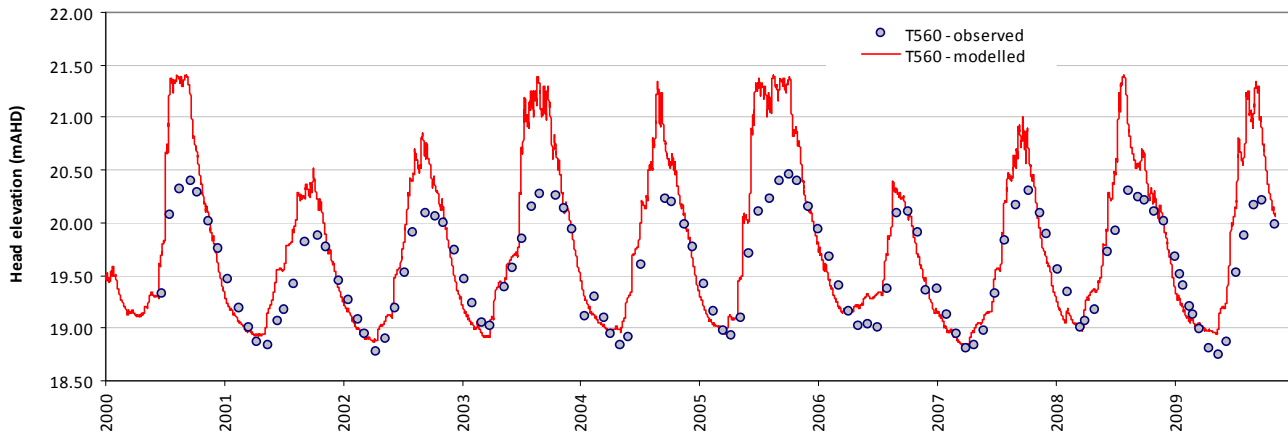
Inundated area: Model



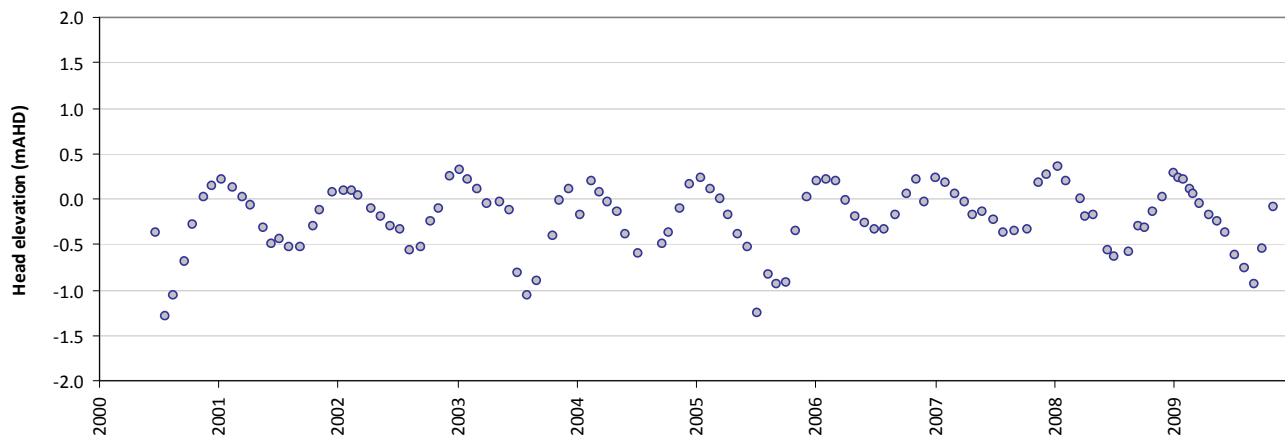
Elliot Road wetland system calibration plots

T560

Modelled vs observed time-series plot - T560



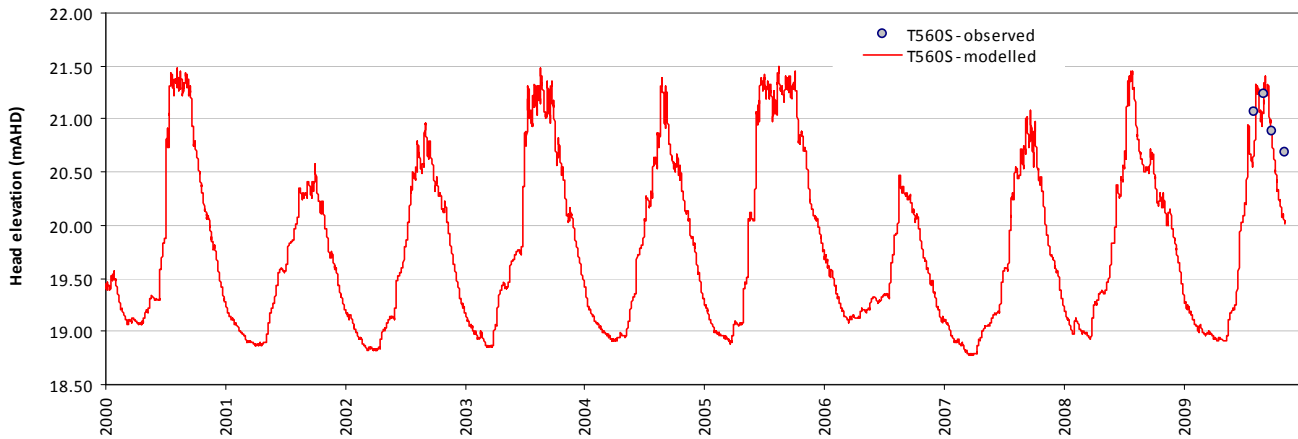
Residual time-series plot - T560



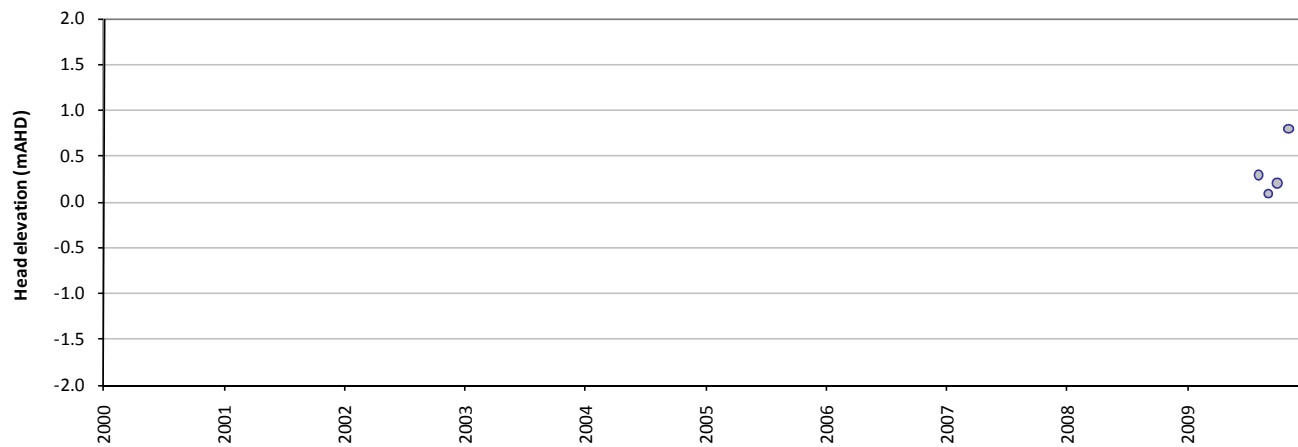
Statistics	
Mean error (ME)	-0.10
Mean absolute error (MAE)	0.30
Root mean square error (RMSE)	0.40
Standard deviation of residuals (STDres)	0.39
Correlation coefficient (R)	0.89
Nash Sutcliffe correlation coefficient (R2)	0.35

T560S

Modelled vs observed time-series plot - T560S



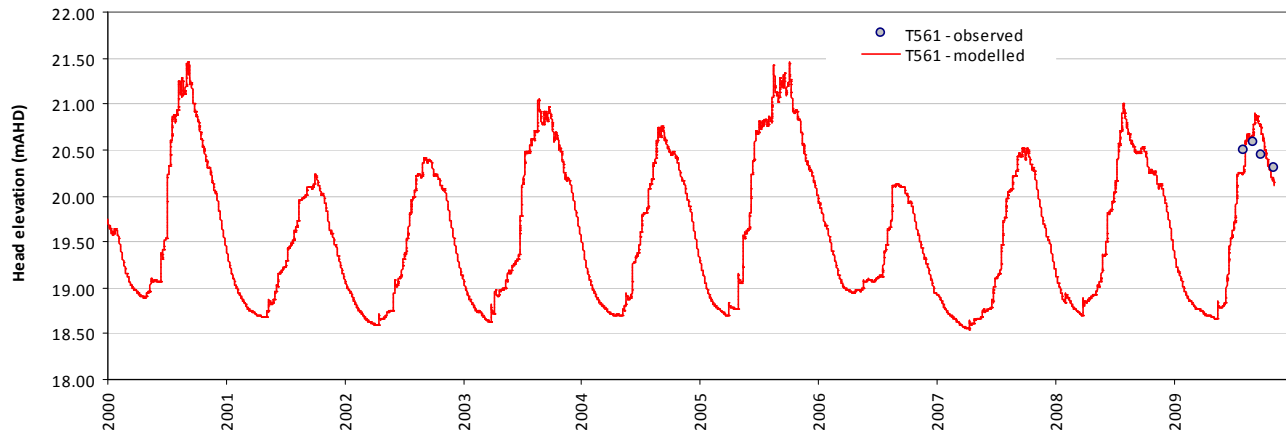
Residual time-series plot - T560S



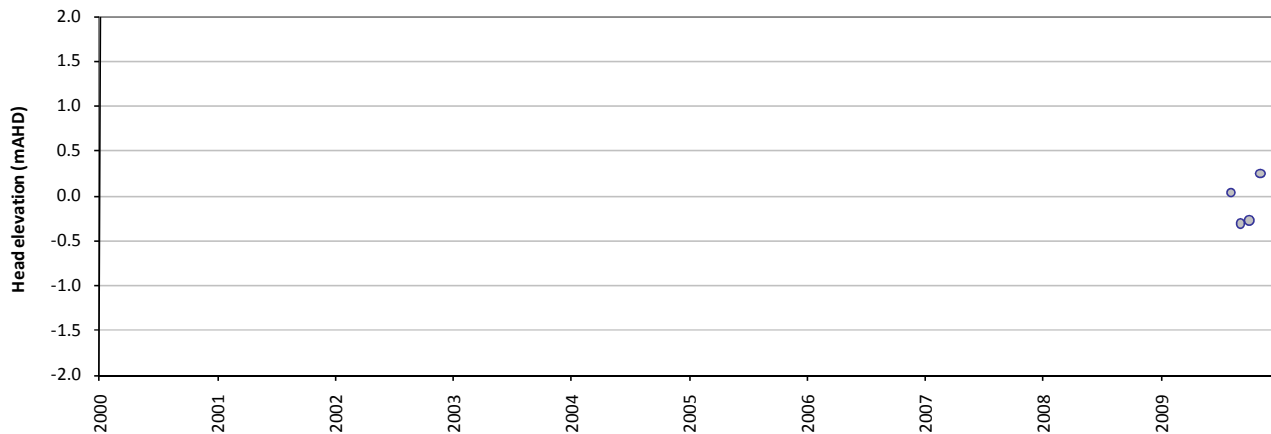
Statistics	
Mean error (ME)	0.35
Mean absolute error (MAE)	0.35
Root mean square error (RMSE)	0.44
Standard deviation of residuals (STDres)	0.27
Correlation coefficient (R)	0.95
Nash Sutcliffe correlation coefficient (R2)	-3.50

T561

Modelled vs observed time-series plot - T561



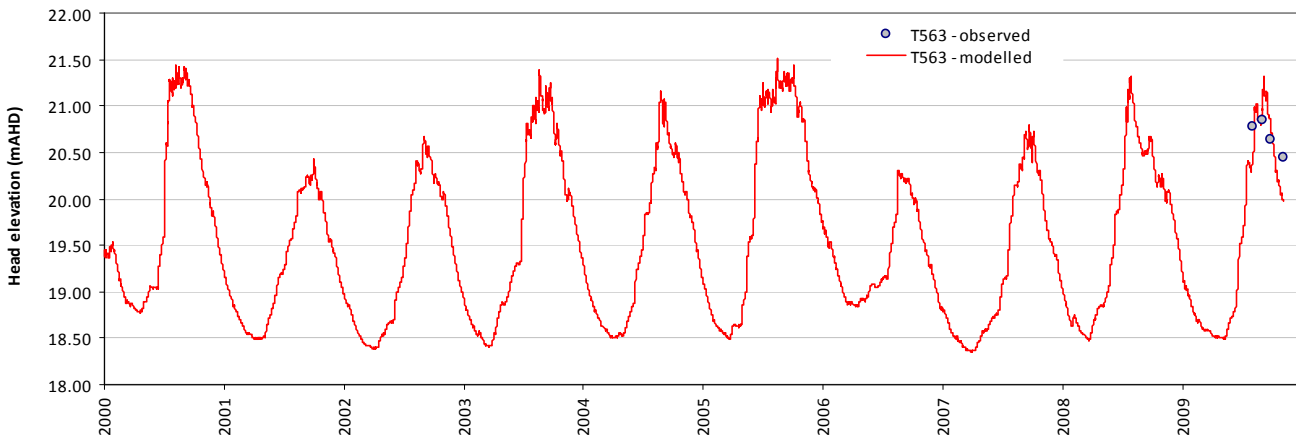
Residual time-series plot - T561



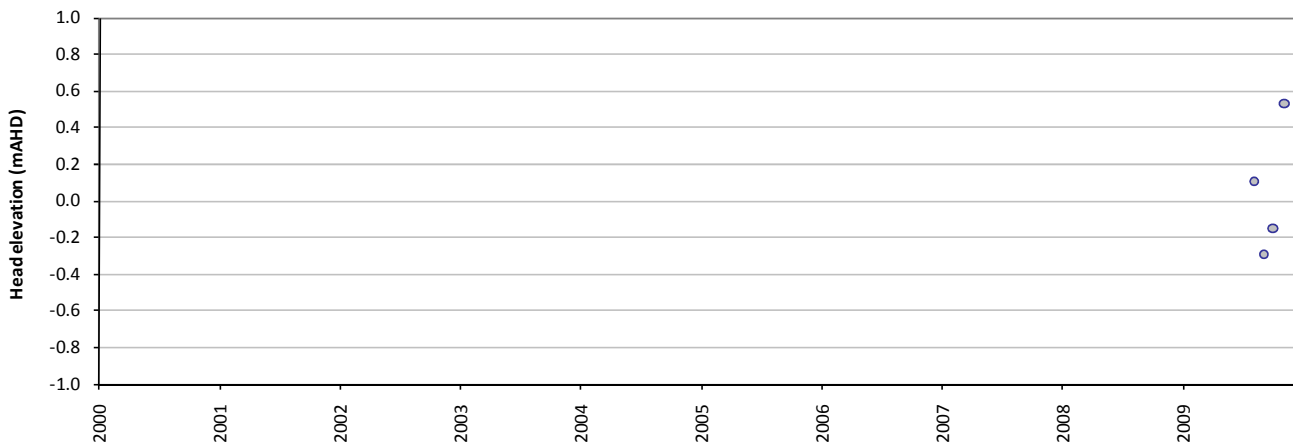
Statistics	
Mean error (ME)	-0.07
Mean absolute error (MAE)	0.23
Root mean square error (RMSE)	0.25
Standard deviation of residuals (STDres)	0.24
Correlation coefficient (R)	0.89
Nash Sutcliffe correlation coefficient (R2)	-4.93

T563

Modelled vs observed time-series plot - T563



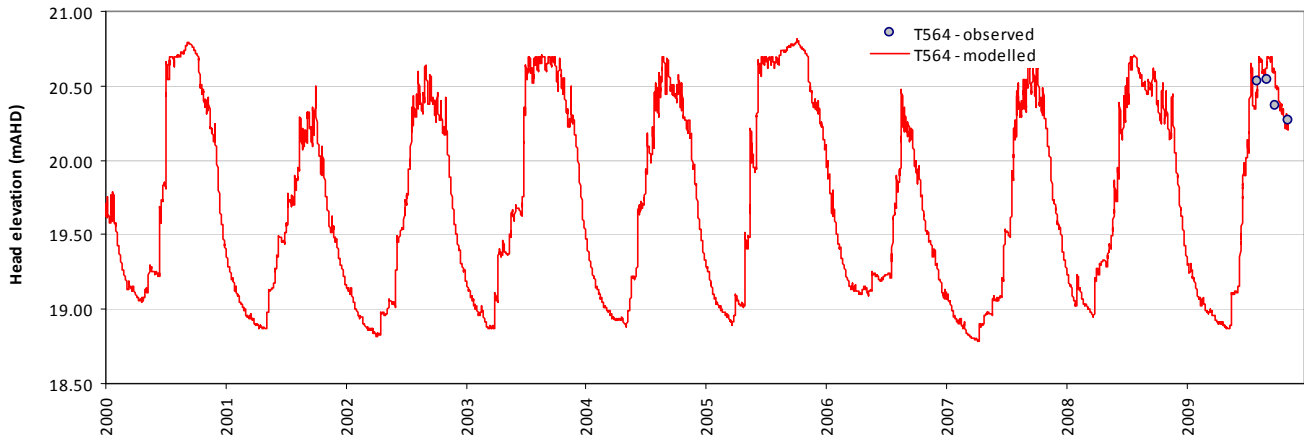
Residual time-series plot - T563



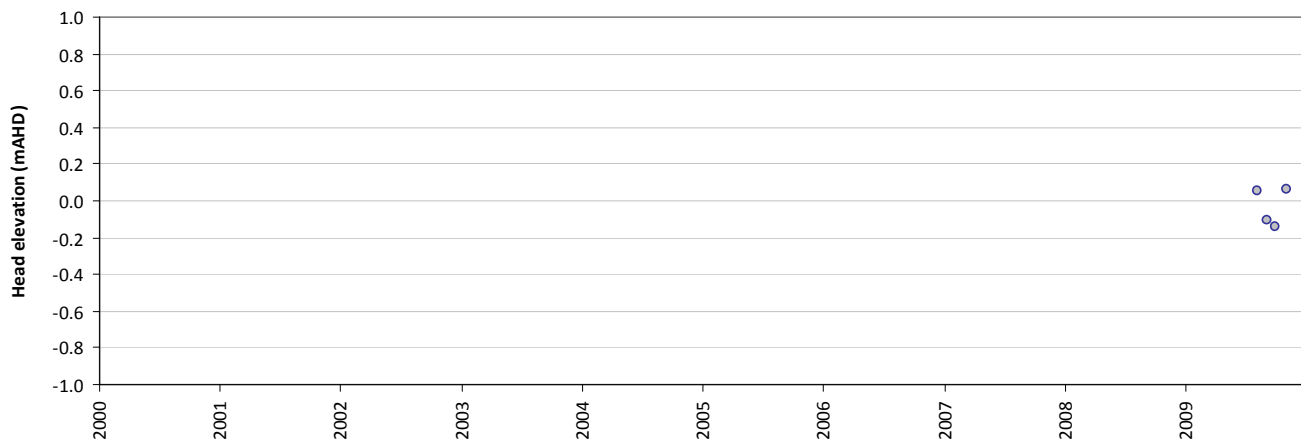
Statistics	
Mean error (ME)	0.06
Mean absolute error (MAE)	0.29
Root mean square error (RMSE)	0.32
Standard deviation of residuals (STDres)	0.32
Correlation coefficient (R)	0.88
Nash Sutcliffe correlation coefficient (R2)	-3.32

T564

Modelled vs observed time-series plot - T564



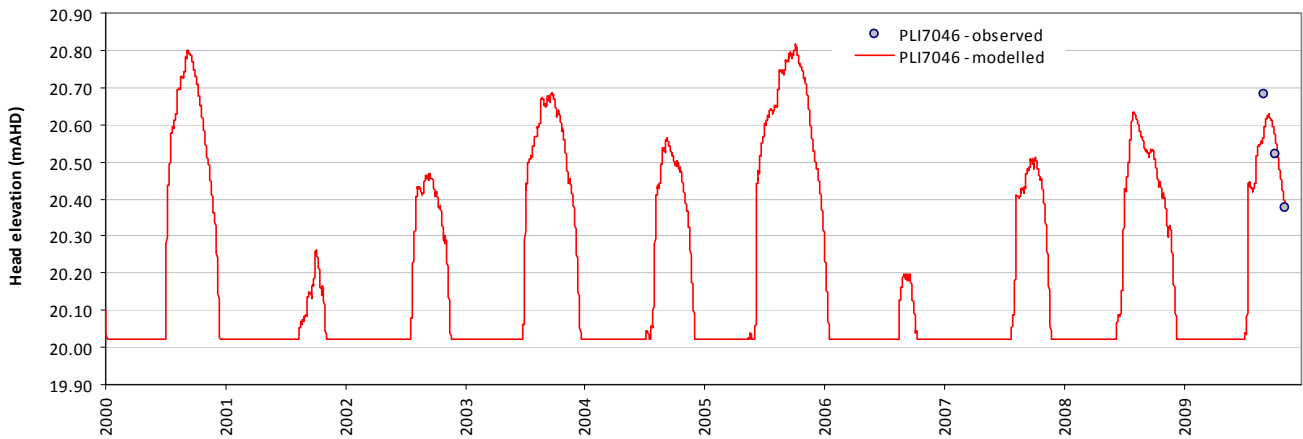
Residual time-series plot - T564



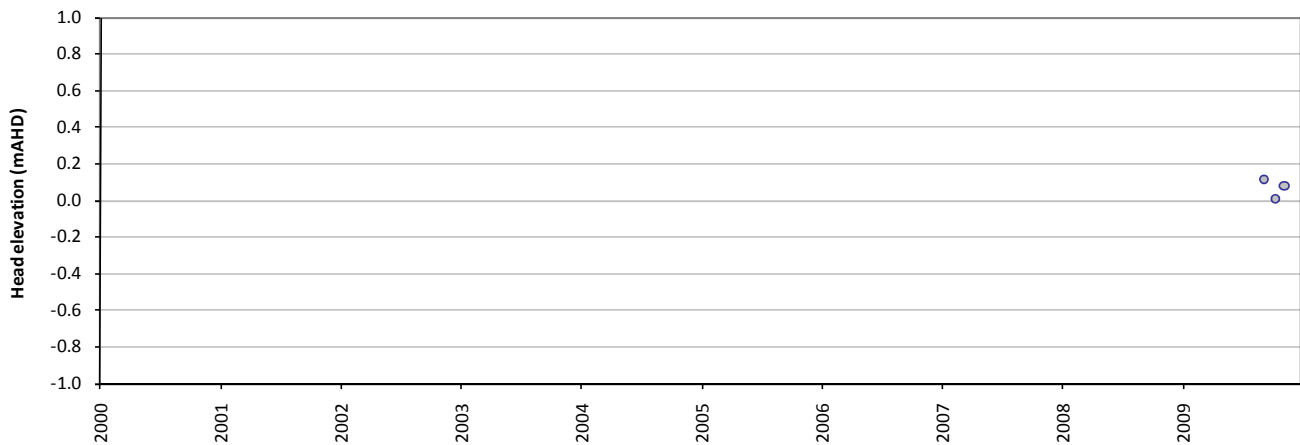
Statistics	
Mean error (ME)	0.01
Mean absolute error (MAE)	0.10
Root mean square error (RMSE)	0.11
Standard deviation of residuals (STDres)	0.11
Correlation coefficient (R)	0.89
Nash Sutcliffe correlation coefficient (R2)	0.12

PLI7046

Modelled vs observed time-series plot - PLI7046



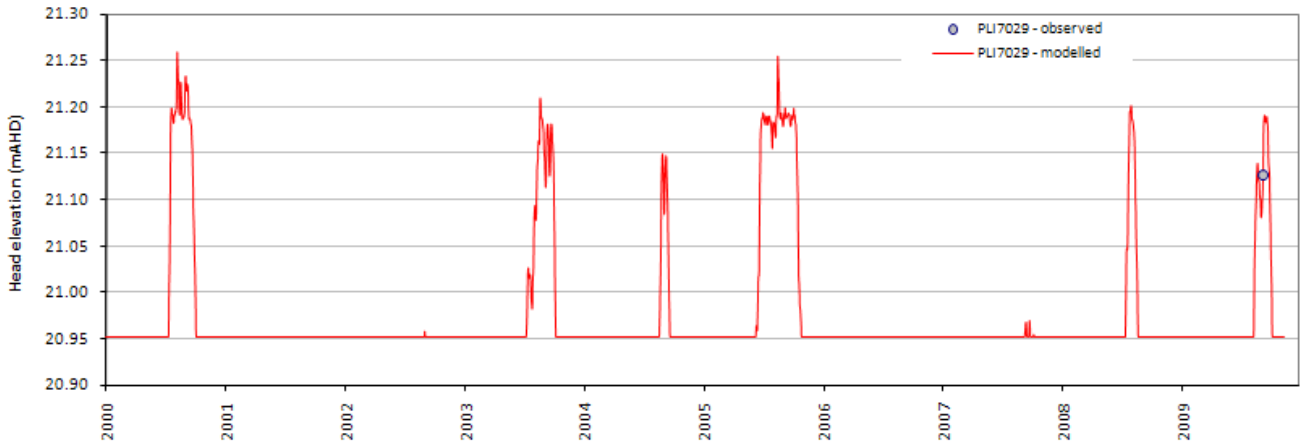
Residual time-series plot - PLI7046



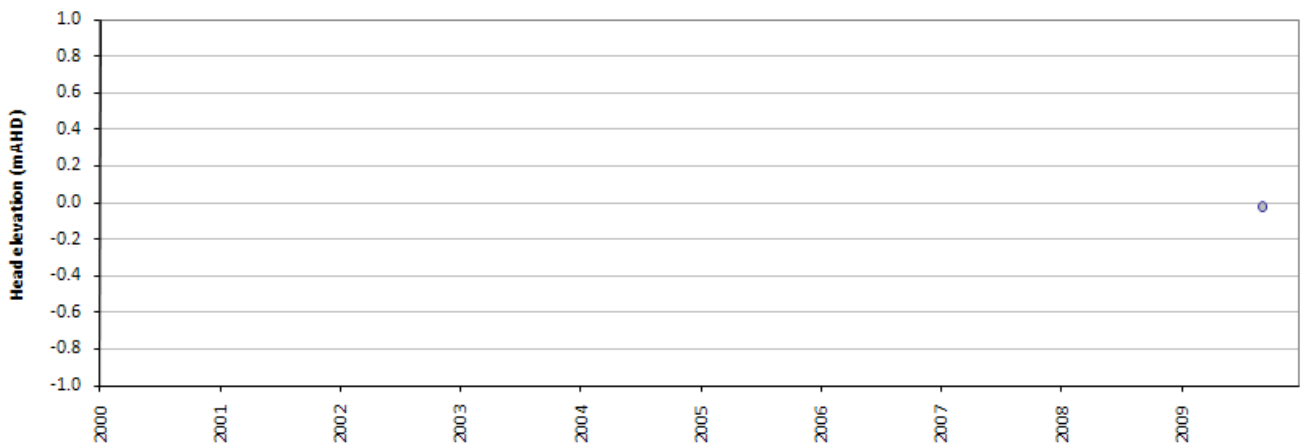
Statistics	
Mean error (ME)	0.07
Mean absolute error (MAE)	0.07
Root mean square error (RMSE)	0.08
Standard deviation of residuals (STDres)	0.05
Correlation coefficient (R)	0.92
Nash Sutcliffe correlation coefficient (R2)	0.55

PLI7029

Modelled vs observed time-series plot - PLI7029



Residual time-series plot - PLI7029



Statistics	
Mean error (ME)	0.00
Mean absolute error (MAE)	0.00
Root mean square error (RMSE)	-
Standard deviation of residuals (STDres)	-
Correlation coefficient (R)	-
Nash Sutcliffe correlation coefficient (R2)	-

Appendix F: Lakes Road wetland system calibration statistics and plots

Lakes Road wetland system calibration statistics

Table F-1: Lakes Road wetland system calibration statistic for observed vs modelled heads.

Description	Observed	Modelled	Residual	Abs residual
sum (m)	1738	1680	57.6	
average (m)	11.51	11.13	0.38	0.49
median (m)	13.19	12.44	0.26	0.35
min (m)	4.21	4.06	-0.57	
max (m)	17.35	17.58	1.70	
range (m)	13.14	13.52	2.27	

Table F-1: Lakes Road wetland system summary statistic for observed vs modelled heads.

Description	Symbol	Value
Count	n	151
Sum of squares (m ²)	SSQ	65
Mean sum of squares (m ²)	MSSQ	0.43
Root mean square (m)	RMS	0.66
Scaled root mean square (%)	SRMS	4.99
Sum of residuals (m)	SRMS	74.0
Mean sum of residuals (m)	MSR	0.49
Scaled mean sum of residuals (%)	SMSR	3.73
Coefficient of determination ()	CD	0.99

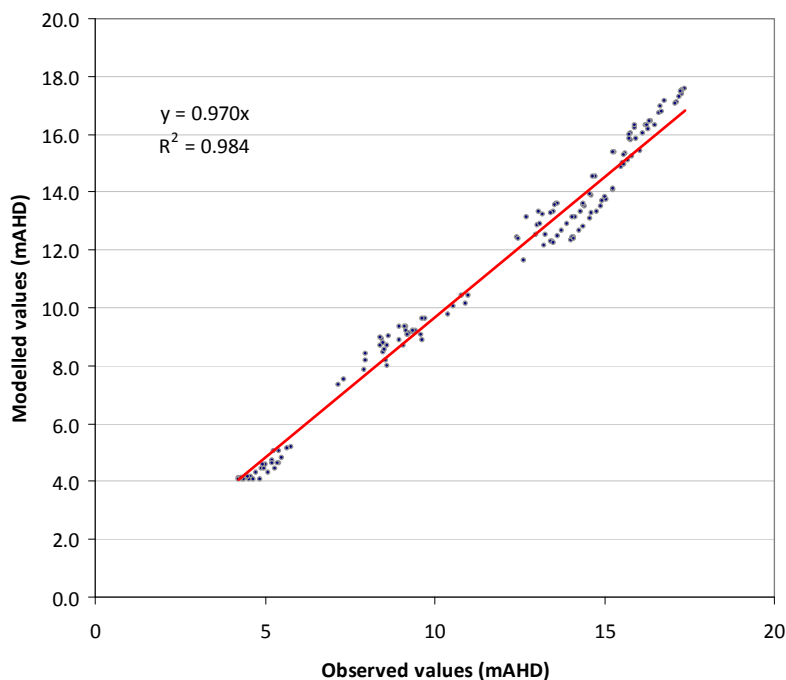


Figure F-1: Lakes Road wetland system scatterplot for observed vs modelled groundwater levels

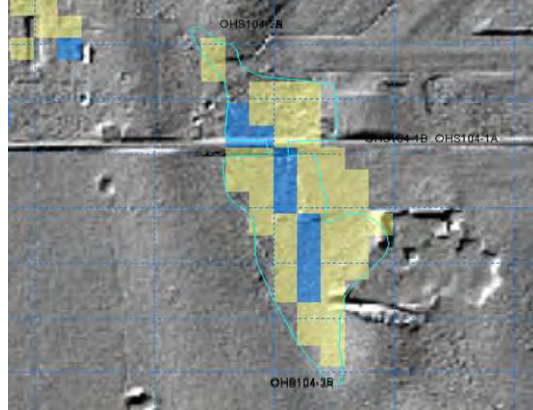
Airfield wetland aerial photos vs modelled data

Aerial Photo: December 2003



SwanCoastPlain_S_04_40cm_z50.ecw

Inundated area: Model

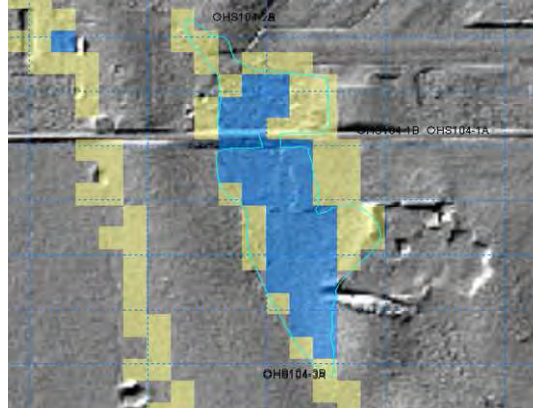


Aerial Photo: December 2005



swancoastplain_South_2006_20cm_z50.ecw

Inundated area: Model

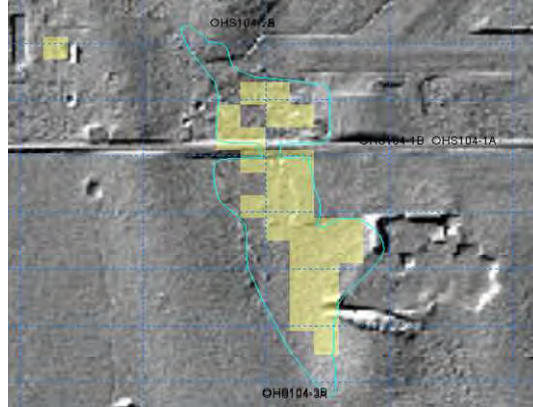


Aerial Photo: December 2006



SwanCoastPlain_South_2007_20cm_z50.ecw

Inundated area: Model



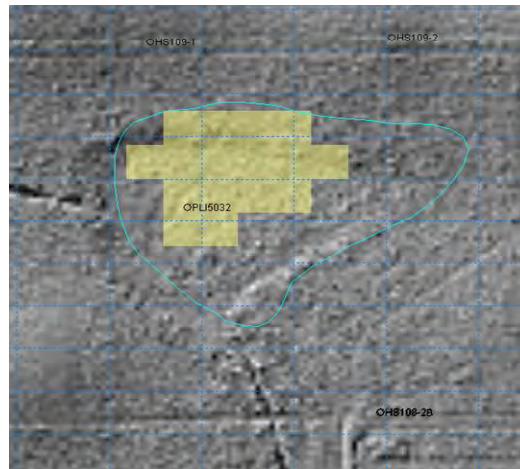
Greyhound Road wetland aerial photos vs modelled data

Aerial Photo: December 2003



SwanCoastPlain_S_04_40cm_z50.ecw

Inundated area: Model

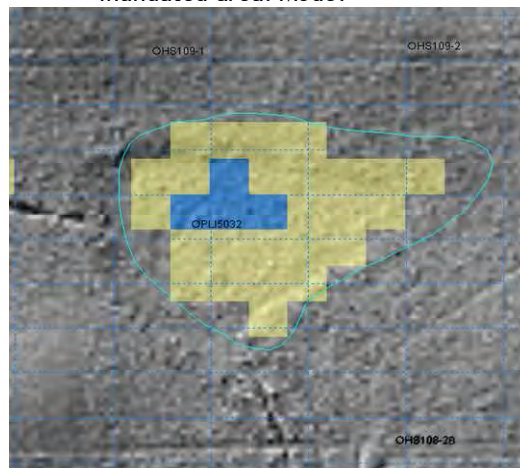


Aerial Photo: December 2005



swancoastplain_South_2006_20cm_z50.ecw

Inundated area: Model

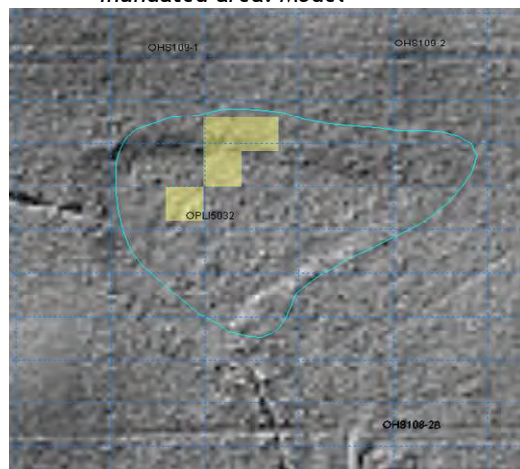


Aerial Photo: December 2006



SwanCoastPlain_South_2007_20cm_z50.ecw

Inundated area: Model



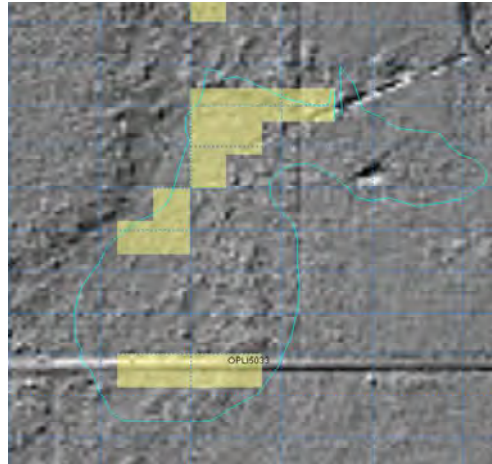
Lakes Road wetland aerial photos vs modelled data

Aerial Photo: December 2003

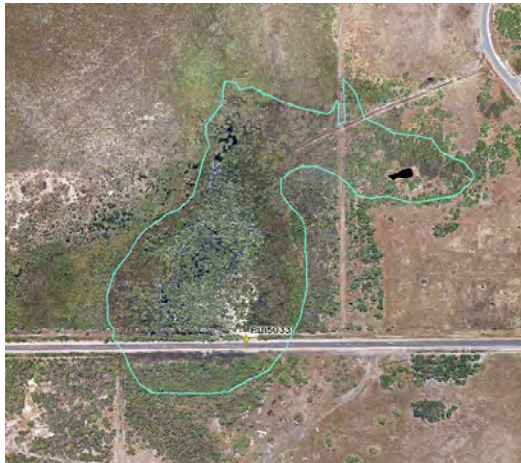


SwanCoastPlain_S_04_40cm_z50.ecw

Inundated area: Model

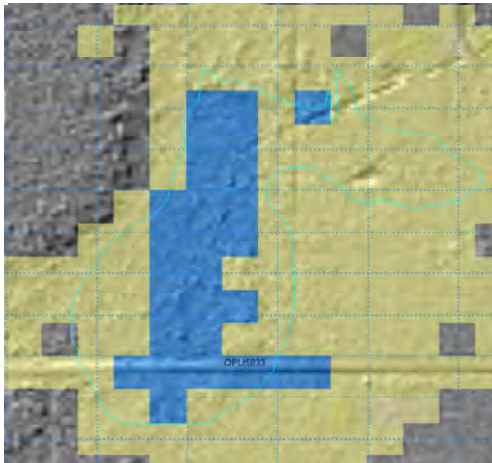


Aerial Photo: December 2005



swancoastplain_South_2006_20cm_z50.ecw

Inundated area: Model



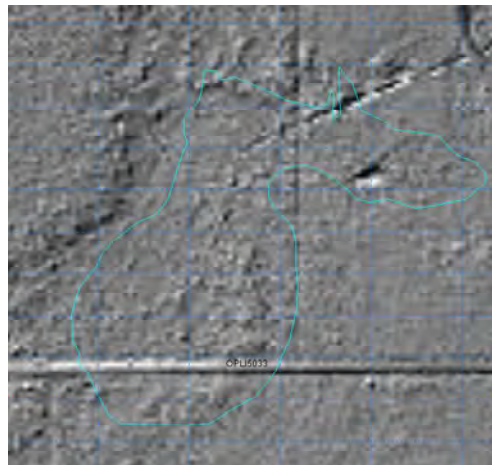
(2nd December)

Aerial Photo: December 2006



SwanCoastPlain_South_2007_20cm_z50.ecw

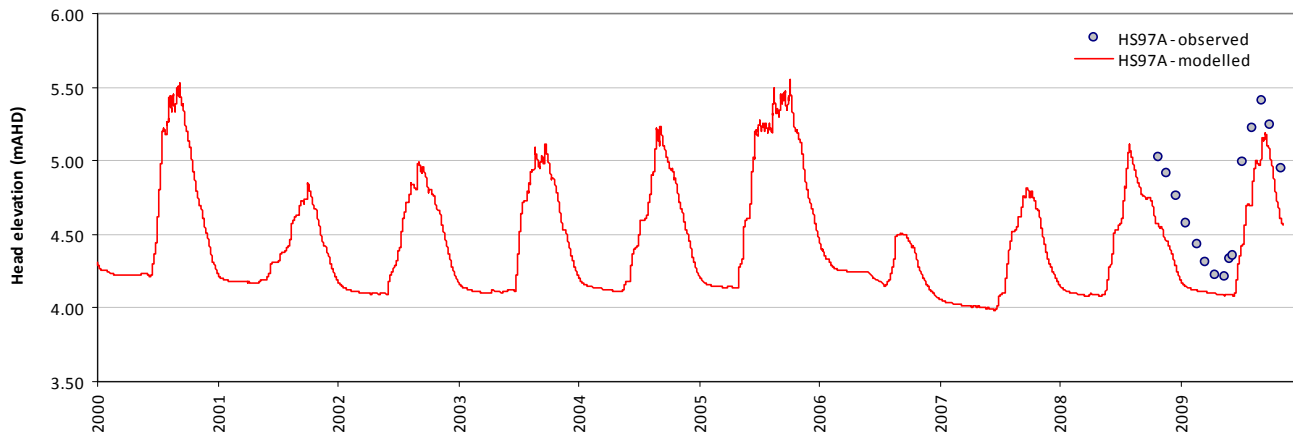
Inundated area: Model



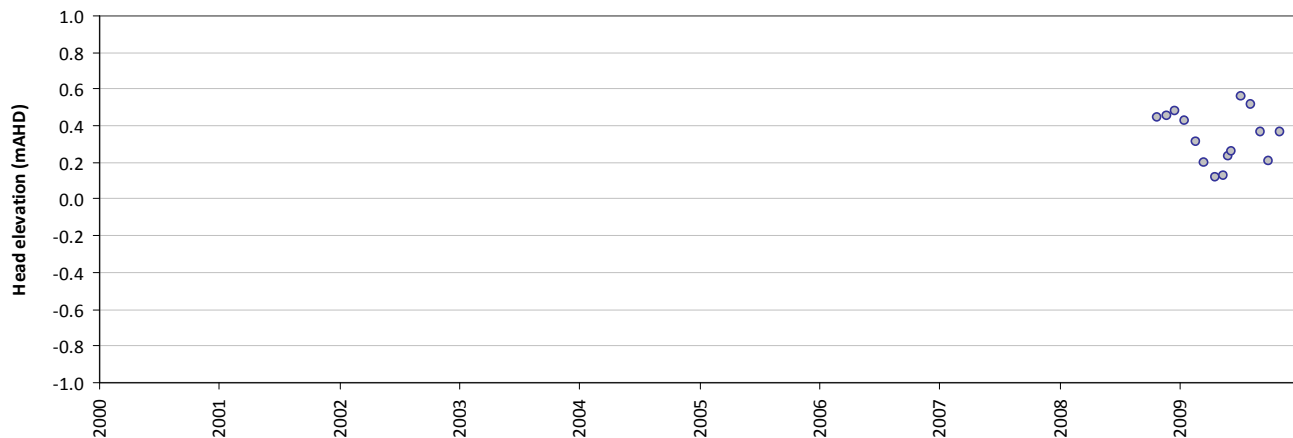
Lakes Road wetland system calibration plots

HS97A

Modelled vs observed time-series plot - HS97A



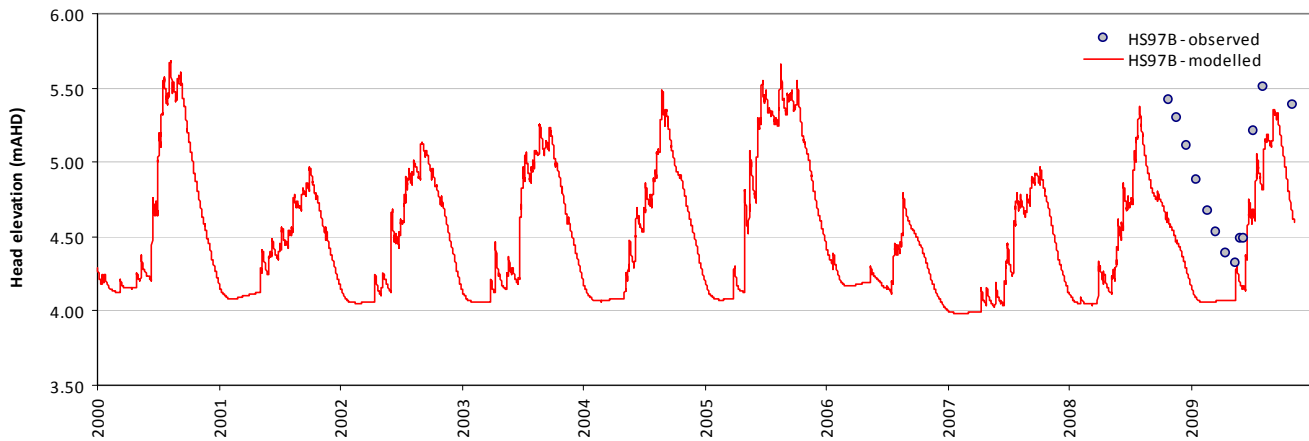
Residual time-series plot - HS97A



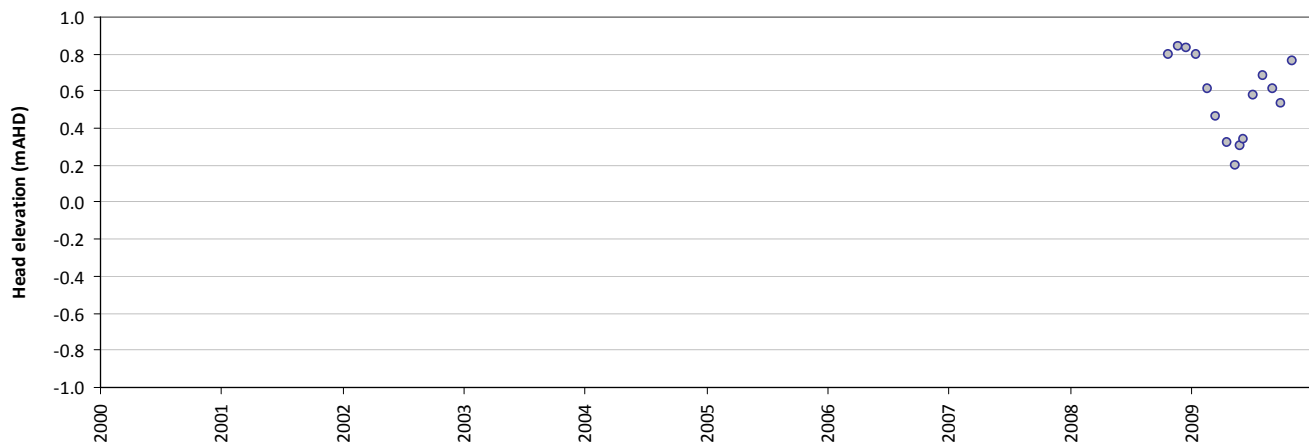
Statistics	
Mean error (ME)	0.34
Mean absolute error (MAE)	0.34
Root mean square error (RMSE)	0.34
Standard deviation of residuals (STDres)	0.14
Correlation coefficient (R)	0.94
Nash Sutcliffe correlation coefficient (R2)	0.13

HS97B

Modelled vs observed time-series plot - HS97B



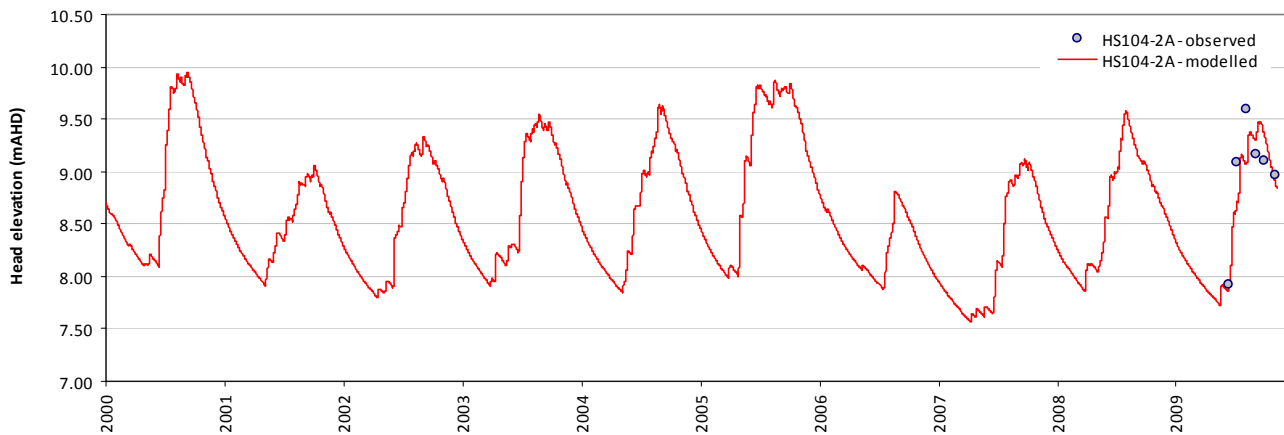
Residual time-series plot - HS97B



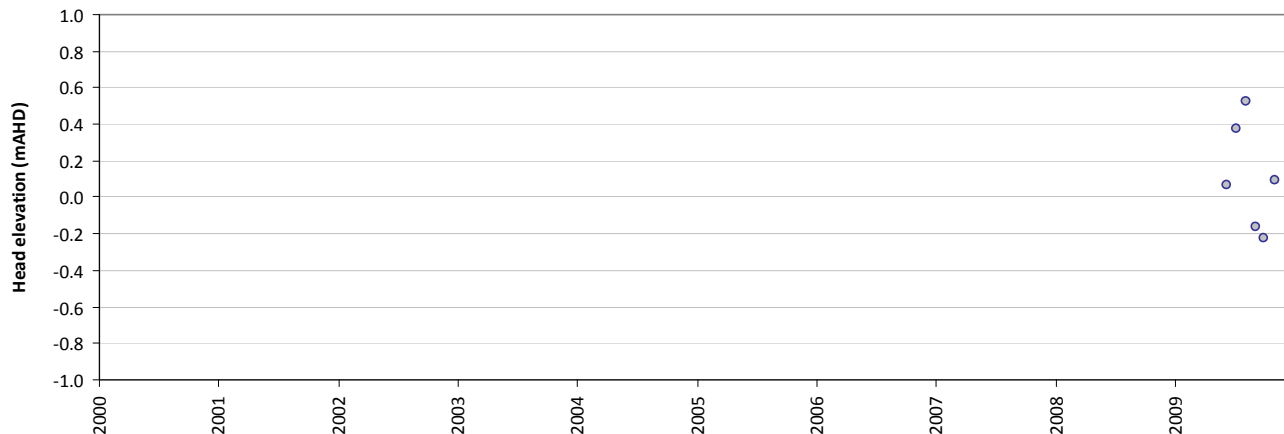
Statistics	
Mean error (ME)	0.58
Mean absolute error (MAE)	0.58
Root mean square error (RMSE)	0.58
Standard deviation of residuals (STDres)	0.21
Correlation coefficient (R)	0.92
Nash Sutcliffe correlation coefficient (R2)	-0.62

HS104-2A

Modelled vs observed time-series plot - HS104-2A



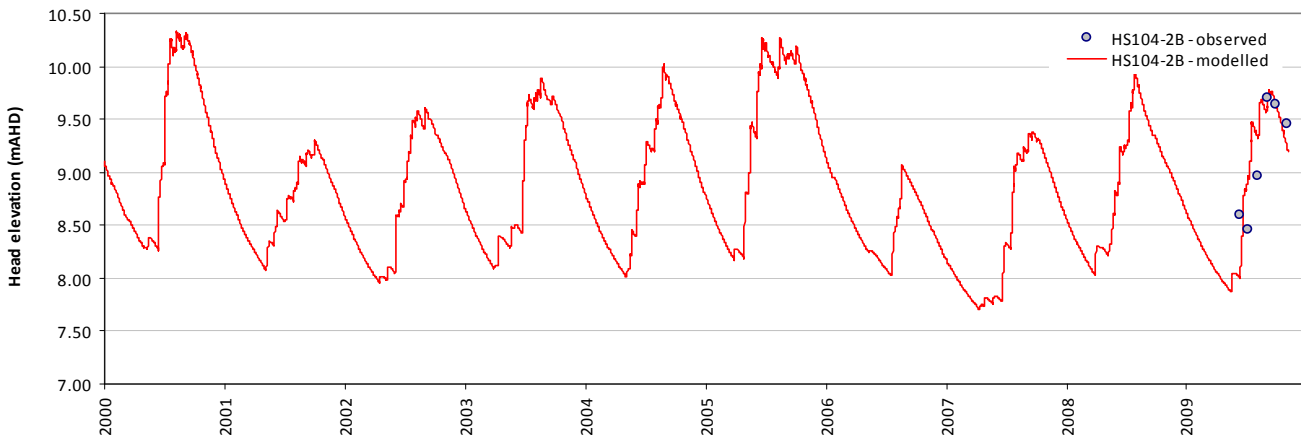
Residual time-series plot - HS104-2A



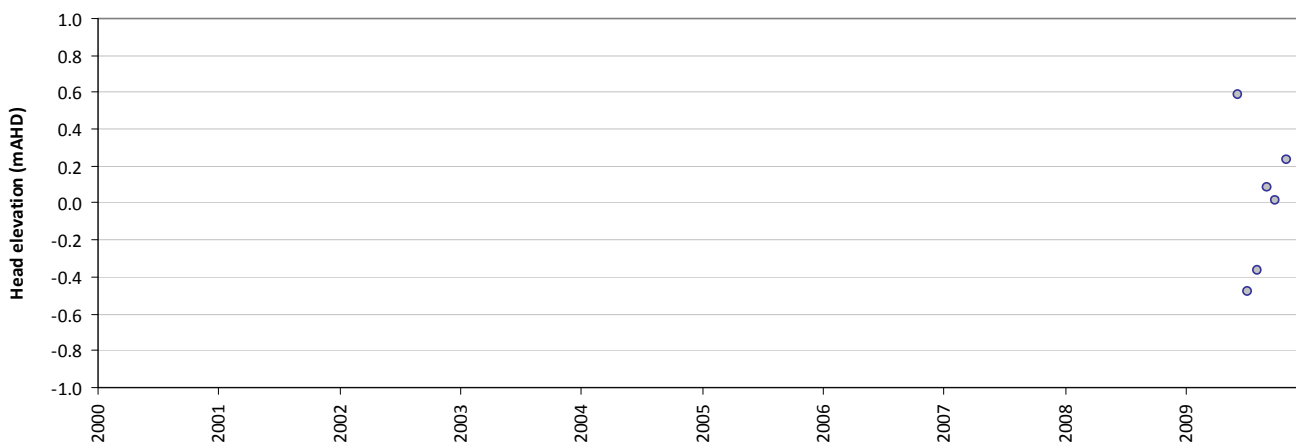
Statistics	
Mean error (ME)	0.11
Mean absolute error (MAE)	0.24
Root mean square error (RMSE)	0.24
Standard deviation of residuals (STDres)	0.27
Correlation coefficient (R)	0.86
Nash Sutcliffe correlation coefficient (R2)	0.67

HS104-2B

Modelled vs observed time-series plot - HS104-2B



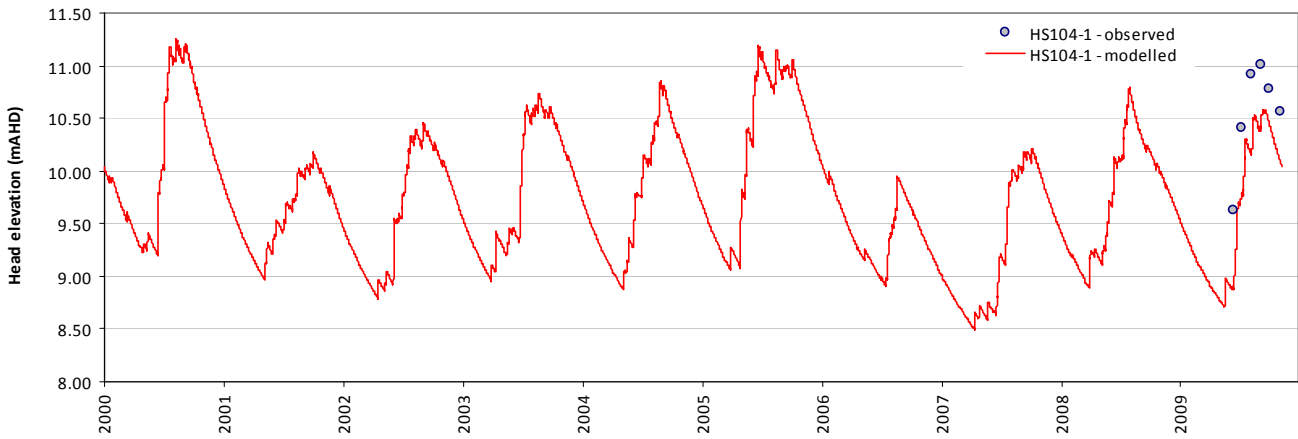
Residual time-series plot - HS104-2B



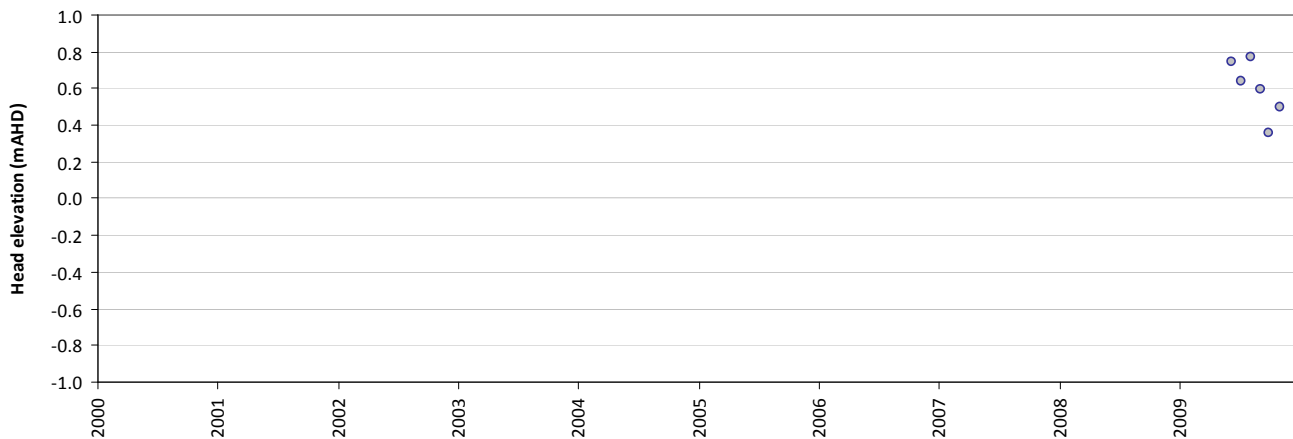
Statistics	
Mean error (ME)	0.01
Mean absolute error (MAE)	0.29
Root mean square error (RMSE)	0.29
Standard deviation of residuals (STDres)	0.36
Correlation coefficient (R)	0.77
Nash Sutcliffe correlation coefficient (R2)	0.48

HS104-1

Modelled vs observed time-series plot - HS104-1



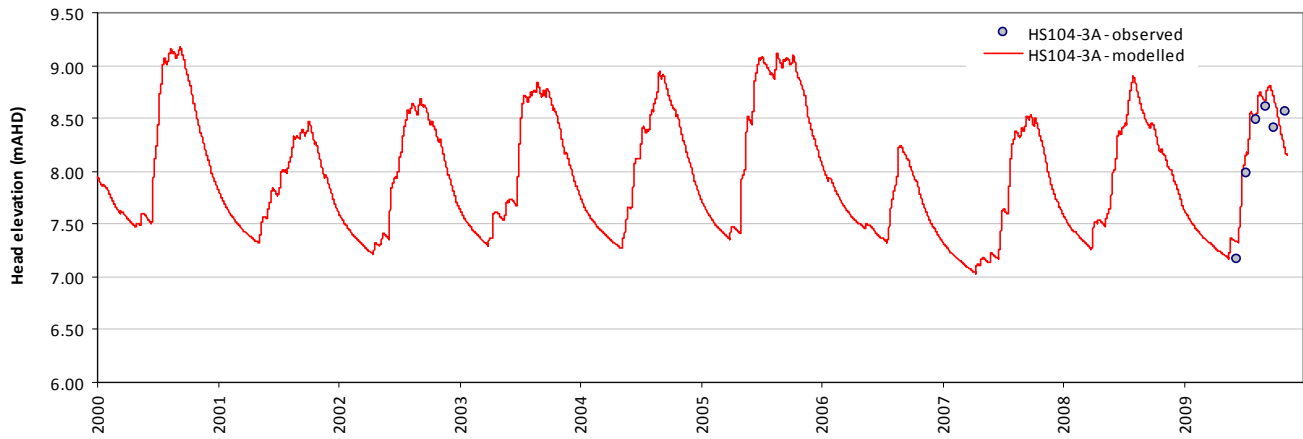
Residual time-series plot - HS104-1



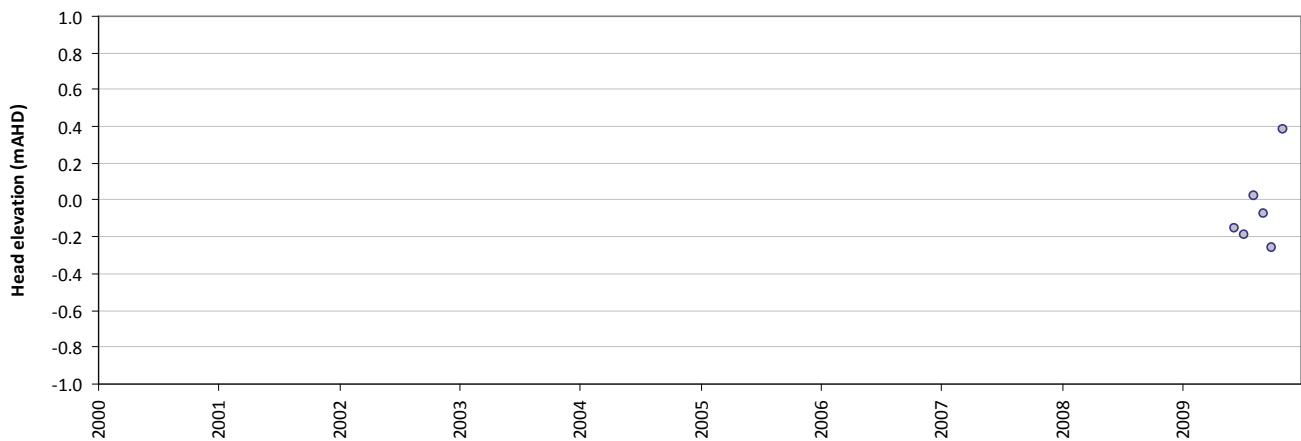
Statistics	
Mean error (ME)	0.60
Mean absolute error (MAE)	0.60
Root mean square error (RMSE)	0.60
Standard deviation of residuals (STDres)	0.14
Correlation coefficient (R)	0.97
Nash Sutcliffe correlation coefficient (R2)	-0.79

HS104-3A

Modelled vs observed time-series plot - HS104-3A



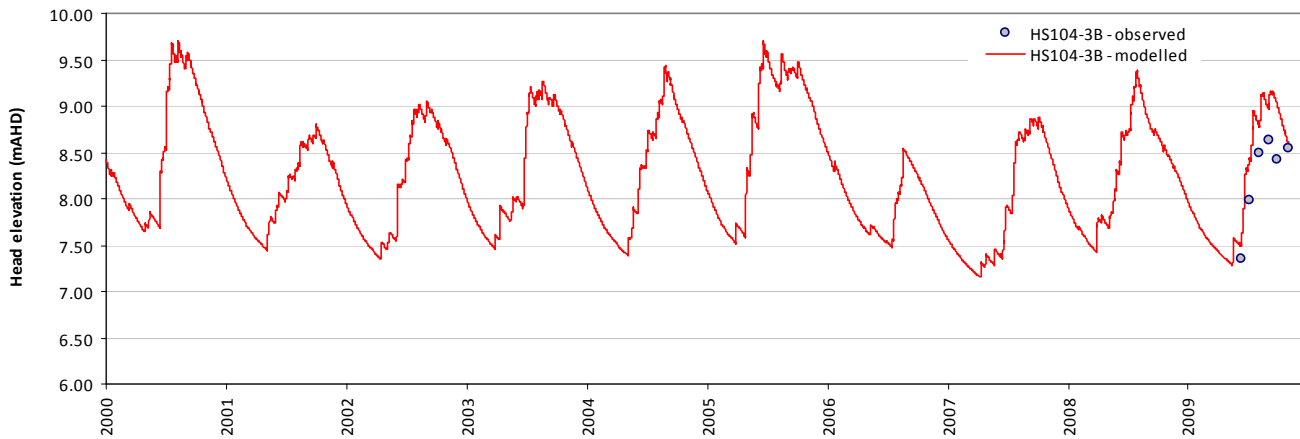
Residual time-series plot - HS104-3A



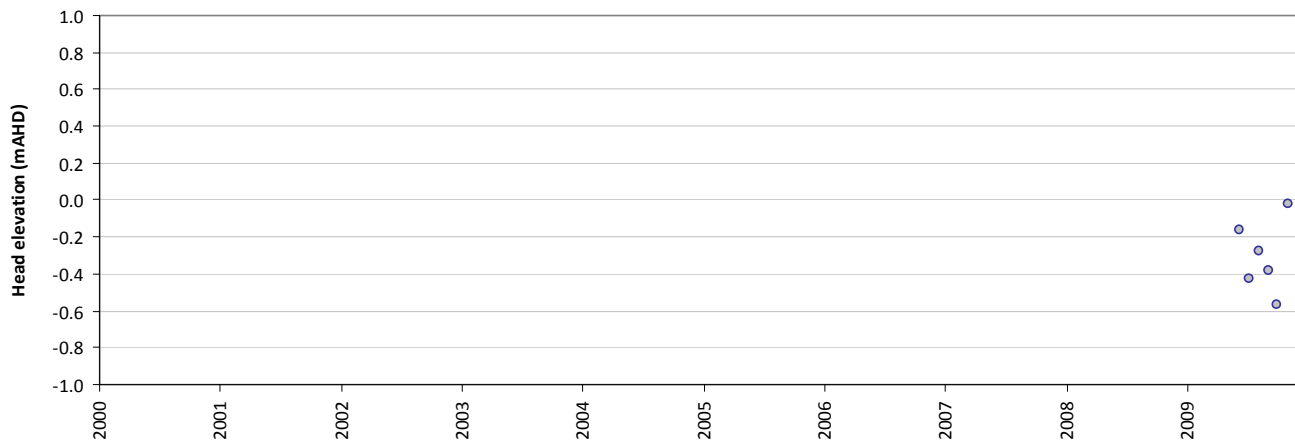
Statistics	
Mean error (ME)	-0.04
Mean absolute error (MAE)	0.18
Root mean square error (RMSE)	0.18
Standard deviation of residuals (STDres)	0.21
Correlation coefficient (R)	0.91
Nash Sutcliffe correlation coefficient (R2)	0.82

HS104-3B

Modelled vs observed time-series plot - HS104-3B



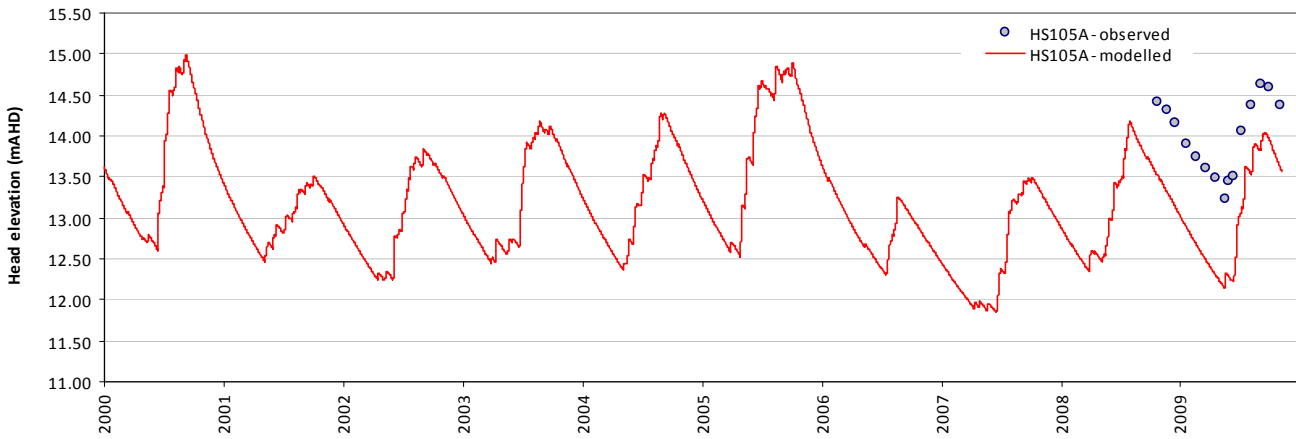
Residual time-series plot - HS104-3B



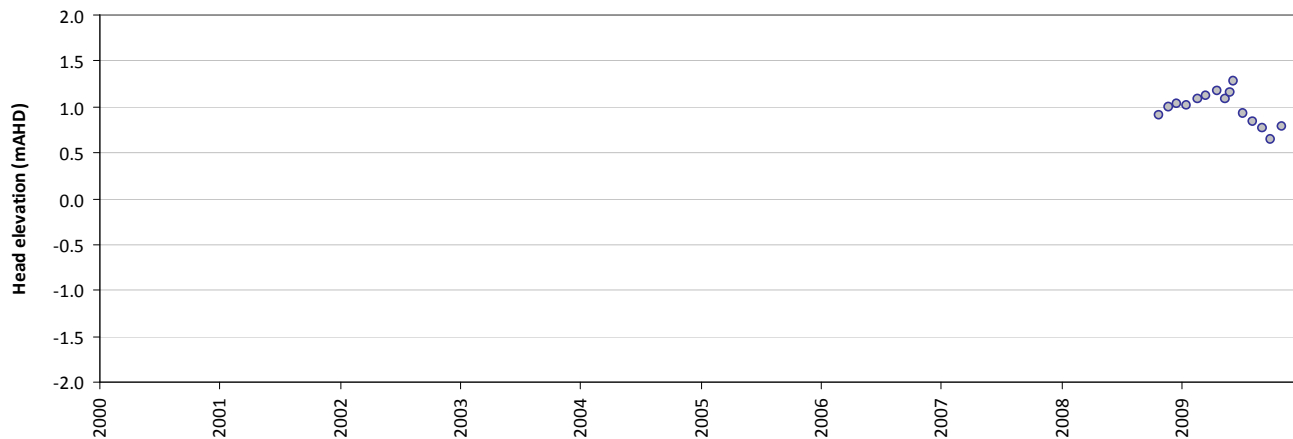
Statistics	
Mean error (ME)	-0.31
Mean absolute error (MAE)	0.31
Root mean square error (RMSE)	0.31
Standard deviation of residuals (STDres)	0.18
Correlation coefficient (R)	0.94
Nash Sutcliffe correlation coefficient (R2)	0.37

HS105A

Modelled vs observed time-series plot - HS105A



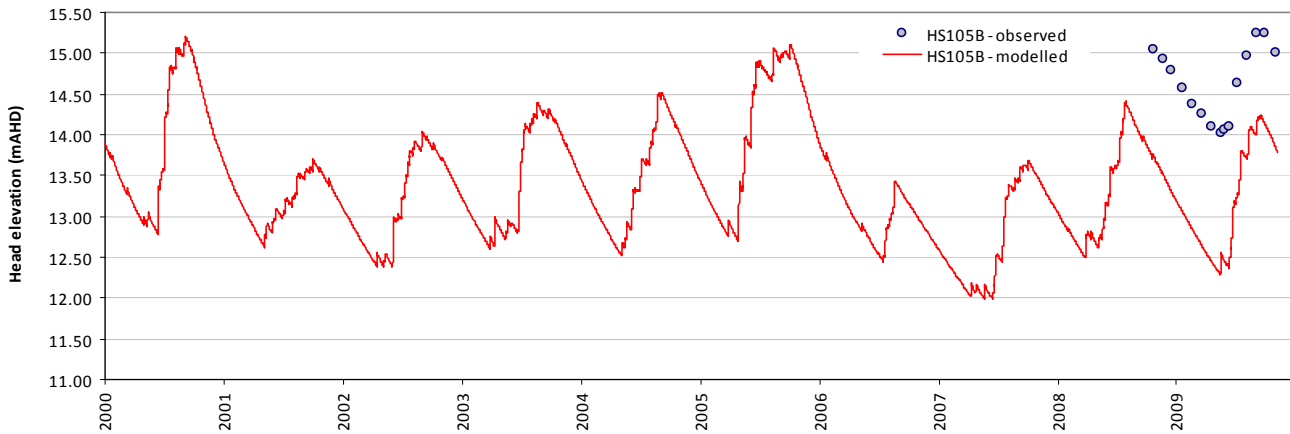
Residual time-series plot - HS105A



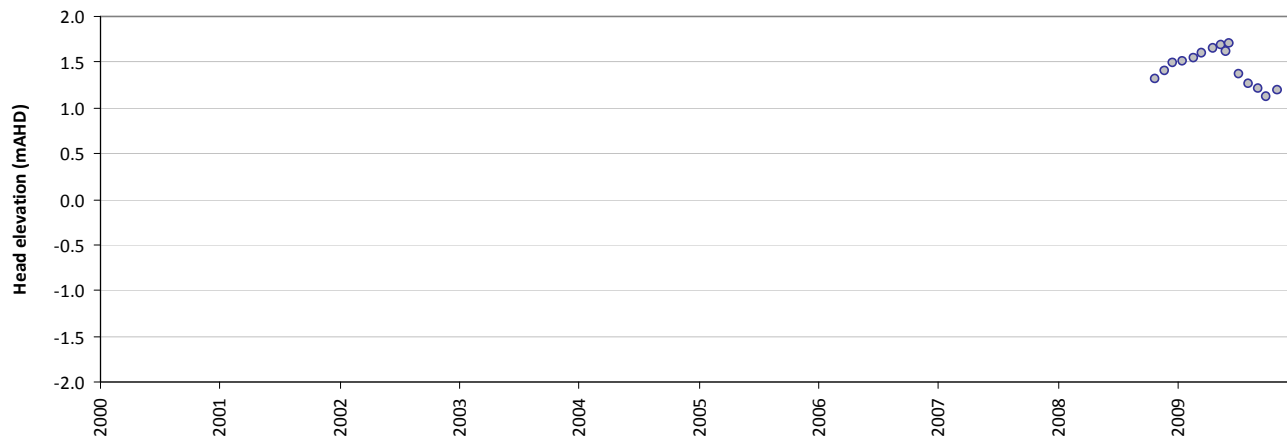
Statistics	
Mean error (ME)	0.99
Mean absolute error (MAE)	0.99
Root mean square error (RMSE)	0.99
Standard deviation of residuals (STDres)	0.17
Correlation coefficient (R)	0.99
Nash Sutcliffe correlation coefficient (R2)	-4.06

HS105B

Modelled vs observed time-series plot - HS105B



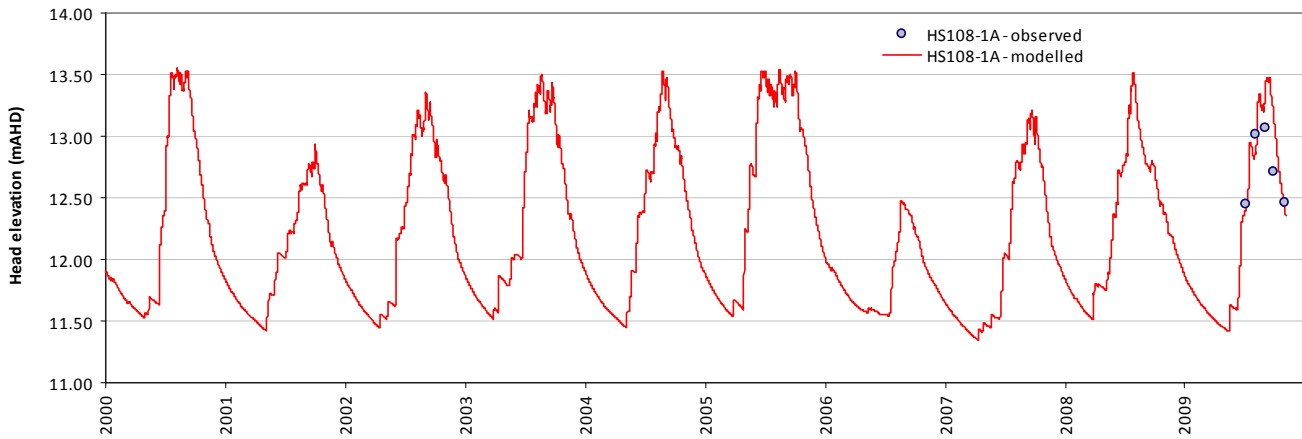
Residual time-series plot - HS105B



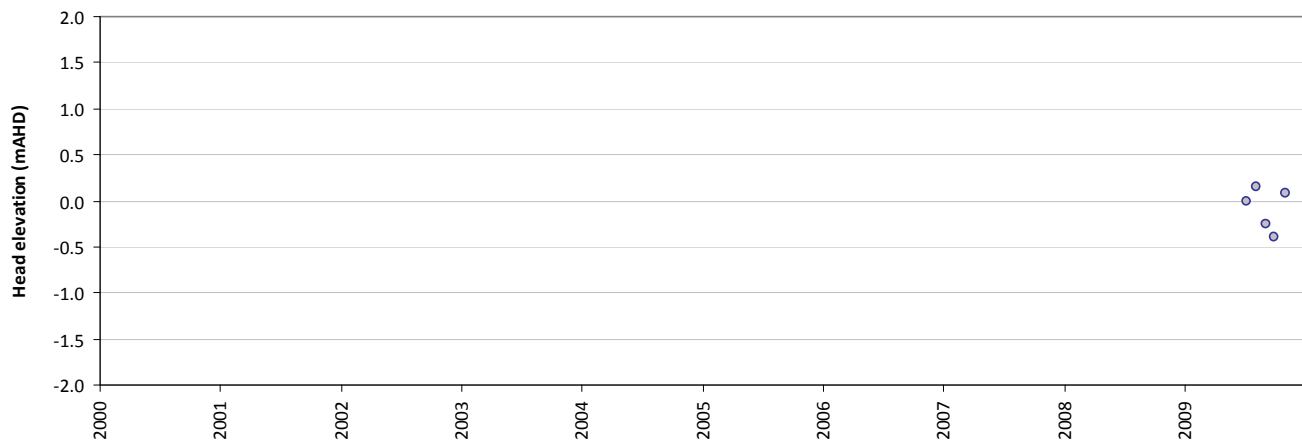
Statistics	
Mean error (ME)	1.44
Mean absolute error (MAE)	1.44
Root mean square error (RMSE)	1.44
Standard deviation of residuals (STDres)	0.19
Correlation coefficient (R)	1.00
Nash Sutcliffe correlation coefficient (R2)	-10.47

HS108-1A

Modelled vs observed time-series plot - HS108-1A



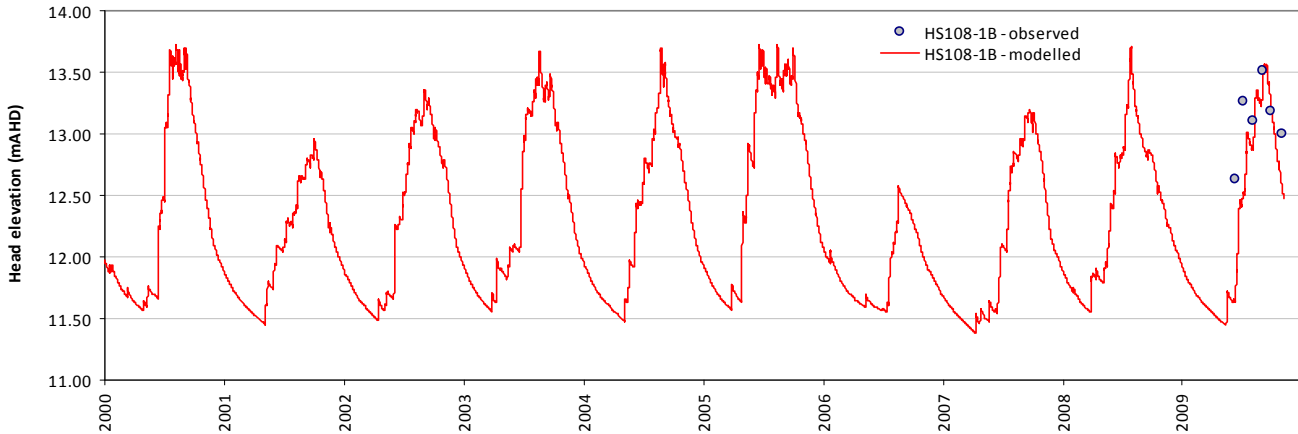
Residual time-series plot - HS108-1A



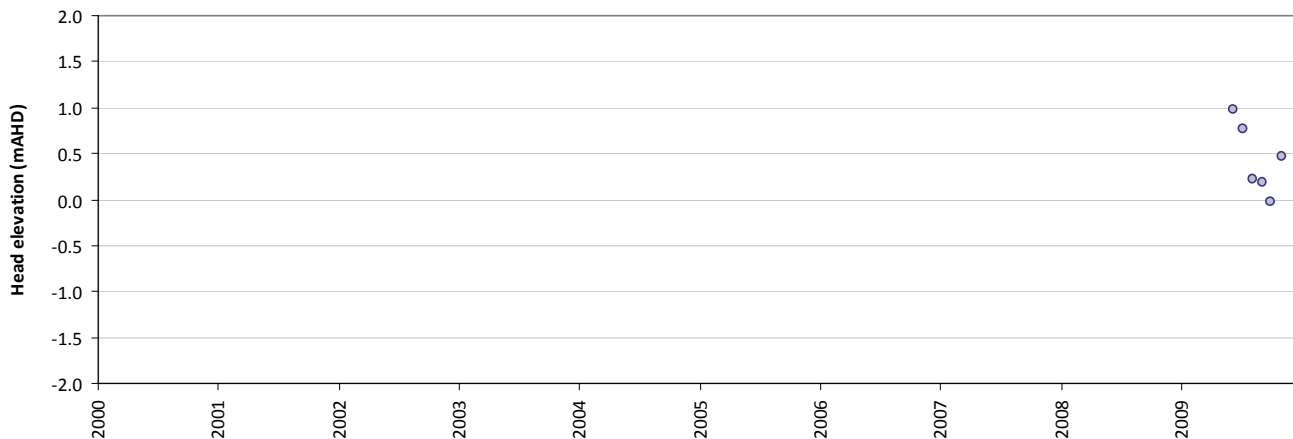
Statistics	
Mean error (ME)	-0.08
Mean absolute error (MAE)	0.18
Root mean square error (RMSE)	0.18
Standard deviation of residuals (STDres)	0.21
Correlation coefficient (R)	0.83
Nash Sutcliffe correlation coefficient (R2)	0.28

HS108-1B

Modelled vs observed time-series plot - HS108-1B



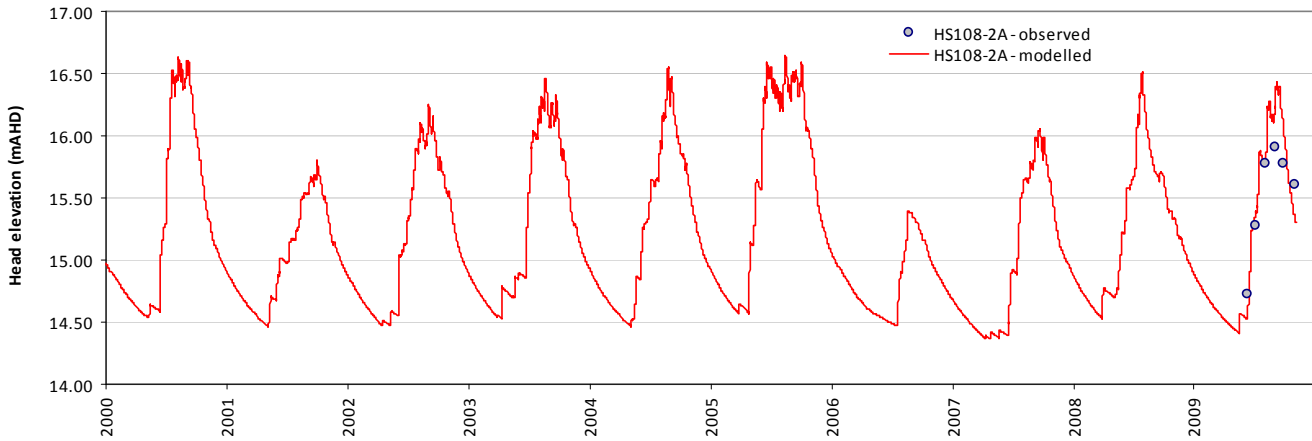
Residual time-series plot - HS108-1B



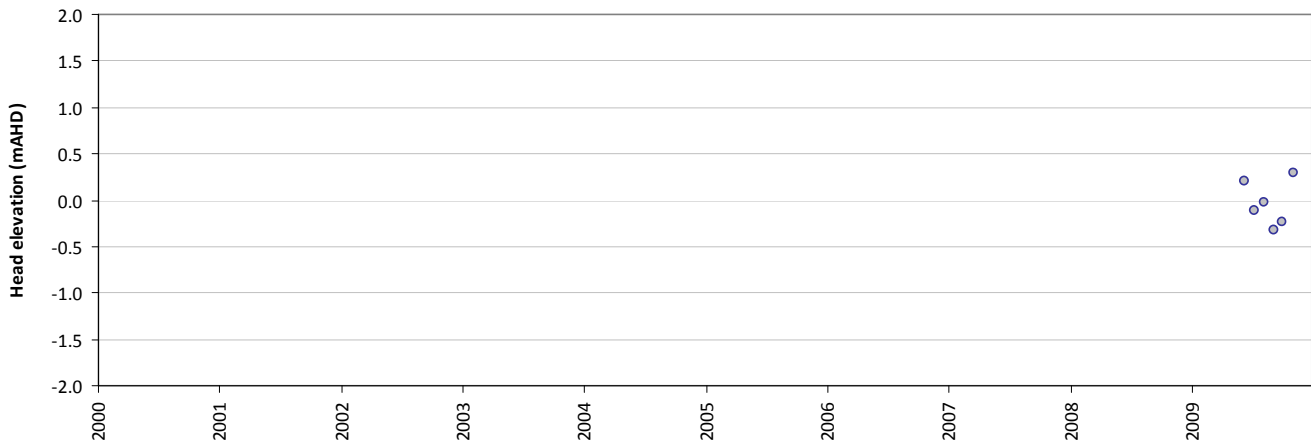
Statistics	
Mean error (ME)	0.43
Mean absolute error (MAE)	0.44
Root mean square error (RMSE)	0.44
Standard deviation of residuals (STDres)	0.35
Correlation coefficient (R)	0.87
Nash Sutcliffe correlation coefficient (R2)	-3.19

HS108-2A

Modelled vs observed time-series plot - HS108-2A



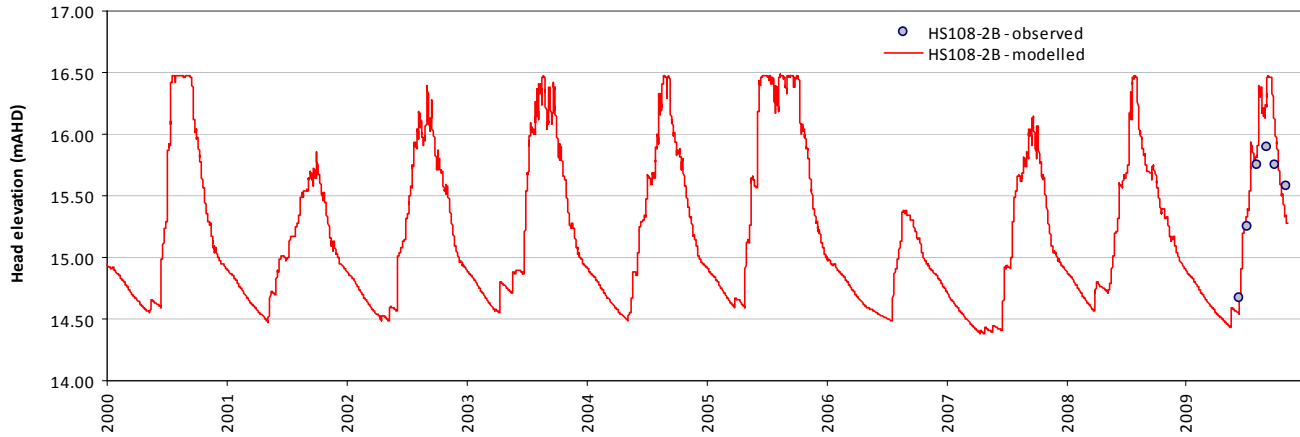
Residual time-series plot - HS108-2A



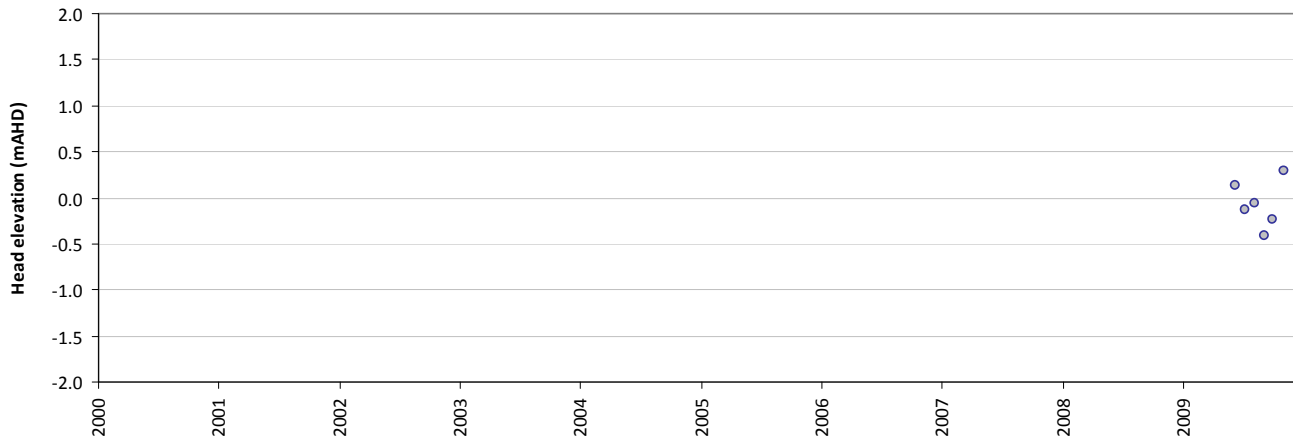
Statistics	
Mean error (ME)	-0.03
Mean absolute error (MAE)	0.20
Root mean square error (RMSE)	0.20
Standard deviation of residuals (STDres)	0.22
Correlation coefficient (R)	0.95
Nash Sutcliffe correlation coefficient (R2)	0.70

HS108-2B

Modelled vs observed time-series plot - HS108-2B



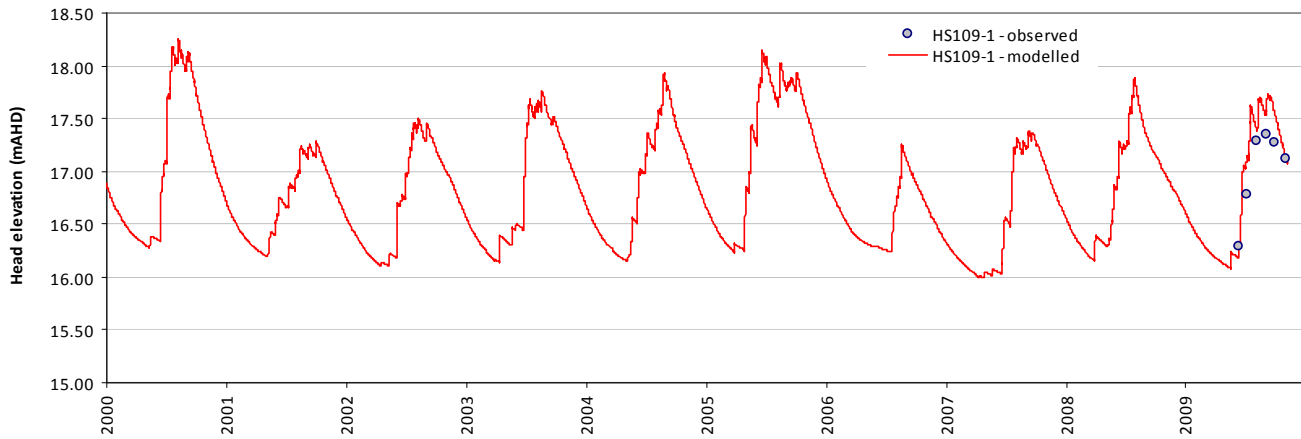
Residual time-series plot - HS108-2B



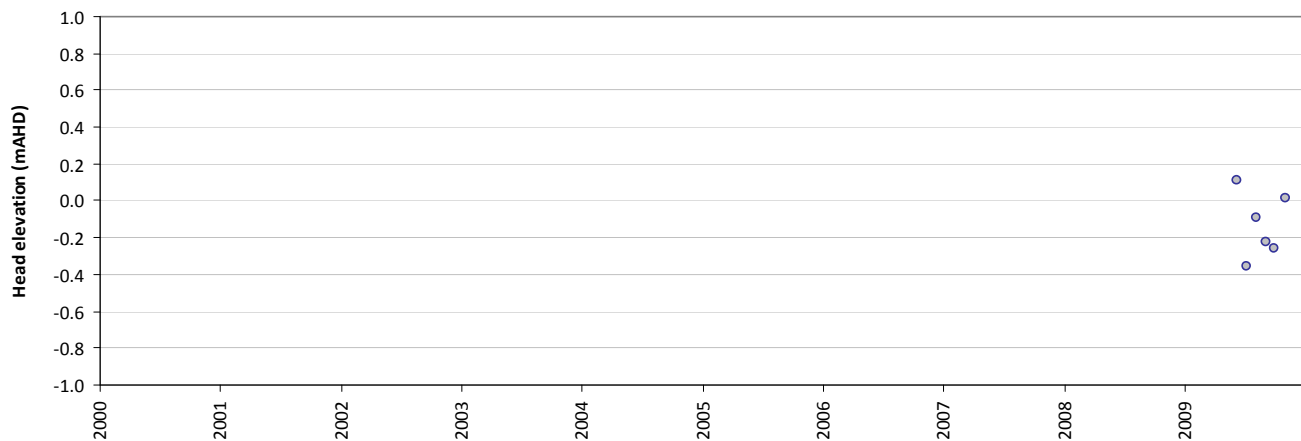
Statistics	
Mean error (ME)	-0.07
Mean absolute error (MAE)	0.21
Root mean square error (RMSE)	0.21
Standard deviation of residuals (STDres)	0.23
Correlation coefficient (R)	0.94
Nash Sutcliffe correlation coefficient (R2)	0.65

HS109-1

Modelled vs observed time-series plot - HS109-1



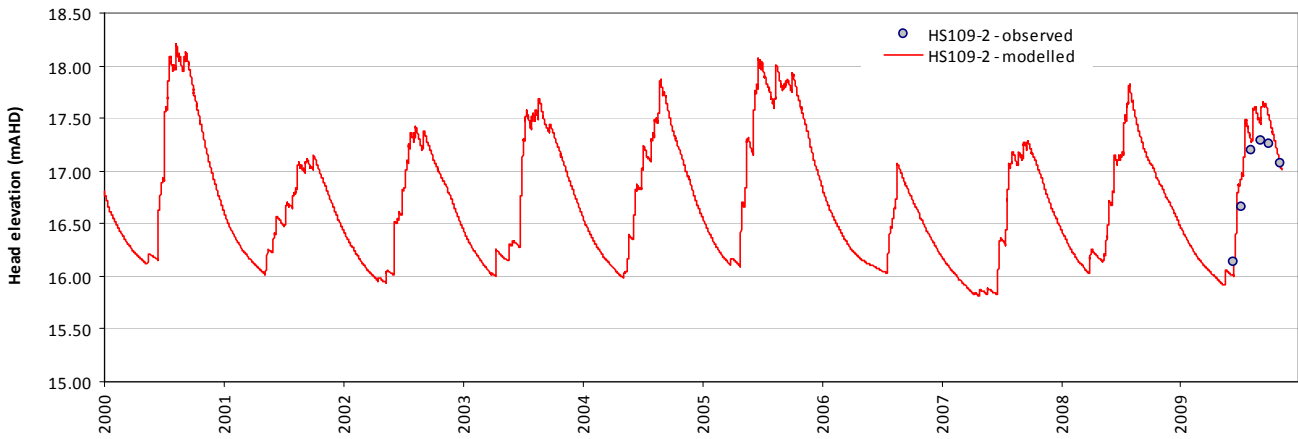
Residual time-series plot - HS109-1



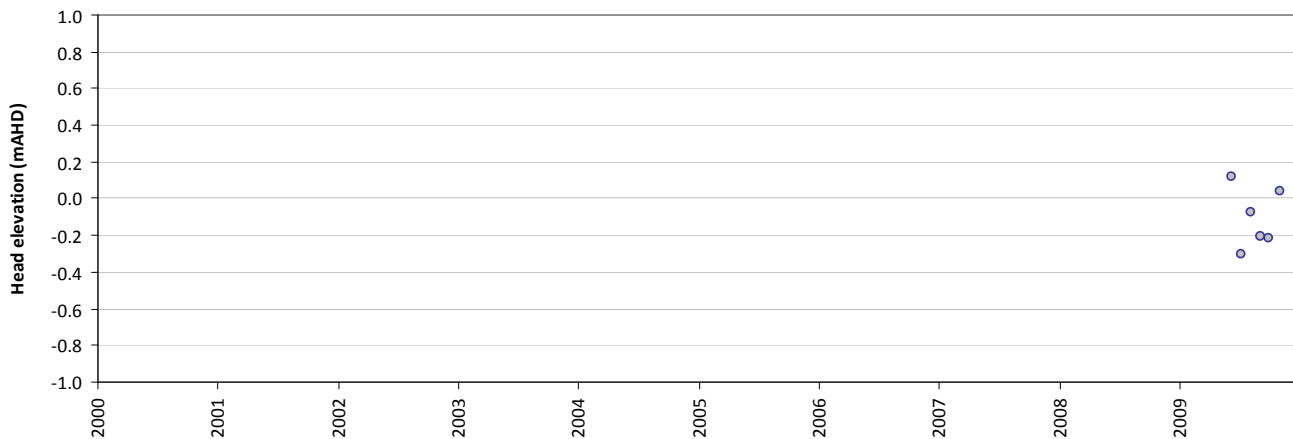
Statistics	
Mean error (ME)	-0.14
Mean absolute error (MAE)	0.17
Root mean square error (RMSE)	0.17
Standard deviation of residuals (STDres)	0.16
Correlation coefficient (R)	0.95
Nash Sutcliffe correlation coefficient (R2)	0.69

HS109-2

Modelled vs observed time-series plot - HS109-2



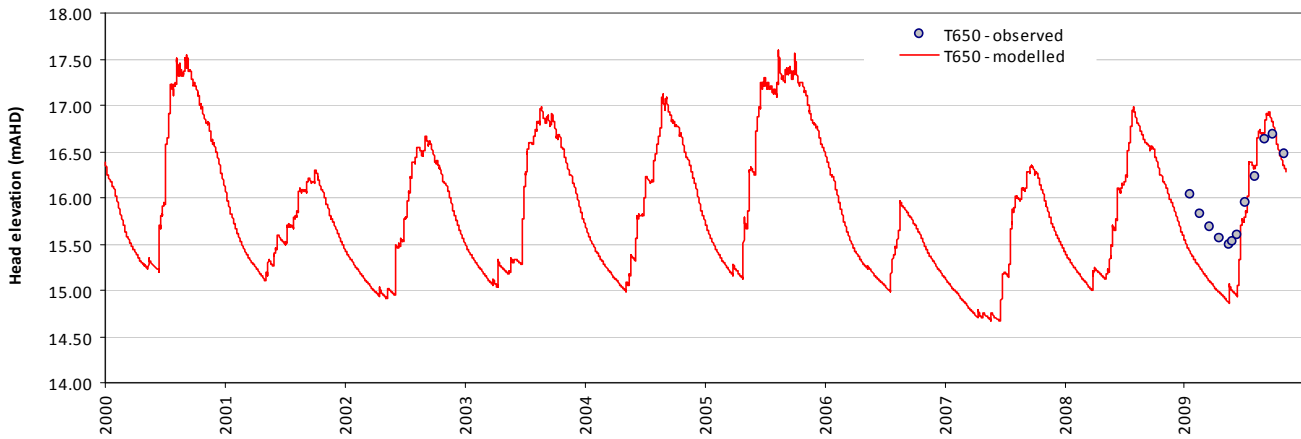
Residual time-series plot - HS109-2



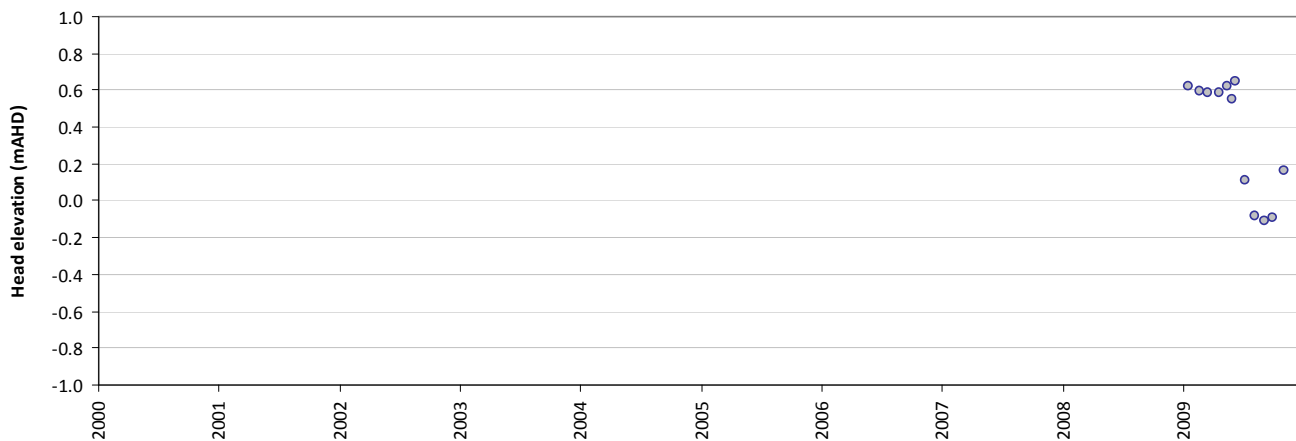
Statistics	
Mean error (ME)	-0.11
Mean absolute error (MAE)	0.16
Root mean square error (RMSE)	0.16
Standard deviation of residuals (STDres)	0.15
Correlation coefficient (R)	0.97
Nash Sutcliffe correlation coefficient (R2)	0.81

T650

Modelled vs observed time-series plot - T650



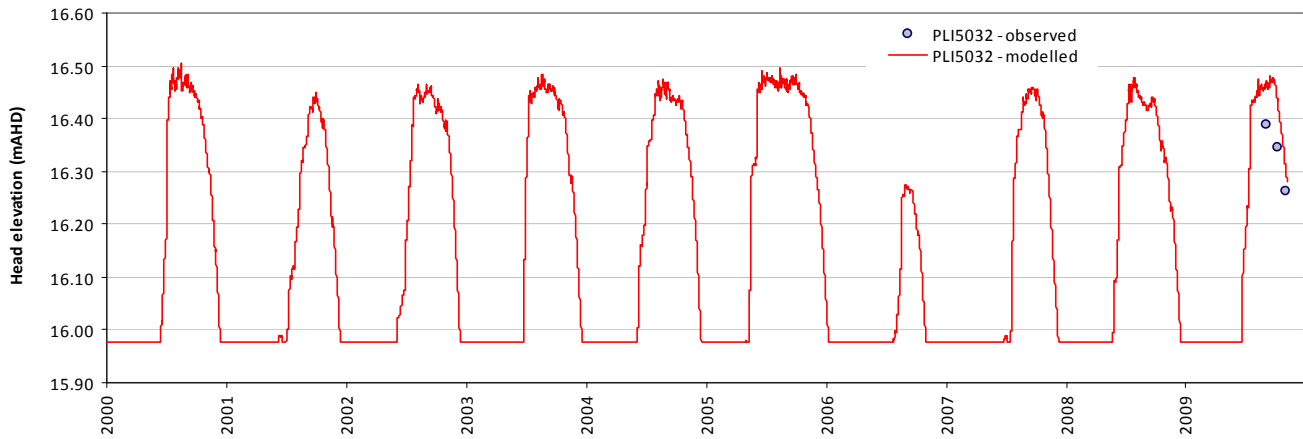
Residual time-series plot - T650



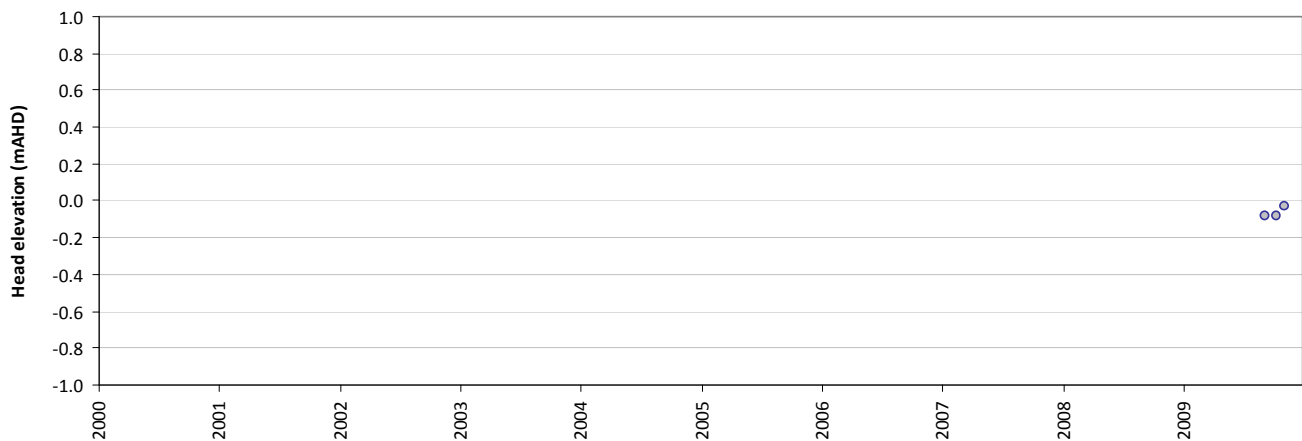
Statistics	
Mean error (ME)	0.35
Mean absolute error (MAE)	0.40
Root mean square error (RMSE)	0.40
Standard deviation of residuals (STDres)	0.31
Correlation coefficient (R)	0.97
Nash Sutcliffe correlation coefficient (R2)	-0.23

PLI5032

Modelled vs observed time-series plot - PLI5032



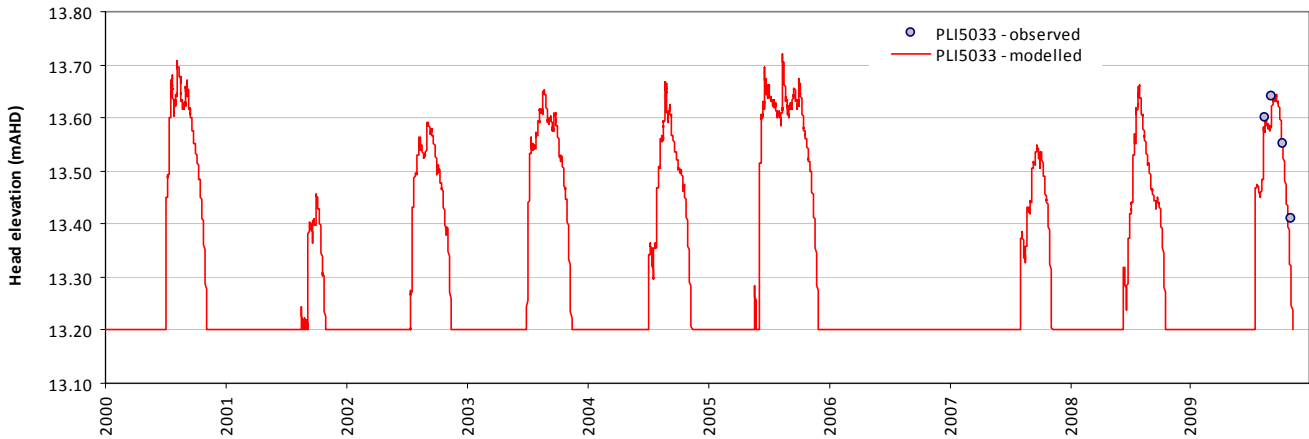
Residual time-series plot - PLI5032



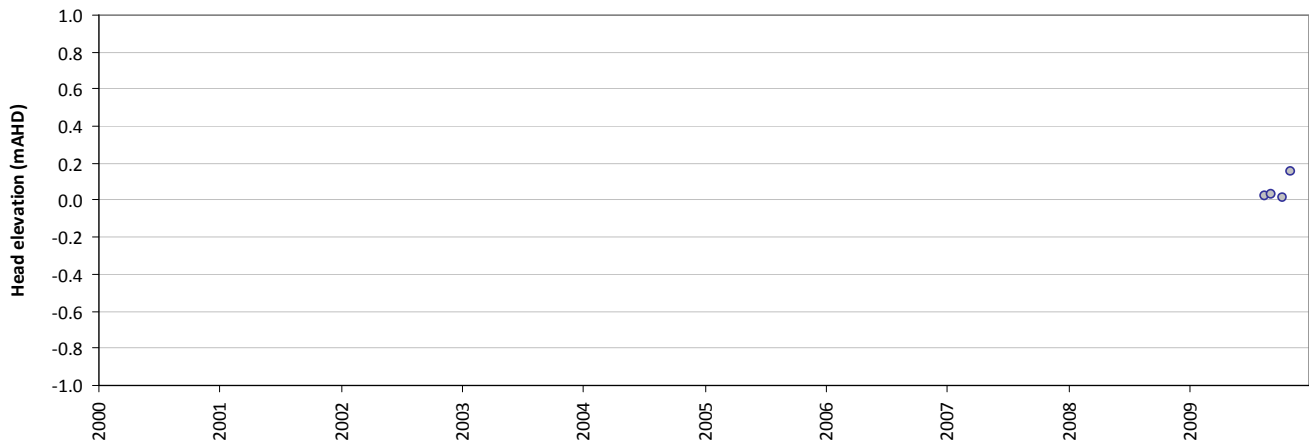
Statistics	
Mean error (ME)	-0.07
Mean absolute error (MAE)	0.07
Root mean square error (RMSE)	0.07
Standard deviation of residuals (STDres)	0.02
Correlation coefficient (R)	0.98
Nash Sutcliffe correlation coefficient (R2)	-0.81

PLI5033

Modelled vs observed time-series plot - PLI5033



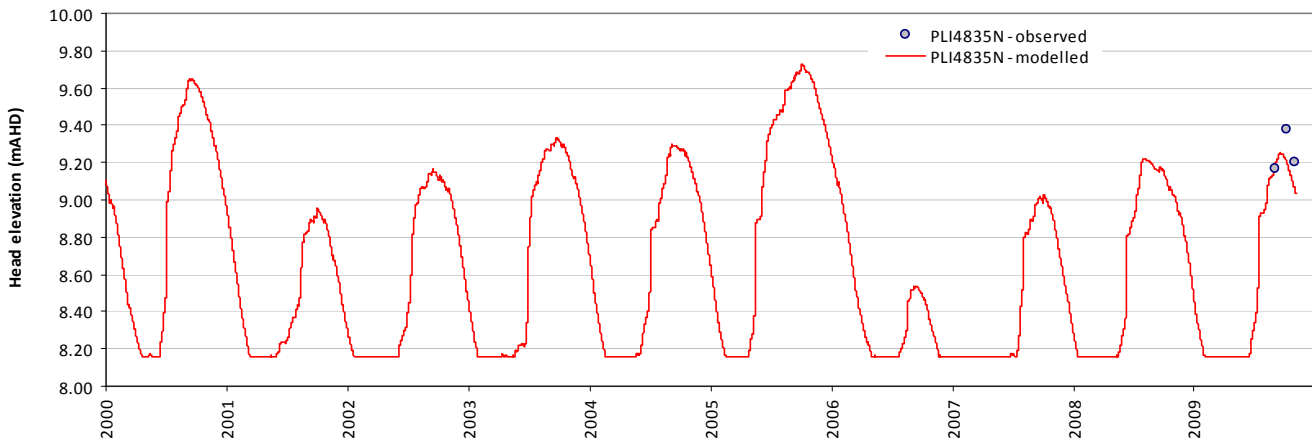
Residual time-series plot - PLI5033



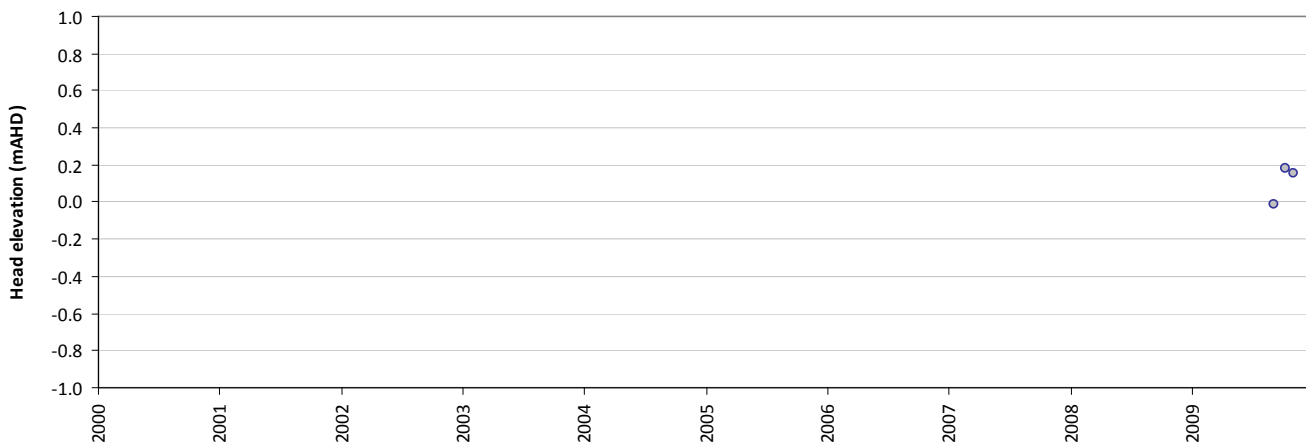
Statistics	
Mean error (ME)	0.05
Mean absolute error (MAE)	0.05
Root mean square error (RMSE)	0.05
Standard deviation of residuals (STDres)	0.06
Correlation coefficient (R)	0.98
Nash Sutcliffe correlation coefficient (R2)	0.18

PLI4835N

Modelled vs observed time-series plot - PLI4835N



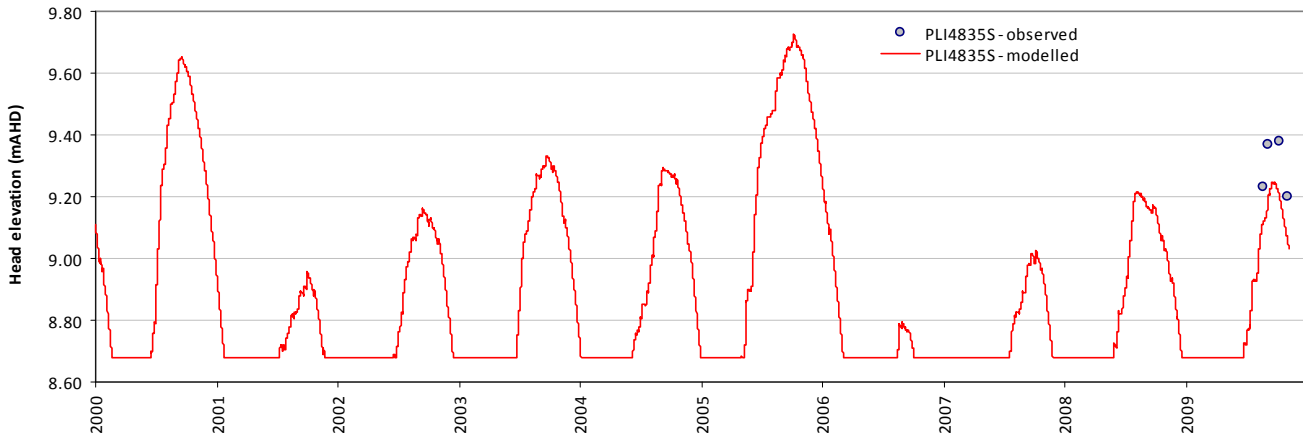
Residual time-series plot - PLI4835N



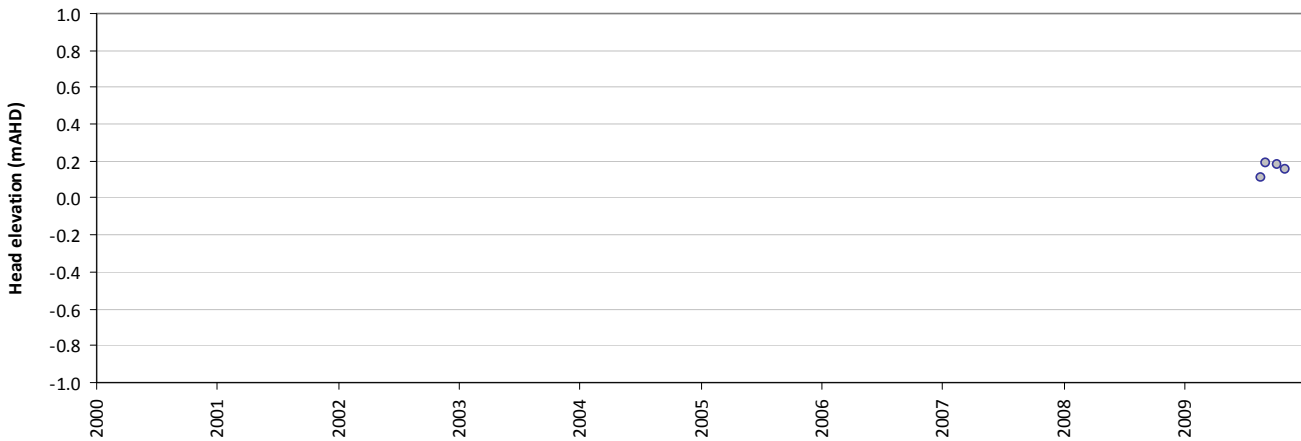
Statistics	
Mean error (ME)	0.11
Mean absolute error (MAE)	0.11
Root mean square error (RMSE)	0.11
Standard deviation of residuals (STDres)	0.08
Correlation coefficient (R)	0.49
Nash Sutcliffe correlation coefficient (R2)	-1.14

PLI4835S

Modelled vs observed time-series plot - PLI4835S



Residual time-series plot - PLI4835S



Statistics	
Mean error (ME)	0.17
Mean absolute error (MAE)	0.17
Root mean square error (RMSE)	0.17
Standard deviation of residuals (STDres)	0.02
Correlation coefficient (R)	1.00
Nash Sutcliffe correlation coefficient (R2)	-3.28

Appendix G: Phillips Road wetland system calibration statistics and plots

Phillips Road wetland system calibration statistics

Table G-1: Phillips Road wetland system calibration statistic for observed vs modelled heads.

Description	Observed	Modelled	Residual	Abs residual
sum (m)	315	317	-1.2	
average (m)	5.09	5.11	-0.02	0.37
median (m)	4.01	4.06	-0.09	0.27
min (m)	2.42	2.90	-0.85	
max (m)	8.28	7.98	1.29	
range (m)	5.86	5.09	2.13	

Table G-1: Phillips Road wetland system summary statistic for observed vs modelled heads.

Description	Symbol	Value
Count	n	62
Sum of squares (m ²)	SSQ	13.51
Mean sum of squares (m ²)	MSSQ	0.22
Root mean square (m)	RMS	0.47
Scaled root mean square (%)	SRMS	7.97
Sum of residuals (m)	SRMS	22.6
Mean sum of residuals (m)	MSR	0.37
Scaled mean sum of residuals (%)	SMSR	6.23
Coefficient of determination (I)	CD	1.24

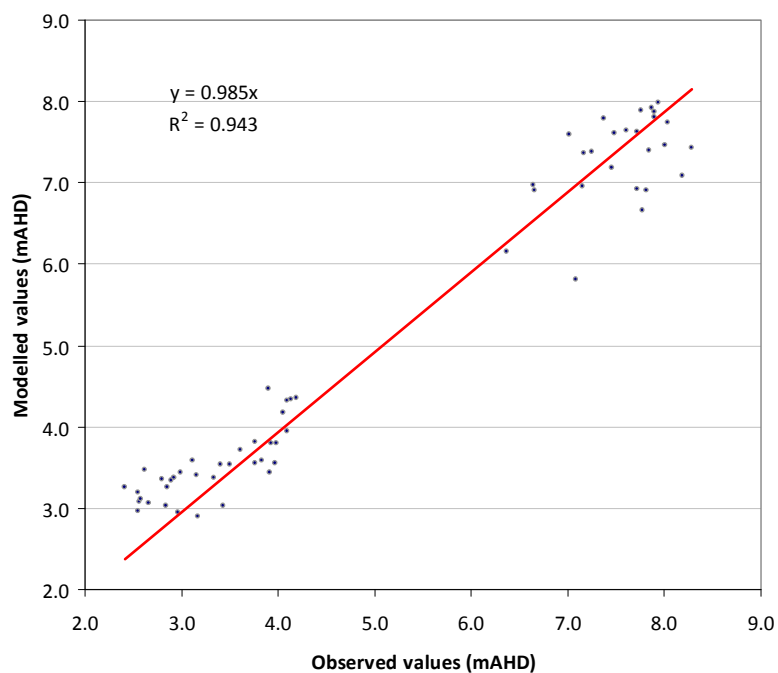


Figure G-1: Phillips Road wetland system scatterplot for observed vs modelled groundwater levels

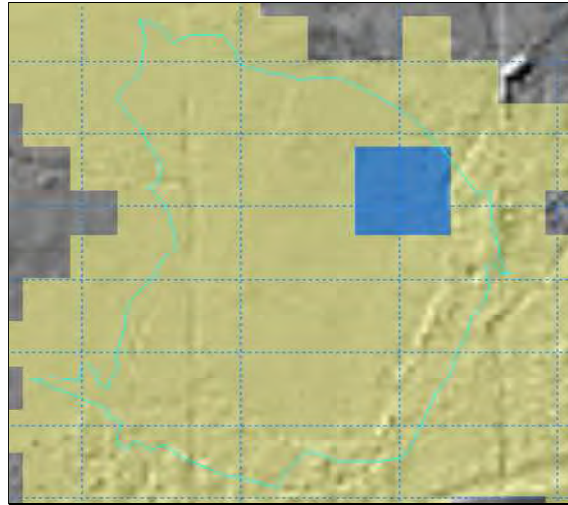
Phillips Road wetland aerial photos vs modelled data

Aerial Photo: December 2005



swancoastplain_South_2006_20cm_z50.ecw

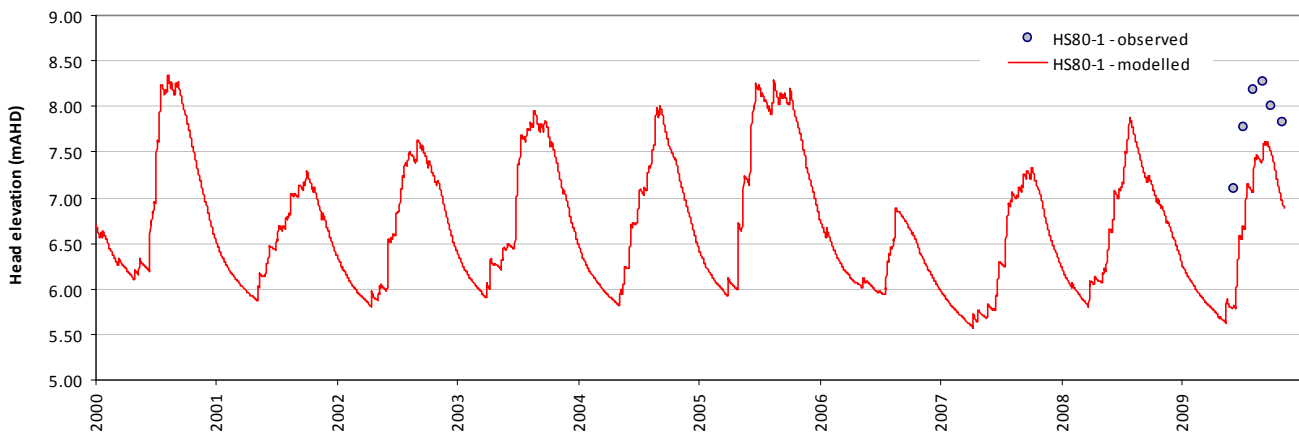
Inundated area: Model



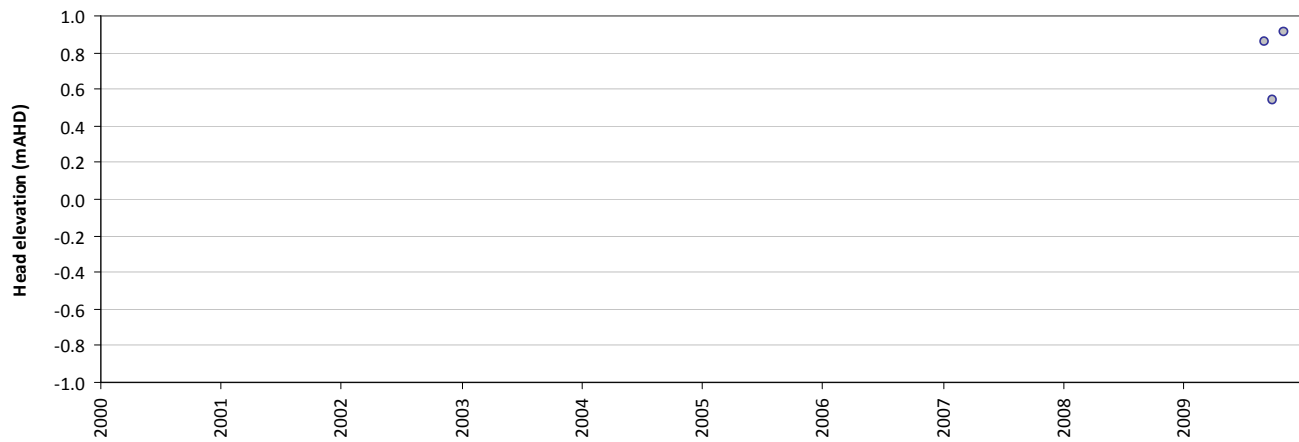
Phillips Road wetland system calibration plots

HS80-1

Modelled vs observed time-series plot - HS80-1



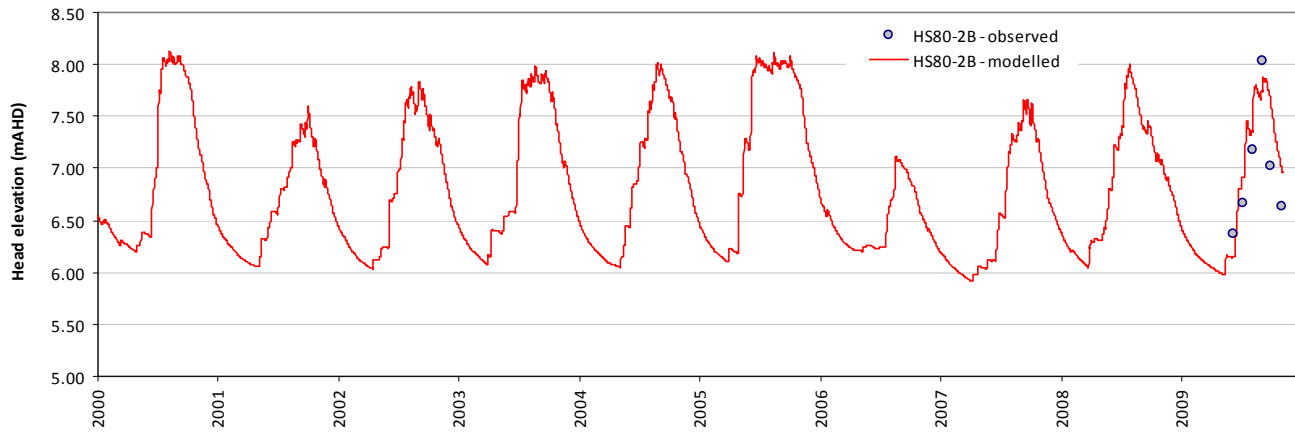
Residual time-series plot - HS80-1



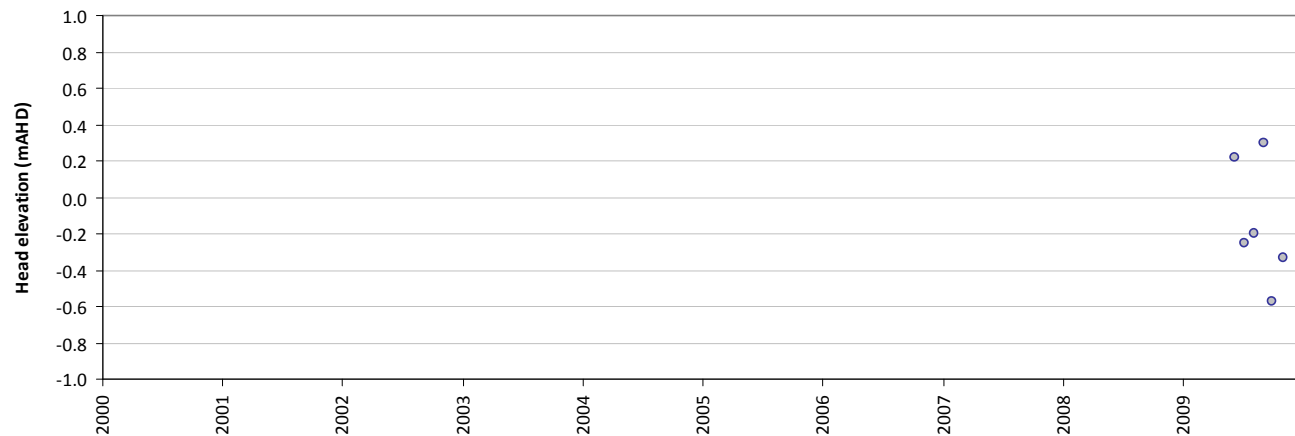
Statistics	
Mean error (ME)	0.97
Mean absolute error (MAE)	0.97
Root mean square error (RMSE)	0.99
Standard deviation of residuals (STDres)	0.24
Correlation coefficient (R)	0.94
Nash Sutcliffe correlation coefficient (R2)	-5.52

HS80-2B

Modelled vs observed time-series plot - HS80-2B



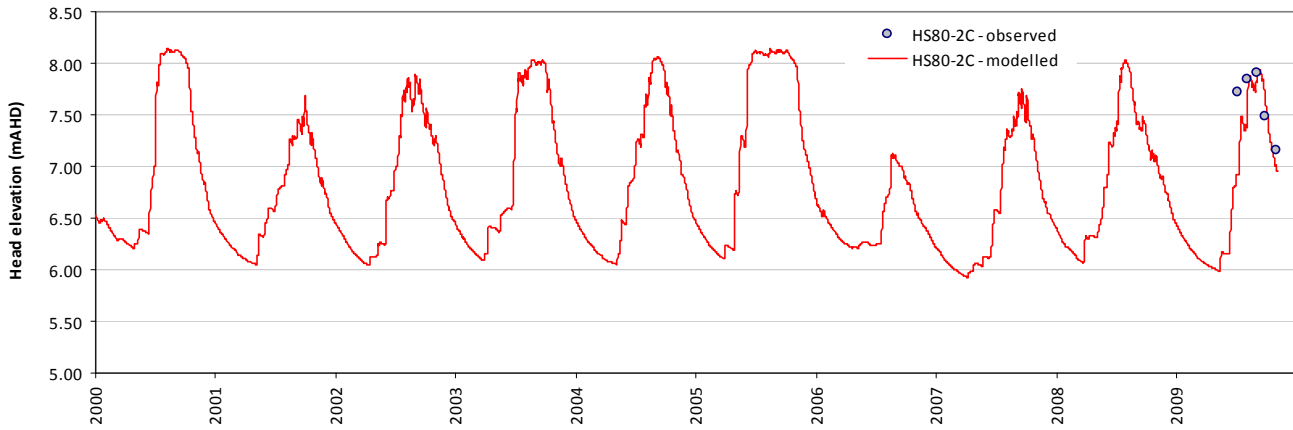
Residual time-series plot - HS80-2B



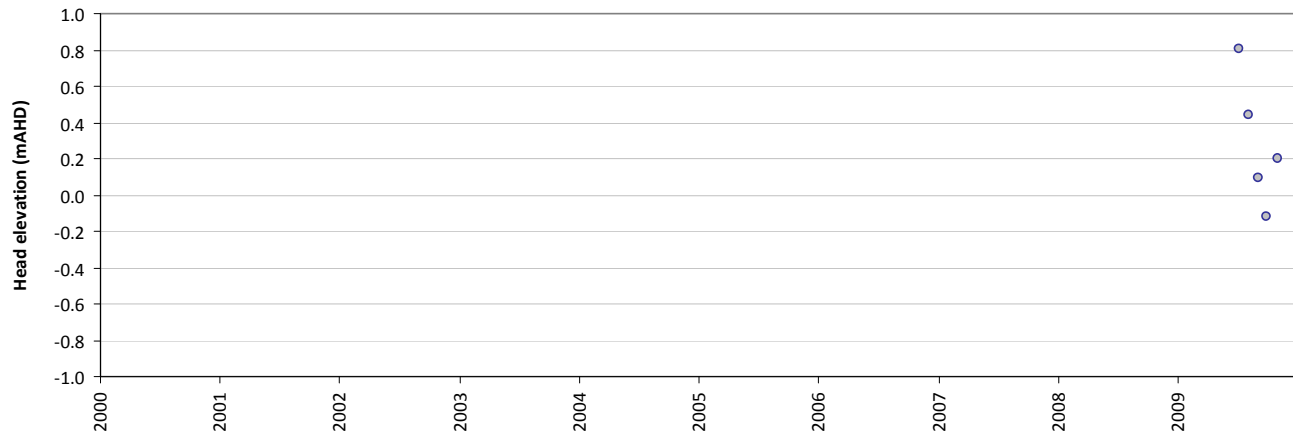
Statistics	
Mean error (ME)	-0.14
Mean absolute error (MAE)	0.31
Root mean square error (RMSE)	0.34
Standard deviation of residuals (STDres)	0.31
Correlation coefficient (R)	0.84
Nash Sutcliffe correlation coefficient (R2)	0.61

HS80-2C

Modelled vs observed time-series plot - HS80-2C



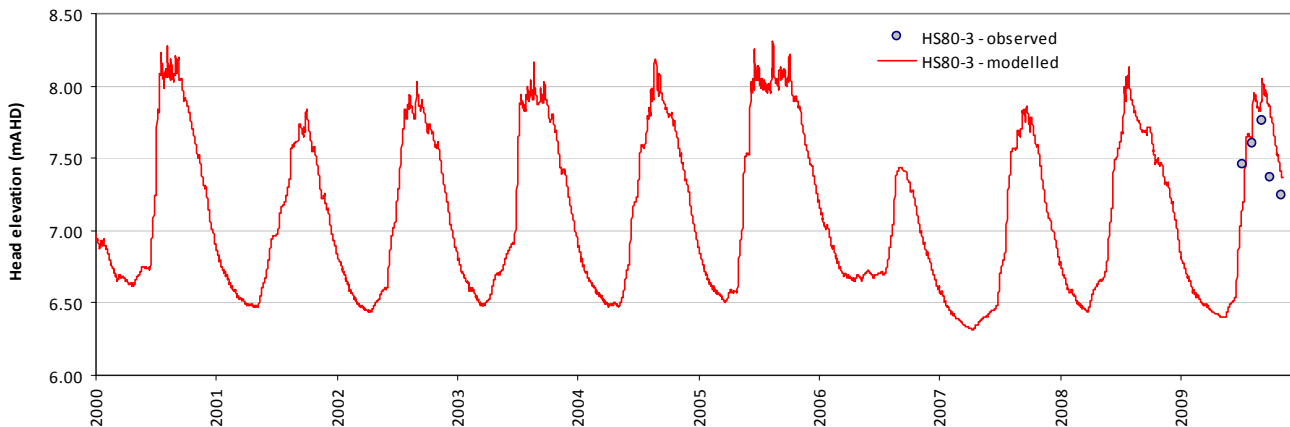
Residual time-series plot - HS80-2C



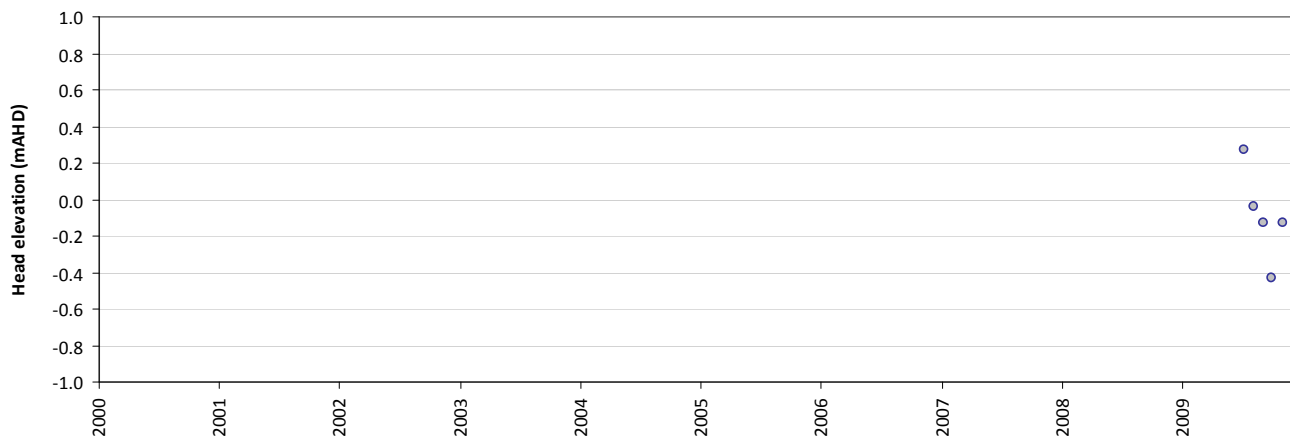
Statistics	
Mean error (ME)	0.28
Mean absolute error (MAE)	0.33
Root mean square error (RMSE)	0.42
Standard deviation of residuals (STDres)	0.32
Correlation coefficient (R)	0.51
Nash Sutcliffe correlation coefficient (R2)	-1.45

HS80-3

Modelled vs observed time-series plot - HS80-3



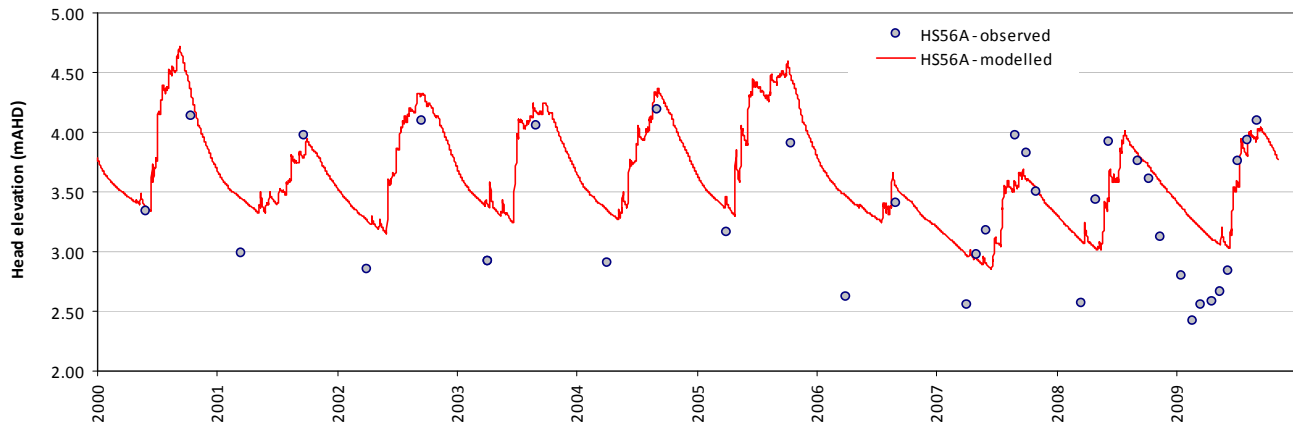
Residual time-series plot - HS80-3



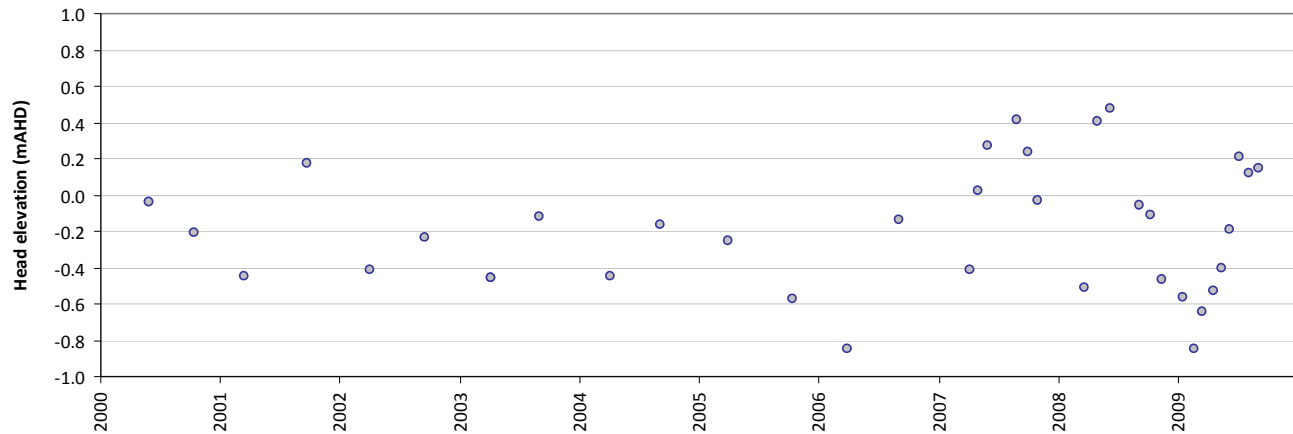
Statistics	
Mean error (ME)	-0.09
Mean absolute error (MAE)	0.20
Root mean square error (RMSE)	0.24
Standard deviation of residuals (STDres)	0.22
Correlation coefficient (R)	0.55
Nash Sutcliffe correlation coefficient (R2)	-0.84

HS56A

Modelled vs observed time-series plot - HS56A



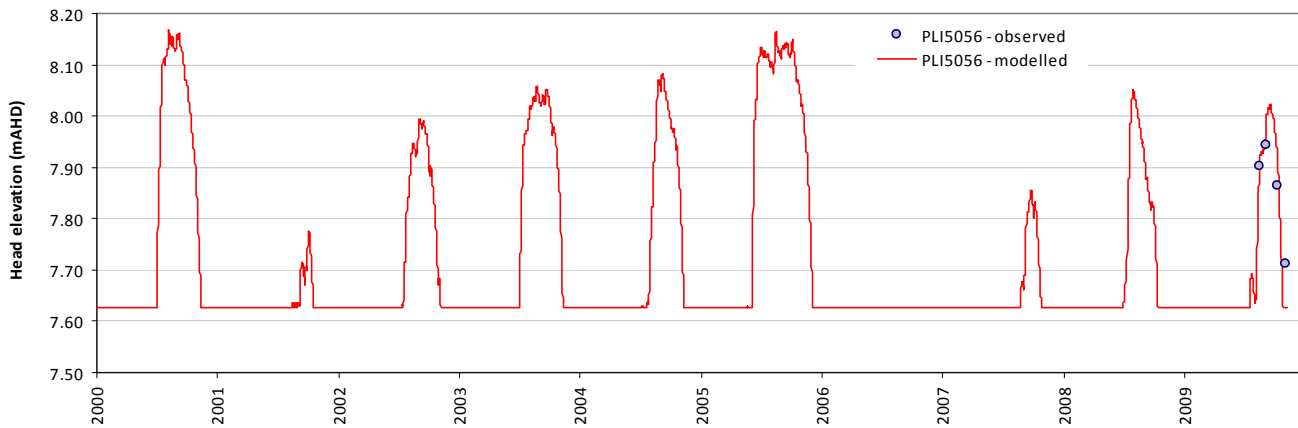
Residual time-series plot - HS56A



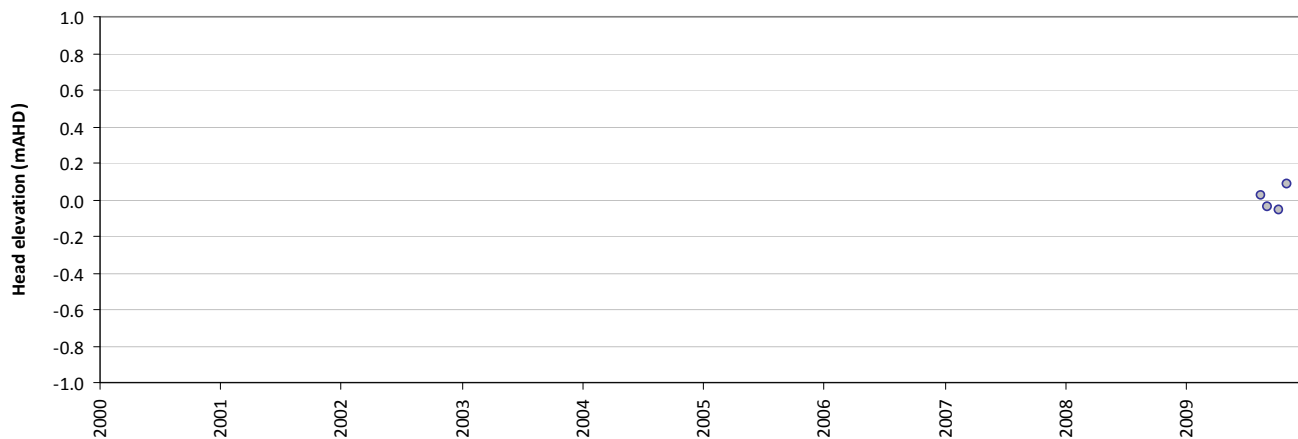
Statistics	
Mean error (ME)	-0.20
Mean absolute error (MAE)	0.34
Root mean square error (RMSE)	0.40
Standard deviation of residuals (STDres)	0.34
Correlation coefficient (R)	0.79
Nash Sutcliffe correlation coefficient (R2)	0.50

PLI5056

Modelled vs observed time-series plot - PLI5056



Residual time-series plot - PLI5056



Statistics	
Mean error (ME)	0.01
Mean absolute error (MAE)	0.05
Root mean square error (RMSE)	0.06
Standard deviation of residuals (STDres)	0.06
Correlation coefficient (R)	0.96
Nash Sutcliffe correlation coefficient (R2)	0.59



Water Science
technical series

Looking after all our water needs

Department of Water

168 St Georges Terrace, Perth, Western Australia
PO Box K822 Perth Western Australia 6842
Phone: (08) 6364 7600
Fax: (08) 6364 7601
www.water.wa.gov.au

5944 00 0610